SR-5

Coastal Hydraulic Models

by

Robert Y. Hudson, Frank A. Herrmann, Jr., Richard A. Sager,

Robert W. Whalin, Garbis H. Keulegan,

Claude E. Chatham, Jr., and Lyndell Z. Hales

SPECIAL REPORT NO. 5

MAY 1979

Prepared for

U.S. ARMY, CORPS OF ENGINEERS

COASTAL ENGINEERING RESEARCH CENTER

Kingman Building

Fort Belvoir, Va. 22060

U.S. Army Coastal Engineering Research Center
Kingman Building
Fort Belvoir, Virginia 22060

REPORT DOCUMENTATION PAGE

READ INSTRUCTIONS BEFORE COMPLETING FORM

1. REPORT NUMBER: SR-5	2. GOVT ACCESSION NO.
3. RECIPIENT'S CATALOG NUMBER	
4. TITLE (and Subtitle): COASTAL HYDRAULIC MODELS	5. TYPE OF REPORT & PERIOD COVERED: Special Report
	6. PERFORMING ORG. REPORT NUMBER
7. AUTHOR(s): Robert Y. Hudson, Frank A. Herrmann, Jr., Richard A. Sager, Robert W. Whalin, Garbis H. Keulegan, Claude E. Chatham, Jr., and Lyndell Z. Hales	8. CONTRACT OR GRANT NUMBER(s)
9. PERFORMING ORGANIZATION NAME AND ADDRESS: U.S. Army Engineer Waterways Experiment Station, P.O. Box 631, Vicksburg, Mississippi 39180	10. PROGRAM ELEMENT, PROJECT, TASK AREA & WORK UNIT NUMBERS: F31234
11. CONTROLLING OFFICE NAME AND ADDRESS: Department of the Army, Coastal Engineering Research Center (CEREN-CD), Kingman Building, Fort Belvoir, VA 22060	12. REPORT DATE: May 1979
	13. NUMBER OF PAGES: 531
14. MONITORING AGENCY NAME & ADDRESS(if different from Controlling Office)	15. SECURITY CLASS. (of this report): UNCLASSIFIED
	15a. DECLASSIFICATION/DOWNGRADING SCHEDULE

16. DISTRIBUTION STATEMENT (of this Report)

Approved for public release; distribution unlimited

17. DISTRIBUTION STATEMENT (of the abstract entered in Block 20, if different from Report)

18. SUPPLEMENTARY NOTES

19. KEY WORDS (Continue on reverse side if necessary and identify by block number)

Coastal erosion	Fixed-bed models	Model construction
Coastal harbors	Hydraulic models	Model design
Coastal structures	Hydraulic similitude	Model verification
Estuaries	Inlets	Movable-bed models

20. ABSTRACT (Continue on reverse side if necessary and identify by block number)

This is a comprehensive report describing the use of hydraulic models to assist in the solution of complex coastal engineering problems. This report provides information for use by both the laboratory research engineer and the field design engineer on the capabilities and limitations of coastal hydraulic modeling procedures. The report is intended to provide sufficient information to document the state-of-the-art of scale modeling practiced by the U.S. Army Engineer Waterways Experiment Station (WES); and for field design engineers

(Continued)

and other laboratory research engineers to better understand the principles of scale models and the application of these principles in the design, construction, and operation of scale hydraulic models in the solution of problems involving the interaction of waves, tides, currents, and related sediment movements in estuaries, coastal harbors, coastal erosion, and stability of coastal structures and inlets.

PREFACE

This report is published to provide coastal engineers with sufficient information for an understanding of the capabilities and limitations of coastal hydraulic models. It also provides the laboratory engineer with valuable information concerning the design, construction, and operation of physical models. The work was carried out by the U.S. Army Engineer Waterways Experiment Station (WES) under the coastal engineering research program of the U.S. Army Coastal Engineering Research Center (CERC).

This report is one of a series of reports to be published to form a Coastal Engineering Manual.

The report includes information on physical modeling of waves, tides, currents, and the related sediment movement, structure and harbor design problems in the coastal zone pertinent to interests of navigation, beach erosion, and control of storm-generated flooding. The report was intended to be a comprehensive state-of-the-art review; however, because information concerning new procedures is relatively slow in being published, and because detailed information on model design, construction, and operation is often not available in the literature, the primary emphasis is on the state-of-the-art of physical coastal modeling at WES. The report draws extensively from the open literature, particularly the sections on similitude, coastal harbors, and coastal structures. Continual improvements to the state-of-the-art in coastal hydraulic modeling since this report was prepared, have already outdated some parts. In this report the term *verification* is the process of adjusting model parameters until the model can reproduce measured prototype data, and normally checking the adjustment by assuring the model reproduces at least two separate sets of prototype data. Abbreviations in this report conform to the U.S. Government Printing Office Style Manual.

This report was prepared by WES and authored by (indicated for each of the seven Sections) Robert Y. Hudson, formerly Chief, Wave Dynamics Division; Frank A. Herrmann, Jr., Assistant Chief, Hydraulics Laboratory; Richard A. Sager, Chief, Estuaries Division; Dr. Robert W. Whalin, Chief, Wave Dynamics Division; Dr. Garbis H. Keulegan, Special Assistant to the Chief of the Hydraulics Laboratory; Claude E. Chatham, Jr., Chief, Wave Research Branch; and Dr. Lyndell Z. Hales, Wave Research Branch; under the general supervision of Henry B. Simmons, Chief, Hydraulics Laboratory. During the preparation of this report, the Commander and Directors of WES were Brig. Gen. E.D. Peixotto, Col. G.H. Hilt, and Col. John L. Cannon. The Technical Director at WES was Mr. Frederick R. Brown.

R.A. Jachowski, Chief, Coastal Design Criteria Branch, was the CERC contract monitor for the report, under the general supervision of G.M. Watts, formerly Chief, Engineering Development Division.

Comments on this publication are invited.

Approved for publication in accordance with Public Law 166, 79th Congress, approved 31 July 1945, as supplemented by Public Law 172, 88th Congress, approved November 1963.

TED E. BISHOP
Colonel, Corps of Engineers
Commander and Director

CONTENTS

TABLES

FIGURES

CONTENTS

FIGURES--Continued

FIGURES--Continued

FIGURES--Continued

FIGURES--Continued

FIGURES--Continued

FIGURES--Continued

CONTENTS

FIGURES--Continued

FIGURES--Continued

CONVERSION FACTORS, U.S. CUSTOMARY TO METRIC (SI)
UNITS OF MEASUREMENT

U.S. customary units of measurement used in this report can be converted to metric (SI) units as follows:

Multiply	by	To obtain
inches	25.4	millimeters
	2.54	centimeters
square inches	6.452	square centimeters
cubic inches	16.39	cubic centimeters
feet	30.48	centimeters
	0.3048	meters
square feet	0.0929	square meters
cubic feet	0.0283	cubic meters
yards	0.9144	meters
square yards	0.836	square meters
cubic yards	0.7646	cubic meters
miles	1.6093	kilometers
square miles	259.0	hectares
knots	1.852	kilometers per hour
acres	0.4047	hectares
foot-pounds	1.3558	newton meters
millibars	1.0197×10^{-3}	kilograms per square centimeter
ounces	28.35	grams
pounds	453.6	grams
	0.4536	kilograms
ton, long	1.0160	metric tons
ton, short	0.9072	metric tons
degrees (angle)	0.01745	radians
Fahrenheit degrees	5/9	Celsius degrees or Kelvins[1]

[1]To obtain Celsius (C) temperature readings from Fahrenheit (F) readings, use formula: $C = (5/9)(F - 32)$.

To obtain Kelvin (K) readings, use formula: $K = (5/9)(F - 32) + 273.15$.

COASTAL HYDRAULIC MODELS

I. INTRODUCTION

by
R.Y. Hudson

1. Purpose and Scope.

This report provides information on hydraulic scale models of coastal engineering problems for design engineers to properly evaluate the usefulness of such models as an aid in obtaining practical solutions to difficult coastal problems. Sufficient information is presented so that the state-of-the art of scale modeling of the most important types of coastal problems can be discerned. These problems include: (a) the effects of wind waves, long-period seiche-type waves, tsunamis, wind setup (storm surge), and astronomical tides on currents and sediment movement in the coastal zone and estuaries; (b) the functional efficiency of coastal structures; (c) the effects of coastal structures on littoral currents and beach erosion and accretion; and (d) the stability of coastal structures when subjected to the forces of waves and currents. The structures considered, and the natural forces to which they are subjected, are those that are pertinent to navigation, beach erosion, sediment transport and deposition in estuaries, pollution, and the control of wave-generated flooding. Coastal problems are discussed under the general headings of estuaries, coastal harbors, coastal erosion, stability of coastal structures, and inlets. Hydraulic scale-model technology, considered as an engineering tool, is discussed with respect to (a) its historical development; (b) similitude relations; (c) field data required; (d) model design, operation, and interpretation of results; (e) application, advantages, and disadvantages; and (f) general time and cost estimates for typical model studies.

2. Historical Development of Hydraulics and Scale-Model Techniques.

Although there is evidence that the control of water through canals for irrigation purposes occurred in several parts of the world (e.g., Egypt, Mesopotamia (mostly present-day Iraq), India, Pakistan, and China) nearly 5,000 years ago, the study of hydraulics in a scientific manner was actually begun by Leonardo da Vinci, in Italy, about the year 1500 (Rouse and Ince, 1957). The first known scale-model experiments were conducted by an English engineer (John Smeaton) during the period 1752-53, to determine the performance of water wheels and windmills; a French professor (Ferdinand Reech) in 1852, was the first to express what is now known as the Froude criterion of similitude (Rouse and Ince, 1957). The earliest known tests on a movable-bed river model were conducted by another Frenchman (Louis J. Fargue) in 1875 (Gibson, 1936; Rouse and Ince, 1957; Ippen, 1970). In Fargue's tests the model riverbanks were fixed and sand was spread over the bottom. The depth scale was 1:100, and the width and time scales were arbitrarily assumed. In 1885, tests using a movable-bed model

of the River Mersey were conducted by Osborne Reynolds in England. In these tests, sand was used as the bed material and the time element was first considered. A linear-scale distortion factor of 33 was used. The work of Reynolds was continued by L.F. Vernon-Harcourt (Gibson, 1936; Rouse and Ince, 1957; Ippen, 1970), who used bed materials of sand and lighter weight sediments such as charcoal and pumice. Vernon-Harcourt expressed his thoughts on the basis for trusting the results of movable-bed scale models as follows:

> "If I can succeed in demonstrating with the model that the originally existing conditions can be reproduced typically; and if, moreover, by placing regulating works in the model, the same changes can be reproduced that were brought about by the training works actually built, then I am sure that I can take the third most important step, namely, of investigating, with every promise of success, the probable effect of the projects that have been proposed. . . ."

This principle of movable-bed model verification has since been proven very reliable, although as yet there has been no rigorous proof of its sufficiency. This is in contrast to the excellent derivations showing the accuracy that can be obtained on fixed-bed models in which the phenomena studied involve only two major forces, and where adequate equations are known for the remaining, secondary forces. Most hydraulic and coastal engineering problems fall within this category.

The first hydraulic laboratory designed for experimental work on movable-bed models began operating in 1898 in Dresden, Germany, under the direction of Hubert Engels (Reynolds, 1929). The first hydraulic laboratory at an American engineering school was founded at Lehigh University in 1887 by Mansfield Merrimen (Rouse and Ince, 1957). The Miami Conservancy District, Ohio, constructed test facilities in 1915 to study the hydraulic jump and the design of stilling basins. The hydraulic laboratory of the University of Iowa was founded in 1918 (Rouse and Ince, 1957). At the insistence of John R. Freeman, a notable American hydraulic engineer, who was impressed with the work of German hydraulic laboratories in the early twenties, a bill was passed in Congress that authorized construction of a hydraulic laboratory in the United States. As a result of this, and because of the magnitude and difficulty of the flood-control problems caused by the 1927 flood on the Mississippi River, the U.S. Army Engineer Waterways Experiment Station (WES) was founded in Vicksburg, Mississippi, in 1929 (Tiffany, 1968). Since then the WES has grown from a small hydraulic laboratory with an annual dollar work volume near $50,000 and about a dozen civilian employees to a large, diverse engineering laboratory of the U.S. Army, Corps of Engineers with an annual work program of about $50 million in FY 1976 and more than 1,400 civilian employees.

The conduct of hydraulic scale models was the primary mission of WES at the outset and for several years thereafter. At present the Hydraulics Laboratory of WES conducts both hydraulic research and hydraulic

model studies; however, the scope of the WES mission has been expanded over the years until now, in addition to hydraulics, research is conducted in such engineering fields as soils and foundations, concrete, flexible pavements, nuclear weapons effects, mobility, environmental effects, geology, terrain analysis, expedient surfacing, soil dynamics, and rock mechanics.

The establishment of the U.S. Army Corps of Engineers, Beach Erosion Board (BEB), was authorized by Congress in 1930 (Quinn, 1977). The BEB's first laboratory facility was a small wave tank constructed in 1932 at Fort Humphreys (now Fort Belvoir), Virginia. This laboratory was moved to Washington, D.C., in 1934. BEB Technical Reports 1 and 2, published in 1941 and 1942, titled, "A Study of Progressive Oscillatory Waves" and "A Summary of the Theory of Oscillatory Waves," respectively, have become classics in the literature in this field. The BEB was abolished by Congress in 1963 and most of its functions were vested in the Coastal Engineering Research Center (CERC). The CERC's missions are to: (a) conceive, plan, and conduct research and development to provide a better understanding of shore processes, winds, waves, tides, surges, and currents as they apply to navigation improvements, flood and storm protection, beach erosion control, and coastal engineering works; (b) furnish technical assistance as directed by the Chief of Engineers in the conduct of studies made by other elements of the Corps of Engineers with the view of devising effective means of preventing erosion of shores of coastal and lake waters by waves and currents; and (c) publish information and data concerning coastal phenomena and research and development projects that are useful to the Corps of Engineers and the public. Other functions assigned to CERC by the Chief of Engineers are: (a) assist the Chief of Engineers in planning and designing coastal works, including determination of probable effects of such works on adjacent shorelines; establishment of hurricane protection criteria; evaluation of effectiveness of proposed coastal navigation improvements; and review for technical adequacy of studies, plans, and specifications for beach erosion control and other coastal engineering works; (b) provide staff support to the Coastal Engineering Research Board in conduct of its functions; (c) maintain liaison through appropriate Army and Governmental agencies with domestic and foreign institutions having the same interests in order to evaluate the effect of other efforts on the U.S. coastal research program; and (d) provide consulting services on coastal engineering problems to other elements of the Corps of Engineers and other Governmental agencies as directed.

The work accomplished by WES and CERC, and other laboratories in the United States, Europe, and Japan, has advanced the state-of-the-art in coastal engineering research, and in the procedures used in the conduct of hydraulic scale-model studies of coastal engineering problems, to the extent that scale-model studies are conducted in connection with virtually all coastal and other hydraulic engineering projects.

3. Use of Models to Aid in Solution of Coastal Problems.

As indicated in the discussion of the historical development of hydraulics and hydraulic models, the scale model has played an increasing role

in the design of hydraulic structures and coastal works in the United States since about 1930. Important model techniques and procedures have been developed, instrumentation has improved, and simulation of more complicated phenomena has become possible through experience and basic research. Engineering experience and the use of analytical methods in the solution of design problems are still important factors in the design of engineering works. For many of the complex problems in coastal engineering, especially those concerning the effects of wave action, the best approach to the problem of obtaining the optimum balance between the functional, stability, and economical aspects of design is the use of scale models and the formation of a close alliance between the design engineer and the laboratory engineer. The design engineer should also be appraised of the test results so that there can be a constant interplay and feedback from the test results, testing program, and design concepts.

LITERATURE CITED

GIBSON, A.H., "Tidal River Models," *Institution of Civil Engineers Journal*, London, England, Vol. 3, Supplement to No. 8, Oct. 1936.

IPPEN, A.T., "Hydraulic Scale Models," *Osborne Reynolds and Engineering Science Today*, J.D. Jackson and D.M. McDowell, eds., Barnes and Noble, New York, 1970.

QUINN, M., "The History of the Beach Erosion Board, U.S. Army, Corps of Engineers, 1930-63," MR 77-9, U.S. Army, Corps of Engineers, Coastal Engineering Research Center, Fort Belvoir, Va., Aug. 1977.

REYNOLDS, K.C., "Notes on Laws of Hydraulic Similitude as Applied to Experiments of Models," App. 14, *Hydraulic Laboratory Practice*, American Society of Mechanical Engineers, New York, 1929.

ROUSE, H., and INCE, S., "History of Hydraulics," Iowa Institute of Hydraulics Research, State University of Iowa, Iowa City, Iowa, 1957.

TIFFANY, J.B., ed., "History of the Waterways Experiment Station," U.S. Army Engineer Waterways Experiment Station, Vicksburg, Miss., 1968.

II. PRINCIPLES OF SIMILARITY, DIMENSIONAL ANALYSIS, AND SCALE MODELS

by
R.Y. Hudson and G.H. Keulegan

The requirements for similarity between hydraulic scale models and their prototypes can be established on the bases of dynamical considerations, dimensional analysis, and differential equations. The use of scale models in the solution of hydraulic problems is based on the application of several relationships generally known as the laws of hydraulic similitude. These laws, which are based on the principles of fluid mechanics, define the requirements necessary to ensure correspondence between flow conditions of a scale model and its prototype. In a majority of hydraulic engineering problems, the degree of correspondence is limited because it is not possible to obtain a model fluid that has the required viscosity, surface tension, and elastic modulus to obtain exact similitude unless the linear scale is such that the model is as large, or nearly so, as its prototype. Although complete similitude is not usually feasible, the laws for complete similitude are known and, from experience, it is known that to impose complete similarity in model tests is unnecessary. A very important part of a model engineer's job is to justify his selected departures from complete similarity and, when necessary, apply theoretical corrections to compensate for them.

1. Dynamic Similarity.

Dynamic similarity between a model and its prototype involves geometric and kinematic similarity and Newton's laws of motion. If parts of a model have the same shape as the corresponding parts of the prototype, the two systems are geometrically similar, and the following relation exists between corresponding linear dimensions:

$$L_m = L_r L_p \,. \tag{2-1}$$

The subscripts m and p refer to model and prototype, respectively, and L_r is the scale of length. (This definition shows that the often-used term "small-scale model" is difficult to define. The term "scale model" is perferred--the size of the model compared with its prototype is indicated by the value of L_r.)

Kinematics deals with space-time relationships; thus, kinematic similarity indicates a similarity of motion between model and prototype. Two particles, one in the model and the other in the prototype, that correspond to each other are said to be homologous. Kinematic similarity of two systems is obtained if homologous particles are at homologous points at homologous times (American Society of Civil Engineers, 1942). The time intervals in the two systems must have a constant ratio,

$$T_m = T_r T_p \tag{2-2}$$

In geometrically similar models, kinematic similarity is assured when there is dynamic similarity.

Two systems are dynamically similar if there is similarity of masses and forces (i.e., if there is kinematic similarity, if the ratios of the masses of the various homologous particles or objects that are involved in the motion occurrences are equal, and if the ratios of the homologous forces that affect the motion occurrence of the homologous objects are equal). Thus,

$$M_m = M_r M_p \tag{2-3}$$

and

$$F_m = F_r F_p \,. \tag{2-4}$$

In the types of fluid mechanics problems involved in coastal and estuarine engineering projects, the forces on system elements consist of the kinetic reaction due to the inertia of an element's mass (F_i), gravity (F_g), viscous shear (F_μ), surface tension (F_{st}), elastic compression (F_e), and the pressure force resulting from or connected with the motion (F_{pr}). It follows from Newton's second law of motion that the vector sum of the active forces on an element is equal to the element's mass reaction to those forces,

$$F_i = F_g + F_\mu + F_{st} + F_e + F_{pr} \,. \tag{2-5}$$

For overall similarity, the ratio of the inertia forces, model to prototype, must equal the ratio of the vector sum of the active forces,

$$\frac{(F_i)_m}{(F_i)_p} = \frac{(F_g + F_\mu + F_{st} + F_e + F_{pr})_m}{(F_g + F_\mu + F_{st} + F_e + F_{pr})_p} \,. \tag{2-6}$$

Also, dynamic similitude is not obtained unless

$$\frac{(F_i)_m}{(F_i)_p} = \frac{(F_g)_m}{(F_g)_p} = \frac{(F_\mu)_m}{(F_\mu)_p} = \frac{(F_{st})_m}{(F_{st})_p} = \frac{(F_e)_m}{(F_e)_p} = \frac{(F_{pr})_m}{(F_{pr})_p} \,. \tag{2-7}$$

All but one of these ratios may be regarded as independent quantities, with that one ratio being determined after the others are established. The pressure ratio is usually regarded as the dependent variable; thus, it is not used in the process of determining the scale relationship for the type of studies under consideration (Warnock, 1950). However, there are other types of hydraulic flow problems in which the pressure force is a primary variable and is used in determining the scale relationships, model to prototype.

No model fluid is known that has viscosity, surface tension, and elastic modulus characteristics such as to satisfy equation 2-7. However, since one or more of the forces may not contribute to the flow phenomenon under consideration, and others may have only a slight effect

or may be related to the most important force, a particular state of fluid motion can often be simulated in a scale model by considering that either gravity forces or viscous forces predominate. Since inertial reaction is always present in the flow phenomenon, it follows that inertial forces must be considered in any particular flow situation. Equation 2-7 is used to express the ratio between the applicable forces for given flow conditions. To express these forces in usable terms their physical equivalents in terms of length (L), mass (M), gravitational acceleration (g), density (ρ), dynamic viscosity (μ), modulus of elasticity (E), surface tension (σ), and pressure (p) may be used. Thus,

$$F_i = \text{mass} \times \text{acceleration} = (\rho L^3)(V^2/L) = \rho L^2 V^2 \qquad (2\text{-}8a)$$

$$F_g = \text{mass} \times \text{gravitational acceleration} = \rho L^3 g \qquad (2\text{-}8b)$$

$$F_\mu = \text{viscosity} \times \frac{\text{velocity}}{\text{distance}} \times \text{area} = \mu VL \qquad (2\text{-}8c)$$

$$F_{st} = \text{unit surface tension} \times \text{length} = \sigma L \qquad (2\text{-}8d)$$

$$F_e = \text{modulus of elasticity} \times \text{area} = EL^2 \qquad (2\text{-}8e)$$

$$F_{pr} = \text{unit pressure} \times \text{area} = pL^2 \qquad (2\text{-}8f)$$

a. The Froude Number. Based on equations 2-7 and 2-8a and when gravitational forces predominate,

$$\frac{(F_i)_m}{(F_i)_p} = \frac{(F_g)_m}{(F_g)_p}, \quad \text{or} \quad \frac{(\rho L^2 V^2)_m}{(\rho L^2 V^2)_p} = \frac{(\rho L^3 g)_m}{(\rho L^3 g)_p}$$

from which

$$\frac{V_m^2}{g_m L_m} = \frac{V_p^2}{g_p L_p} \qquad (2\text{-}9)$$

and, with subscript r indicating the model-to-prototype ratios,

$$\frac{V_r}{(g_r L_r)^{1/2}} = 1. \qquad (2\text{-}10)$$

The dimensionless quantity $V/(gL)^{1/2}$ is called the Froude number F_n; the required equality of the Froude number, model-to-prototype, which indicates that the ratio of gravitational to inertial forces in a model should equal the corresponding ratio in the prototype, is known as the Froude model law.

b. The Reynolds Number. When viscous forces predominate,

$$\frac{(F_i)_m}{(F_i)_p} = \frac{(F_\mu)_m}{(F_\mu)_p}, \quad \text{or} \quad \frac{(\rho L^2 V^2)_m}{(\rho L^2 V^2)_p} = \frac{(\mu VL)_m}{(\mu VL)_p}$$

from which

$$\frac{L_m V_m}{\nu_m} = \frac{L_p V_p}{\nu_p} \tag{2-11}$$

where $\nu = \mu/\rho$, the kinematic viscosity, and

$$\frac{L_r V_r}{\nu_r} = 1 . \tag{2-12}$$

The dimensionless quantity LV/ν is called the Reynolds number R_n; the required equality of this number, model to prototype, as indicated by equation 2-12, is known as the Reynolds model law.

c. The Weber and Mach-Cauchy Numbers. When surface-tension effects predominate, the ratio between surface tension and inertia forces gives

$$\frac{V_r}{(\sigma_r/\rho_r L_r)^{1/2}} = 1 \tag{2-13}$$

and

$$\frac{V}{(\sigma/\rho L)^{1/2}}$$

is known as Weber's number W_n. If all forces other than those resulting from elastic compression are neglected, the ratio between elastic and inertia forces gives

$$\frac{V_r}{(E_r/\rho_r)^{1/2}} = 1 \tag{2-14}$$

and

$$\frac{V}{(E/\rho)^{1/2}}$$

is the Mach or Cauchy number M_n. Surface-tension effects are seldom encountered in coastal engineering problems in the prototype, but they are involved with some of the phenomena when reduced in magnitude in scale models. The resulting scale effects can, in most cases, be reduced satisfactorily in model studies by proper selection of the linear scale. The Mach-Cauchy law also has little application in engineering problems involving the flow of water; however, it is useful for those problems concerning the flow of gases at velocities exceeding the speed of sound and the design of structural models where the elastic forces are important.

d. Similitude Ratios. The model-prototype relationships for the different flow characteristics (velocity, time, force, etc.) can be obtained directly from the derived dimensionless ratios, equations 2-10 to 2-14. For example, with the Froude number the same in model and prototype, and with $g_m = g_p$,

$$\frac{V_m^2}{L_m} = \frac{V_p^2}{L_p} \tag{2-15a}$$

from which

$$V_r = L_r^{1/2} \tag{2-15b}$$

and, since $L = VT$

$$T_r = L_r^{1/2} . \tag{2-16}$$

Since force is mass times acceleration

$$F_r = M_r \frac{dV_r}{dT_r} = \frac{L_r^3 \rho_r V_r}{T_r} = L_r^2 \rho_r V_r^2 = L_r^3 \frac{\gamma_r}{g_r} \frac{V_r}{T_r} . \tag{2-17a}$$

Substituting the values of V_r and T_r from equations 2-15a and 2-16 and considering that $g_m = g_p$,

$$F_r = L_r^3 \gamma_r . \tag{2-17b}$$

Other ratios for the Froude-law condition, and for other types of phenomena where the Reynolds, Weber, or Mach-Cauchy number must be adhered to, can be derived in a manner similar to the above. The derived relationships for the conditions that occur frequently in coastal engineering flow problems (i.e., where gravitational or viscous forces predominate) are listed in Table 2-1.

e. Importance of Reynolds and Froude Numbers.. The Reynolds and Froude numbers are of great importance to hydraulic engineers because they provide the necessary conditions, in addition to that of geometric similarity, for flow similitude between model and prototype for those types of flow in which the compressibility and surface-tension effects can be neglected. If the Reynolds number is numerically the same in model and prototype there will be dynamic similarity with respect to inertia and viscous forces. The model can be used to study all problems that involve the flow of liquids where viscous forces predominate, surface tension is negligible, and gravity has no effect on the flow (such as the flow of liquids through pressure conduits), the motion of deeply submerged bodies (when surface and internal waves do not occur), or flow patterns around objects (when the velocities are not so high as to cause cavitation). Thus, there are few problems in coastal engineering that can be studied on scale models using Reynolds number as the sole criterion for similarity. For many problems in hydraulics and coastal engineering it is sufficient for similitude that the Froude number be the same in model and prototype; e.g., models of spillways, open-channel flow, short slucies

Table 2-1. Similitude ratios.

Characteristic	Dimension	Froude No.	Reynolds No.
Geometric			
Length	L	L_r	L_r
Area	L^2	$(L_r)^2$	$(L_r)^2$
Volume	L^3	$(L_r)^3$	$(L_r)^3$
Kinematic			
Time	T	$(L\rho\gamma^{-1})_r^{1/2}$	$(L^2\rho\mu^{-1})_r$
Velocity	LT^{-1}	$(L\gamma\rho^{-1})_r^{1/2}$	$(\mu L^{-1}\rho^{-1})_r$
Acceleration	LT^{-2}	$(\gamma\rho^{-1})_r$	$(\mu^2 L^{-3}\rho^{-2})_r$
Discharge	L^3T^{-1}	$(L^{5/2}\gamma^{1/2}\rho^{-1/2})_r$	$(L\mu\rho^{-1})_r$
Kinematic viscosity	L^2T^{-1}	$(L^{3/2}\gamma^{1/2}\rho^{-1/2})_r$	$(\mu\rho^{-1})_r$
Dynamic			
Mass	M	$(L^3\rho)_r$	$(L^3\rho)_r$
Force	MLT^{-2}	$(L^3\gamma)_r$	$(\mu^2\rho^{-1})_r$
Density	ML^{-3}	ρ_r	ρ_r
Specific weight	$ML^{-2}T^{-2}$	γ_r	$(\mu^2 L^{-3}\rho^{-1})_r$
Dynamic viscosity	$ML^{-1}T^{-1}$	$(L^{3/2}\rho^{1/2}\gamma^{1/2})_r$	μ_r
Surface tension	MT^{-2}	$(L^2\gamma)_r$	$(\mu^2 L^{-1}\rho^{-1})_r$
Volume elasticity	$ML^{-1}T^{-2}$	$(L\gamma)_r$	$(\mu^2 L^{-2}\rho^{-1})_r$
Pressure intensity	$ML^{-1}T^{-2}$	$(L\gamma)_r$	$(\mu^2 L^{-2}\rho^{-1})_r$
Momentum and impulse	MLT^{-1}	$(L^{7/2}\rho^{1/2}\gamma^{1/2})_r$	$(L^2\mu)_r$
Energy and work	ML^2T^{-2}	$(L^4\gamma)_r$	$(L\mu^2\rho^{-1})_r$
Power	ML^2T^{-3}	$(L^{7/2}\gamma^{3/2}\rho^{-1/2})_r$	$(\mu^3 L^{-1}\rho^{-2})_r$

and tubes, stilling basins, and surface wave phenomena. However, every effort should be made in the model design to minimize the effects of viscous forces. In harbor wave action models, for instance, the bottom friction effects may be appreciable in the model, whereas they are negligible in nature. Thus, in wave action models, long reaches in shallow water should be avoided and the wave heights in such areas should be corrected by theoretical means. If it were possible to satisfy both the Froude and Reynolds model laws simultaneously, most of the fluid-flow phenomena that occur in hydraulic and coastal engineering problems could be simulated with considerable accuracy, and without the necessity of making scale-effect corrections. However, this would require that

$$\frac{V_r}{(g_r L_r)^{1/2}} = \frac{L_r V_r}{\nu_r} \tag{2-18a}$$

which, because $g_r = 1$, reduces to

$$\frac{L_r^{3/2}}{\nu_r} = 1 . \tag{2-18b}$$

This relationship shows that when either the model fluid or the linear scale of the model is selected, the value of the other is fixed. It can also be shown that the use of a reasonable linear scale will result in a required viscosity for the model fluid that does not exist. For example, a linear scale of 1/10 will result in a viscosity scale of 1/30, and since water is the prototype fluid in most coastal engineering problems, no such model fluid can be found. For those phenomena in which forces are exerted by a moving fluid on an immersed object, the forces may be evaluated by the drag-force equation,

$$F = C_D A \rho V^2 \tag{2-19}$$

where $C_D = f$ (R_n, shape of object). For a given shape, the value of C_D will vary with R_n over a certain range of R_n. Thus, when C_D is constant the drag forces will be modeled accurately using the Froude model law; i.e., from equation 2-17b,

$$F_r = \rho_r V_r^2 L_r^2 = L_r^3 \gamma_r$$

and there would be no need for a scale-effect correction.

2. Similarity by Dimensional Analysis.

Dimensional analysis treats the general forms of equations that describe natural phenomena, and the theory of dimensional analysis is an algebraic theory of dimensionally homogeneous functions. If the form of an equation does not depend on the fundamental units of measurement, it is considered dimensionally homogeneous. Any mathematical equation of motion must be dimensionally homogeneous if it is physically correct, and each term in the equation must contain identical powers of each of

the dimensions when the terms are reduced to basic dimensions of mass, length, and time (MLT) or force, length, and time, (FLT). These two systems, i.e., the MLT and the FLT systems, are interrelated through Newton's law, $F = Ma$ or $F = ML/T^2$. By use of this relation, conversion from one system of units to another can be made.

The application of the method of dimensional analysis to a particular phenomenon in engineering is based on the assumption that certain variables are independent variables of the problem, and that all the other variables involved, except the dependent variable, are redundant or irrelevant. The listing of the variables, except for simple cases, requires considerable insight into the natural phenomenon. Although the application of the principles of dimensional analysis is complicated in some cases, it is simple for a large number of problems and is useful in both analytical and experimental work. Some of these uses are to:

(a) Aid memory in writing formulas.

(b) Check the dimensional homogeneity of equations.

(c) Determine a conversion factor for changing system of units.

(d) Develop general functional equations of fluid-flow phenomena expressed in terms of dimensionless parameters.

(e) Obtain partial solutions of complex problems.

(f) Plan tests and present experimental results in a condensed and systematic manner.

(g) Provide dimensionless ratios of terms that can be used as the bases for scale-model design and interpreting the test results.

The details of the methods of dimensional analysis were developed primarily by Rayleigh (1899), Buckingham (1914), and Bridgman (1922). The theory of dimensional analysis has been treated in considerable depth by van Driest (1946), Birkhoff (1950), and Langhaar (1951). Ruark (1935) and Birkhoff (1950) have explained another method, called inspectional analysis, which supplements the dimensional analysis method. Their method is reported to be capable of providing all the information that can be obtained by dimensional analysis and, in certain cases, it can provide more information. The mathematical rigor and the more philosophical aspects of the subject are not discussed in this report; however, the above references may be consulted if a detailed study of the methods of dimensional and inspectional analysis is desired.

The best method of analyzing fluid-flow problems is by direct mathematical solution. However, since most problems confronted by the coastal engineer are complex and many variables are involved in the differential equations of motion, direct mathematical solutions are not possible. For these types of problems dimensional analysis can, in many instances, be used to great advantage. The method of dimensional analysis developed

by Rayleigh (1899) does not differ basically from that of Buckingham (1914) but the latter method is preferred because, according to Langhaar (1951), it does not involve the construction of an infinite series as in the Rayleigh method. If n variables are connected by an unknown dimensionally homogeneous equation, Buckingham's theorem, generally known as the π (pi) theorem, shows that the equation can be expressed in the form of a relationship among $n - k$ dimensionless products, where k is the number of fundamental dimensions in the problem and $n - k$ is the number of products in a complete set of dimensionless products (π terms) of the variables, and that each π term will have $k + 1$ variables of which one must be changed from term to term. Thus, given a set of n variables $A_1, A_2, \ldots A_n$ in which A_1 depends on only the independent variables $A_2, A_3, \ldots A_n$, the general function can be written in the form

$$A_1 = f(A_2, A_3, \ldots A_n) \tag{2-20a}$$

which can be written

$$f'(A_1, A_2, A_3, \ldots A_n) = 0 \; ; \tag{2-20b}$$

also,

$$f''(\pi_1, \pi_2, \pi_3, \ldots \pi_{n-k}) = 0 \; . \tag{2-20c}$$

The variables of each π term must appear in this exponential form to make each π term dimensionless. Buckingham's contention that there will be $n - k$ dimensionless products is now known to be a good general rule, but it is not always true (Langhaar, 1951; van Driest, 1946). Van Driest has shown that, to be generally true, the statement should be:

> "The number of dimensionless products in a complete set is equal to the total number of variables minus the maximum number of these variables that will not form a dimensionless product."

Langhaar, using the algebra of determinants to study this problem, obtained the following necessary condition, which is equivalent to that of van Driest:

> "The number of dimensionless products in a complete set is equal to the total number of variables minus the rank of their dimensional matrix."

Numerous examples showing the application of dimensional analysis to engineering problems, involving different types of electrical, mechanical, and fluid-flow phenomena, are presented in the literature by different authors. The example selected in this instance is the general case of fluid motion. According to Rouse (1938), the only variables that can influence fluid motion are (a) those linear dimensions necessary to define the geometrical boundary conditions (a, b, c, d, etc.); (b) the kinematic and dynamic characteristics of flow (such as a characteristic velocity V or a discharge Q, a time t, or an acceleration dv/dt, a pressure increment Δp, and a pressure gradient dp/dx, or a resisting

force F); and (c) the fluid properties (density ρ, specific weight γ, viscosity μ, surface tension σ, and elastic modulus E). If it is assumed that, for the flow problem being investigated, all of these variables are involved in the prototype or model flow, or both,

$$f'(a, b, c, d, V, \Delta p, \rho, \gamma, \mu, \sigma, E) = 0 . \qquad (2\text{-}21)$$

Since there are 3 fundamental dimensions (L, T, M or L, T, F) and 11 variables, the final functional relationship (according to Buckingham, 1914) must contain 8 π terms, with 3 variables common to each. The three common variables must also contain each of the fundamental dimensions at least once. Selecting a characteristic length a, density ρ, and velocity V as the three common variables, with the remaining eight terms appearing singly in each group with a negative exponent (the selection of a, ρ, and V, and the use of a negative exponent for the remaining eight variables in the π terms were selected in such a way as to obtain π terms that are in the form of the different types of numbers obtained previously by dynamical reasoning; other forms of the π terms would have been correct, but would not have been as useful as model scale ratios or for experimental analysis) the functional equation is

$$\phi(\pi_1, \pi_2, \pi_3, \pi_4, \ldots \pi_8) = 0 \qquad (2\text{-}22)$$

in which

$$\pi_1 = a^{x_1} V^{y_1} \rho^{z_1} b^{-1} ,$$

$$\pi_2 = a^{x_2} V^{y_2} \rho^{z_2} c^{-1} ,$$

$$\pi_3 = a^{x_3} V^{y_3} \rho^{z_3} d^{-1} ,$$

$$\pi_4 = a^{x_4} V^{y_4} \rho^{z_4} \Delta p^{-1} ,$$

$$\pi_5 = a^{x_5} V^{y_5} \rho^{z_5} \gamma^{-1} ,$$

$$\pi_6 = a^{x_6} V^{y_6} \rho^{z_6} \mu^{-1} ,$$

$$\pi_7 = a^{x_7} V^{y_7} \rho^{z_7} \sigma^{-1} ,$$

and

$$\pi_8 = a^{x_8} V^{y_8} \rho^{z_8} E^{-1} .$$

Expressing the quantities in each π term in their respective dimensional units (L, T, and M), and placing the sum of their exponents equal to zero (which assures that each π term will be dimensionless), there will be three dimensionless unknowns and three simultaneous linear equations for

each π term. The solution of each set of simultaneous equations gives the exponents of each variable in each π term, as follows:

$$\pi_1 = (L)^{x_1}\left(\frac{L}{T}\right)^{y_1}\left(\frac{M}{L^3}\right)^{z_1}(L)^{-1} . \qquad (2\text{-}23)$$

For L,

$$x_1 + y_1 - 3z_1 - 1 = 0 .$$

For T,

$$-y_1 = 0 .$$

For M,

$$z_1 = 0 .$$

Thus,

$$x_1 = 1, \quad y_1 = 0, \quad z_1 = 0 ,$$

and

$$\pi_1 = \frac{a}{b} .$$

Similarly,

$$\pi_2 = \frac{a}{c} ,$$

and

$$\pi_3 = \frac{a}{d} .$$

$$\pi_4 = (L)^{x_4}\left(\frac{L}{T}\right)^{y_4}\left(\frac{M}{L^3}\right)^{z_4}\left(\frac{M}{LT^2}\right)^{-1} . \qquad (2\text{-}24)$$

For L,

$$x_4 + y_4 - 3z_4 + 1 = 0 .$$

For T,

$$-y_4 + 2 = 0 .$$

For M,

$$z_4 - 1 = 0 .$$

Thus,

$$x_4 = 0, \quad y_4 = 2, \quad z_4 = 1 ,$$

and

$$\pi_4 = \frac{V^2\rho}{\Delta p} = \frac{V^2}{\Delta p/\rho} .$$

In a similar manner it can be shown that

$$\pi_5 = \frac{V^2\rho}{a\gamma} = \frac{V^2}{ag} ,$$

$$\pi_6 = \frac{Va}{\mu/\rho} = \frac{Va}{\nu} ,$$

$$\pi_7 = \frac{V^2a}{\sigma/\rho} ,$$

and

$$\pi_8 = \frac{V^2}{E/\rho} .$$

π_4 is known as the Euler number, which is taken as the dependent variable since it contains the essential characteristics of the flow itself.

π_5, π_6, π_7, and π_8 are in the form of the Froude, Reynolds, Weber, and Mach-Cauchy numbers, respectively. Thus,

$$\frac{V^2}{\Delta p/\rho} = CQ'\left(\frac{a}{b}, \frac{a}{c}, \frac{a}{d}, F_n, R_n, W_n, M_n\right) \tag{2-25}$$

in which C is a constant independent of the choice of dimensional units and of the variation of the π terms. The function Q' is also free from dimensional influences, provided that all variables in the relationship are expressed in units of the same dimensional system. If necessary to study the variation of velocity in a fluid-flow problem, equation 2-25 can be converted to the form:

$$V = C'Q''\left(\frac{a}{b}, \frac{a}{c}, \frac{a}{d}, F_n, R_n, W_n, M_n\right)\left(\frac{\Delta p}{\rho}\right)^{1/2} . \tag{2-26}$$

The above exercise in dimensional analysis has not given any information as to the form of the function Q'' or the value of C'. However, the π theorem has reduced the number of essential terms and produced parameters independent of dimensional units. The form of the function and values of the constant, for different types of flow conditions, must be determined by analytical reasoning, experiment, or a combination of reasoning and experiment. Equation 2-25 can also be used to establish the requirements of similitude for scale models of fluid-flow problems and to indicate the terms that must be investigated to determine scale effects.

3. Similarity by Differential Equations.

If the differential equations that govern a phenomenon are known they may give more insight into the laws of similarity than the use of dimensional analysis of the variables that are known to influence or are suspected of influencing the phenomenon. This is especially true if it is desired to ascertain the laws of similarity for models with distorted scales. If a phenomenon can be described with sufficient accuracy by differential equations, the equations, after being converted to dimensionless form, provide the basis of determining transfer parameters between model and prototype. The transfer parameters obtained in this manner also show, automatically, whether scale distortion can or cannot be used. The equations arising in physical investigations can be reduced to dimensionless forms in several ways, as in the following example. The equation of motion of a simple pendulum is

$$\ell \frac{d^2\theta}{dt^2} + g \sin \theta = 0 \tag{2-27a}$$

where ℓ is the length of pendulum, g the acceleration of gravity, and θ the angle of the pendulum with the vertical in circular measure. If

the terms in equation 2-27a are divided by g, it is then in the dimensionless form

$$\frac{\ell}{g}\frac{d^2\theta}{dt^2} + \sin\theta = 0 . \qquad (2\text{-}27b)$$

Let $\tau = t/T$, where T is the period of the pendulum and τ is dimensionless, from which $dt = T\,d\tau$, $dt^2 = T^2\,d\tau^2$, and, by substitution,

$$\frac{\ell}{gT^2}\frac{d^2\theta}{d\tau^2} + \sin\theta = 0 . \qquad (2\text{-}27c)$$

In equation 2-27c each term is dimensionless. This equation shows that, for any two pendulums governed by this equation, the solution for θ will be the same, i.e.,

$$\theta_m = \theta_p ,$$

at corresponding times if

$$\frac{\ell_m}{g_m T_m^2} = \frac{\ell_p}{g_p T_p^2} \qquad (2\text{-}28)$$

or for two pendulums in the same location (from eq. 2-16),

$$\frac{T_m}{T_p} = \left(\frac{\ell_m}{\ell_p}\right)^{1/2} .$$

The following examples relate to fixed-bed harbor wave action models. Other examples of the use of differential equations to obtain the requirements for similarity between scale models and their full-scale counterparts are given by Langhaar (1951), Duncan (1953), Keulegan (1966), and Young (1971).

a. Undistorted Model (Intermediate Depth Waves, $0.05 < d/\lambda < 0.5$). The system of differential equations underlying the wave motion applicable to waves of small amplitude and moderate periods in intermediate depths, is considered to determine the conditions for similarity between model and prototype. In this examination, the frictional effects, which are nearly always small in nature and can usually be made negligible in the model, or can be accounted for by analytical or experimental means, are ignored and the flow everywhere is assumed irrotational. Thus, it will be assumed that motions are created from rest and, accordingly, a velocity potential ϕ exists in a three-dimensional domain of x, y, z points. Various texts show that $\phi = \phi\,(x,y,z,t)$, which gives the velocity components

$$u = -\frac{\partial\phi}{\partial x},\quad v = -\frac{\partial\phi}{\partial y},\quad w = -\frac{\partial\phi}{\partial z} \qquad (2\text{-}29)$$

and satisfies the Laplacian

$$\frac{\partial^2\phi}{\partial x^2} + \frac{\partial^2\phi}{\partial y^2} + \frac{\partial^2\phi}{\partial z^2} = 0 \qquad (2\text{-}30)$$

at every point in the region of the model or the prototype. At the solid boundaries

$$\frac{\partial\phi}{\partial n} = 0 \qquad (2\text{-}31a)$$

i.e., the velocity component normal to the solid boundary vanishes. Let x_o, y_o, z_o be a point on the solid boundary and ℓ, m, n be the direction cosines of the normal to the boundary at this point. Equation 2-31a may now be written as

$$\ell \frac{\partial\phi}{\partial x} + m \frac{\partial\phi}{\partial y} + n \frac{\partial\phi}{\partial z} = 0 . \qquad (2\text{-}31b)$$

If the equation of the solid boundary is in the form

$$f(x,y,z) = 0 , \qquad (2\text{-}32)$$

an alternate expression to equation 2-31b is

$$\frac{\partial f}{\partial x}\frac{\partial\phi}{\partial x} + \frac{\partial f}{\partial y}\frac{\partial\phi}{\partial y} + \frac{\partial f}{\partial z}\frac{\partial\phi}{\partial z} = 0 . \qquad (2\text{-}33)$$

The velocity potential needs to satisfy two boundary conditions, the dynamic and the kinematic. Assuming that the pressure over the water surface is constant, and equal to zero, then the dynamic surface condition takes the form

$$\frac{\partial\phi}{dt} + g\eta = 0, \quad z = 0 . \qquad (2\text{-}34)$$

The kinematic surface condition, assuming that products such as $u(\partial h/\partial x)$ can be ignored, takes the form

$$\frac{\partial\phi}{\partial z} + \frac{\partial\eta}{\partial t} = 0, \quad z = 0 \qquad (2\text{-}35)$$

where η is the surface elevation, measured from the undisturbed water level, and the z-axis is drawn vertically upward. The conditions for similarity between model and prototype can be readily obtained after the

relations in equations 2-29 to 2-35 are changed into dimensionless forms. This is accomplished by expressing time in terms of a characteristic time, T_c, the horizontal lengths in terms of a characteristic length, L_c, and the vertical lengths in terms of a characteristic depth, d_c. The selection of a characteristic time would depend on the particular phenomenon being studied. For example, when the resonance phenomena of a harbor are to be investigated, the characteristic time could be the fundamental seiche period of the harbor basin; or, for the ordinary harbor problems that involve periodic inputs, the period of the entering waves may be taken as the characteristic T_c. The characteristic length L_c could be the width of an important location in the harbor area, such as the outer input line occupied by the wave generator of the model. When it is unnecessary that the generator occupy the entire length of the outer input line, the entrance to the harbor may be taken as the input line and the characteristic length L_c. The characteristic depth, d_c, can be taken as the average depth along the outer input line or the harbor entrance. Introducing the following dimensionless variables and a dimensionless velocity potential:

$$X = \frac{x}{L_c}, \quad Y = \frac{y}{L_c}, \quad Z = \frac{z}{d_c},$$

$$\tau = \frac{t}{T_c}, \quad \eta' = \frac{\eta}{d_c},$$

and

$$\Phi = \frac{\phi T_c}{L_c^2}$$

the equation of the bottom configuration can be expressed as

$$f\left(\frac{x_o}{L_c}, \frac{y_o}{L_c}, \frac{z_o}{d_c}\right) = 0 \tag{2-36a}$$

or

$$F(X,Y,Z) = 0, \quad x = x_o, \text{ etc.} \tag{2-36b}$$

Letting the parameter N express the ratio of the characteristic horizontal length to the characteristic depth, i.e.,

$$N = \frac{L_c}{d_c}$$

and introducing the new variables in equations 2-30, 2-33, 2-34, and 2-35, there is obtained

$$\frac{\partial^2\Phi}{\partial X^2} + \frac{\partial^2\Phi}{\partial Y^2} + \frac{N^2\partial^2\Phi}{\partial Z^2} = 0 \tag{2-37}$$

$$\frac{\partial F}{\partial X}\frac{\partial \Phi}{\partial X} + \frac{\partial F}{\partial Y}\frac{\partial \Phi}{\partial Y} + N\frac{\partial F}{\partial Z}\frac{\partial \Phi}{\partial Z} = 0 \tag{2-38}$$

$$\frac{\partial \Phi}{\partial Z} + \frac{\partial \eta'}{\partial \tau} = 0, \quad Z = 0 \tag{2-39}$$

$$\frac{\partial \Phi}{\partial \tau} + N^{-2} K \eta' = 0 \tag{2-40}$$

where

$$K = \frac{gT_c^2}{d_c}. \tag{2-41}$$

The solution of the wave problem for a particular environment would be

$$\Phi = \Phi(X, Y, Z, N, K, \tau) \tag{2-42}$$

and

$$\eta' = \eta'(X, Y, Z, N, K, \tau). \tag{2-43}$$

Equations 2-42 and 2-43 are the bases for establishing the conditions for obtaining similarity between model and prototype. The corresponding times are given by the relation

$$(\tau)_m = (\tau)_p \tag{2-44}$$

and for similarity,

$$(N)_m = (N)_p \tag{2-45}$$

and

$$(K)_m = (K)_p. \tag{2-46}$$

Equation 2-45 states that similarity between model and prototype will be obtained only when the linear scales are not distorted. Also, equation 2-46 states that for corresponding times, i.e.,

$$\left(\frac{t}{T_c}\right)_m = \left(\frac{t}{T_c}\right)_p.$$

K must have the same value in model and prototype. Thus, from equation 2-41

$$\left(\frac{gT_c^2}{d_c}\right)_m = \left(\frac{gT_c^2}{d_c}\right)_p \tag{2-47}$$

which is a Froude relationship. If L_r be the linear scale of the model, and since the model is not distorted in scale,

$$(d_c)_m = L_r(d_c)_p \tag{2-48}$$

Introducing this relation in equation 2-47, the relationship for the wave periods is

$$(T_c)_m = L_r^{1/2}(T_c)_m . \tag{2-49}$$

Since equation 2-43 applies to any point in the model, and therefore for points on the input line, and if η_1 is the surface elevation at the line,

$$(\eta_1')_m = (\eta_1')_p \tag{2-50}$$

or

$$\left(\frac{\eta_1}{d_c}\right)_m = \left(\frac{\eta_1}{d_c}\right)_p . \tag{2-51}$$

Equations 2-49 and 2-51 are the two conditions for similarity between model and prototype. The transference equation for velocities is obtained by combining equation 2-29 and the dimensionless variables $X = x/L_c$, and $\Phi = \phi T_c/L_c^2$, where it can be shown that

$$\frac{uT_c}{L_c} = \frac{\partial \Phi}{\partial X} \tag{2-52}$$

and

$$\left(\frac{uT_c}{L_c}\right)_m = \left(\frac{uT_c}{L_c}\right)_p . \tag{2-53a}$$

Also, since the model is to be undistorted in scale,

$$\left(\frac{uT_c}{d_c}\right)_m = \left(\frac{uT_c}{d_c}\right)_p . \tag{2-53b}$$

An alternate relationship can be obtained by introducing equation 2-47, where

$$\left(\frac{u}{g^{1/2}d_c^{1/2}}\right)_m = \left(\frac{u}{g^{1/2}d_c^{1/2}}\right)_p . \tag{2-54}$$

The above results were derived supposing that the particle velocities and the steepness of the waves are small. However, for the validity of the results, these restrictions are unnecessary. The transfer numbers for the periods, the surface elevations, and the particle velocities were developed for situations where the bottom friction is negligible. In models with a small linear-scale number L_r, friction can attain appreciable values near the coastal areas, in which case the runup and reflection will not be properly reproduced. Also, the potential theory derivation specifically and tacitly excludes the incidence of breaking

waves, so that the transfer numbers derived are valid only in the areas from the entrance line up to the position of the breaks. In these situations, recourse to analysis and to experimental data relative to runup, reflection, and reformation is necessary to make the proper adjustment of the model indicated in the critical areas.

b. Distorted Model (Long Waves, $0 < d/\lambda < 0.05$). In the case of long waves the relationship of times for the corresponding events in a distorted model and its prototype is also readily established by differential equations. A departure from the system of equations used above for undistorted models is indicated for ease in development. In long waves, where wavelengths are large compared with water depths, vertical accelerations are negligible and pressures in the liquid are hydrostatic

$$p = \rho g(\eta + z) . \tag{2-55}$$

The velocity components u and v are independent of z and are functions of x, y, and t. The dynamic surface conditions are

$$\frac{\partial u}{\partial t} = -g \frac{\partial \eta}{\partial x} ; \quad \frac{\partial v}{\partial t} = -g \frac{\partial \eta}{\partial y} . \tag{2-56}$$

These are equivalent to equation 2-34. Taking the equation of the free surface in the form

$$F(x, y, z, t) = z - \eta , \quad z = \eta \tag{2-57}$$

the surface kinematic condition, stating that a particle on the surface remains on the surface, is

$$\frac{\partial \eta}{\partial t} + u \frac{\partial \eta}{\partial x} + v \frac{\partial \eta}{\partial y} - w = 0 , \quad z = \eta . \tag{2-58}$$

This corresponds to equation 2-35 if second-order terms are neglected. Taking the equation of the rigid bottom surface in the form

$$F(x, y, z) = z + d , \quad z = -d \tag{2-59}$$

the bottom surface condition, stating that particles on the bottom surface move along that surface, is

$$u \frac{\partial d}{\partial x} + v \frac{\partial d}{\partial y} + w = 0 , \quad z = -d , \tag{2-60}$$

which corresponds to equation 2-33. Taking the condition of continuity

$$\frac{\partial u}{\partial x} + \frac{\partial v}{\partial y} + \frac{\partial w}{\partial z} = 0 \tag{2-61}$$

which corresponds to equation 2-30. Multiply equation 2-61 by dz and integrate between the limits $z = -d$ and $z = 0$. The result, after using the boundary conditions (eqs. 2-58 and 2-60), and neglecting second-order terms, is

$$\frac{\partial \eta}{\partial t} + \frac{\partial}{\partial x}(ud) + \frac{\partial}{\partial y}(vd) = 0 . \tag{2-62}$$

Introducing the relations from equation 2-56, the following field equation for the water surface displacements is obtained.

$$\frac{\partial^2 \eta}{\partial t^2} - g\frac{\partial}{\partial x}\left(d\frac{\partial \eta}{\partial x}\right) - g\frac{\partial}{\partial y}\left(d\frac{\partial \eta}{\partial y}\right) = 0 . \tag{2-63}$$

One of the boundary conditions to be associated with the field equation is the input along a given input line

$$\eta = \eta_1 (t); \quad x = x_1, \quad y = y_1 . \tag{2-64}$$

The boundary condition associated with the coastal boundary could be of two types. If the waters are limited by fixed vertical boundaries, then on these boundaries

$$\ell\frac{\partial \eta}{\partial x} + m\frac{\partial \eta}{dy} = 0 \tag{2-65}$$

where ℓ and m are the direction cosines of the normal to the coastline. For a changing coastline, the boundary condition is somewhat complicated. Let x_2, y_2 be a point on the coastline and the maximum displacements in x and y directions during a runup be S_{11} and S_{12}, given by

$$S_{11} = \int_0^{T/4} u_2 \, dt, \quad S_{12} = \int_0^{T/4} v_2 \, dt \tag{2-66}$$

where u_2 and v_2 are the component velocities of the particle at the edge line. These velocities are independent of the beach slope in the case of inundations and will be identical with the particle velocities of the vertical section passing through the edge of the undisturbed waters. Summarizing,

$$\eta = \eta_1; \quad x = x_1, \quad y = y_1 \tag{2-67}$$

$$\frac{\partial u}{\partial t} + g\frac{\partial \eta}{\partial x} = 0 \tag{2-56a}$$

$$\frac{\partial v}{\partial t} + g\frac{\partial \eta}{\partial y} = 0 \tag{2-56b}$$

and

$$\frac{\partial^2 \eta}{\partial t^2} - g\frac{\partial}{\partial x}\left(d\frac{\partial \eta}{\partial x}\right) - g\frac{\partial}{\partial y}\left(d\frac{\partial \eta}{\partial y}\right) = 0 . \tag{2-63}$$

The differential equations above must be placed into dimensionless forms, as were those for the potential problem discussed previously. For this purpose a characteristic length L_c is introduced to measure horizontal distances, a characteristic depth d_c to measure vertical distances, and a characteristic time T_c to measure times. The selection of these quantities is governed to a considerable extent by the geometry of the environment under consideration. For example, if the problem involved tsunamis in a bay similar to that of Hilo Bay, Hawaii (Palmer, Mulvihill, and Funasaki, 1967), L_c would be the length of the bay, d_c the depth at the bay mouth, and T_c the critical period of the bay oscillations. The following dimensionless variables are then introduced:

$$X = \frac{x}{L_c}, \quad Y = \frac{y}{L_c}, \quad Z = \frac{z}{d_c},$$

$$U' = \frac{u}{(gd_c)^{1/2}} \quad V' = \frac{v}{(gd_c)^{1/2}}, \quad \eta' = \frac{\eta}{d_c}, \quad \Theta = \frac{d}{d_c},$$

and

$$\tau = \frac{t}{T_c}.$$

These variables imply that particle velocities are measured in terms of $(gd_c)^{1/2}$, vertical distances in terms of d_c, horizontal distances in terms of L_c, and times in terms of T_c. Introducing these variables in equations 2-56 and 2-63 to obtain, in the following order,

$$\frac{\partial^2 \eta'}{d\tau^2} - \frac{\partial}{\partial X}\left(\Theta \frac{\partial \eta'}{\partial X}\right) - \frac{\partial}{\partial Y}\left(\Theta \frac{\partial \eta'}{\partial Y}\right) = 0 \qquad (2\text{-}68)$$

$$\frac{\partial U'}{\partial \tau} + K' \frac{\partial \eta'}{\partial X} = 0 \qquad (2\text{-}69)$$

and

$$\frac{\partial V'}{\partial \tau} + K' \frac{\partial \eta'}{\partial Y} = 0 \qquad (2\text{-}70)$$

where

$$K' = \frac{(gd_c)^{1/2} T_c}{L_c}. \qquad (2\text{-}71)$$

The solution of the wave problem for a particular environment would be equations of the form

$$\eta' = \eta'(X, Y, \tau, K', \Theta) \qquad (2\text{-}72)$$

$$U' = U'(X, Y, \tau, K', \Theta) \qquad (2\text{-}73)$$

and

$$V' = V'(X, Y, \tau, K', \Theta). \qquad (2\text{-}74)$$

Equations 2-72, 2-73, and 2-74 are the bases for establishing the conditions for similarity between the distorted model and the prototype. These equations will serve to represent (identically) the quantities of the model and prototype, provided that K' has the same value in model and prototype and the input at the entrance of the model is the same as that in the prototype. More specifically, at corresponding times

$$\tau_m = \tau_p \tag{2-75}$$

and at corresponding locations

$$X_m = X_p, \quad Y_m = Y_p ; \tag{2-76}$$

then,

$$\eta'_m = \eta'_p \tag{2-77}$$

$$U'_m = U'_p \tag{2-78}$$

and

$$V'_m = V'_p \tag{2-79}$$

provided that

$$K'_m = K'_p \tag{2-80}$$

and, at the input line or at the entrance of the model given by $f(X_1,Y_1) = 0$

$$(\eta'_1)_m = (\eta'_1)_p \, . \tag{2-81}$$

From equation 2-80, and using equation 2-71 which defines K',

$$(T_c)_m = \frac{(L_c)_m}{(L_c)_p} \frac{(d_c)_p^{1/2}}{(d_c)_m^{1/2}} (T_c)_p \, . \tag{2-82}$$

Denoting the scale of horizontal lengths by $(L_\eta)_r$ and the scale distortion by $\overline{DF}$, i.e.,

$$(L_h)_m = (L_h)_r (L_h)_p \tag{2-83}$$

and

$$(d_c)_m = \overline{DF} (L_h)_r (d_c)_p \tag{2-84}$$

to obtain

$$(T_c)_m = (L_h)_r^{1/2} \overline{DF}^{-1/2} (T_c)_p \tag{2-85}$$

which relates the period of the fundamental seiche-type oscillations in the model with those of the prototype. The input to the model is defined as the variation of the water surface elevation at the entrance of the model area. For a periodically varying input

$$\eta_1 = a_1 \cos \frac{2\pi t}{T} \tag{2-86}$$

where T is the period of oscillation of the test waves. In accordance with equation 2-81, since

$$\left(\frac{\eta_1}{d_c}\right)_m = \left(\frac{a_1}{d_c} \cos 2\pi \frac{\tau T_c}{T}\right)_m \tag{2-87a}$$

and

$$\left(\frac{\eta_1}{d_c}\right)_p = \left(\frac{a_1}{d_c} \cos 2\pi \frac{\tau T_c}{T}\right)_p \tag{2-87b}$$

then,

$$\left(\frac{a_1}{d_c}\right)_m = \left(\frac{a_1}{d_c}\right)_p \tag{2-88}$$

and

$$\left(\frac{T_c}{T}\right)_m = \left(\frac{T_c}{T}\right)_p . \tag{2-89}$$

The relations expressed by equations 2-85, 2-88, and 2-89 are the conditions necessary to assure similarity of long-wave action, model to prototype, for distorted-scale models. For corresponding times and corresponding locations, from equations 2-77, 2-78, and 2-79,

$$\left(\frac{\eta}{d_c}\right)_m = \left(\frac{\eta}{d_c}\right)_p \tag{2-90}$$

$$\left(\frac{u}{g^{1/2} d_c^{1/2}}\right)_m = \left(\frac{u}{g^{1/2} d_c^{1/2}}\right)_p \tag{2-91}$$

and

$$\left(\frac{v}{g^{1/2} d_c^{1/2}}\right)_m = \left(\frac{v}{g^{1/2} d_c^{1/2}}\right)_p . \tag{2-92}$$

In distorted-scale models the boundary condition of equation 2-65, associated with fixed vertical walls, remains unchanged for the model and the prototype, since ℓ and m have like values for the model and the prototype. The boundary condition of equation 2-66 is also unaffected by scale

distortion for long waves, if the runup is in the form of inundation by water with horizontal flow. These types of runup are modeled correctly by distorted-scale models. The first relation in equation 2-66 may be written

$$\frac{S_{11}}{L_c} = \frac{\sqrt{gd_c} \times T_c}{L_c} \times \frac{T}{T_c} \int_o^{1/4} \frac{u_2}{\sqrt{gd\tau_c}} \tag{2-93}$$

Therefore, from equations 2-82, 2-89, and 2-91,

$$\left(\frac{S_{11}}{L_c}\right)_m = \left(\frac{S_{11}}{L_c}\right)_p \tag{2-94}$$

and, similarly,

$$\left(\frac{S_{12}}{L_c}\right)_m = \left(\frac{S_{12}}{L_c}\right)_p , \tag{2-95}$$

LITERATURE CITED

AMERICAN SOCIETY OF CIVIL ENGINEERS, "Hydraulic Models," Manual of Engineering Practice No. 25, Committee of the Hydraulics Division on Hydraulic Research, 1942.

BIRKHOFF, G., *Hydrodynamics*, Princeton University Press, Princeton, N.J., 1950, 186 pp.

BRIDGMAN, P.W., *Dimensional Analysis*, Yale University Press, New Haven, Conn., 1922, 112 pp.

BUCKINGHAM, E., "On Physically Similar Systems: Illustrations of the Use of Dimensional Equations," *Physical Review*, Vol. 4, 1914.

DUNCAN, W.J., *Physical Similarity and Dimensional Analysis*, E. Arnold, ed., London, England, 1953, 156 pp.

KEULEGAN, G.H., "Model Laws for Coastal and Estuarine Models," *Estuary and Coastline Hydrodynamics*, A.T. Ippen, ed., McGraw-Hill, New York, 1966, pp. 691-710.

LANGHAAR, H.L., *Dimensional Analysis and Theory of Models*, Wiley, New York, 1951, 106 pp.

PALMER, R.Q., MULVIHILL, M.E., and FUNASAKI, G.T., "Study of Proposed Barrier Plans for the Protection of the City of Hilo and Hilo Harbor, Hawaii," Technical Report No. 1, U.S. Army Engineer Division, Pacific Ocean, Ft. Shafter, Hawaii, Nov. 1967.

RAYLEIGH, LORD, "On the Viscosity of Argon as Affected by Temperature," *Proceedings of the Royal Society of London*, Vol. LXVI, 1899-1900, pp. 68-73.

ROUSE, H., *Fluid Mechanics for Hydraulic Engineers*, McGraw-Hill, New York, 1938, 422 pp.

RUARK, A.E., "Inspectional Analysis," *Journal, Elisha Mitchell Scientific Society*, Vol. 51, No. 1, Aug. 1935.

VAN DRIEST, E.R., "On Dimensional Analysis and the Presentation of Data in Fluid-Flow Problems," *Journal of Applied Mechanics*, Vol. 13, No. 1, Mar. 1946, pp. A34-A40.

WARNOCK, J.E., "Hydraulic Similitude," *Engineering Hydraulics*, H. Rouse, ed., Wiley, New York, 1950, pp. 136-176.

YOUNG, D.F., "Basic Principles and Concepts of Model Analysis," *Experimental Mechanics, Journal of the Society for Experimental Stress Analysis*, Vol. 11, No. 7, July 1971, pp. 325-336.

III. ESTUARIES

by
Frank A. Herrmann, Jr.

1. Introduction.

The term *estuary* is classically defined as the lower reaches of a stream (a river or a creek conveying upland discharges) where the effects of the tide may be distinguished; i.e., where a periodic rise and fall of the water surface may occur in consonance with the astronomic forces alone, or where periodic reversals of current direction may also occur. Recently, much broader definitions of estuaries have developed. One broad definition (used in this report) describes all coastal waters from the ocean to the limits of tidal effects as estuaries, to include bays, rivers, creeks, fjords, coastal inlets, straits, sounds, lagoons, labyrinthine mazes of channels meandering through marshes and deltas, and artificial canals (only if the canals exhibit tidal effects). (U.S. Army Engineer Waterways Experiment Station, 1969.)

Estuaries are immensely valuable resources, which serve as habitats for migratory waterfowl, fish, and shellfish, as sources of water supply, and as arteries of commerce; thus, their preservation is of great importance. In a natural condition, before man altered their characteristics, estuaries were much more satisfactory for wildlife and as sources of water supply. However, as commerce began to grow and ship sizes increased, natural channels were inadequate, and it became necessary to enlarge and straighten the channels at critical reaches. These initial works, which were relatively minor in scope, were often ineffective. Historically, the first estuarine problems were associated with the need to improve the waterway for navigation. The dimensions of the channels required to accommodate the larger ships had to keep pace with increasing ship size, and these enlarged channels began to create significant changes in the regimen of the estuary (U.S. Army Engineer Waterways Experiment Station, 1969).

Improvements in the interest of navigation pose a number of associated problems, and their solutions in turn give rise to other problems which may be termed "side effects." Other problems, not related to navigation, also arise due to increased populations and associated activities along the course of the estuary; e.g., the problem of deterioration of water quality. Popular demands to abate estuarine pollution are at a very high level and are not likely to decrease until the associated problems are resolved. Estuarine problems are broadly classified as: (a) those indirectly related to, or resulting from, navigation or navigation improvements, and (b) those due to factors not directly traceable to navigation or to navigation improvements. Table 3-1 lists the estuarine problems for each classification (the order of presentation has no significance) (U.S. Army Engineer Waterways Experiment Station, 1969).

Hydraulic modeling is a problem-solving technique that requires the development, construction, verification, and testing of a scale model of

Table 3-1. Estuarine problems.

Due to navigation or navigation improvements	Not directly traceable to navigation or navigation improvements
Channel dimensions and layouts	Effects of landfills
Shoaling	Effects of bridges and embankments
Disposal of dredged material	Hurricane and storm surges
Salinity problems	Tsunami surge problems
Erosion and deposition along shorelines	Diversion and changes of upland discharges
Changes in regimen	Shoreline scour and deposition
Pollution (heat, chemical, organic)	Pollution (heat, chemical, organic)
Ecologic and environmental problems	Estuary ecology and environment
Jetties and groins	Coastal marshlands
	Levees and dikes

a particular prototype situation. It allows an investigator to study various aspects of prototype behavior without observing and testing the prototype itself. Although a model might not reproduce all prototype phenomena, it must be designed to yield the desired design decision parameters (parameters on which decisions are based, such as tides, currents, salinities, etc.). Basically, models are used as aids in the planning process. In certain cases, model results may, within themselves, provide sufficient information on which to base certain decisions; in other cases, modeling may be only one step or a small part of the planning process necessary to make a decision or develop a design (Simmons, Harrison, and Huval, 1971).

Estuary modeling is usually restricted to modeling water-related problems where tidal action provides the major amount of system energy. In some cases, other phenomena such as riverflow, wind waves, and storm surges are of major importance, with tidal action merely a part of the physical processes that control the system.

Estuary modeling techniques have been applied to two major problem types: (a) Predicting effects of construction in areas subject to tidal action, and (b) establishing base-line conditions against which future changes can be measured. Predicting the effects of changes caused by construction has been the major use of estuary modeling. Establishing base-line conditions in areas of anticipated changes has been a more recent application which has grown from the need for guidelines against which possible future developments may be compared (U.S. Army Engineer Waterways Experiment Station, 1969).

Modeling techniques are an important planning tool for a number of reasons. It is both easier and faster to initiate changes and test their effects in a model than in the prototype. The testing of many alternatives in a model represents only a modest financial investment; prototype testing of the same alternatives would probably be a prohibitively expensive major undertaking. Prototype testing of tidal-related problems is time consuming, and often the results are of less than desirable quality or quantity. It would be impractical to test a sufficient number of

prototype alternatives to assure that the final solution is the most desirable (U.S. Army Engineer Waterways Experiment Station, 1969).

Most problem areas concerned with tidal modeling techniques are listed in Table 3-1. Environmental considerations are inherent in most of these problem areas and are of primary consideration in predicting construction effects. Some problems are quite amenable to modeling; others are not (U.S. Army Engineer Waterways Experiment Station, 1969). Sedimentation problems are a general class which has resisted accurate quantitative solution by hydraulic modeling, although modeling techniques provide highly useful qualitative information.

Tidal modeling techniques are generally classified as: hydraulic (also referred to as physical or scale) modeling and mathematical modeling. Hydraulic modeling is performed by designing, constructing, verifying (adjusting or proving), and testing a scale model of the prototype situation. Mathematical modeling requires developing, constructing, verifying, and testing a set of mathematical or logical expressions for a solution (usually on a high-speed digital computer) which yields the desired parameters. Other modeling techniques such as electronic analogs and hybrid computers are also used on certain problems; however, hydraulic and mathematical modeling are the most widely used tidal modeling techniques (U.S. Army Engineer Waterways Experiment Station, 1969). In this report, only hydraulic modeling will be discussed.

All models of estuaries have one common characteristic; i.e., the models cannot be a completely accurate simulation of all of the complex phenomena inherent in tidal waterways. To approximate complete model-prototype similarity, a hydraulic model of an estuary should reproduce the geometry and boundary roughness of the prototype and be able to simulate the following (individually and collectively) as they vary with tidal cycle time at all points in the system:

(a) Water surface elevations;

(b) current velocities and directions;

(c) salinities;

(d) physical characteristics of sediments;

(e) transportation, deposition, and scour of sediments;

(f) parameters reflecting water quality, such as dissolved oxygen, temperature, viscosity, diffusion of introduced pollutants, etc.;

(g) freshwater and saltwater discharges into the estuary, and the turbulent intermixing within the water mass; and

(h) effects of winds on setup, waves, local water currents, mixing, diffusion, etc.

Simulation of all of these estuarine phenomena is unnecessary to solve every problem. In model studies of certain problems, some of the

phenomena would be completely irrelevant and others would be so nearly irrelevant as to be negligible. The recommended approach to the design of an estuary model would be to first select the prototype phenomena which would significantly affect, or be affected by, the problem to be studied (or by possible solutions), and then to design the model to simulate the selected phenomena with acceptable accuracy. Since equations cannot be developed to express the highly complex interrelationships between the many variables involved in the modeling of a major estuary, extensive prototype data collection programs must be carried out to support adjustment of the model to attain and prove the necessary degree of similitude.

The use of hydraulic models to predict the effects of construction in estuaries began in 1885 when Professor Osborne Reynolds constructed and tested a small-scale model of the Mersey Estuary in England. This model was constructed with an erodible bed of sand, molded initially to an earlier hydrographic survey of the estuary, and was operated through a great number of tidal cycles to determine if observed changes in channel and shoal conditions could be reproduced as observed in nature. Professor Reynolds concluded that the model reproduced known changes in bed configurations with enough accuracy to be used for prediction of future events; consequently, the remainder of his study involved installing a variety of possible remedial works in the model and testing to determine which plan or plans produced the most desirable channel conditions in the estuary from the viewpoint of developing channels for navigation (U.S. Army Engineer Waterways Experiment Station, 1969).

The first estuary model at the U.S. Army Engineer Waterways Experiment Station (WES) was constructed for Winyah Bay, South Carolina, in the early 1930's. This study was followed by several other model studies of tidal inlets and parts of estuaries; however, all of these models reproduced only relatively small sections of the systems involved, and were equipped with flow and elevation control devices at each end to simulate the dynamics of tidal flow in the problem areas. The trend toward constructing large, ocean-to-river comprehensive models of estuaries at WES began about 1940, when it was realized that density (salinity) phenomena played a significant role in estuarine hydraulics and in the resultant sedimentation and flushing characteristics of estuaries. Accordingly, model laws and techniques were developed for operating estuary models with both saltwater and freshwater, as well as for adjusting the resistance of the models in such a manner that both vertical and lateral current velocity distributions of nature were reproduced to scale in the models. As a result of these developments, it is now possible to reproduce (with acceptable accuracy) the distributions of both current velocity and salinity throughout the models, the resultant density-induced vertical circulation that exists in nature, and the extent of saltwater intrusion as affected by tide and freshwater inflow (U.S. Army Engineer Waterways Experiment Station, 1969).

After a physical model has been properly adjusted and verified, many of the effects of planned construction in the estuary involved can be

predicted with quantitative accuracy. The types of construction in estuaries normally accomplished by the U.S. Army, Corps of Engineers, include:

(a) Construction of new channels or the deepening of existing channels for navigation purposes;

(b) construction of dikes, jetties, sediment traps, and sand-bypassing facilities to alleviate sedimentation;

(c) construction and operation of dams and reservoirs to reduce flood damage and to resolve water supply problems;

(d) dredging of new tidal inlets or the stabilization and improvement of existing inlets for small-craft or deep-draft navigation; and

(e) construction and operation of barriers for control of flooding by storm surges (U.S. Army Engineer Waterways Experiment Station, 1969).

Various aspects of fixed-bed models of estuaries are discussed later in this section, with emphasis on practices used at WES. Since most movable-bed model studies of estuaries are confined to the immediate entrance area, this type of model is discussed in Section VII.

2. Model Design Considerations.

a. Similitude Relations. Since gravitational forces are predominant in tidal flows, it can be demonstrated that the model and prototype Froude numbers, F_n, must be equal. Therefore, using equation (2-9),

$$\frac{V_m^2}{g_m L_m} = \frac{V_p^2}{g_p L_p}$$

where $V^2/(gL)$ is the Froude number. For distorted-scale models, depth is taken as the characteristic length; thus,

$$\frac{V_m^2}{g_m (L_v)_m} = \frac{V_p^2}{g_p (L_v)_p} \tag{3-1}$$

or

$$\frac{V_r}{\left(g_r (L_v)_r\right)^{1/2}} = 1 \ . \tag{3-2}$$

This can also be shown by inspection of the pertinent differential equation (also referred to as inspectional analysis). According to

Harleman (1971), one-dimensional tidal motion in estuaries can be described by the continuity and momentum equations as follows:

$$b\frac{\partial h}{\partial t}+\frac{\partial Q}{\partial x}-q=0 \tag{3-3}$$

and

$$\frac{\partial Q}{\partial t}+U\frac{\partial Q}{\partial x}+Q\frac{\partial U}{\partial x}+g\frac{\partial h}{\partial x}A+g\frac{Q|Q|}{AC_h^2R}=0\ . \tag{3-4}$$

In inspectional analysis, the differential equations must first be transformed into dimensionless form. Birkhoff (1950) has shown that for similitude the dimensionless coefficients must be equal in model and prototype. Harleman (1971) has shown that the dimensionless coefficients of the fourth and fifth terms of equation 3-4 can be written as

$$\left(\frac{1}{F_n}\right)$$

and

$$\left(\frac{gL_h}{C_h^2L_v}\right)$$

where F_n is the Froude number and C_h is the Chezy coefficient. These coefficients must be equal in model and prototype for the two systems to be dynamically similar.

It then follows from the first coefficient that

$$V_r = \left(g_r(L_v)_r\right)^{1/2}$$

and since $g_r = 1$

$$V_r = (L_v)_r^{1/2}\ . \tag{3-5}$$

From this basic relation and the continuity equation it can be shown that

$$Q_r = (L_h)_r(L_v)_r^{3/2} \tag{3-6}$$

and

$$T_r = (L_h)_r(L_v)_r^{-1/2}\ . \tag{3-7}$$

From the second coefficient it follows that

$$\frac{g_r(L_h)_r}{(C_h)_r^2(L_v)_r} = 1\ ,$$

and since $g_r = 1$

$$(C_h)_r = \left(\frac{(L_h)_r}{(L_v)_r}\right)^{1/2} \tag{3-8}$$

which shows that the roughness scale is a function only of the linear scale-distortion ratio. In terms of the Manning roughness n

$$n_r = \frac{(L_v)_r^{2/3}}{(L_h)_r^{1/2}} \quad . \tag{3-9}$$

This can be stated in terms of the distortion ratio $\overline{DF} = (L_v)_r/(L_h)_r$ as follows:

$$n_r = \frac{(L_v)_r^{2/3}}{(L_h)_r^{1/2}} \frac{(L_h)_r^{2/3}}{(L_h)_r^{2/3}} = \overline{DF}^{2/3} (L_h)_r^{(2/3-1/2)}$$

$$n_r = \overline{DF}^{2/3} (L_h)_r^{1/6} \tag{3-10}$$

The effect of scale distortion on the roughness ratio can now be shown as follows:

$(L_v)_r$	$(L_h)_r$	$\overline{DF}$	n_r
1/100	1/100	1	0.464
1/100	1/1,000	10	1.47
1/100	1/2,000	20	2.08

Thus, the higher the degree of distortion used in the model, the greater the roughness which is required in the model. For large distortions, boundary roughness alone may not yield a sufficient model roughness. Then, it is necessary to use some type of vertical roughness element which extends throughout the entire water depth.

Keulegan (1951, 1966) has shown that, in distorted-scale models of mixed estuaries, the salinity (or density) ratio should be unity. That is

$$s_r \text{ or } \rho_r = 1 \, . \tag{3-11}$$

However, Harleman (1971) states that, whereas the salinity scale should be unity for models of highly stratified estuaries, there is no strict necessity for this scaling in models of mixed estuaries. The general requirement, based on the Richardson number, is that

$$\left(\frac{\Delta\rho}{\rho}\right)_r = 1 \, . \tag{3-12}$$

This requirement is most conveniently satisfied by using a density ratio of unity (the general practice).

Harleman (1971) has shown that, based on inspectional analysis of the one-dimensional mass transfer equation

$$\frac{\partial s}{\partial t} + U\frac{\partial s}{\partial x} = \frac{1}{A}\frac{\partial}{\partial x}\left(AE'\frac{\partial s}{\partial x}\right) \tag{3-13}$$

the dispersion coefficient scale can be determined for areas of significant vertical density gradients. The dimensionless coefficient for the left-hand term is

$$\frac{E'_o}{U_o L} ;$$

therefore, the dispersion coefficient ratio is

$$E'_r = U_r\left(L_h\right)_r = V_r\left(L_h\right)_r$$

or

$$E'_r = \left(L_v\right)_r^{1/2}\left(L_h\right)_r . \tag{3-14}$$

In regions of salinity-induced density gradients, verification of model salinity conditions against prototype observations ensures that the mass dispersion process is satisfactorily reproduced in the model.

However, for uniform density areas (no longitudinal or vertical salinity gradients), Harleman (1971) and Fischer and Holly (1971) state that there is a direct conflict between the required dispersion coefficient ratio determined by inspectional analysis (eq. 3-14) and the ratio predicted on the basis of observed vertical and horizontal distributions in both prototype and model. From the Taylor-Elder equation

$$E_L = 5.9d\left(gRS_E\right)^{1/2} \tag{3-15}$$

where d is the depth of flow, R the hydraulic radius, and S_E the slope of energy gradient. Harleman (1971) shows that in this case the dispersion coefficient ratio should be

$$\left(E_L\right)_r = \frac{\left(L_v\right)_r^{1/2}}{\left(L_h\right)_r^{1/2}} . \tag{3-16}$$

For a model with a horizontal scale of 1:1,000 and a vertical scale of 1:100, equation (3-14) gives E'_r = 1:10,000; whereas equation (3-16) gives $(E_L)_r$ = 1:316.

However, this analysis does not consider the roughness elements commonly used in distorted-scale tidal models. The vertical roughness strips generate large-scale mixing by eddies which may be on the order

of 100 feet (prototype) in diameter. Fischer and Hanamura (1975) have shown that the effect of the roughness strips on momentum exchange is considerably greater than that of the boundary shear in the model. Model test results showed that the roughness strips dominate the velocity distributions in the model, and the dispersion coefficient is thus a function of the roughness strips. They conclude that agreement of transverse mixing between model and prototype is possible through a proper combination of strip widths and velocities, but that such agreement should be investigated in each case.

Near-field dispersion of heated discharges is dominated by momentum entrainment in the immediate vicinity of the discharge where inertia of the jet is more important than density differences. Since the three-dimensional turbulence structure of the jet cannot be distorted, near-field heat dispersion cannot be directly reproduced in a distorted-scale model if vertical exchange is important.

In the far field, heat dispersion is governed by convective spread of the plume over the surface of the receiving waters, mass transport of the plume by ambient currents, diffusion and dispersion due to turbulence in the receiving waters, and surface heat exchange. The steady-state form of the equation governing conservation of heat in an advective, turbulent-flow field is (Stolzenbach, 1971; Zitta and Douglas, 1975)

$$u\frac{\partial T}{\partial y}+v\frac{\partial T}{\partial y}+w\frac{\partial T}{\partial z}=\frac{\partial}{\partial x}\left(E_x\frac{\partial T}{\partial x}\right)+\frac{\partial}{\partial y}\left(E_y\frac{\partial T}{\partial y}\right)+\frac{\partial}{\partial z}\left(E_z\frac{\partial T}{\partial z}\right) \qquad (3\text{-}17)$$

where

u = velocity in the x direction
T = temperature
v = velocity in the y direction
w = velocity in the z direction
E = dispersion coefficient

By inspectional analysis, it can be determined that

$$E_{x_r} = E_{y_r} = V_r\left(L_h\right)_r = \left(L_v\right)_r^{1/2}\left(L_h\right)_r \qquad (3\text{-}18)$$

$$E_{z_r} = \frac{V_r\left(L_v\right)_r^2}{\left(L_h\right)_r} = \frac{\left(L_v\right)_r^{5/2}}{\left(L_h\right)_r} \qquad (3\text{-}19)$$

where it has been previously determined that the appropriate velocity scale for a distorted-scale model is $V_r = \left(L_v\right)_r^{1/2}$.

The equation describing heat loss from the free surface of a well-mixed body of water with an artificial heat input is (Stolzenbach, 1971; Zitta and Douglas, 1975)

$$\rho c \overline{V} \frac{\partial T}{\partial t} = -KA(T - T_e) + H \qquad (3\text{-}20)$$

where

ρ = density of water
c = specific heat of water
$\overline{V}$ = volume of water body
K = net surface heat exchange coefficient
A = surface area
T_e = equilibrium temperature
H = artificial heat input

It can be shown that the surface heat exchange scale is

$$K_r = \frac{(L_v)_r^{3/2} \left(\frac{\Delta\rho}{\rho}\right)_r^{1/2}}{(L_h)_r} \quad . \qquad (3\text{-}21)$$

Since the density ratio is normally unity, this reduces to

$$K_r = \frac{(L_v)_r^{3/2}}{(L_h)_r} \quad . \qquad (3\text{-}22)$$

One of the peculiarities of equation (3-22) is that if $(L_h)_r$ = 1:1,000 and $(L_v)_r$ = 1:100 (common scales in tidal models), then K_r = 1.0

Because sediment transport processes are very complex and poorly understood, reliable sedimentation similitude relations cannot be developed. Model simulation of sediment transport is therefore empirical and depends on a trial-and-error procedure to develop an appropriate testing technique by which to reproduce known sedimentation patterns.

Although scale relations can be determined for various phenomena by analytical means, there is still no assurance that a distorted-scale model will accurately reproduce prototype-flow conditions without comparing model and prototype observations. This is the result of not being able to determine the distribution of roughness (including density gradient-induced mixing) throughout the prototype. Therefore, it is necessary to carefully adjust the model roughness until measured prototype tides, velocities, and salinities are accurately reproduced. This process is referred to as model verification.

b. Selection of Model Scales. The "ideal" scales and/or distortion for the various types of studies conducted in a particular model are often conflicting. For example, it has been shown analytically that the ideal

scales for surface heat exchange in heat dispersion studies are 1:1,000 horizontally and 1:100 vertically (10:1 distortion); however, if the model is subjected to movable-bed testing, the maximum desirable distortion is about 5:1. Therefore, the model designer must exercise a considerable amount of judgment in the selection of the "best" scales for the model.

In general, the scale selection is based on several rather practical considerations. The vertical scale must be large enough to permit accurate water level measurements and to provide sufficient water depth in which to make measurements of velocities, salinities, etc., at various depths. The horizontal scale should be small to minimize the cost of model construction or to yield a model size which will fit an existing site. The scale distortion should be small enough to permit satisfactory reproduction of all phenomena to be considered in the model investigation. Probably most importantly, it must be determined that the scales selected will result in turbulent-flow conditions in the model throughout most of the tidal cycle.

The vertical scale most commonly used for estuarine models at WES is 1:100. With existing instrumentation, this is the smallest scale with which it is possible to determine water surface elevations to within ±0.1 foot prototype. The 1:100-scale is also convenient for making depth or elevation measurements on the model. In addition, this scale is normally on the order of the smallest vertical scale which will ensure that model flow is turbulent. Thus, vertical scales smaller than 1:100 are seldom, if ever, used. For models of very shallow estuaries, this scale may result in model water depths which create undesirable capillary effects and which are too small for use of existing velocity meters. In such cases, increasing the vertical scale to about 1:60 or 1:80 is necessary.

Horizontal scales usually vary from 1:300 to 1:2,000, depending on the nature of the problems to be investigated, available space, and construction costs. Since the area of the model increases with the square of the horizontal scale, doubling the horizontal scale quadruples the area of the model.

The vertical scale is usually selected first, and selection of the horizontal scale is based on the degree of scale distortion which can be tolerated. Distortion ratios (horizontal:vertical) most commonly used are 3:1, 5:1, 10:1, and 20:1. The higher distortion ratios obviously result in smaller models and lower construction costs. Generally, a distortion ratio of 3:1 to 5:1 is used if a part of the model will subsequently be converted to movable bed. These low distortion ratios are also required if qualitative tests of wave climate are conducted in the model. For most models not requiring movable-bed studies, a distortion ratio of 10:1 is satisfactory for a wide range of investigations including tides, currents, salinity intrusion, shoaling distribution, dye dispersion, heat dispersion, and hurricane surges. For this degree of distortion, it is not desirable to conduct even highly qualitative wave climate tests or movable-bed shoaling studies. If use of the model is

restricted to studies of tides, circulation patterns, salinity intrusion, and hurricane surges in broad, unrestricted waterways, a distortion ratio as high as 20:1 can be used. However, in past models with such a distortion, it was found extremely difficult to achieve a satisfactory reproduction of vertical velocity and salinity distributions in well-defined channels.

After the vertical and horizontal scales have been selected, it is necessary to ensure that the flow in the model will be turbulent throughout most of the tidal cycle. Turbulent flows will exist when the Reynolds number, dV/ν, for the model is on the order of 1400. In most instances the vertical scale should be greater than 1:150 to satisfy this criterion. This requires that comprehensive estuary models be built to distorted scales, since it is normally economically infeasible to use a horizontal scale greater than about 1:300 (the largest feasible scale is usually on the order of 1:500 to 1:1,000).

c. Scale Effects. There are several significant scale effects common to estuary models. The distortion of linear scales directly influences the required model roughness (eqs. 3-8 and 3-10). Since the roughness ratio increases with the distortion ratio, models with high distortions may require so much artificial roughness that the flow regimen is severely disrupted throughout the vertical to achieve the proper degree of mixing. However, it is not as significant a factor in broad, shallow bays with a small tidal range where flows are naturally low and mixing is primarily generated by wind.

The flow through an inlet, canal, or structure is dependent on its resistance (roughness) characteristics. The reliability of results of tests on proposed openings of this nature will depend on ensuring that their flow characteristics are properly modeled. For this reason it is usually necessary to conduct flow calibration tests in an undistorted-scale model (usually a flume-type facility). After the flow characteristics have been determined in the undistorted-scale model, the opening is subjected to calibration tests in a distorted-scale model (still in the flume) during which its width or shape is altered to produce the required flow characteristics. The final configuration is then constructed in the distorted-scale estuary model. (A detailed discussion of undistorted-scale modeling is presented in Section VII.)

A similar scale-effects problem is encountered for flow through pile structures (e.g., pile dikes). If the structure is modeled according to the horizontal scale, the openings between piles are likely to be so small that surface tension will adversely affect flow through the structure. Previous flume tests have determined that the vertical scale should be used in modeling the horizontal dimensions of such structures.

Short-period wave action cannot be accurately reproduced with the distortion ratios commonly used in estuary models. Short-period waves are generated in the models only to simulate the effects of wave energy on the resuspension and movement of sediments in the model.

The characteristics of the waves generated in the model are determined by trial and error, although prototype wave characteristics are used to guide the development of model waves.

It should be noted that no sedimentation scales are actually used in estuary model studies. Time and volume scales are developed during the shoaling verification, but these are only empirical estimates of the scales and, therefore, should be used only for determining the relative merits of various proposed plans. Fixed-bed shoaling tests should not be conducted for longer durations than the verification period.

Since it is impractical to reproduce local wind effects during hurricane-surge tests or the time decay of pollutants during dispersion tests, the results of these tests must be analytically adjusted to account for these effects. It is also infeasible to control the surface heat exchange coefficient of the model during heat-dispersion tests, and the model results must be adjusted accordingly.

The effect of the Earth's rotation is to generate a deflecting force on flowing water particles which is referred to as the Coriolis force. This force is given by Defant (1961) as

$$C = 2V\omega \sin \phi \qquad (3\text{-}23)$$

where V is the horizontal velocity, ω the angular velocity of Earth's rotation, and ϕ the latitude. The effect of the Coriolis force is to cause flows to veer to the right in the Northern Hemisphere and to the left in the Southern Hemisphere. For this force to be correctly modeled, the model should rotate faster than the Earth by a factor equal to the model time scale. To rotate an even moderate-sized estuary model would obviously be infeasible since the model would have to be constructed on a special platform. However, the Delft Hydraulics Laboratory (1968) found that the Magnus Force on a rotating cylinder in a parallel flow is analogous to the Coriolis force, and developed a rotating cylinder (Coriolis top) to simulate the desired effect. The Coriolis effect can also be simulated in the model by adjustment of the model roughness to reproduce prototype lateral velocity and salinity gradients, which are the result of Coriolis forces.

d. Model Limits. The primary considerations in determining the model limits or boundaries of an estuary model are the upper reaches of the estuary and the ocean and their effects on the study. Therefore, the upstream (river) and downstream (ocean) limits will actually be boundary condition control points. Since it is impossible to predict changes in tides, currents, salinities, etc., at these boundary points which might result from the study, the model limits must be established beyond the zone of influence of the area to be studied.

The upstream model limit of a fixed-bed estuary model should usually be located upstream from the extent of saltwater intrusion. If this is not possible, a boundary control system must be constructed in which the

salinity at the model limit can be varied with time throughout a tidal cycle (and perhaps seasonally) and with depth (if there is a vertical salinity gradient at that point). Such a control system is not only costly, but it also complicates operation of the model. This presents two serious drawbacks to the model testing capabilities: (a) the effects of any plan under investigation on the upstream extent of saltwater intrusion cannot be determined, and (b) any condition in the model where salinity conditions at the model limit are not known from prototype observations cannot be reproduced. These are rather severe restrictions to the use of the model in defining the environmental impact of projects being investigated and defining the existing salinity regimen for conditions for which no prototype data are available.

Since the proper tidal conditions at the upstream end of the model must be reproduced, it is necessary either to extend the model to the head of tide or to provide a tide-generating mechanism at the upstream model limit. This decision is usually made on the basis of the cost of constructing that part of the channel upstream from the problem areas to be investigated compared to the cost of a secondary tide generator. The part of the channel that is well beyond the areas of investigation can be reproduced as a labyrinth (Fig. 3-1). The space available for the model site may determine if the use of a secondary tide generator is necessary. If a secondary tide generator is used at the upstream model limit, the change in tidal elevations, phases, or prism at that point which may be caused by a plan under investigation cannot be determined. This is not usually a serious limitation to the model as long as the study area is well downstream from the model limit.

To conserve shelter space or to keep the model entirely inside the shelter, it is often necessary to introduce artificial bends in confined channels. This procedure does not adversely affect the hydraulic or salinity conditions of the model, although detailed investigations of flow patterns cannot be made in the immediate vicinity of an artificial bend. Examples of bends introduced into two models are shown in Figures 3-2 and 3-3. A labyrinth at the upstream end of a model is an extreme example of folding the model to conserve space. In this case, the natural form roughness may be greatly altered and extensive model roughness adjustment may be required in the labyrinth. No model measurements other than tidal elevations should be made in the labyrinth.

The limits of the model ocean are somewhat nebulous to define. To properly reproduce saltwater intrusion into the estuary, the model ocean should extend seaward to a prototype depth contour at least 10 to 20 feet deeper than any entrance channel which is investigated in the model. If the entrance area is investigated, the seaward model limit should be far enough offshore that the ocean boundary does not significantly affect current patterns in the immediate vicinity of the entrance. If entrance jetties are investigated, the offshore boundary should be far enough offshore that currents between the ends of the jetties and the model limits are not adversely affected by the model configuration. The model limits should be located far enough upcoast and downcoast of the entrance that

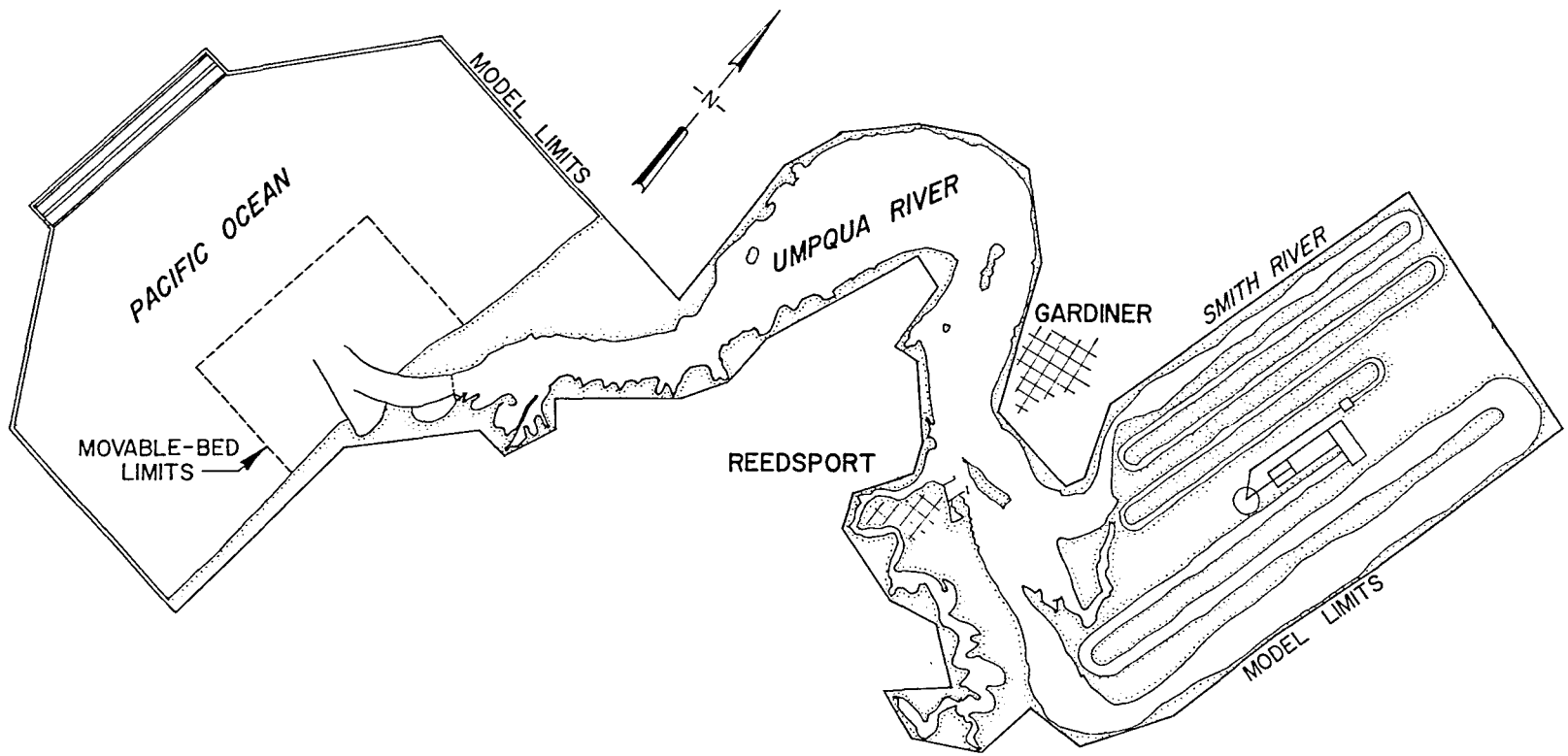

Figure 3-1. Umpqua River Estuary model (after Fisackerly, 1970).

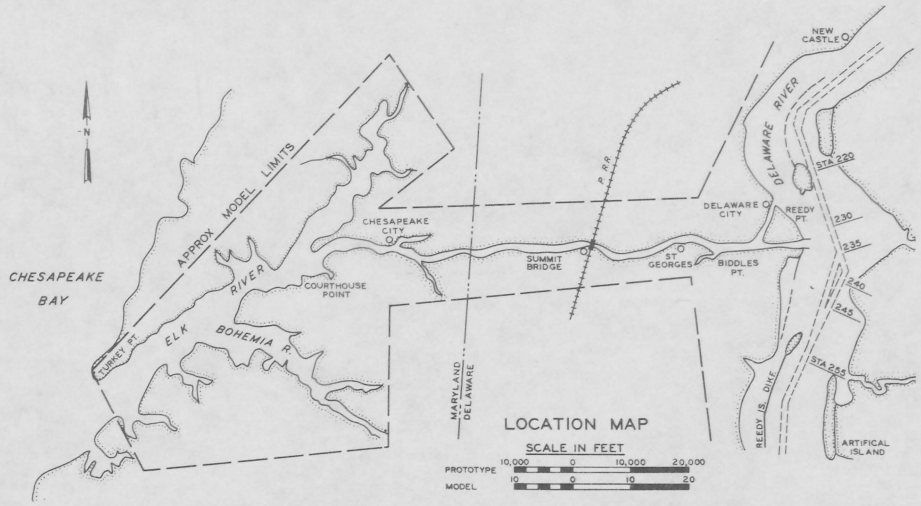

PROTOTYPE CONFIGURATION

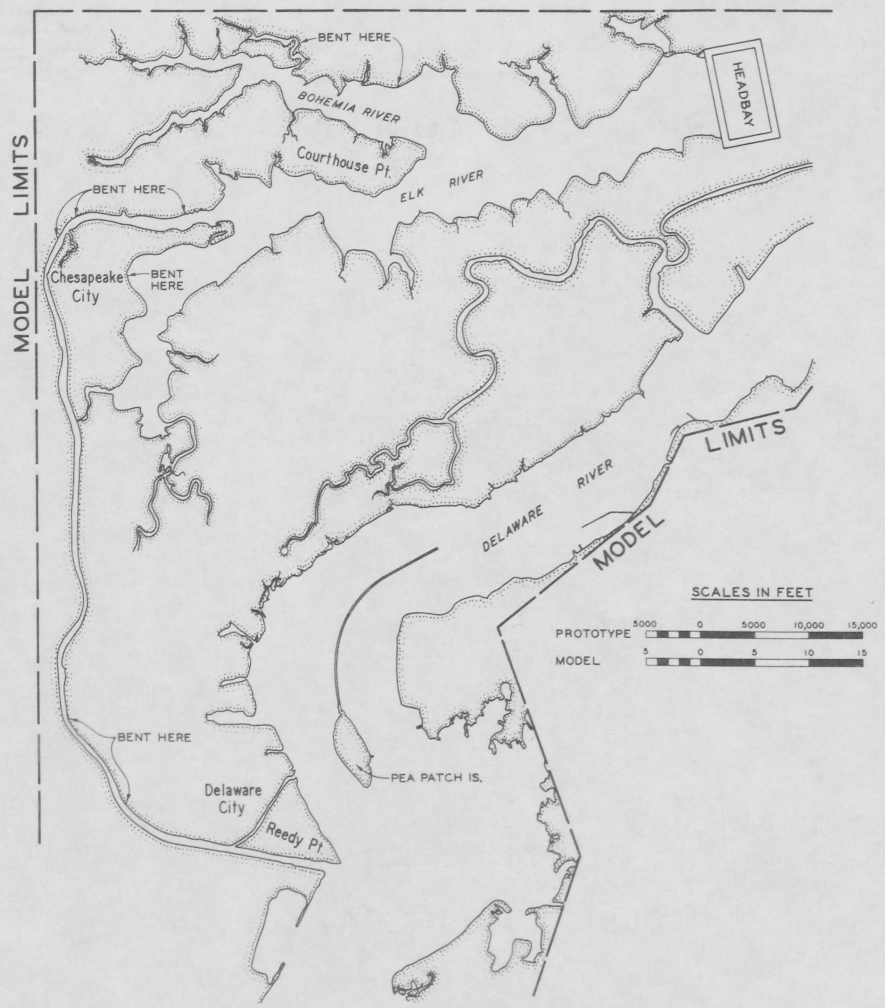

MODEL CONFIGURATION

Figure 3-2. Artificial bends in C&D Canal, Delaware River model (after Boyd, et al., 1973).

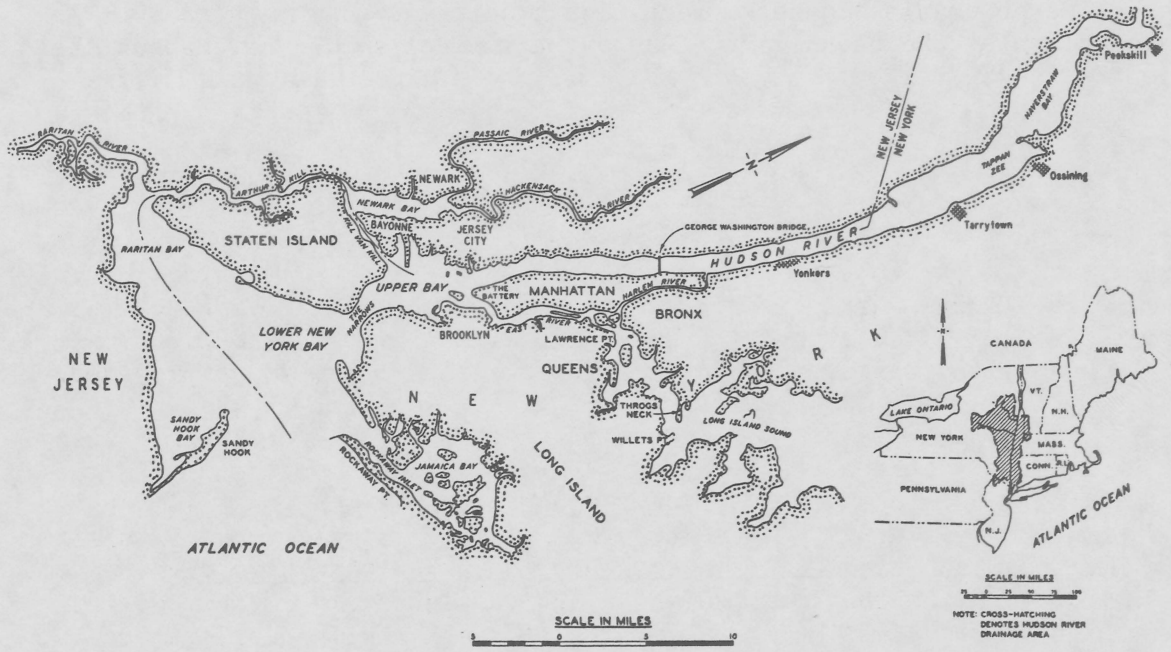

PROTOTYPE CONFIGURATION

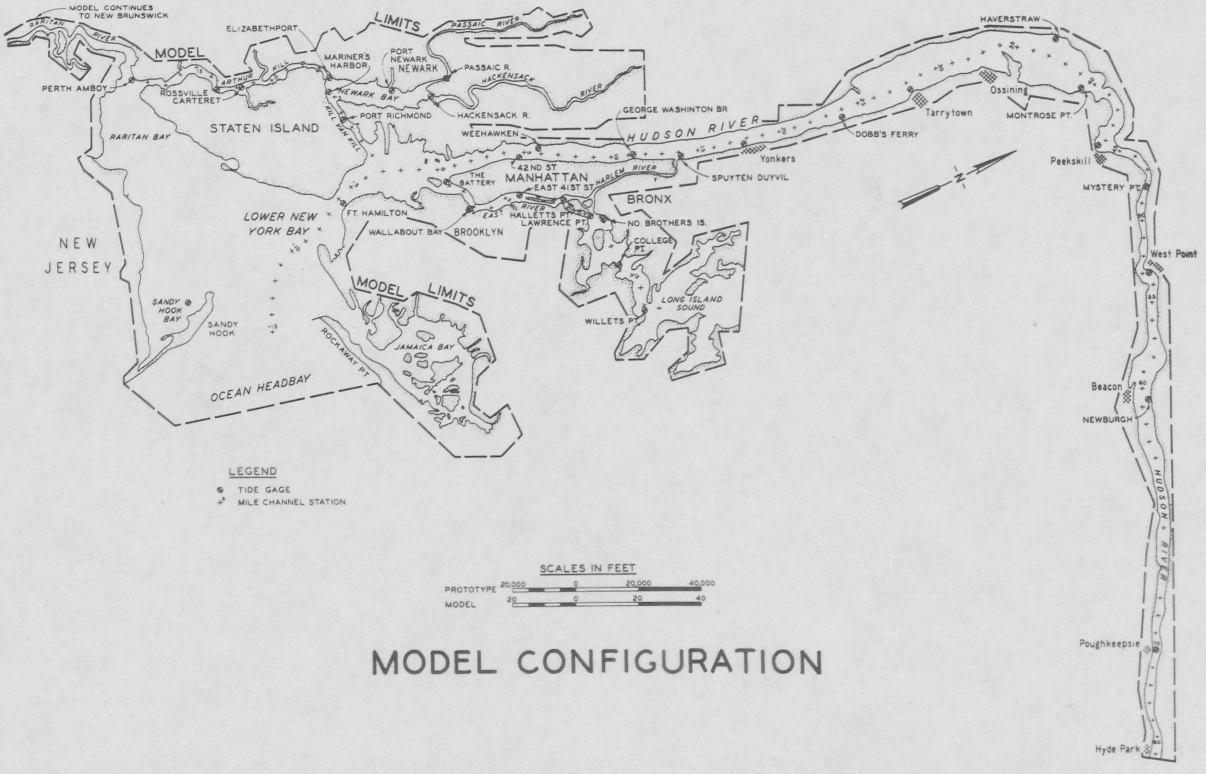

MODEL CONFIGURATION

Figure 3-3. Artificial bend in Hudson River, New York Harbor model (after Simmons and Bobb, 1965).

these side boundaries do not affect flow conditions in the entrance. As a general rule, the ocean part of an estuary model should have about the same area as the estuary part of the model to avoid operational difficulties with the tide generator.

Finally, the upper (vertical) model limit must be established. The bank line must be constructed to a somewhat higher elevation than the highest tide level to be reproduced in order to provide some degree of freeboard. This freeboard is generally taken as about 5 feet (prototype). If hurricane surges are generated in the model, the model overbank area must include all prototype areas subject to inundation by the highest surge to be investigated. Again, a 5-foot freeboard should be provided.

e. Field Data Required. Because of various scale effects in estuary models and the attendant need for adjusting the model roughness, a large amount of field data must be obtained to ensure that the model is capable of reproducing prototype phenomena. This requirement is even more stringent for those phenomena which are simulated rather than directly modeled. For example, rather than reproducing a scaled wind field in the models, the effects of wind action on the mixing of freshwater and saltwater are simulated by fans which blow down on the water surface in a random pattern or by bubbling air through the water column. Similarly, sedimentation is simulated by developing an operating technique by trial and error which will duplicate known shoaling patterns; however, no attempt is made to actually scale the sediment or to determine the sedimentation time scale by analytical means.

Prototype surveys required vary widely with the characteristics of the estuary and the problems to be investigated. Data required on most estuary models include hydrographic and topographic surveys, tidal elevations, current velocities (magnitude and direction), salinities, freshwater inflows, and shoaling rates and patterns. In addition, data on wave climate and dye and heat dispersion are often required.

To ensure that the model results are valid over the range of tidal and freshwater inflow conditions that can normally be expected to occur, hydraulic and salinity field surveys are necessary for various tidal conditions or freshwater inflows. Typically, two or three such surveys are required. For example, if there is a wide variation of tidal range, surveys may be made for neap and spring tides with normal freshwater inflow. If tidal variations are small, surveys are made for various inflow conditions without regard to tidal range. A long-term salinity survey may also be useful where salinities are observed periodically at a limited number of locations to determine seasonal fluctuations.

(1) Hydrographic Surveys. In order for the model to be an accurate geometric replication of the prototype, detailed hydrographic surveys are required of the entire area to be included in the model. National Ocean Survey (NOS) boat sheets may be used for this purpose; however, the sheets have limited value because they frequently do not show recent conditions. Project (condition) surveys by the U.S. Army

Corps of Engineers are usually current but are generally limited to the immediate vicinity of a Corps of Engineers' project such as a navigation channel. If the available surveys are several years old, and there is doubt as to their accuracy, cross-channel profiles should be obtained at about 1/4-mile intervals to verify old surveys. In areas where the bed is subject to rapid change, hydrographic surveys should be scheduled to essentially coincide with the velocity and salinity surveys. The hydrographic surveys must include the intertidal zone between mean low water (MLW) and mean high water (MHW). Recent aerial photos, especially of the bank line, are helpful in confirming the location of structures along the shore.

(2) Topographic Surveys. Topographic surveys are required to determine the overbank slopes immediately adjacent to the MHW line. These surveys should extend to about 10 feet above MHW. If the model is used for hurricane-surge protection studies, the topographic surveys must cover all areas which may be subject to inundation during a surge for existing or proposed conditions. In a large estuary model (i.e., Chesapeake Bay or Delaware Bay) the topography can be obtained from U.S. Geological Survey (USGS) quadrangle sheets and supplemented with field surveys as required.

(3) Tidal Observations. Tide records must be obtained along the length of the estuary and major tributaries. Depending on the complexity of the system, tide records should usually be obtained at intervals of 10 to 20 percent of the length included in the model. Examples of tide gage layouts for estuaries of various sizes and complexities are shown in Figures 3-4 to 3-8. If possible, a gage should be located in the ocean, even if the datum of the gage cannot be accurately established. The data from this gage are valuable in determining whether a significant choking of the tide occurs through the estuary mouth. The datum of each gage should be determined to an accuracy of ±0.1 foot, and all the gages should be referenced to a common horizontal datum, such as mean sea level. The gages should be put into operation about 3 months before the velocity and salinity surveys and operated continuously throughout these surveys and for an additional 2 months.

(4) Current Velocity and Direction. Velocity metering stations must be established on several ranges across the estuary and major tributaries. These current ranges should be spaced (as for the tidal stations) at intervals of 10 to 20 percent of the length of that part of the estuary in which model studies are conducted. It is usually unnecessary to obtain velocity data upstream from the problem area, since that part of the model can usually be satisfactorily adjusted using only tidal data. If the problem area is confined strictly to the entrance area, three or four velocity ranges may suffice. Depending on the width and shape of the cross-sectional area of the estuary at each range, one to five velocity stations should be located on each range. As many as 11 stations on a single range have been required on ranges across wide, deep estuaries such as Chesapeake Bay (Fig. 3-4). For channels in the upstream reaches of the estuaries or tributaries, a single station may be sufficient

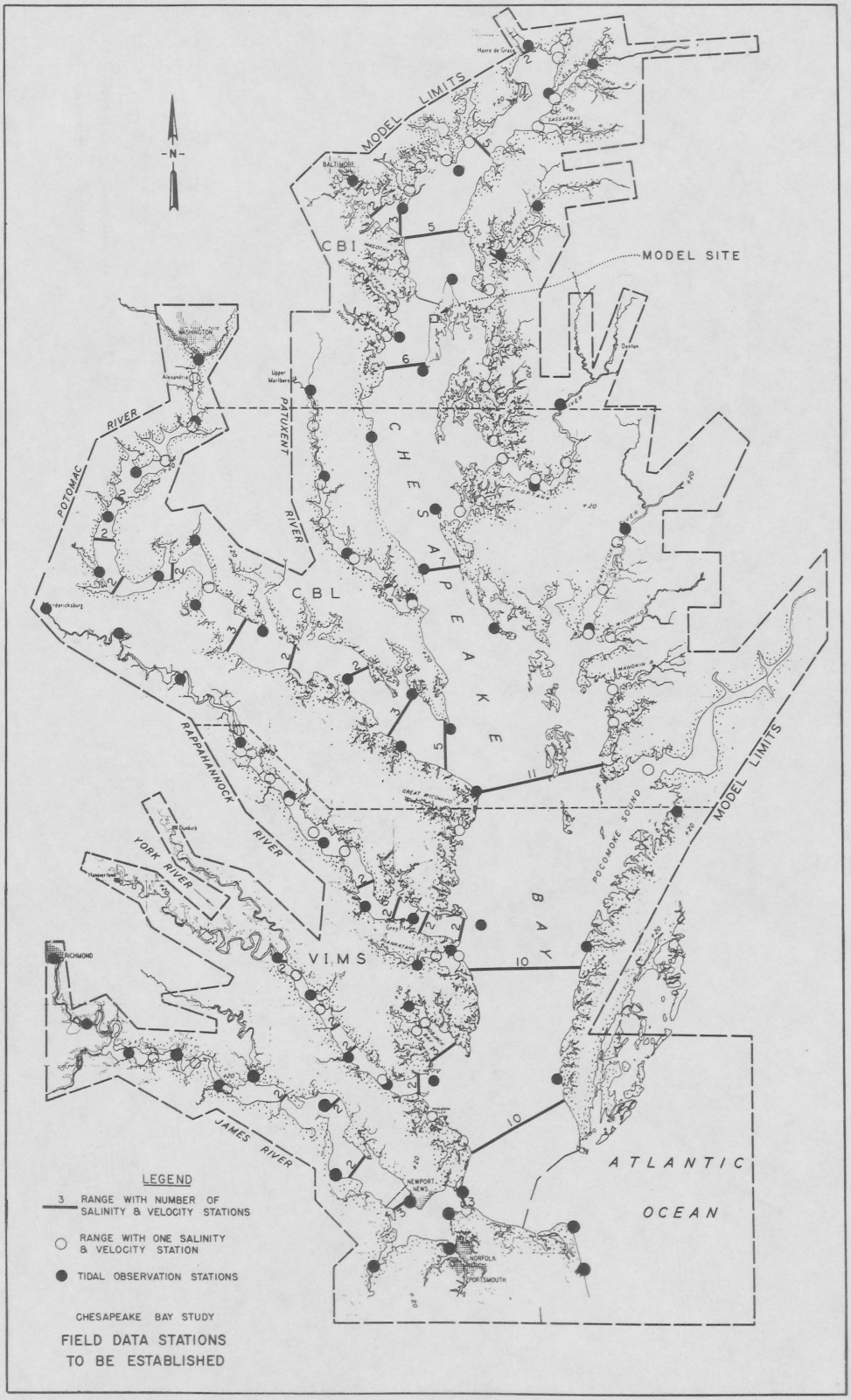

Figure 3-4. Chesapeake Bay model (after U.S. Army Engineer District, Baltimore, 1970).

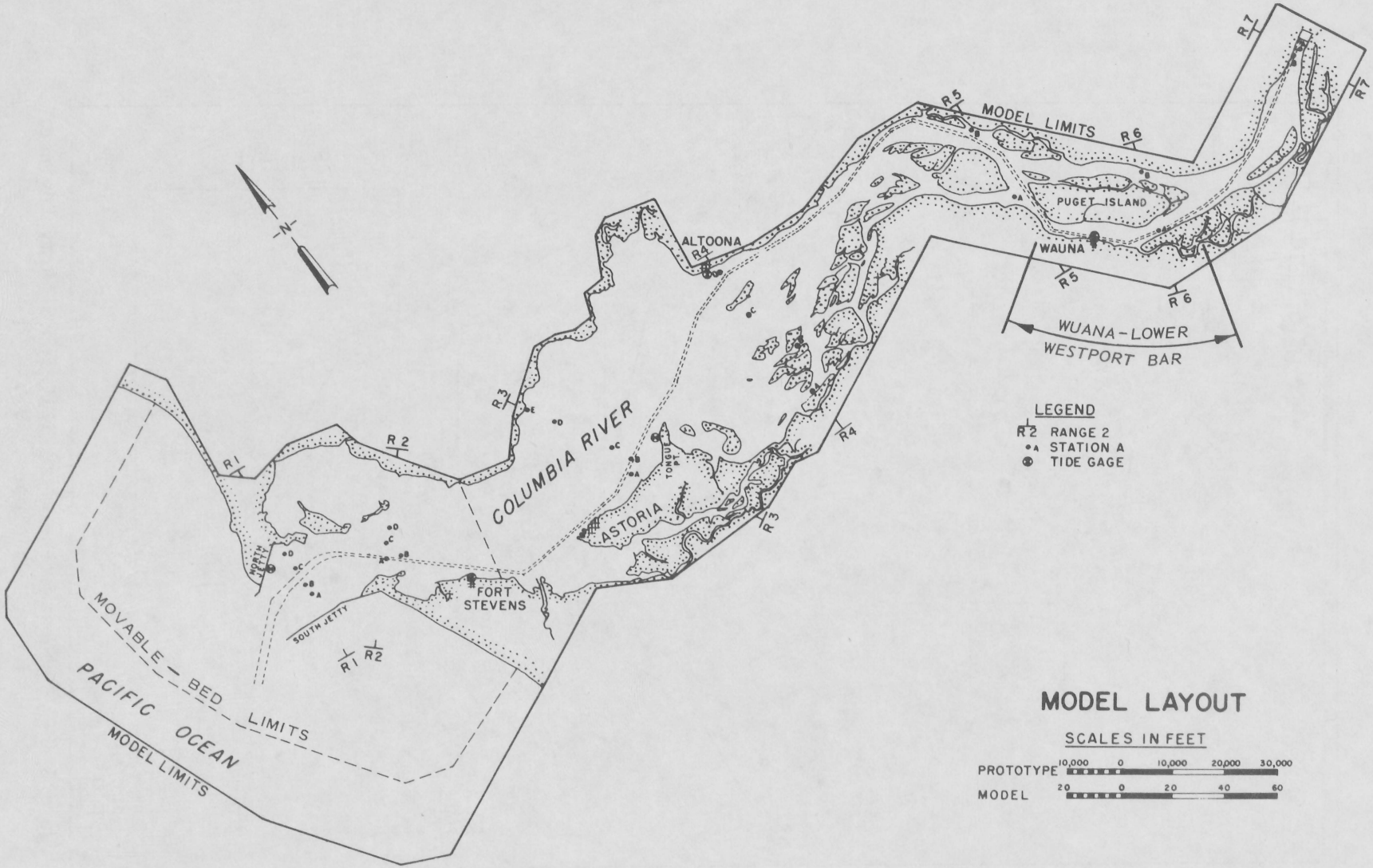

Figure 3-5. Columbia River Estuary model (after Herrmann, 1968, 1971).

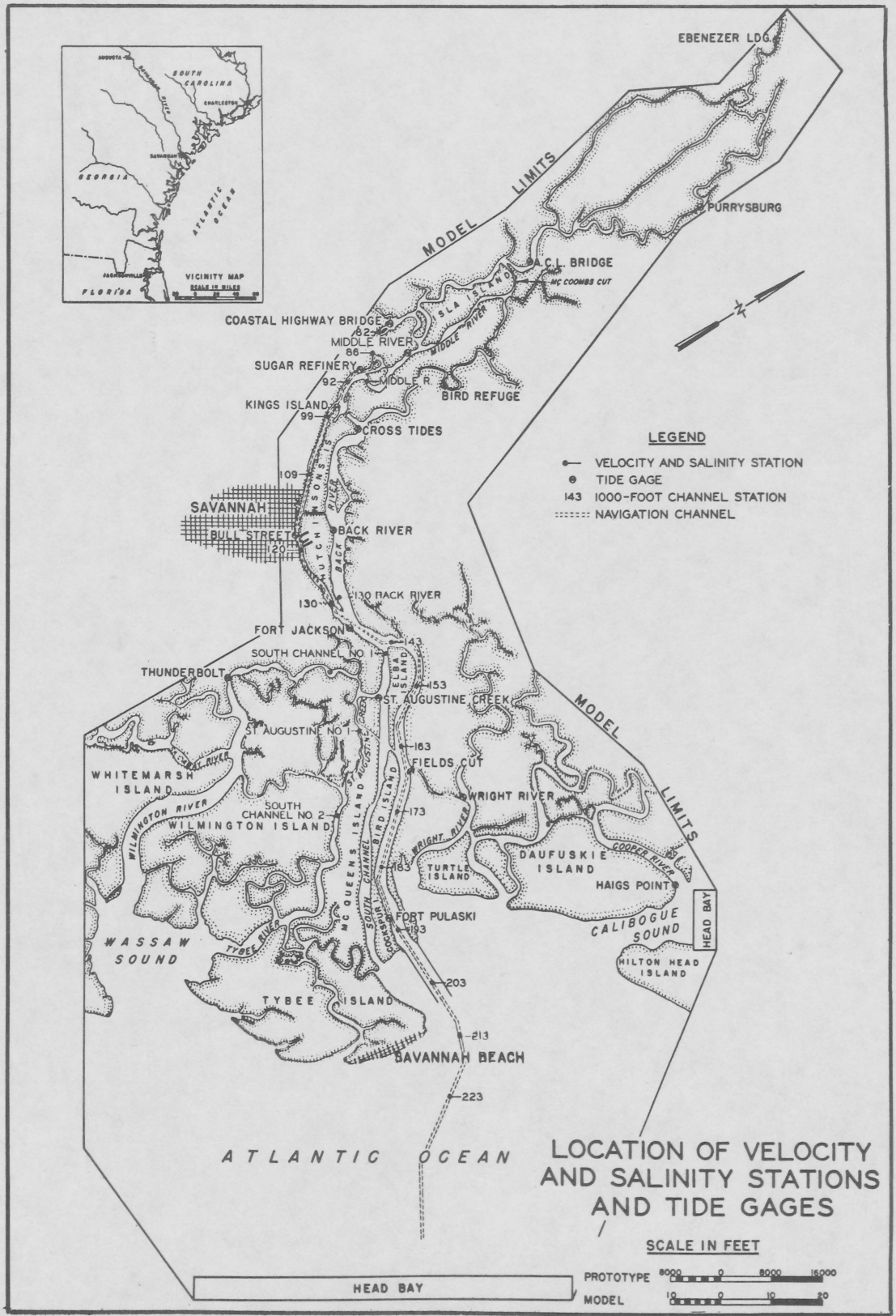

Figure 3-6. Savannah Harbor model (after U.S. Army Engineer Waterways Experiment Station, 1961).

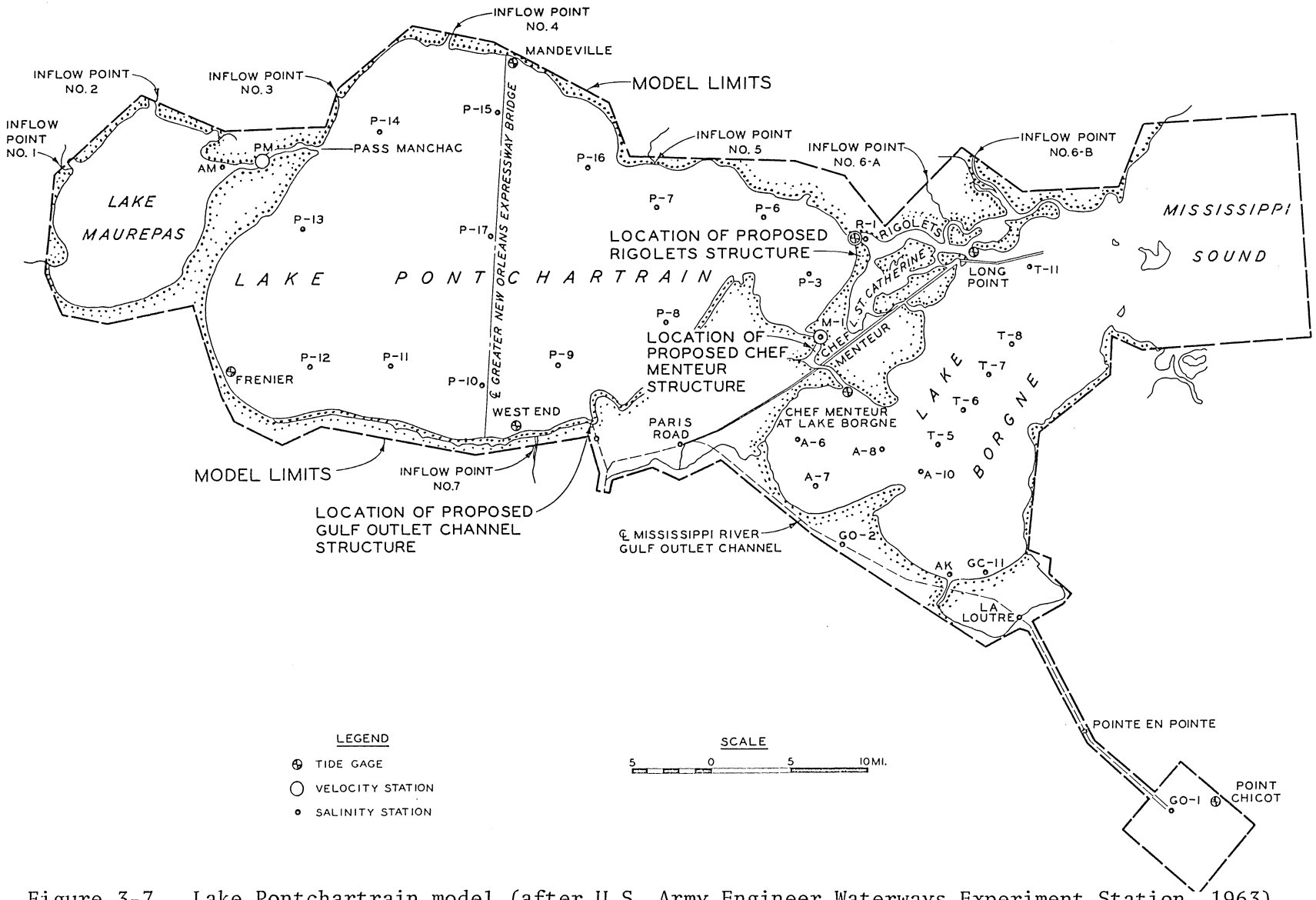

Figure 3-7. Lake Pontchartrain model (after U.S. Army Engineer Waterways Experiment Station, 1963).

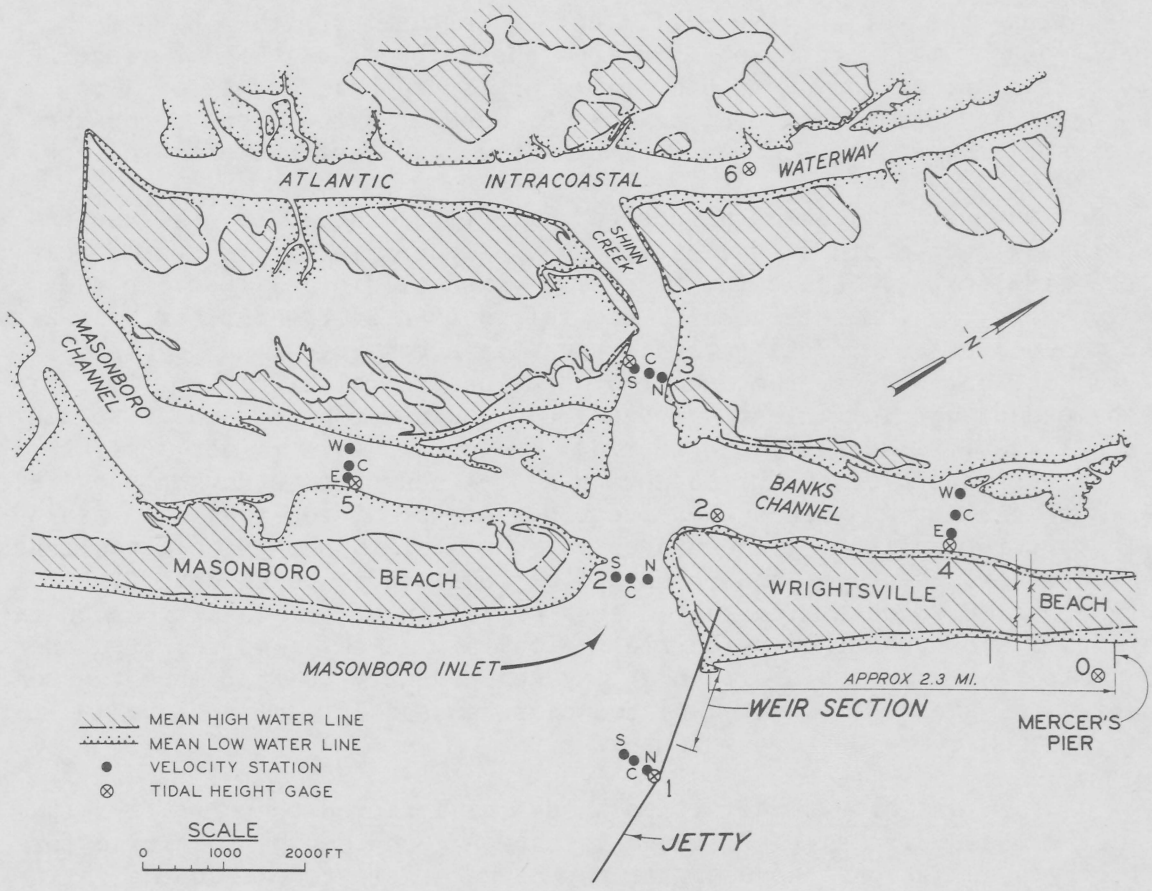

Figure 3-8. Prototype data stations, Masonboro Inlet (Sager and Seabergh, 1977).

(Fig. 3-6). Examples of velocity station layouts are shown in Figures 3-4 to 3-8. Velocity observations should be made at various depths on each station. In depths of 6 feet or less, only the middepth observations are required; in depths of about 6 to 15 feet, only surface and bottom observations are normally required. In greater depths, the vertical observation interval depends largely on the expected degree of salinity stratification. In well-mixed estuaries, surface, middepth, and bottom observations are sufficient; in estuaries with a higher degree of stratification, observations should be made at the surface and bottom and at the 1/4-depth points or at depth intervals of 6 to 10 feet. Surface measurements should be made at 1 to 3 feet below the water surface, and bottom measurements at 2 to 4 feet above the bottom.

Current velocities (magnitude and direction) should be observed at each designated depth at each station at 1/2-hour intervals over a complete tidal cycle. Where the tides are mixed or diurnal (Pacific and gulf coasts), a complete tidal cycle refers to a 24.84-hour period; where the tides are semidiurnal (Atlantic coast), a complete tidal cycle is a 12.42-hour period. If the number of stations is relatively small, it is recommended that sufficient personnel and equipment be assembled to monitor all stations during a single tidal cycle. If this is not possible, the survey should be conducted during as few consecutive days as possible and during a period when successive tides are predicted to have a reasonably uniform amplitude. In such cases, one station should be established as the control station, and it should be monitored on each day of the survey period to determine the effects of varying tidal conditions on the magnitude and phasing of velocities. To minimize the time required to complete the survey, a single boat may concurrently monitor more than one station, if the stations are located close enough for the boat to monitor each station every 30 to 45 minutes.

(5) Salinity. Salinities should be measured concurrently with velocity measurements at all ranges, stations, and depths specified for velocity observations; however, it may be necessary to extend the salinity survey upstream to the extent of saltwater intrusion. These data are sufficient to define the lateral and vertical salinity distributions throughout the system for particular freshwater inflow conditions and to evaluate the change of the salinity with tidal phase in all critical areas. However, if the velocity measuring program does not cover a significant part of the year to adequately evaluate the response of the salinity regimen to major changes in freshwater inflow, a supplemental long-term program of salinity measurements may be required. This can be accomplished by establishing a network of key salinity stations throughout the system, and salinity observations can be made at intervals (e.g., at the time of high water slack every few days) over a period of time in which freshwater inflow varies from minimum to maximum. The sampling network for the long-term salinity survey can be random, in which case the variation of salinity with time is determined at each point; or the stations can be located along the length of the main channel, in which case the longitudinal salinity profile for each sampling period is also determined. Both types of measurements have previously been successful,

and their results are adequate to evaluate the long-term response of the salinity regimen to variations in freshwater inflow.

Salinity can be determined either by laboratory analysis (titration or conductivity) of samples taken from the estuary or by in situ measurements with conductivity or inductance meters. In the latter case, some physical samples must also be obtained to ensure that the meter calibration remains stable throughout the survey period.

(6) Freshwater Inflow. Freshwater inflows (mean daily flows) from all tributaries to the estuary must be determined for about 2 weeks before and during the velocity and salinity survey. Inflow data are also required during long-term salinity observation programs, but in this case mean weekly flows may be satisfactory, depending on the inflow and the estuary volume. During low freshwater discharge periods, very small individual discharges (e.g., industrial discharges of well water) may become a significant part of the total freshwater inflow and should be monitored.

(7) Dye Dispersion. Although field dye-dispersion tests have not generally been used for model verification, the tests should be done if dye-dispersion tests are conducted in the model. A fluorescent dye should be released continuously over a 2-week period or preferably, until a stable dye regimen is established throughout the estuary. Thus, it should be made during a period of relatively uniform freshwater inflow, and may require a continuous release for 6 weeks or more. Data analysis will be complicated by dye decay, etc., during such a long period. The dye should be released at a location about two-thirds the distance from the entrance to the upper limit of the model. Dye concentrations should be determined at surface and bottom at numerous stations located throughout the estuary. The velocity and salinity station locations may be satisfactory, although additional stations along the channel centerline may be desirable. The concentrations should be determined at the times of local high and low water slack at daily intervals during the period of rapid dye buildup, but the sampling frequency can be reduced to intervals of 3 to 7 days during the latter stages of the test.

(8) Heat Dispersion. If tests are made of the heat dispersion from an existing powerplant, water temperatures should be monitored in the field for use in model verification. Surface temperatures should be measured on several ranges across the plume at about 1,000-foot intervals both upstream and downstream from the discharge point, and vertical temperature profiles should be obtained at several stations in the survey area. The survey coverage should be sufficient to identify the limits of the 0.6° Celsius (1° Fahrenheit) temperature rise contour. At least one station should be located outside the thermal plume upstream from the discharge point and one station downstream to define the ambient water temperature. In designing the layout of the field survey stations, it is helpful to first obtain infrared aerial photos of the area to determine the size and shape of the thermal plume. Similar aerial photos should be taken during the actual survey to obtain a better synoptic view of the

thermal patterns than can be obtained with contact measurements. An example of a water temperature observation network is shown in Figure 3-9.

(9) Sedimentation. Only those data required for verification of shoaling patterns in a fixed-bed model are discussed in this section. Requirements for movable-bed models are discussed in Section VII. Many model shoaling investigations are conducted in existing navigation channel projects. In this case, available periodic hydrographic surveys of a channel by the Corps of Engineers or other responsible agency will probably be sufficient for use in the model study. Channel surveys of several representative years (at least two, but preferably three or more surveys) should be analyzed to determine the distribution of shoaling throughout the length of the channel. The channel should be subdivided into several sections (usually longitudinal), and the volumes of shoaling between dredging operations determined for each section for each year. This information is determined from the postdredging survey for 1 year and the predredging survey for the following year. In this manner the average percentile distribution of shoaling along the channel can be determined. If shoaling tests are required over the entire width of the estuary, or if no navigation channel exists, hydrographic surveys over a much broader area are required. Again, surveys are required for a period of several years, and should be of sufficient detail and accuracy to develop scour-and-fill maps for the area to be studied. The only information required of the nature of the sediments is the grain size or even a very qualitative indication of whether the material consists of clays, silts, or sand.

3. Model Construction.

a. Construction Procedures. There are several basic methods of estuary model construction. For example, the model can be constructed of individual slabs, or it can be of essentially continuous construction. The construction control points can be parallel templates (male or female), templates which follow a given contour, or rods for which the top (or bottom) elevations are set to the desired model elevation. Only the general practice of WES will be discussed here.

The model construction effort actually begins by laying out the horizontal control grid on the maps from which the model will be built. Parallel gridlines should be established at 2- to 3-foot intervals along the length of the model. In areas of low relief such as in broad, shallow bays or offshore, grid intervals of 4 to 6 feet can be used. The gridlines should generally be laid out about normal to the main channel within the estuary or normal to the shoreline in the offshore area. Although it is convenient for all gridlines to be parallel or perpendicular to each other, a rather irregular grid system should sometimes be developed.

After the grid system has been developed, cross-sectional profiles are determined for each grid and transferred to template material (typically hardboard; e.g., Masonite). Sheet metal templates corrode in saltwater and should be avoided in estuary models. Typical templates are shown in Figure 3-10.

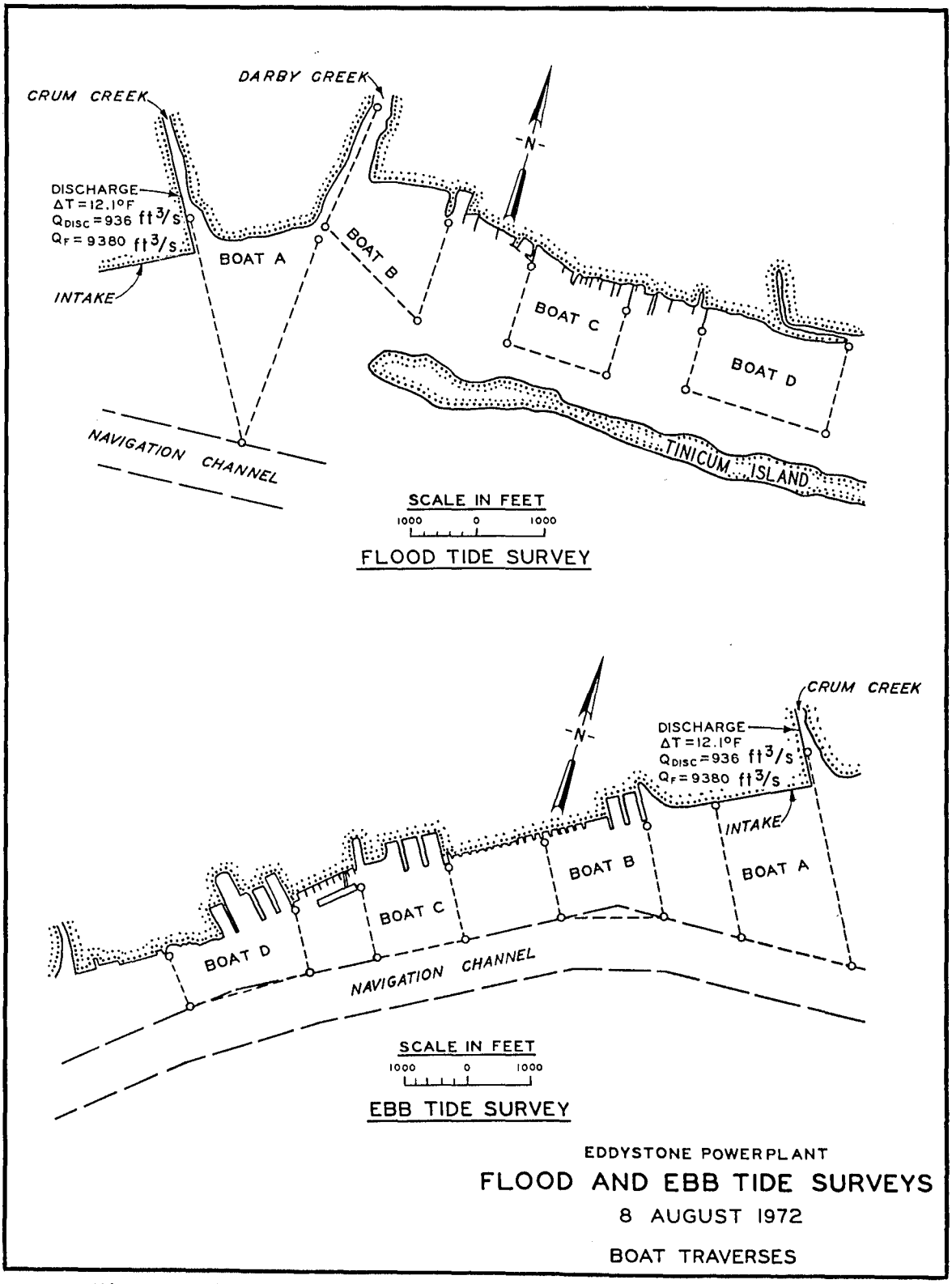

Figure 3-9. Prototype temperature stations, Delaware River (after Trawle, 1976).

Figure 3-10. Rough-graded templates.

The model grid system is located on the model site to delineate areas which may require rough grading with heavy equipment. The grid system is then accurately established on the site for use in positioning templates. The templates are set by nailing to wooden stakes and are roughly graded (Fig. 3-10). The ground between the templates is then smoothed to an elevation about 4 to 6 inches below the final model grade. Sand is placed between the templates and smoothed to within 2 or 3 inches of the final grade, and the templates are final graded. The templates are then painted with a sealer to provide a waterproof joint between the concrete and the template, and twenty-penny nails are driven through the templates to prevent differential settlement of the concrete slabs. At this point (Fig. 3-11), the model is ready for paving.

Concrete grout (cement, sand, and water) is poured between the templates and rough graded by screeds (only for areas of very low relief) or critical contours are sketched in the wet grout to define details between the templates (Fig. 3-12). The concrete is then molded to conform to the sketching. During the molding process, both the position and elevation of physical features between the templates are accurately checked. The concrete surface is finished, and roughness is added to the model while the concrete is still wet (Fig. 3-13).

Different types of model roughness are used, often in a single model. In relatively deep water, boundary roughness will probably not generate sufficient mixing for satisfactory reproduction of vertical salinity gradients. In this case, vertical roughness elements (strips, rods, or bars) are used. At WES, copper or stainless-steel strips of widths varying between about 0.25 and 1.0 inch are preferred. The tops of the strips are cut off just below the elevation of low water to avoid interference with surface currents. The strips are initially placed about 1 per 1 to 5 square feet (normally considerably more than required), and the excess strips are bent down during the verification process. In shallow water and areas of low velocity, the turbulence generated by vertical roughness elements will not yield sufficient model friction; therefore, boundary roughness is used. This can be achieved by scratching the concrete surface before it sets, adding a thin layer of stucco and roughening it with a mason's float, or by applying gravel, small cubes, etc., to the model bed. It may be necessary to smooth or further roughen the boundary roughness during the verification process.

If an investigation of a new or enlarged navigation channel is planned, a trough is constructed in the model on the proper alinement of sufficient width and depth to permit installation of the enlarged channel at a later date. The trough is then filled with concrete and molded to the existing conditions (Fig. 3-14).

Concurrent with construction of the model, construction and installation of model appurtenances is accomplished. Installation of drainpipes (and sometimes water supply pipes) must be done before pouring the concrete.

b. Tide Generation. Several different types of tide generation mechanisms are employed at the various hydraulic laboratories throughout the

Figure 3-11. Model ready for paving.

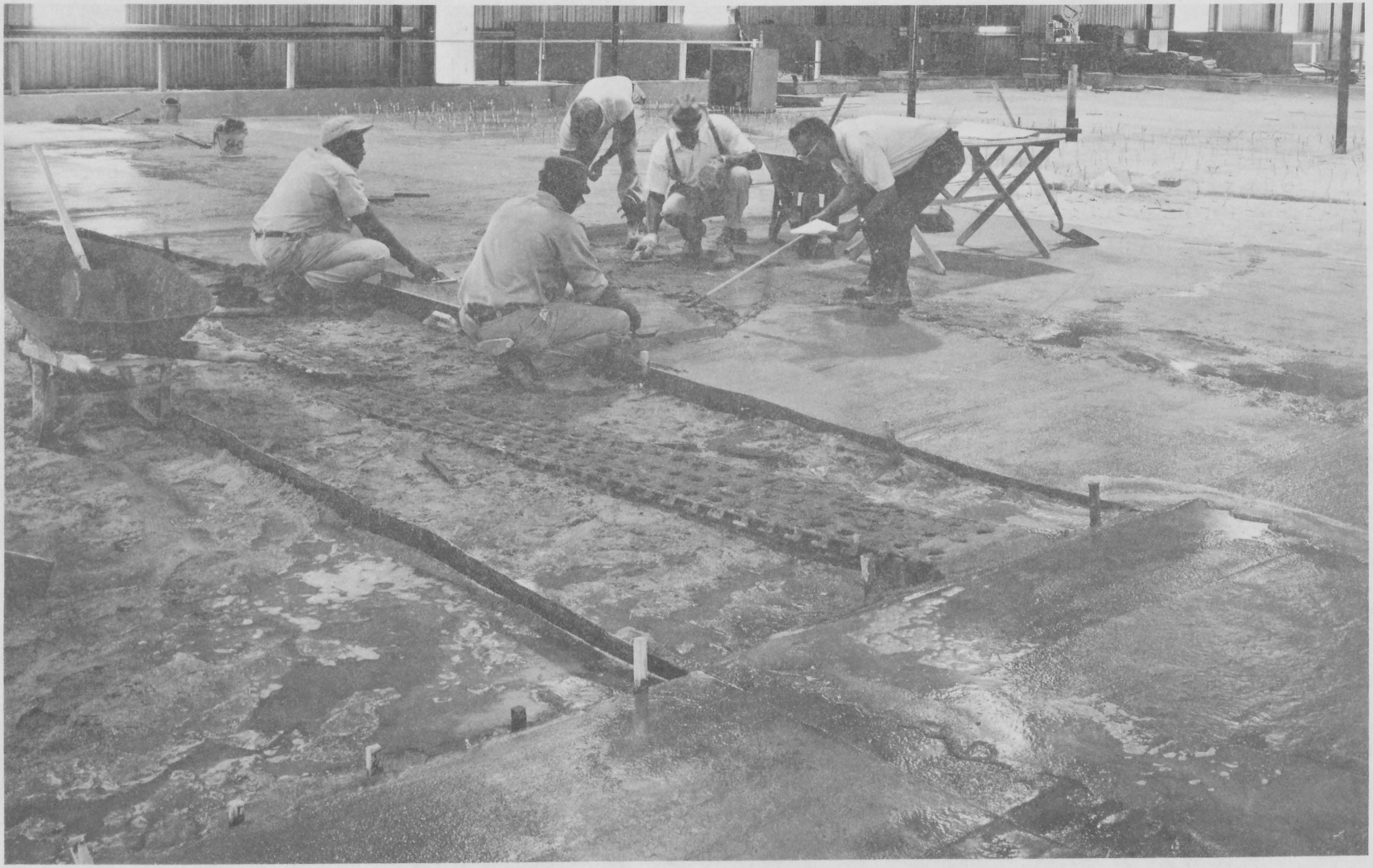

Figure 3-12. Sketching details before molding.

Figure 3-13. Completed section of model.

Figure 3-14. Trough for later installation of enlarged channel.

world, including physical displacement, pneumatic displacement, pumped inflow and gravity outflow, and gravity inflow and gravity outflow (with pumping between the return and supply sumps). Only the latter two systems (used by the Corps of Engineers) are discussed in this section.

The type used most extensively by the Corps is the pumped inflow and gravity outflow system, shown schematically in Figure 3-15. This system is programed (mechanically, pneumatically, or digitally) to maintain a differential between a constant-pumped inflow of saltwater to the model and a variable gravity return flow to the supply sump as required to reproduce the desired tidal characteristics at a control station located in the ocean or in the lower part of the estuary. In models with a very large tidal volume, it is often desirable to provide a supplemental control on the pumped inflow by installing a programed valve on the inflow line. The pumped inflow is reduced during the falling tide and increased during the rising tide to reduce the fluctuation in discharge through the gravity return line. With mechanical or pneumatic programing of the outflow, the system is generally limited to repetitive reproduction of a single tide. The control unit must be reprogramed to reproduce any other tide.

Since computer or digital control offers a high degree of flexibility, any desired sequence of tides can be reproduced in the model. A computer control system can also be used to convert analog signals received from model sensors (water levels, salinity, velocity, and temperature) to digital signals and store the data on magnetic tapes or disks for later analysis. A schematic diagram of an Automatic Data Acquisition and Control System (ADACS) is shown in Figure 3-16. A supplemental control on the pumped inflow, if required, can also be programed on the computer control system.

Another concept using the pumped inflow and gravity outflow principle requires the use of a movable overflow weir (Fig. 3-17). Saltwater is pumped into a headbay between the weir and the model. The weir is programed to move up and down as required to generate the desired tide, and the overflow is returned to the sump. Alternatively, either a flap gate or radial gate can be used as the weir.

Gravity inflow and gravity outflow (with pumping between return and supply sumps) is used in the Chesapeake Bay model. A schematic diagram of the system is shown in Figure 3-18. The reason for using this scheme is to provide a sufficient inflow capacity to generate hurricane surges in addition to tides.

Often, it is necessary or desirable to terminate an estuary model downstream from the head of tide (i.e., upstream boundary within effects of tide). If the upstream tidal prism cannot be simulated by using a labyrinth or simple storage basin, a secondary tide generator should be provided. A simplified pumped inflow and gravity outflow or pumped outflow and gravity inflow system is generally used for this purpose. In either case, water is removed from the upstream end of the model during the rising tide and returned to the model during the falling tide.

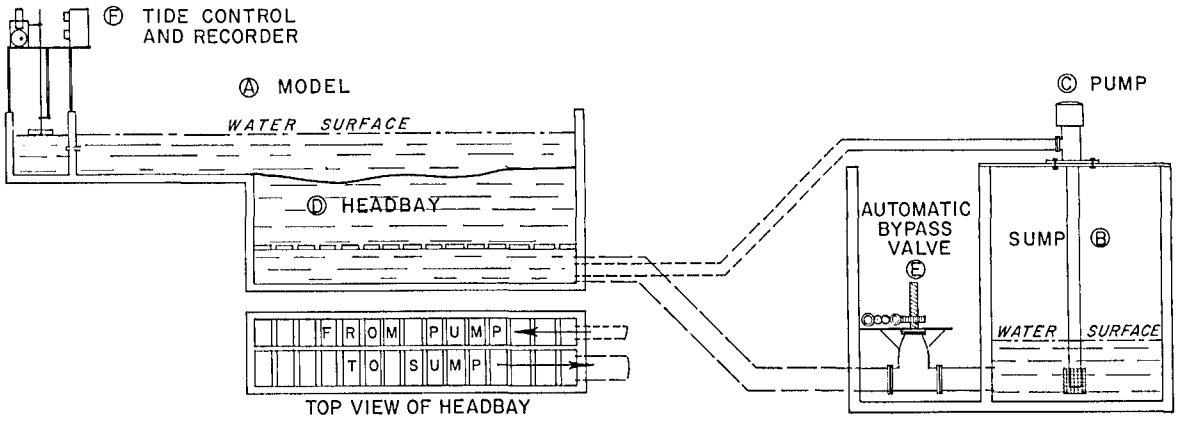

OPERATION OF TIDE GENERATOR

THE WATER SURFACE IN THE MODEL (A) IS APPRECIABLY HIGHER THAN IN THE SUMP (B). A PUMP (C) LOCATED IN THE SUMP DISCHARGES A CONSTANT AMOUNT OF WATER INTO ONE SIDE OF A DIVIDED HEADBAY (D). DISCHARGE FROM THE MODEL TO THE SUMP IS CONTROLLED BY AN AUTOMATIC VALVE (E). OPERATION OF THE AUTOMATIC VALVE IS DICTATED BY THE TIDE CONTROL (F) LOCATED IN THE MODEL. WHEN THE TIDE IS RISING IN THE MODEL, THE AUTOMATIC VALVE IS ALMOST CLOSED SO THAT MOST OF THE WATER REMAINS IN THE MODEL. WHEN THE TIDE IS FALLING IN THE MODEL, THE VALVE IS ALMOST OPEN SO THAT ALL THE WATER FROM THE PUMP, PLUS THE DESIRED AMOUNT OF WATER FROM THE MODEL RETURNS TO THE SUMP. THE TIDE CONTROL MAINTAINS THE PROPER VALVE OPENING AT ALL TIMES AS REQUIRED TO REPRODUCE ANY DESIRED TIDE IN THE MODEL.

Figure 3-15. Operation of pumped inflow and gravity outflow tide generator.

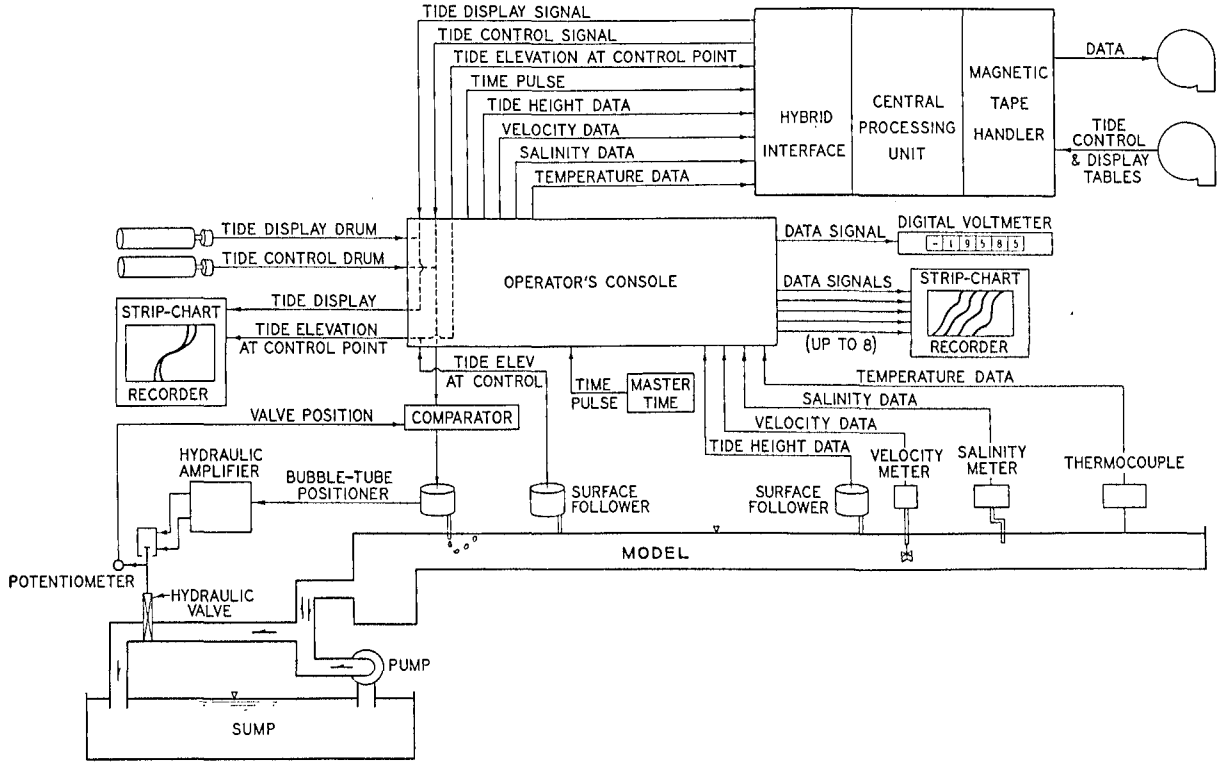

Figure 3-16. Automatic Data Acquisition and Control System (ADACS).

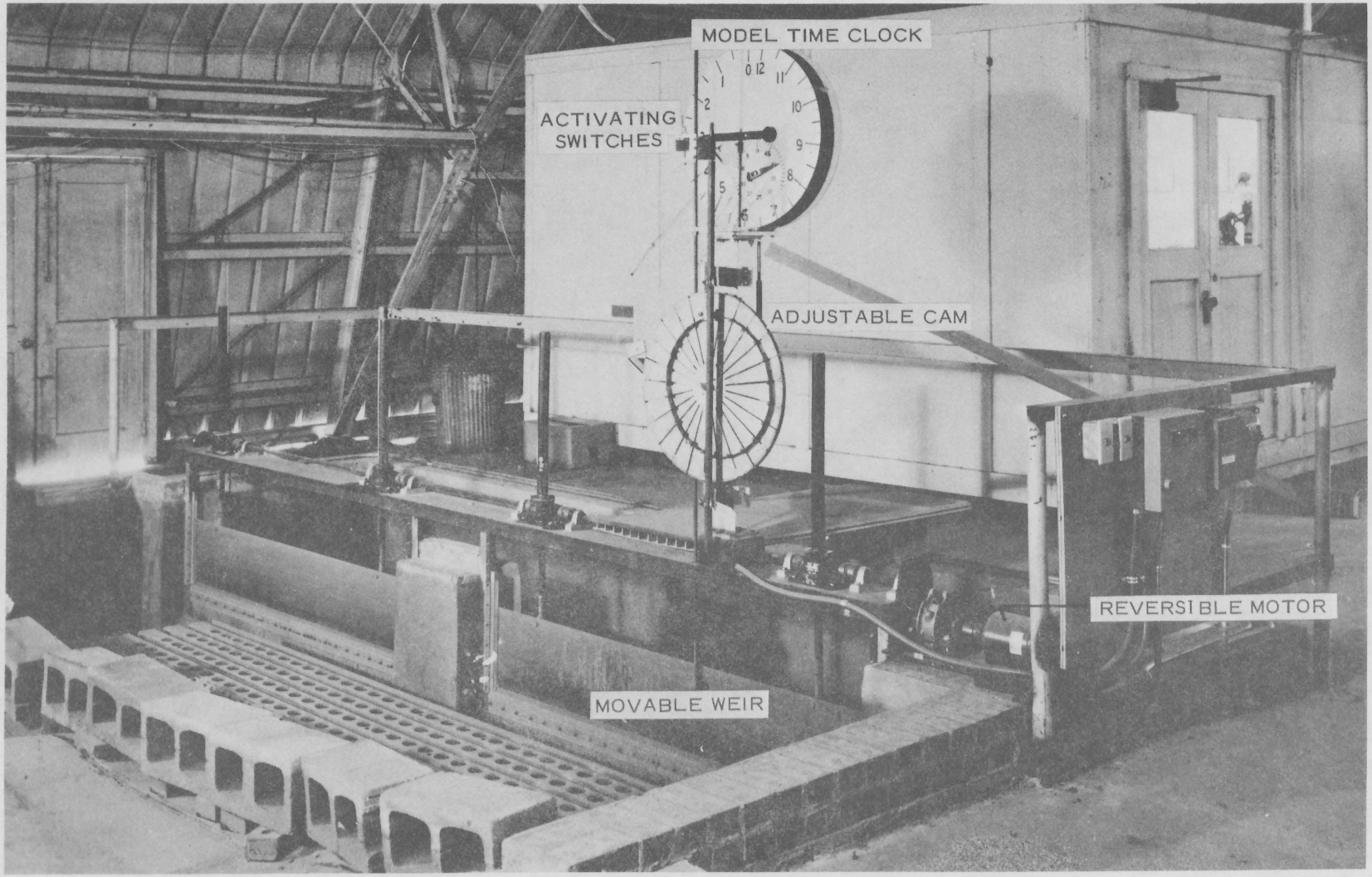

Figure 3-17. Mechanically programed overflow weir tide generator.

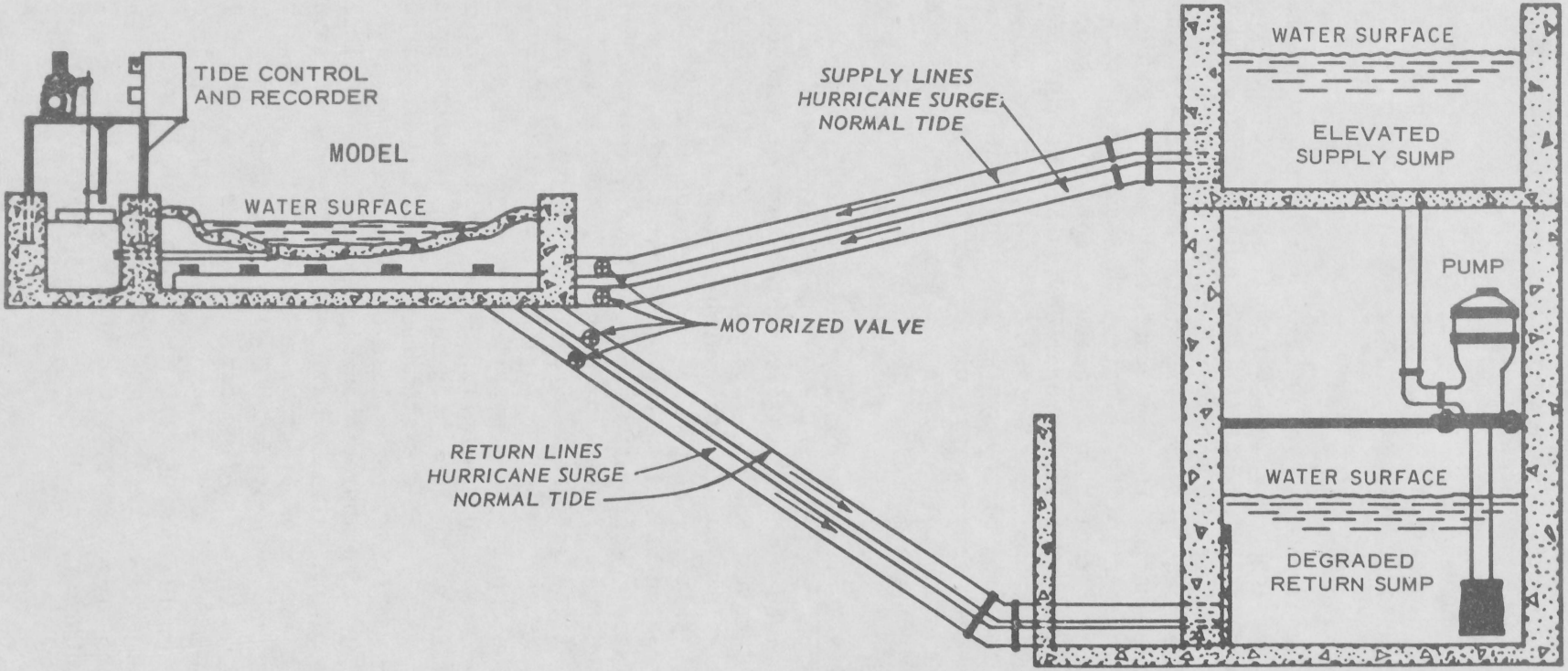

Figure 3-18. Gravity inflow and gravity outflow tide generator.

c. Model Appurtenances, Instrumentation, and Measurements. Estuary models are equipped with the necessary appurtenances to reproduce and measure all pertinent phenomena such as tidal elevations, hurricane surges, saltwater intrusion, current velocities, freshwater inflow, waves, littoral currents, mass (dye) dispersion, heat dispersion, and sedimentation. Tide generators were discussed previously; other model appurtenances are described below.

(1) Water Supply Sump. The water supply sump is the reservoir from which saltwater is pumped into the model; the saltwater returns to the sump from the model via the gravity return line. The sump is normally of sufficient size to store the entire volume of the model (at least the saltwater part of the model); therefore, during model operations, it is usually less than one-quarter full. Because salt must be added to the sump to maintain a constant ocean salinity, the sump must be rather turbulent and have a good circulation to achieve rapid mixing and, if necessary, rapid dissolving of salt. Proper design of the return line, supply line, and supply pump bypass line can result in sufficient mixing conditions. A supplemental mixing system is often required; however, in this case, two pumps are generally required, one to lift water from the sump to the model, and one to circulate and mix water in the sump with the water returned from the model.

(2) Salinity Control. Normally, freshwater is introduced into an estuary model in the upstream reaches, moves downstream into the model ocean, and becomes mixed with saltwater. Water must be removed from the model ocean at the same rate as the freshwater inflow rate in order to maintain a constant volume in the model-sump system. Since the discharge is contaminated with salt, it cannot be recycled and must be wasted. To maintain a constant ocean salinity, the salt lost in the waste-water discharge must be replaced. Most estuary models have a relatively small salt consumption, and the salt replenishment is accomplished by merely dumping finely granulated salt into a riser on the gravity return line or directly into the sump. Models with large freshwater inflows normally have a large salt consumption, and a salt brine injection system (Lixator) is used which eliminates manual handling of the salt. A Lixator is basically a container filled with rock salt into which water is added to dissolve the salt (Fig. 3-19). The system is designed to discharge a fully saturated brine. In addition to the loss of salt from the system, the freshwater inflow causes an appreciable dilution in the model ocean. Since increasing the ocean salinity only with the saltwater required for tide generation is a very slow process, additional circulation between the sump and model ocean is provided. The inflow and outflow lines carry considerably more flow than required for tide generation, thus increasing the exchange rate between model and sump. Models with a large ocean and substantial freshwater inflows usually develop a thin layer of relatively freshwater on the surface of the ocean. To minimize this effect, supplemental skimming weirs are often provided which remove this water from the ocean surface and return it to the sump where the salinity is increased to the proper value.

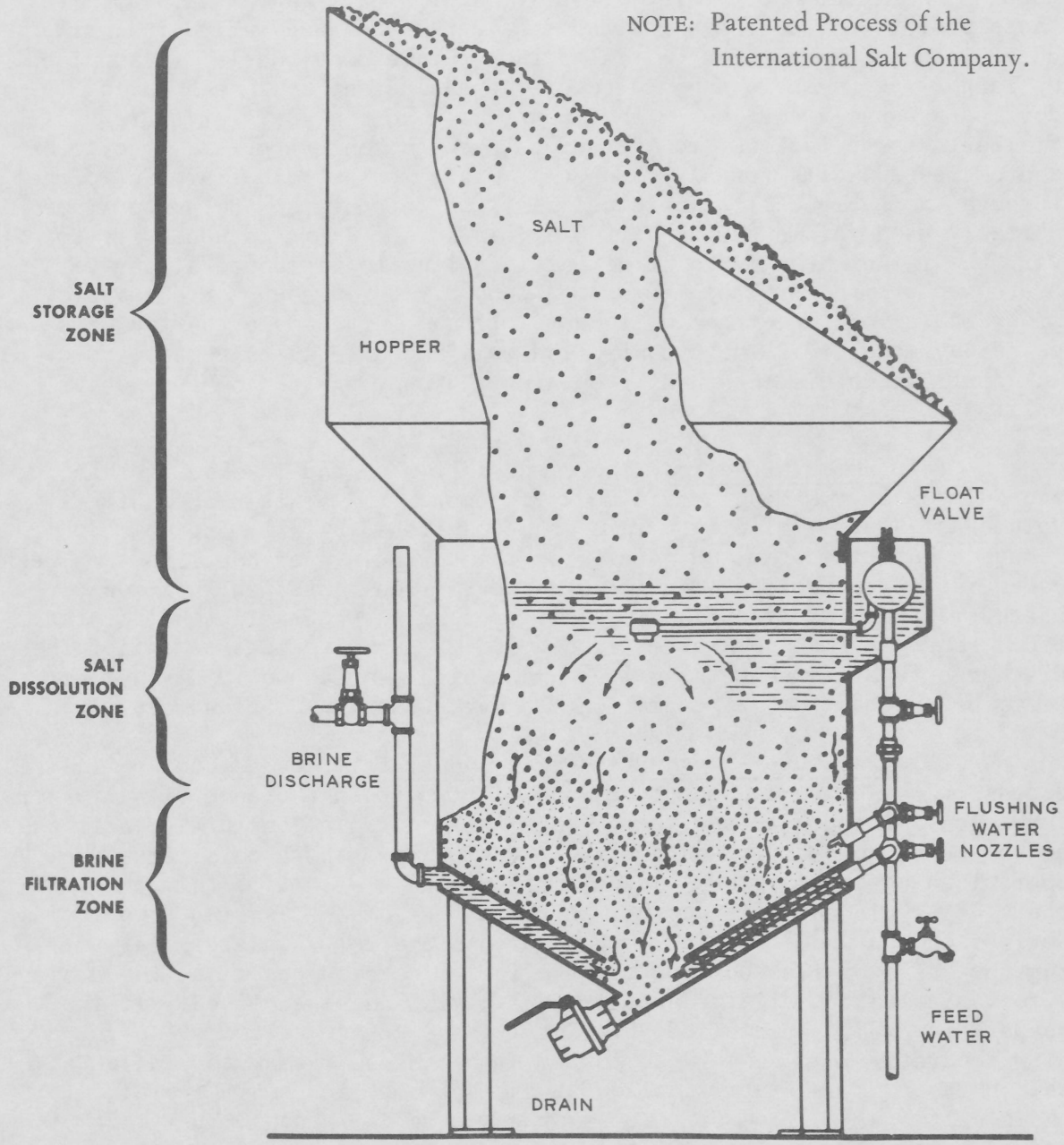

Figure 3-19. Lixator ® (after International Salt Company, 1965; patented process of the International Salt Company, copyright 1965).

(3) Freshwater Inflow Control. All tributary rivers with significant freshwater inflows are equipped with flow control devices of various types. The inflows of streams with minor freshwater inflows are combined with those of nearby tributaries of significant inflow or with those of several other minor streams, and the combined inflow is introduced into the model at a central point. Since most models are supplied by large water systems subject to pressure fluctuations, each inflow device is usually equipped with a constant head tank or a pressure controller. Large inflows are introduced through Venturi meters or over sharp-crested weirs (usually V-notch). Intermediate flows are introduced through Van Leer (California pipe) weirs or rotameters. Rotameters are normally used for measuring very small inflows. If it is necessary to vary the inflow at a large number of locations to reproduce a long-term hydrograph or to vary the inflow continuously throughout a tidal cycle, programable inflow devices will be required. For example, on the Chesapeake Bay model, digitally controlled multiple-orifice valves are used. The desired flow is obtained by opening the appropriate combination of orifices.

(4) Skimming Weirs. The mixed saltwater and freshwater that accumulates in the model ocean must be removed to maintain a constant volume and source salinity. This is accomplished by skimming weirs which remove a quantity of mixed water from the surface layer equal to the freshwater inflow to the model. Either a long, fixed-elevation, horizontal, sharp-crested weir or a floating weir is used, depending on whether the tidal range is small or large, respectively. Precise measurement of the discharge from the skimming weir is made by a V-notch weir, a Van Leer weir, or a rotameter, depending on the magnitude of the flow rate.

(5) Saltwater-Freshwater Inflow Separator. Occasionally, it is necessary to locate the upstream model limit within the zone of saltwater intrusion. In such a case, the artificial control of salinity conditions at the model boundary is necessary. This can present a considerable operational problem, since the salinity may vary with time throughout the tidal cycle and with depth. If the estuary is well mixed, two inflow devices can be used, one for freshwater and one for saltwater. By varying the ratio of flow between the two inflow meters with time, the desired time variation of salinity at the model limit can be achieved. If the estuary is highly stratified and exhibits a distinct saltwater wedge, a flow separator is necessary to permit simultaneous freshwater inflow at the surface and saltwater outflow at the bottom. A freshwater inflow pit and a saltwater outflow pit are separated by a horizontal plate which is hinged so that its lower elevation can be set to that of the saltwater interface. An observation pit with a glass panel is located beside the separator to permit visual observations and measurements of the saltwater interface. Freshwater flows are introduced above the separator plate, and saltwater flows out under the plate by gravity.

(6) Hurricane Surge Generator. A surge generator must be provided for models used to investigate hurricane surges. Only the methods of surge generation used by the Corps are described, and they include

displacement by horizontal plunger, displacement by vertical plunger, and gravity inflow. Hurricane surges could be generated in the model ocean with an independent pumped inflow and gravity outflow system similar to that used for tide generation, except that the large amplitude of the surges would require a very large pump and sump, pipes, and valves. Since construction of the system would be costly, a displacement surge generator is normally used. A horizontal displacement surge generator consists of a reservoir (or basin), adjacent to and integral with the model ocean, that contains a volume of water somewhat larger than that of the largest surge to be studied. The surge is reproduced by programing the forward and backward movement of a motorized, relatively watertight bulkhead located in the basin. The bulkhead is operated in such a manner that its forward motion displaces water from the surge basin into the model ocean at any desired rate, thus reproducing the rising phase of the selected surge; its backward motion permits water to flow from the model ocean into the basin, thus producing the falling phase of the surge hydrograph. The bulkhead drive motor is a three-phase type to permit the necessary reversal in direction, and a positive, infinitely variable (PIV) speed control unit is installed in the drive mechanism to permit a highly accurate control of the bulkhead speed. A vertical displacement hurricane surge generator is similar in basic concept, except that a large caisson is driven down into the reservoir to displace water into the model or driven up out of the basin to allow water to flow out of the model. The drive mechanism on the caisson consists of a variable-speed power supply connected to hydraulic jacks on the caisson. For very large models, the use of a displacement surge generator may be infeasible. In this case, either pumped or gravity inflow can be used. In pumped inflow, a large pumping system and a large sump are required; in gravity inflow, a large elevated supply sump is required in addition to a return sump. For the Chesapeake Bay model, the gravity inflow system was selected (shown schematically in Fig. 3-18). During operation for normal tides, the supply sump is only partly full, but just before generation of a hurricane surge the sump is filled with the volume required for the surge to be studied. During the falling phase of the surge hydrograph, water flows from the model by gravity into the return sump.

(7) Wave Generators. If sedimentation studies are required in the entrance to the estuary, the model ocean is usually equipped with one or more wave generators to reproduce the effects of ocean waves on the transportation and deposition of sediments. The wave generators are normally a vertical plunger-type and can be quickly adjusted to produce the desired wave height and period so that the model waves will move the model bed material (sediment) in the same manner as prototype waves produce bed movement in the prototype. The wave generators are mounted on wheels for ease in moving from place to place in the model ocean to generate waves from various directions.

(8) Littoral Current Generator. During entrance area shoaling studies (particularly movable-bed studies) it is often necessary to artificially generate littoral currents. The littoral current system consists of an intake-outflow header with ports at regular intervals at each end of

the model ocean connected through a pump (Fig. 3-20). By controlling the water direction and flow rate, a littoral current in either direction and of any desired strength can be induced in the model ocean. Flow direction can be controlled either by a bypass line equipped with appropriate valves around the pump or by a reversible pump.

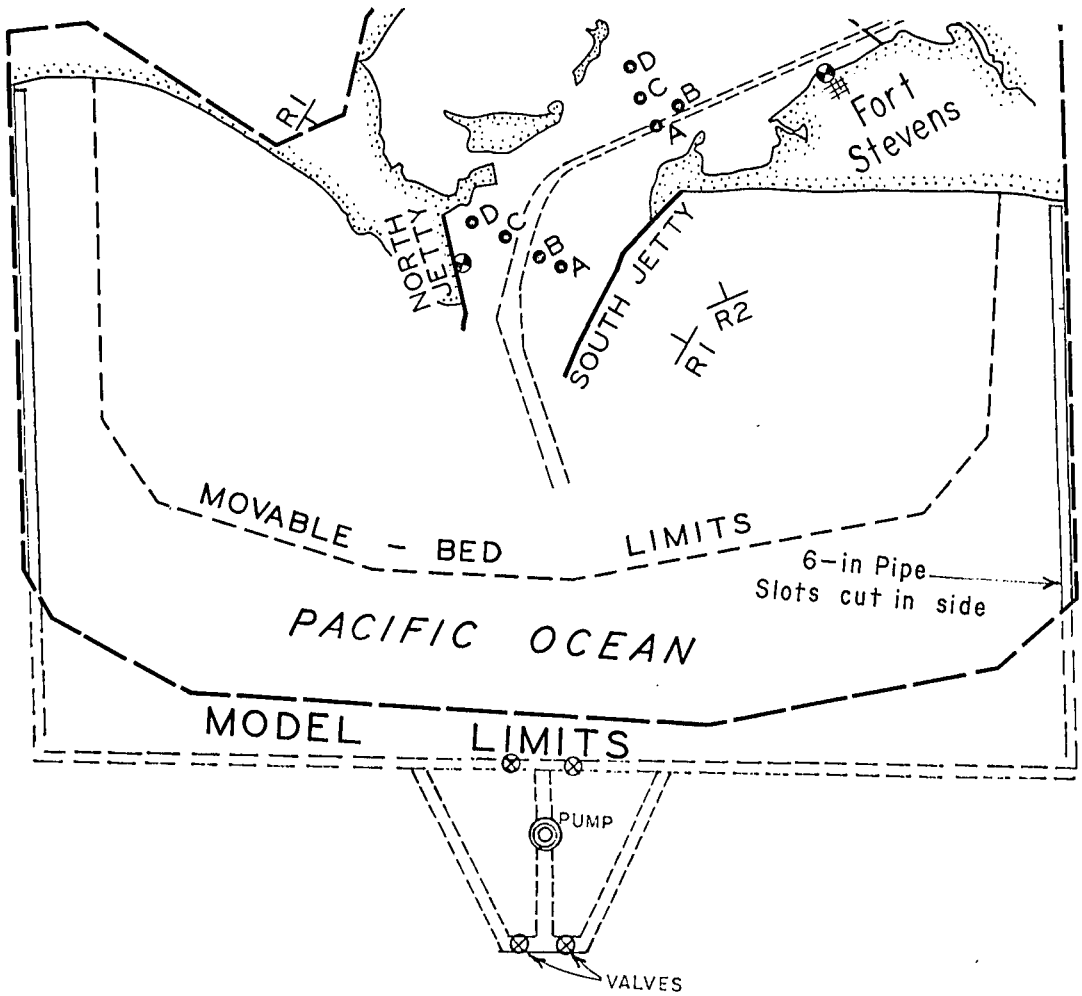

Figure 3-20. Typical littoral current generator.

(9) Powerplant Simulators. During heat-dispersion tests the powerplant cooling water is withdrawn from the appropriate location in the model and at the proper flow rate, heated to reproduce the desired temperature differential, and then discharged at the appropriate location in the model. The inflow rate is measured by a rotameter, the inflow temperature is monitored, and the heaters are set to produce the desired temperature differential.

(10) Shoaling Injection Apparatus. In fixed-bed shoaling studies a simulated sediment is introduced into the model in a manner determined by trial and error. Two basic types of model sediments are used: (a) granulated plastic or nylon, and (b) finely ground gilsonite. The plastic

or nylon materials are generally placed by hand directly on the model bed, injected into the model as a slurry from a tank through a hose equipped with a flared nozzle, or injected as a slurry through a perforated trough. If an injection of the plastic or nylon material at a uniform rate over an extended period of time is necessary, an injection system consisting of a material reservoir, a rotating distribution wheel, and an electric drive motor with a variable-ratio gearbox is used. At the correct injection time, the mechanism is activated by a cam on the tide generator and operated until the injection period has been completed. Gilsonite is injected into the model as a slurry from a circular tank through perforated pipes. The tank is equipped with motor-operated mixing blades to maintain a uniform consistency of the slurry. The slurry is introduced by gravity or pumped flow from the tank into the perforated pipes during the injection period.

(11) Shoaling Recovery Apparatus. The plastic or nylon materials are recovered with a flared nozzle connected by a hose to an aspirator and discharged into a tub for decontamination, or with a jet pump connected to a hydrocyclone for separation of the water and material. Gilsonite is recovered with either the aspirator apparatus or the jet pump; however, separation by the hydrocyclone is not very effective.

(12) Dye Injection Apparatus. A given weight of powdered fluorescent dye is thoroughly mixed with a known volume of water and stored in a tank. The tanks are equipped with a system of valves, tubes, and rotameters to control the desired inflow ratio at the injection location.

(13) Salinity and Dye Samplers. Water samples are withdrawn from the model by suction, either orally by model technicians or by a vacuum pump. In the first method, the samples are obtained in a small pipette (typically 25 cubic centimeters) by suction applied to a short piece of tubing attached to the pipette. For obtaining simultaneous, multidepth samples, a multidepth sampler which consists of a number of single samplers designed to withdraw simultaneous samples at various depths at one position is used. Multidepth samples can be withdrawn either by suction applied orally or from a vacuum pump connected to a central manifold, which in turn is connected to tubes running to each sampling location. This latter device enables simultaneous sampling at all desired depths at all sampling stations throughout the model. Samples can also be withdrawn continuously (or intermittently) over a complete cycle to obtain an integrated sample. The sampling system is similar to the multidepth sampler described above, except that the sample container must be larger.

(14) Saltwater-Freshwater Mixing Simulators. Occasionally, the proper degree of mixing of saltwater and freshwater cannot be achieved through the use of roughness elements or model boundary roughness. This is particularly true for models of broad, shallow estuaries with small tidal ranges where wind action is the primary mixing agent. The use of a simulator is then necessary to achieve the proper degree of mixing.

For this purpose, small oscillating room fans are placed throughout the model in the pattern and number determined during the model verification process. The fans are directed down on the water surface rather than across the surface. In estuaries with low tidal range and low freshwater inflow, mixing in the navigation channels is often primarily due to the passage of deep-draft ships. Simulation of this type mixing can be achieved by releasing air bubbles at a low rate at intervals along the bottom of the channel.

(15) Ship Simulators for Sediment Resuspension. In estuaries where current velocities are weak, the movement and deposition of sediments in the navigation channel may be strongly influenced by the passage of deep-draft ships. Deposited sediments are resuspended and subsequently moved by the weak tidal currents. Since the model tidal currents are also too weak to move the deposited sediment along the bed of the model, a ship simulator is used to resuspend the sediment. The ship simulator consists of a small propellor which can be rotated at various speeds in either direction. It is towed back and forth along the navigation channel during shoaling tests.

(16) Water Level Measurement. Water level is usually measured with manually operated point gages, recording float gages, electronic water level followers, air-capacitance gages or air-bubbling systems. Point gages can be mounted permanently or on portable racks. If it is necessary to obtain a continuous record of the water (as during a hurricane surge), one of the other types of measuring devices must be used. The recording float gage consists of a float-supported pen which inks a continuous record of water level on a roll of recording paper on a drum, which in turn is mounted on a tripod permanently located at gaging stations. The electronic water level follower detects conductivity through probes continuously moved up and down by a servo drive, thus continuously making and breaking contact with the water. The air-capacitance gage is also mounted on a servomechanism, but this gage monitors the position of the water surface by maintaining a constant electrical capacitance in the air gap between the gage and the water surface. Vertical movement of the gage probes is recorded on a strip chart, or the voltage outputs can be converted to digital signals and recorded on magnetic tape. The bubble tube positioner follows the water level by moving the bubble tube up or down as required to maintain a constant pressure at the open end (bottom) of the tube. Water level changes are detected by a potentiometer on the servo drive. Bubbler systems are also available which determine water level directly from the pressure in a fixed bubble tube. Water level can be determined to within ±0.001 foot with any of these instruments, and is generally the accuracy of duplicating identical conditions on the model.

(17) Current Velocity Meters. Current velocity is normally measured by miniature Price-type current meters (Fig. 3-21) capable of measuring velocities as low as 0.02 foot per second (~0.01 knot). Their calibration is quite stable unless the meters are damaged or the jeweled bearings become fouled. Because five cups (constructed of plastic or

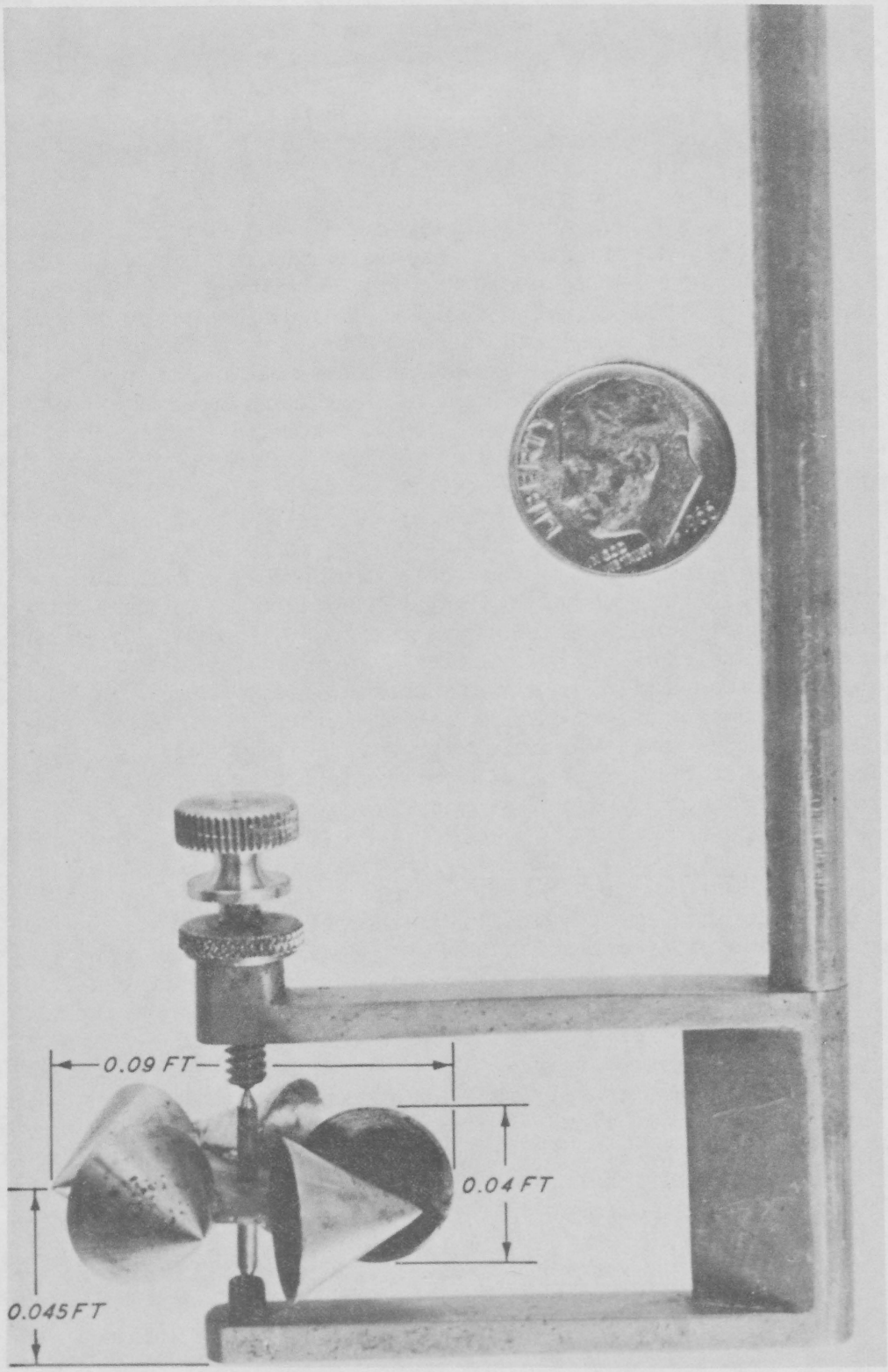

Figure 3-21. Model velocity meter.

metal) are mounted on a vertical axis, the meter is insensitive to current direction. In operation, the number of wheel revolutions per 10-second period is determined visually and converted directly into prototype velocity. A photo cell, fiber optics, an electronic counting circuit, and an alternating current-direct current converter have been added to provide automatic velocity measurements. Light is transmitted to the reflective surface on the cups and back to the photodiode through fiber optics. The pulsations of the photodiode are thus directly proportional to velocity. The sampling frequency is quite flexible. Miniature electromagnetic current meters are being developed which should further improve the ease and accuracy of obtaining velocity measurements. Advantages of such sensors include the lack of inertia (which would improve the response to accelerating and decelerating flow) and automatic determination of velocity vectors. The limitations of the current velocity meters used in estuary models should be considered before making close comparisons between model and prototype velocity data. In models with commonly used vertical scales, the centerline of the meter cup or vane is 3 to 5 feet (prototype) above the bottom, whereas field measurements are usually about 2 feet above the bottom. The model velocities are commonly determined over an interval equivalent to 3 to 16 minutes (depending on the model scales and the type of meter), whereas prototype velocity observations are often made in less than 1 minute. For common model scales, the horizontal spread of the entire meter cup or vane wheel is equivalent to 50 to 100 feet (depending again on the scales and type of meter). However, prototype velocity meters have a horizontal spread of less than 1 foot. Thus, the distortion of areas (model to prototype) results in comparison of prototype point velocities with model mean velocities for a much larger area. The same is true for the vertical area. The accuracy of the model velocity meters is on the order of ±0.25 foot per second (prototype).

(18) Current Velocity Photos. In areas where velocities are very small throughout most of the tidal cycle or where water depth is too shallow for a velocity meter, velocity can be determined by timing the travel of a float over a measured distance. Surface current velocities can also be determined from time-exposure photos of confetti floating on the water surface. The camera lens is opened by a solenoid activated by the tide generator and closed by an accurate timing device. A bright light is flashed immediately before the camera lens is closed, resulting in a bright spot at approximately the end of each confetti streak which indicates the direction of flow. Current velocities can be determined from the photos by determining the length scale of the photo, measuring the length of a confetti streak, and knowing the length of the time exposure. An example of a current pattern photo is shown in Figure 3-22.

(19) Salinity Measurement. Salinity concentration is measured either by chemical titration with silver nitrate or conductivity measurement. Based on the sample volumes normally used for analysis, salinity concentrations determined by titration are considered accurate to within ±0.02 part per thousand. The conductivity meter assembly consists of a set of three temperature-compensated conductivity cells, a cell switch, a conductivity indicator, and a digital readout. The conductivity cells

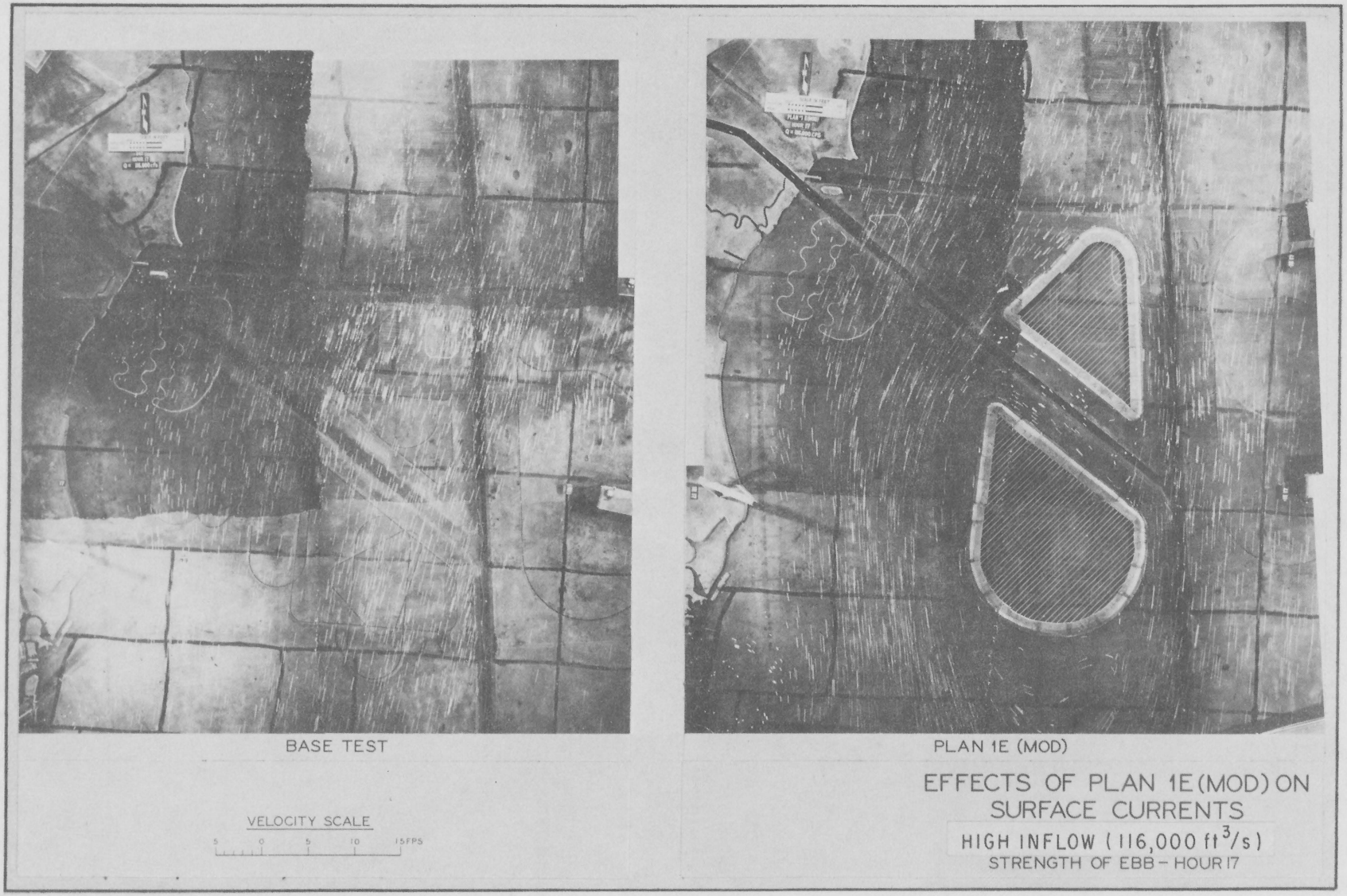

Figure 3-22. Typical current pattern photo (Lawing, Boland, and Bobb, 1975).

are 5-cubic centimeter pipettes into which the samples are drawn by suction. Each cell is equipped with two platinum electrodes and a thermocouple. Separate conductivity cells are used for samples between 0.0 and 1.0, 1.0 and 10.0, and 10.0 and 40.0 parts per thousand; the cells are accurate to within ±0.03, ±0.30, and ±0.50 parts per thousand, respectively. The cells are frequently calibrated to ensure accuracy, but the calibration has been determined quite stable. The accuracy to which a model can be expected to duplicate salinities at any given point from cycle to cycle for identical conditions is about ±3 to 5 percent.

(20) Dye Concentration Measurement. Fluorescent dye tracers are used to determine dispersion patterns and rates. Pontacyl Brilliant Pink, Uranine and Rhodamine WT dyes are most commonly used in models. Dye concentrations are determined to within about ±3 percent by a Turner Model III fluorometer. Since this instrument is sensitive to temperature changes, all samples should be analyzed at a uniform temperature. In most dye-dispersion tests, the dye is released at a point source and then moves in high concentration clouds along the model for several tidal cycles until the dye spreads throughout the estuary. These clouds move away from the injection point with the ebb and flood currents and form detached areas of comparatively high dye concentration which are discernable for several tidal cycles thereafter. Therefore, dye concentrations measured at points 1 foot apart in the model differ greatly. The same phenomenon occurs in nature and is probably responsible for the reported difficulty in analysis of results of similar full-scale studies in the field.

(21) Temperature Measurement. During heat-dispersion tests, water temperatures are measured either by an extensive array of thermocouples and multichannel recorders or by thermistors with individual or multichannel recorders. Temperature differentials are accurately measured to within ±0.5° Fahrenheit (±0.3° Celsius) with the thermocouples or ±0.2° Fahrenheit (±0.1° Celsius) with the thermistors.

(22) Sedimentation Measurement. At the conclusion of a fixed-bed model shoaling test, the model sediment deposited within the limits of marked areas (e.g., 1,000-foot-long sections of a navigation channel) is recovered with the apparatus discussed previously. After most of the water has been separated from the model sediment, the material is then measured volumetrically in graduated cylinders. The limit of accuracy of repeating identical shoaling tests is about ±10 percent. Assuming that a satisfactory shoaling verification has been achieved, the model and prototype shoaling rates can be related. Although the model shoaling test results must be considered qualitative, the model predictions will give a reasonable indication of prototype shoaling rates.

4. Model Verification.

The worth of any model study is completely dependent on verification of the ability of the model to produce, with a reasonable degree of accuracy, the results which can be expected to occur in the prototype

under given conditions. Therefore before any model tests are undertaken of proposed improvement plans, it is essential that the required similitude is first established between the model and prototype and that all significant scale relationships between the two are determined.

Verification of a fixed-bed estuary model is generally accomplished in three phases: (a) Hydraulic verification, which ensures that tidal elevations and times, and current velocities and directions are in proper agreement with the prototype; (b) salinity verification, which ensures that salinity phenomena in the model correspond to those of the prototype for similar conditions of tide, ocean salinity, and freshwater inflow; and (c) fixed-bed shoaling verification, which assures acceptable reproduction of prototype shoaling distribution. In addition, dye-dispersion verification is accomplished if the results of a prototype dye-tracer study are available.

Since discrepancies between model and prototype observations are likely, the effects of various plans tested in the model on the basis of model-to-prototype comparisons should not be evaluated. Therefore, after the model has been verified, a series of observations is made throughout the model to define "existing" or "base" conditions in the model. The plan test results are then evaluated on the basis of model-to-model comparisons to determine the changes caused by the plan.

a. Tides.. The objective of the model tidal adjustment is to obtain an accurate reproduction of prototype tidal elevations and phases throughout the model. Prototype tidal data from several gages located throughout the length of the estuary are required. The prototype tide gages must have been operated continuously throughout the velocity, salinity, and dye-tracer surveys.

Because of limitations on the availability of personnel and equipment, most prototype current and salinity surveys are conducted over a period of several consecutive days, rather than obtaining all data simultaneously in a single day. Therefore, during a prototype survey there can be significant variations of tidal range. To avoid the time-consuming and expensive procedure of adjusting a model to reproduce all of the tides during the prototype metering program, a single tide is usually selected which approximates an average tidal condition for the metering period; the model is then adjusted for reproduction of tides, currents, and salinities (for that metering period) for only the single tide. Verification using tidal constituents is discussed in Section VII.

With the model operated with freshwater only (saltwater is not required at this stage), the primary tide generator is adjusted so that the tide generated in the ocean causes an accurate reproduction of the prototype tide at the control tide gage (located in the ocean or near the mouth of the estuary). The appropriate freshwater inflows are reproduced in all tributaries to the estuary during the verification process. The secondary tide generator (if used) and the model roughness are then progressively adjusted until the prototype tidal elevations and phases are reproduced to scale throughout the model. This adjustment is aimed at

reproduction of average tidal volumes and discharges, and little, if any, attention is paid to current velocities. If the control tide gage is located inside the estuary, at least limited tidal information is required for the ocean near the estuary mouth in order to properly adjust the model roughness between the ocean and the control gage. If available, data from temporary National Ocean Survey (NOS) tide gages within the study area are often useful. This process is usually repeated for various conditions of tidal range and freshwater inflow to ensure that the gross model roughness distribution is valid for a wide range of known conditions.

In estuaries with extensive marshes which are inundated at high tide, the alternate waterflow into and out of the areas comprises a considerable part of the tidal prism. In such cases it may be necessary to accomplish the tidal adjustment in two phases, since different types of model roughness are used in the deep channel and tidal marsh areas. First, a neap tide is reproduced in the model and the channel roughness is adjusted until tidal elevations in the channels are reproduced as accurately as possible. A spring tide is then reproduced, and the marsh roughness is adjusted until proper tidal elevations are obtained throughout the model.

Although a redistribution of the model roughness is made during the current (and possibly salinity) adjustment, tidal elevations are checked to ensure that the tidal reproduction is still accurate. Examples of the tidal verification achieved in various estuary models are presented in Figures 3-23 and 3-24.

b. Currents. During a substantial part of the current adjustment, the introduction of saltwater into the model is still unnecessary. After it has been determined that average tidal volumes and discharges are being reproduced with reasonable accuracy (tidal adjustment), the depth-average prototype velocity is determined at hourly or 1/2-hour intervals throughout a tidal cycle at several points on ranges across the estuary. The lateral distribution of velocity (prototype) as a function of time during the tidal cycle can then be determined for each velocity range and compared to measurements in the model. Extensive alterations in the lateral distribution of model roughness are usually necessary to bring the lateral velocity distribution in the model into agreement with that of the prototype. The total amount of roughness between tide gages cannot be altered significantly, because of the necessity of maintaining an accurate tidal adjustment. During this stage of the model adjustment, it is unnecessary to achieve an accurate reproduction of the absolute magnitude of velocities; only the lateral distribution is needed. Therefore, the prototype velocity data need not be corrected for moderate differences in tidal range between the tide which occurred when the prototype velocities were measured and the tide reproduced in the model. However, the prototype velocity observations for each range must all be made during a single tide or corrected to represent conditions for a single tide. As for the tidal adjustment, the process is repeated for various conditions of tidal range and freshwater inflow to ensure that the lateral roughness distribution is valid for a wide variety of known conditions.

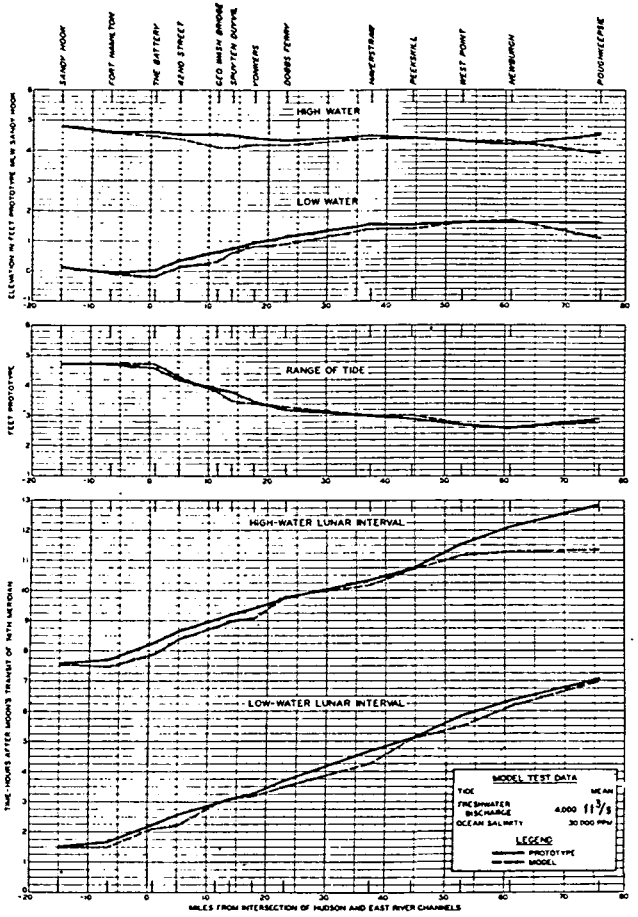

Figure 3-23. Verification of tides, New York Harbor model (after Simmons and Bobb, 1965).

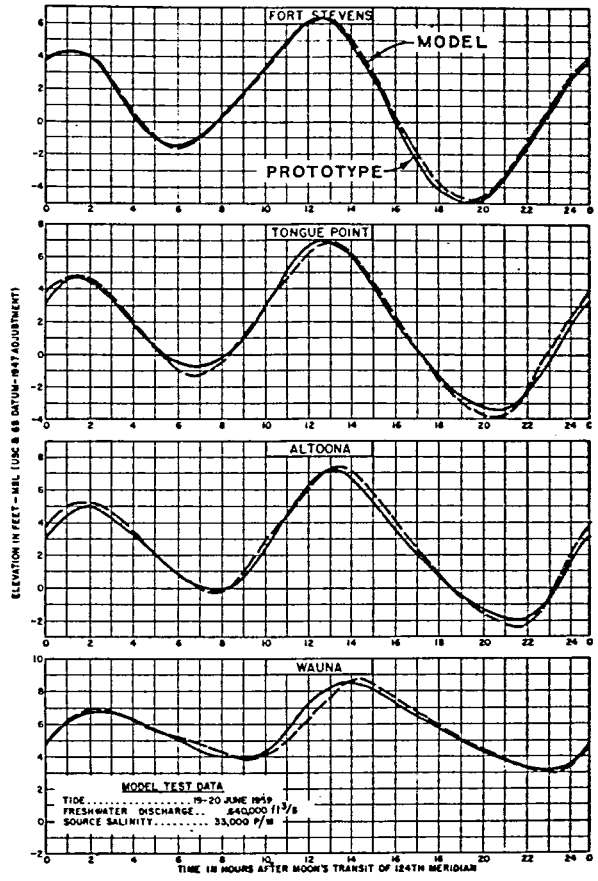

Figure 3-24. Verification of tides, Columbia River Estuary model (Herrmann, 1968).

The next step of the current adjustment consists of operating the model with saltwater in the ocean. For a representative tide, the model roughness distribution is refined to achieve accurate reproduction of velocity distribution both laterally and vertically. During this phase, the lateral distribution of velocity (model and prototype) is determined at various depths across each velocity range rather than as a depth average. It is sometimes necessary during this phase of the model adjustment to bend some (or most) of the vertical roughness elements in half in order to concentrate more of the flow resistance near the bed.

If the prototype velocity data have been collected over a long period of time, there may be no short term (i.e., 1 week or less) during which sufficient velocity data were collected throughout the entire estuary. In this case, reproduction of velocity distribution rather than absolute magnitude is emphasized to avoid the necessity for reproducing all the combinations of tide and freshwater inflow during which prototype velocity data were obtained. After the velocity distributions have been satisfactorily reproduced, a few prototype tide-inflow conditions must be reproduced to ensure that velocity magnitudes are accurately reproduced in various areas throughout the estuary. If the prototype velocity data have been collected in comprehensive, short-term surveys, greater emphasis can be placed on the reproduction of velocity magnitudes. As discussed previously, a single tide from each short-term survey is selected as representative of that survey, and only this tide is reproduced in the model. Since the magnitude of current velocity is strongly influenced by tidal range, an adjustment to many of the prototype velocities may be necessary to represent conditions for the tide reproduced in the model. The prototype velocity adjustment can often be based on a simple correlation between tidal range and maximum ebb and flood velocities at a given station (Fig. 3-25). The maximum ebb and flood velocities for the tide being reproduced can be determined from such a plot and compared to the maximum velocity observed. The appropriate percentage correction is then made to all velocities observed at that station.

Two particular difficulties are often encountered during the velocity verification. Depending on the type of prototype velocity meter used, vertical motion of the survey boat can cause the recorded velocity to be considerably greater than the actual velocity. This is particularly troublesome in the entrance to an estuary, where the survey boat is subject to continuous wave action. In this case, model reproduction of the lateral and vertical velocity distributions must be emphasized rather than velocity magnitude. In confined channels of tributaries or the upstream reaches of the estuary, current velocities are greatly influenced by the magnitude of the freshwater inflow. If the reported prototype freshwater flow rate is inaccurate, an accurate velocity verification in such areas cannot be achieved. The freshwater inflow rate must then be adjusted as necessary to obtain the proper velocities.

Although a further refinement of model roughness may be required during the salinity verification, velocities are checked to ensure that

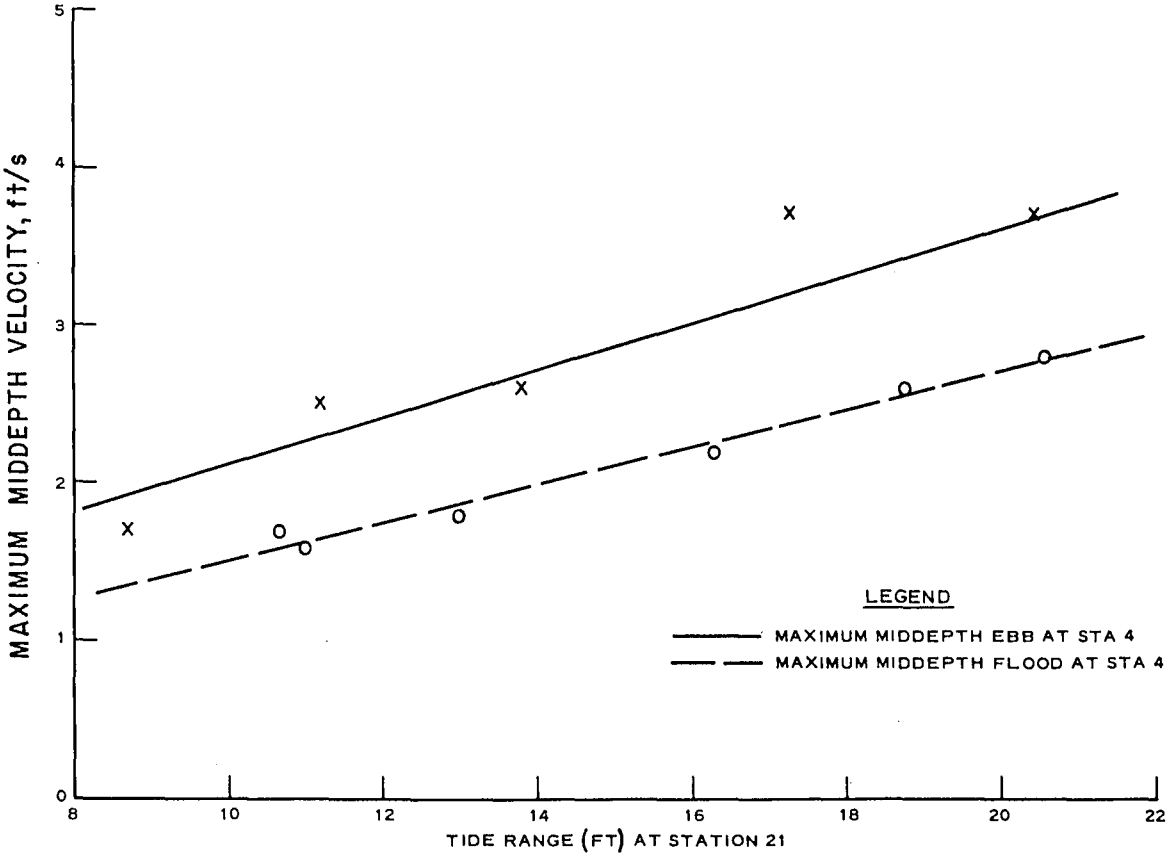

Figure 3-25. Typical correlation between tidal range and maximum velocity, Gastineau Channel model (Herrmann, 1972).

the current reproduction is still accurate. Examples of velocity verification achieved in various estuary models are presented in Figures 3-26 and 3-27.

The flow predominance method of presenting current velocity reduces magnitude, direction, and duration of the currents to a single expression that defines what percentage of total flow at any given point is toward the ocean (ebb) and what percentage is away from the ocean (flood). This expression is derived from a conventional plot of velocity versus time over a tidal cycle at any given point. The areas subtended by both the ebb and flood parts of the curve are measured (or calculated) and summarized. The area subtended by the ebb part of the curve is then divided by the total area to determine what percentage of the total flow is in the ebb direction. This calculation is performed for both model and prototype velocity data to determine the time-average vertical flow distribution. This information is used in addition to the time-varying vertical velocity distribution in adjusting the model roughness. The flow predominance data are useful in determining the vertical flow distribution at a given station (shown in Fig. 3-28), or in determining the longitudinal distribution of flow along the length of the estuary at particular depths (shown in Fig. 3-29).

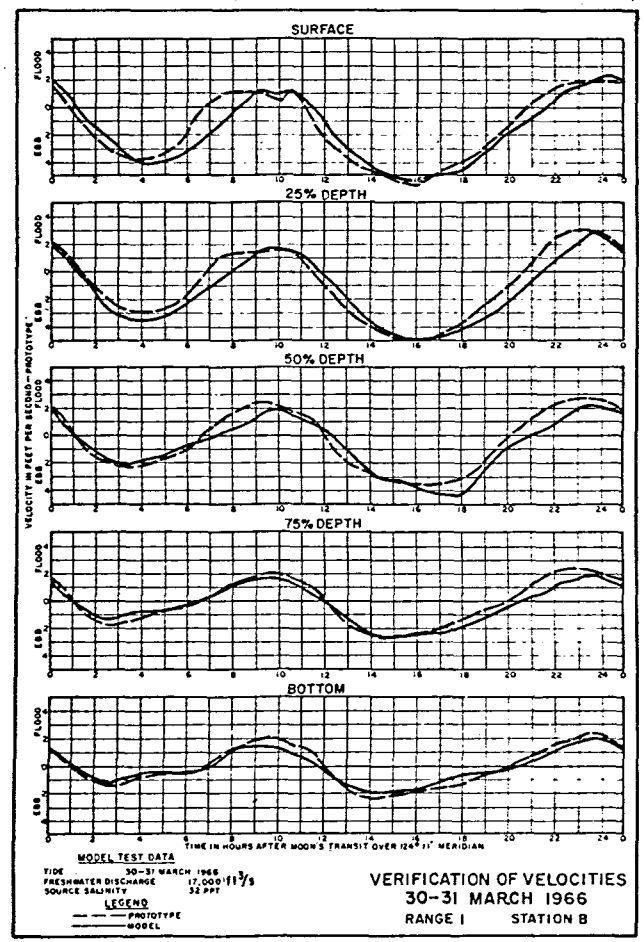

Figure 3-26. Verification of current velocities, Umpqua River Estuary model (Fisackerly, 1970).

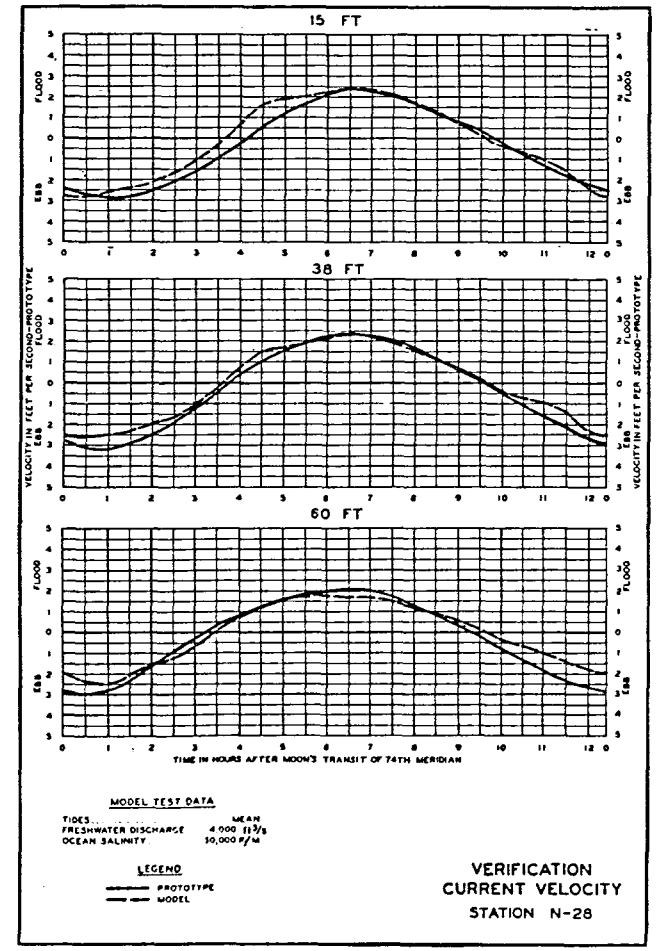

Figure 3-27. Verification of current velocities, New York Harbor model (Simmons and Bobb, 1965).

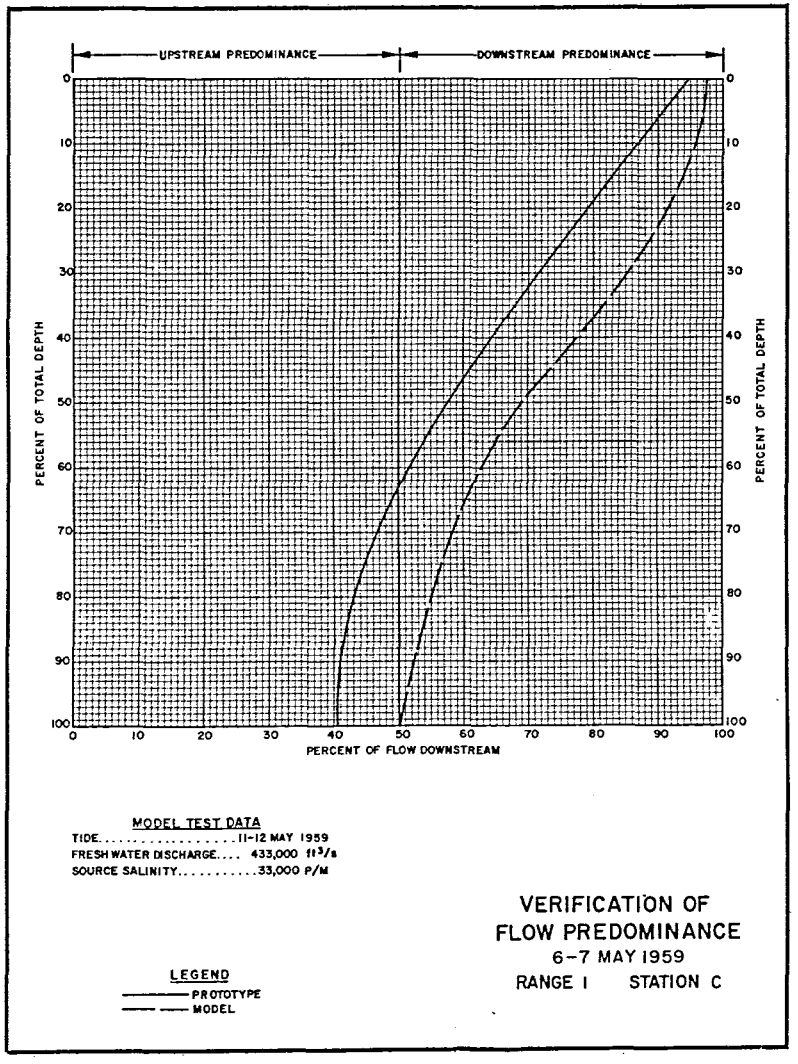

Figure 3-28. Verification of flow predominance, Columbia River Estuary model (Herrmann, 1968).

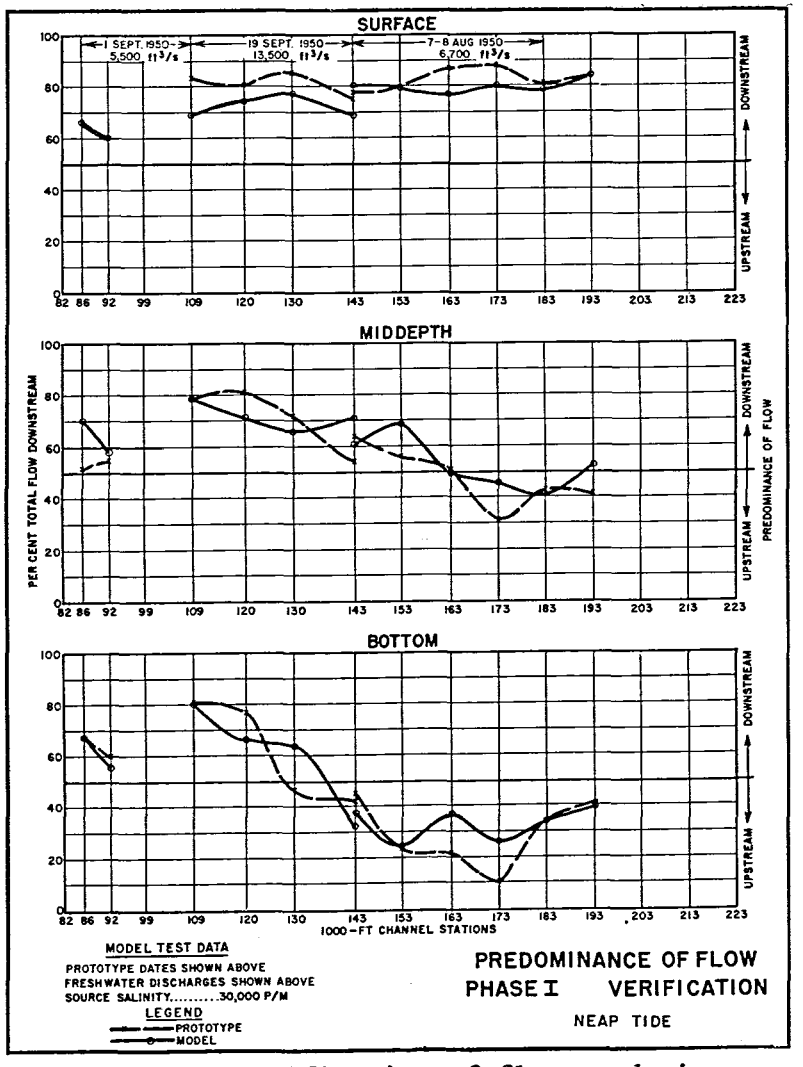

Figure 3-29. Verification of flow predominance, Savannah Harbor model (U.S. Army Engineer Waterways Experiment Station, 1961).

c. Salinity. Depending on the nature of the tests to be conducted in the model, salinity verification is achieved in either one or two phases. The first, and often the only, phase involves the reproduction of the salinity conditions which were obtained during the quasi-steady-state conditions of a single tidal cycle; the second phase involves reproduction of transient, long-term salinity conditions as affected by seasonal variations in freshwater inflow.

The first step in the quasi-steady-state verification process is to determine the proper source salinity. Selection of the proper salinity for the ocean water supply system is usually based on the maximum bottom salinity observed during the prototype metering program at the deepest station on the range closest to the ocean. If subsequent model tests show that the maximum salinity at this location is affected by freshwater inflow, the source salinity will have to be increased until the proper maximum salinity is reproduced. Because the model salinity conditions are completely artificial and temporary at the time model operation is initiated, the model should be operated until salinity conditions have stabilized before making detailed salinity measurements in the model. After stability has been achieved, samples are withdrawn from the model at hourly (prototype) intervals at the stations and depths for which prototype data are available. As in the velocity verification, a representative tide from the prototype survey period is reproduced in the model; however, because tidal range has little, if any, effect on numerical salinity concentrations in many estuaries, it is often unnecessary to adjust salinities observed during different tides as long as the freshwater inflow conditions are the same. Drastic changes from the tidal range of the previous day should be avoided. In this manner it is possible to demonstrate that the effects of tide on short-term (one tidal cycle) phasing and fluctuations in concentration of salinity are accurately reproduced. Further refinements to the model roughness to achieve a satisfactory salinity verification are usually unnecessary. However, modification of the skimming weirs may be necessary to remove excess freshwater from the surface of the model ocean to prevent dilution of the source salinity. Note that quasi-steady-state conditions in the model are used to represent prototype conditions which are actually transient. When prototype salinity conditions are changing rapidly in response to significant variations in the freshwater inflow, the model cannot be expected to accurately reproduce these conditions with a quasi-steady-state test. Other unusual conditions during the prototype survey may also result in a rather poor verification; e.g., heavy winds immediately preceding or during the prototype survey may result in a higher than normal degree of mixing. However, local rainfall may result in a surface layer of freshwater over a large area of the estuary. An example of quasi-steady-state salinity verification is shown in Figure 3-30.

In broad, shallow bays with low tidal ranges (common along the Gulf of Mexico), tidal currents are generally of insufficient strength to generate a high degree of mixing between saltwater and freshwater. However, these estuaries are typically well mixed by wind-generated wave action. In estuary models of this type, the artificial roughness normally used

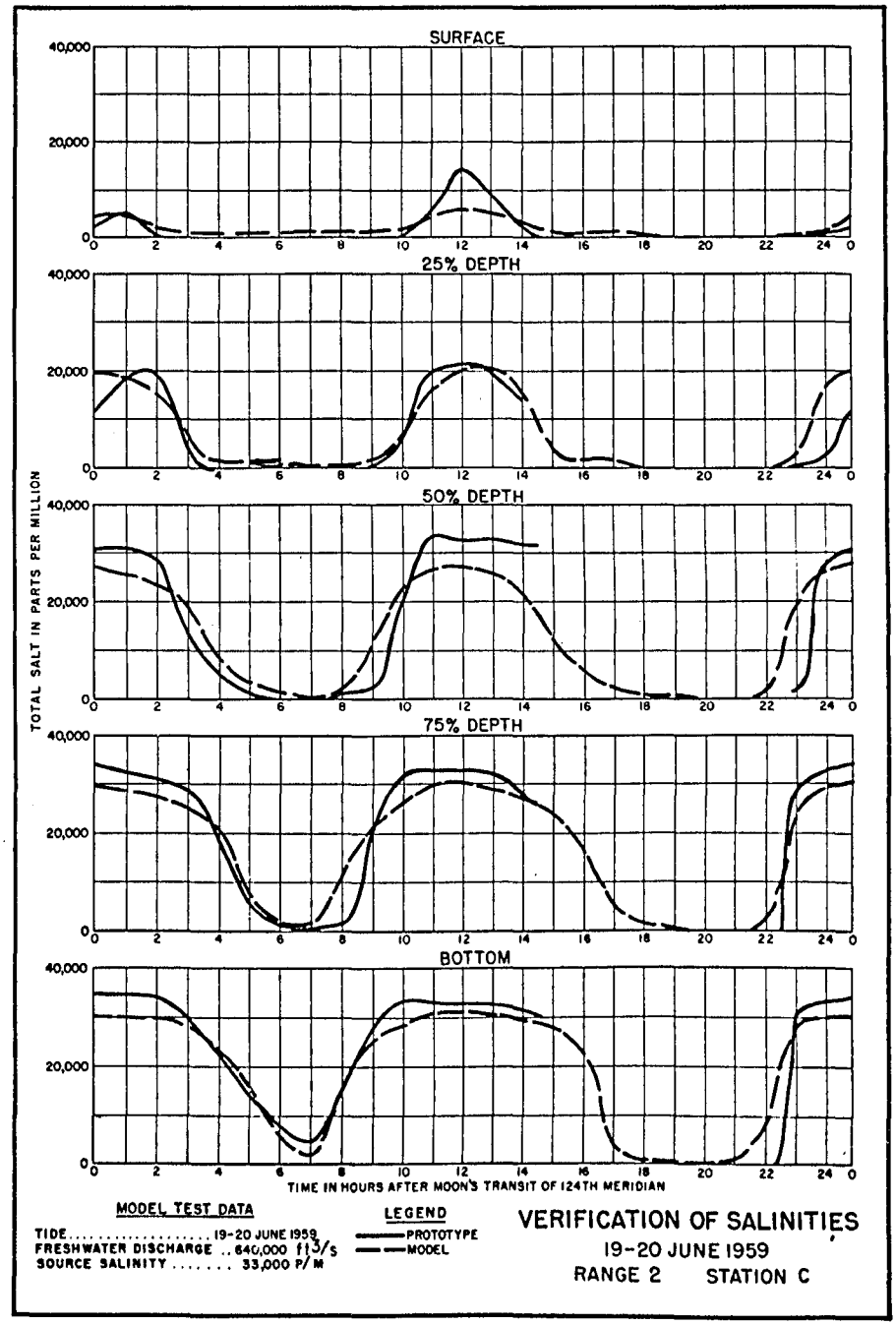

Figure 3-30. Verification of tidal-cycle salinities, Columbia River Estuary model (Herrmann, 1968).

does not generate sufficient turbulence to reproduce the proper degree of mixing, and the models tend to be more stratified than their prototype counterparts. To obtain proper model salinity mixing, oscillating fans are mounted on stands and positioned to blow down on the model water surface in a pattern designed to prevent the establishment of unnatural surface eddy patterns (Fig. 3-31). The number and position of the fans are determined by trial and error to achieve the proper vertical salinity gradients. The mixing index (or salinity ratio) is determined for both model and prototype at various locations throughout the estuary by dividing surface salinity by bottom salinity and multiplying by 100 to convert the result to a percentage. Examples of the degree to which the mixing index has been reproduced are shown in Figure 3-32 and in Table 3-2.

Table 3-2. Lake Pontchartrain mixing indices.[1]

Station	Prototype	Model	Station	Prototype	Model
GC-11	100.0	100.0	P-7	95.0	97.0
T-5	98.0	85.0	P-8	100.0	100.0
T-6	101.0	83.0	P-9	100.0	100.0
T-7	101.0	100.0	P-10	101.0	90.0
T-8	98.0	100.0	P-11	99.0	97.0
A-6	99.0	96.0	P-12	100.0	89.0
A-8	99.0	88.0	P-13	99.0	100.0
A-10	100.0	91.0	P-14	94.0	69.0
M-1	100.0	91.0	P-15	91.0	91.0
R-1	97.0	93.0	P-16	100.0	100.0
P-6	100.0	97.0	P-17	99.0	98.0
Avg.				98.7	93.4

[1] Salinity ratios (U.S. Army Engineer Waterways Experiment Station, 1963).

The first step in the long-term salinity verification is also determination of the proper source salinity. Periods of high freshwater discharge may result in a considerable dilution of salinities immediately offshore of the estuary entrance. Thus, the model source salinity may have to be varied on a seasonal basis to achieve proper salinity verification in the estuary. These tests usually are conducted using a repetitious mean tide. The freshwater inflows are set to reproduce prototype conditions at the beginning of the survey, and the model is operated until salinity conditions for that prototype day are achieved. At that point, reproduction of the freshwater inflow hydrographs in the main stream and all tributaries is started and continued to the model time scale. The model hydrographs are usually stepped on a weekly (prototype) basis.

The results of the long-term salinity verification can be presented as the variation of salinity with time at given points, as salinity profiles along the channel at various times, or as plots of constant isochlors or isohalines at various times on a map of the estuary. An example of the

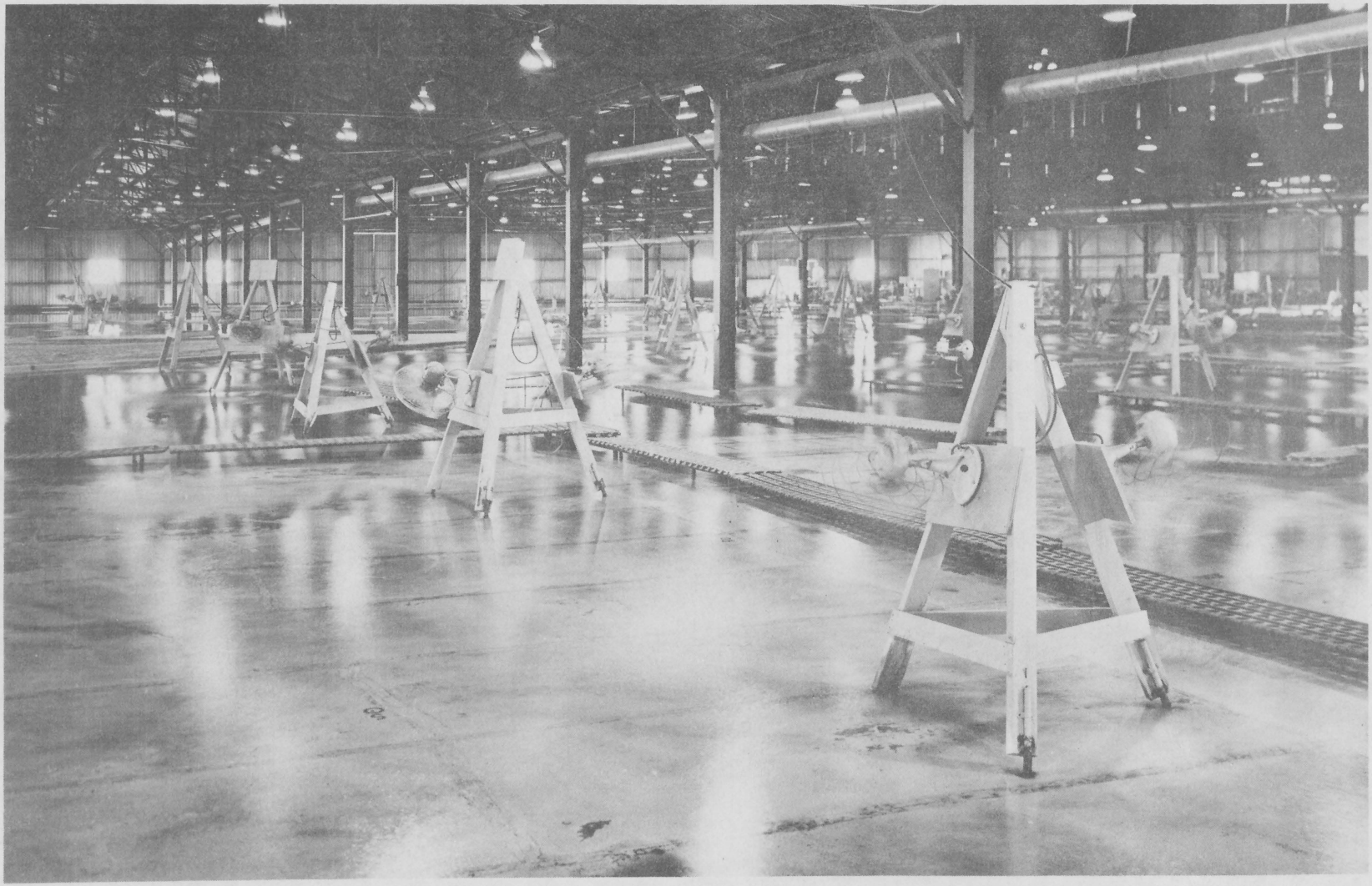

Figure 3-31. Oscillating fans for mixing.

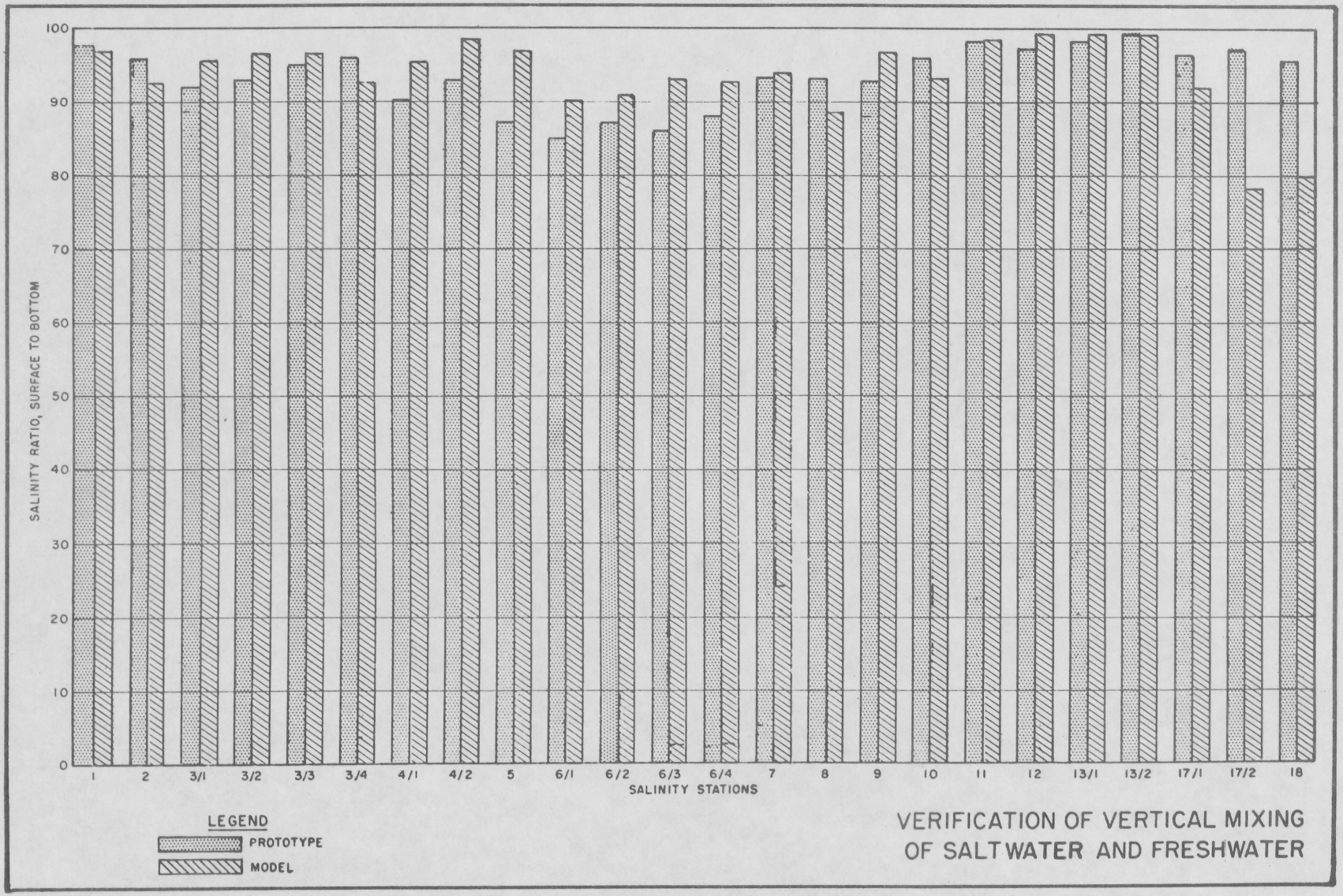

Figure 3-32. Verification of salinity ratios, Matagorda Bay model (Simmons and Rhodes, 1966).

reproduction of the salinity profiles in the Delaware River during a period when the salinity front was advancing upstream is shown in Figure 3-33; an example of longer term salinity verification covering the period when the salinity front advanced and retreated is shown in Figure 3-34.

d. Hurricane Surges. Because of the infeasibility of reproducing winds in an estuary model, prototype hurricane surge hydrographs must be adjusted to remove the effects of local winds. The model test results reflect only the gravitational component of the surge and must be adjusted to account for the local wind effects. The reproduction of normal tides in conjunction with reproduction of hurricane surges is often suspended because the contributions of normal tides to the total surge elevations are often relatively small and can be easily added to the model results by computer techniques. When separately adding the normal tide to the model surge results, the phase of tide with respect to the surge and the tidal range can be varied to determine the maximum and minimum effects of the tide on the height of the peak surge. Removal of the tide factor greatly simplifies the model operation procedure. If normal tides and hurricane surges are generated concurrently, the tide generator is adjusted to reproduce the desired tide; then the surge generator is adjusted to produce the observed water level history at the control gage. Because the model roughness has previously been adjusted for normal tides and currents, any adjustments to the roughness for accurate reproduction of the hurricane surge are usually unnecessary. However, some modification to the overbank roughness in areas subject to surge flooding may be necessary. An example of hurricane-surge verification for a case where the prototype data include normal tide and local wind effects is shown in Figure 3-35. Figure 3-36 illustrates a case where local wind effects have been removed from the prototype data.

e. Shoaling. (Since this report was prepared, a hybrid modeling technique has been developed for sedimentation studies. A physical model is used to determine the hydrodynamic conditions which are then used to drive a numerical sedimentation model.) The basic objective of the fixed-bed model shoaling verification is to identify a synthetic sediment that will move and deposit under the influence of the model forces in the same manner that the natural sediments move and deposit under the influence of the natural forces. Because no satisfactory similitude laws have been developed for estuarine sedimentation, the development of the modeling shoaling test procedure is more an art than a science at this time. The appropriate time and volume scales for the shoaling tests must be determined by trial and error.

Many variables are involved in identifying a suitable operating technique for use in the model, and each must be resolved by trial and error in the model. The most significant variables include: (a) Shape, size, gradation, and specific gravity of the synthetic sediment; (b) method, location, duration, and quantity of synthetic sediment injection; (c) rate of freshwater inflow; (d) magnitude of tide; (e) height, direction, and period of ocean waves; (f) length of model operation; and (g) readjustment of model roughness. The model water temperature must be closely monitored,

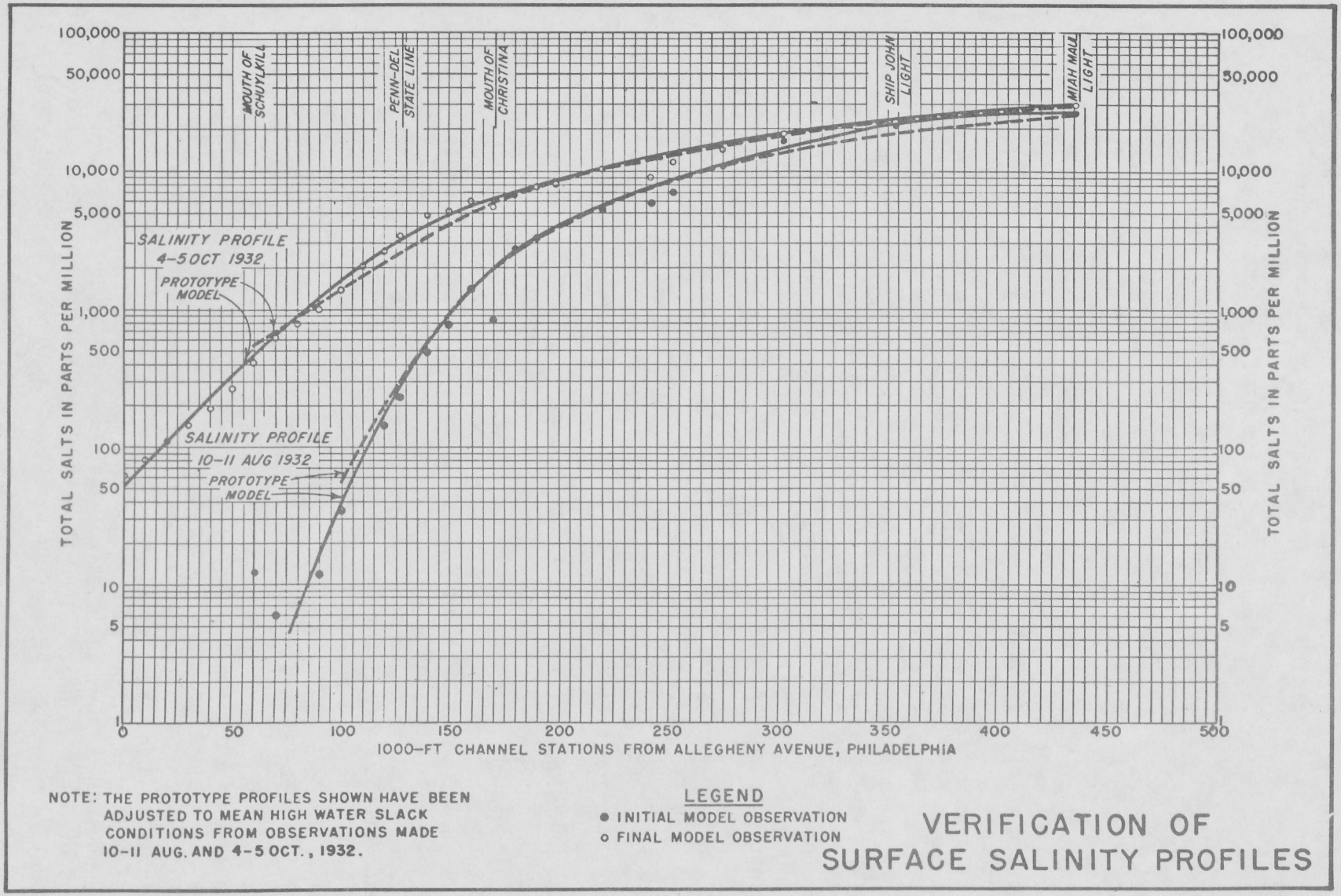

Figure 3-33. Verification of long-term salinity profiles, Delaware River model (U.S. Army Engineer Waterways Experiment Station, 1956).

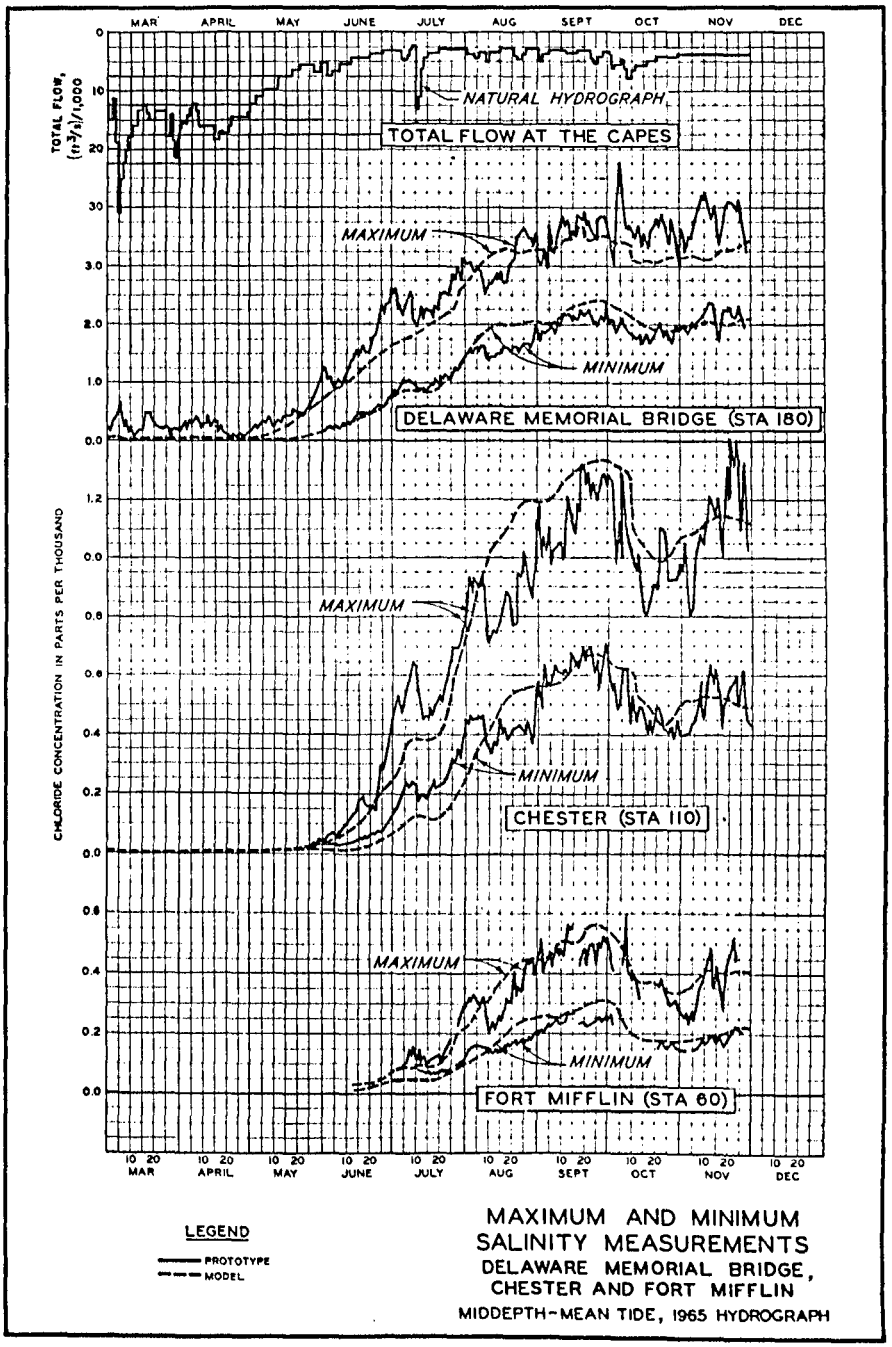

Figure 3-34. Verification of long-term salinity conditions, Delaware River model (after Simmons, Harrison, and Huval, 1971).

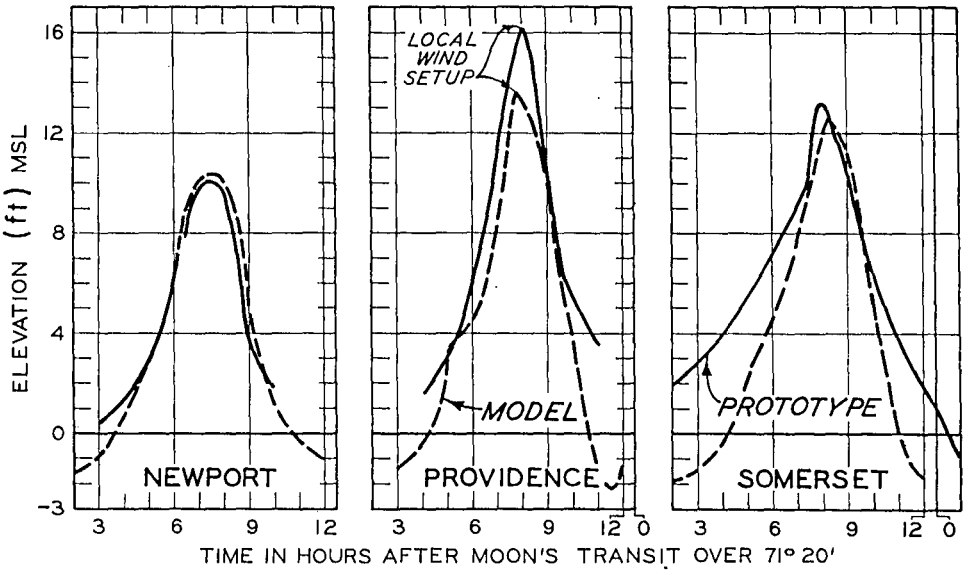

Figure 3-35. Verification of hurricane surge, Narragansett Bay model (after Simmons, 1964).

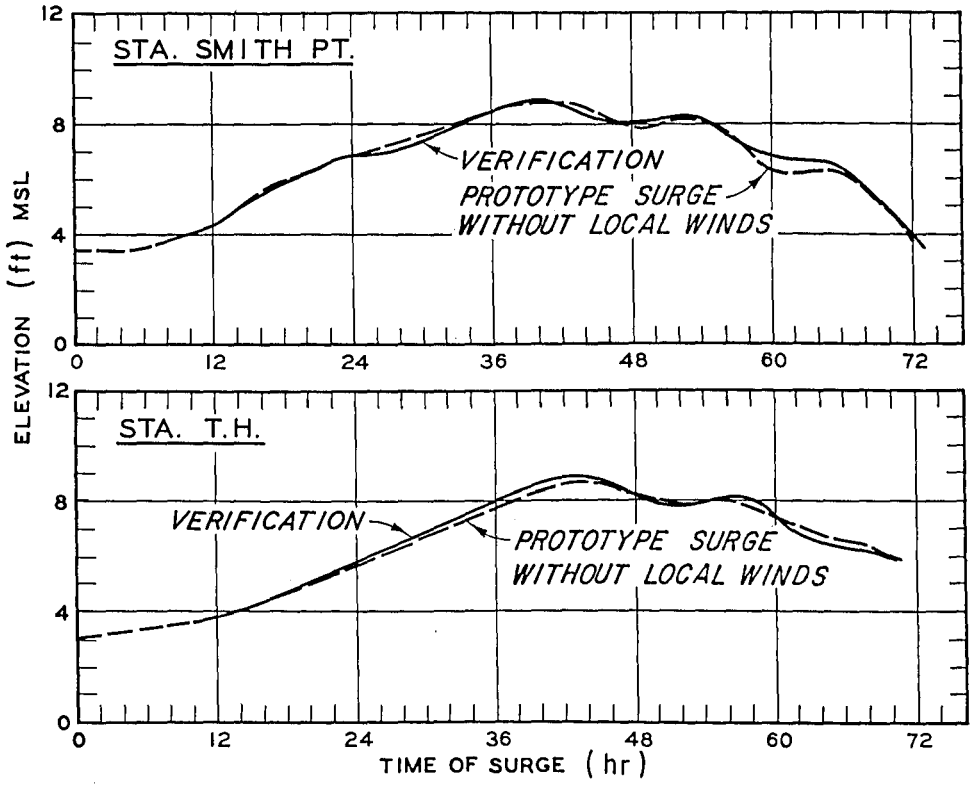

Figure 3-36. Verification of hurricane surge, Galveston Bay surge model (Brogdon, 1969).

since similar shoaling tests run with different water temperatures often give significantly different results. In general, finely ground gilsonite is used to simulate suspended sediments, and granulated plastic, nylon, or other similar material is used to simulate bedload sediments. Gilsonite is an asphaltic base material with a specific gravity of about 1.03; it is usually graded to pass a Tyler No. 24 screen (0.8 millimeter), and is retained on a Tyler No. 35 screen (0.4 millimeter). No attempt is made to model the characteristics (e.g., fall velocity) of a particular suspended sediment. Commonly used granulated materials (with specific gravities) include polystyrene (1.03 to 1.09), nylon (1.13 to 1.15), Tenite Butyrate (1.18 to 1.20), coal (1.4), and naturalite (1.7). These materials are available in various regular shapes such as cubes and cylinders or in irregular crushed shapes. The selected material is usually injected into the model in a slurry as either a point or line source, although it is occasionally spread over the entire problem area before starting the model. After completion of the injection of the shoal material, the model is normally operated for several tidal cycles to allow enough time for the material to be dispersed by the currents and deposited. Waves should only be generated when the shoaling problem area is in the estuary entrance area and thus subject to ocean wave action. Because of the distorted model scales, waves in the model that represent prototype conditions cannot be reproduced; rather, the model waves are adjusted to simulate the degree of agitation required so the model sediments can be moved and deposited by the tidal currents.

Because the shoaling test technique is developed by trial and error, the validity of the shoaling verification is highly dependent on the quality and quantity of the available prototype data. Surveys of the problem area should be available for a period of at least 2 and preferably 3 or more years, in order that average annual conditions can be determined. The problem area is subdivided into sections, and the average annual prototype shoaling rate is determined for each section. These rates are then converted to percentages of the shoaling rate for the entire problem area, and this is the percentage distribution that is reproduced in the model. When an acceptable reproduction of the distribution pattern has been achieved, the volume of material recovered from the problem area in the model can be equated to the prototype shoaling rate to establish an approximate shoaling volume scale. The duration of the model test can also be equated to the prototype period for which the shoaling rate was developed to determine the shoaling test time scale. Examples of shoaling verifications are presented in Figures 3-37 to 3-39.

Since all conditions cannot be exactly duplicated between model and prototype, an exact duplication of the shoaling distribution pattern cannot be expected; e.g., the effects of overdepth or advance maintenance dredging may be difficult to simulate in the model unless the dredging practice is consistent from year to year. Because the models are fixed bed, the effects of local scour or nearby deposition, and the changes in cross section resulting from scour or unusual dredging cannot be simulated. At the termination of a model shoaling test, all material in motion deposits immediately in place, resulting in some model shoaling

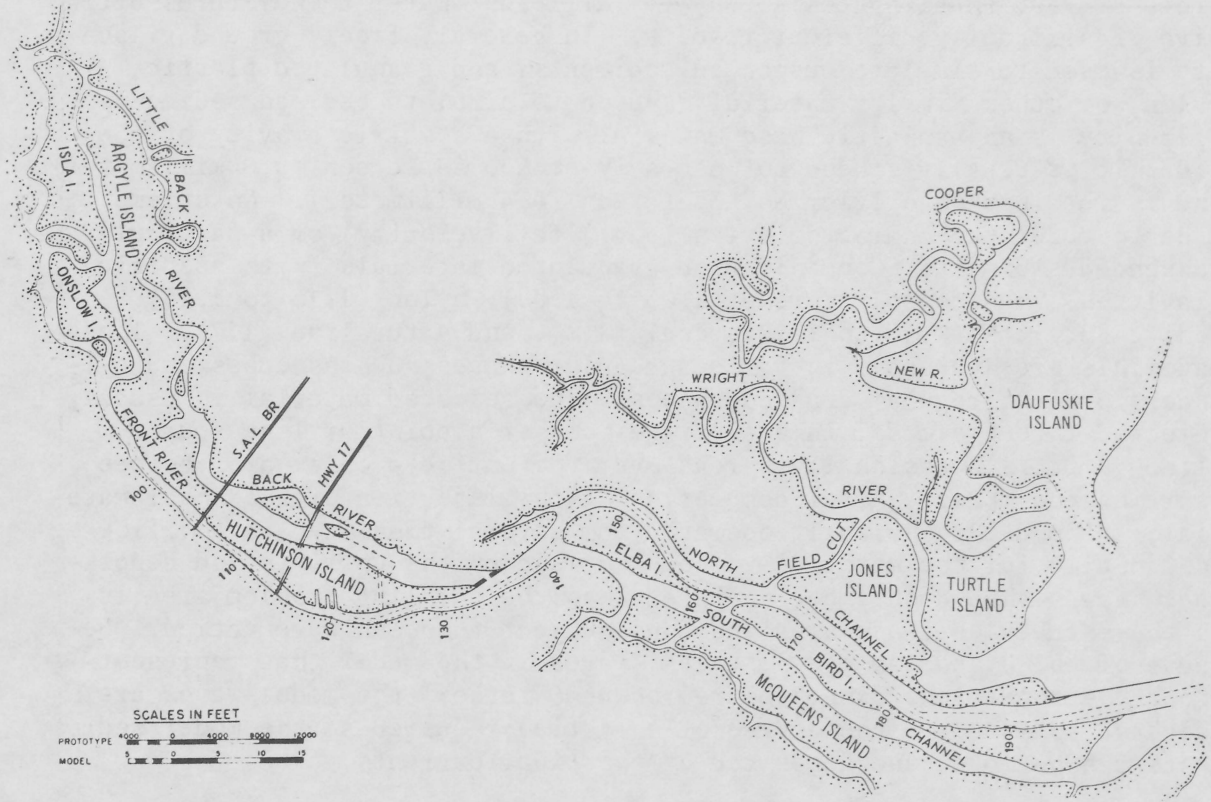

CHANNEL LAYOUT

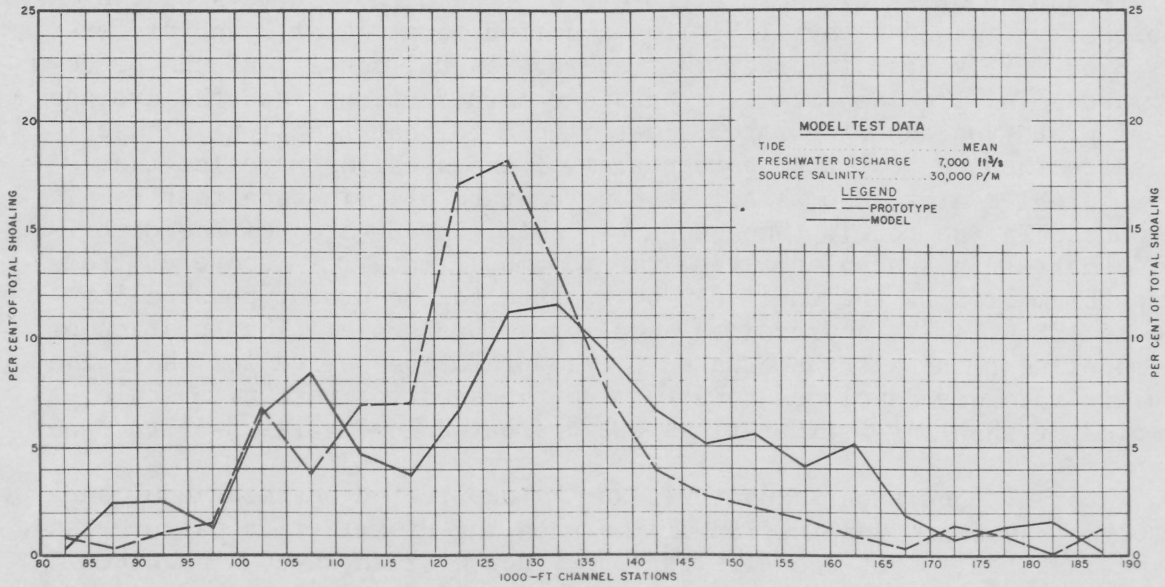

SHOALING DISTRIBUTION

Figure 3-37. Verification of shoaling distribution, Savannah Harbor model (after U.S. Army Engineer Waterways Experiment Station, 1961).

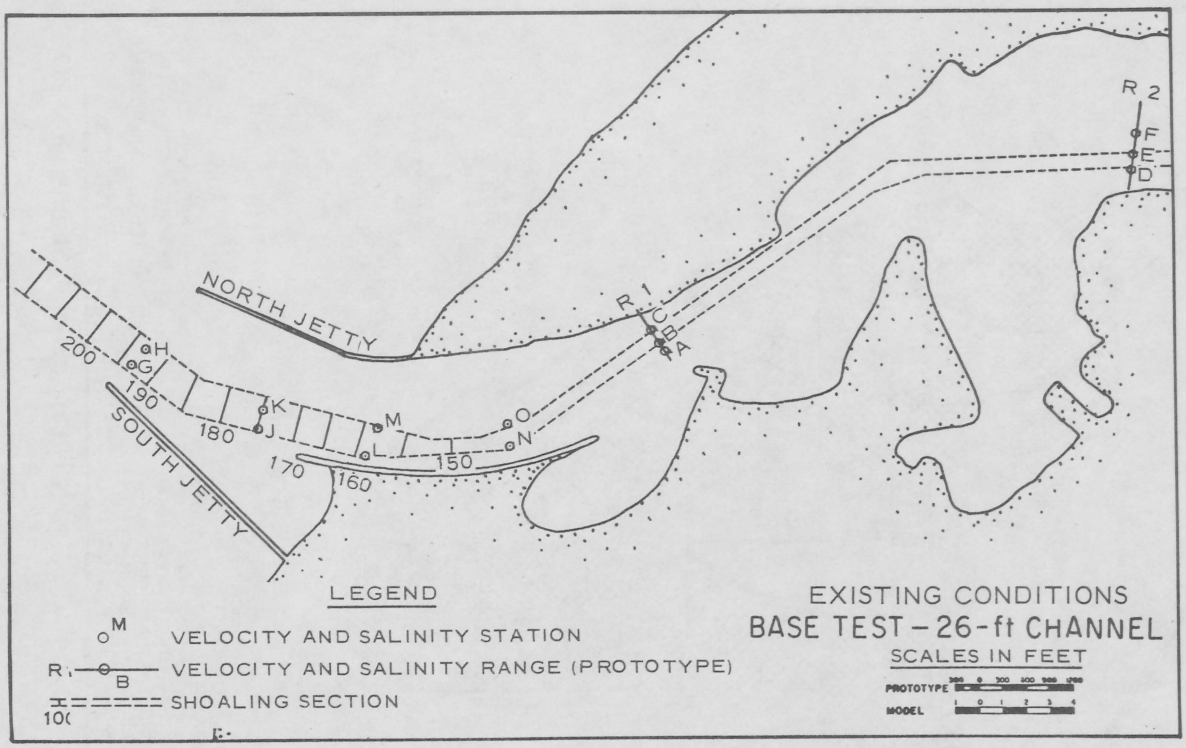

CHANNEL LAYOUT

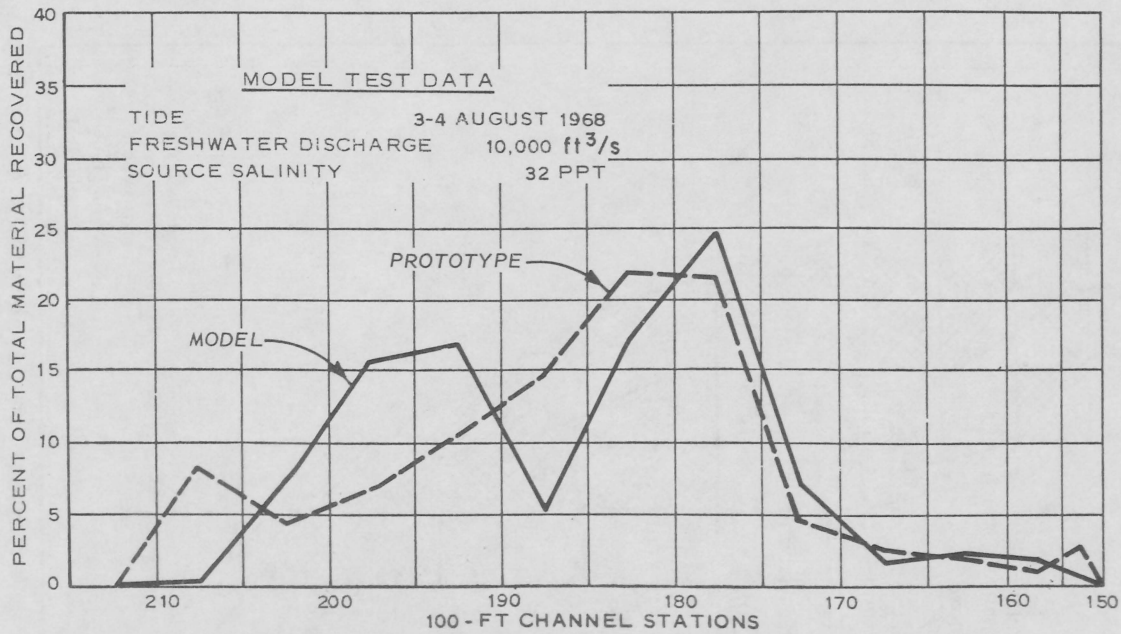

SHOALING DISTRIBUTION

Figure 3-38. Verification of shoaling distribution, Umpqua River Estuary model (after Fisackerly, 1970).

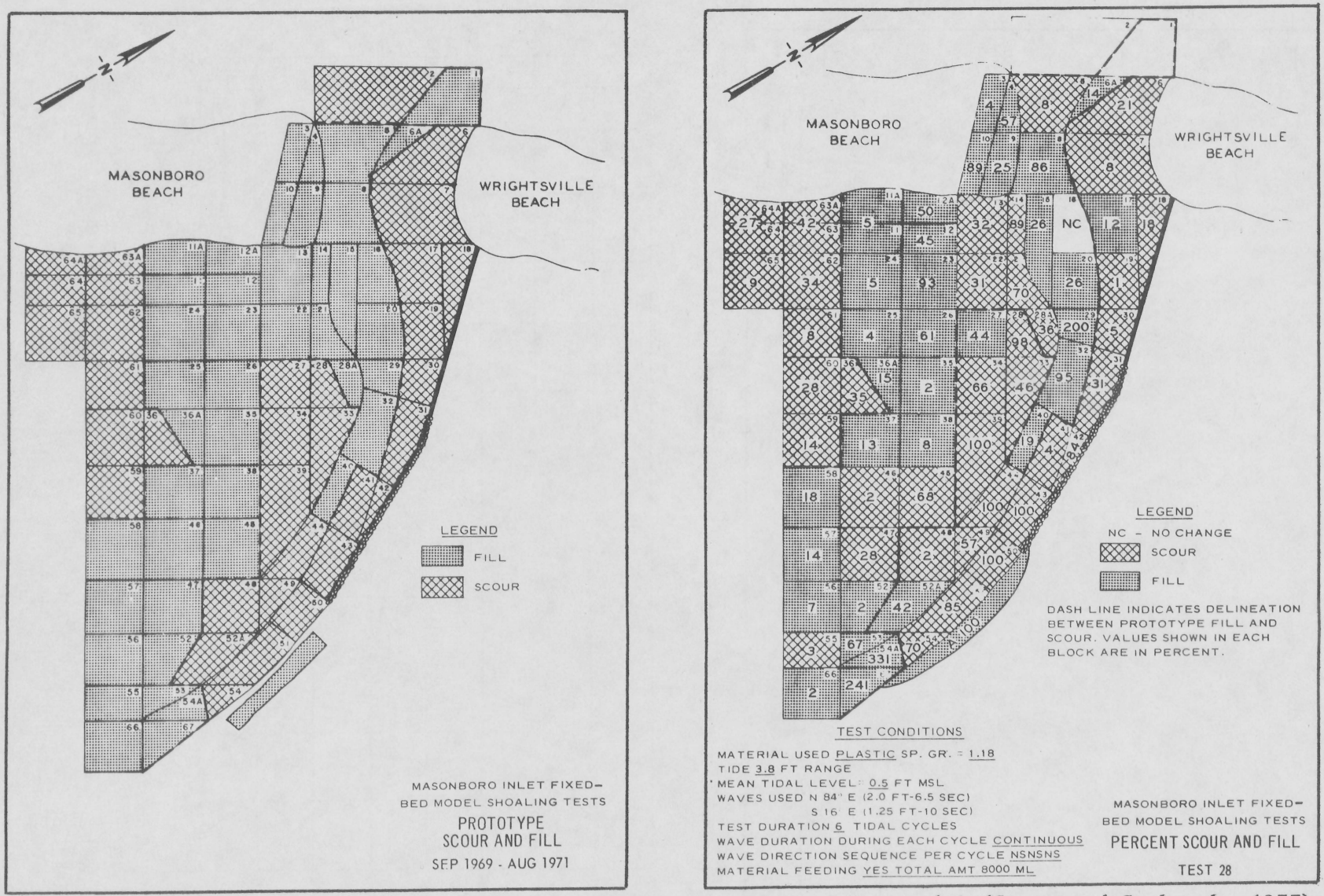

Figure 3-39. Verification of shoaling distribution, Masonboro Inlet model (Sager and Seabergh, 1977).

in reaches that experience none in the prototype. Dredge-disposal practices are normally not reproduced in the model. If there is a return of material to the channel from the disposal area, this source of material may not be reproduced in the model shoaling tests.

If prototype data are not available for a detailed shoaling verification, any model shoaling tests are of a highly qualitative, rather than quantitative, nature. The relative shoaling tendencies of the various plans tested can be compared but shoaling rates cannot be predicted. In this case, the only verification possible is the intuitive judgment of the model operator as to whether or not the model shoaling pattern looks reasonable. The development of more than one shoaling test technique may be necessary to simulate the effects of various possible primary sediment sources.

f. Dye Dispersion. Verification of dye dispersion is normally not accomplished because field dye-dispersion data are usually not available. However, the data were available in suitable form at the proper time for use in the San Diego Bay model. Because the prototype injection rate was very low, direct scaling of the dye release in the model was not possible. However, it was necessary to properly scale the density of the prototype dye release (1:1) and to make the release at the correct location and at the scaled times. A satisfactory verification was achieved (see Fig. 3-40).

g. Heat Dispersion. Verification of heat dispersion has never been accomplished at WES for a particular project investigation. This is usually because no heated discharge exists at the time the model study is conducted. To determine the validity of far-field thermal dispersion tests in a distorted-scale model, a heat-dispersion verification was conducted for three existing powerplants in the Delaware Estuary (Trawle, 1976). Figure 3-41 shows comparisons of model and prototype thermal plumes at the Eddystone powerplant, which is located in the intermediate salinity zone of the estuary. The results demonstrated that this model (scales 1:100 vertically and 1:1,000 horizontally) can be used effectively for trend predictions of far-field thermal plume characteristics.

5. Utilization of Scale Models.

a. Problems Susceptible to Model Analysis. Hydraulic models are highly valuable tools in investigations of physical (as opposed to biological) phenomena in estuaries. A wide range of phenomena can be reproduced or simulated in hydraulic models, and a wide range of problems or projects are susceptible to model investigations. However, there are definite limitations to the capabilities of hydraulic models. The capabilities and limitations of fixed-bed models are discussed below.

The various phenomena which can be reproduced or simulated in hydraulic models include tides, tidal currents, density currents, littoral currents, currents generated by riverflows, salinity, mass dispersion, heat dispersion, shoaling, hurricane surges, tsunami surges, and the

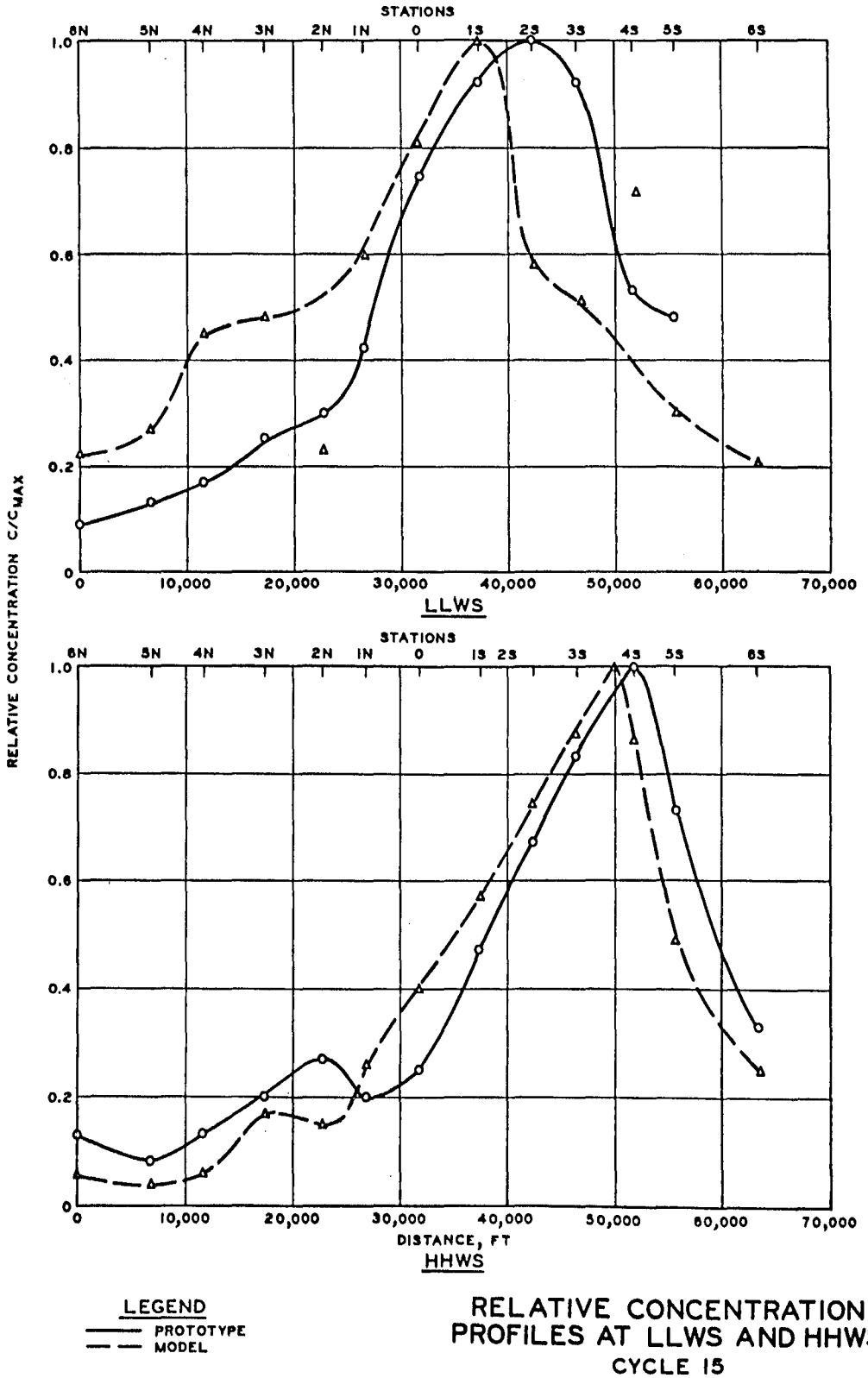

Figure 3-40. Verification of dye dispersion, San Diego Bay model (Fisackerly, 1974).

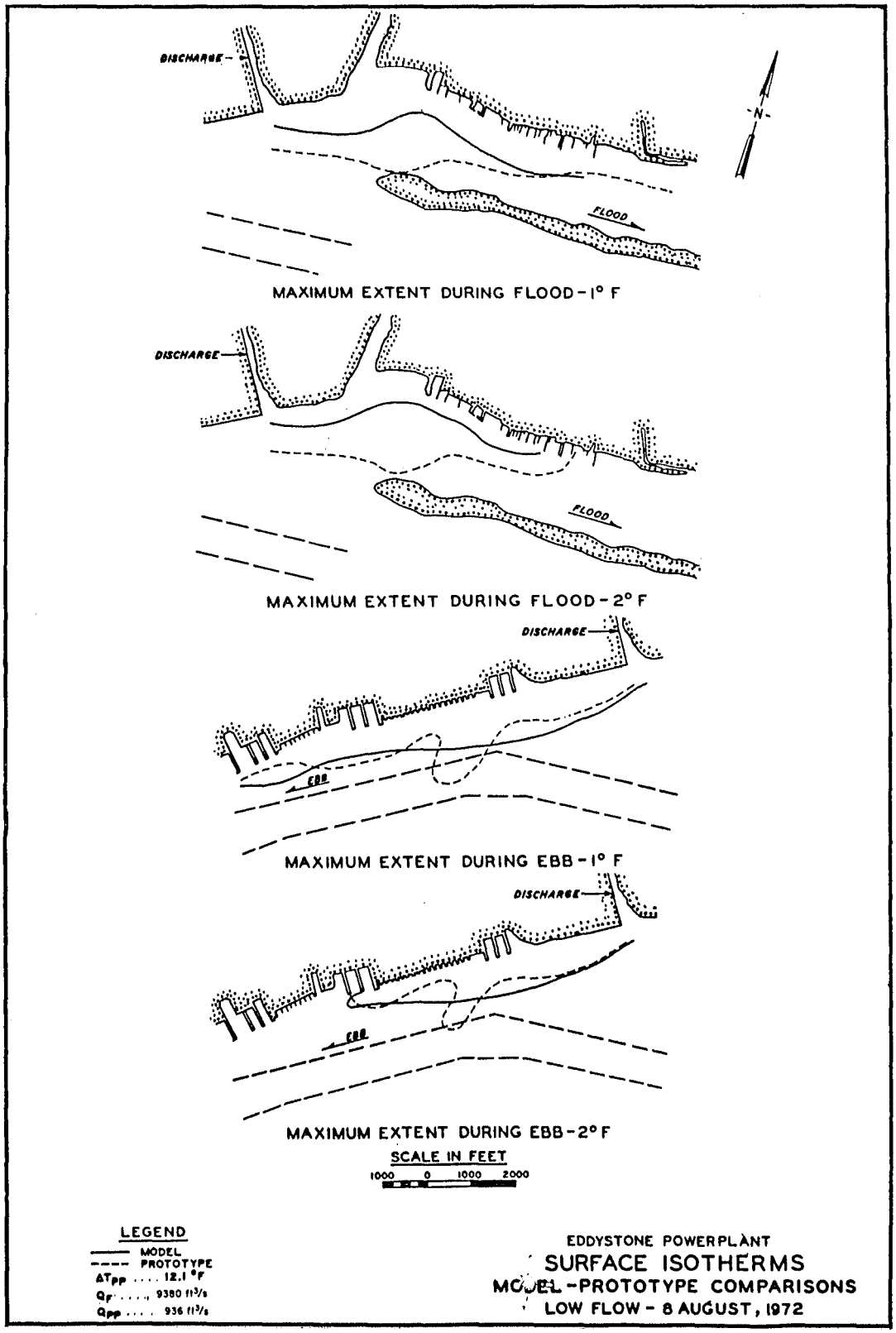

Figure 3-41. Verification of heat dispersion, Delaware River model (after Trawle, 1976).

general effects of wave and ship action on the resuspension of sediments. Although wind-induced currents and water level setup can be reproduced, it is generally not economically feasible to construct a large estuary model in a wind tunnel with the capability of generating winds from various directions. Coriolis forces can be simulated, but comprehensive estuary models cannot be rotated unless they are constructed to very small scales.

The rise and fall of a tide or surge and its progression upstream can be accurately modeled. Not only can the magnitude, phasing, and direction of currents be reproduced at a particular point, but the longitudinal, lateral, vertical and temporal velocity distributions are reproduced. The same is true for salinity. Thus, the physical model provides a time-varying, three-dimensional representation of the hydraulic and salinity regimens of the estuary. Presently, only physical models are capable of providing such three-dimensional representations.

Although it is possible to model the dispersion of pollutants in three dimensions and with time, the model tracer is usually a conservative dye (i.e., no decay with time). The physical model results must, therefore, be treated analytically before they can be applied to field conditions. For dispersion of thermal and other pollutant discharges, far-field dispersion can be modeled, but the near-field dispersion cannot be accurately reproduced in a distorted-scale model, if vertical exchange in the discharge jet is important.

A qualitative reproduction of shoaling patterns and distributions can be achieved by the empirical development of a model operating technique. However, the technique does not reproduce the changes in cohesion of deposited materials, the effect of internal shearing of the flows on aggregation or dispersion of suspended sediments, suspended-sediment concentrations, flocculation, or resuspension of sediments by wave action inside the estuary.

The various problems or projects often investigated in fixed-bed physical models include:

(a) navigation channels (existing, new, enlarged, or realined);

(b) navigating conditions (current velocities and patterns);

(c) sediment traps and turning basins;

(d) manmade inlets or canals;

(e) training works (jetties, groins, dikes, channel constrictions, etc);

(f) port facility siting;

(g) landfills (commercial or industrial sites, highways, airport runways, diked disposal areas, etc.);

(h) open-water disposal areas (submerged or above water);

(i) hurricane or tsunami surge protection;

(j) bridge and tunnel crossings;

(k) shore erosion control (qualitative);

(l) discharges of wastes (municipal, industrial, and thermal);

(m) freshwater supply (municipal, industrial, and agricultural);

(n) salinity control structures; and

(o) upstream control or diversion of freshwater inflow.

In addition to investigations of proposed projects, the models are often used to define existing prototype conditions for various situations where no field data are available, to provide data with which other models (physical or mathematical) are adjusted and verified, and to provide boundary conditions required in the operation of other models.

Studies of navigation channels are usually conducted to determine ways to minimize maintenance dredging requirements or to determine maintenance requirements for a new or modified project. The effects of the new or modified project on such environmental factors as tides, currents, salinities, and dispersion must be determined; also it must be determined that velocities and current patterns are not hazardous to navigation. Studies of other navigation-related projects (manmade inlets and canals, training works, sediment traps and turning basins, and port facility siting) are usually concerned with essentially the same types of problems. Qualitative studies of the potential for bank erosion are made during investigations of new inlets, canals, or training works by defining the current velocities and patterns adjacent to the shoreline.

Landfill studies usually include determination of the effects on dispersion patterns, tides, currents, and salinities. If the fill is located near an existing navigation channel, its effect on channel shoaling is also determined. Studies of submerged open-water disposal areas usually concentrate on the dispersal of sediments from the disposal area (i.e., where the sediments redeposit). For submerged disposal-bank or disposal-island projects, studies will also determine their effects on current and circulation patterns, dispersion patterns, tides, and salinities. Studies of hurricane and tsunami barriers are concerned not only with ensuring that the desired degree of flood protection is provided, but also with developing the number and location of tidal passages required in the barriers to preserve existing tidal, hydraulic, salinity, and dispersion regimens under normal (nonsurge) conditions.

Bridge- and tunnel-crossing studies will define current velocity conditions which are encountered during construction and will determine shoaling and other environmental factors. Qualitative shore erosion studies are made to determine areas which may be subjected to scouring velocities and to develop protection works (dikes, groins, etc.).

Waste-discharge studies will define zones of influence for existing or proposed outfall locations and will determine optimum outfall locations. These studies are usually limited to tests of conservative dye or thermal dispersion.

Studies of freshwater supplies will determine whether or not the supply is safe from saltwater contamination during low freshwater-flow periods and will determine the effects of the freshwater withdrawal on salinity conditions downstream. If regulation of the salinity of one body of water is desired by introducing or regulating flow from another water body, model studies will determine the size and location of the control structure and the rate of the regulated flow required to achieve the desired salinity. Upstream projects often alter the freshwater inflow to an estuary by regulating the flow (seasonally for flood control projects or daily for hydroelectric projects) or by diverting freshwater flow from or into the estuary. In any case, the effects of such projects may have a significant impact on salinity and dispersion conditions in the estuary. If large changes in salinity conditions are indicated, the investigation should be expanded to determine the effects on shoaling distribution.

After model verification has been completed, the model can be used to obtain more extensive and detailed data on existing conditions than are available from the prototype. These data can provide a baseline for use in evaluating the effects of proposed projects, and can also lead to an improved understanding of prototype phenomena. For example, the model can be used to determine the effects of tidal range, changes in mean sea level, differences in sustained freshwater inflow, hurricane surges, etc., on the extent of saltwater intrusion, salinity distribution, and general dispersion characteristics throughout the estuary.

b. Advantages and Disadvantages of Scale Models. Modeling techniques are an exceedingly important planning tool for a number of reasons. It is easier and faster to initiate changes and test the effects in a model than in the prototype. The testing of many alternatives in a model represents only a modest financial investment; prototype testing of the same alternatives would probably be a prohibitively expensive major undertaking. Prototype testing of tidal-related problems is time consuming, and the results are often of less than desirable quality or quantity. To test a sufficient number of prototype alternatives to assure that the final solution is the most desirable would usually be impossible (Simmons, Harrison, and Huval, 1971). In addition, model testing of various alternatives may prevent irreversible damage to the estuary which might be caused by an unsatisfactory design.

The hydraulic model has been developed and used to solve many estuarine problems involving physical processes. Only the hydraulic model is presently capable of simulating fluid flows with variable densities in three dimensions. Many problems which cannot now be expressed mathematically can be solved by the hydraulic model. Those problems which can be expressed mathematically often require basic data to evaluate coefficients in the equations which, in particular instances, may be obtained at a far less cost and time in laboratory flumes or hydraulic models than in nature. The hydraulic model study method has certain other advantages. It is a highly useful method of visually demonstrating alternative plans of improvement to the public and to representatives of local, State and Federal agencies. The model has great value in decision-making on estuary improvements, providing the necessary understandable information by observation. The model can also be a research tool, and undefined problems or principles in the prototype can be discovered and solved by operation of a hydraulic model (U.S. Department of the Army, 1969).

The hydraulic model has shortcomings, not the least of which is the apparently great first cost for construction and verification. Changes in conditions and alternative plans are more time consuming to study in a physical model than in a mathematical model. The technique provides little information on suspended-sediment concentrations in the estuary or on patterns of resuspension of fine-grained sediments throughout the estuary (U.S. Department of the Army, 1969). Phenomena which cannot be reproduced in fixed-bed hydraulic models include shoreline erosion, bottom scour, decay of pollutants, chemical interactions, turbidity, flocculation, photosynthesis, respiration, evaporation, solar radiation, refraction and diffraction (simultaneously) of short-period waves, and biological processes.

c. Complementarity of Scale and Mathematical Models. Extensive use of both physical and mathematical models has shown that the two problem-solving methodologies complement each other to a great extent. Although the use of an existing well-verified mathematical model would probably result in savings of time and money, physical scale modeling of tidal phenomena is usually reliable in providing accurate values of decision parameters for a wider range of problems than its mathematical modeling counterpart. In some cases, the two modeling techniques have been applied to the same prototype, an advantage of using different modeling capabilities to perform given parts of the study in the most economical manner (Simmons, Harrison, and Huval, 1971).

Mathematical models are often used to provide input data for physical scale models more economically than this input could be generated from other sources (and vice versa). Mathematical models are also used to set the closed boundaries of physical models by establishing limits beyond which phenomena do not affect the problem areas or by providing computed open-boundary conditions. Either approach would allow physical modelers to reduce a model area at a commensurate savings in construction and testing. Relatively simple mathematical models have been used for

exploratory feasibility studies to point out specific problem areas within a large study area. This knowledge allows a physical modeler to study in detail and at larger scale only those specific areas and might again preclude much model construction and testing effort. Rather simplified mathematical models have also been used to calculate and control tidal and salinity inputs to physical scale models (Simmons, Harrison, and Huval, 1971).

Physical scale models have been used to provide input to mathematical models. In a general way, observations of a physical model running under test conditions often lead to ideas and correct conclusions which would not have been realized under another set of circumstances. Most empirically based computation formulas (such as Manning's equation) have been derived as a result of laboratory testing. Scale models also provide boundary and initial conditions as well as discharge coefficients for a mathematical model. In addition, physical scale modeling is used to obtain dispersion coefficients which are then used in mathematical models to simulate tidal transport phenomena. Mathematical models are often easily verified by using hydraulic scale models (Simmons, Harrison, and Huval, 1971).

Table 3-3 summarizes (in a simplified listing) some of the chief advantages and disadvantages of the two types of models. However, in deciding which modeling technique (if any) is appropriate for solution of specific problems, experienced investigators should be consulted.

Table 3-3. Physical models versus mathematical models.[1]

Advantages	Disadvantages
Physical models	
Best description of three-dimensional flow	High cost
Extensive operational experience	Difficulty of modification
Ease of visualization	Distortion effects
Best simulation of salinity effects	Limited long-range development
Ability to reproduce several phenomena in a single model	Measurement difficulty
Mathematical models	
High repeatability and precision of measurements	Cannot reproduce three-dimensional density gradients
Data and model storage and retrievability	Storage grid-size limitations
Computational speed	High computer cost
Compatibility with other models	Computational stability problems
Ability to expand and improve models	Boundary condition definition
Verification and modification simplicity	Integration limits—time and scale
Low cost after development	High initial development cost
	Mathematical equation formulation problem

[1] Simmons, Harrison, and Huval, 1971.

Physical models have a long history and have been refined to a sound predictive technique. On the other hand, comprehensive mathematical models have only been introduced recently, but the modeling techniques are expected to continue to be rapidly developed and used for tidal modeling. Physical model techniques should also be continually improved, refined, and reduced in cost to provide some of the answers to tidal problems that cannot now be obtained in any other way (Simmons, Harrison, and Huval, 1971).

d. Predictive Capabilities. Physical hydraulic models have long been successfully used to predict the response of estuaries to alterations such as dredging, landfills, constricting works, and flow alterations. Model predictions of tidal elevations and phases, current velocities, circulation patterns, and salinity intrusion are considered highly reliable; however, little attention has been given to a careful comparison of model predictions and prototype conditions after the proposed modifications to the system have been made. Other phenomena, such as pollutant and sediment transport, which are considered to be reproduced only qualitatively in physical models, have similarly suffered from a lack of study to determine the relative merits of modeling them.

There are several reasons for the lack of comparison between model prediction and prototype behavior, which is termed postconstruction verification or model confirmation. First, resources are seldom available to follow up on a project if it is functioning satisfactorily. Other problems usually demand attention and money that might be applied to followup studies. Second, many projects are changed before construction due to considerations that are not pertinent to the model study; thus, detailed comparisons are not possible unless costly additional model tests are conducted. Finally, if model results show a project to be infeasible, it is not constructed; consequently, comparison is not possible. The limited number of confirmation investigations on Corps of Engineers model study predictions includes hydraulic characteristics of the St. Johns River (Fortson, 1970), and shoaling characteristics of the Alameda Naval Air Station (U.S. Army Engineer Waterways Experiment Station, 1950), and in the Delaware River (U.S. Army Engineer Waterways Experiment Station, 1947).

The increasing environmental awareness in recent years has resulted in a demand for more detailed model predictions of many estuarine phenomena. Recognizing the need for postconstruction verification of model studies to provide more reliable results, the Office, Chief of Engineers (OCE), authorized WES in 1971 to begin a series of confirmation studies. The primary objective of these studies was to define the degree of accuracy to which the results of tests conducted in physical hydraulic models predict the changes induced by modifications to estuarine systems. A secondary objective was to improve modeling techniques such that the value of physical model studies may be increased.

The first study in this series evaluated the predictions made in the Delaware River model for the effects of a navigation channel enlargement project between Philadelphia and Trenton (Letter and McAnally, 1975).

The channel-deepening project between Philadelphia and Trenton caused significant, but not large, changes in the hydrodynamic and salinity regimen of the estuary. The magnitude of the changes induced was much larger than the fluctuations due to the imperfect repeatability of the model, but not great enough to strain the initial calibration of the model. Therefore, the deepening project constituted a valid test of the capability of the model to predict the changes in the estuarine system caused by projects of that scale.

The original verification was considered very good, and this study concluded that the accuracy of the model predictions was as good as the original verification. Tidal phenomena, current velocities, and the salinity regimen of the estuary have been predicted by the model with accuracy for the postconstruction conditions.

The results of this study show not only the validity of the Delaware River model predictions but also the necessity of interpreting the results in general terms rather than for specific point values. The model is very accurate for predicting changes and general trends for the estuary, but a particular value at a particular time and place should not be considered completely quantitative in all cases. Physical hydraulic models used with proper caution to avoid too literal an interpretation of the results, are of significant value as a decisionmaking tool.

Several additional confirmation studies presently underway or planned will consider a variety of projects, estuarine phenomena, types of estuaries, and model scales.

6. Examples of Model Studies Conducted.

a. Navigation Channel Shoaling--Columbia River Estuary.

(1) Project. South jetty rehabilitation, improvement of entrance channel by construction of a new jetty, and enlargement of existing navigation channel.

(2) References. Herrmann and Simmons (1966); Herrmann (1968, 1971, 1974).

(3) Laboratory. WES.

(4) Test Period. South jetty (August 1963 to January 1964); Wauna-Lower Westport Bar (August 1964 to October 1965); jetty B (January to May 1967).

(5) Problems. The authorized length of the south jetty (Fig. 3-42) is about 6.6 miles with a top elevation of +24 feet mean lower low water (MLLW). In 1941, a terminal block was constructed 3,900 feet shoreward of the outer end of the structure; by 1960, the jetty needed extensive rehabilitation shoreward of the terminal block. The entrance channel dimensions are 48 feet deep and 0.5 mile wide over a distance of about

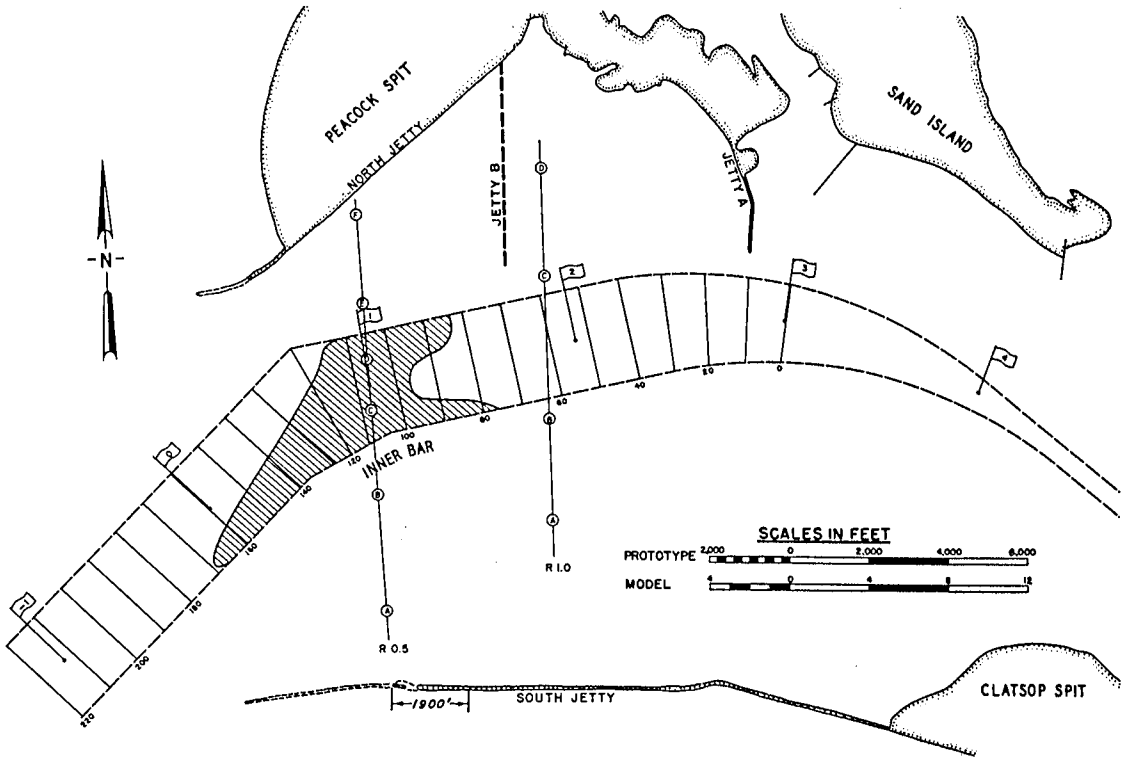

Figure 3-42. Columbia River entrance (after Herrmann and Simmons, 1966; Herrmann, 1974).

5 miles, and the average annual maintenance dredging amounts to about 2.3 to 2.5 million cubic yards. A 5,300-foot-long jetty B (Fig. 3-42) was authorized for the Columbia River entrance to reduce maintenance dredging in the entrance channel. The Wauna-Lower Westport Bar (Fig. 3-5) is located between river miles 41 and 45 on the Columbia River and is considerably upstream from the extent of saltwater intrusion. For the 35- by 500-foot channel, the average annual maintenance dredging was about 315,000 cubic yards. Model tests were made to determine the changes in hydraulic and shoaling characteristics that would be effected by enlarging the channel to 40 by 600 feet and to develop an optimum improvement plan to minimize the cost of maintenance dredging in the enlarged channel.

(6) Purpose of Model Study. The model study was conducted to determine: (a) the need for and to develop optimum plans for rehabilitation of existing entrance jetties, (b) the most effective means of reducing the cost of maintenance dredging in the navigation channels, and (c) the effects of the proposed interior channel enlargement from 35 by 500 feet to 40 by 600 feet.

(7) The Model. The Columbia River Estuary model reproduced the lower 52 miles of the estuary (see Fig. 3-5) and was constructed to linear scales of 1:500 horizontally and 1:100 vertically. The model (a combination fixed- and movable-bed type) was about 560 feet long, 130 feet wide at its widest point, and covered an area of about 48,000 square feet.

The model was initially constructed as a fixed-bed model throughout; however, provisions were made to convert the entrance area to a movable-bed model at a later date to investigate the effects of various plans on bed configuration in the entrance. The primary tide generator was located in the model ocean, and a secondary tide generator reproduced the proper ebb and flood discharges at the upstream end of the model, since the tidal influence extended about 50 miles beyond the upstream model limit.

(8) Test Procedures. The model was operated with saltwater and freshwater for all fixed-bed tests. Since the sediments in the lower Columbia River Estuary consist primarily of fine sand with a grain size of 0.15 to 0.3 millimeter, a granulated material was used as the fixed-bed model shoaling material. Shoaling test techniques were developed by trial and error at each of the seven problem areas investigated rather than developing a single comprehensive testing procedure for the entire model. In each case it was determined that polystyrene (S.G. = 1.08) was the most appropriate material.

(9) Summary of Test Results. The test results indicated that rehabilitation of the existing outer end of the south jetty would not significantly benefit the hydraulic, salinity, or shoaling characteristics of the entrance area as a whole, although some additional protection to vessel traffic from ocean wave action would probably be effected by the rehabilitation. However, the tests also indicated that, if the seaward 1,900 feet of the above-water part of the jetty (Fig. 3-42) were allowed to degrade to an elevation of about -15 feet MLLW, shoaling of the entrance channel could be reduced by about 21 percent (Fig. 3-43). This

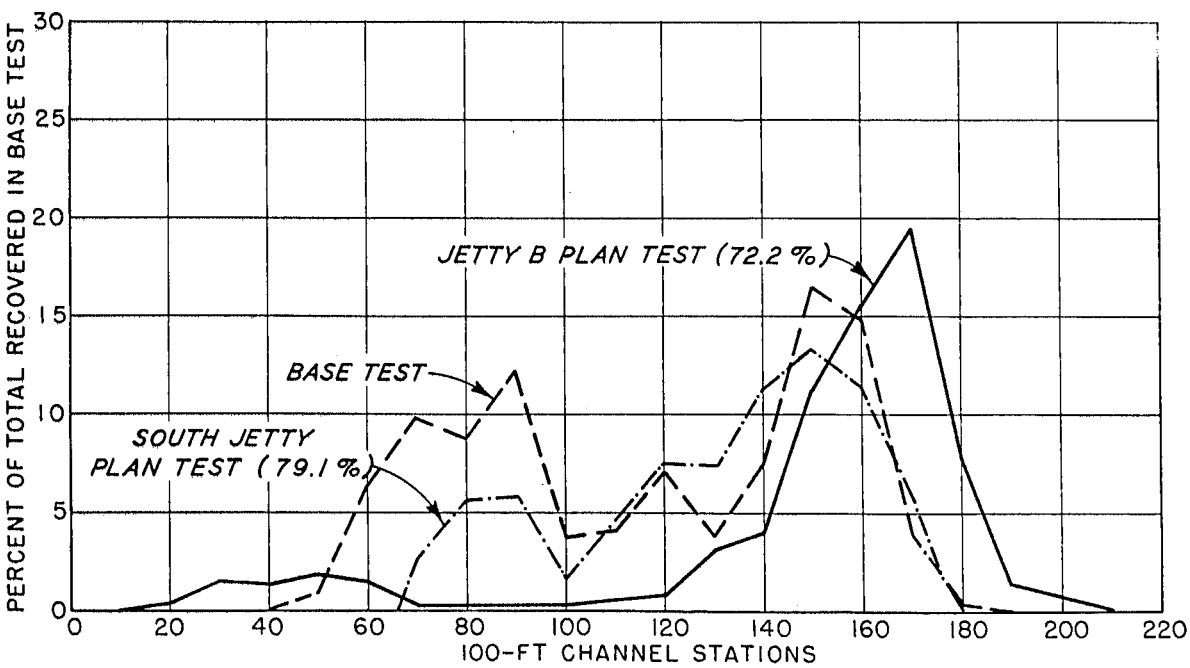

Figure 3-43. Effects of south jetty plan 2 and jetty B on Columbia River entrance shoaling (after Herrmann, 1974; Herrmann and Simmons, 1966).

plan was adopted, thus saving $4,570,000 in planned jetty rehabilitation. In addition, a substantial maintenance dredging cost savings will result when the jetty has naturally deteriorated to -15 feet MLLW.

Tests of jetty B indicated that channel shoaling would be reduced by about 28 percent and that the upstream peak in the shoaling distribution pattern would be eliminated (Fig. 3-43). In addition, the structure would cause a very significant change in vertical mixing in the entrance. As a result, middepth and bottom salinities would be generally reduced, while surface salinities would be generally increased (Fig. 3-44). The maintenance dredging savings from this plan would not be sufficient to justify the initial cost of the structure, estimated to be $12 million in 1958.

The results of the Wauna-Lower Westport Bar (Fig. 3-45) tests indicated that enlarging the channel without supplemental improvements would increase the rate of shoaling by about 76 percent and would create a new peak in the shoaling distribution pattern (Fig. 3-46). The best improvement plan tested consisted of four pile dikes with lengths of 400 to 1,100 feet and three large disposal area fills as shown in Figure 3-45. Model tests indicated that this plan would reduce shoaling in the enlarged channel by about 30 percent and eliminate shoaling in the upstream 2,500 feet of the bar (Fig. 3-47). The dikes and fills were constructed in the prototype about 1 year before enlarging the channel. The plan was so effective that new work dredging requirements for the enlarged channel were reduced by 42 percent by the natural scouring action of the newly constructed dikes. Thus, the plan resulted in an initial savings of about $334,000. Future savings will result from the reduced shoaling as compared to an unimproved, but enlarged, channel.

In 1969, it was estimated that the annual maintenance dredging savings from the south jetty and Wauna-Lower Westport Bar studies would amount to $125,000 (U.S. Department of the Army, 1969). In addition, programed construction expenditures of $4,570,000 (south jetty rehabilitation) were saved and an authorized project estimated to cost $12 million (construction of jetty B) was dropped. The total cost of the model study, which included investigations of several other problems, was about $1.2 million.

b. Environmental Impact of Navigation Channel Enlargement--James River.

(1) Project. Deepening existing navigation channel from -25 to -35 feet mean sea level (MSL).

(2) Reference. U.S. Army Engineer Waterways Experiment Station (1966).

(3) Laboratory. WES.

(4) Test Period. September 1964 to September 1966.

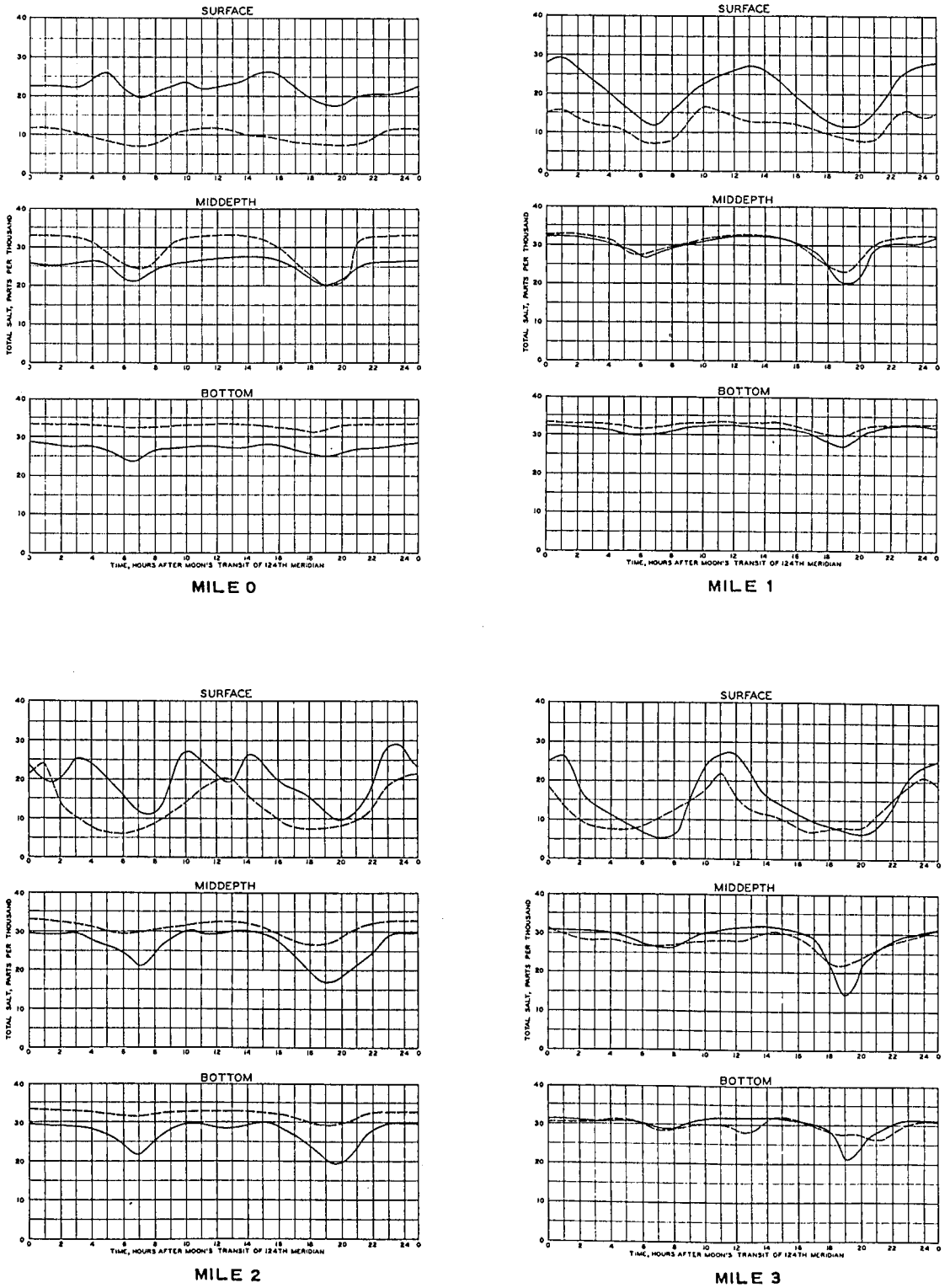

Figure 3-44. Effects of jetty B on Columbia River entrance salinities (after Herrmann, 1974).

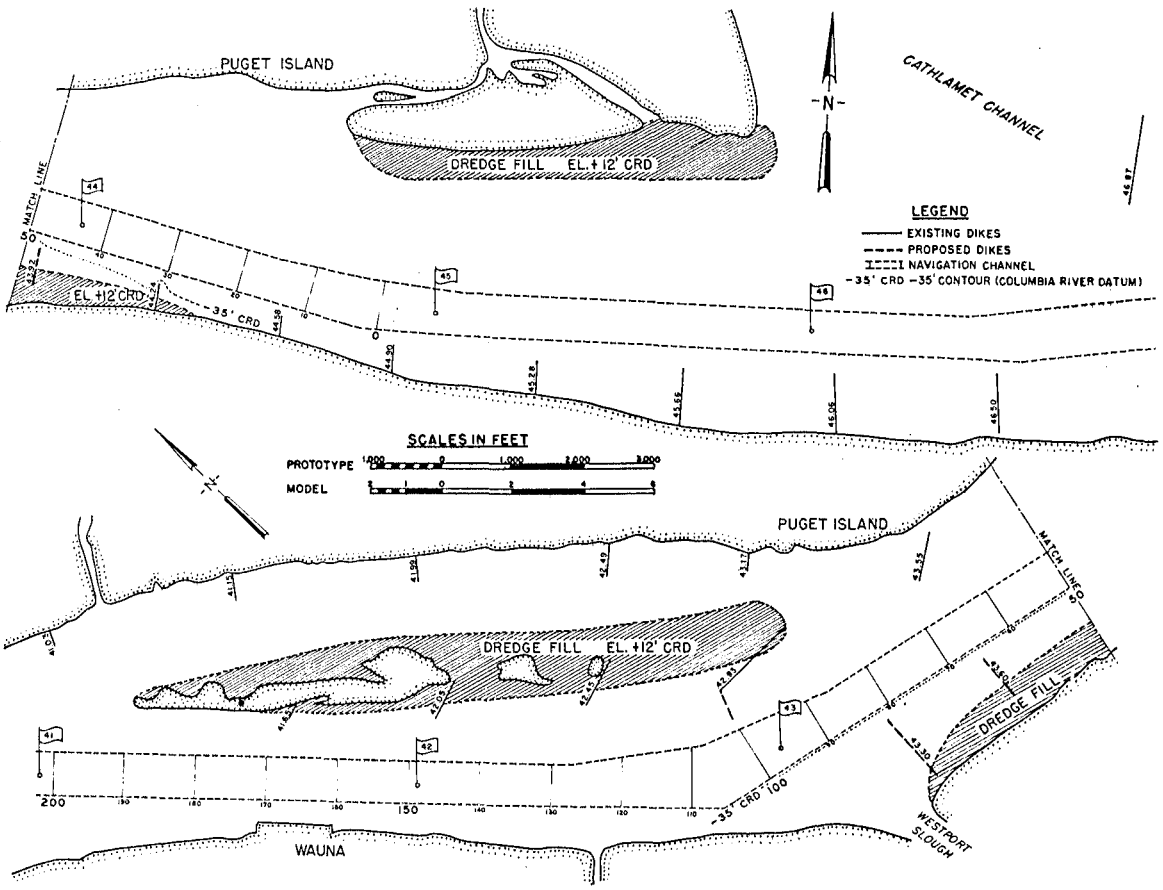

Figure 3-45. Elements of Wauna-Lower Westport Bar improvement plan, Columbia River Estuary (after Herrmann, 1971).

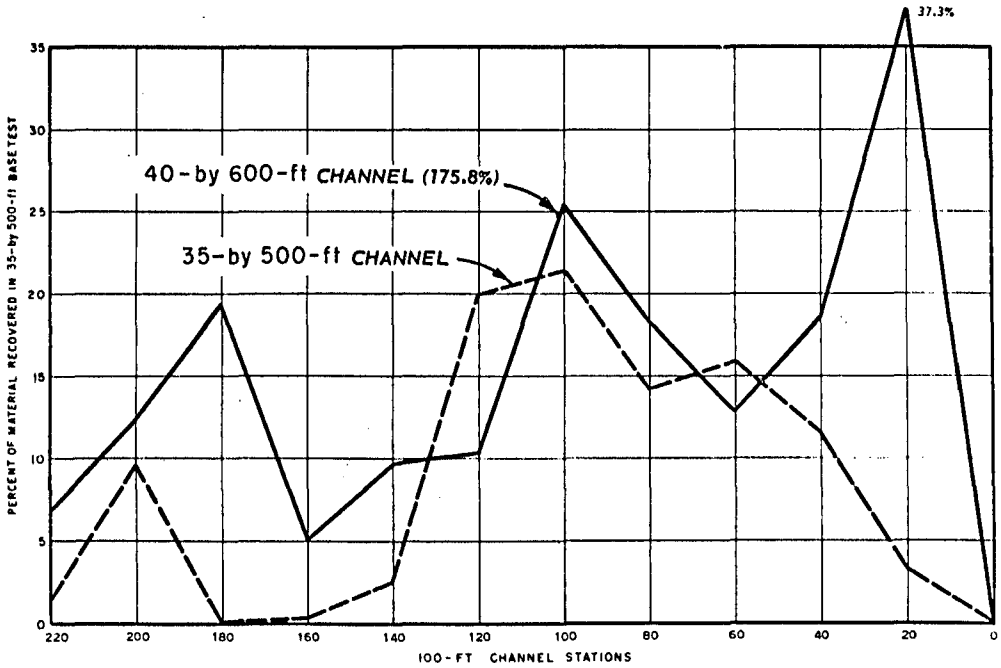

Figure 3-46. Effects of enlarged channel on shoaling at Wauna-Lower Westport Bar, Columbia River Estuary (after Herrmann, 1971).

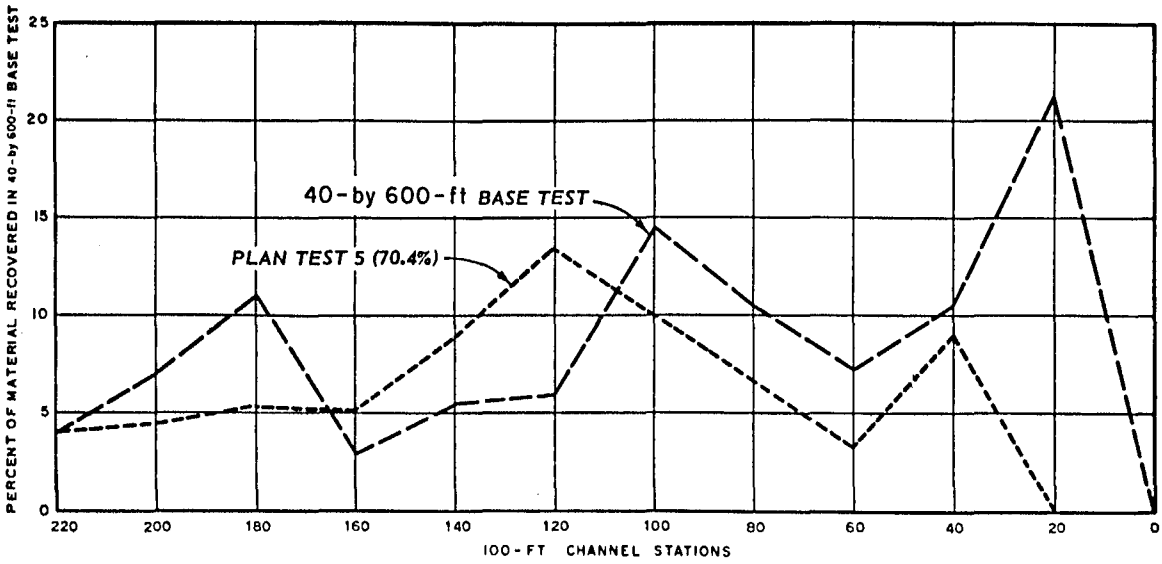

Figure 3-47. Effects of improvement plan on shoaling at Wauna-Lower Westport Bar, Columbia River Estuary (after Herrmann, 1971).

(5) Problem. A reach of the James River just upstream from the James River Bridge is the major source of seed oysters for the $5 million per annum Chesapeake Bay oyster industry. Plans to dredge a deeper channel would probably need revising if deepening would adversely affect hydraulic or salinity conditions over the seed oysterbeds.

(6) Purpose of Model Study. A comprehensive model of the James River was used to determine the probable effects of a proposed 10-foot increase in the depth (from -25 to -35 feet MLW) of the navigation channel between Newport News and Richmond on salinities and currents in the estuary as a whole and especially over the seed oysterbeds.

(7) The Model. The model (Fig. 3-48), constructed to linear scales of 1:1,000 horizontally and 1:100 vertically, was about 550 feet long and 130 feet wide at its widest point.

(8) Test Procedures. The model tests involved reproduction of low, medium, and high sustained freshwater inflows into the James River and its principal tributaries, together with reproduction of an average ocean tide. Measurements of salinities and currents were made throughout the problem reach at hourly and 1/2-hour intervals, respectively, over a complete tidal cycle; the results were generally averaged (time and depth) to determine the average velocity and average salinity values. These data were intended to demonstrate the effects of the proposed channel deepening on the entire estuary, as well as in areas used for seed oysterbeds.

(9) Summary of Test Results. Figure 3-49 shows the effects of the 35-foot channel on time- and depth-averaged salinities at sampling stations located in and immediately adjacent to the navigation channel for the three inflow conditions tested. The figure shows that the effects were negligible for a river discharge of 11,500 cubic feet per second, that average channel salinities were increased by about 0.1 to 0.8 part per thousand for a discharge of 3,200 cubic feet per second and that average channel salinities were increased by about 0.1 to 0.4 part per thousand for a discharge of 1,000 cubic feet per second. Figures 3-50, 3-51, and 3-52 show the changes in time- and depth-averaged salinities at stations in the seed oysterbeds for the various river discharges. Over the entire seed oysterbed area, average salinity was decreased by 0.2 part per thousand at 11,500 cubic feet per second, and was increased by 0.2 and 0.4 part per thousand at 3,200 and 1,000 cubic feet per second, respectively. Similar information developed for the effects of the enlarged channel on velocities in the problem area indicated that average flood and ebb velocities over the entire area would be changed on the order of ±0.2 foot per second.

It was concluded that the proposed 10-foot deepening of the channel would have no significant effects on tides, currents, or salinities in the James River in the reach between the James River Bridge and Fort Eustis, which includes the important seed oysterbeds.

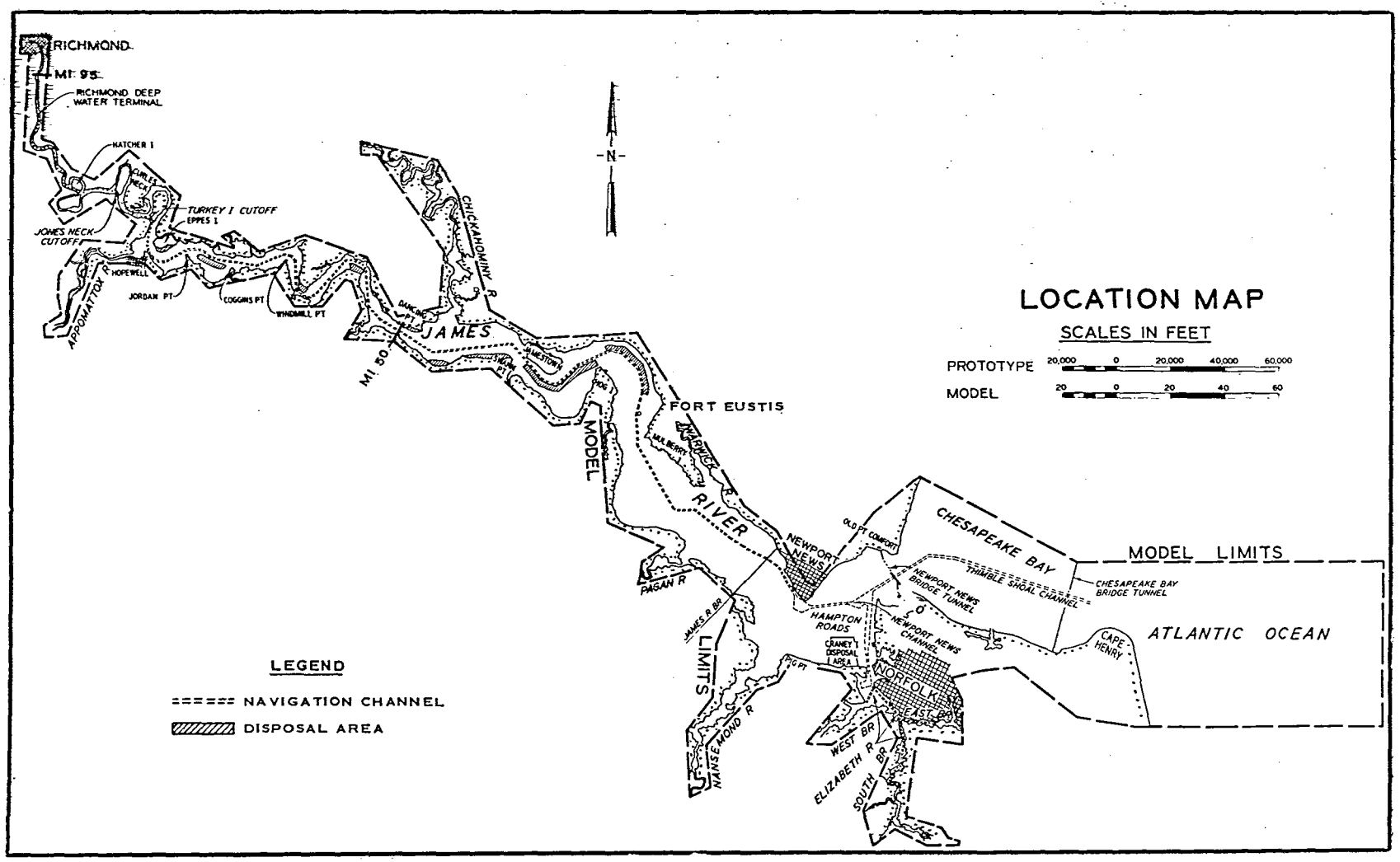

Figure 3-48. James River model (after U.S. Army Engineer Waterways Experiment Station, 1966).

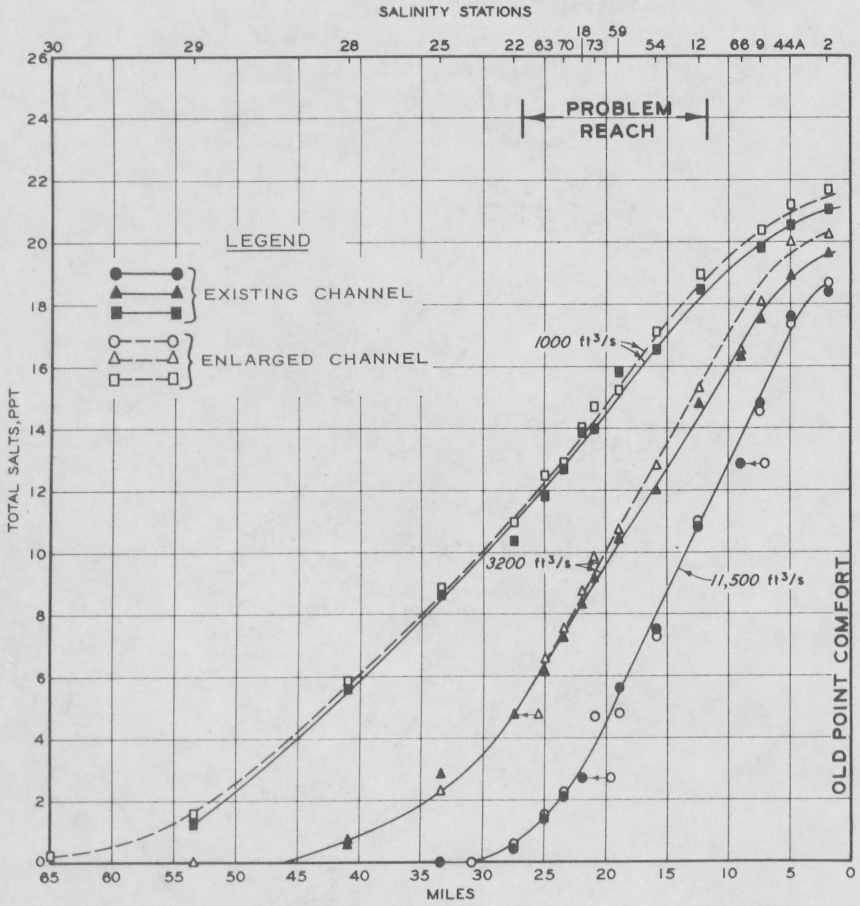

Figure 3-49. Effects of channel enlargement on salinity profiles, James River (after U.S. Army Engineer Waterways Experiment Station, 1966).

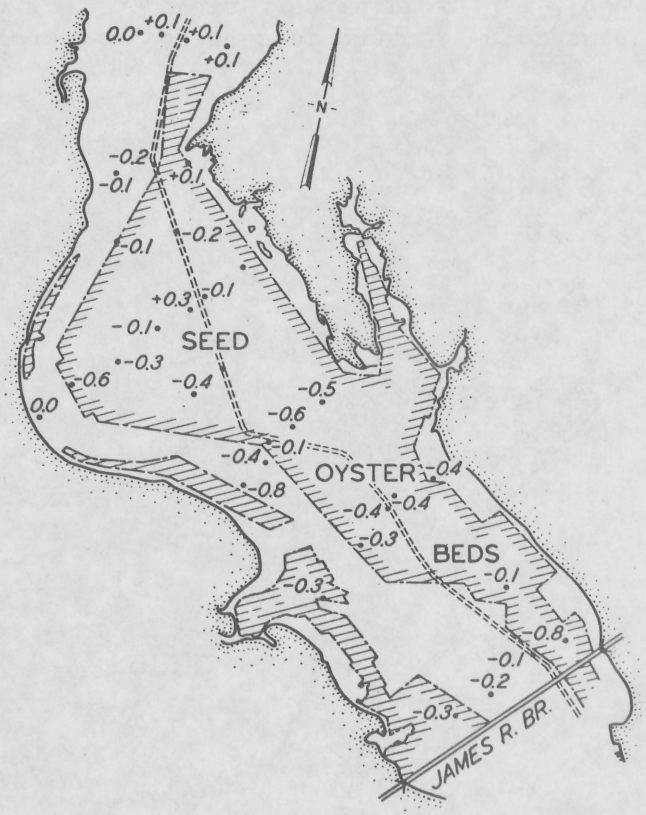

Figure 3-50. Effects of channel enlargement on average salinities, Q = 11,500 cubic feet per second, James River (after U.S. Army Engineer Waterways Experiment Station, 1966).

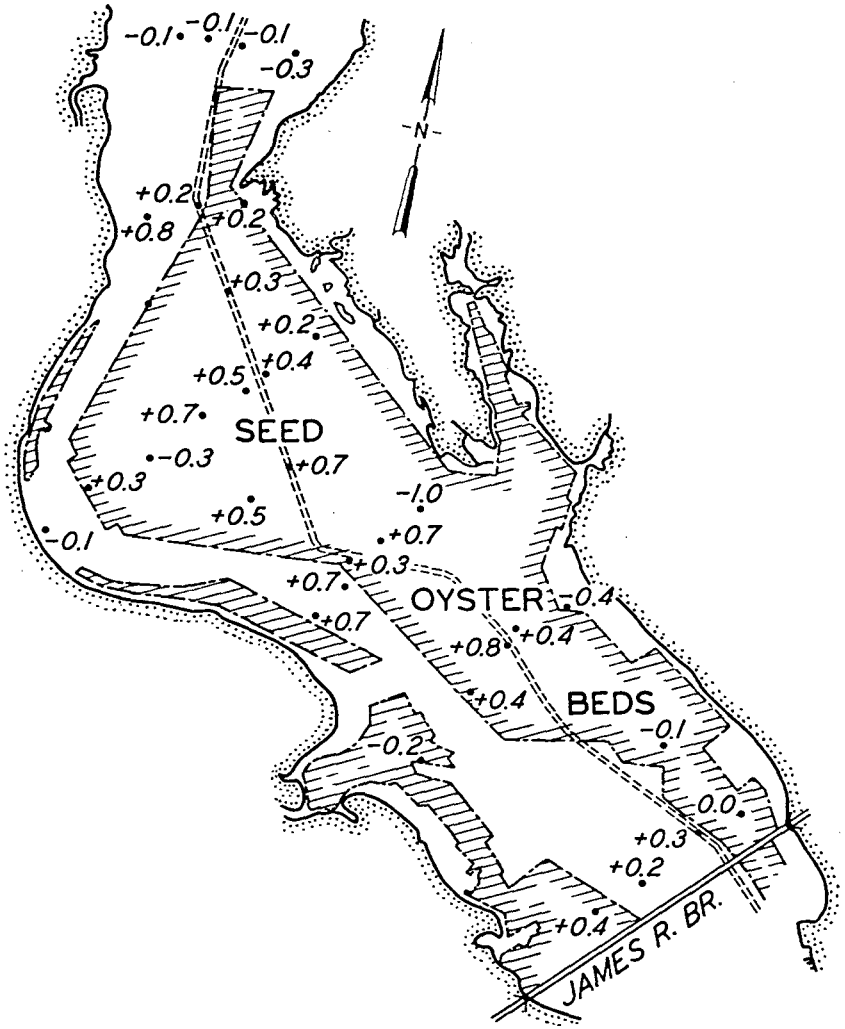

Figure 3-51. Effects of channel enlargement on average salinities, Q = 3,200 cubic feet per second, James River (after U.S. Army Engineer Waterways Experiment Station, 1966).

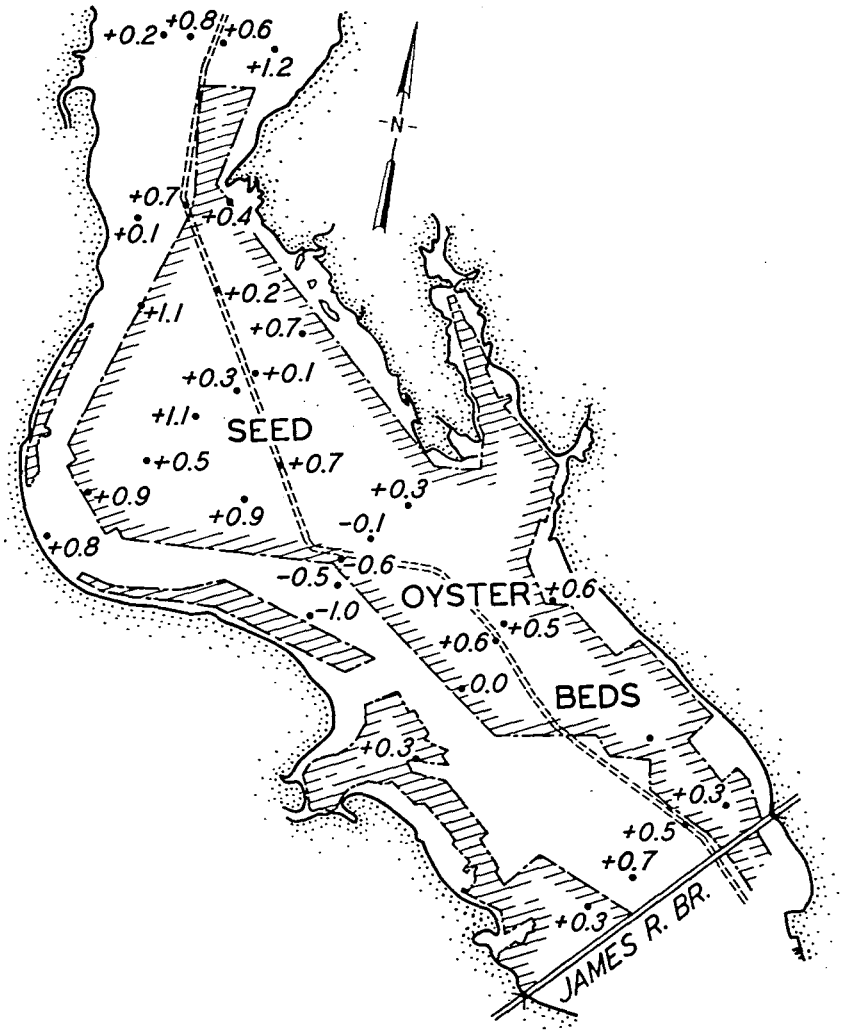

Figure 3-52. Effects of channel enlargement on average salinities, Q = 1,000 cubic feet per second, James River (after U.S. Army Engineer Waterways Experiment Station, 1966).

c. Navigation Conditions--Umpqua River Estuary.

(1) Project. Improvement of navigation conditions in existing navigation channel.

(2) Reference. Fisackerly (1970).

(3) Laboratory. WES.

(4) Test Period. October 1965 to May 1968.

(5) Problem. An adverse crosscurrent existed in the entrance area. No actual measurements of the crosscurrent were available, and only a general description of the phenomena was provided by tug skippers. Barge tow crossings over the entrance bar are usually made on the flood tide. A barge proceeding seaward in the channel on the south side of the entrance encounters a shear current to the north near the seaward end of the training jetty which forces the tug or barge onto the middle grounds. The Umpqua River entrance is shown in Figure 3-53.

(6) Purpose of Model Study. Model tests were conducted to obtain an optimum layout of the entrance area jetty system to (a) improve current patterns in the entrance from the standpoint of navigation, and (b) minimize the cost of maintenance dredging.

(7) The Model. The model (see Fig. 3-1) was constructed to linear scales of 1:300 horizontally and 1:100 vertically, was about 280 feet long, 100 feet wide at its widest point, and covered an area of about 10,000 square feet. The model was a combination fixed- and movable-bed model which was initially constructed as a fixed-bed model, with provisions to later convert the entrance area to movable bed if necessary.

(8) Test Procedures. Crosscurrent observations were obtained by means of time-exposure photos of a staff-type float, weighted so that the bottom was 10 feet below the water to represent the depth of a loaded oceangoing barge.

(9) Summary of Test Results. In the model, a crosscurrent was created by generating waves which approached from the northwest quadrant. Waves approaching from that direction tended to pile up water in the angle between the south jetty and the training jetty, resulting in a head differential between this area and the navigation channel which generates the crosscurrent. The condition is accentuated during the flood phase of the tide, because a part of the tidal flow naturally enters into the angle between the jetties, and the outflow from the angle must turn more than 90° to flow upstream in the main channel.

Photos of the crosscurrent for existing (base test) conditions and for three of the various plans tested are shown in Figure 3-54. Elimination of the angle between the south and training jetties by extending the training jetty to the outer end of the south jetty (plan 1 in Fig.

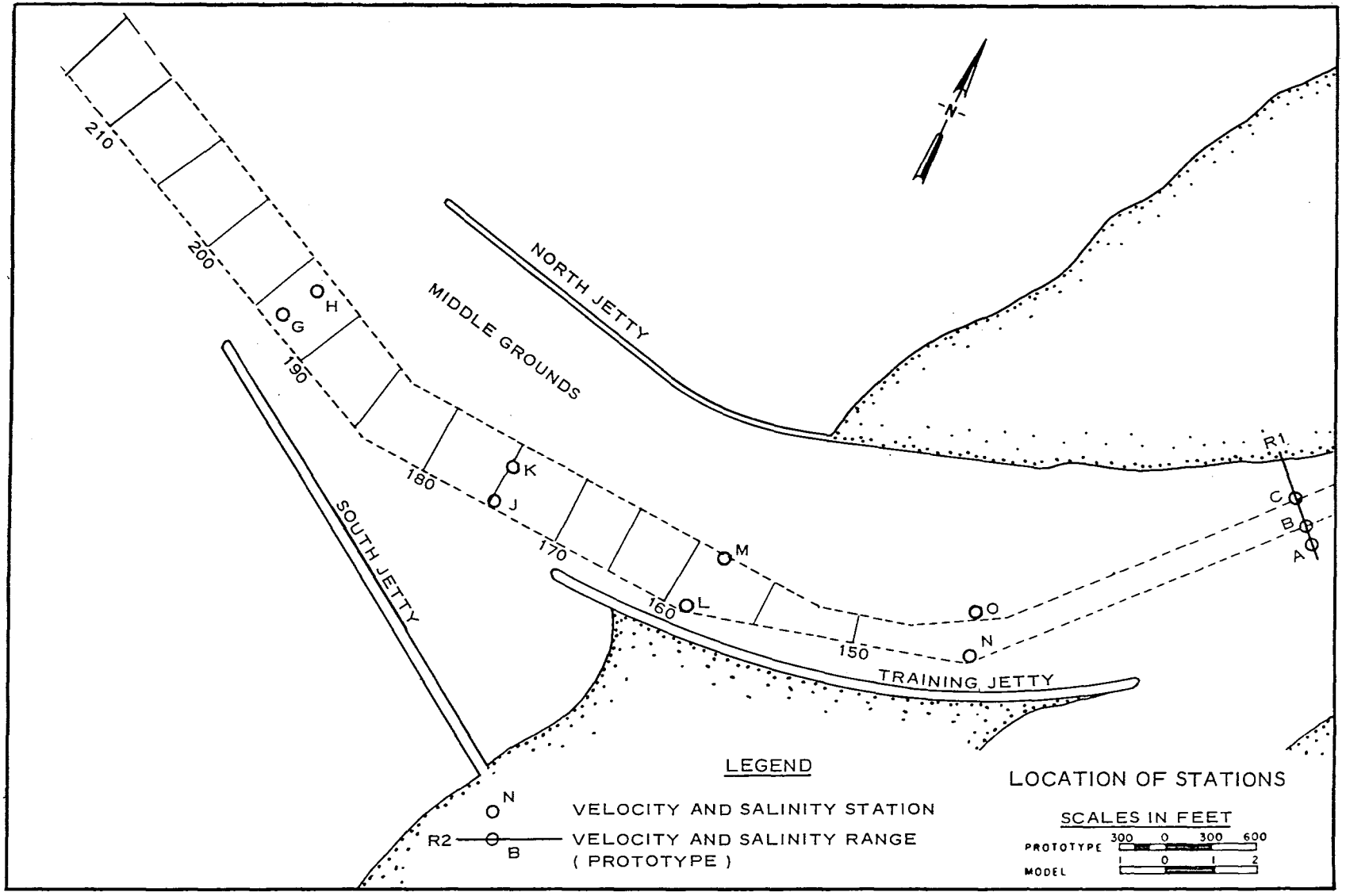

Figure 3-53. Umpqua River entrance (after Fisackerly, 1970).

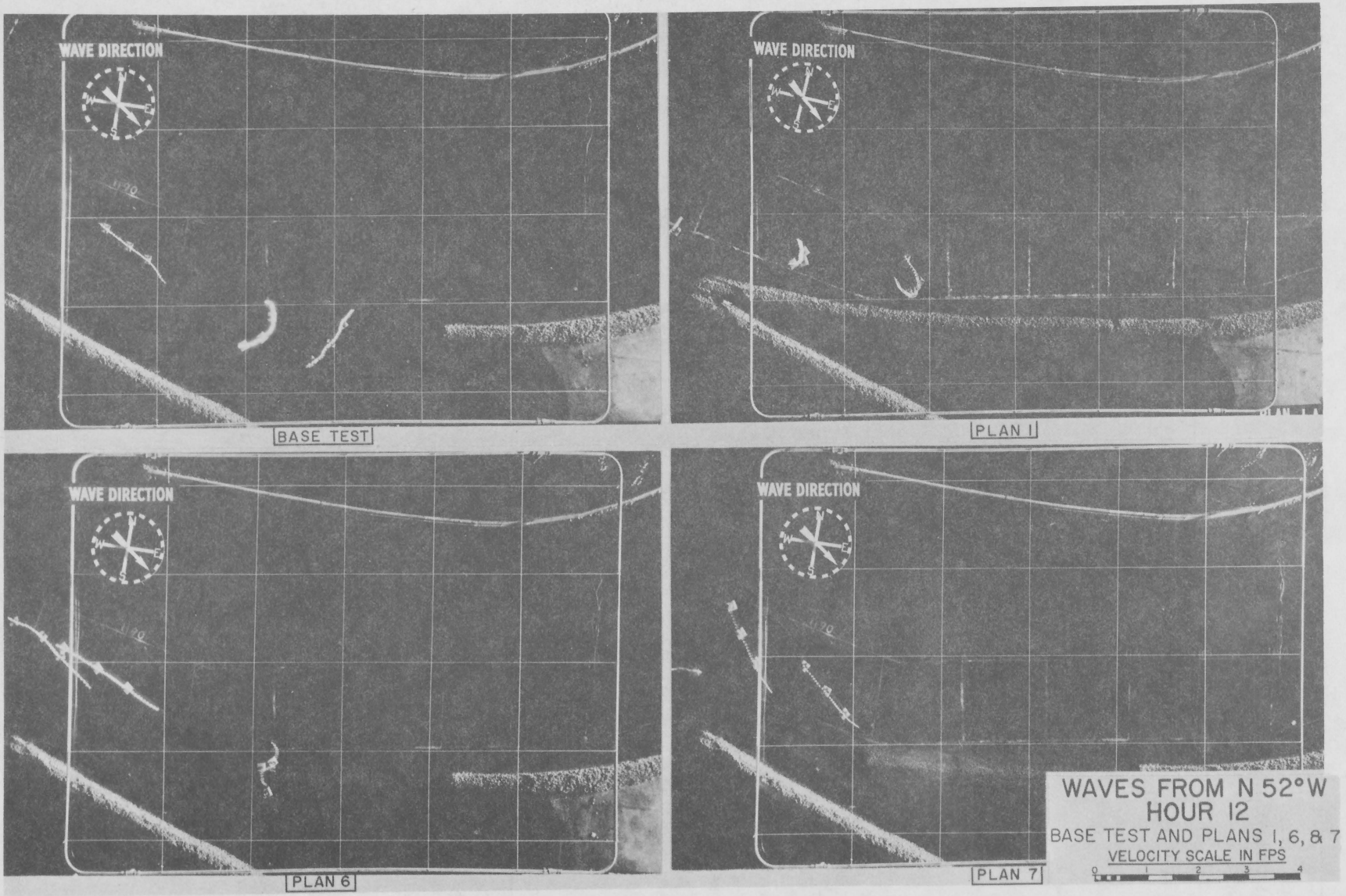

Figure 3-54. Crosscurrents in Umpqua River entrance (Fisackerly, 1970).

3-54) completely eliminated the crosscurrent. Shorter extensions of the training jetty reduced the strength and duration of the crosscurrent but did not eliminate it.

d. Training Structures--Delaware River.

(1) Project. Rehabilitation of existing dikes.

(2) Reference. U.S. Army Waterways Experiment Station (1956, 1964).

(3) Laboratory. WES.

(4) Test Period. April to November 1963.

(5) Problem. Reedy Island Dike (Fig. 3-55), constructed in 1887 to 1917 to a total length of 17,000 feet, was designed to concentrate flow into the main channel east of Reedy Island and thus reduce serious shoaling that occurred in that part of the estuary at the time the dike was constructed. Pea Patch Dike, constructed in 1930-34 to a total length of 19,000 feet, and Pennsville Dike, constructed in 1942-43 to a length of 5,000 feet, were built for the same basic reasons. At the time of the model studies all three dikes were seriously deteriorated, and estimates for rehabilitating the structures to design conditions showed that expenditures of $5 million each would be required to restore Reedy Island and Pea Patch Island Dikes, and $1,500,000 to restore Pennsville Dike.

(6) Purpose of Model Study. Model tests were conducted to determine: (a) The effects of Reedy Island and Pea Patch Island Dikes on hydraulic conditions in the estuary, and if the flow regimen so required, the extent of dike rehabilitation necessary; and (b) the additional benefits that would be derived from restoring deteriorated sections of Pennsville Dike to a crest elevation of about 2 feet above MHW rather than to the elevation of mean tide level.

(7) The Model. The Delaware Estuary model (Fig. 3-56) reproduced the entire tidal part of Delaware Bay and River from the Capes to Trenton, New Jersey, to linear scales of 1:1,000 horizontally and 1:100 vertically. Before the dike studies, the entire model had been carefully adjusted and verified for tides, tidal currents, and salinity conditions throughout the full range of freshwater inflows.

(8) Test Procedures. All three dikes were subjected to hydraulic tests for existing and design conditions, and for essentially a completely deteriorated condition of each dike. After these tests were completed and the results analyzed, further tests were made with certain parts of the dikes restored to design conditions and other parts left in a deteriorated state.

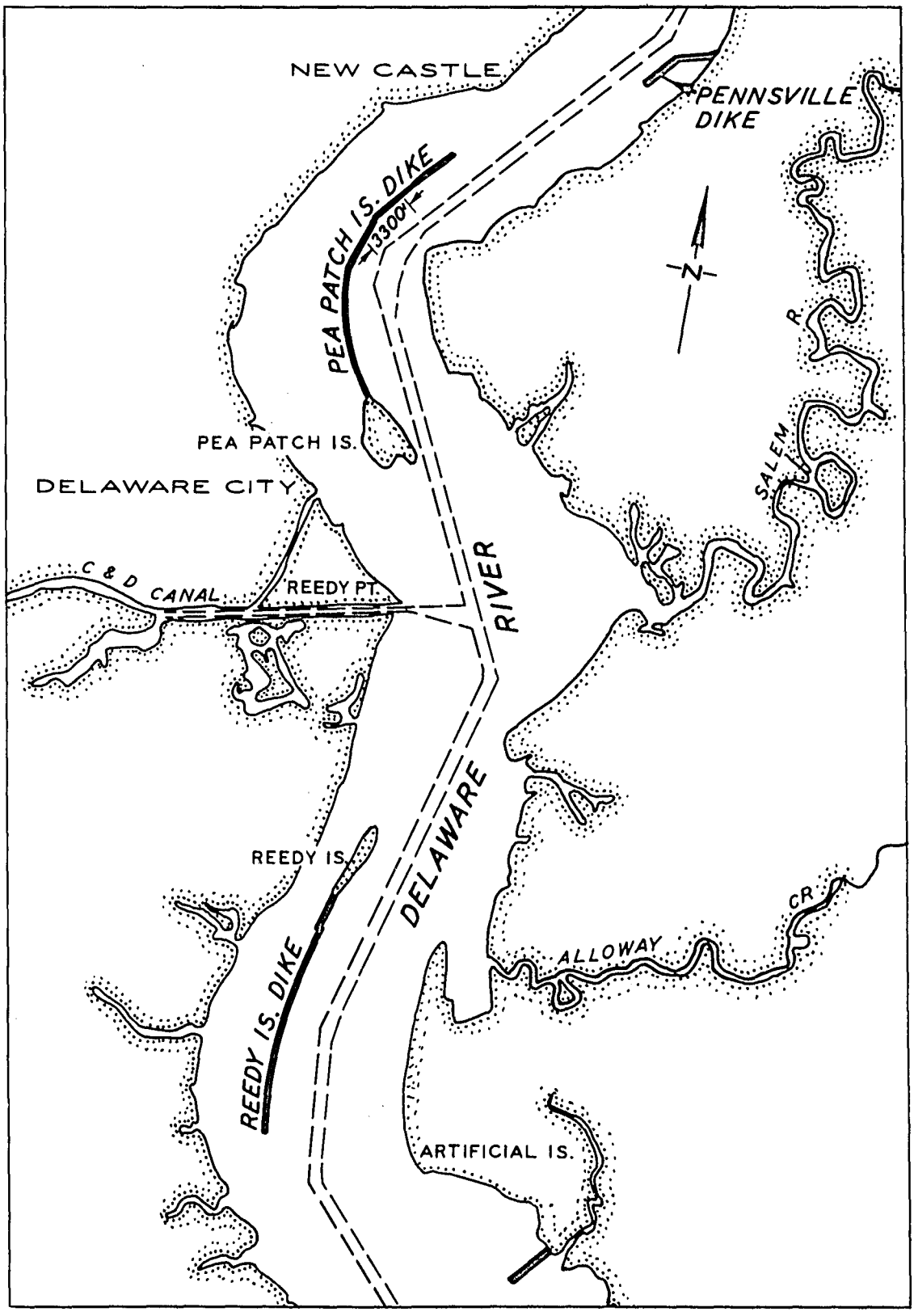

Figure 3-55. Locations of Delaware River dikes (after U.S. Army Engineer Waterways Experiment Station, 1964).

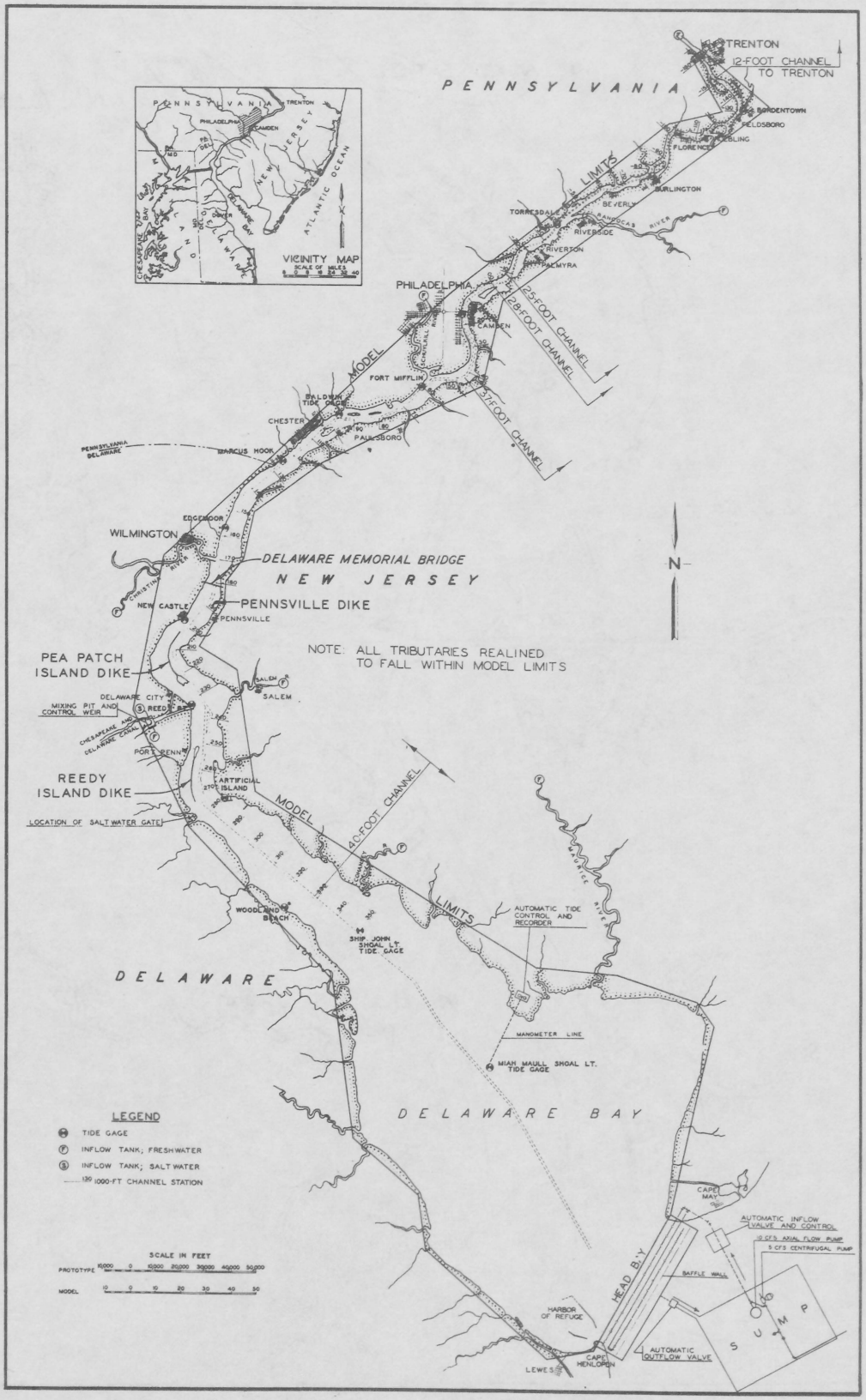

Figure 3-56. Delaware River model (after U.S. Army Engineer Waterways Experiment Station, 1964).

(9) Summary of Test Results. Close examination of flow pattern photos and velocity measurements showed conclusively that all of Reedy Island Dike could be allowed to deteriorate without adverse effects on hydraulic conditions or shoaling. The tests also showed that most of Pea Patch Island Dike could likewise be allowed to deteriorate without adverse effects; however, the results suggested that sufficient benefits would accrue from maintaining the upstream 3,300 feet of the dike to design grade to justify the cost of rehabilitation and maintenance. Tests of the Pennsville Dike showed conclusively that this structure should be rehabilitated and maintained to the design conditions. These tests resulted in a total savings of about $9,100,000 ($5 million for rehabilitation of Reedy Island Dike, and $4,100,000 for rehabilitation of the unnecessary 15,700 feet of Pea Patch Island Dike), and showed that allowing the Reedy Island Dike and part of Pea Patch Island Dike to deteriorate would have no adverse effects on hydraulic or shoaling conditions in the estuary.

e. Disposal Islands--Matagorda Bay.

(1) Project. Deepening existing navigation channel from 12 feet to a 36-foot-deep new entrance, and location of dredged-material disposal.

(2) Reference. Simmons and Rhodes (1966).

(3) Laboratory. WES.

(4) Test Period. December 1959 to September 1962.

(5) Problem. Matagorda Bay is located on the Texas coast between Galveston and Corpus Christi, and until a 36-foot-deep navigation channel to Point Comfort was authorized by Congress, navigation in the bay was limited to a 12-foot-deep channel for barge tows and small craft. The deep-draft project for Matagorda Bay is unique in that, instead of the channel being gradually deepened a few feet at a time as has been the case in most estuarine navigation projects, the channel was dredged in one operation from -12 feet or less to a project depth of -36 feet. Because of the large quantity of material to be dredged in the initial excavation of the channel, and since the dredged material could not be distributed widely in the bay because of potential redistribution of the material to the channel and possible adverse effects on marine life, the question of proper selection of dredge-disposal areas was a highly important one.

(6) Purpose of Model Study. The model study was conducted for the design of a deep-draft navigation channel. Studies were conducted to determine the optimum locations for dredged-material disposal during initial excavation and subsequent maintenance dredging of the channel.

(7) The Model. The Matagorda Bay model was of the fixed-bed type. It reproduced to linear scales of 1:1,000 horizontally and 1:100 vertically the prototype area shown in Figure 3-57. The model was about 200 feet long, 225 feet wide, and covered an area of about 30,000 square

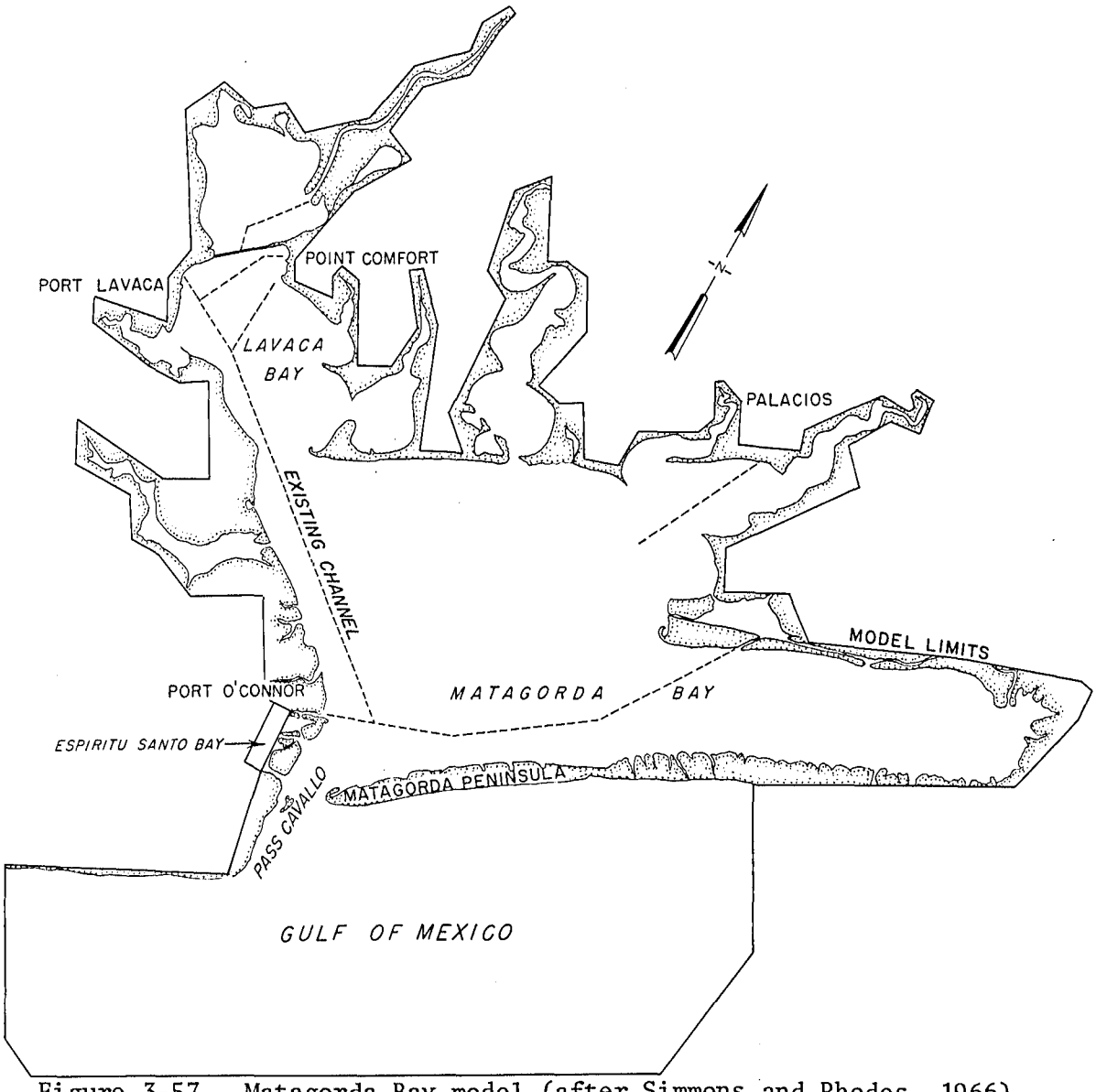

Figure 3-57. Matagorda Bay model (after Simmons and Rhodes, 1966).

feet. Tides and tidal currents were reproduced by a primary tide generator located in the Gulf of Mexico part of the model and a secondary tide generator located at the model limit of the channels which connect Matagorda Bay and Espiritu Santo Bay to the west. This secondary generator reproduced the discharge exchange between the two bays which results from tidal action in each of the bays.

(8) Test Procedures. The model was operated with both saltwater and freshwater so that density effects on current velocity distribution in the deep channels would be reproduced, and the effects of the deep-draft project on the salinity regimen of the bay system could be determined.

(9) Summary of Test Results. The alinement of the new entrance channel, as developed during the model study, is shown in Figure 3-58.

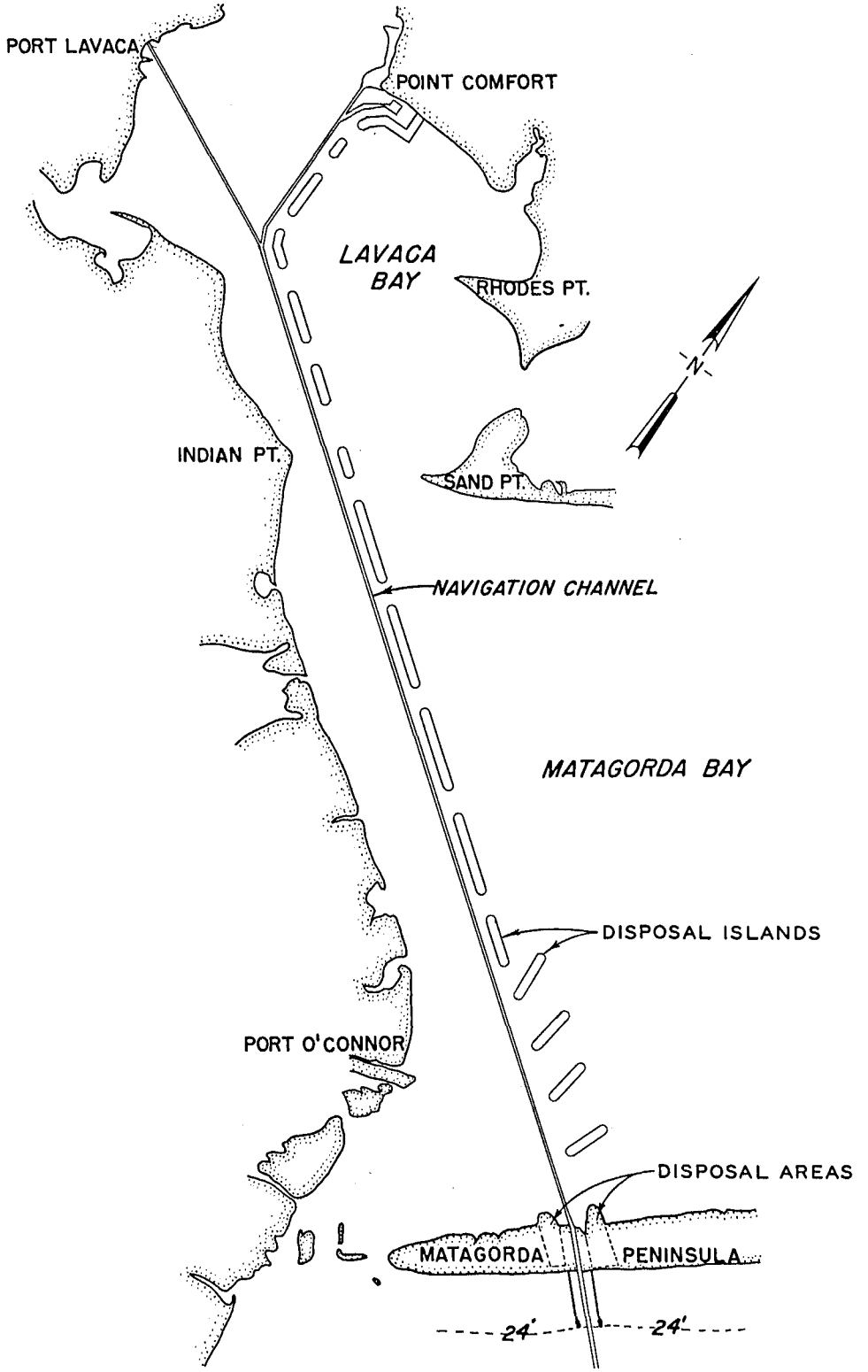

Figure 3-58. Elements of improvement plan, Matagorda Bay (after Simmons and Rhodes, 1966).

After numerous tests, it was determined that a chain of disposal islands, generally following the east side of the navigation channel and with substantial openings between adjacent islands (Fig. 3-58), would neither result in adverse effects on circulation patterns nor cause undesirable crosscurrents in the navigation channel. In the area between Matagorda Peninsula and a point about opposite Port O'Conner, the disposal islands had to be oriented so that the long axes were parallel to the predominant current directions; this increased the widths of openings between adjacent disposal islands to prevent further restriction of the entrance to the bay and the production of crosscurrent velocities and patterns which might be detrimental to navigation (Fig. 3-59).

f. Submerged Disposal Areas--James River.

(1) Project. Evaluation of existing open-water disposal areas adjacent to 35-foot-deep navigation channel.

(2) Reference. Boland and Bobb (1975).

(3) Laboratory. WES.

(4) Test Period. March 1969 to September 1970.

(5) Problems. For a number of years the U.S. Army Engineer District, Norfolk, has been using the open-water disposal technique to dispose of material dredged during maintenance of the existing James River navigation channel extending from deep water in Chesapeake Bay some 100 miles to the city of Richmond, Virginia. It was necessary to determine if the areas used for disposal between Newport News and Hopewell were performing satisfactorily in terms of retaining the placed dredged material and to obtain some idea of the life expectancy of the respective areas.

(6) Purpose of Model Study. The study was conducted to determine if the areas used for dredged-material disposal were performing satisfactorily and to determine their life expectancies. Alternate disposal areas were evaluated as necessary.

(7) The Model. The existing James River model was used (see Fig. 3-48). Adjustment of the model to reproduce prototype tides, currents, and salinities was accomplished before conducting the study, and no additional adjustment for this purpose was required. However, shoaling verification in the problem area had not been accomplished, and tests were conducted to demonstrate the capability of the model to reproduce known prototype shoaling characteristics. Gilsonite was selected as the appropriate model sediment.

(8) Test Procedures. The tests involved placement of lightweight sediments (gilsonite) in the disposal areas, tracing patterns of movement from such areas, and defining the areas where sediments moving from the disposal areas would deposit. If the test results indicated a probable

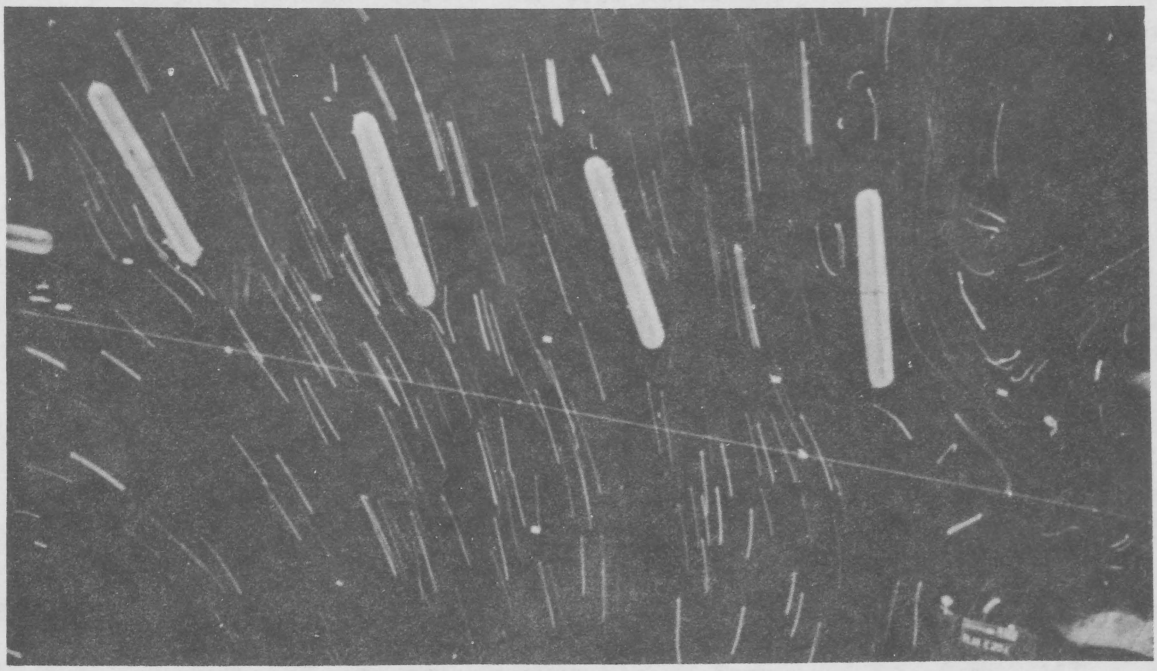

STRENGTH OF EBB FLOW

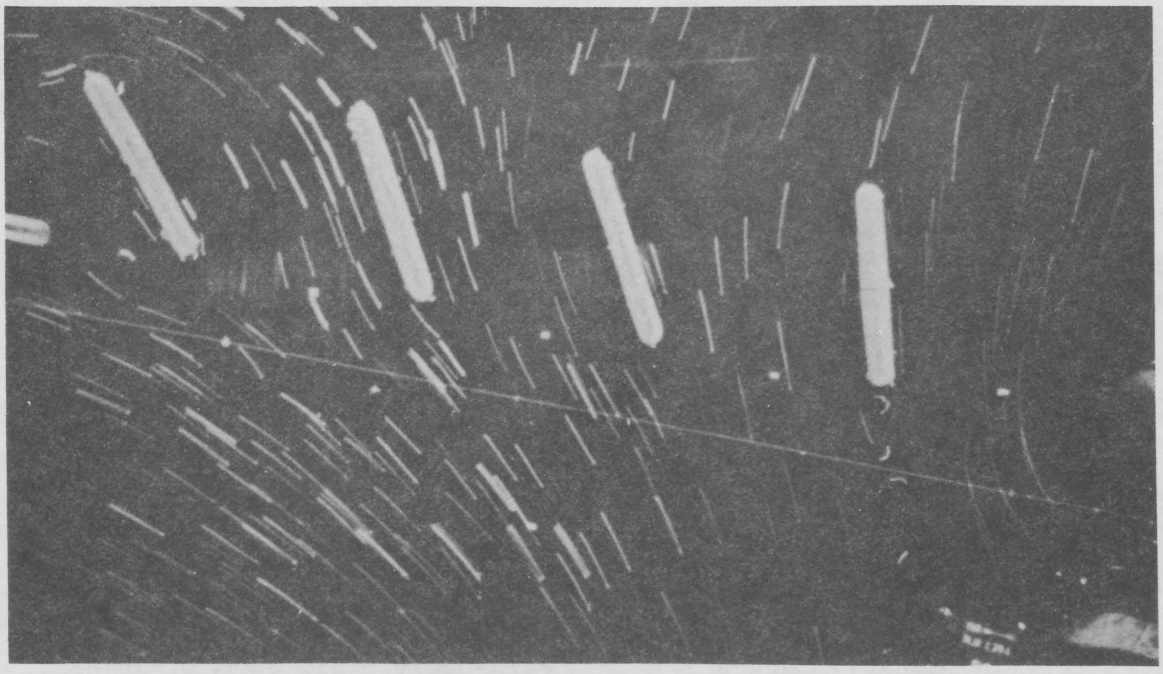

STRENGTH OF FLOOD FLOW

Figure 3-59. Surface current patterns around disposal islands, Matagorda Bay (Simmons and Rhodes, 1966).

excessive rate of return of dredged material to the channel from the existing disposal areas, the tests were expanded to include studies of alternate areas in the same general vicinity to determine if more suitable areas could be defined. For the disposal area tests, the gilsonite water mixture was dumped into the disposal area in the model in a manner to simulate prototype disposal operations. The daily prototype dredge advancement rate was simulated in the model injection operation.

(9) Summary of Test Results. At the Goose Hill shoal reach, material was placed about 1,600 feet south of, and parallel to, the navigation channel. The results of tests in which material was placed only in the upstream half of the present disposal area (Fig. 3-60) indicated that only a very small part of the material from this area returns to the navigation channel. Test results for the downstream half of this disposal area indicated a substantial return of material to the navigation channel (Fig. 3-61). However, a test conducted in which the material was placed in a proposed disposal area on the opposite (north) side of the channel and it was found that no material returned to the navigation channel.

g. Flushing--San Diego Bay.

(1) Project. Proposed second entrance to bay.

(2) Reference. Fisackerly (1974).

(3) Laboratory. WES.

(4) Test Period. May 1967 to September 1968.

(5) Problem. At the present time, the only connection between the Pacific Ocean and San Diego Bay is Zuniga Channel, located at the northwestern end of the bay. Since the more recent navigation facilities are located in the southeastern part of the bay, and more are planned for the near future in that area, a second entrance would greatly reduce the transit time through the bay for commercial vessels and would alleviate some traffic congestion in Zuniga Channel. Because the flushing rate of San Diego Bay is extremely low, it was hoped that a second entrance would expedite flushing and therefore improve the quality of the bay water.

(6) Purpose of Model Study. This study was conducted to determine the feasibility of, and the optimum location for, a second entrance into San Diego Bay and the effects of such an entrance on the tidal heights, current velocities, and circulation patterns throughout the bay and in the second entrance.

(7) The Model. The physical model used for this study reproduced all of San Diego Bay and a part of the Pacific Ocean outside the bay (Fig. 3-62). The model was of fixed-bed construction and was built to linear-scale ratios of 1:500 horizontally and 1:100 vertically. The model was 125 feet long, 100 feet wide, and covered an area of about 12,000 square feet.

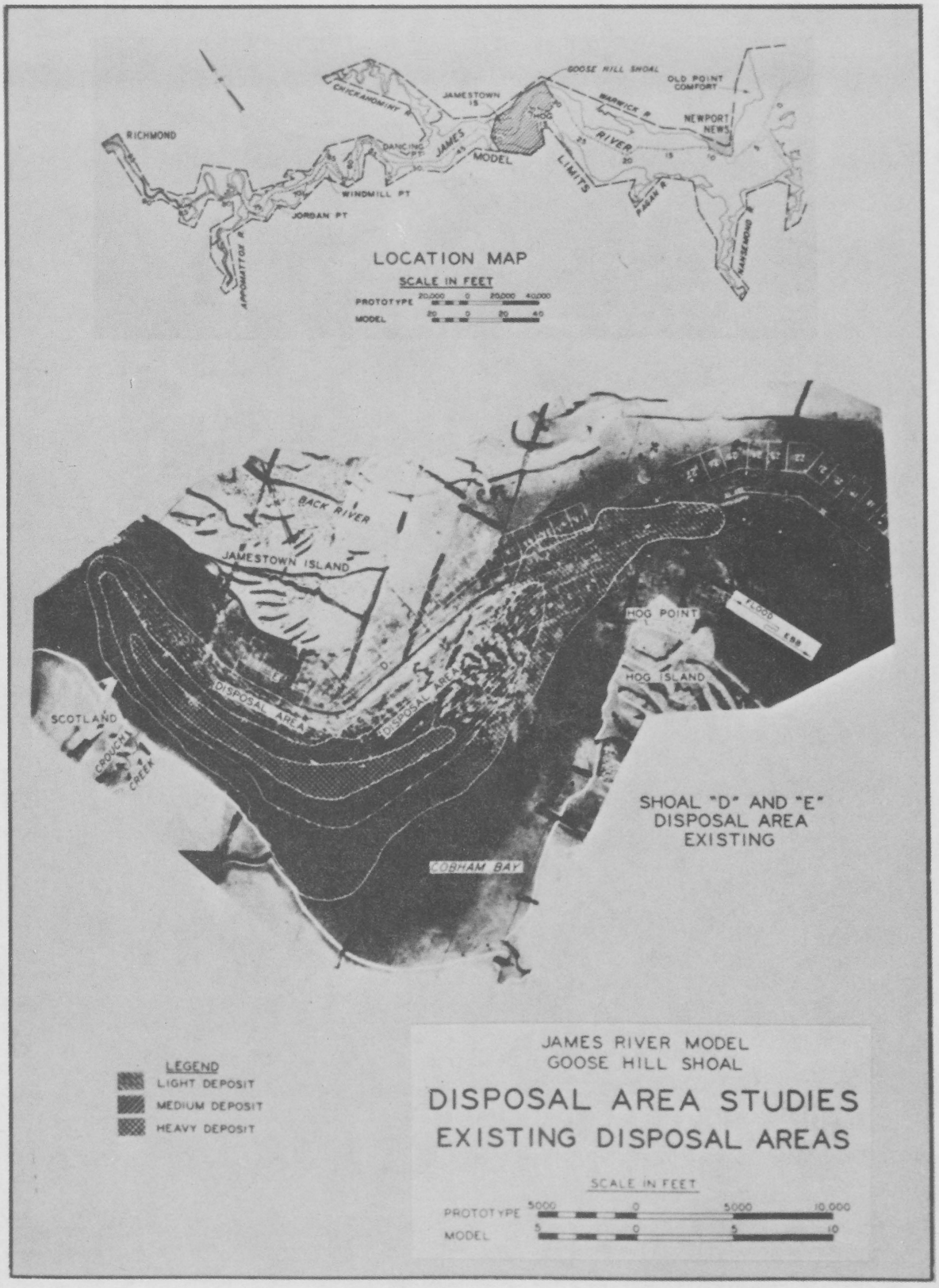

Figure 3-60. Shoaling test results, Upper Goose Hill shoal, James River (after Boland and Bobb, 1975).

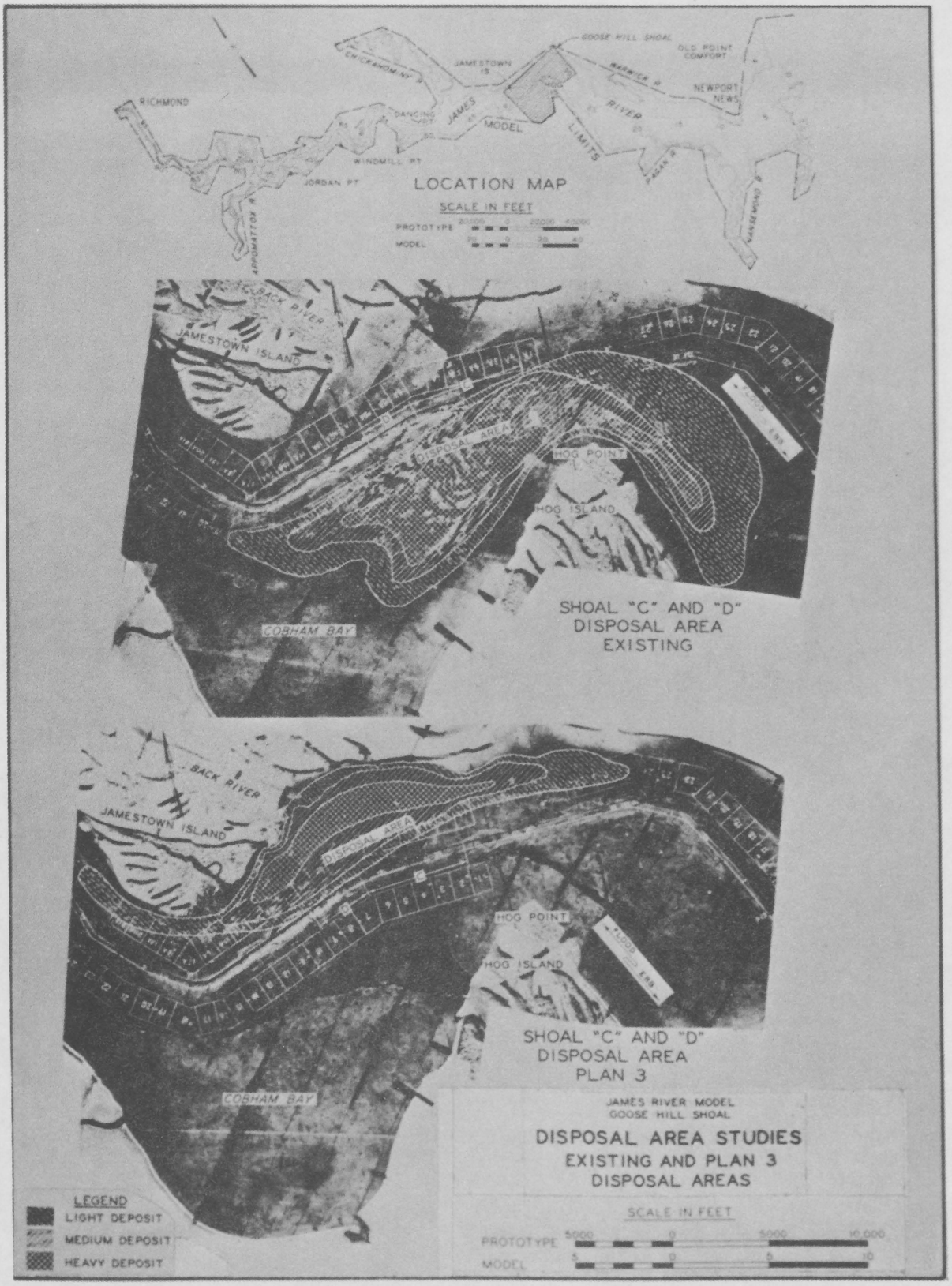

Figure 3-61. Shoaling test results, Lower Goose Hill shoal, James River (after Boland and Bobb, 1975).

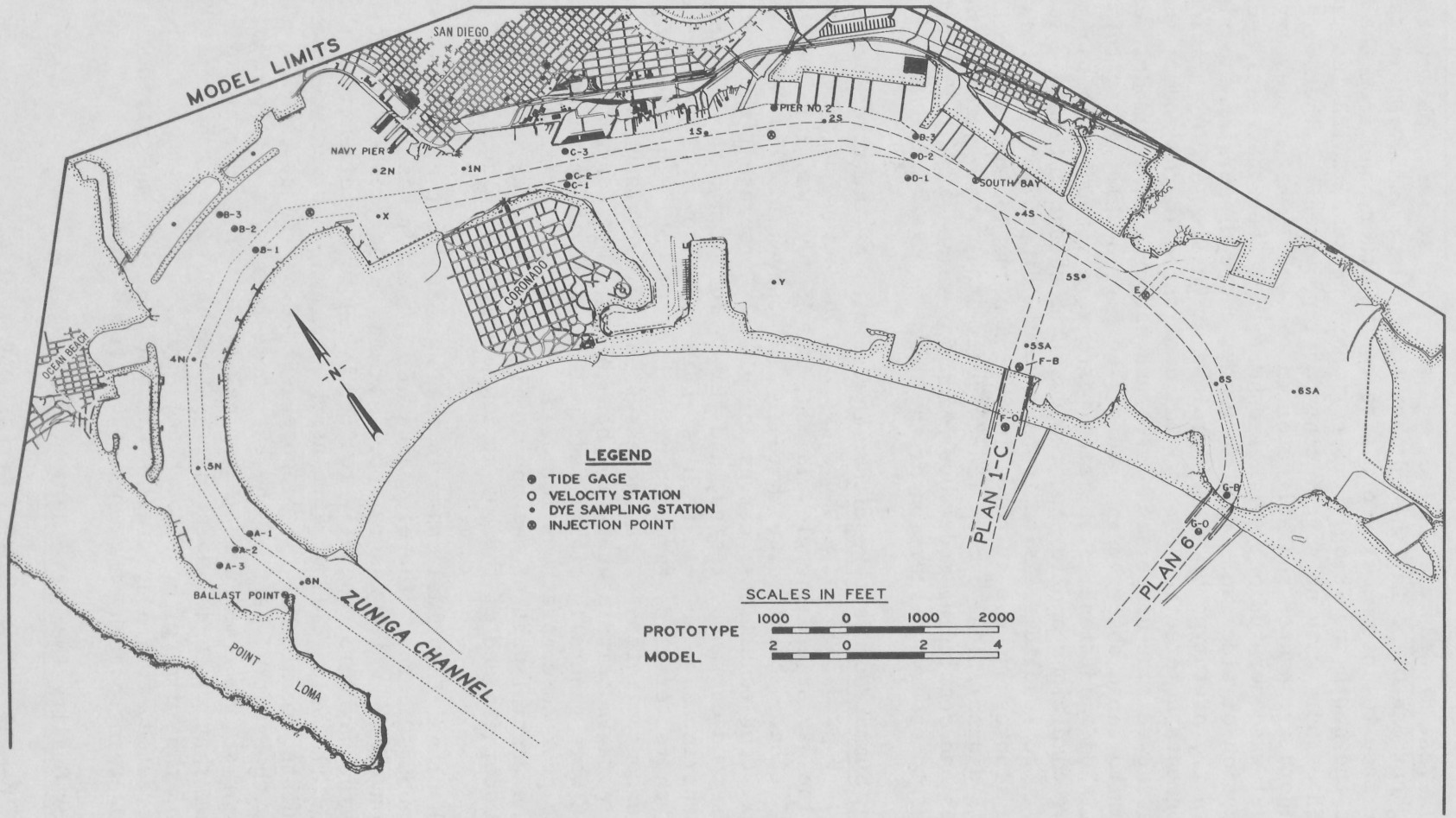

Figure 3-62. San Diego Bay model (after Fisackerly, 1974).

(8) Test Procedures. A thorough study of salinity observations made throughout San Diego Bay showed that the maximum variation in salinity from surface to bottom, from one side to the other, and from the entrance to the south end is only 0.5 part per thousand, which indicates a well-mixed estuary with no significant density currents. Therefore, the use of both freshwater and saltwater in the model was unnecessary, and the model was operated only with freshwater. After the usual hydraulic verification of tides and tidal currents, a dye-dispersion experiment conducted in the prototype by the Federal Water Quality Administration (now Environmental Protection Agency) was duplicated in the model, and the results showed that dispersion rates and patterns in the model were very similar to those observed in nature (see Fig. 3-40). After this had been established, additional dispersion tests were conducted in the model for existing conditions and for the two possible second entrances (see Fig. 3-62). The model dispersion tests involved discharging equal quantities of a fluorescent dye at three injection point locations (see Fig. 3-62) for 15 diurnal tidal cycles (24.84 hours each), then terminating the releases and continuing model operation for an additional 35 diurnal tidal cycles to observe dispersion of the dye.

(9) Summary of Test Results. The results of the three tests are summarized in Figure 3-63 which shows dye concentrations at given stations throughout the bay at tidal cycles 15, 30, and 45 (dye was released during the first 25 tidal cycles) for each test. The curves labeled "base test" represent existing conditions; curves for plan 1-C represent the northerly of the two second entrances tested, and curves for plan 6 the southerly of the second entrances. The test results indicated an overall improvement in flushing characteristics throughout the bay for both plans tested, although dye concentrations were increased during certain phases of the dispersion tests in certain areas for both plans. Dye concentrations for plan 1-C were generally significantly lower than those for plan 6, although the peak concentrations for plan 1-C were higher than those for plan 6 in the central part of the bay at higher high water slack and in the extreme southern end of the bay at lower low water slack.

For both plans, the tidal range in the southern part of the bay was reduced by about 0.5 foot; the elevation of high water was lowered while the elevation of low water was raised. Maximum velocities in the northern part of the bay were generally reduced by 60 to 80 percent; in the southern part the velocities were relatively unchanged or showed increases in the immediate vicinity of the proposed second entrance. A nodal point developed in the central part of the bay where there was little horizontal water movement at any time during the tidal cycle. The current pattern photos showed that the nodal point during the ebb tide was about 6,000 feet south of that during the flood tide. Thus, a net southward circulation was created, with a net inflow through the existing entrance and a net outflow through each of the proposed second entrances.

h. Water Quality--New York Harbor.

(1) Project. Proposed inlet to Sandy Hook Bay.

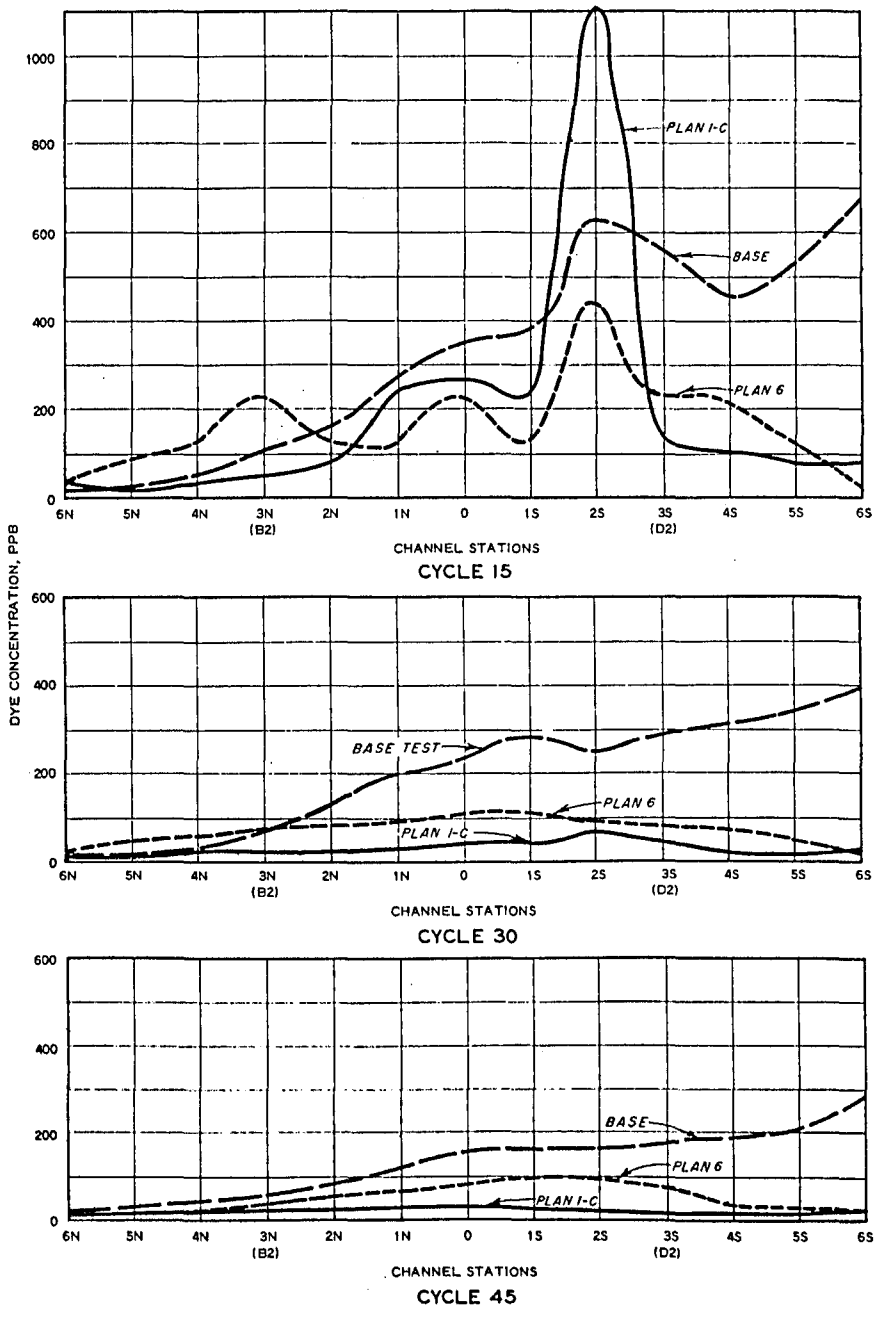

Figure 3-63. Effects of second entrance on dye concentration profiles, San Diego Bay (after Fisackerly, 1974).

(2) References. McNair and Hill (1972); Section VII,8,a of this report.

(3) Laboratory. WES.

(4) Test Period. January 1969 to February 1970.

(5) Problem. The principal purpose of the new inlet was to provide a safer and shorter route for recreation and charter boats between the Shrewsbury-Navesink River complex and the popular fishing grounds lying offshore and to the southeast. Boats presently travel north through Sandy Hook Bay, around the tip of Sandy Hook, then south to the fishing grounds. The proposed inlet would reduce travel distance and time by more than 50 percent and would provide a safer passage by eliminating the need to pass through the rough waters of Sandy Hook Bay. The proposed inlet would be constructed across Sandy Hook Peninsula about 5 miles south of the entrance to New York Harbor (Fig. 3-64). The new inlet, known locally either as Shrewsbury or Sandy Hook Inlet, had proposed dimensions of 250 feet in width and 15 feet in depth at MLW. Before making the final decision on whether to construct the new inlet, it was essential to know its effects on tides, currents, salinities, temperatures, and the flushing characteristics of Sandy Hook Bay and the Shrewsbury-Navesink River complex so that effects of the project on environmental factors throughout the area could be fully evaluated.

(6) Purpose of Model Study. The model studies were conducted to determine the effects of the inlet on (a) water quality in Sandy Hook Bay and the Shrewsbury and Navesink Rivers from the viewpoints of public health, recreation, and fish and wildlife; (b) flooding within the areas as a result of normal tides and hurricane surges; (c) recreational boating and commercial navigation; (d) general shoaling characteristics and maintenance requirements; (e) the optimum location and length of jetties at the ocean end of the proposed inlet; and (f) transmission of wave energy through the inlet into Sandy Hook Bay.

(7) The Model. Two physical models were used for the studies. The first was an undistorted 1:100-scale model (Fig. 3-65) of the area in which the new inlet would be constructed, including appropriate parts of the ocean and bay approaches to the inlet. This section model was about 65 feet long and 30 feet wide. A comprehensive discussion of the section model is presented in Section VII. The second model used was an existing comprehensive model of New York Harbor (Figs. 3-3 and 3-66) constructed to linear scales of 1:1,000 horizontally and 1:100 vertically. The model, extended for this study to include the Shrewsbury-Navesink Rivers and appropriate offshore areas, was about 500 feet long, covered an area of about 25,000 square feet, and was equipped with a primary tide generator in the ocean and secondary tide generators in Long Island Sound and the upstream end of the Hudson River.

(8) Test Procedures. The section model was used to define the hydraulic characteristics of the proposed inlet, to study the details of channel and jetty locations and dimensions, and to determine the amount of wave energy that would be transmitted through the new inlet into Sandy

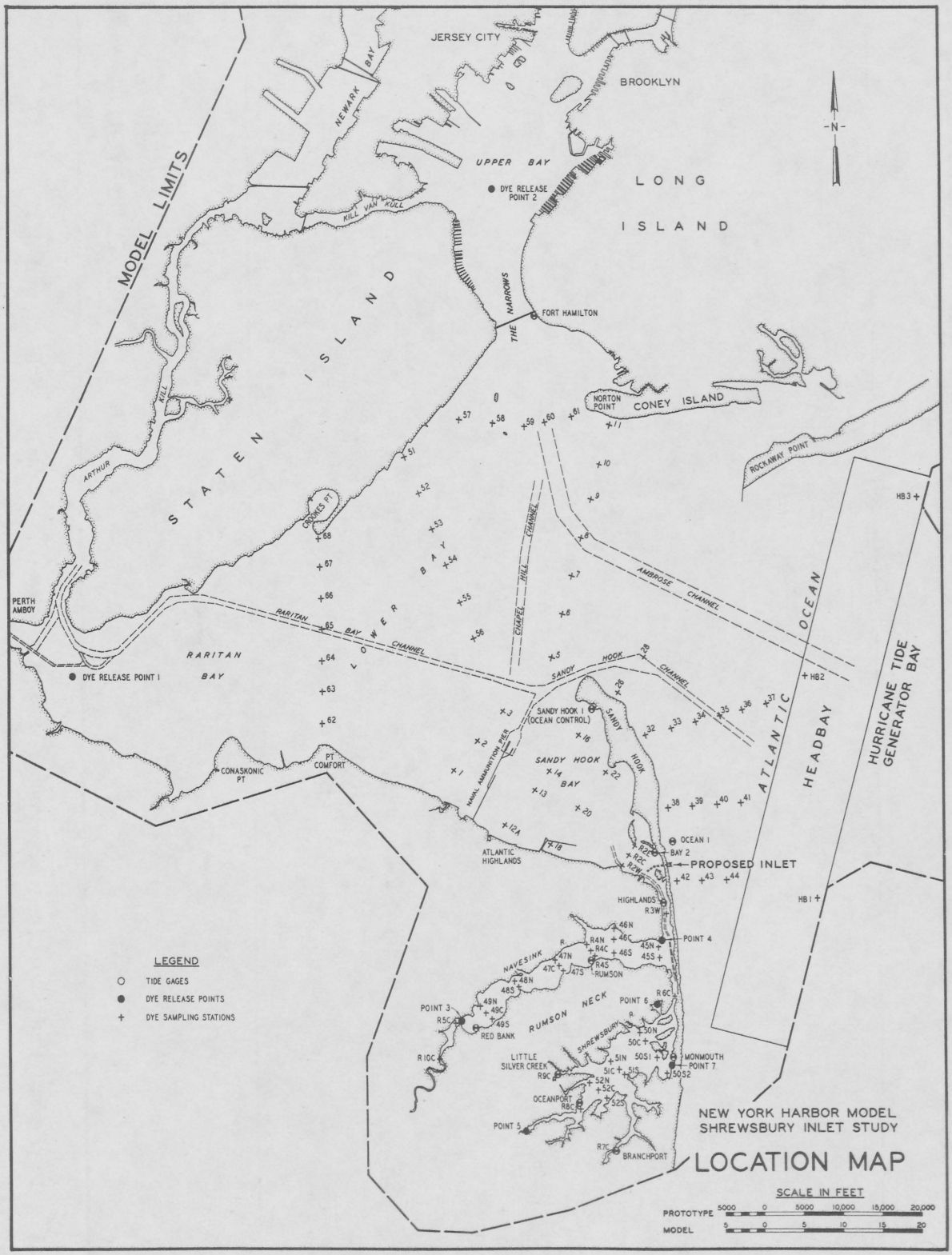

Figure 3-64. Location of proposed Shrewsbury Inlet (after McNair and Hill, 1972).

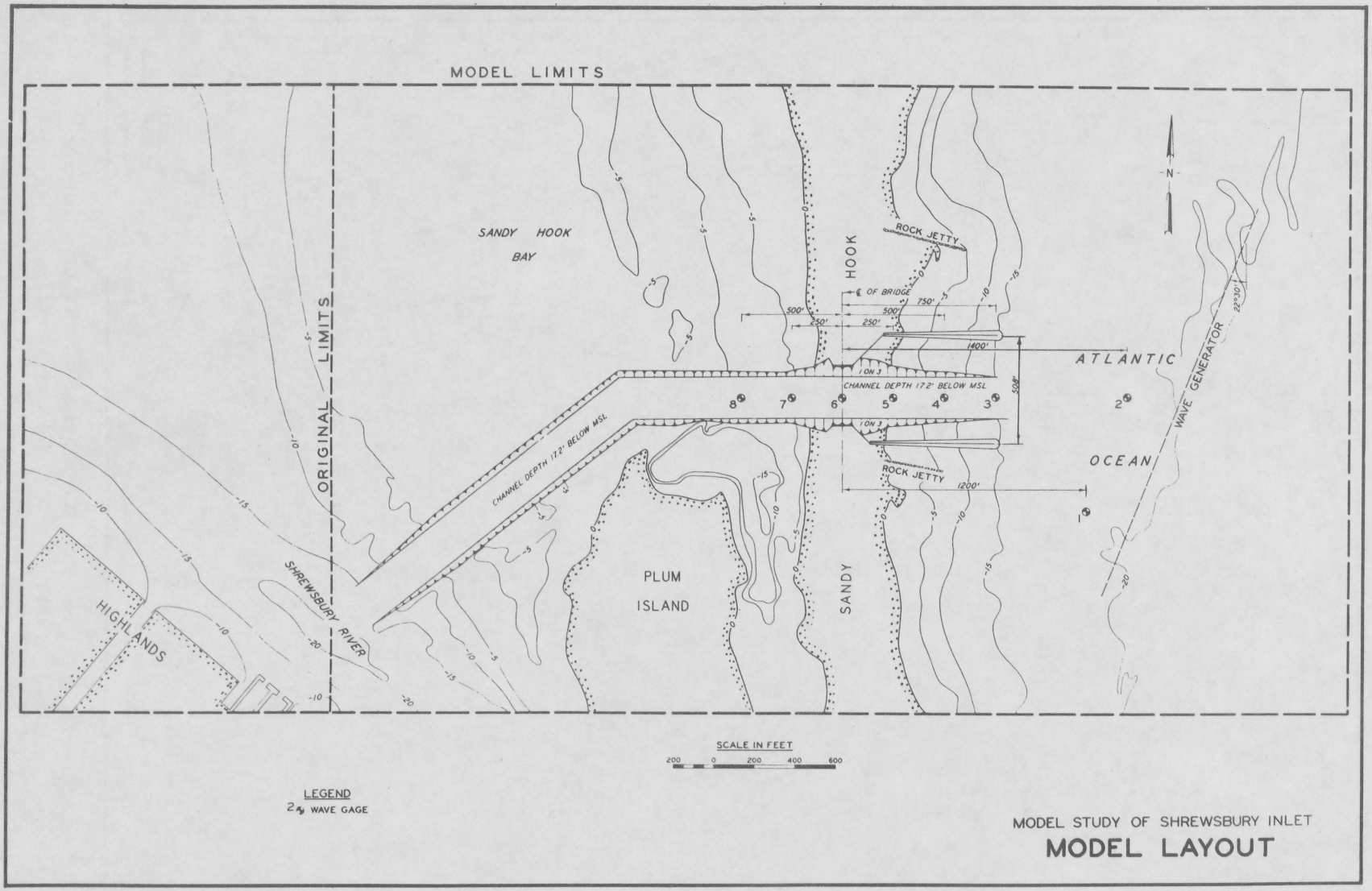

Figure 3-65. Undistorted-scale model of Shrewsbury Inlet (after McNair and Hill, 1972).

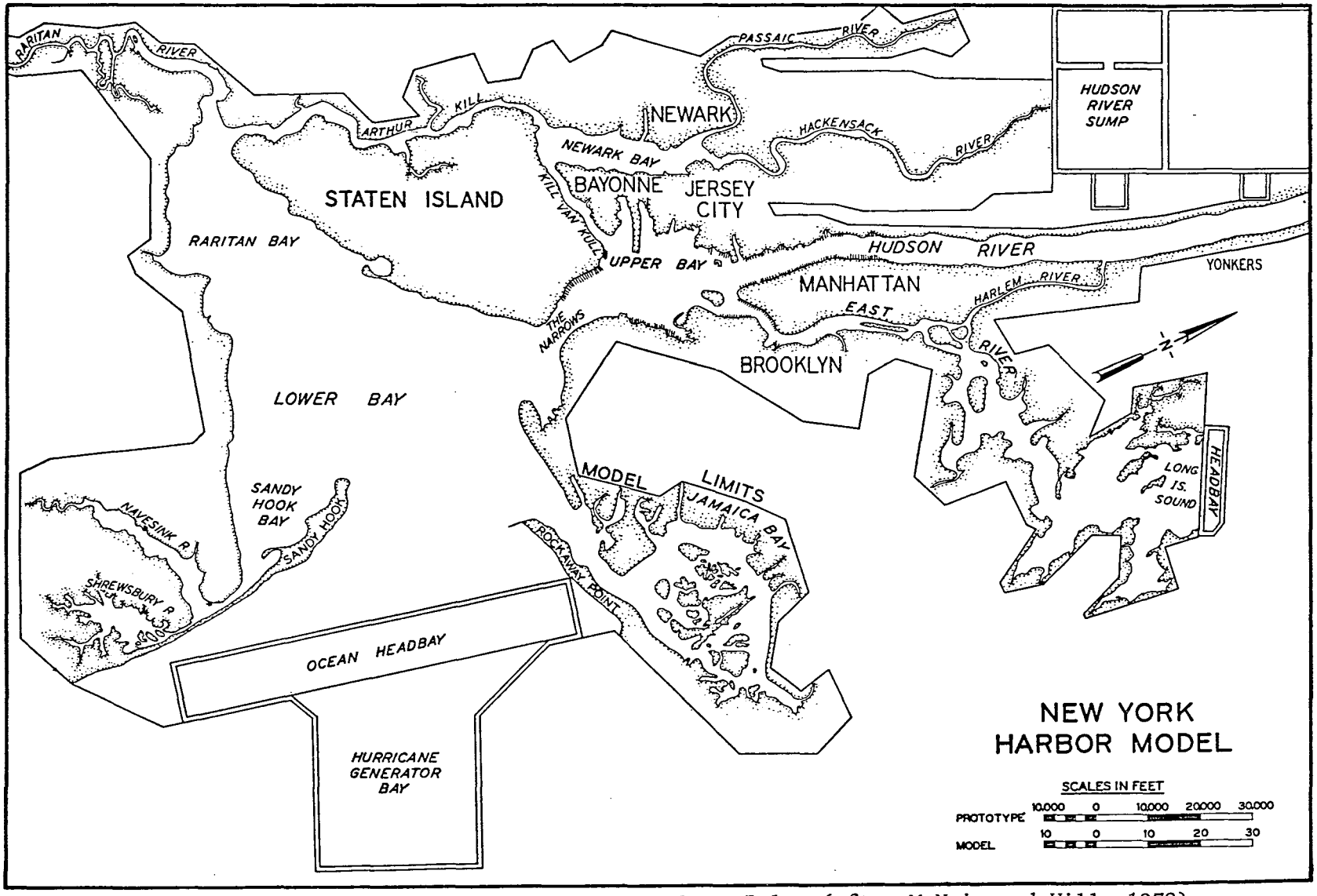

Figure 3-66. Distorted-scale model of Shrewsbury Inlet (after McNair and Hill, 1972).

Hook Bay, with specific reference to the locations of marinas near Highlands, New Jersey. The comprehensive model was used to determine the effects of the new inlet on normal tides, hurricane surges, tidal currents, salinities, temperatures, and the concentrations of pollutants in the study area for various input sources of pollution.

(9) Summary of Test Results. The following results of the model tests are summarized to provide a quick appraisal of the effects of the new inlet on various environmental factors. Table 3-4 shows the effects of the new inlet on average salinities in the major compartments of the study area (Sandy Hook Bay, Shrewsbury River, and Navesink River). The maximum change in average salinity amounted to about 0.3 part per thousand.

Table 3-4. Effects of plan 3 on average salinities.

Test	Chlorides[1]		
	Sandy Hook Bay	Navesink River	Shrewsbury River
Base	16.0	14.3	14.9
Plan 3	16.1	14.0	15.1

[1] Parts per thousand.

The effects of the new inlet on normal tides at three locations in the study area are shown in Figure 3-67 (note that normal tides were essentially unaffected). The effects on water surface elevations for a test involving reproduction of the November 1950 hurricane surge in the harbor are shown in Figure 3-68. The maximum elevation of the surge was not changed by the new inlet, but outflow through the new inlet allowed surge elevations in Sandy Hook Bay to drop slightly faster than for existing conditions.

Figure 3-69 shows current velocities over a complete tidal cycle at three locations in the study area (see Fig. 3-64 for location of stations). Current velocities were not changed significantly by the new inlet, although the time phasing of the current at a station near the new inlet (R2-W) was modified. This information, together with the tidal data, show conclusively that the new inlet would not change existing flow rates and volumes of inflow and outflow between Sandy Hook Bay and Shrewsbury and Navesink Rivers. The inflow and outflow control would remain in the relatively small channel connecting Sandy Hook Bay with the Shrewsbury and Navesink Rivers, and dredging of the new inlet would not change this control section in any way.

Figure 3-70 shows the effects of the new inlet on the rate of change in temperature in the study area for conditions simulating an upwelling of cold ocean water off Sandy Hook (a fairly common occurrence). The rate at which water temperatures decreased in the study area because of such upwelling was essentially the same with the new inlet installed as for existing conditions, thus indicating that the new inlet would have no significant effects on water temperature.

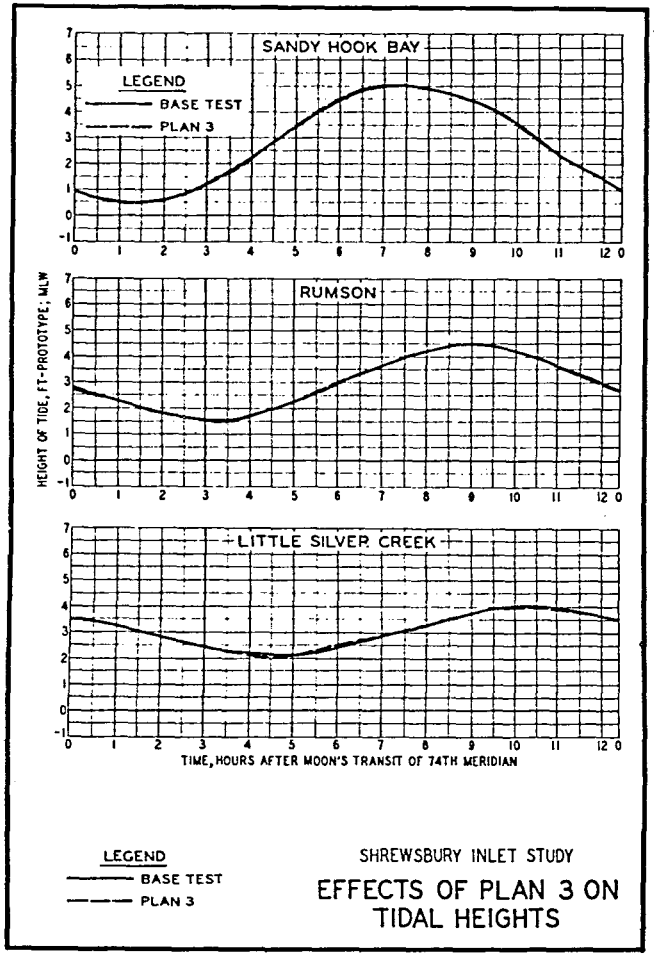

Figure 3-67. Effects of Shrewsbury Inlet on tides (after McNair and Hill, 1972).

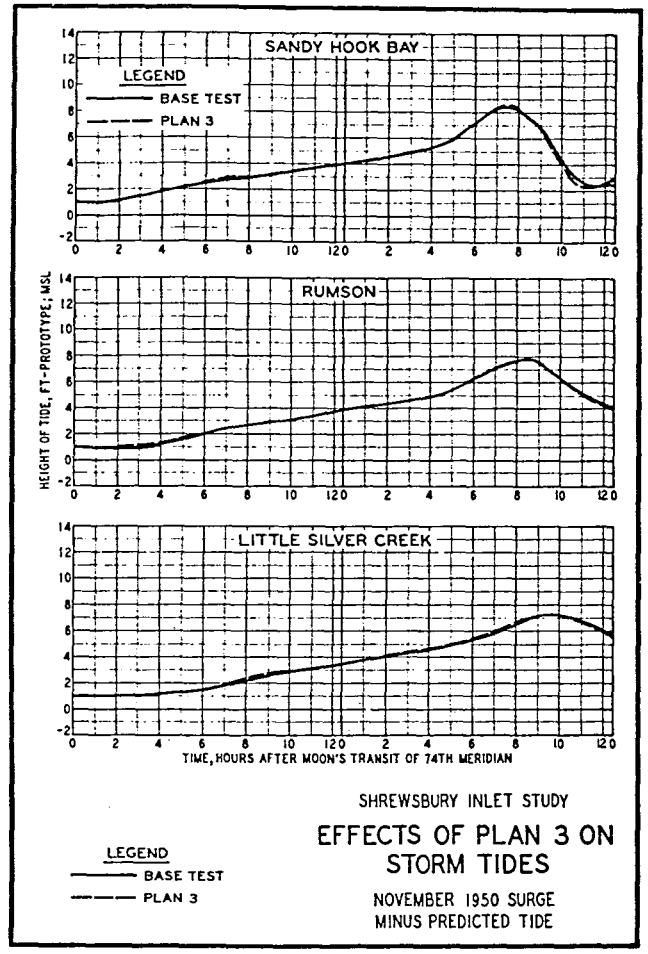

Figure 3-68. Effects of Shrewsbury Inlet on surges (after McNair and Hill, 1972).

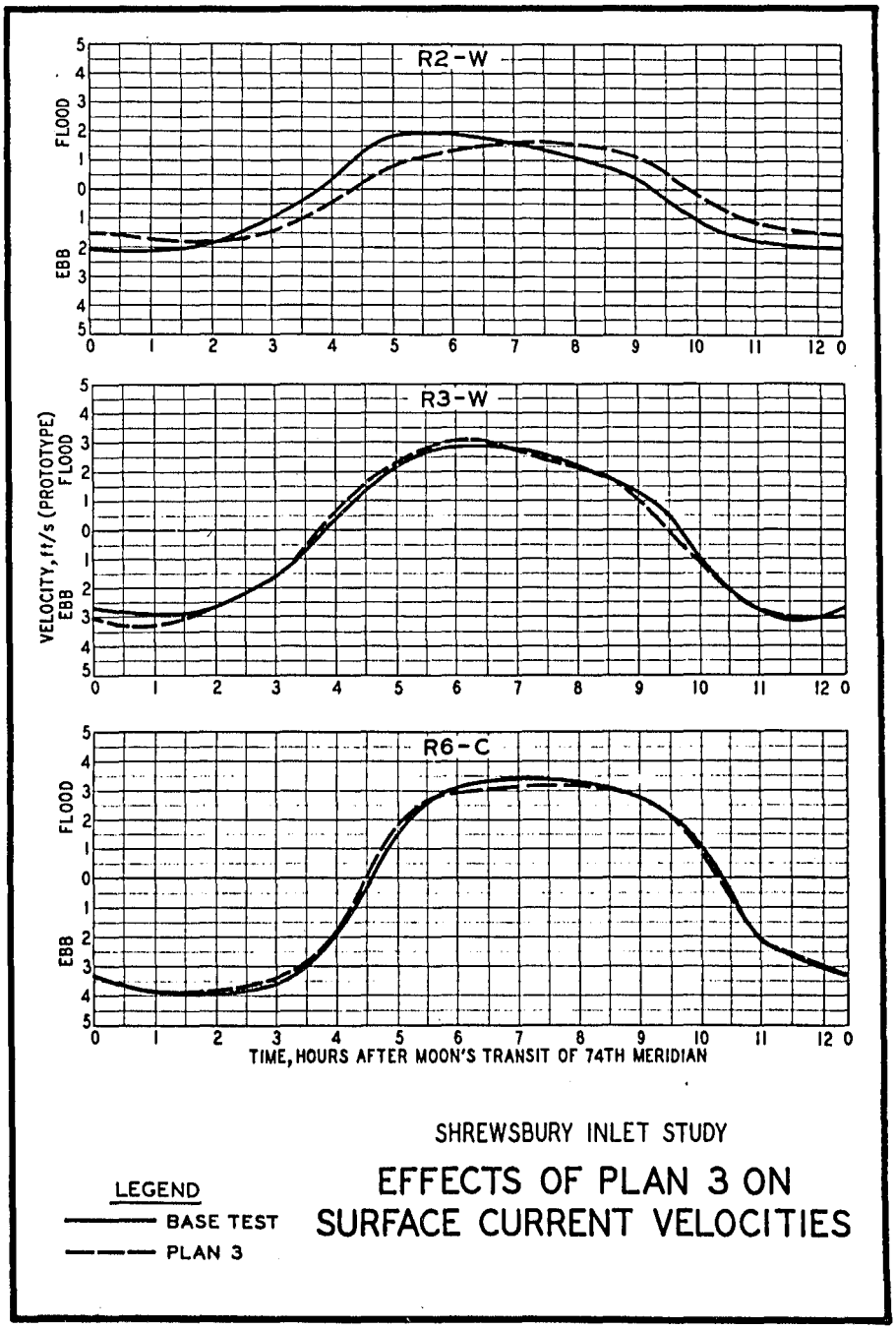

Figure 3-69. Effects of Shrewsbury Inlet on velocities (after McNair and Hill, 1972).

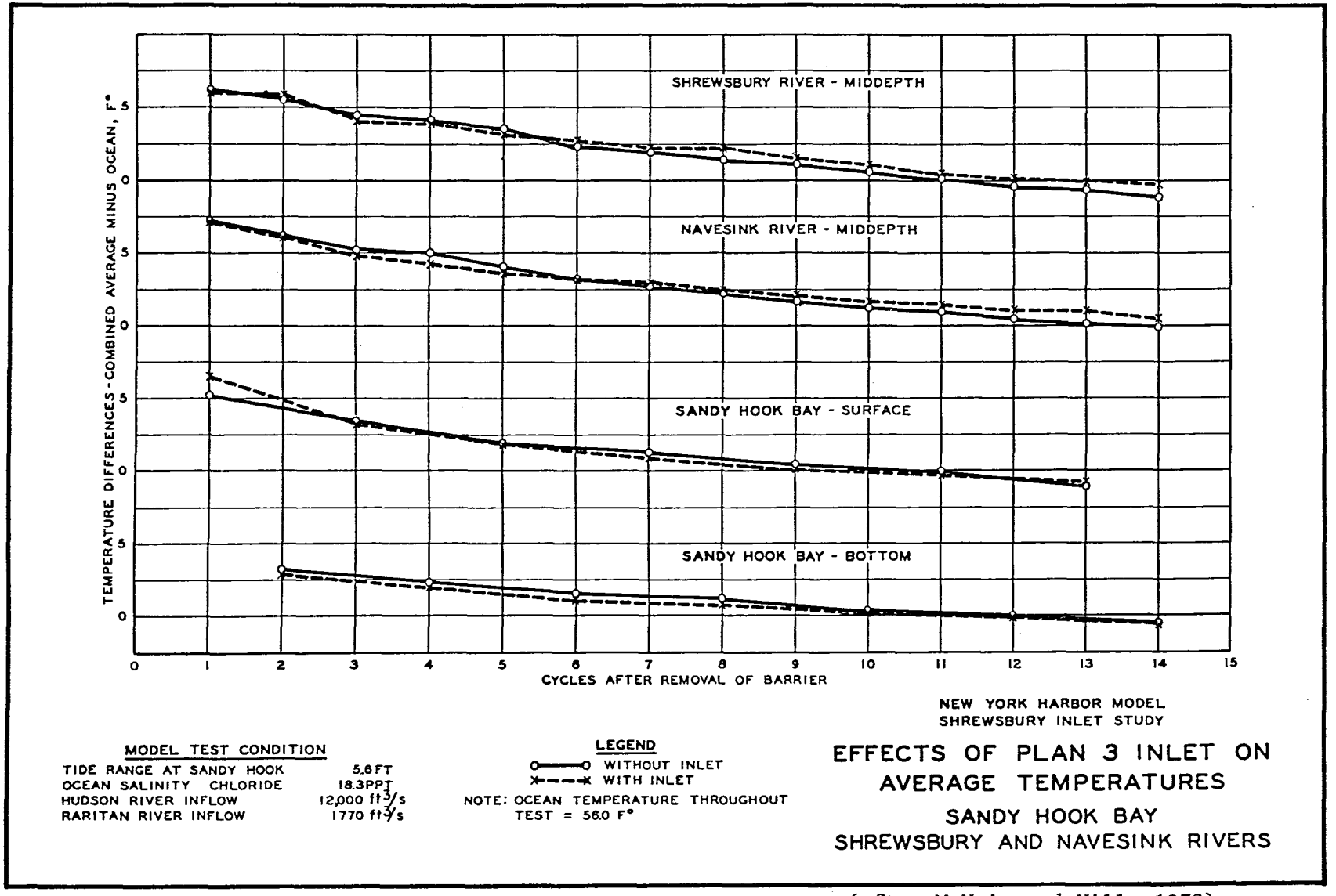

Figure 3-70. Effects of Shrewsbury Inlet on temperatures (after McNair and Hill, 1972).

Three separate tests were made to evaluate the effects of the new inlet on pollution concentrations in the study area. Test results are summarized in Table 3-5. One pollution source was simulated in Raritan Bay (see Fig. 3-64 for location of release point), representing the effluents discharged from the Middlesex County Trunk Sewer Outfall. Pollution concentrations from that source were lower in all three of the major water bodies of the study area with the new inlet installed; this showed that the new inlet would reduce the influx of Raritan Bay wastes to the study area. Table 3-5 presents the results of a similar test series, but simulating the major sewer outfalls in Upper New York Bay (see Fig. 3-64). For this source of pollution, concentrations in all three major water bodies of the study area were increased. Table 3-5 also presents the results of the third pollution test series, for which the local sources of pollution input in the Shrewsbury and Navesink Rivers were simulated (see Fig. 3-64.). For conditions of these local sources, concentrations throughout the study areas were substantially reduced.

Table 3-5. Effects of plan 3 on average dye concentrations.[1]

Test	Sandy Hook Bay	Navesink River	Shrewsbury River
Raritan Bay[2]			
Base	186	99	102
Plan 3	174 (−6 pct)	94 (−5 pct)	96 (−6 pct)
Upper New York Bay[2]			
Base	1,039	649	694
Plan 3	1,072 (+3 pct)	862 (+33 pct)	854 (+23 pct)
Navesink River[2]			
Base	55	372	82
Plan 3	45 (−18 pct)	285 (−24 pct)	39 (−53 pct)
Shrewsbury River[2]			
Base	71	129	634
Plan 3	48 (−33 pct)	75 (−42 pct)	356 (−44 pct)

[1]Dye concentrations in parts per billion;
Initial concentrations = 100,000 parts per billion.

[2]Pollution source.

The reduction in pollution concentrations in the study area from the Raritan Bay source is attributed to the fact that tidal flow in and out of the new inlet reduces the present exchange of flow between Lower New York Bay and Sandy Hook Bay; therefore, less of the polluted water of Lower New York Bay is drawn into the study area. The increase in pollution levels in the study area from Upper New York Bay pollution sources is caused by pollutants (from this source) which disperse largely into the ocean; a small percentage of this waste is then transferred from the ocean to the study area by tidal exchange through the new inlet. The peak dye concentration thus arrived in the study area later during the

plan test than during the base test. Subsequent analysis of the data by the Environmental Protection Agency (EPA) indicated that, because pollutants actually decay with time, water quality in the area would actually be improved as a result of the delay in arrival time. The substantial reduction in pollution from local sources is caused by pollutants flowing out through the new inlet during ebb currents but not completely returning during the subsequent flood currents; thus, the rate of flushing of such pollutants is much faster with the new inlet in place. In summary, the new inlet would reduce pollution concentrations in the study area from all of the three principal sources.

It is emphasized that the actual test data obtained from the model were very comprehensive in nature. Tides, current velocities, and salinities were measured at hourly intervals or less over complete tidal cycles at many stations throughout the study area, and current velocities and salinities were measured at several points in the vertical at each station. In the dye-tracer tests simulating pollutants, surface and bottom samples were obtained for analysis at more than 100 stations in and adjacent to the study area. Time-exposure photos showing surface current patterns and velocities were obtained at hourly intervals throughout the tidal cycle in the new inlet and in all adjacent areas where flows could be affected by the new inlet. All of these test data were furnished to Federal, State, and local agencies concerned with the effects of the inlet on the water quality.

i. Hurricane Surge Protection--Galveston Bay.

(1) Project. Construction of a hurricane surge protection barrier.

(2) References. Marinos and Woodward (1968); Reid and Bodine (1968); Brogdon (1969); Bobb and Boland (1970a, 1970b); Sager and McNair (1973a, 1973b); and Section VII,8,b of this report.

(3) Laboratory. WES (physical models); U.S. Army Engineer District, Galveston, and Texas A&M University (mathematical model).

(4) Test Period. January 1965 to April 1970.

(5) Problem. The Texas coast frequently experiences hurricane surges; therefore, consideration had to be given to protection of this area from inundation resulting from storm surges. A long-range plan was developed by the U.S. Army Engineer District, Galveston, to investigate the feasibility of construction of such protection with the initial effort directed toward the problems surrounding the Galveston Bay complex. The design of an adequate protection system involves not only reducing water heights resulting from hurricane surges, but many other factors such as salinity conditions in the bay, effects of the plan on flushing and circulation characteristics, fish and wildlife, navigation requirements, and flooding of the bay during periods of high upland discharge.

(6) Purpose of Model Study. The physical model studies were conducted to (a) determine the effects of all proposed structures on

normal tides and hurricane surge heights upstream and downstream from barrier sites, current velocities throughout the bay system, the salinity regimen of the bay, and the rates of diffusion and flushing of pollutants discharging into the bay; and (b) provide data that were in turn used to calibrate and improve the numerical model and its capability of predicting surge elevations at other locations along the Texas coast.

(7) Physical Models. At the conception of the Galveston Bay surge study, an existing model of the Houston Ship Channel (Fig. 3-71), constructed to scales of 1:60 vertically and 1:600 horizontally, was available for studies on barrier effects on normal tides, currents, salinities, and dispersion patterns throughout the bay and to determine the number and position of tidal openings in that part of the barrier crossing the bay. This model did not reproduce the entire bay complex and was not equipped with the necessary apparatus for generating hurricane surges. Because it was not economically feasible to add this capability and expand the model, a second general model was constructed for the sole purpose of investigating the effects of the hurricane barriers on surge elevations resulting from a hurricane approaching from the gulf. Since a greater degree of distortion was possible for this type of investigation; the model was constructed to scales of 1:100 vertically and 1:3,000 horizontally. This model (Fig. 3-72) was referred to as the Galveston Bay hurricane surge model. Each of the general models was equipped with the necessary apparatus to satisfactorily reproduce normal tides, current velocities and patterns, and freshwater inflow. In addition, the Houston Ship Channel model was capable of reproducing salinity intrusion and flushing characteristics, and the Galveston Bay surge model was equipped with a hurricane surge generator. Several section models were constructed in a flume (Fig. 3-73) to determine the discharge characteristics of the existing barrier beaches and the proposed navigation and tidal barrier openings. The undistorted-scale section models were constructed to a scale of 1:100; the distorted-scale section models were constructed to the same scales as the Houston Ship Channel model or the Galveston Bay surge model, as appropriate.

(8) Test Procedures. Before initiating testing for the barrier studies, each model had been adjusted to satisfactorily reproduce all pertinent prototype phenomena. The Galveston Bay surge model was adjusted using tide and velocity information obtained in the Houston Ship Channel model and hurricane surge elevation data collected by U.S. Army Engineer District, Galveston, personnel during Hurricane Carla. The prototype hurricane data were first subjected to a numerical analysis, in which the effects of local wind and normal tide were removed. The Galveston Bay surge model was then adjusted to reproduce these modified prototype surge data. Each navigation opening and typical tidal openings to be tested were first calibrated in an undistorted-scale section model to determine the discharge characteristics. The openings were then subjected to similar tests in a distorted-scale section model. During these latter tests, the size or shape of the model openings were adjusted to achieve the same discharge characteristics as determined in the undistorted-scale calibration tests. Photos of the undistorted- and distorted-scale models of the Alpha barrier navigation opening are shown

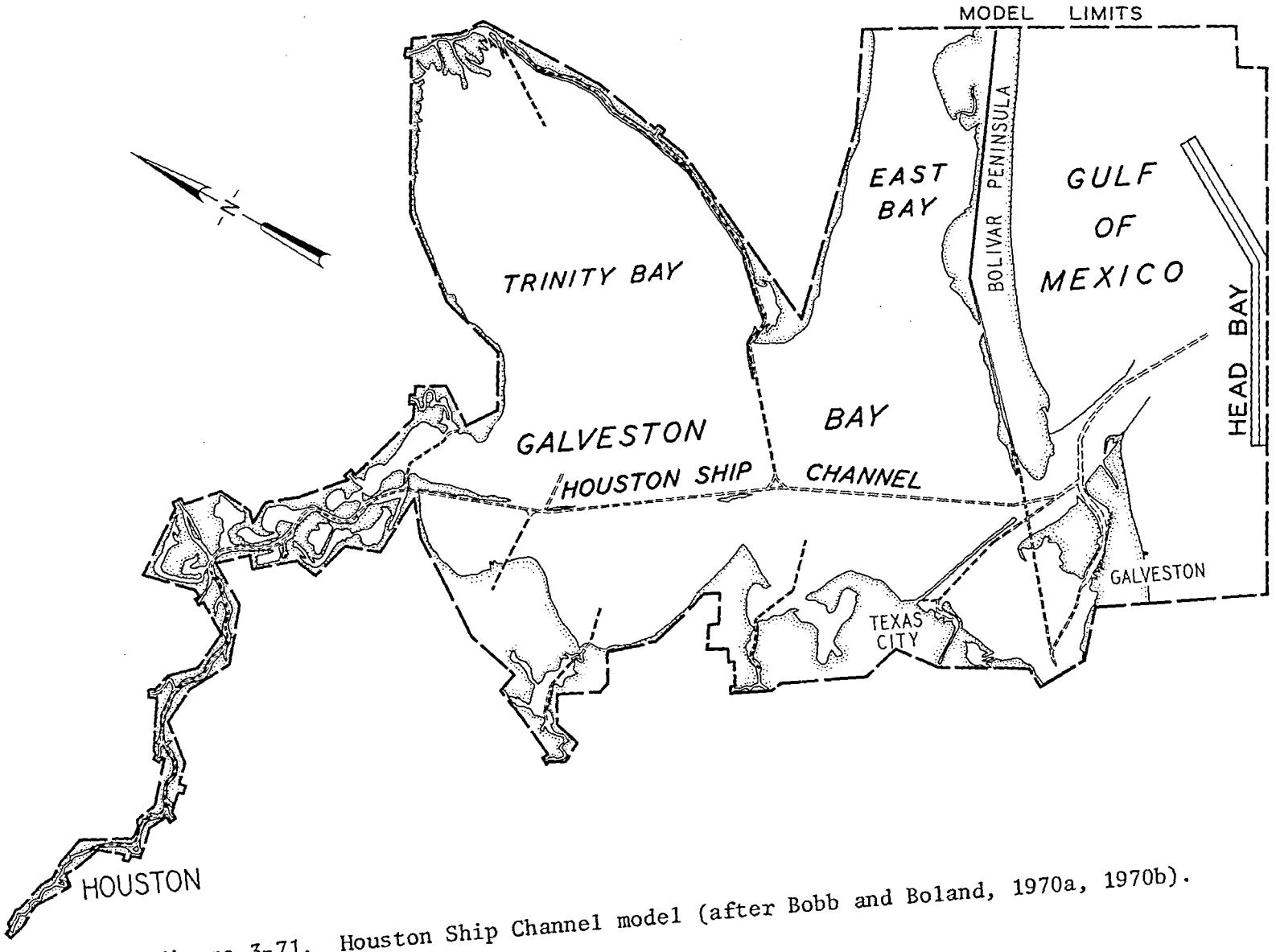

Figure 3-71. Houston Ship Channel model (after Bobb and Boland, 1970a, 1970b).

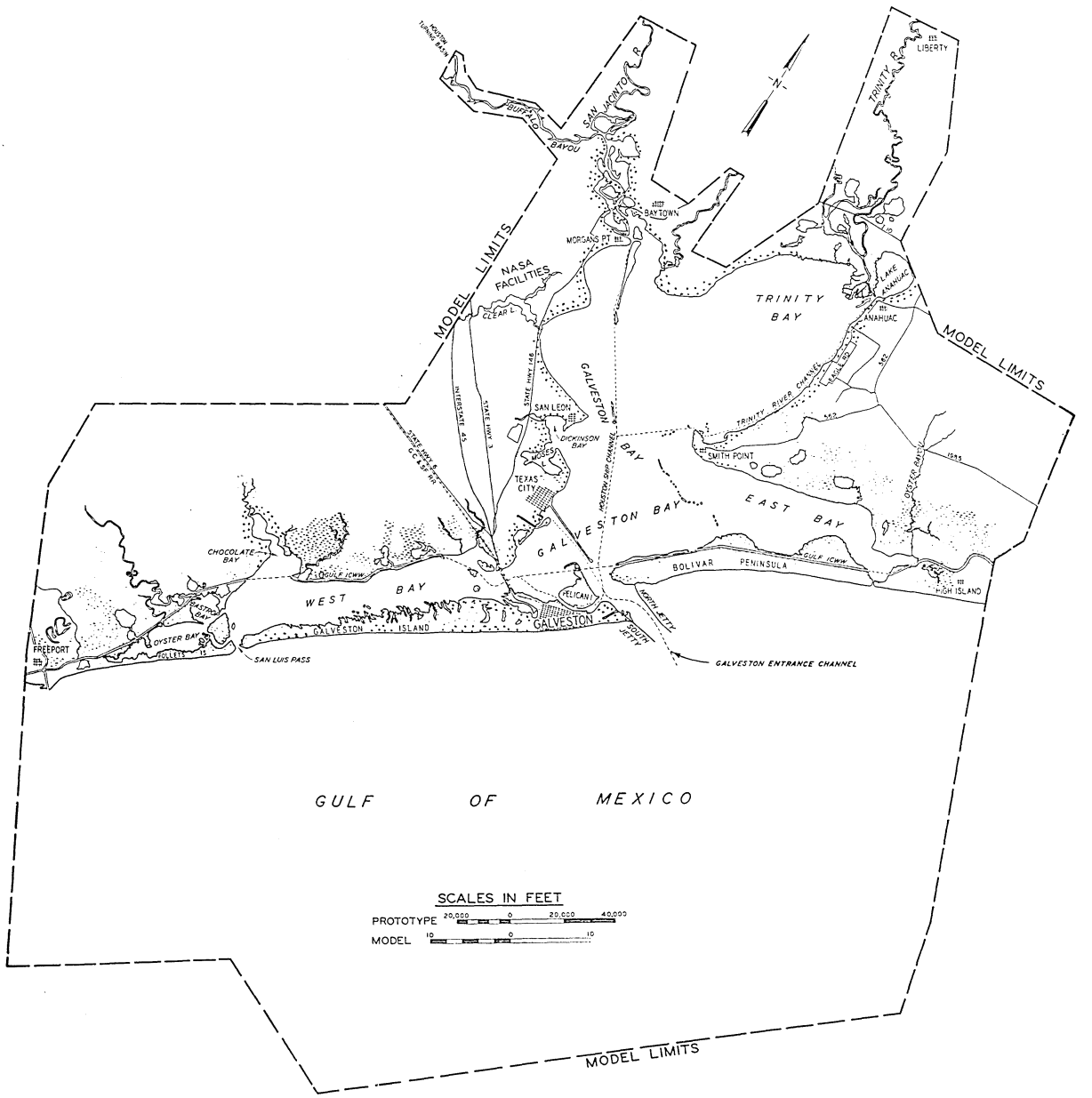

Figure 3-72. Galveston Bay surge model (after Brogdon, 1969).

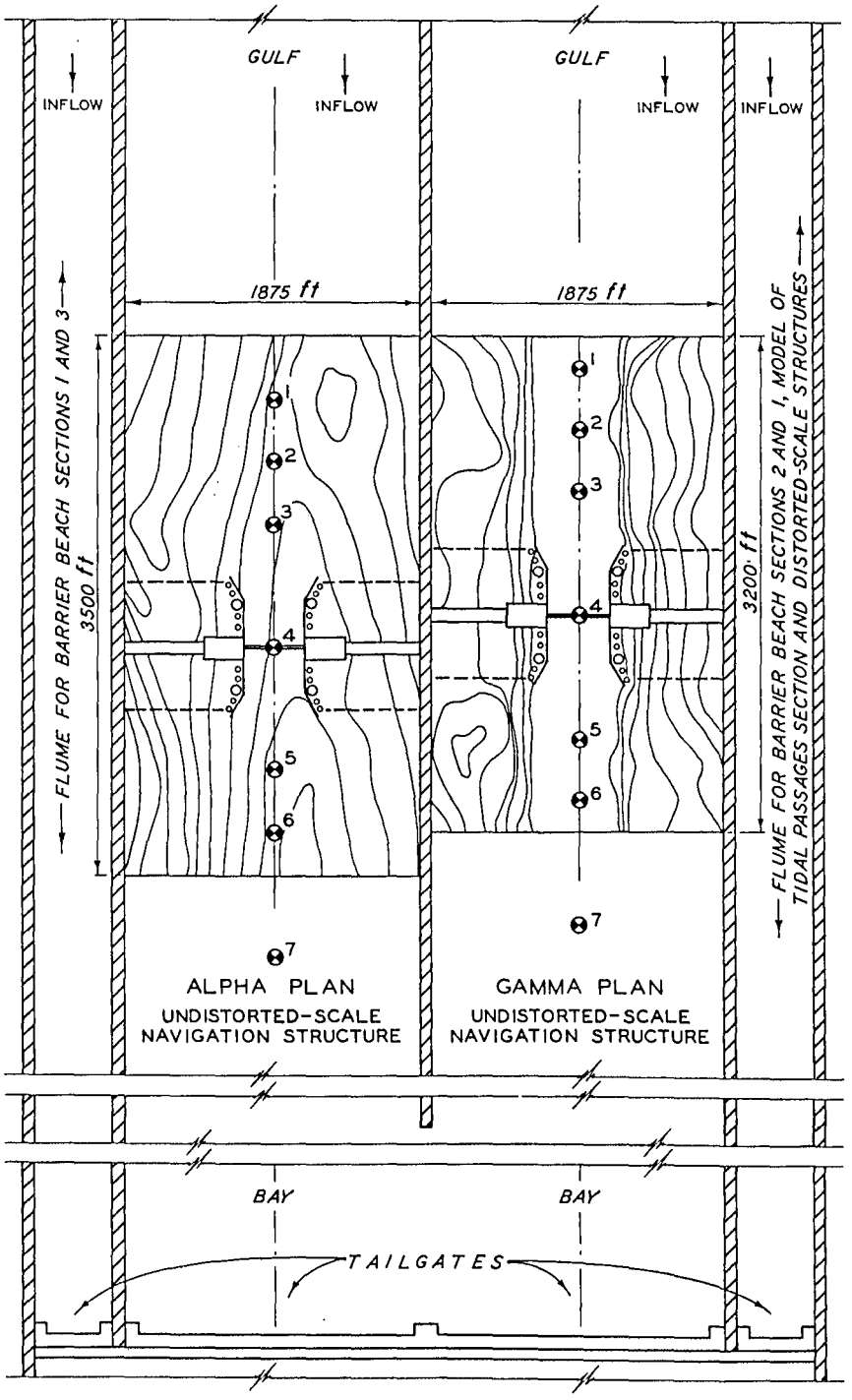

Figure 3-73. Galveston Bay surge study section models (after Sager and McNair, 1973a, 1973b).

in Figure 3-74. Various barrier beach sections were also subjected to undistorted-scale flume tests to determine the appropriate discharge characteristics for use in the mathematical model. Similarly, the Houston Ship Channel model was subjected to detailed tests to determine the discharge characteristics of the entrance and barrier beaches for use in the mathematical model.

(9) Summary of Test Results. The testing program in the surge model consisted of tests with two major barrier plans, designated Alpha and Gamma. The locations of the two plans and two representative tide gages are shown in Figure 3-75. The Alpha plan barrier was located generally just behind the gulf beaches and would protect all low-lying areas adjacent to Galveston Bay complex and tributaries. The Gamma plan barrier was located about 9 miles upstream from the entrance and afforded no protection to the barrier beaches or other low-lying areas downstream of the barrier, including Galveston. These two barriers were tested with gated and ungated navigation openings for three hurricane surge conditions. Since the tidal flow gates would be closed by the time a hurricane surge came inland, only navigation openings in the barriers were involved in surge tests.

Figure 3-76 shows a comparison of three hurricane surge histories at a point near the Galveston Bay entrance. One of the hurricane surges investigated represented a hypothetical (design) surge resulting from a large radius, slow translation (LRST) hurricane that would generate a maximum surge of about 10.5 feet at the Galveston Bay entrance about 100 hours after the wind field arrived at the Continental Shelf. This type of hurricane, even though the peak elevation was lower than the large radius, high translation (LRHT) hurricane, resulted in higher surge elevations landward of the barriers. This is attributed to the slow approach speed of the storm, which allows a gradual water level buildup behind the barriers as a result of the long period of flow through the navigation opening. Typical results of tests conducted with this slow storm and the Gamma and Alpha barriers are shown in Figures 3-77 and 3-78, respectively.

The results of studies conducted on the Galveston Bay surge model indicated that both the Alpha and Gamma hurricane barrier schemes would effectively protect upstream areas from damage caused by hurricane surges originating in the Gulf of Mexico. The degree of protection afforded would be significantly greater with a gated navigation opening than with an ungated opening. The ungated Alpha barrier would provide better protection than the ungated Gamma barrier.

The Houston Ship Channel model (Fig. 3-71) was used to investigate the effects of the two barrier plans (Alpha and Gamma) on tides, currents, salinities, and dye dispersion within the bay system. Tests conducted with the proposed Alpha design plan (Fig. 3-79) indicated no significant effects on tidal elevations, ranges, or times. Maximum current velocities in the navigation opening would be about 4.7 feet per second. Tests further showed that a 20-percent reduction of total area of tidal passages proposed in the original design caused this maximum velocity to be increased to about 5.1 feet per second (which is considered about the

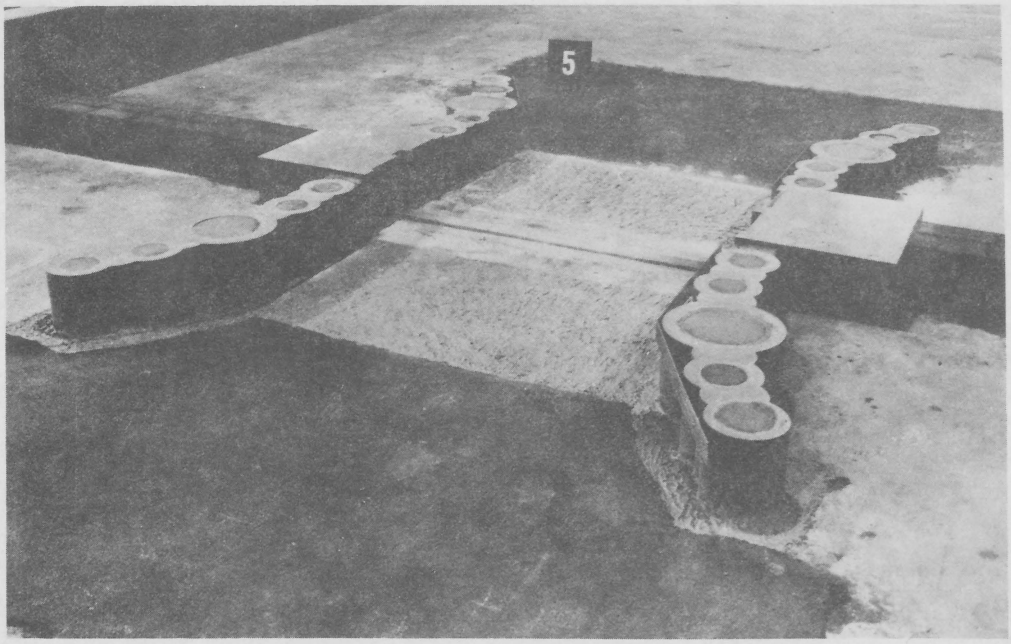

ALPHA PLAN, UNDISTORTED-SCALE MODEL
OF THE NAVIGATION STRUCTURE

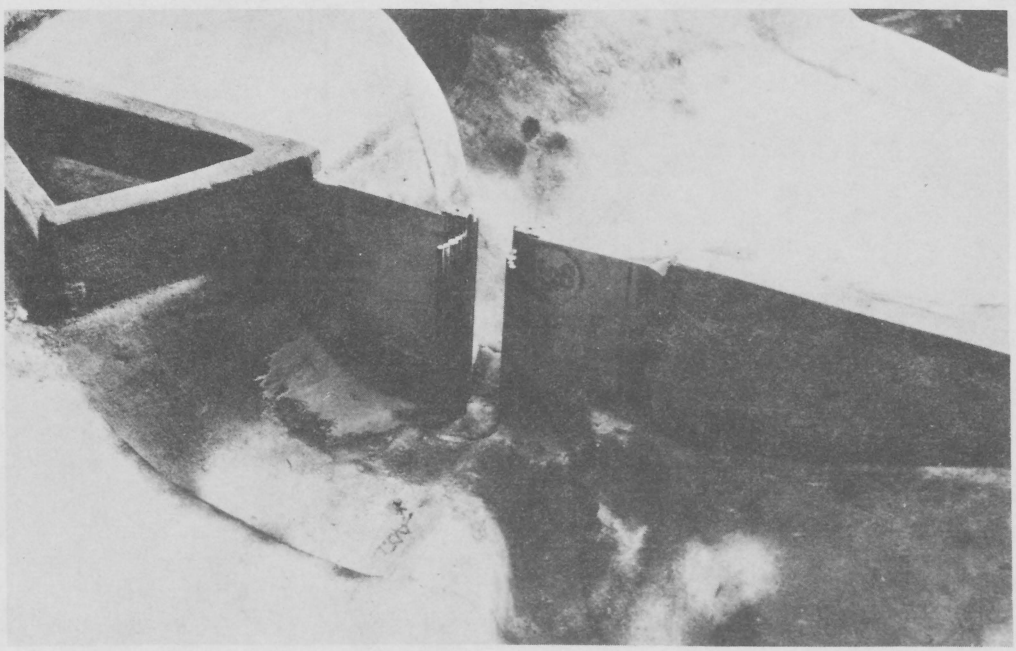

ALPHA PLAN, DISTORTED-SCALE MODEL OF THE
NAVIGATION STRUCTURE, GENERAL VIEW FROM THE GULF

Figure 3-74. Alpha plan navigation structures, Galveston Bay (Sager and McNair, 1973a).

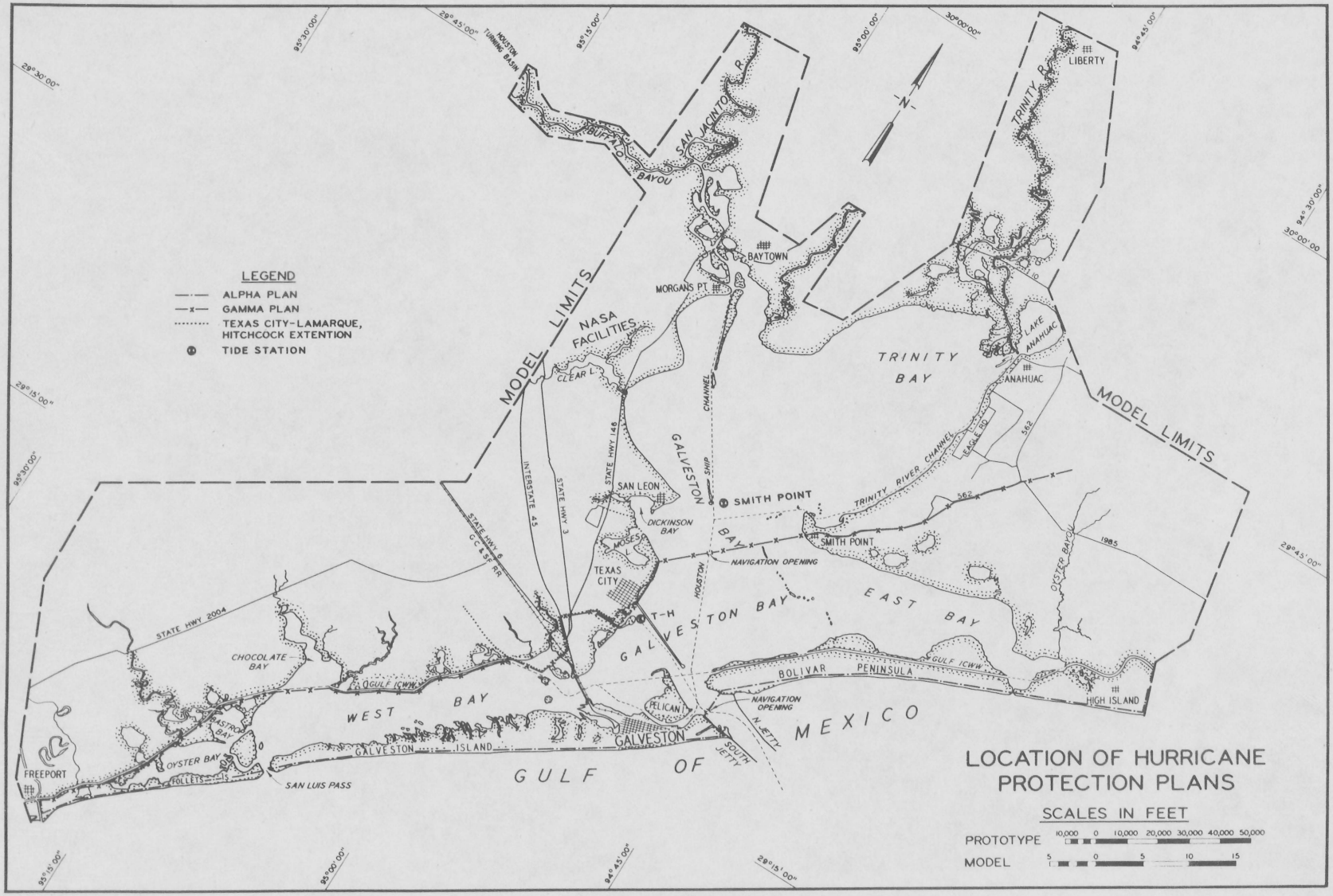

Figure 3-75. Proposed hurricane surge protection barriers, Galveston Bay (after Brogdon, 1969).

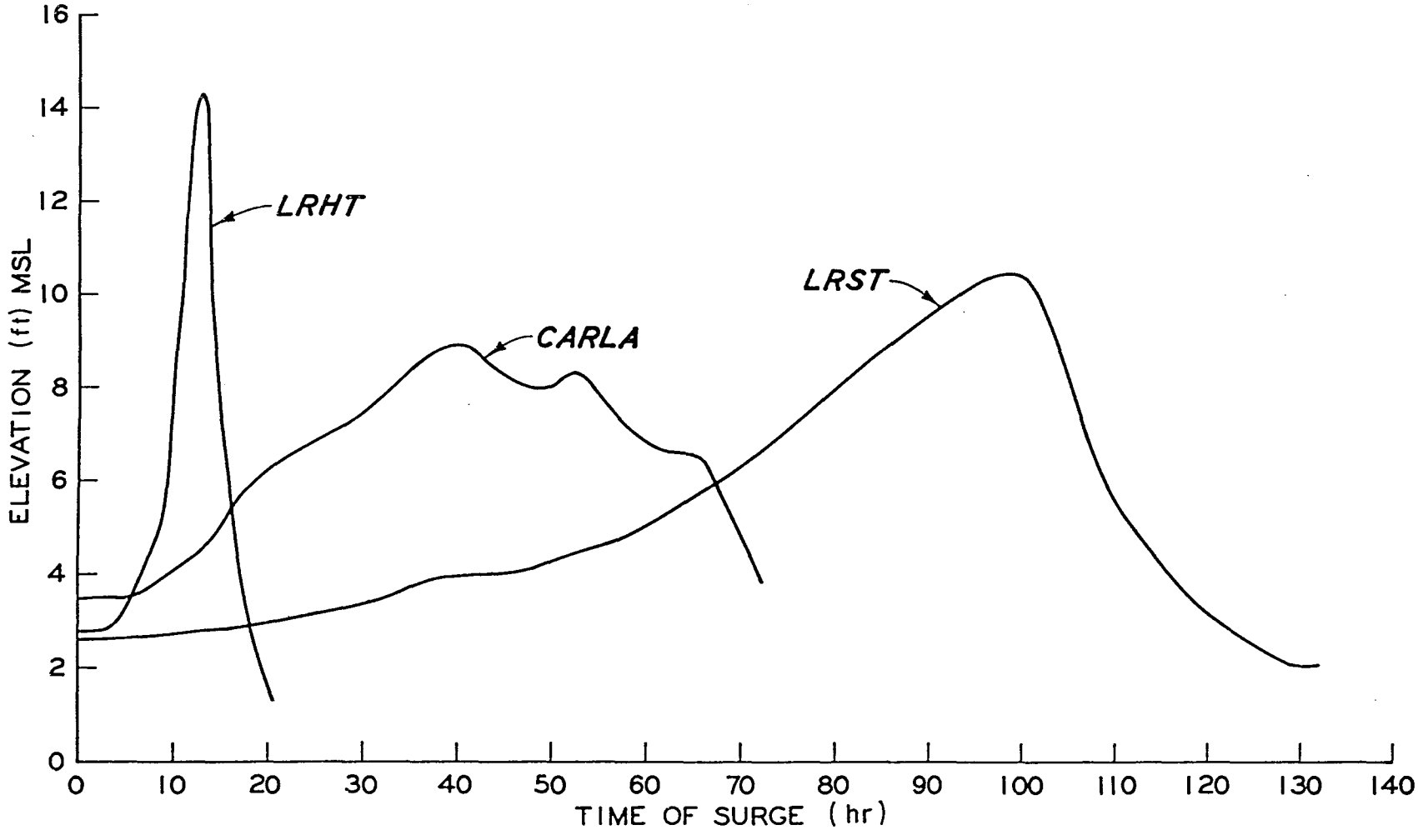

Figure 3-76. Hurricane surge histories, Galveston Bay entrance (after Brogdon, 1969).

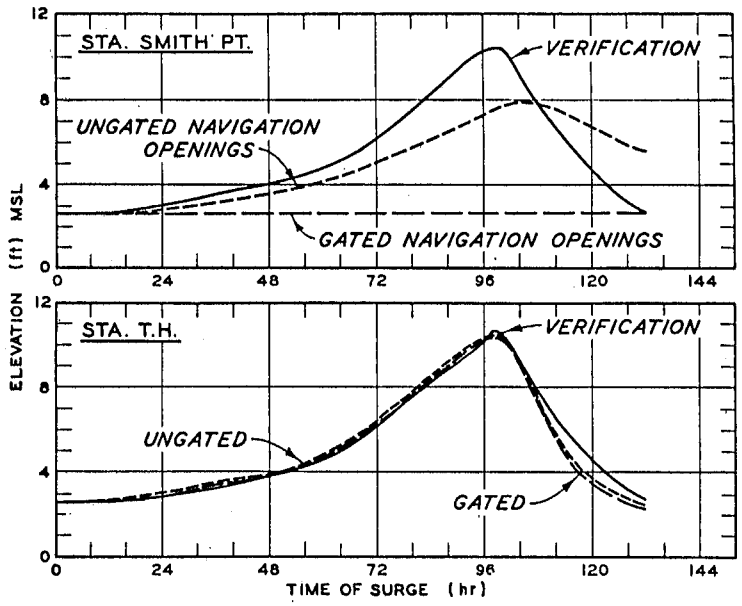

Figure 3-77. Effects of Gamma plan on LRST surge, Galveston Bay (after Brogdon, 1969).

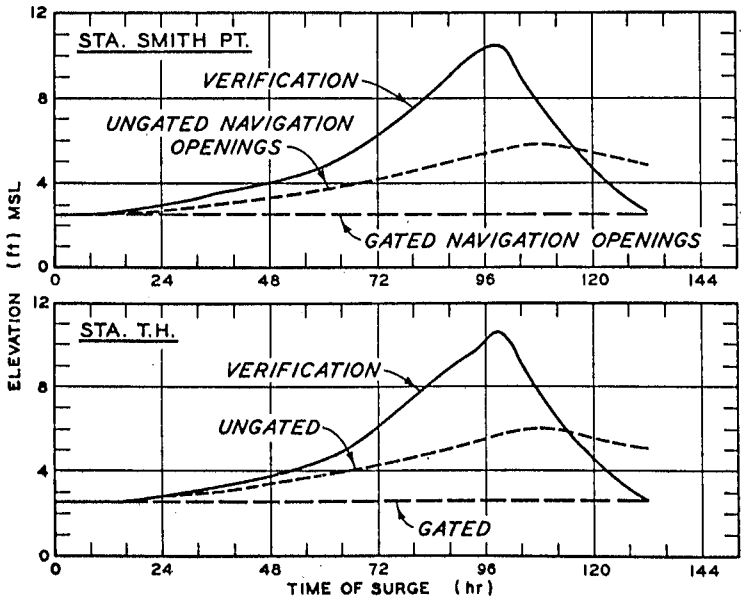

Figure 3-78. Effects of Alpha plan on LRST surge, Galveston Bay (after Brogdon, 1969).

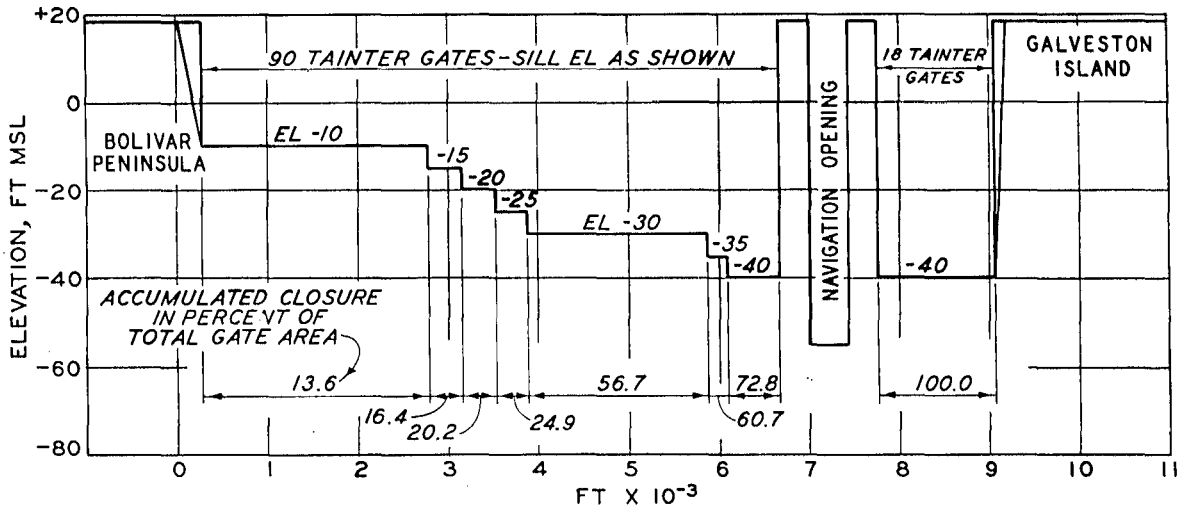

Figure 3-79. Proposed Alpha plan structure, Galveston Bay (Bobb and Boland, 1970a).

maximum allowable for safe navigation), with no significant effects on salinity conditions and on dispersion patterns or rates.

The Gamma barrier (Fig. 3-80) as originally designed would cause tidal ranges downstream of the barrier to increase, the mean tide level to lower, tidal ranges upstream of the barrier to reduce, the tidal prism upstream to reduce, salinities upstream of the barrier to reduce, and concentration of the effluent from the ship channel upstream of Morgan Point to increase (all changes were slight). However, dispersion patterns were relatively unaffected and maximum current velocities were below the maximum allowable. The test results showed that the total cross-sectional area of the tidal passages was not sufficient. Both design barrier plans were subjected to further testing to determine the configuration and total cross-sectional area of the tidal passages required to achieve the minimum effects on conditions within the system.

j. Upstream Flow Regulation--Delaware River.

(1) Project. Regulation of Delaware River freshwater discharge by construction and operation of the proposed Tocks Island Dam.

(2) References. U.S. Army Engineer Waterways Experiment Station (1956); Simmons, Harrison, and Huval (1971).

(3) Laboratory. WES.

(4) Test Period. July and September 1966.

(5) Problem. Since operation of the proposed Tocks Island Dam would modify the annual freshwater discharge characteristics of the Delaware River, it was necessary to determine the environmental impact of such action.

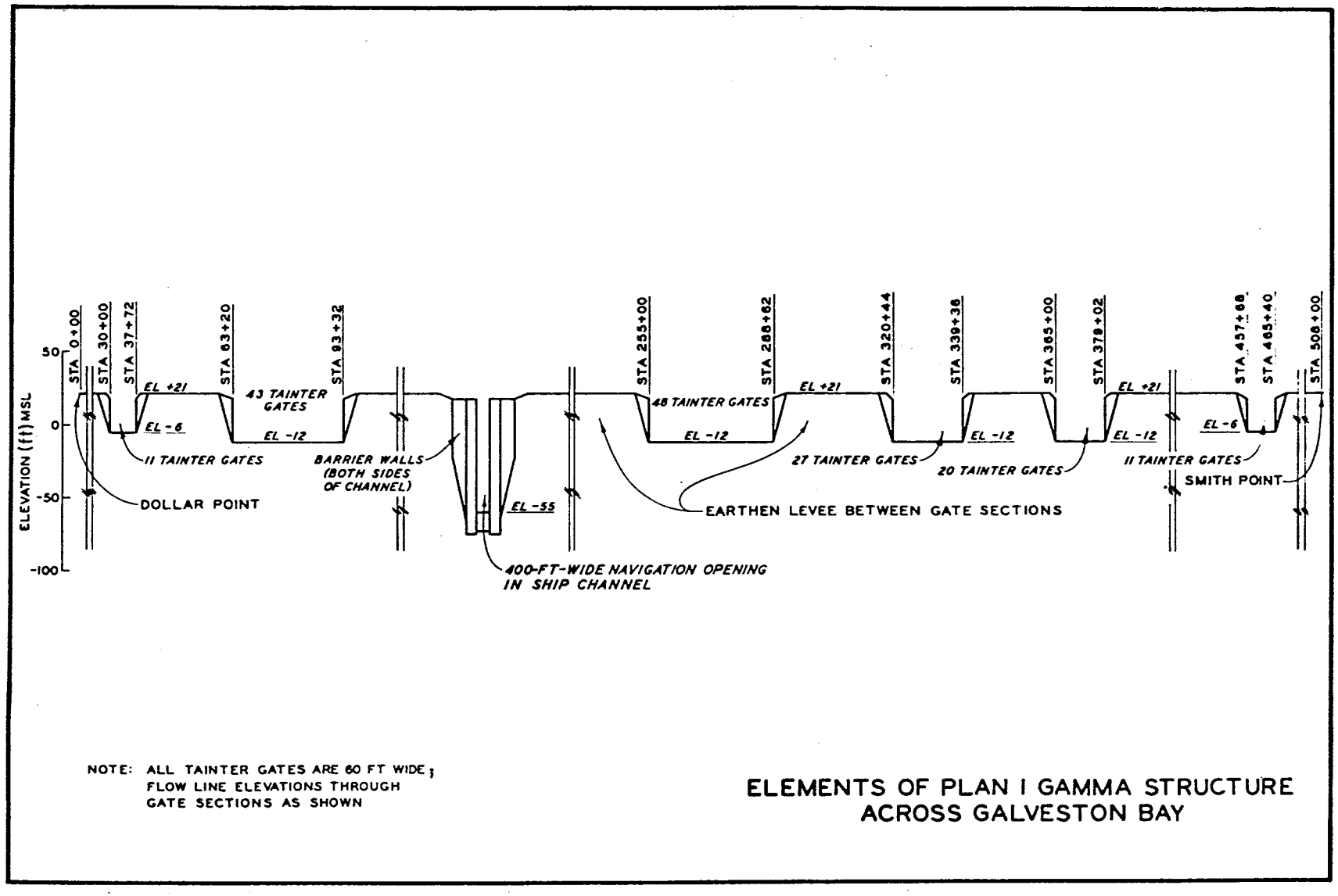

Figure 3-80. Proposed Gamma plan structure, Galveston Bay (Bobb and Boland, 1970a).

(6) Purpose of Model Study. The model study was conducted to determine the influence of modified freshwater inflow on the salinity regimen of the Delaware River estuary.

(7) The Model. The existing Delaware River model (Fig. 3-56) was used; model scales were 1:1,000 horizontally and 1:100 vertically.

(8) Test Procedures. A detailed salinity reverification of the Delaware River model was accomplished before conducting the tests, using freshwater inflows and salinities measured in the prototype between 1 March and 30 November 1965. In the test to determine the effects of Tocks Island Dam on salinity conditions in the estuary, the observed 1965 freshwater hydrograph was modified to reflect the program of storage and release that would have been followed if Tocks Island Dam had been in operation during 1965.

(9) Summary of Test Results. When all necessary field measurements were available, tests were conducted in the Delaware River model to determine what revisions (if any) were needed to reproduce the actual rate of advance of the salinity front and the maximum upstream location of the 250 isochlor for conditions of the 1965 drought. During this drought, a prolonged period of very low flow (about 2,000 cubic feet per second) occurred. After the initial check showed unsatisfactory agreement with the maximum extent of salinity intrusion, the U.S. Army Engineer District, Philadelphia, determined that an additional 200 cubic feet per second entered the river between Trenton and Torresdale as groundwater and well-water discharges. This is an insignificant part of the 12,000 cubic feet per second mean Delaware River flow at Trenton. However, 200 cubic feet per second is critical when drought flows occur on the order of 2,000 cubic feet per second. The model was found to correctly reproduce both the rate of advance and the maximum location of the 250 isochlor when this additional freshwater was introduced into the model.

With the exception of short-term fluctuations in prototype salinities, caused primarily by winds and other meteorological effects not simulated in the model tests, the agreement between model and prototype salinities was very close throughout the test period. Figure 3-81 shows a comparison of the location of the 250 parts per million chloride concentration (isochlor) in the model and prototype for the duration of the test with the natural 1965 hydrograph. The solid line in the figure shows the exact location of the 250 isochlor at high water slack in the model throughout the test, as determined from measurements made every second tidal cycle; the solid black points represent the locations of this concentration at high water slack in the prototype, as determined by the U.S. Army Engineer District, Philadelphia, on a monthly basis. The open points in Figure 3-81 represent the approximate locations of the 250 isochlor as determined from surface salinity profiles made in the prototype by several agencies during the test period. Comparison of model and prototype salinity time histories at selected stations for this reverification are shown in Figure 3-34. The agreement between model and prototype salinities was well within acceptable limits for the entire period of the test.

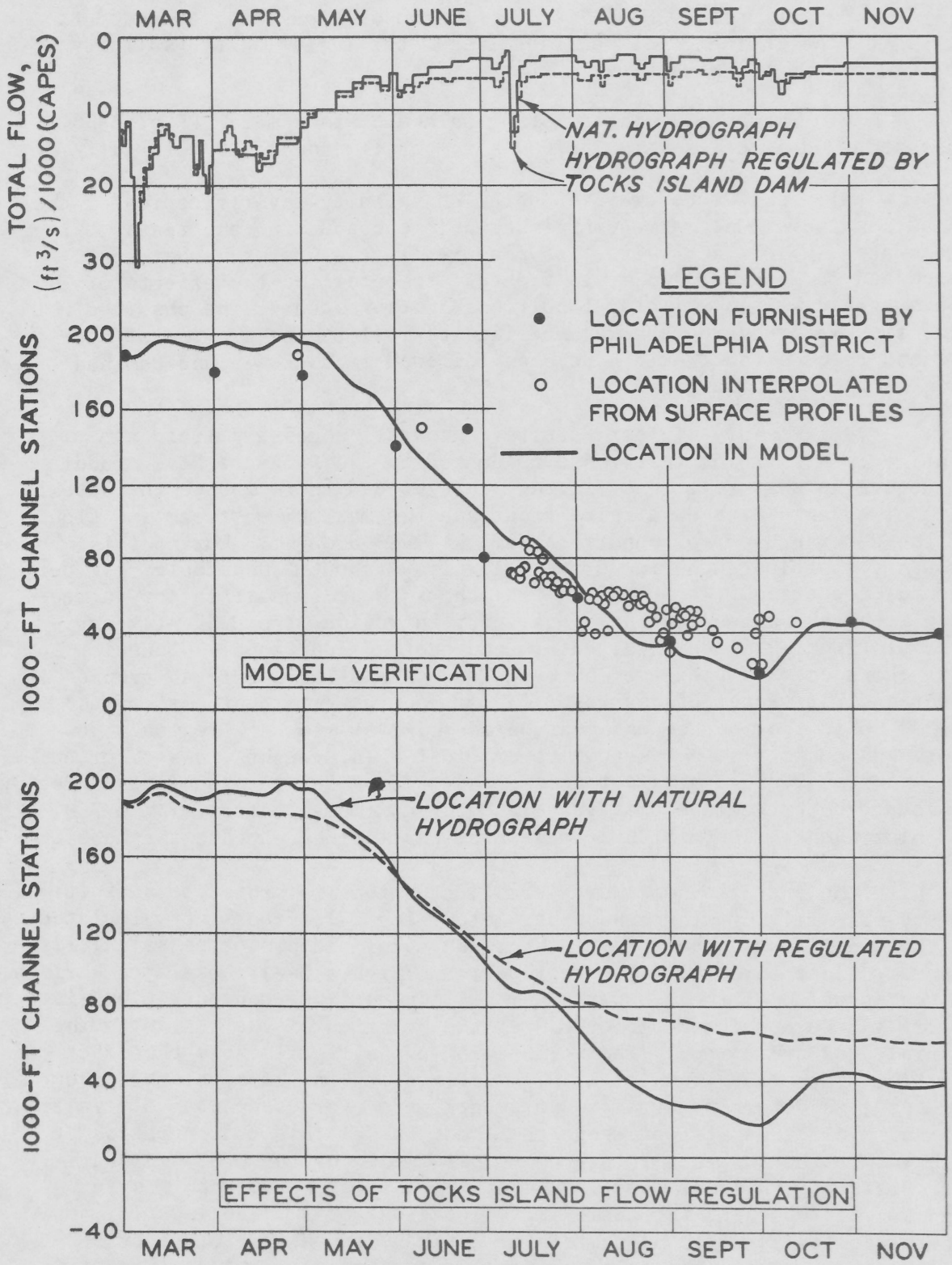

Figure 3-81. Effects of Tocks Island Dam on location of 250 isochlor, Delaware River (after Simmons, Harrison, and Huval, 1971).

The natural and adjusted hydrographs for the Delaware River estuary are shown in the upper part of Figures 3-81 and 3-82. The lower part of Figure 3-81 shows the changes in location of 250 isochlor for the test period as a result of simulated operation of the reservoir; Figure 3-82 shows the change in salinity at high water and low water slacks at Delaware Memorial Bridge, Chester, and Fort Mifflin. Note that both high water slack (maximum) and low water slack (minimum) salinities at all three locations were reduced by the regulated hydrograph, thus showing that salinities would be reduced generally in the upstream part of the estuary during the low flow season. The 250 isochlor was not moved as far downstream during the high inflow period of the regulated hydrograph as for the natural hydrograph; however, the maximum upstream location for the 250 isochlor for the regulated hydrograph was almost 8 miles farther downstream than for the natural hydrograph. Thus, while maximum salinities in the upstream part of the estuary would be significantly reduced by flow regulation (advantageous for water use), minimum salinities in the lower estuary would be increased (may be undesirable for marine life and oyster predator control).

k. Freshwater Supply-Salinity Control--Vermilion Bay.

(1) Project. Construction of a salinity control barrier in Vermilion Bay.

(2) Reference. U.S. Army Engineer Waterways Experiment Station (1959).

(3) Laboratory. WES.

(4) Test Period. December 1955 to December 1966.

(5) Problem. Vermilion Bay (Fig. 3-83) is located on the Louisiana coast between Morgan City and Lake Charles. The bay has a deep and narrow connection to the Gulf of Mexico through Southwest Pass on the south, and a second wide and shallow connection through West and East Cote Blanche Bays and Atchafalaya Bay to the east and southeast. The Vermilion River, a relatively small stream, discharges into the northeast side of Vermilion Bay; the Atchafalaya River, which carries a large freshwater discharge at all times, and Wax Lake Outlet discharge into Atchafalaya Bay.

The Vermilion River is used extensively as a source of water for irrigating rice. During dry seasons, when most irrigation water is used, the rate of pumping from the Vermilion River often exceeds the riverflow, and saltwater from Vermilion Bay moves rapidly upstream and eventually reaches the pump intakes. Considerable damage to the rice crop may then result, either from lack of water needed by the rice if pumping is curtailed, or from the salinity of the water pumped into the ricefields if pumping is continued. Historical salinity data show that the entire bay complex is freshened during the high discharge season on the Atchafalaya River, which usually extends from about February through June. After the

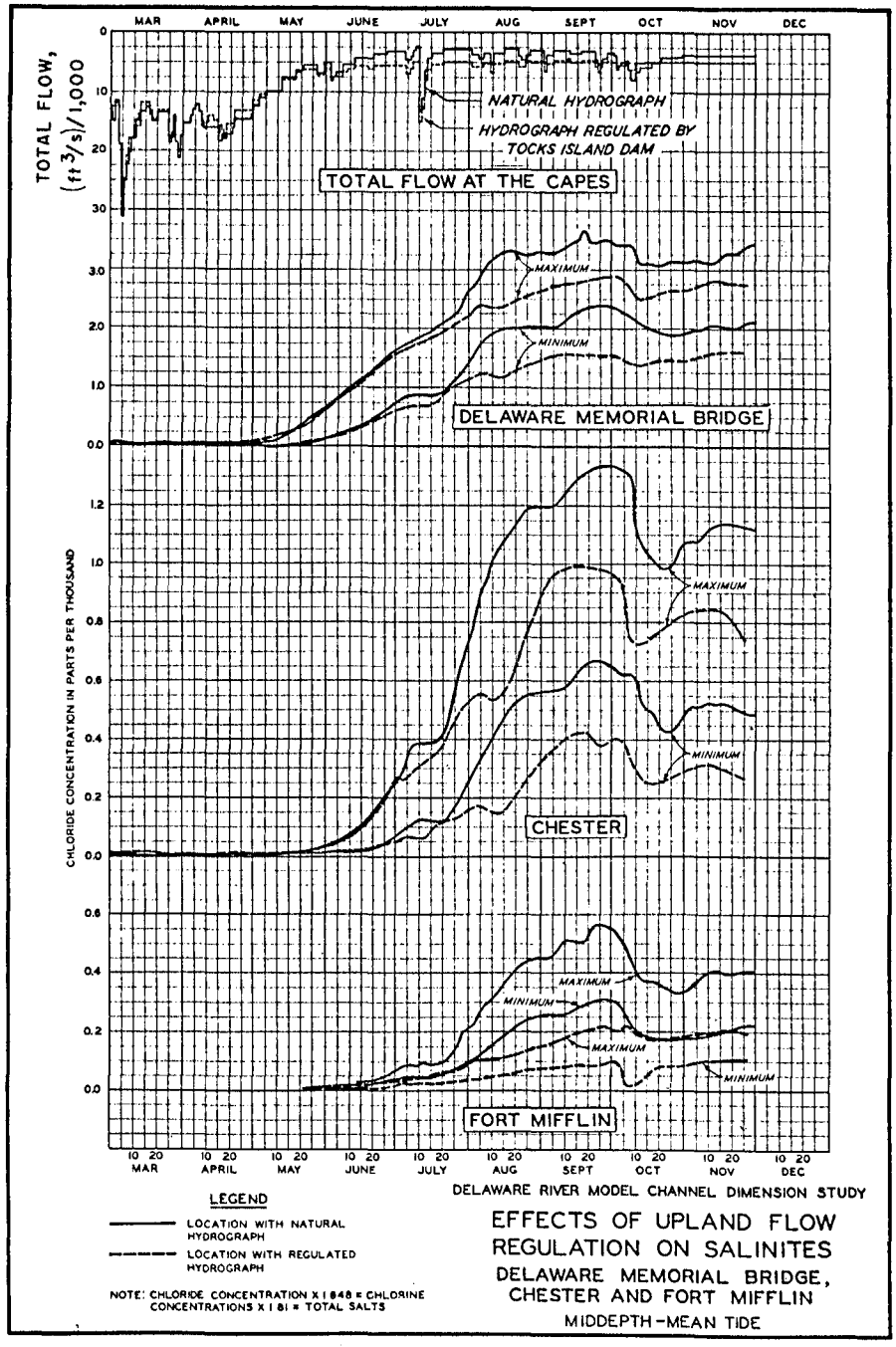

Figure 3-82. Effects of Tocks Island Dam on salinities, Delaware River (after Simmons, Harrison, and Huval, 1971).

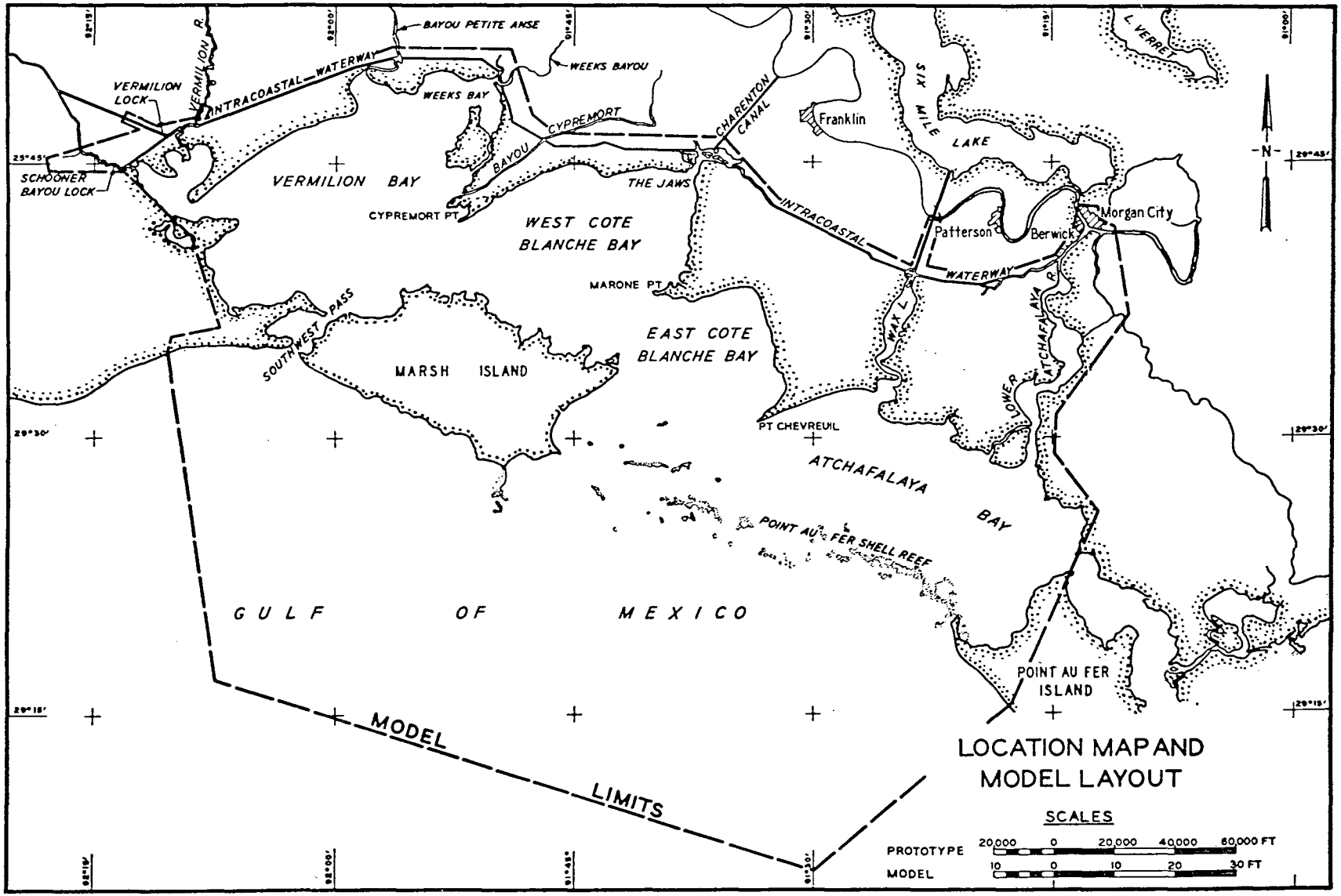

Figure 3-83. Vermilion Bay model (after U.S. Army Engineer Waterways Experiment Station, 1959).

high discharge period, salinities throughout the bays increase gradually, usually reaching a maximum in about September or October (also the period of high use of irrigation water). These data also indicate that the primary source of saltwater into Vermilion Bay is through Southwest Pass, with a secondary source through Atchafalaya Bay and East and West Cote Blanche Bays. Therefore, the possibility was considered that closure of Southwest Pass would reduce the rate of influx of saltwater into Vermilion Bay to such an extent that pumping from the Vermilion River could be continued for an appreciably longer period of time than is now possible.

(6) Purpose of Model Study. The principal objectives of the model study were: (a) to determine whether the closure of Southwest Pass would reduce salinities in Vermilion Bay to concentrations permissible in irrigation; (b) if so, to determine the effects on the reduced salinities of withdrawing 10,000 cubic feet per second for irrigation and industrial use from the north and west parts of the bay; and (c) to obtain data for use, if needed, in evaluating the effects of the Southwest Pass closure on fish and wildlife.

(7) The Model. The Vermilion Bay model (Fig. 3-83) reproduced a part of the Gulf of Mexico, all of Atchafalaya Bay, East and West Cote Blanche Bays, Vermilion Bay, the lower reaches of the Atchafalaya and Vermilion Rivers, and the lower reaches of other streams which contribute freshwater to the bay complex. The model was constructed to linear scales of 1:2,000 horizontally and 1:100 vertically.

(8) Test Procedures. Tides were reproduced by a tide generator located in the Gulf of Mexico part of the model, which also contained provisions for reproducing littoral or alongshore currents from either direction. All freshwater tributaries were equipped with weirs for metering freshwater inflow, and the model was operated with the Gulf of Mexico part filled with saltwater to the salinity scale of 1:1. Because the entire bay complex is quite shallow, usually less than 12 feet in depth, surface wind waves play a significant role in the vertical mixing of saltwater and freshwater, and this effect had to be reproduced in the model to reproduce accurately the salinity regimen of the prototype. Since the reproduction of the wind waves in the distorted-scale model was infeasible, the mixing effects were simulated by oscillating fans positioned to blow in a random pattern on the model water surface.

Two conditions of freshwater inflow were selected for test purposes: the first used prototype freshwater inflow data for 1954 (which represented a year of low inflow), and the second used inflow data for 1955 (which represented a year of normal flow). For both conditions, the model was first operated with Southwest Pass open to establish the salinity regimen for existing conditions, and then the pass was closed and the model test was repeated to establish the regimen following closure of the pass.

(9) Summary of Test Results. Figure 3-84 shows the salinity distribution of the bay system at the time of peak salinities for the low inflow year with Southwest Pass open; Figure 3-85 shows the salinity distribution at the time of peak salinity under similar inflow conditions with the pass closed. Data presented in these two figures show that closure of Southwest Pass reduced the maximum salinity along the west side of Vermilion Bay and near the mouth of the Vermilion River from about 15.0 to about 2.0 parts per thousand, or a reduction in maximum salinity of almost 90 percent. The time of maximum salinity at the location was also delayed from September to January (not shown in the figures), which would cause the time of occurrence of maximum salinity to be delayed until well after the end of the irrigation season instead of occurring within the irrigation season. As a result, the salinity reduction afforded by the plan in the critical irrigation season was greater than 90 percent. Although this plan has not been constructed in nature, the model tests have demonstrated the benefits that would accrue to irrigation interests.

1. Thermal Discharges--James River.

(1) Project. Construction of a nuclear power generating plant.

(2) Reference. Pritchard (1967).

(3) Laboratory. WES (physical model tests); Pritchard-Carpenter, Consultants (collection and analysis of model data).

(4) Test Period of Physical Model. July and October 1966.

(5) Problem. The Virginia Electric and Power Company was constructing the Surry Nuclear Power Station on the James River estuary. The construction site is located approximately 30 miles above the mouth of the James River at Old Point Comfort and 55 miles below Richmond, Virginia. Hog Point is the northernmost point of a peninsula formed by a large bend in the James River estuary (Fig. 3-86). The site of the power station extends across the central part of the peninsula, the river forming both the eastern and western boundaries of the site. The peninsula to the north of the site is a low-lying area of tidal marshes, tidal channels, and islands which serve as a wildfowl refuge, and terminates at Hog Point.

A design of the cooling water discharge system was necessary to minimize the impact of the waste heat on the estuarine environment (particularly the nearby seed oysterbeds) and to minimize the return of waste heat to the cooling water intake. The cooling water intake and discharge were to be located on opposite sides of Hog Point.

(6) Purpose of Model Study. The study was conducted to determine the probable effect of the discharge of waste heat from the condenser cooling water at the Surry Nuclear Power Station on the distribution of temperature in the adjacent James River estuary.

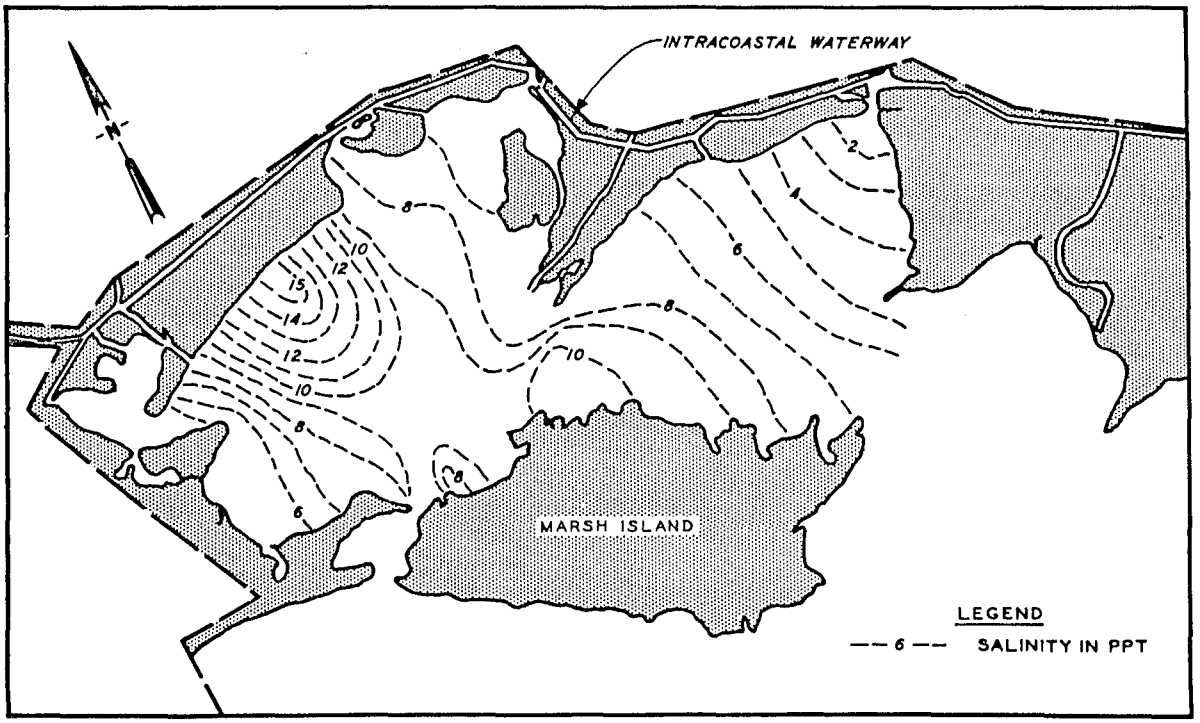

Figure 3-84. High salinity survey, Southwest Pass open, Vermilion Bay (after U.S. Army Engineer Waterways Experiment Station, 1959).

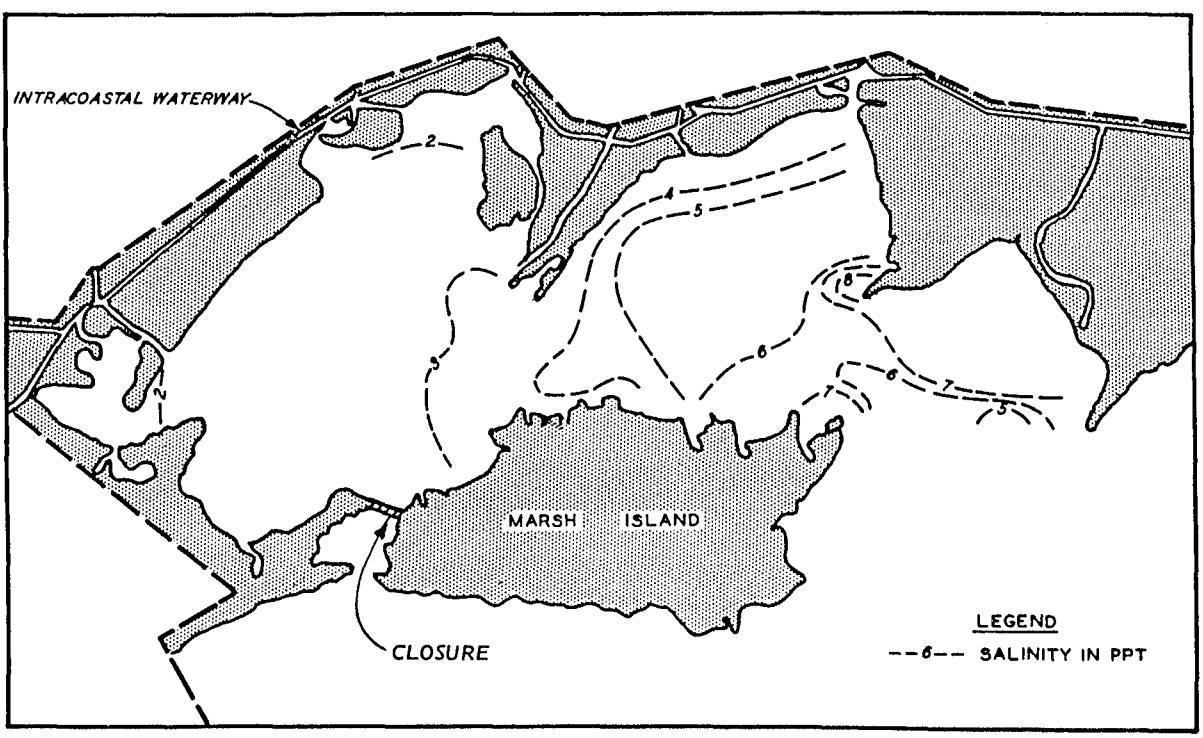

Figure 3-85. High salinity survey, Southwest Pass closed, Vermilion Bay (after U.S. Army Engineer Waterways Experiment Station, 1959).

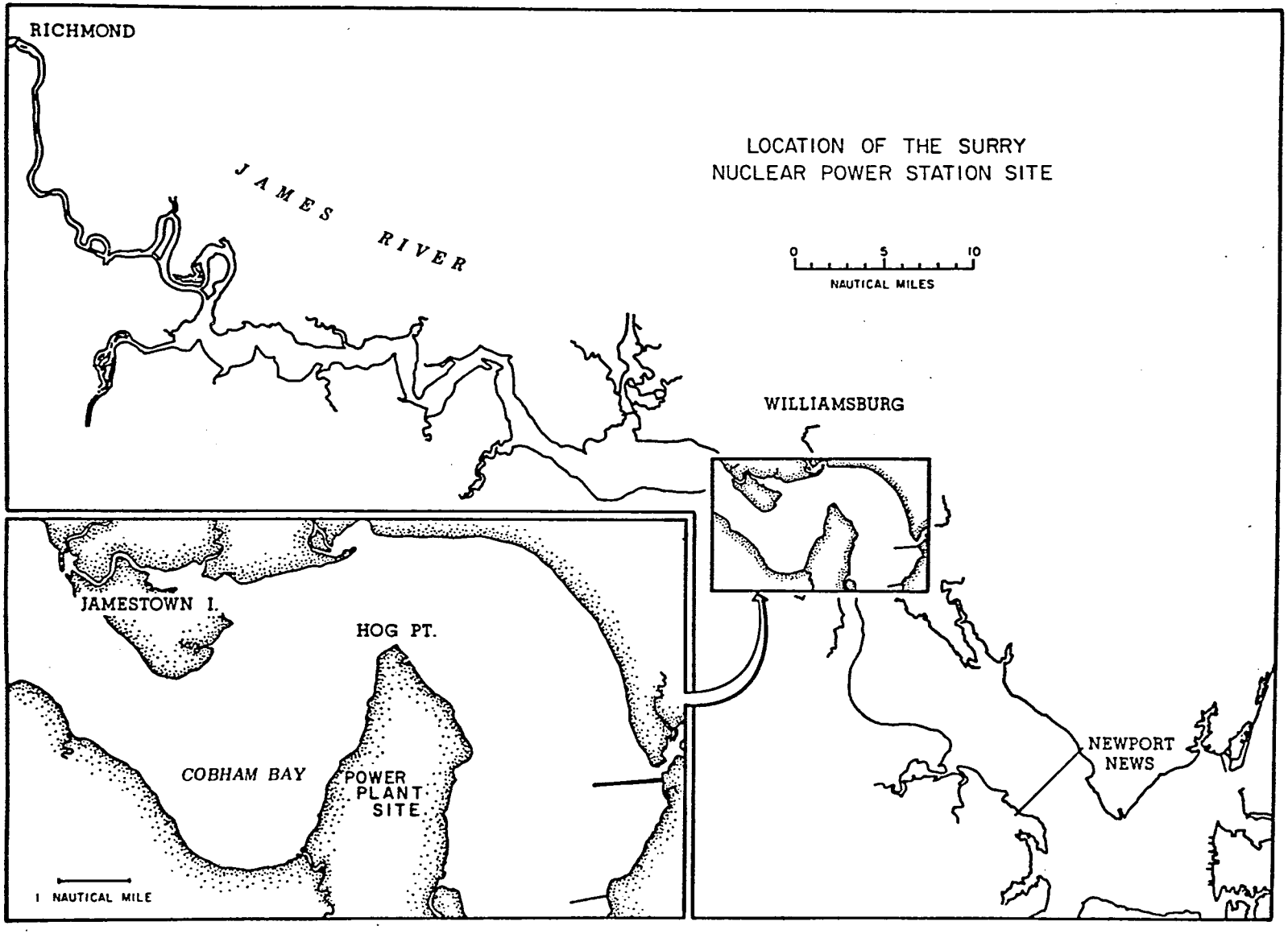

Figure 3-86. Location of Surry Nuclear Power Station, James River (after Pritchard, 1967).

(7) The Model. The existing James River model (see Fig. 3-48) was used for this study; model scales were 1:1,000 horizontally and 1:100 vertically. The model was operated by WES personnel; the data were collected and analyzed by Pritchard-Carpenter, Consultants.

(8) Test Procedures. Two series of model tests were conducted to define the extent of the thermal plumes from the station in order to determine whether the discharge point should be on the upstream or downstream side of the island. The water temperature observations made in the physical model were adjusted analytically (Pritchard, 1967) to correct for the difference in surface heat exchange coefficients between model and prototype and wind effects (which were not reproduced in the model).

One of the main purposes of the first series of tests was to determine the degree of mixing produced by discharging the condenser cooling water as a jet having an initial velocity equal to or larger than the tidal velocity in the estuary. On the basis of these studies, it was determined that a discharge velocity of 6 feet per second would be most suitable for design of the condenser discharge structure.

Tests were conducted during this series with a simulated heat rejection at the condensers of 5.2×10^9 British thermal units per hour, corresponding to a single 850-megawatt unit, and at 12×10^9 British thermal units per hour, corresponding to a total of 1,764 megawatts electrical power production. Temperatures in the model were measured using a rapid response thermistor bead mounted on a motor-driven trolley structure which ran across the model on a 16-foot-long aluminum bean. A single run consisted of setting the beam across the model at a designated cross section, and running the thermistor sensor across the model to obtain a plot of temperature versus lateral distance made on a strip-chart recorder. At each location, runs were made each 1.5 hours throughout a tidal cycle. During the July test series, a total of 496 temperature runs was made.

For the second test series, improvements were made in the temperature measuring system so that two thermistor bead sensors were towed across the model on each run. The sensors were placed 18 inches apart, representing a prototype distance of 1,500 feet. Near the discharge structure, one run provided data for two adjacent temperature cross sections. Farther away from the discharge, where the horizontal temperature gradients were small, the two simultaneous sections provided a check on the consistency of the data. About 489 temperature runs were made, each consisting of at least one (and in many cases two) record of surface termperature across a section of the estuary.

In a special test to determine the surface heat exchange coefficient for the model, Cobham Bay was blocked off from the rest of the model by a long rubber dam. Motor-driven paddle wheels were mounted in the enclosed area to circulate the water at a speed corresponding to the mean tidal current. Thermistor bead temperature sensors were placed at several locations in the enclosed water area. Water from this area was circulated through the heaters until the temperature in the enclosed area

was 11° Celsius (20° Fahrenheit) above the ambient water temperature in the adjacent model. A temperature-time record was then made as the water in the enclosed basin cooled. The rate of cooling provided a measure of the surface heat exchange coefficient.

Because the tests continued over several days during each series, the base or ambient temperature of the water in the model varied. Therefore, it was necessary to monitor the water temperature in the model in areas which were sufficiently removed from the station site so that the temperature of these areas represented the ambient water temperature. During both series of tests, fixed thermistor bead temperature sensors were placed in the model at selected positions upstream and downstream from the plant site.

(9) Summary of Test Results. For plan 1, the intake point was located about 8,000 feet offshore in about 20 feet of water on the downstream side, and the discharge was through a canal emptying into Cobham Bay on the upstream side. The excess temperature distributions at the times of high and low water slacks of the tidal cycle for conditions of a 2,000-cubic foot per second freshwater riverflow are shown in Figure 3-87. Although the thermal plume (1° Celsius isotherm; not shown in the figure) extended downstream to the intake point at low water slack, the intake point was located at the bottom and was unaffected by the surface temperature.

For plan 2, the intake point was located about 3,000 feet offshore in about 10 feet of water in Cobham Bay on the upstream side, and the discharge canal emptied into the main channel on the downstream side. Figure 3-88 presents test results similar to those for plan 1. In this case, the thermal plume at low water slack extended for a considerable distance downstream and would alter temperatures in valuable seed oysterbeds. The upstream extent of the plume at high water slack did not influence temperatures at the intake point.

On the basis of the model results, the discharge canal was located on the upstream side of the power station to avoid potential detrimental effects to the seed oysterbeds.

m. Definition of Existing Conditions--Delaware River.

(1) Project. No specific project was related to this study.

(2) References. U.S. Army Engineer Waterways Experiment Station (1954, 1956).

(3) Laboratory. WES.

(4) Test Period. December 1950 to March 1954.

(5) Problem. Tests are often conducted in a model to define hydraulic and salinity regimens for conditions where prototype data are

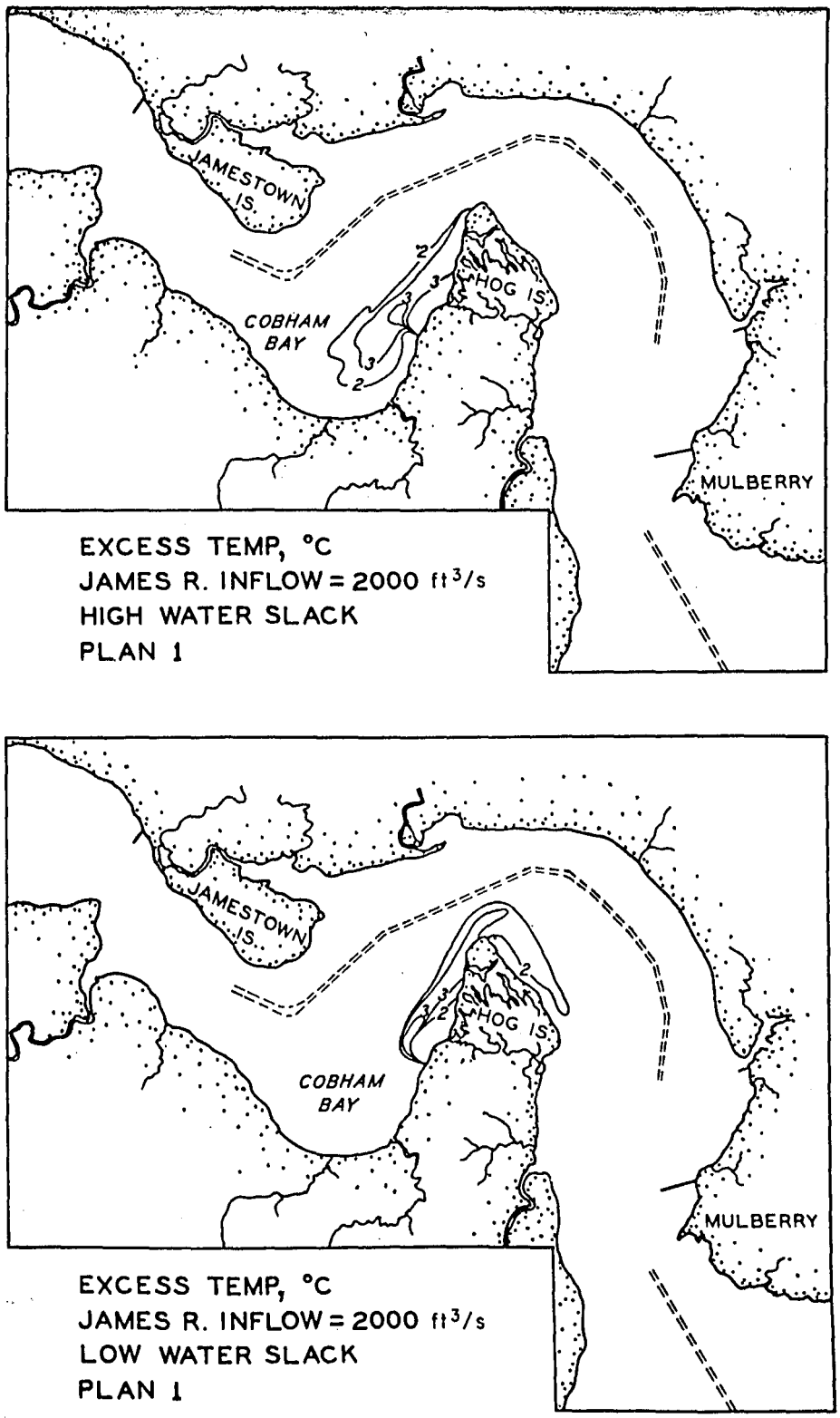

Figure 3-87. Excess temperature distributions, Surry Nuclear Power Station, plan 1, James River (after Pritchard, 1967).

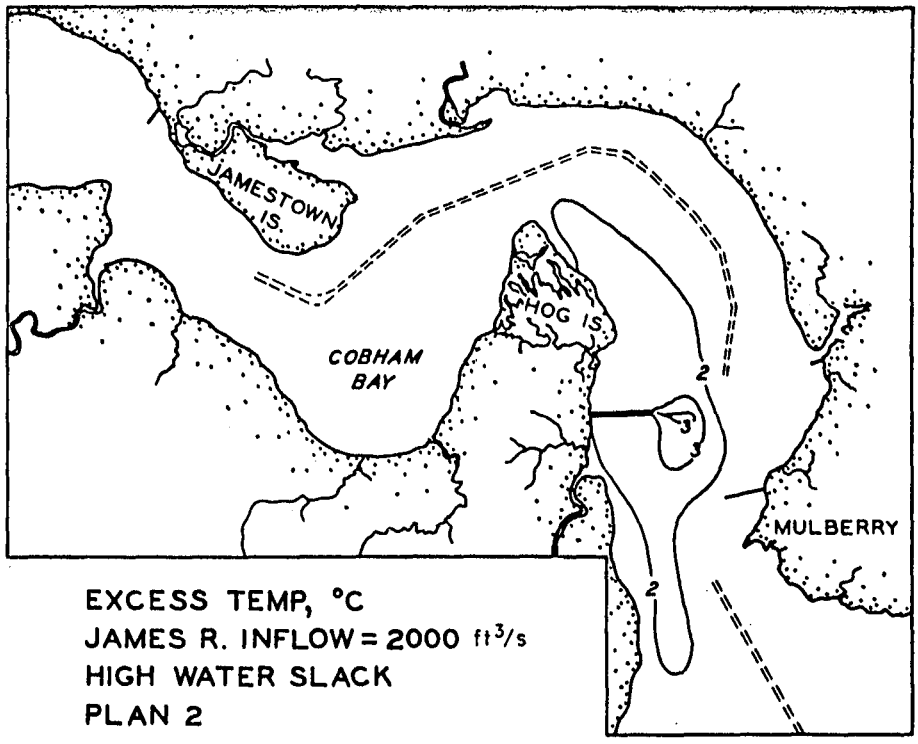

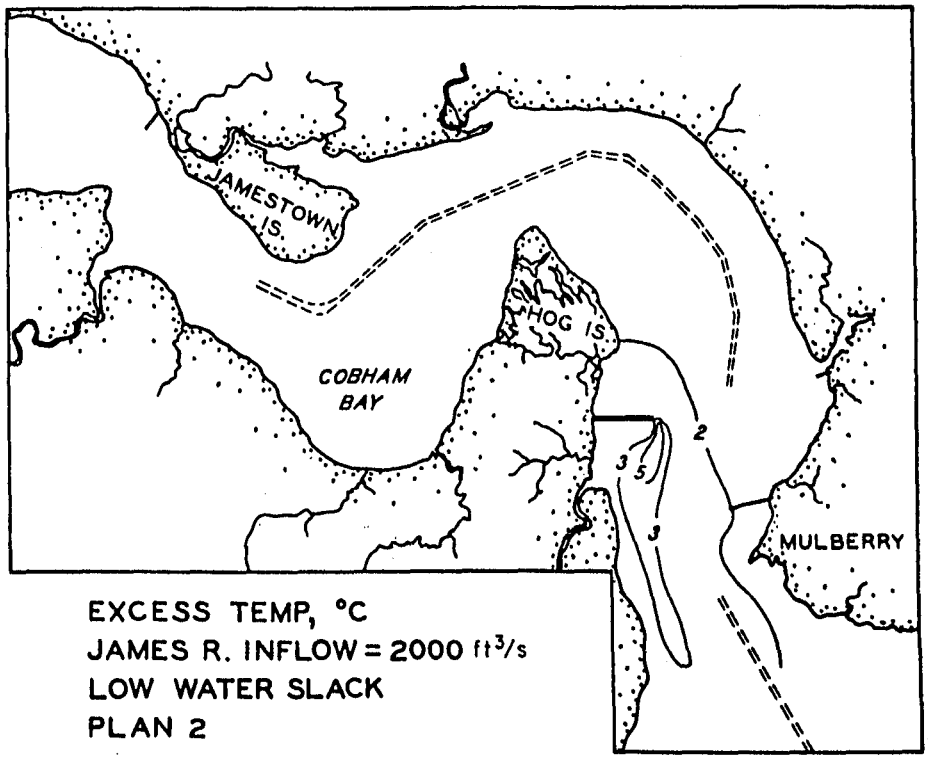

Figure 3-88. Excess temperature distributions, Surry Nuclear Power Station, plan 2, James River (after Pritchard, 1967).

unavailable. The tests may be necessary because of the high cost of obtaining field data (compared to the cost of obtaining the data in an existing model), or because the transient and uncontrollable prototype conditions prohibit the definition of quasi-steady-state conditions from field data. Such studies obviously cannot be made until the hydraulic and salinity verifications of the model have been completed.

Salinity intrusion in the Delaware River estuary constitutes a serious problem when freshwater discharge conditions are such that saltwater intrudes upstream beyond the Delaware-Pennsylvania State line, since upstream from this point the river water is used extensively for industrial purposes. The maximum salinity concentration that can be tolerated by certain industries located on the river is on the order of 50 parts per million of chlorine (50 isochlor). When the salinity of the river water at the plant sites exceeds this value, either the water must be treated chemically to remove the objectionable constituents or water of satisfactory quality must be obtained from another source. Either method is very expensive because of the large quantities of water involved.

(6) Purpose of Model Study. A series of tests was conducted in the Delaware River model to determine the effects of each principal factor known or believed to affect the nature and extent of salinity intrusion in the estuary.

(7) The Model. The Delaware River model (Fig. 3-56) was a fixed-bed type with scales of 1:1,000 horizontally and 1:100 vertically.

(8) Test Procedures. For most of these tests, constant freshwater inflows were used.

(9) Summary of Test Results. It had long been recognized that freshwater discharge into the Delaware River estuary was the major factor governing the extent of salinity intrusion therein, since saltwater has intruded as far upstream as Philadelphia during periods of extremely low freshwater discharge and has been forced as far downstream as Artificial Island during large floods. However, the proper correlation of the extent of salinity intrusion with freshwater discharge has never been possible, since the freshwater discharge in the prototype rarely, if ever, remains stable for a sufficient period of time to produce an equivalent stable salinity regimen. Therefore, one of the problems for the model study was determination of the relationship between sustained freshwater discharge and stable salinity conditions over a fairly wide range of freshwater discharges. The results of such tests would show the sustained freshwater discharge required to hold the critical salinity concentration (50 isochlor) at the Delaware-Pennsylvania State line.

Six tests were conducted in the model to determine the relationship between sustained freshwater discharge and salinity distribution throughout the estuary for mean tide conditions. These tests involved reproduction of sustained freshwater discharges in the Delaware River including the Schuylkill River of 5,000, 7,000, 9,000, 10,600, 13,000, and 16,475 cubic feet per second.

Bottom salinity distribution curves at high water slack for all freshwater discharges tested are shown in Figure 3-89. The curves were developed from detailed information to clearly show the effect of sustained freshwater discharge on horizontal salinity distribution throughout the estuary and the horizontal shift of a given isochlor with change in freshwater discharge.

Results of these tests determined that sustained freshwater discharges of about 12,000 and 10,600 cubic feet per second would hold the 50 and 100 isochlors, respectively, at the Delaware-Pennsylvania State line. Additional tests were conducted to determine the length of time required to reestablish the 100 isochlor at the State line following periods of mean (16,475 cubic feet per second) and low (2,000 cubic feet per second) discharge (results are shown in Fig. 3-90).

Tests to determine the effects of tidal range on salinity distribution throughout the estuary were conducted for conditions of mean freshwater discharge (16,475 cubic feet per second) and of low freshwater discharge (5,000 cubic feet per second). The tests for mean freshwater discharge were made to determine the effects of tidal range on salinity distribution for normal conditions; the tests for low freshwater discharge were made to determine the effects of tidal range for critical conditions of salinity intrusion (when the salinity front was well upstream from the Delaware-Pennsylvania State line). Tests were conducted for neap, mean, and spring tides. The results are summarized in Figures 3-91 and 3-92 and indicate that the extent of salinity intrusion in the estuary increases slightly as the tidal range decreases. The differences in salinity at any given point in the estuary for the various tidal ranges were less for the tests of low freshwater discharge than for the tests of mean freshwater discharge.

Mean annual sea level at the entrance to the Delaware River estuary rose about 0.5 foot between about 1920 and 1950. To determine the effect of changes in sea level of this order of magnitude on salinity intrusion and distribution throughout the estuary, tests were made for the 1948 mean sea level and with the sea level raised 0.5 foot above and lowered 0.5 foot below the 1948 level. Each of these tests was made for mean conditions of tide and freshwater discharge.

Bottom salinity distribution curves at high water slack for the three elevations of sea level indicate that the extent of salinity intrusion in the estuary increases as sea level rises (Fig. 3-93). Other characteristics of the salinity distribution curves for the three conditions appear to be identical. The upstream shift of equal isochlors as sea level rises is believed to be attributable to corresponding increases in cross-sectional area of the estuary with increase in sea level.

7. Time and Cost Estimates.

A generalization of the time and cost requirements for estuary models is difficult because of the wide variety of model sizes, problems to be

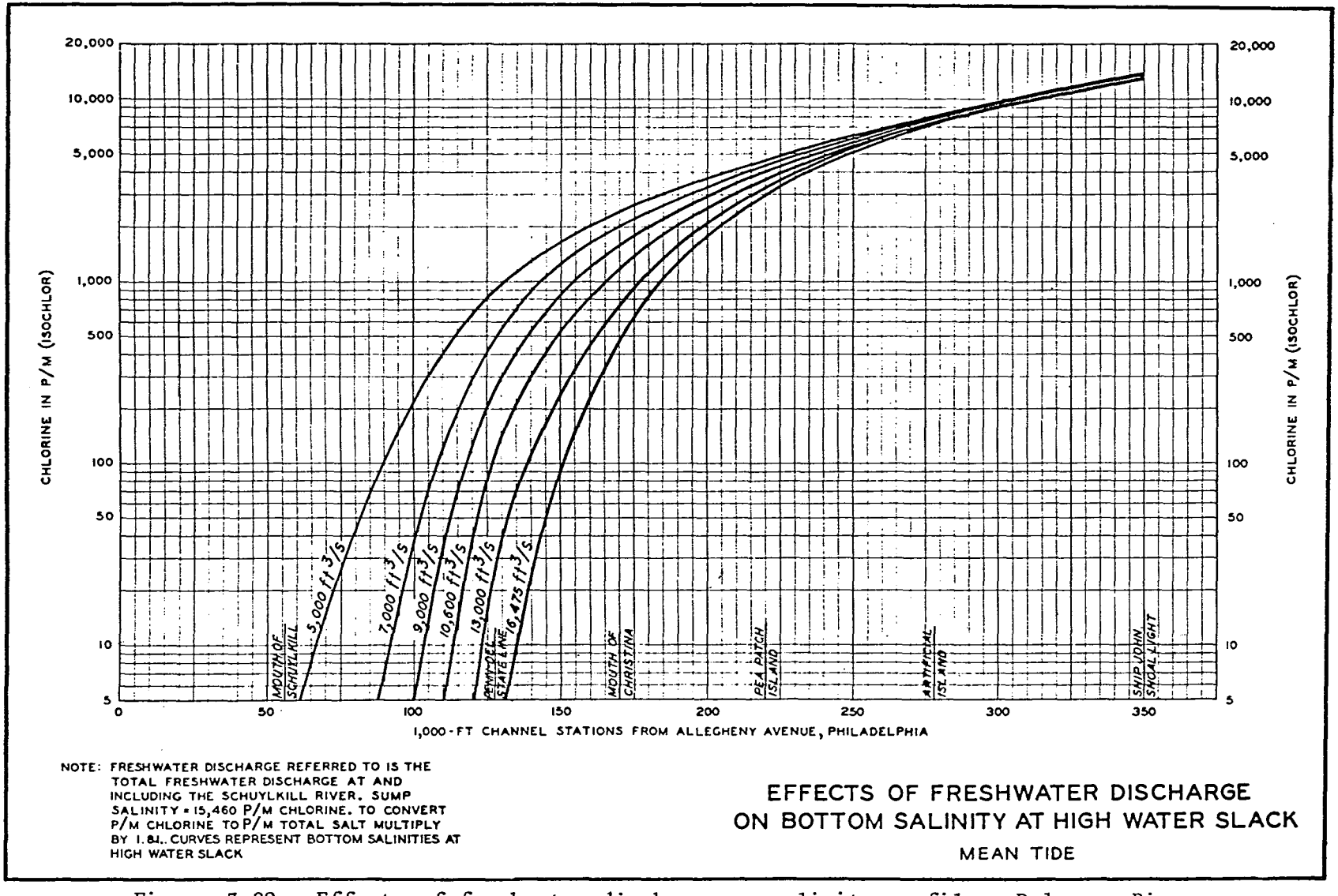

Figure 3-89. Effects of freshwater discharge on salinity profiles, Delaware River (after U.S. Army Engineer Waterways Experiment Station, 1954).

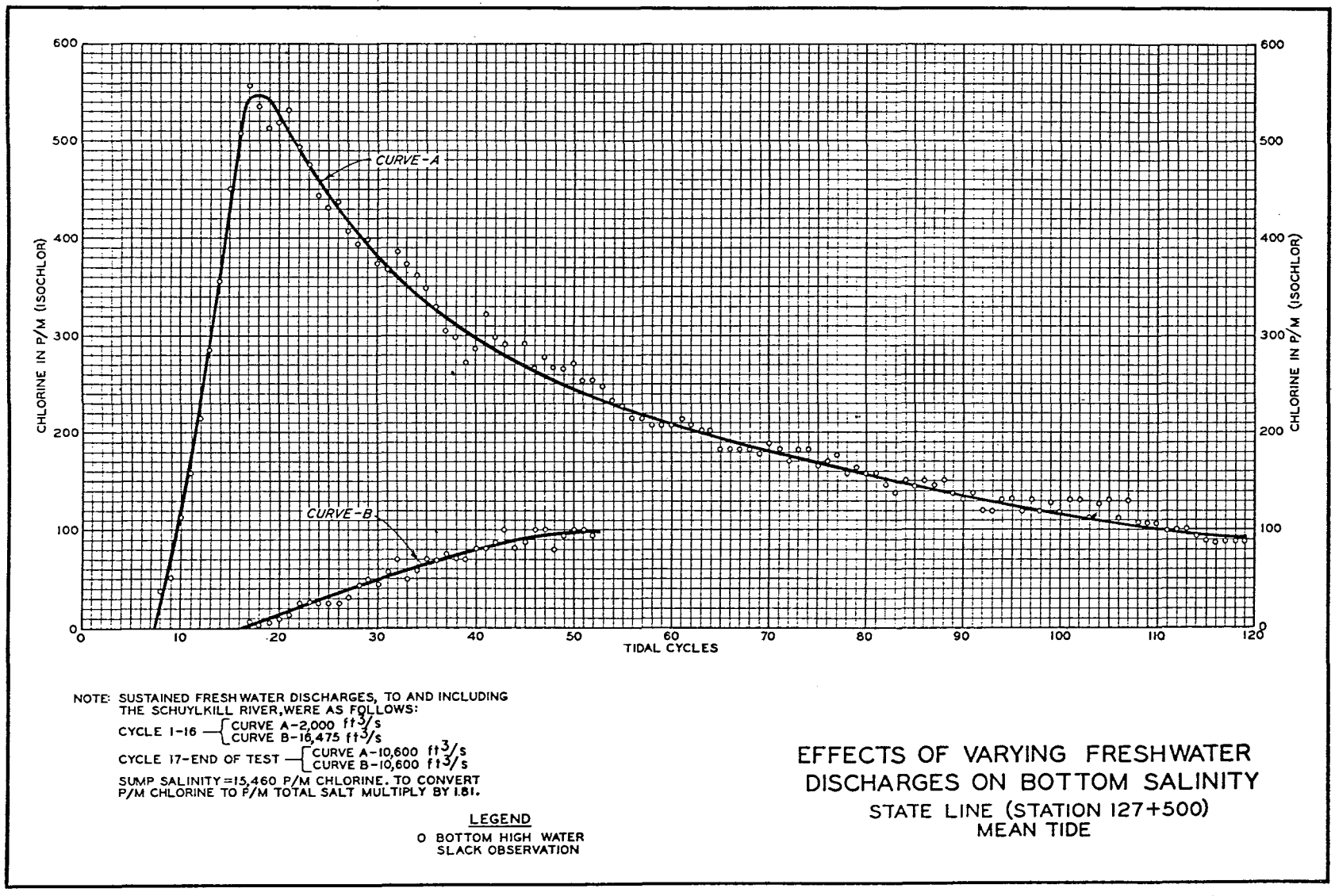

Figure 3-90. Time required to reestablish salinity conditions at State line, Delaware River (U.S. Army Engineer Waterways Experiment Station, 1954).

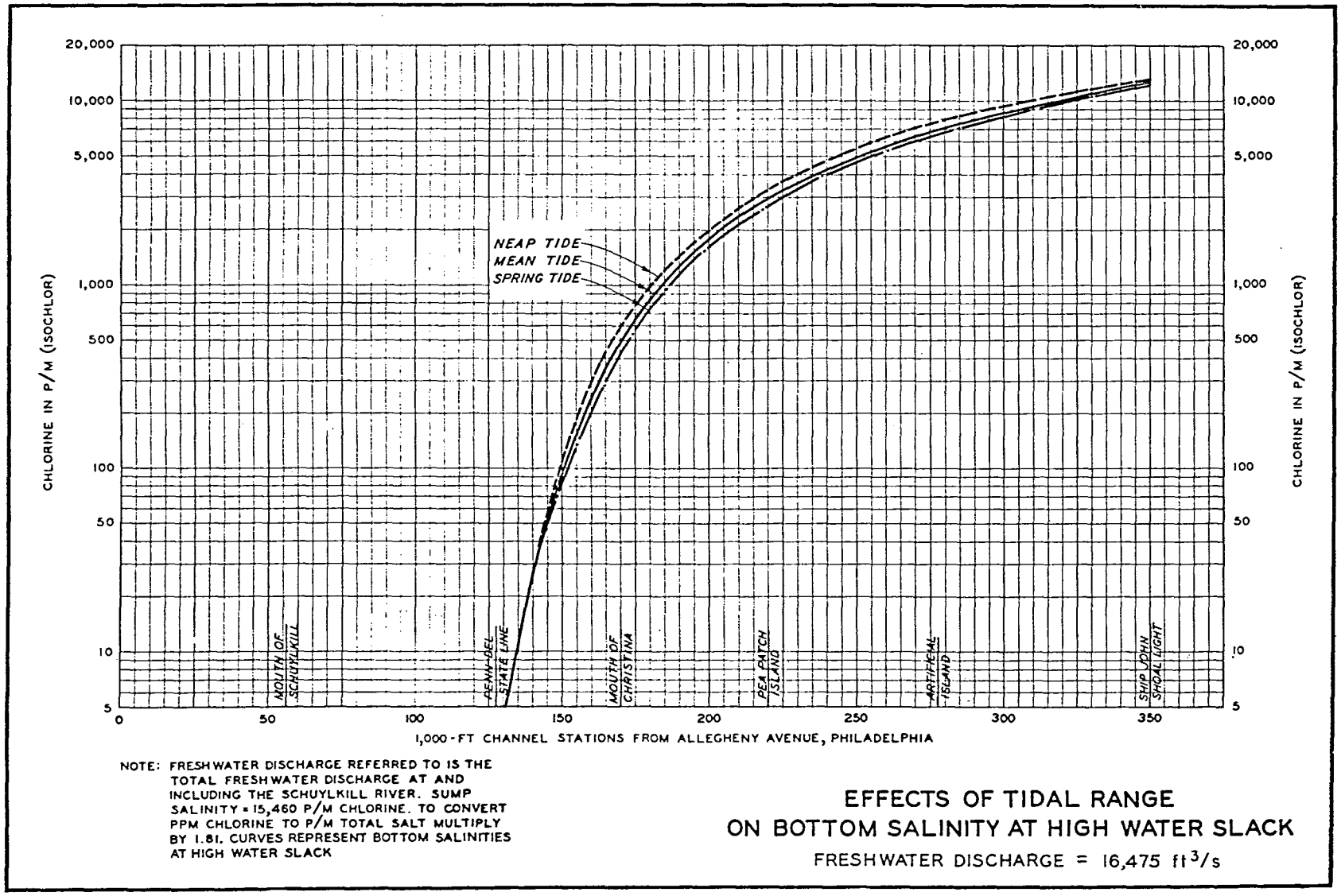

Figure 3-91. Effects of tidal range on salinity profiles for mean freshwater discharge, Delaware River (after U.S. Army Engineer Waterways Experiment Station, 1954).

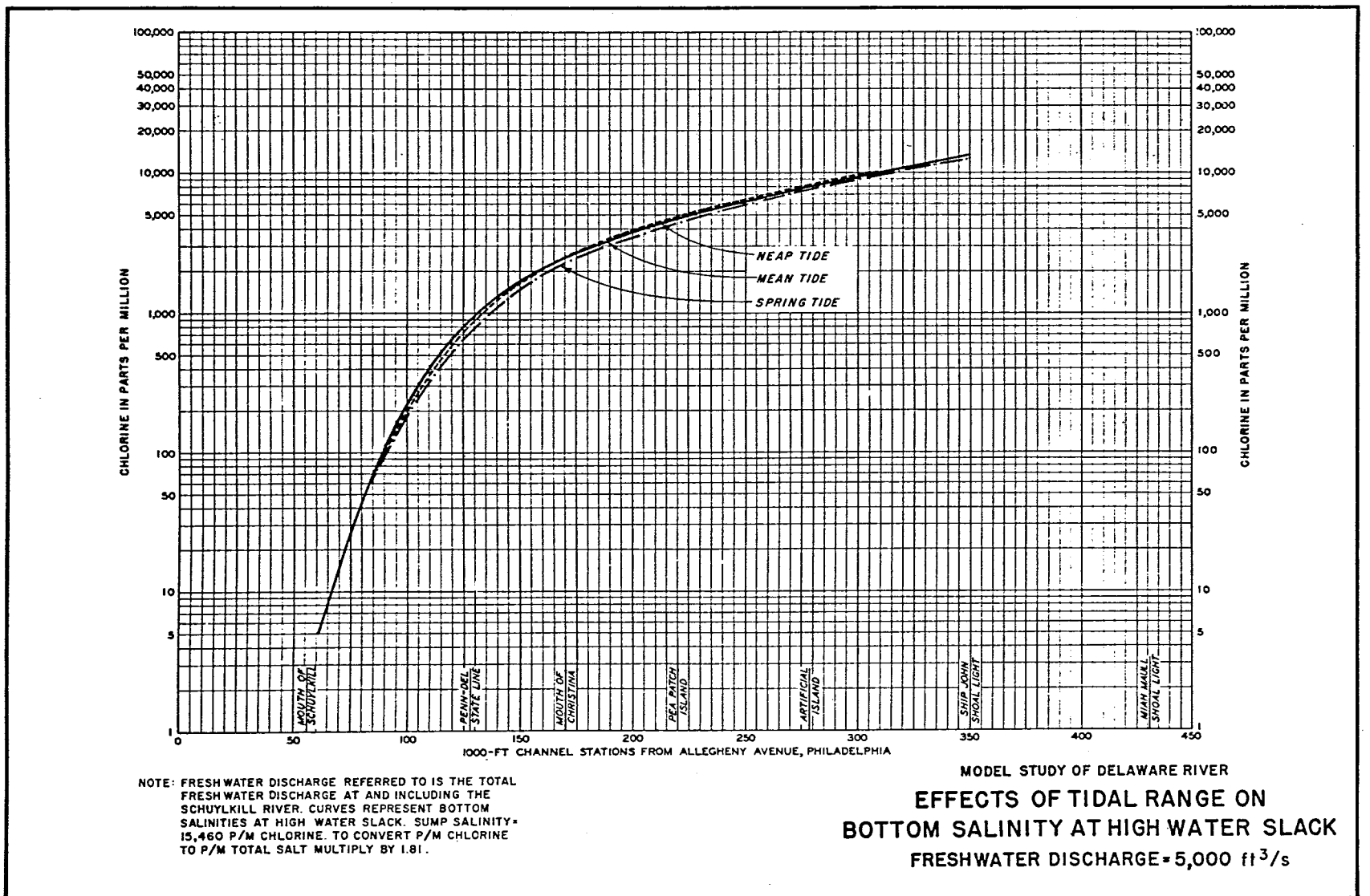

Figure 3-92. Effects of tidal range on salinity profiles for low freshwater discharge, Delaware River (after U.S. Army Engineer Waterways Experiment Station, 1954).

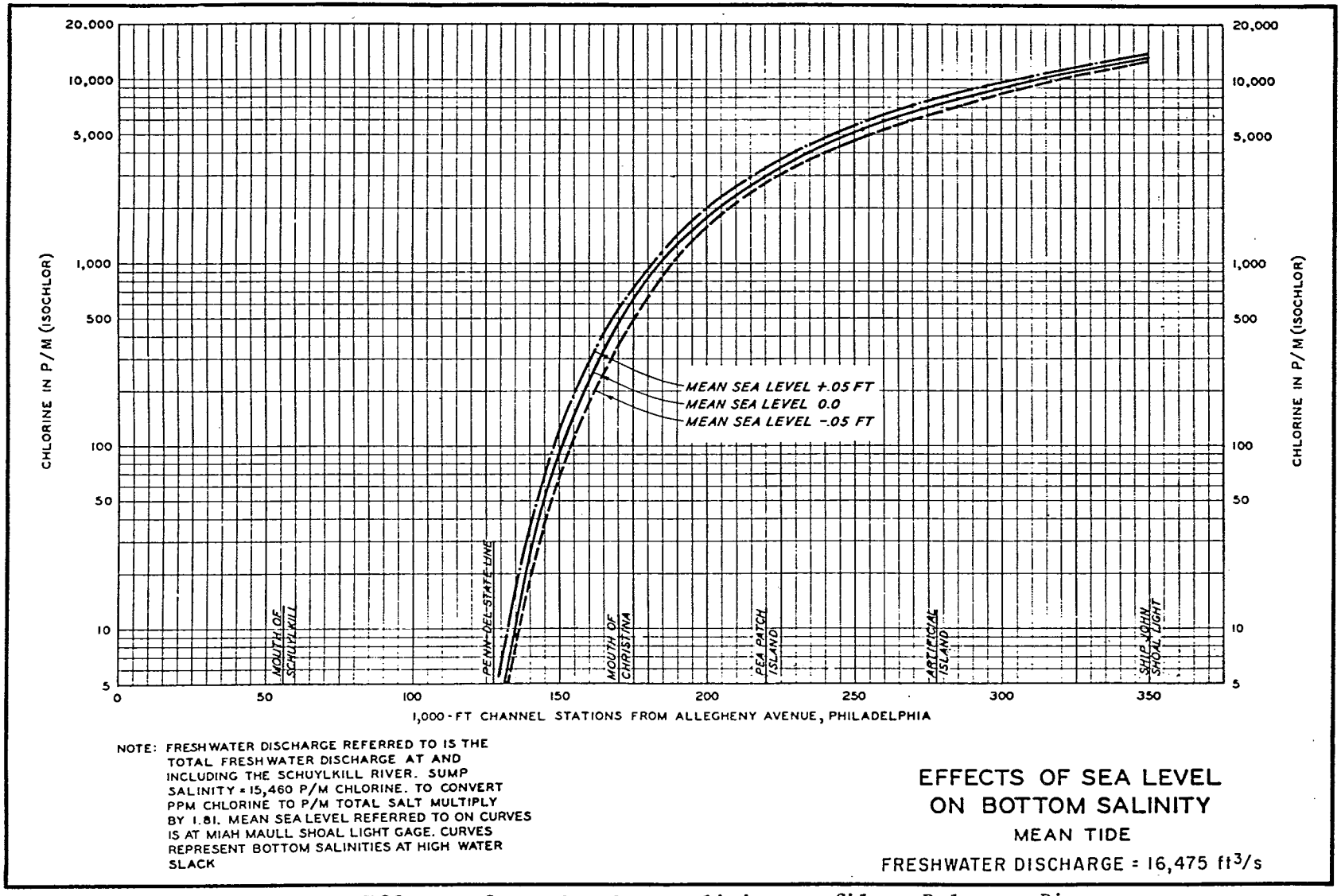

Figure 3-93. Effects of sea level on salinity profiles, Delaware River (after U.S. Army Engineer Waterways Experiment Station, 1954).

investigated, and amount of detail required from test results. Estuary models generally vary in size from about 5,000 to 60,000 square feet, excluding extremes such as the Gastineau Channel model (1,600 square feet) and the Chesapeake Bay model (340,000 square feet). The cost of model design and construction varies not only with the area of the model but also with the complexity of the model geometry (i.e., pier slips, braided channels, etc., as opposed to relatively flat bay bottoms, straight channels, etc.). Design and construction costs by WES have been on the order of $12 to $15 per square foot (March 1976); however, this does not normally include the (direct) cost of major appurtenances (such as tide generators, wave generators, hurricane surge generators, water supply pumps, etc.), the model shelter, water supply sump, or model instrumentation. These items are obtained with plant funds, and WES is reimbursed by indirect charges to all projects. Construction time also varies with both the size and complexity of the model (generally 1 to 8 months). Most of the model design is accomplished before initiating model construction; however, the design effort is usually continued into the early stages of construction. The design is usually initiated 1 to 3 months before construction. If prototype hydraulic, salinity, and shoaling data are available, they can be analyzed during this period.

After completion of the model construction, a substantial period of time is required for model verification. Since this is a trial-and-error process, it is difficult to predict the time and cost required even for a specific case. The time required for hydraulic and salinity verification varies from about 3 to 15 months, depending on the size of the model, the complexity of the estuary, the amount of prototype data available, the number of conditions (combinations of tide and freshwater discharge) to be reproduced, the skill of the model personnel, and "luck." Operating costs during this period will vary from about $8,000 to $15,000 per month (March 1976) depending on the number of operating personnel, the amount of support (shops, molding, photography, drafting, etc.), and the amount of materials (especially salt) required. Fixed-bed shoaling verification can also be a lengthy process requiring from 2 weeks to 3 months for each reach to be studied. Monthly costs for shoaling verification will often be 10 to 20 percent less than during hydraulic and salinity verifications because fewer operating personnel are required.

The testing program for a *single* study will generally require from 1 month to 1 year. However, *several* studies will probably be conducted during the life of any one model. Operating costs will average about $10,000 to $15,000 per month (March 1976). Costs may be significantly higher during extensive water quality studies because of the greater personnel and data reduction requirements.

After completion of a model study the results are either published in a single comprehensive report or in a series of reports on specific studies conducted in the model. Test results are furnished to the sponsor in preliminary form as soon as they are available. Preparation and publication of a final report usually requires about 6 months at a cost of approximately $10,000 (March 1976).

The Columbia River estuary model (48,000 square feet) was constructed in 1961-62. Design and construction required about 11 months at a cost of approximately $230,000. Hydraulic and salinity verification required about 15 months at a cost of approximately $125,000. Shoaling verifications were performed at various channel reaches during individual studies. Testing for about 20 separate studies was carried out over about 6 years. Total cost of the model was approximately $1.2 million.

The Mobile Bay model (30,000 square feet) was constructed in 1972. Design and construction required about 4 months at a cost of approximately $153,000; hydraulic and salinity verification required about 12 months at a cost of $77,000. Testing to develop the best plan for dredged-material disposal areas for the proposed Theodore Ship Channel required 11 months and $113,000; preparation and publication of the final report cost $10,000. The total cost was approximately $353,000.

LITERATURE CITED

BIRKHOFF, G., *Hydrodynamics, A Study in Logic, Fact, and Similitude*, Princeton University Press, Princeton, N.J., 1955.

BOBB, W.H., and BOLAND, R.A., Jr., "Effects of Proposed Barriers on Tides, Currents, Salinities, and Dye Dispersion for Normal Tide Conditions," Report 2, Technical Report H-69-12, *Galveston Bay Hurricane Surge Study*, U.S. Army Engineer Waterways Experiment Station, Vicksburg, Miss., July 1970a.

BOBB, W.H., and BOLAND, R.A., Jr., "Effects of Plan 2 Alpha and Plan 2 Gamma Barriers on Tides, Currents, Salinities, and Dye Dispersion for Normal Tide Conditions," Report 3, Technical Report H-69-12, *Galveston Bay Hurricane Surge Study*, U.S. Army Engineer Waterways Experiment Station, Vicksburg, Miss., July 1970b.

BOLAND, R.A., Jr., and BOBB, W.H., "Evaluation of Disposal Areas in James River; Hydraulic Model Investigation," Miscellaneous Paper H-75-1, U.S. Army Engineer Waterways Experiment Station, Vicksburg, Miss., Jan. 1975.

BOYD, M.B., et al., "Enlargement of the Chesapeake and Delaware Canal; Hydraulic and Mathematical Model Investigation," Technical Report H-73-16, U.S. Army Engineer Waterways Experiment Station, Vicksburg, Miss., Oct. 1973.

BROGDON, N.J., Jr., "Effects of Proposed Barriers on Hurricane Surge Heights; Hydraulic Model Investigation," Technical Report H-69-12, Report 1, *Galveston Bay Hurricane Surge Study;* U.S. Army Engineer Waterways Experiment Station, Vicksburg, Miss., Sept. 1969.

DEFANT, A., *Physical Oceanography*, Vol. 1, Pergamon Press, New York, 1961, 729 pp.

DELFT HYDRAULICS LABORATORY, "The Earth's Rotation in Hydraulic Models," *Hydro Delft*, Delft, The Netherlands, No. 11, Apr. 1968, pp. 1-5.

FISACKERLY, G.M., "Estuary Entrance, Umpqua River, Oregon; Hydraulic Model Investigation," Technical Report H-70-6, U.S. Army Engineer Waterways Experiment Station, Vicksburg, Miss., May 1970.

FISACKERLY, G.M., "San Diego Bay Model Study; Hydraulic Model Investigation," Technical Report H-74-12, U.S. Army Engineer Waterways Experiment Station, Vicksburg, Miss., Nov. 1974.

FISCHER, H.B., and HANAMURA, T., "The Effect of Roughness Strips on Transverse Mixing in Hydraulic Models," *Water Resources Research*, Vol 11, No. 2, Apr. 1975, pp. 362-364.

FISCHER, H.B., and HOLLEY, E.R., "Analysis of the Use of Distorted Hydraulic Models for Dispersion Studies," *Water Resources Research*, Vol. 7, No. 1, Feb. 1971, pp. 46-51.

FORTSON, E.P., Jr., "Capabilities of Hydraulic Models," Miscellaneous Paper H-70-5, U.S. Army Engineer Waterways Experiment Station, Vicksburg, Miss., May 1970.

HARLEMAN, D.R.F., "Physical Hydraulic Models," *Estuarine Modeling: An Assessment*, Water Pollution Control Research Series 16070 DZV, Water Quality Office, Environmental Protection Agency, Washington, D.C., Feb. 1971, pp. 215-263.

HERRMANN, F.A., Jr., "Hydraulic and Salinity Verification," Report 1, Technical Report No. 2-735, *Model Studies of Navigation Improvements, Columbia River Estuary*, U.S. Army Engineer Waterways Experiment Station, Vicksburg, Miss., Dec. 1968.

HERRMANN, F.A., Jr., "40-Ft Channel Studies; Wauna-Lower Westport Bar," Report 3, Section 1, Technical Report No. 2-735, *Model Studies of Navigation Improvements, Columbia River Estuary*, U.S. Army Engineer Waterways Experiment Station, Vicksburg, Miss., Feb. 1971.

HERRMANN, F.A., Jr., "Navigation Channel Improvement, Gastineau Channel, Alaska; Hydraulic Model Investigation," Technical Report H-72-9, U.S. Army Engineer Waterways Experiment Station, Vicksburg, Miss., Nov. 1972.

HERRMANN, F.A., Jr., "Entrance Studies; Jetty A Rehabilitation, Jetty B, and Outer Bar Channel Relocation," Report 2, Section 4, Technical Report No. 2-735, *Model Studies of Navigation Improvements, Columbia River Estuary*, U.S. Army Engineer Waterways Experiment Station, Vicksburg, Miss., July 1974.

HERRMANN, F.A., Jr., and SIMMONS, H.B., "Entrance Studies; Fixed-Bed Studies of South Jetty Rehabilitation," Report 2, Section 1, Technical Report No. 2-735, *Model Studies of Navigation Improvements, Columbia River Estuary*, U.S. Army Engineer Waterways Experiment Station, Vicksburg, Miss., Aug. 1966.

INTERNATIONAL SALT COMPANY, *The Sterling Brine Handbook*, Clarks Summit, Pa., 1965, 32 pp.

KEULEGAN, G.H., "Fifth Progress Report on Model Laws for Density Currents, Distorted Models in Density Current Phenomena," Report 1188, U.S. Department of Commerce, National Bureau of Standards, Washington, D.C., Oct. 1951.

KEULEGAN, G.H., "Model Laws for Coastal and Estuarine Models," *Estuary and Coastline Hydrodynamics*, A.T. Ippen, ed., McGraw-Hill, New York, 1966, pp. 691-710.

LAWING, R.J., BOLAND, R.A., and BOBB, W.H., "Effects of Proposed Theodore Ship Channel and Disposal Areas on Tides, Currents, Salinities, and Dye Dispersion," Report 1, Technical Report H-75-13, *Mobile Bay Model Study*, U.S. Army Engineer Waterways Experiment Station, Vicksburg, Miss., Sept. 1975.

LETTER, J.V., Jr., and McANALLY, W.H., Jr., "Assessment of Predictive Capabilities; Hydrodynamics of the Delaware River Estuary Model," Report 1, Research Report H-75-3, *Physical Hydraulic Models*, U.S. Army Engineer Waterways Experiment Station, Vicksburg, Miss., June 1975.

MARINOS, G., and WOODWARD, J.W., "Estimation of Hurricane Surge Hydrographs," *Journal of the Waterways and Harbors Division*, Vol. 94, No. WW2, May 1968, pp. 189-216.

McNAIR, E.C., and HILL, T.C., "Summary Report; Model Studies of Shrewsbury Inlet," Miscellaneous Paper H-72-2, U.S. Army Engineer Waterways Experiment Station, Vicksburg, Miss., Mar. 1972.

PRITCHARD, D.W., "Temperature Distribution in the James River Estuary Which Will Result from the Discharge of Waste Heat from the Surry Nuclear Power Station," Virginia Electric and Power Company, Richmond, Va., Aug. 1967.

REID, R.O., and BODINE, B.R., "Numerical Model for Storm Surges in Galveston Bay," *Journal of the Waterways and Harbors Division*, Vol. 94, No. WW1, Feb. 1968, pp. 33-58.

SAGER, R.A., and McNAIR, E.C., Jr., "Effects of Proposed Barriers on Hurricane Surge Heights; Hydraulic Model Investigation; Appendix A: Calibration Tests," Technical Report H-69-12, *Galveston Bay Hurricane Surge Study*, U.S. Army Engineer Waterways Experiment Station, Vicksburg, Miss., Mar. 1973a.

SAGER, R.A., and McNAIR, E.C., Jr., "Effects of Proposed Barriers on Tides, Currents, Salinities, and Dye Dispersion for Normal Tide Conditions; Hydraulic Model Investigation; Appendix B: Calibration Tests," Technical Report H-69-12, *Galveston Bay Hurricane Surge Study*, U.S. Army Engineer Waterways Experiment Station, Vicksburg, Miss., Mar. 1973b.

SAGER, R.A., and SEABERGH, W.C., "Fixed-Bed Hydraulic Model Results," App. 1, GITI Report 6, *Comparison of Numerical and Physical Hydraulic Models, Masonboro Inlet, North Carolina*, U.S. Army, Corps of Engineers, Coastal Engineering Research Center, Fort Belvoir, Va., and U.S. Army Engineer Waterways Experiment Station, Vicksburg, Miss., June 1977.

SIMMONS, H.B., "Protection of Narragansett Bay from Hurricane Surges, Summary Report; Hydraulic Model Investigation," Technical Report No. 2-662, U.S. Army Engineer Waterways Experiment Station, Vicksburg, Miss., Oct. 1964.

SIMMONS, H.B., and BOBB, W.H., "Hudson River Channel, New York and New Jersey; Plans to Reduce Shoaling in Hudson River Channels and Adjacent Pier Slips," Technical Report No. 2-694, U.S. Army Engineer Waterways Experiment Station, Vicksburg, Miss., Sept. 1965.

SIMMONS, H.B., HARRISON, J., and HUVAL, C.J., "Predicting Construction Effects by Tidal Modeling," Miscellaneous Paper H-71-6, U.S. Army Engineer Waterways Experiment Station, Vicksburg, Miss., Apr. 1971.

SIMMONS, H.B., and RHODES, H.J., "Matagorda Ship Channel Model Study, Matagorda Bay, Texas; Hydraulic Model Investigation," Technical Report No. 2-711, U.S. Army Engineer Waterways Experiment Station, Vicksburg, Miss., Jan. 1966.

STOLZENBACH, K.D., "Heated Surface Discharges: Three-Dimensional Temperature Distribution," *Engineering Aspects of Heat Disposal from Power Generation*, R.M. Parsons Laboratory for Water Resources and Hydrodynamics, Department of Civil Engineering, Massachusetts Institute of Technology, Cambridge, Mass., unpublished, June 1971.

TRAWLE, M.J., "Experiments in the Delaware River Model," Report 2, Research Report H-75-2, *Heat Dispersion in Physical Estuarine Models*, U.S. Army Engineer Waterways Experiment Station, Vicksburg, Miss., Feb. 1976.

U.S. ARMY ENGINEER DISTRICT, BALTIMORE, "The Chesapeake Bay Plan of Study," Baltimore, Md., June 1970.

U.S. ARMY ENGINEER WATERWAYS EXPERIMENT STATION, "Model Study of Plans for Elimination of Shoaling in Deepwater Point Range, Delaware River," Technical Memorandum No. 2-231, Vicksburg, Miss., May 1947.

U.S. ARMY ENGINEER WATERWAYS EXPERIMENT STATION, "Review of Model Study for Breakwater Location, Alameda Naval Air Station," Miscellaneous Paper No. 5-63, Vicksburg, Miss., Mar. 1950.

U.S. ARMY ENGINEER WATERWAYS EXPERIMENT STATION, "Salinity Tests of Existing Channel," Report 2, Technical Memorandum No. 2-337, *Delaware River Model Study*, Vicksburg, Miss., June 1954.

U.S. ARMY ENGINEER WATERWAYS EXPERIMENT STATION, "Hydraulic and Salinity Verification," Report 1, Technical Memorandum No. 2-337, *Delaware River Model Study*, Vicksburg, Miss., May 1956.

U.S. ARMY ENGINEER WATERWAYS EXPERIMENT STATION, "Effects of Proposed Closure of Southwest Pass on the Regimen of Vermilion Bay, Louisiana; Hydraulic Model Investigation," Technical Report No. 2-494, Vicksburg, Miss., Mar. 1959.

U.S. ARMY ENGINEER WATERWAYS EXPERIMENT STATION, "Savannah Harbor Investigation and Model Study; Results of Model Investigations; Model Verification and Results of General Studies," Vol. III, Section 1, Technical Report No. 2-580, Vicksburg, Miss., Oct. 1961.

U.S. ARMY ENGINEER WATERWAYS EXPERIMENT STATION, "Effects on Lake Pontchartrain, Louisiana, of Hurricane Surge Control Structures and Mississippi River-Gulf Outlet Channel; Hydraulic Model Investigation," Technical Report No. 2-636, Vicksburg, Miss., Nov. 1963.

U.S. ARMY ENGINEER WATERWAYS EXPERIMENT STATION, "Delaware River Model Study; Dike Rehabilitation," Technical Memorandum No. 2-337, Report 4, Vicksburg, Miss., May 1964.

U.S. ARMY ENGINEER WATERWAYS EXPERIMENT STATION, "Effects of a Proposed 35-Foot Channel to Richmond on Currents and Salinities over the Seed Oyster Beds in James River; Hydraulic Model Investigation," Miscellaneous Paper, 2-912, Vicksburg, Miss., Sept. 1966.

U.S. ARMY ENGINEER WATERWAYS EXPERIMENT STATION, "Special Analytic Study of Methods for Estuarine Water Resources Planning," Technical Bulletin No. 15, Committee on Tidal Hydraulics, Vicksburg, Miss., Mar. 1969.

U.S. DEPARTMENT OF THE ARMY, "Guidelines for Evaluating Estuary Studies, Models and Comprehensive Planning Alternatives," Washington, D.C., Aug. 1969.

ZITTA, V.L., and DOUGLAS, G.W., "State of the Art," Report 1, Research Report H-75-2, *Heat Dispersion in Physical Estuarine Models,* U.S. Army Engineer Waterways Experiment Station, Vicksburg, Miss., June 1975.

IV. COASTAL HARBORS

by
R.Y. Hudson

1. Introduction.

A port consists of a harbor with the necessary marine terminal facilities for the mooring of vessels during loading and unloading, and for the storage of goods awaiting transshipment. A harbor is an area of water that is protected from wave action to the extent that vessels are provided safe anchorage and satisfactory mooring, loading, and unloading conditions. Coastal harbors are either natural or artificial. Natural harbors are located in bays or other coastal indentations that provide complete or partial protection from storm wave action. Natural harbors with only partial protection may require the construction of breakwaters for additional protection from wave action. Artificial harbors are created by the construction of breakwaters when the selected location is not protected by natural coastline configurations. Harbors are also classified according to use; e.g., harbors of refuge, military harbors, fish harbors, large commercial harbors which are usually a part of a port complex, and small-craft harbors. Small-craft harbors are either harbors of refuge or marinas (American Society of Civil Engineers, 1969; Dunham and Finn, 1974). Harbors of refuge are usually located on a remote coastal area and are designed especially for boats in distress and for the transient boater. Marinas are small-craft harbors with the required facilities to moor and service recreational boats. Combining the commercial venture and the recreational aspects of small-craft harbors, marinas provide a logical location for the sale, outfitting, repair, and manufacture of pleasure craft.

Until recently, commercial harbors were located in coastal areas where oceangoing commerce and inland river, rail, or motor transportation systems were adequate and in adequately protected waters with depths to accommodate the number and size of vessels required to service the industry of the hinterland area. For this type of harbor, the functions of the design engineer consisted primarily in (a) the layout of the harbor facilities to provide vessels entering and leaving the harbor with adequate turning basins and navigation channels, (b) the location and structural design of the necessary piers and wharfs, and (c) the location and structural design of any required breakwaters to ensure adequate protection of moored vessels from wave action. Although the science of harbor design, especially small-craft harbors (Dunham and Finn, 1974), has progressed rapidly in recent years, the work of the designer has become more complex. The lack of good natural harbor sites and the constantly increasing size and draft of new ships (especially the tanker fleet of private industry), complicate the selection of a suitable coastal area which provides adequate depths (either natural or dredged), is near existing trade routes, and is in an area where the existing raw materials and industry can supply interstate and foreign commerce to the extent necessary to support a large harbor-port complex. To locate a site for

such a harbor is not only difficult, but the necessity to design the harbor to provide adequate protection for the larger ships from wave action becomes more acute. In addition, the problem of keeping harbor and port accommodations in balance with the requirements of "superships," now in operation or proposed, is international in scope and importance.

A great interest in small-boat ownership has developed in recent years. About 50.5 million people in the United States participated in recreational boating in 1976, more than 10 million boats used U.S. waterways and harbors, and about 6,000 small-craft harbors, and yacht and boating clubs provided berthing spaces and other services to boat owners (Cahners Publishing Co., Inc., 1977).

The problems of harbor design in providing adequate protection from wave action include: (a) Location of the harbor to ensure that the maximum possible protection from wave action is obtained; (b) determination of the location, alinement, height, and type of breakwater required to provide adequate wave protection; (c) determination of the best location, orientation, and dimensions of navigation openings to provide vessels safe and easy passage into and out of the harbor without impairing the wave protection characteristics of the harbor works; and (d) the positioning of spending beaches and other forms of wave absorbers inside the harbor area. Except for the deepwater harbors required for the new and large deep-draft vessels, either in use or proposed, the engineer is seldom consulted in the selection of sites for large commercial harbors, since most locations have been determined by industrial, transportation, and other economic requirements. However, in the case of small-craft harbors, the engineer is more likely to be employed at the start of the project, and is in a good position to provide the proper technical input to the problems of site selection. The first step in the solution of harbor problems is to select the types of waves for which protection will be required, and to obtain enough information relative to wave dimensions, directions of approach, and frequency of occurrence to enable the judicious selection of design wave characteristics. The complexity of wave action phenomena and the complicated geometry of most harbors cause difficulty in obtaining adequate answers to design problems strictly by analytical means. Thus, the hydraulic scale model is commonly used as an aid in the planning of harbor development, and in the design and layout of breakwaters and wave absorbers to obtain optimum protection from wave action.

In designing harbors, the engineer is concerned with the (a) short-period waves generated by stormwinds (those generated by local or near-local storms are usually referred to as "sea," and waves generated by distant storms, when they arrive at or near shore, as "swell") with periods from about 1 to 25 seconds and heights from about 1 to 40 feet or more; (b) intermediate-period waves with periods from about 25 seconds to 2 minutes; and (c) long-period waves from about 2 minutes to 1 hour. The origins of the intermediate- and long-period parts of the wave spectra that generate forced oscillations in harbor basins, which in turn may cause troublesome or damaging ship or boat surging, are not specifically known; however, the origins are believed to be the result of atmospheric

pressure differentials, wind setup, surf beats, shelf resonance, edge waves, internal waves, and tsunamis. The heights of the intermediate- and long-period waves range from about 1 inch to 3 feet for the forced oscillation, seich-type waves, and up to 30 feet or more for tsunamis. Tides are also long-period waves, but they are seldom reproduced in harbor wave action models. Instead, selected stillwater levels, representing high and low stages of the tide, and considering the effects of local wind setup and hurricane surge, are used for testing. Waves are also conveniently classified according to the ratio of water depth to wavelength, d/λ, called *relative depth*. Eagleson and Dean (1966) suggested the following classification (Table 4-1) of small-amplitude waves according to relative depth.

Table 4-1. Classification of small-amplitude waves (Eagleson and Dean, 1966).

Range of d/λ	Wave type
0 to 0.05	Shallow-water waves
0.05 to 0.5	Intermediate-depth waves
0.5 to ∞	Deepwater waves

Shallow-water and deepwater waves are also referred to as long and short waves, respectively. The classification according to the wave period is useful because the magnitudes of movements (roll, pitch, heave, surge, sway, and yaw), for vessels moored elastically at piers in the ordinary manner, are sensitive to the period of the incident waves measured in terms of the resonant periods of oscillation of the moored vessel. Likewise, amplitudes of the oscillations of the water masses in harbor basins are sensitive to the period of the incident waves measured in terms of the resonant periods of oscillations of the basin waters. According to Wilson (1967), the critical oscillations for ordinary-sized ships moored in commercial harbors with elastic lines lie in the intermediate-period wave range from about 25 seconds to 2 minutes. Raichlen (1968) states that the critical oscillations for the ordinary-sized boats that moor in small-craft harbors lie in the short-period wave range of about 10 seconds and less. The classification of waves according to relative depth is useful because the wave velocity and the degree of refraction of waves approaching a problem area from deep water through water of decreasing depth is a function of the d/λ ratio. The phenomenon of wave diffraction is also a function of relative depth.

The perimeter walls of most harbor basins are usually prime wave reflectors, and the reflection coefficient increases as the wave period increases. Thus, for intermediate- and long-period waves the harbor boundaries are nearly perfect wave reflectors, and standing-wave systems are generated in the harbor basins for such waves with little reduction in energy due to friction. Such waves oscillating in harbor basins are usually called *seiches*, a French term which was used originally to designate the free oscillations of relatively long-period standing waves in lakes or other enclosed bodies of water. Seiches in lakes were usually caused by the piling up of water on the windward side of the lake (wind

setup), due to the tractive force of stormwinds blowing over the water surface in one direction, and the consequent release of the water when the wind shifted in direction or was reduced in speed over a short period of time. However, common usage of seiche now applies to both free and forced oscillations of enclosed and semienclosed bodies of water. Seiches in harbor basins are forced oscillations with periods that are generally determined by the periods of the incident waves which enter the basins from the ocean area surrounding the harbor, rather than the natural or free oscillation periods of the basin. A resonant oscillation occurs when the period of the forcing oscillation is equal to the period of the fundamental (gravest mode) or a harmonic of the natural period of oscillation of the basin waters. Water oscillations with periods greater than those of the third harmonic of the fundamental are believed to be rare, except for harbor basins that are somewhat rectangular in shape, because the energy in the higher harmonics can be dissipated more easily by imperfect reflections from the irregular boundaries. Standing wave systems with periods in the intermediate- and long-wave range have large horizontal excursions in the nodal areas, even when the vertical amplitudes are as small as 6 inches to 1 foot. Ships moored elastically in or near the nodal areas of such oscillations in a harbor basin are subjected to oscillatory forces that can cause mooring lines to break and damage the ship or pier or, at a minimum, make loading or unloading of cargo difficult or impossible. The resonant motion of a moored vessel is a function of the vessel's mass and the length, number, position, and elasticity of the mooring lines. Thus, resonant ship motions may occur when the water masses in the harbor basin are not oscillating in a resonant mode. However, the worst conditions for the shipowner would be when both the harbor-basin waters and the moored ship were oscillating in resonance with the forcing oscillations from outside the harbor.

The above discussion shows that the designer of a harbor faces a formidable task where relatively large vessels are moored elastically for loading and unloading cargo, and where the harbor is exposed to relatively long-period waves. From a practical approach, the designer should determine the wave energy spectrum that exists outside the harbor and then select water depths and horizontal dimensions of the harbor basins to detune the basins from the peaks in the intermediate- and long-period part of the energy spectrum of the outside waves. The detuning of the harbor basins is difficult, if not impossible, except for one or two of the incident wave periods, because the basin geometry and dimensions are largely determined by the requirements of ship navigation into and out of the different harbor basins, the required turning basin areas, and the water depths necessary to accommodate the larger, deep-draft vessels. For optimum mooring conditions, the harbor designer should be able to detune the oscillating characteristics of the moored ships from both the periods of the outside forcing function and the resonant periods of the water masses in the harbor basins. This stage of the detuning process, to be successful, would require that the energy spectrum of the forcing oscillation contain a minimum of peaks, and that the harbor designer has both the authority to establish the method of ship mooring and the technical information and ability to determine the characteristics of the mooring

system required to reduce ship oscillations sufficiently to meet the surge criteria for different classes of ships and loading conditions. Unfortunately, little reliable data are available from which to obtain the answers to this problem. More theoretical and experimental investigations are needed to provide the design engineer with the necessary tools to solve the harbor-basin and ship mooring design problems.

Theoretically, the problems of designing small-craft harbors are closely related to those problems for the relatively large, commercial vessel harbor, but the short-period part of the wave energy spectrum is the important consideration when the harbor is used to berth small craft. This is especially true for marinas where the boats are for recreational use and are moored by the average boater and left unattended except for the weekend or longer periods of time. However, more prototype wave data are generally available, mostly from hindcast studies, and with the proper selection of breakwater position, length, crest height, and degree of imperviousness, and if adequate space is allowed for the use of wave absorbers in the critical parts of the harbor perimeter, the wave climate in the berthing areas can usually be reduced satisfactorily. The problems of devising satisfactory mooring methods for small craft are not as intractable as are those for the larger ships, although the problems are somewhat similar in their theoretical aspects. Raichlen (1968) provides some valuable information for use as a guide in mooring small craft, but additional studies are needed to place the solution of small-craft mooring problems on a sounder scientific basis.

2. Similitude Relations.

a. Geometrically Similar (Undistorted-Scale) Models. Ideally, all harbor wave action model studies that are performed to determine optimum plans for providing adequate wave protection for moored vessels should be conducted using models constructed geometrically similar to their prototype harbors. Fortunately, the size and depth of most harbors and the order of magnitude of the horizontal dimensions of short-period storm waves (periods usually range from about 2 to 5 seconds for lakes of small to moderate size, about 5 to 10 seconds for large lakes and near-local ocean storm waves, and about 10 to 20 seconds for severe storm waves generated in ocean areas located a considerable distance from the harbor) are such that undistorted-scale models can be used. Few harbors are of a size and depth to be feasible for use in undistorted-scale models for intermediate- and long-period waves. In nature, surface wind waves are propagated by the restoring force of gravity, and surface tension and friction forces, although present, are not usually of sufficient magnitude to affect wave action significantly within the areas reproduced by scale models. Thus, harbor wave action models where short-period wind waves cause a problem are designed in accordance with the Froude model law and are constructed geometrically similar to their prototypes. After the linear scale, L_r, has been selected, the model-to-prototype relationships necessary for model design, construction, and operation, the interpretation of model results and the transference of model test data to corresponding prototype units can be derived in terms of the linear scale

from the Froude model law, and simple relationships for area, volume, force, etc., as follows:

(1) Velocity. Velocity ratios are obtained directly from the Froude model law (eq. 2-9, Section II)

$$\frac{V_m}{(g_m L_m)^{1/2}} = \frac{V_p}{(g_p L_p)^{1/2}} ,$$

from which

$$\frac{V_m}{V_p} = \left(\frac{g_m}{g_p}\frac{L_m}{L_p}\right)^{1/2}$$

and

$$V_r = (g_r L_r)^{1/2} . \qquad (4\text{-}1)$$

(2) Time. Since length equals velocity times time,

$$L_r = V_r T_r , \quad V_r = \frac{L_r}{T_r} = (g_r L_r)^{1/2} ,$$

and

$$T_r = L_r^{1/2} g_r^{-1/2} = \left(\frac{L_r}{g_r}\right)^{1/2} \qquad (4\text{-}2)$$

(3) Force. Since force equals mass times acceleration,

$$F_r = M_r \frac{dV_r}{dT_r} = L_r^3 \frac{\gamma_r}{g_r}\frac{V_r}{T_r} . \qquad (4\text{-}3a)$$

Substituting the values of V_r and T_r from equations (4-1) and (4-2)

$$F_r = L_r^3 \gamma_r . \qquad (4\text{-}3b)$$

(4) Weight. Weight equals volume times specific weight; therefore,

$$W_r = L_r^3 \gamma_r . \qquad (4\text{-}4)$$

(5) Energy. Energy is a force times distance; therefore,

$$E_r = F_r L_r = L_r^4 \gamma_r . \qquad (4\text{-}5)$$

Similarly, for area, volume, discharge, and pressure,

$$A_r = L_r^2 \tag{4-6}$$

$$\overline{V} = L_r^3 \tag{4-7}$$

$$Q_r = L_r^{5/2} \tag{4-8}$$

and

$$p_r = \frac{F_r}{L_r^2} = \frac{L_r^3 \gamma_r}{L_r^2} = L_r \gamma_r \, . \tag{4-9}$$

Essentially, $g_r = 1$ and this should be considered when referring to the model scales (derived above) in Table 4-2. The similarity relations for undistorted wave models, derived by the method of differential equations, are also presented in Section II,3.

Table 4-2. Derived model scales.

Characteristic	Dimension	Model-to-prototype scale
Length	L	L_r
Area	L^2	$A_r = L_r^2$
Volume	L^3	$\overline{V}_r = L_r^3$
Time	T	$T_r = L_r^{1/2}$
Velocity	L/T	$V_r = L_r^{1/2}$
Discharge	L^3/T	$Q_r = L_r^{5/2}$
Force	F	$F_r = L_r^3 \gamma_r$
Weight	F	$W_r = L_r^3 \gamma_r$
Pressure	F/L^2	$p_r = L_r \gamma_r$
Energy	FL	$E_r = L_r^4 \gamma_r$

b. Geometrically Dissimilar (Distorted-Scale) Models. Linear-scale distortion (where the horizontal length scale is not the same as the scale of vertical lengths) is used in hydraulic models of harbor wave action problems when the wave periods, and also wavelengths, are of a magnitude that requires the use of excessively large models, and when the water depths in the prototype are such that the use of an undistorted scale would result in depths in the model so small that the friction effects would be excessive. The use of distorted-scale models also provides easier measurement of wave heights, especially for long-period,

seiche-type waves which have small wave heights in the prototype. Thus, distorted scales are used when the departure from geometric similarity serves a definite purpose, and the use of the model is limited to those problems for which the resulting scale effects are minor. The accuracy of such models depends primarily on the degree of scale distortion and the prototype water depths relative to wavelength.

For long, shallow-water waves of small amplitude, and $0 < d/\lambda < 0.05$, in which the wave velocity is given by the relation

$$V = (gd)^{1/2} , \tag{4-10}$$

distorted-scale models reproduce wave refraction and diffraction and resonant periods accurately. For all types of waves, the bottom-friction effects in distorted-scale models are less than those in undistorted models. Wave reflection effects are increased by scale distortion. For long waves, the velocity scale can be determined directly from equation (4-10) as follows (eq. 2-9, Section II);

$$\frac{V_m}{V_p} = \left(\frac{g_m}{g_p}\frac{d_m}{d_p}\right)^{1/2}$$

or, since $g_m = g_p$, and all vertical lengths (L_v) in the model are measured in accordance with the depth ratio; i.e.,

$$\frac{d_m}{d_p} = \frac{(L_v)_m}{(L_v)_p} ,$$

$$V_r = (L_v)_r^{1/2} . \tag{4-11}$$

This is the same relationship that is obtained by use of the Froude model law with the water depth as the linear dimension. If the horizontal lengths are designated L_h, the scale of horizontal lengths as $(L_h)_m/(L_h)_p = (L_h)_r$, and the distortion factor (a number greater than unity) as $\overline{DF}$, then

$$\overline{DF} = \frac{(L_v)_r}{(L_h)_r} . \tag{4-12}$$

Based on the designations above, the time ratio is derived as follows:

$$T_r = \frac{(L_h)_r}{V_r} = \frac{(L_h)_r}{(L_v)_r^{1/2}}$$

or

$$T_r = \frac{(L_h)_r^{1/2}}{(\overline{DF})^{1/2}} . \tag{4-13}$$

The derivations above are for the special case in which the waves are of sufficient length relative to depth that the wave velocity is a function only of gravity and the water depth. In the general case, for small-amplitude waves,

$$V = \left(\frac{g\lambda}{2\pi} \tanh \frac{2\pi d}{\lambda}\right)^{1/2} \tag{4-14}$$

and the velocity ratio, with $g_m = g_p$, is

$$\left(\frac{V_m}{V_p}\right)^2 = \frac{\lambda_m}{\lambda_p} \frac{\tanh \frac{2\pi d_m}{\lambda_m}}{\tanh \frac{2\pi d_p}{\lambda_p}} . \tag{4-15}$$

Thus, since wavelength is a horizontal dimension,

$$V_r = (L_h)_r^{1/2} \frac{\left(\tanh \frac{2\pi d_m}{\lambda_m}\right)^{1/2}}{\left(\tanh \frac{2\pi d_p}{\lambda_p}\right)^{1/2}} \tag{4-16a}$$

and the time ratio is $T_r = (L_h)_r / V_r$, or

$$T_r = (L_h)_r^{1/2} \frac{\left(\tanh \frac{2\pi d_p}{\lambda_p}\right)^{1/2}}{\left(\tanh \frac{2\pi d_m}{\lambda_m}\right)^{1/2}} . \tag{4-17a}$$

Also, since (eq. 4-12)

$$\overline{DF} = \frac{(L_v)_r}{(L_h)_r} = \frac{d_m}{d_p} \times \frac{\lambda_p}{\lambda_m} ,$$

equation (4-16) becomes

$$V_r = (L_h)_r^{1/2} \frac{\left(\tanh \frac{2\pi d_p \overline{DF}}{\lambda_p}\right)^{1/2}}{\left(\tanh \frac{2\pi d_p}{\lambda_p}\right)^{1/2}} \tag{4-16b}$$

and equation (4-17a) becomes

$$T_r = \left(L_h\right)_r^{1/2} \frac{\left(\tanh \frac{2\pi d_p}{\lambda_p}\right)^{1/2}}{\left(\tanh \frac{2\pi d_p \overline{DF}}{\lambda_p}\right)^{1/2}} . \qquad (4\text{-}17b)$$

These equations show that, for intermediate-depth waves, the velocity and time ratios are dependent on the local prototype relative depths, the horizontal scale, and the distortion factor. Thus, for wave periods and depths such that $0.05 < d/\lambda < 0.5$, scale distortion has the effect of distorting the wave refraction patterns compared with the prototype patterns and those obtained from models with undistorted scale.

Distorted-scale models of waves that fall within the category of intermediate-depth waves can be used to obtain the correct refraction patterns as the waves approach a harbor, but then the accuracy of the resonance conditions within the harbor basins is sacrificed. The refraction patterns in a distorted-scale model and the prototype will be similar if

$$\frac{d_m}{\lambda_m} = \frac{d_p}{\lambda_p} \qquad (4\text{-}18)$$

or

$$\frac{d_p}{\lambda_p} = \frac{\left(L_v\right)_r d_p}{\lambda_m} \qquad (4\text{-}19)$$

and

$$\lambda_p = \frac{1}{\left(L_v\right)_r} \lambda_m . \qquad (4\text{-}20)$$

Since

$$\lambda = \frac{gT^2}{2\pi} \tanh \frac{2\pi d}{\lambda} \qquad (4\text{-}21)$$

$$\frac{gT_p^2}{2\pi} \tanh \frac{2\pi d_p}{\lambda_p} = \frac{1}{\left(L_v\right)_r} \frac{gT_m^2}{2\pi} \tanh \frac{2\pi d_m}{\lambda_m} \qquad (4\text{-}22)$$

and, in accordance with equation (4-18),

$$\tanh \frac{2\pi d_p}{\lambda_p} = \tanh \frac{2\pi d_m}{\lambda_m} . \qquad (4\text{-}23)$$

Thus, equation (4-22) reduces to

$$T_p^2 = \frac{1}{(L_v)_r} T_m^2 \qquad (4\text{-}24a)$$

or, to obtain similar refraction patterns, model-to-prototype, in distorted-scale models,

$$T_m = T_p (L_v)_r^{1/2} \ . \qquad (4\text{-}24b)$$

3. Model Design.

a. Field Data Required. The following information and field data are needed for hydraulic model studies of harbor wave action problems:

(1) Statistical data describing the wave environment.

(2) Tide data referred to a standard datum.

(3) Accurate depth contours within the harbor area and outside the harbor to a sufficient depth seaward to allow the construction of refraction diagrams or orthogonals from deep water to the harbor area for the different deepwater directions of wave approach. The depth contours should be referred to the same datum as that used for the tide data.

(4) Topographic and hydrographic maps of the harbor and adjacent land area showing locations of all pertinent harbor and shoreline structures. The maps should be referred to the same horizontal control and vertical datum as those used to show depth contours.

(5) Construction details of existing and proposed breakwaters, jetties, wave absorbers, seawalls, piers, and docks.

(6) Details of existing and proposed plans for the dredging of turning basins and navigation channels.

(7) The resonant wave periods for both surge and sway (fore-and-aft motion of the vessel parallel to the dock line and sideways motion perpendicular to the dock line, respectively) of all types and classes of large vessels expected to moor in the harbor. The resonant wave periods should be obtained for the type of mooring-line assembly used for each type and class of vessel. For small craft it is usually unnecessary to obtain resonant wave periods for motions other than those of surge fore and aft.

(8) The maximum allowable wave height for each type and class of vessel as a function of wave period.

Items (1) to (6) provide data needed to design and construct the model and select the test waves and stillwater level conditions. Items (7) and (8) provide information for analyzing the test data to obtain the best harbor-basin arrangement and the most efficient breakwater plan for reducing wave action conditions within the harbor to tolerable levels for the types and sizes of vessels that will moor in the harbor basins. The ideal harbor for the movement of moored vessels is a harbor where the geometry and depths are such that the water masses in individual basins within the harbor are not tuning to any of the incident wave periods, and where moored vessels are not excited to resonant oscillations by the incident waves. Waves in nature are complex and contain different wave periods in the same train. The size, shape, and depths of harbor basins are also determined primarily by the type and size of vessels that frequent the harbor. Thus, all resonant phenomena cannot be excluded by avoiding the harbor-basin dimensions that are critical to incident wave periods. Likewise, it is not possible to exclude from the harbor all vessels that are of a size that, with the normal mooring-line assembly, are excited to abnormal oscillations by the forcing function of the incident waves. Some relief can be obtained by variations in the elasticity, size, and tautness of lines, but the necessity of allowing for changes in tide level makes it difficult without sophisticated mooring tension apparatus.

The short-period wave data needed for harbor wave action models are similar to those required for stability models of coastal structures (see Sec. VI). The significant deepwater wave heights and periods ($H_{1/3}$ and $T_{1/3}$, respectively) from the different directions of approach are usually selected for use in testing, and these deepwater waves are projected into the positions of the wave generator by existing wave refraction techniques. However, for complicated inshore bathymetry, wave refraction and shoaling effects become more complex, and there is a need for a more reliable method of selecting shallow-water test-wave dimensions and directions for both stability and harbor wave action model studies. The heights of intermediate- and long-period waves that cause objectionable surge oscillations of moored ships are relatively small, even in harbor basins that are excited by resonant wave periods. Thus, it is difficult and usually impractical, to obtain model input data for such waves in areas other than those within the harbor basins or immediately outside the breakwaters. Measurable wave heights are generally easier to obtain in the antinodal areas where the vertical motion of the water is maximum; however, this may pose a problem for any but the most simple geometry in mooring areas. If the mooring area is in the form of a slip where the adjacent docks are impervious to the flow of water, a simple two-dimensional oscillation of the standing wave system occurs, and a wave gage in the shoreward end of the slip is in an antinodal area and near enough to the ships docked in the slip so that there should be good correlation between the recorded heights and periods of the waves and the surge amplitude of the ships. When the mooring basin geometry is more open and complex in plan form, the positions of the nodal and antinodal areas are item functions of the wave period, and the selection of satisfactory gage locations becomes difficult. Considerable help in

the location of intermediate- and long-period wave gages can be obtained from mathematical models where the modes of oscillation of the harbor areas for different wave periods are plotted by digital computer techniques.

The resonant wave periods of vessels that frequent a harbor can be obtained from model studies of individual vessels in which the vessel's shape, size, mass distribution, and weight, and the characteristics of the mooring-line assembly, are reproduced to acquire dynamic similarity, model-to-prototype. This information should be complemented by prototype wave data correlated with actual vessel observations with respect to the severity of surge oscillations. Both types of data are difficult, expensive, and time consuming to obtain, and sufficient data of these types can seldom be acquired to allow accurate analysis of harbor wave action problems. Without this information, the harbor wave action model will reliabily show which of several plans is the best for intermediate- and long-period wave action in the different basins of the harbor, but it cannot ensure that the best of several plans will be satisfactory for the surge and sway of vessels moored elastically at docks within the harbor. This situation is also true for short-period waves in small-craft harbors, at least in principle. However, experience has shown that small-craft harbors are usually satisfactory, with respect to the breaking of lines and boat damage, if the wave heights in the harbor basins can be reduced to about 1 foot or less. Raichlen (1968) has stated that the motions of small craft may be reduced by the proper design of mooring systems and the imposition of certain mooring restrictions, rather than the drastic and expensive reduction of wave energy that is allowed to enter the harbor basins.

The tsunami data needed for the conduct of a harbor wave action model are essentially the same as those needed when the waves are short- or intermediate-period waves. Design and operation of the model and the interpretation of model test results require that the frequency of occurrence of tsunamis with different periods and wave heights, from the different directions of approach, be available for locations in the ocean corresponding to the shallow-water positions of the wave generator. However, tsunamis in the open ocean are so long and their heights so small that deepwater tsunami data are exceedingly difficult to obtain and such data, sufficient for harbor model studies, are not presently available. Since the tsunami problem areas of the United States are limited to the west coast and to some coasts of Hawaii, considerable data are available for these areas. These data consist of the frequency of occurrence for tsunamis of different heights and periods as measured in bays, coastal zones, and harbors in the problem areas (Cox, 1964; Wiegel, 1965). The directions of the wave fronts at the ocean limits of a proposed model are determined by wave refraction studies in which the wave rays are projected from the earthquake epicenters where the major tsunamis originate. A digital computer program, written specifically for tsunami refraction, has been used in a study concerning the design of a proposed tsunami model of Crescent City Harbor, California (Keulegan, Harrison, and Mathews, 1969).

b. Selection of Linear Scale.

(1) Short-Period Waves. Coastal harbor models in which the problem involves the protection of mooring basins from the attack of short-period wind waves are designed in accordance with Froude's law and are constructed geometrically similar to the prototype harbor. The linear scale is selected so that internal friction and surface tension forces are negligible, compared with gravity forces. The linear scale should also be selected so that the reduction of model wave heights by bottom friction in the viscous boundary layer is negligible, or is such that the lack of similarity of the friction forces, model-to-prototype, can be corrected by analytical and experimental methods. The harbor wave action model must usually reproduce the complete prototype harbor, with enough upcoast and downcoast distances to allow the littoral current to generate, and with enough ocean area to allow the waves to generate in depths of water so that the refraction of waves, between the wave generator and the harbor, will reproduce correctly. Thus, in most instances, a prototype area of considerable size must be reproduced in the model; since economical considerations require the selection of a linear scale so that the model will be as small as possible consistent with the need for accurate test results, a trade-off situation between cost of model construction and the magnitude of scale effects is usually encountered. The linear scale must also be selected so that model wave heights obtained in the problem areas are of sufficient magnitude for accurate measurement. Experience has shown that, considering the size of harbors, the depths of water, the wave dimensions encountered, and the type of wave gages and model shelter area usually available (and considering other factors mentioned above), the linear scales selected for harbor wave action models where short-period waves are the cause of the problem are usually within the range of about 1:75 to 1:150, model-to-prototype.

(2) Intermediate- and Long-Period Waves. The intermediate- and long-period waves of primary interest to harbor wave action conditions are the relatively long-period, small-amplitude waves with periods ranging from about 20 or 25 seconds to 2 to 3 minutes. For ordinary commercial vessels, the critical range of wave periods for vessels moored with the commonly-used elastic mooring-line assemblies is between about 25 seconds and 2 minutes. During the last decade, vessels of about 250,000-ton displacement or more have been constructed and placed in operation. When harbors become available that have sufficient navigable depths to accommodate these large vessels, the range of critical wave periods will increase unless more sophisticated mooring assemblies are devised. However, the problems of selecting linear scales and designing hydraulic models for study of mooring problems should not be affected appreciably. The selection of linear scales and the design of harbor models for intermediate- and long-period waves are more difficult than the problems encountered when the model study involves only short-period wind waves. There are several reasons for this situation. One reason is that the ocean area that should be reproduced in the model increases with wavelength, and wavelength increases as the square of the wave period for deepwater waves and for intermediate-depth waves at equal relative

depths, and with the product $d^{1/2}T$ for long waves. The wave steepnesses of intermediate- and long-period waves are also small, and this results in nearly perfect reflection of these waves from beach slopes as flat as about 1:100. This causes problems of scale selection in two ways: (a) Since longer period waves easily reflect from the beach and harbor areas of the model, and because it is infeasible to reproduce a sufficiently large ocean area to allow complete tests before the reflected waves reach the wave generator (located along the boundary of the ocean area of the model), and because waves of long period and small steepness are difficult to absorb without appreciable reflection from the face of the absorber, a large part of the ocean area reproduced in the model (including the area in front of the wave generator) must be filled with wave-absorber material; and (b) the periods of long waves and the resulting high reflection coefficients even on flat beach slopes result in the phenomena of bay and shelf resonance which, in turn, if the harbor is located on a continental shelf or in a bay, or both, can make it necessary to include the bay and shelf in the modeled area. If the shelf is comparatively narrow, long-period oscillations of the shelf waters may occur within the range of critical wave periods of the moored ships. Biesel and Le Mehaute (1955) have stated that when the shapes of both the coast and the shelf are complex, the use of a small preliminary model may be necessary to reproduce a large part of the coast and shelf together with a considerable part of the adjacent ocean area seaward of the shelf.

Because of the situation discussed above, and the ever-present economical and practical considerations, the use of distorted-scale models is necessary in most instances. In such models the vertical and horizontal linear scales are unequal, and

$$\left(\frac{L_m}{L_p}\right)_v > \left(\frac{L_m}{L_p}\right)_h .$$

A few harbor models with the problem of intermediate-period waves have been conducted using undistorted scales of about 1:100; however, most of these studies are conducted using distorted scales. The vertical scales for such models usually range from about 1:50 to 1:100, and the distortion factor is usually from about 3 to 5; e.g., the Los Angeles-Long Beach Harbor model designed and constructed in 1972 had a vertical scale of 1:100 and a horizontal scale of 1:400. For preliminary models where the modes of oscillation are of primary interest, and where the waves and water depths are such that the long-wave velocity relation, $V = (gd)^{1/2}$, is applicable, the horizontal-scale ratio can be decreased and the distortion factor increased. The degree to which the model can be reduced in size and depth is dependent on the accuracy desired. For waves and water depths where the long-wave velocity relation is not applicable, and where the wave velocity is a function of both water depth and wavelength, the error in wave refraction increases as the wave period decreases for a given distortion factor.

c. Scale Effects.

(1) Short-Period Waves and Undistorted, Linear-Scale Models. Although harbor models with the problem of short-period waves are designed in accordance with Froude's law and are constructed geometrically similar to the prototype, the conditions of similitude are not met completely in most instances because friction forces cannot be modeled correctly. Waves are attenuated by surface tension, internal friction, and friction in the bottom boundary layer. Friction effects also reduce the amount of wave energy that is transmitted through pervious coastal structures such as rubble-mound breakwaters and jetties. Bottom friction and the energy loss as waves are transmitted through rubble-mound breakwaters are exaggerated in harbor models and these phenomena constitute the major scale-effect problems in the design of short-period, wave action models. If the linear-scale ratio (L_r) is too small, surface tension can affect the wave velocity, resulting in errors in wave refraction, and internal friction can considerably reduce the wave heights. The effects of surface tension on wave velocity are shown in Figure 4-1. According to Keulegan (1950a), the expression for the variation of wave height with time, due to internal friction, is

$$\frac{H_t}{H_{t=o}} = e^{-8\pi^2 \nu t/\lambda^2} \tag{4-25}$$

and, if t' is the time required to reduce the wave height 50 percent,

$$t' = 0.0088 \frac{\lambda^2}{\nu} . \tag{4-26}$$

In terms of wave period (T) and the distance of wave travel in time t', (x), and with a temperature of 21° Celsius (70° Fahrenheit) ($\nu = 1.059 \times 10^{-5}$), equation (4-26) reduces to

$$x_p = 111{,}750\ T^5 \left(\tanh \frac{2\pi d}{\lambda}\right)^3 . \tag{4-27}$$

The effects of internal friction on the reduction of wave height for relatively small wave periods are shown in Figure 4-2. The figure shows that the effects of surface tension and internal friction can be made negligible in harbor wave action models by the proper selection of linear scale. The law of variation of the wave height with distance due to friction in the viscous boundary layer for a train of progressive oscillatory waves in a rectangular channel of uniform cross section, is (Keulegan, 1950b)

$$\frac{H_2}{H_1} = e^{-\alpha x_p} , \tag{4-28}$$

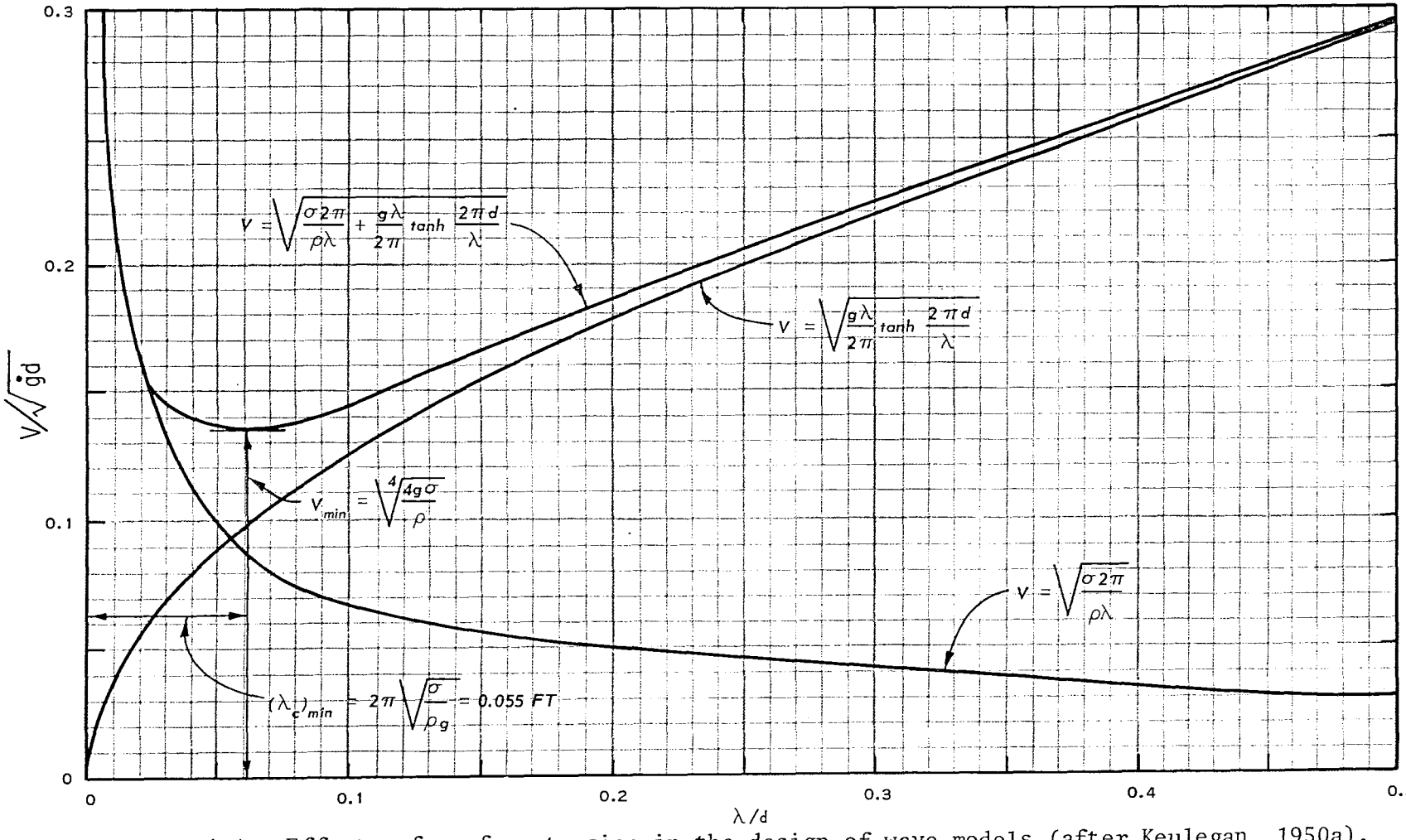

Figure 4-1. Effects of surface tension in the design of wave models (after Keulegan, 1950a).

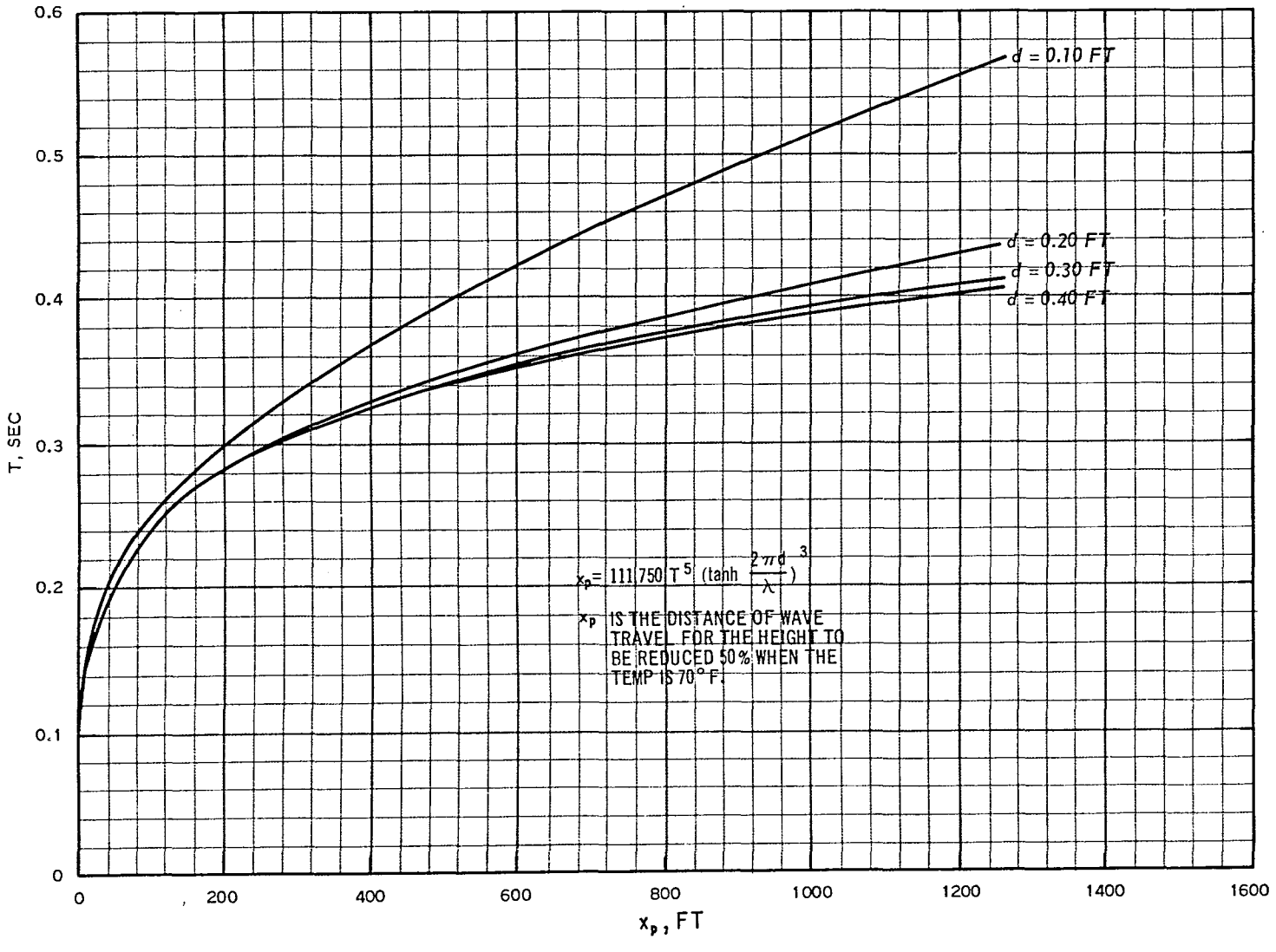

Figure 4-2. Effects of internal friction in the design of wave models (after Keulegan, 1950a).

where

$$\alpha = \frac{2}{VB}\left(\frac{\pi\nu}{T}\right)^{1/2}\left(\frac{\lambda \sinh\frac{4\pi d}{\lambda} + 2\pi B}{\lambda \sinh\frac{4\pi d}{\lambda} + 4\pi d}\right) \tag{4-29}$$

and

V = wave velocity

B = flume width

H_1 = wave height at $x_p = 0$

H_2 = height after the wave has traveled a distance x_p in water of depth d.

If the flume width is many times greater than the water depth, equation (4-29) reduces to

$$\alpha = \frac{4\pi^{3/2}\nu^{1/2}T^{1/2}}{\lambda^2\left(\sinh\frac{4\pi d}{\lambda} + \frac{4\pi d}{\lambda}\right)} \tag{4-30}$$

which is the same as that of Eagleson and Dean (1966). According to Keulegan (personal comunication, 1977) the values of α as determined from equation (4-30) should be increased about 25 percent, or

$$\alpha = \frac{5\pi^{3/2}\nu^{1/2}T^{1/2}}{\lambda^2\left(\sinh\frac{4\pi d}{\lambda} + \frac{4\pi d}{\lambda}\right)}. \tag{4-31}$$

This increase is deemed necessary because of the energy losses due to the contamination of the water surface by dust and oily molecules. The effects of bottom friction in harbor wave action models, including the suggested 25-percent increase in α, are shown in Figures 4-3 and 4-4. The figures show that (a) effects of bottom friction in the prototype (linear scale of 1:1) are negligible within the area and travel distances reproduced in ordinary wave action models; (b) linear scales less than about 1:100 can seldom be used; (c) energy loss due to bottom friction becomes appreciable as the water depths become small; and (d) wave heights measured in harbor wave action models should be corrected to minimize the scale effects due to bottom friction. The correction coefficients can be calculated from equations (4-28) and (4-31).

If rubble-mound breakwaters and wave absorbers are modeled geometrically similar to their prototype structures, there is relatively more wave reflection from the model structures and relatively less wave transmission through the model structures compared with the prototype, unless

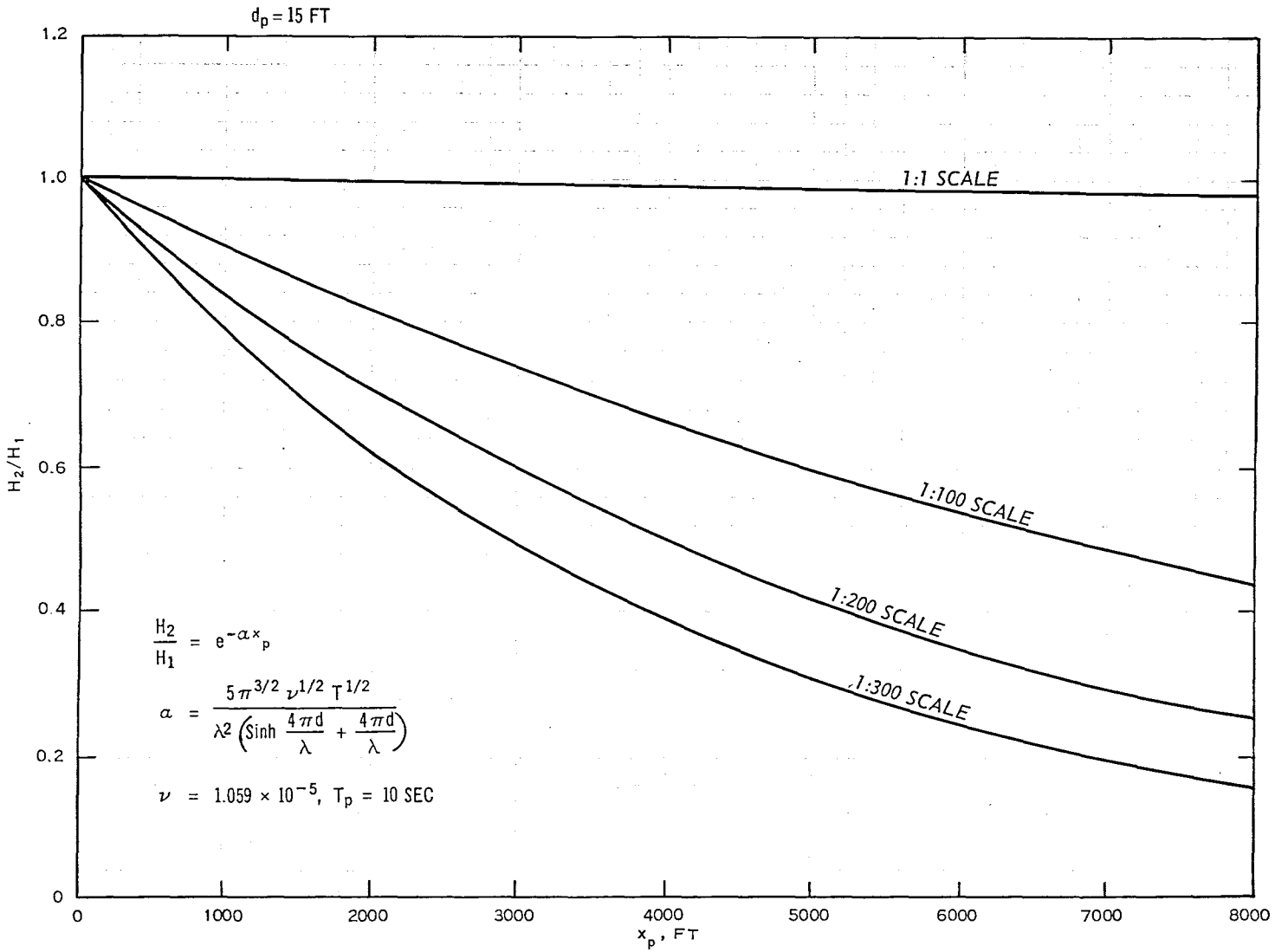

Figure 4-3. Effects of bottom friction in the design of wave models, d_p = 15 feet (after Keulegan, 1950b; personal communication, 1977).

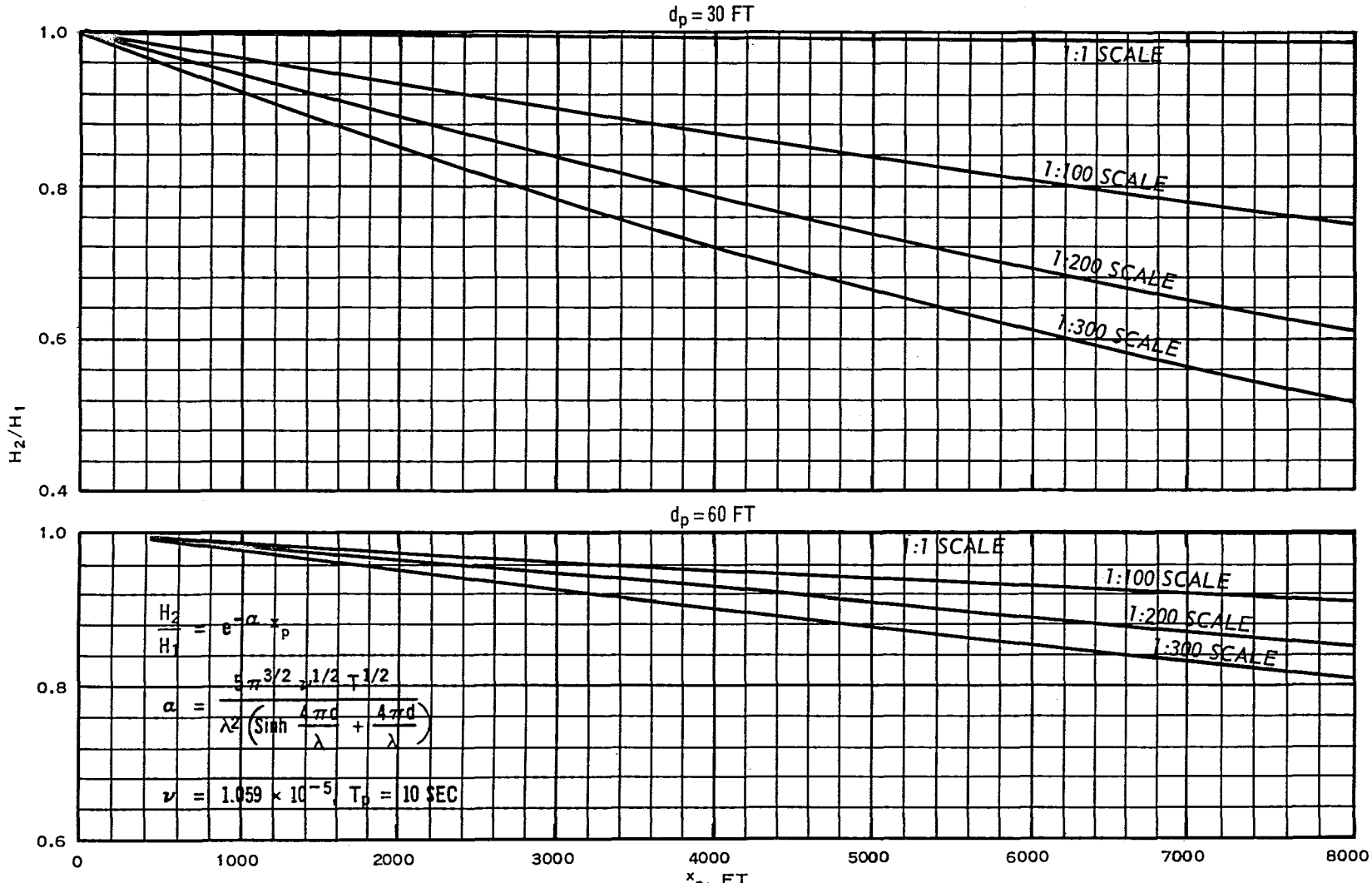

Figure 4-4. Effects of bottom friction in the design of wave models, d_p = 30 and 60 feet (after Keulegan, 1950b, personal communication, 1977).

the model scale is large enough to ensure that the motion is fully turbulent in the model. For most harbor model studies, the linear scales are relatively small and the scale effects in wave reflection and transmission are appreciable. Le Mehaute (1965) stated that scale effects for both wave reflection and transmission can be reduced by using model quarrystone sizes in the protective cover layers and the core material larger than those determined by the linear scale of the model; i.e.,

$$\frac{D_m}{D_p} = K \frac{L_m}{L_p} \tag{4-32}$$

where D is the effective stone diameter, L_m/L_p the linear scale, and K a coefficient greater than one. The value of K for the armor units in the protective cover layer, the characteristics of which determine the reflection coefficient for a rubble breakwater or wave absorber with a given slope, is not the same as the value of K for the core material, which determines to a large extent the wave transmission characteristics of the breakwater. This is especially true if the crest of the core material section is high relative to the total height of the structure. The values of K, for both wave reflection and wave transmission through the voids of the breakwater or wave absorber, can best be determined by experiment. Approximate values of K for wave transmission can be obtained from a nomograph by Le Mehaute (1965) based on analytical considerations and available experimental data (Fig. 4-5). The variables of this nomograph are defined as follows:

> $\Delta H/\Delta L$ is the gradient of the head loss through the voids in the core material part of the breakwater section. ΔH is the height of the incident wave, H_i, and ΔL the average width of the core material section. D_p is the effective quarrystone diameter of the prototype core material in centimeters, and is taken to be the 10 percent smaller than quarrystone from the core material gradation curve. P is the porosity of the core material ($0 < P < 1$).

Le Mehaute (1965) assumes that the gradation curves of the core material in model and prototype are the same, or $P_m = P_p$. The use of the nomograph to estimate the size of model core material necessary to minimize the scale effects in wave transmission through the voids of a breakwater core (scale effects are assumed to be negligible insofar as transmission through the outer armor-unit cover layers are concerned) is given in the following example.

Given:

$$(H_i)_p = \Delta H = 15 \text{ ft},$$
$$\Delta L = 50 \text{ ft},$$
$$\frac{L_m}{L_p} = \frac{1}{100},$$
$$D_p = 0.50 \text{ ft} = 15.2 \text{ cm, and}$$
$$P_p = 0.35.$$

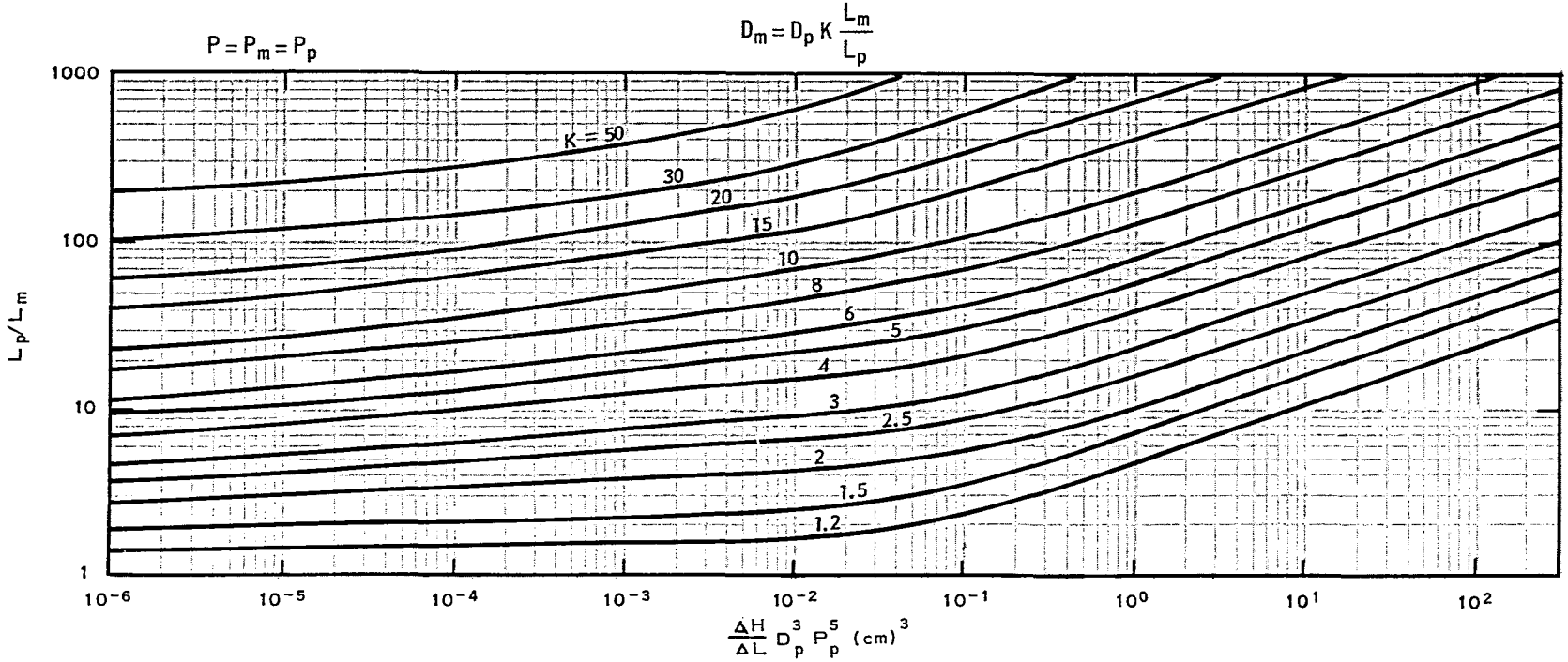

Figure 4-5. Similitude of permeability for core material, geometrical similar models (Le Mehaute, 1965).

Then,

$$\frac{\Delta H}{\Delta L} D_p^3 p^5 = \frac{15}{50} \times (15.2)^3 \times (0.35)^5$$

$$= 0.30 \times 3512 \times 0.00525$$

$$= 5.53 \text{ cm}^3 .$$

From Figure 4-5, for the above-calculated value of $(\Delta H/\Delta L) D_p^3 p^5$ and a linear scale of 1:100, K = 5.0. Using this value of K and equation (4-32), the diameter of the 10 percent smaller than stones in the model core material is

$$D_m = \frac{5.0 \times 0.5}{100} = 0.025 \text{ ft} .$$

The other stones in the model core material would be increased in size in the same proportion.

Keulegan (1973) has given the following equations for wave transmission through model and prototype rubble-mound structures in core materials with a porosity of 0.46. The equations for wave transmission through prototype structures, when $R_n > 2000$, are

$$\left(\frac{H_i}{H_t}\right)_p = 1 + \gamma_p \left(\frac{H_i}{2d}\right)_p \left(\frac{\Delta L}{\lambda}\right)_p \quad (4\text{-}33)$$

and

$$\gamma_p = 2.11 \left(\frac{\lambda}{D}\right)_p \left(gd \frac{T^2}{\lambda^2}\right)_p^{4/3} . \quad (4\text{-}34a)$$

The corresponding equations for wave transmission through model structures, when $20 < R_n < 2000$, are

$$\left(\frac{H_i}{H_t}\right)_m^{2/3} = 1 + \gamma_m \left(\frac{H_i}{2d}\right)_m^{2/3} \left(\frac{\Delta L}{\lambda}\right)_m \quad (4\text{-}35)$$

and

$$\gamma_m = 14.7 \left(\frac{\nu T}{D\lambda}\right)_m^{1/3} \left(\frac{\lambda}{D}\right)_m \left(gd \frac{T^2}{\lambda^2}\right)_m^{4/3} . \quad (4\text{-}36a)$$

If the relations above are generalized for the effects of porosity, assuming, as suggested by Le Mehaute, that the function of porosity is $F(P) = P^{-5}$, equations (4-34a) and (4-36a) become

$$\gamma_p = \frac{P_p^{-4}}{10.6} \left(\frac{\lambda}{D}\right)_p \left(gd \frac{T^2}{\lambda^2}\right)_p^{4/3} \quad (4\text{-}34b)$$

and

$$\gamma_m = \frac{P_m^{-4}}{1.52}\left(\frac{\nu T}{\lambda^2}\right)_m^{1/3}\left(\frac{\lambda}{D}\right)_m\left(gd\,\frac{T^2}{\lambda^2}\right)_m^{4/3} . \qquad (4\text{-}36b)$$

In the above equations by Keulegan, the Reynolds number is

$$R_n = \frac{PH_i\lambda D}{2dT\nu} , \qquad (4\text{-}37)$$

where

H_i = incident wave height

H_t = transmitted wave height

d = water depth

T = wave period

ν = kinematic viscosity

D = characteristic linear dimension of the 10 percent smaller than quarrystone in the core material

ΔL = average width of the core material section

g = acceleration of gravity

P = porosity of the core material; i.e.,

$$P = \frac{\overline{V}_T - \overline{V}_v}{\overline{V}_T} , \qquad (4\text{-}38)$$

where subscripts T and v refer to total volume and volume of voids, respectively. The use of Keulegan's equations to minimize scale effects in wave transmission is based on the requirement that, to obtain similarity,

$$\left(\frac{H_i}{H_t}\right)_m = \left(\frac{H_i}{H_t}\right)_p . \qquad (4\text{-}39)$$

Thus, prototype values of H_i, T, d, λ, P, ΔL, and D are substituted in equations (4-33) and (4-34b) to determine $(H_i/H_t)_p$. This value (from eq. 4-39 equals $(H_i/H_t)_m$), together with the model values of H_i, T, d, λ, ΔL, and ν, is then substituted in equations (4-35) and (4-36b) to determine the required value of D_m. The corresponding value of K can then be determined from equation (4-32).

The methods of Le Mehaute (1965) and Keulegan (1973) for the determination of K are compared in Table 4-3. The experiments by Keulegan were conducted using stones of nearly equal diameter with a porosity of 0.46. Thus, for ease of calculation, the comparison was made using a porosity of 0.46 for both the model and prototype core material. A more reasonable value for P_p for quarry-run core material is about 0.35 to 0.40, depending on the gradation. The linear scale of the model, used in the comparison, was 1:100, and the viscosity was 1.059×10^{-5}, corresponding to a temperature of 21° Celsius (70° Fahrenheit). The water depths, wave dimensions, and quarrystone sizes used represent the ranges of these variables commonly found in prototype structures. Keulegan's equations and Table 4-3 show that the porosity and size of the core material quarrystone have an appreciable effect on the wave transmission coefficient (H_i/H_t). Thus, it is important that accurate values of these variables are obtained for the core material used in the prototype structures. Keulegan's equations also show that adjustments can be made in both the ratios P_m/P_p and D_m/D_p to obtain practical solutions to the problem of minimizing scale effects in wave transmission through rubble-mound breakwaters. Generally, the problems of obtaining dynamic similarity for wave transmission through rubble-mound breakwaters should be the subject of future analysis and experimentation. However, until the results of these studies become available, such scale effects are considered to be reduced appreciably by Le Mehaute's nomograph and Keulegan's equations, and by the proper selection of linear scale. The most accurate of the two methods is unknown; however, it is presently recommended that the value of K used in the model design should be the average of the values obtained by the two methods, or

$$K = \frac{K_L + K_K}{2} \quad . \tag{4-40}$$

Table 4-3. Values of K according to Le Mehaute (1965) and Keulegan (1973) for undistorted-scale models, L_r = 1:100.

d_p (ft)	T_p (s)	$(H_i)_p$ (ft)	D_p (ft)	K_L [1]	K_K [1]	$\frac{K_L}{K_K}$
15	5	7.5	0.25	6.0	4.6	1.30
15	5	7.5	0.75	3.5	2.7	1.30
15	10	7.5	0.25	6.0	4.2	1.43
15	10	7.5	0.75	3.5	2.5	1.40
30	10	15.0	0.25	5.5	4.0	1.38
30	10	15.0	0.75	3.0	2.3	1.31
30	15	15.0	0.25	5.5	3.9	1.41
30	15	15.0	0.75	3.0	2.3	1.31
45	15	25.0	0.25	5.0	3.7	1.35
45	15	25.0	0.75	2.7	2.2	1.23
45	20	25.0	0.25	5.0	3.6	1.39
45	20	25.0	0.75	2.7	2.2	1.23

[1] Subscripts L and K refer to Le Mehaute and Keulegan, respectively.

A similar relation can be established for the core of rubble-mound stability models to ensure that the pressures in the underlayers, which may affect the stability of the armor units in the protective cover layer, are in similitude. The linear scales of such models usually range from about 1:40 to 1:50.

In harbor wave action model studies where short-period waves are studied, scale effects in wave reflection from the outer breakwaters are usually not critical. In such studies, waves reflecting from the outer breakwaters can be reduced satisfactorily by wave absorbers around the ocean perimeter of the model and in front of the wave generator. However, when reflected waves from the breakwaters affect the test results adversely, the increase in wave reflection from the breakwaters due to scale effects can be reduced by wire-mesh screens placed on the ocean-side of the structure. The quarrystone in the protective cover layers of the breakwaters would then be sized in accordance with the linear scale of the model. The proper value of the reflection coefficient would be obtained by special two-dimensional tests in a wave flume. In these special tests the model would be as large as possible, preferably with a linear scale between 1:10 and 1:20, depending on the size of the prototype structure, the prototype water depth and wave dimensions, the dimensions of the available wave flume, and the capacity of the wave generator.

(2) Intermediate- and Long-Period Waves and Distorted-Scale Models. When the problem involves intermediate- and long-period seiche-type waves, harbor models must reproduce a large ocean area because of the long wavelengths involved and because the absorption of reflected waves in the ocean area of the model requires the reproduction of large, additional ocean areas to provide space for the wave absorbers and filters needed to absorb the reflected waves. Exceptionally large absorber-filter areas are required in such models because waves with large periods and small heights are difficult to absorb without considerable reflection from the outer boundaries of the absorber or filter material. The necessity of reproducing such large areas in seiche-type models and the ever-present need to conserve funds require a selection of relatively small linear scales. The use of small linear scales results in excessive bottom friction losses in the model, relative to the small losses in the prototype, if geometrically similar models are used (see Figs. 4-3 and 4-4); therefore, distorted linear scales are usually adopted to reduce the friction effects. The use of the distorted-scale model, in which the horizontal scale $(L_h)_r$ is smaller than the vertical scale $(L_v)_r$, also allows the use of larger wave heights in the model. This increase in model wave heights provides an easier measurement of waves. In undistorted linear-scale models, major scale effects are related to bottom friction effects and the energy loss as waves are transmitted through the voids of rubble breakwaters and wave absorbers. In distorted-scale models the effects of bottom friction on the reduction of wave heights with travel distance are reduced in magnitude as a result of the increased depths and decreased distances of wave travel, compared with undistorted models. However, the bottom slopes and the slopes of coastal

structures (such as rubble-mound breakwaters, jetties, and wave absorbers) are steeper in distorted-scale models than in the prototype or in geometrically similar models; this causes increased wave reflections in distorted models. Scale effects in wave diffraction and refraction may occur in distorted models, depending on the degree of distortion and the ratios of depth to wavelengths that must be reproduced. The total effects of energy loss by friction (including damping due to bottom and internal friction, entrance losses and losses in the voids of rubble-mound breakwaters, and wave absorbers around the perimeter of harbor basins) also cause scale effects in the amplification factor and the sharpness, or Q value, of frequency-response curves at resonance. Therefore, special efforts must be made to devise methods of reducing such scale effects as much as possible. Although the effects on test results due to procedures of model operation cannot be strictly classified as scale effects, the maximum peak values of frequency-response curves can be in error if the increment is too large between wave periods used in the tests.

Bottom friction effects are usually negligible in distorted-scale models; however, in instances where deemed necessary the reduction of wave height with distance of wave travel can be determined from the equations developed by Keulegan (1950b); i.e., equations (4-28) and (4-31). Scale effects due to wave reflection from beach slopes and all types of reflective surfaces can be reduced somewhat by the distortion of wave heights; i.e., the arbitrary increase of wave heights compared with values obtained by application of the vertical scale of the model. This partial reduction of the reflection coefficient is explained by the arbitrary increase in wave heights which results in the increase of values of wave steepness, H/λ, and by the reflection coefficient which decreases as the wave steepness increases. For structures that are located where their reflection coefficients are critical to the problem being investigated (especially rubble-mound structures in which the reflection coefficients are exaggerated because of scale effects related to the lack of fully turbulent flow in the voids of the structure), the reflection coefficients can be reduced satisfactorily by wire-mesh screens placed on the structure slopes, together with a moderate increase in the size of the quarrystones in the outer cover layers of the structure. As in the case described for geometrically similar models, the proper values of reflection coefficients in the model should be determined by the conduct of special, two-dimensional flume tests. Tests would first be made with a large linear scale, in which the Reynolds number is large enough to ensure fully turbulent flow to determine, as nearly as possible, the reflection coefficients of the prototype structures. Tests would then be conducted on the corresponding model structures to determine the optimum combination of wire-mesh screen (or other types of wave filters that have low reflection coefficients) and the use of distorted (enlarged) quarrystone sizes in the structures.

The similitude of refraction can be maintained in distorted-scale models when the waves are long enough relative to depth that the wave velocity is given by the relation $V = (gd)^{1/2}$ (see Sec. IV,2,b). Biesel

and Le Mehaute (1955) have shown that this equation is valid within about 5 percent when

$$d < 0.2T^2 \tag{4-41}$$

where d and T are in feet and seconds, respectively. It was also shown that, on distorted-scale models and with prototype quantities d and T, equation (4-41) becomes

$$d_p < \frac{0.2T_p^2}{\overline{DF}^2} \quad . \tag{4-42}$$

The utility of this equation is in model design. Most distorted-scale, harbor wave action models are conducted to determine the optimum harbor basin and breakwater arrangements to ensure satisfactory mooring and navigation conditions. For such problems, the critical wave periods range from about 20 to 200 seconds. By use of equation (4-42), the maximum depths that can be reproduced in the model areas where wave refraction is important to the problem can be quickly determined. Table 4-4 gives the maximum depth for accurate wave refraction for common values of T and $\overline{DF}$ as determined from this equation. Since the degree of distortion allowable is limited by the reflection error that can be tolerated, after correction to the extent possible by the procedures described earlier, nearly all model studies of this type show that it is infeasible to select model scales such that refraction will be modeled correctly for all wave periods. Determination as to whether the degree of error in the refraction patterns is acceptable is made by comparing computed refraction patterns for the distorted and undistorted conditions (Eagleson, 1960). In the design and operation of distorted-scale models (designed as discussed above), the transference equations for velocity and time are (from eqs. 4-11 and 4-13):

$$V_r = (L_v)_r^{1/2}$$

and

$$T_r = \frac{(L_h)_r^{1/2}}{\overline{DF}^{1/2}}$$

for the special case where the d/λ ratio is such that the wave velocity is given by the relation $V = (gd)^{1/2}$. For the general case, where the relationship (from eq. 4-14)

$$V = \left(\frac{g\lambda}{2\pi} \tanh \frac{2\pi d}{\lambda}\right)^{1/2}$$

Table 4-4. Values of $(d_p)_{max}$ as a function of T_p and $\overline{DF}$.

T_p (s)	$\overline{DF}$ 2.0	3.0	4.0	5.0
	$(d_p)_{max}$ (ft)			
20	20.0	8.9	5.0	3.2
25	31.2	13.9	7.8	5.0
30	45.0	20.0	11.3	7.2
45	101.0	45.0	25.3	16.2
60	180.0	80.0	45.0	28.8
75	281.0	125.0	70.3	45.0
90	405.0	180.0	101.0	64.8
120	720.0	320.0	180.0	115.0
180	1,620.0	720.0	405.0	259.0
210	2,205.0	980.0	551.0	353.0
240	2,880.0	1,280.0	720.0	461.0

must be used to obtain the correct values for wave velocity, the equations (from eqs. 4-16b and 4-17b)

$$V_r = (L_h)_r^{1/2} \frac{\left(\tanh \frac{2\pi d_p \overline{DF}}{\lambda_p}\right)^{1/2}}{\left(\tanh \frac{2\pi d_p}{\lambda_p}\right)^{1/2}}$$

and

$$T_r = (L_h)_r^{1/2} \frac{\left(\tanh \frac{2\pi d_p}{\lambda_p}\right)^{1/2}}{\left(\tanh \frac{2\pi d_p \overline{DF}}{\lambda_p}\right)^{1/2}}$$

must be used. The use of these relationships does not provide similarity of refraction for those conditions of d/λ where the wave velocity is not given accurately by the relation $V = (gd)^{1/2}$, as explained above; however, this use does ensure that the wavelengths on the model are scaled accurately by the horizontal linear scale $(L_h)_r$. This ensures accurate simulation of wavelengths relative to harbor-basin dimensions, which ensures correct simulation of modes of oscillation in the basins for all wave periods and, therefore, the occurrence of resonance at correct wave periods.

The use of the applicable equation (4-13) or (4-17a), if the equation $V = (gd)^{1/2}$ can be used with sufficient accuracy in wave velocity calculations, also ensures accurate simulation of wave diffraction. However, if a distorted-scale model is operated in such a way as to obtain accurate

refraction patterns as the waves approach the harbor and shoreline, by using the distorted time scale (from eq. 4-24b) described in Section IV,2,b,

$$T_r = (L_v)_r^{1/2}$$

then the resulting wavelengths are longer than those obtained by application of the horizontal linear scale of the model, and accurate simulation of modes of oscillation and resonance in the harbor basins is not achieved. The use of this method of obtaining similarity of refraction in the ocean and beach areas of the model also results in the loss of similarity of diffraction. Similarity of diffraction requires that the linear scales for horizontal distances on the model be equal to the wavelength scale, or

$$(L_h)_r = (L_\lambda)_r \ . \qquad (4\text{-}43)$$

Rubble-mound breakwaters and wave absorbers in distorted-scale models have distorted slopes that are steeper than their counterparts in geometrically similar models. Therefore, the scale effects in wave reflection are increased in distorted-scale models compared with undistorted-scale models. Scale effects in wave transmission are also appreciable in distorted-scale models. The nomograph in Figure 4-5 can be used to determine the size of the model core material required to obtain similarity of wave transmission if the inverted linear scale, L_p/L_m, on the vertical axis is replaced by

$$\left[(L_h)_r\,(L_v)_r^{1/2}\right]^{-2/3}$$

and the relation between D_m and D_p, equation (4-32), is replaced by

$$\frac{D_m}{D_p} = K(L_h)_r \ . \qquad (4\text{-}44)$$

These changes are reflected in Figure 4-6.

Keulegan's (1973) equations for wave transmission through rubble-mound structures (eqs. 4-33, 4-34a, 4-35, and 4-36a) can also be used to minimize scale effects of wave transmission in distorted-scale models if equation (4-44) is used to determine the relation between D_m and D_p. The use of Keulegan's equations are simplified somewhat for wave periods and depths in which the wave velocity is given with sufficient accuracy by the relation $V = (gd)^{1/2}$. This is because the term for long waves

$$\left(gd\,\frac{T^2}{\lambda^2}\right)^{4/3}$$

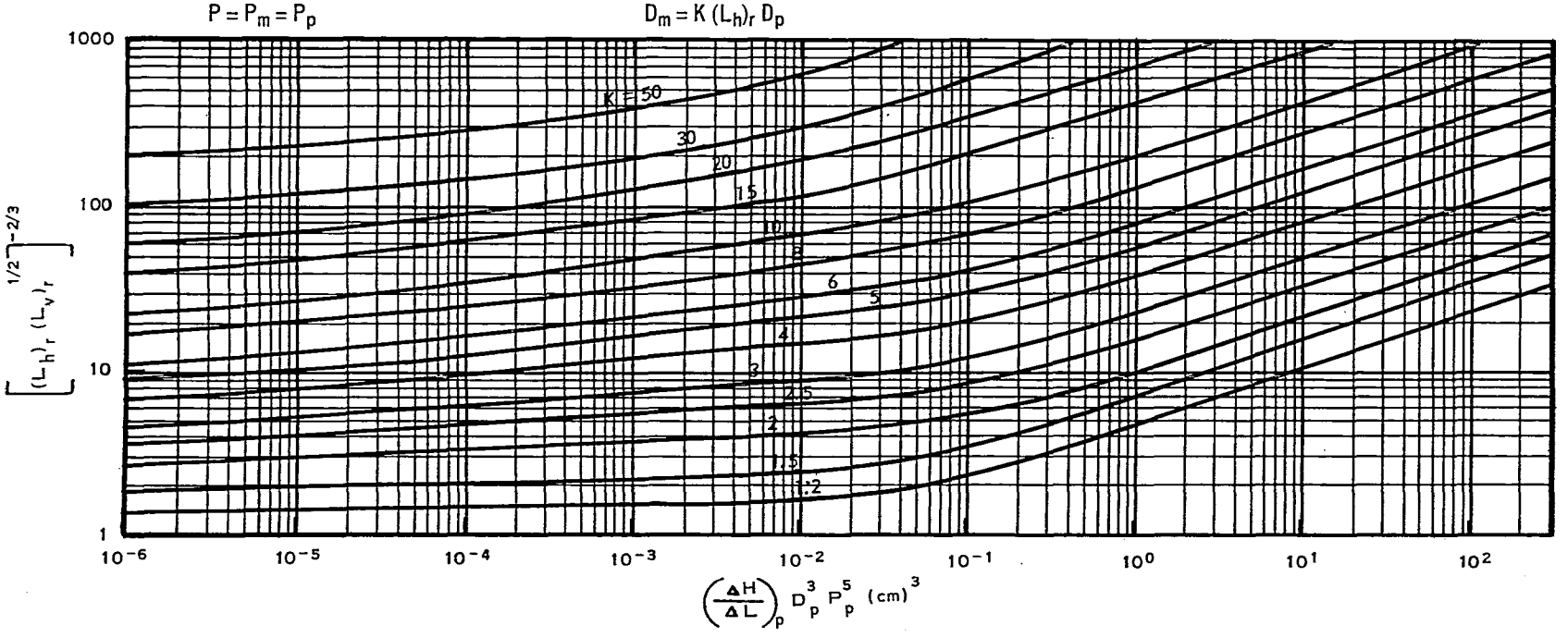

Figure 4-6. Similitude of permeability for core material in distorted-scale models (Le Mehaute, 1965).

in equations (4-34a), (4-34b), (4-36a), and (4-36b) is equal to unity. The methods of Le MeHaute and Keulegan for the determination of K have been compared in Table 4-5 for common values of P_p, $(\Delta L)_p$, D_p, d_p, T_p, and $(H_i)_p$, a distortion factor of 4, a vertical scale of 1:100, and a kinematic viscosity corresponding to a temperature of 21° Celsius (70° Fahrenheit). The values of $(\Delta L)_p$ and d_p were 45 and 30 feet, respectively. Values of p_p, D_p, T_p, and $(H_i)_p$ were 0.40 foot; 0.25, 0.50, and 0.75 foot; 60, 120, and 180 seconds; and 1.0 and 2.0 feet; respectively. It was assumed that $p_m = p_p$.

Table 4-5. Values of K according to Le Mehaute and Keulegan for distorted-scale models.[1]

d_p (ft)	T_p (s)	$(H_i)_p$ (ft)	D_p (ft)	K_L [2]	K_K [2]	$\frac{K_L}{K_K}$
30	60	1.0	0.25	17.0	6.6	2.58
30	120	1.0	0.25	17.0	6.6	2.58
30	180	1.0	0.25	17.0	6.6	2.58
30	60	1.0	0.50	12.0	4.9	2.45
30	120	1.0	0.50	12.0	4.9	2.45
30	180	1.0	0.50	12.0	4.9	2.45
30	60	1.0	0.75	9.5	4.2	2.26
30	120	1.0	0.75	9.5	4.2	2.26
30	180	1.0	0.75	9.5	4.2	2.26
30	60	2.0	0.25	14.8	6.3	2.35
30	120	2.0	0.25	14.8	6.3	2.35
30	180	2.0	0.25	14.8	6.3	2.35
30	60	2.0	0.50	10.5	4.7	2.24
30	120	2.0	0.50	10.5	4.7	2.24
30	180	2.0	0.50	10.5	4.7	2.24
30	60	2.0	0.75	8.5	3.9	2.18
30	120	2.0	0.75	8.5	3.9	2.18
30	180	2.0	0.75	8.5	3.9	2.18

[1] $(L_h)_r = 1{:}400$; $(L_v)_r = 1{:}100$.

[2] Subscripts L and K refer to Le Mehaute and Keulegan, respectively.

As in the case of short-period waves and geometrically similar models, the problems of obtaining dynamic similarity for wave transmission in distorted-scale models should be further investigated; meanwhile, the results of investigations by Le Mehaute (1965) and Keulegan (1973) can be used to minimize the scale effects to the extent that satisfactory results can be obtained for most practical problems. Because of the difference in the results of the two methods, and because it is not known which of the two methods is the most accurate, the values of K used in design of model structures are again recommended to be the average of those calculated by the two methods in accordance with equation (4-40).

A form of scale effect in models where intermediate and long waves are investigated is caused by the reflection of wave energy from the ocean boundaries of the model. It is common practice to use wave absorbers around the ocean boundaries of the model and in front of the wave generator. If these absorbers are not adequate, the wave energy that is radiated from the harbor and wave reflections from breakwaters and adjacent beaches will be trapped in the ocean basin part of the model and will distort the amplification factors or the frequency-response curves of the harbor basins. Considerable work relating to this problem has been accomplished by Ippen and Raichlen (1962), Goda and Ippen (1963), Ippen and Goda (1963), Keulegan (1968), and others, but satisfactory design procedures to ensure sufficient absorption of wave reflections from the ocean boundaries of harbor wave action model studies of intermediate- and long-period waves are not presently available.

Another form of scale effect in intermediate- and long-period wave action models is the differences in the response characteristics of harbor basins, model-to-prototype, caused by the lack of similarity in the dissipation of wave energy in harbor basins. Lee and Raichlen (1971) described this problem and concluded that sufficiently accurate answers are not currently available to design engineers and that additional research in this area is needed.

4. Model Construction and Operation.

a. Construction. Harbor wave action models are constructed in shelters to provide protection against the elements and to ensure that airflow across the water surface does not form ripples or small gravity waves. Such extraneous waves are within the range of wave heights measured in the model, and may, therefore, interfere with obtaining accurate test data. The height of shelter for this type of model should be such that good photos of wave patterns can be obtained. Except for models of small harbors with limited problem areas, camera heights of 30 to 40 feet are preferred. Harbor wave action models are constructed of sheet steel, sheet aluminum, or masonite templets graded to an accuracy of about ±0.002 foot. The templets are placed about 2 to 3 feet apart in the offshore ocean areas where the depth contours are generally regular and there are no abrupt bottom slopes, and about 0.5 to 1.5 feet apart in the more rugged and irregular parts of the harbor area. The space between the templets is filled to about 0.2 foot of the top with sand, the sand is compacted, and the remaining space between the sand bed and the tops of the templets is filled with a cement mortar mix using mason sand with one part cement and three parts sand. Because wave height reduction with distance traveled in harbor wave action models occurs primarily by energy loss in the viscous boundary layer at the rigid bottom, and because dissipation of energy is not a function of bottom roughness if the roughness elements do not extend beyond the viscous boundary layer, a slick, metal-troweled finish of the cement mortar mix is unnecessary. A semislick finish is usually used. Figure 4-7 shows a harbor model under construction where masonite screeds were used in the offshore areas and

Figure 4-7. Harbor model under construction.

sheet-aluminum screeds were used alongshore. Harbor structures in the model are constructed of various materials depending on the type of prototype structure. Rubble-mound breakwaters, jetties, and wave absorbers are constructed of quarrystone or concrete blocks, and the sizes of the material are adjusted as necessary to obtain approximate similarity of wave reflection and transmission coefficients. Impervious, vertical-wall breakwaters and jetties are reproduced in concrete, and piers supported by piles are reproduced using a sheet metal or wood top with heavy-gage wire or solder rod used as piling. The perimeter walls of the model are usually constructed of brick. A freshwater supply is preferable because of the necessity to keep the model as clean as possible. Leakage of water from the model is minimized by an elastic sealer which is applied to the upper part of the templets and in all joints and cracks in the model.

b. Operation.

(1) Short-Period Wave Models. Before actual model operation is begun, prototype wave data for deepwater conditions are transferred to the outer contour limits of the model by wave-refraction techniques; the wave directions and heights for the range of wave periods that occur in nature and are important to the problems under consideration, are then selected for use in the investigation. The dimensions and directions selected for the test waves must ensure a realistic test of the improvement plans proposed or devised during the model study to permit accurate determination of the optimum plan. In most harbor model studies the reproduction of tidal variations in the water surface is unnecessary. Therefore, it is customary to use selected stillwater levels for the different tests. The stillwater levels should be selected so that the various wave-induced phenomena that are dependent on water depths are accurately reproduced in the model. These phenomena are the refraction of waves within the harbor area, the overtopping of harbor structures by wave action, the reflection of wave energy from harbor structures, and the transmission of wave energy through porous structures. A few of the most important factors contributing to selection of the optimum model stillwater level are: (a) The maximum amount of wave energy that can reach a given area will ordinarily do so during the period of a severe storm that coincides in time with the highest water level normally experienced in the area; (b) severe storms moving onshore are characteristically accompanied by an additional increase in the normal water level due to wind setup and mass transport, whereas storms moving offshore tend to lower the water level; and (c) a relatively high stillwater level in the model is beneficial in minimizing the effects of bottom friction, which can be excessive in shallow areas of small-scale models. Therefore, in consideration of the various factors contributing to and affected by the stillwater level in the prototype, and in view of the tendency toward more conservative results from the model investigation, a model stillwater level should be selected that closely approximates the higher water stages that normally prevail during severe storms in the prototype. This entails the study of water level records in the prototype locality, with proper attention given to the higher levels experienced in the area in the past. The test data obtained during the

testing program include wave height measurements at several selected locations throughout the harbor area, photos of wave patterns (as shown in Figs. 4-8 and 4-9), float measurements to obtain current patterns due to breaking waves, and visual observations of wave action in the model. Wave heights are measured by electrical wave height gages and are recorded electrically with multichannel oscillographs. The waves are produced by the displacement of water incident to the periodic motion of a wave generator in the form of a plunger, flap, or bulkhead. A wave generator with a trapezoidal plunger is shown in Figure 4-10; a vertical bulkhead generator is shown in Figure 4-11.

(2) Intermediate- and Long-Period Wave Models. Operation of these models is similar to short-period wave models, except that the phenomenon of harbor-basin resonance becomes a primary problem that must be taken into consideration. Effects of the damping coefficient on the response curve (where the amplification factor is plotted versus the wave frequency or wave period) must be determined and care must be taken to obtain, as nearly as possible, similarity of friction in the harbor basins. Wave heights are measured as before and the modes of oscillation are determined for each wave period that is judged important to the problem under consideration. Currents at navigation openings and other restricted areas in the harbor also become important for the long-period wave part of the spectrum, and these currents are usually measured in model studies of this type.

5. Examples of Model Studies Conducted.

A large number of undistorted, short-period wave action model studies have been conducted worldwide, including about 35 at WES. Model studies of the intermediate- and long-period seiche-type have been smaller in number; only five were conducted at WES. Only a few model studies on tsunamis protection have been conducted; the only one in the United States was conducted by the U.S. Army Engineer Division, Pacific Ocean, concerning proposed breakwater plans of Hilo Harbor and the city of Hilo, Hawaii, for protection from tsunami damage (Palmer, Mulvihill, and Funasaki, 1967).

Selected examples of investigations concerning short-, intermediate-, and long-period model studies are discussed below.

a. Harbor Wave Action Studies, Short-Period Waves, and Undistorted-Scale Models.

(1) Marina del Rey, Venice, California.

(a) Project. Improvement in wave conditions.

(b) Reference. Brasfeild (1965).

(c) Laboratory. WES.

(d) Test Period. January to May 1963.

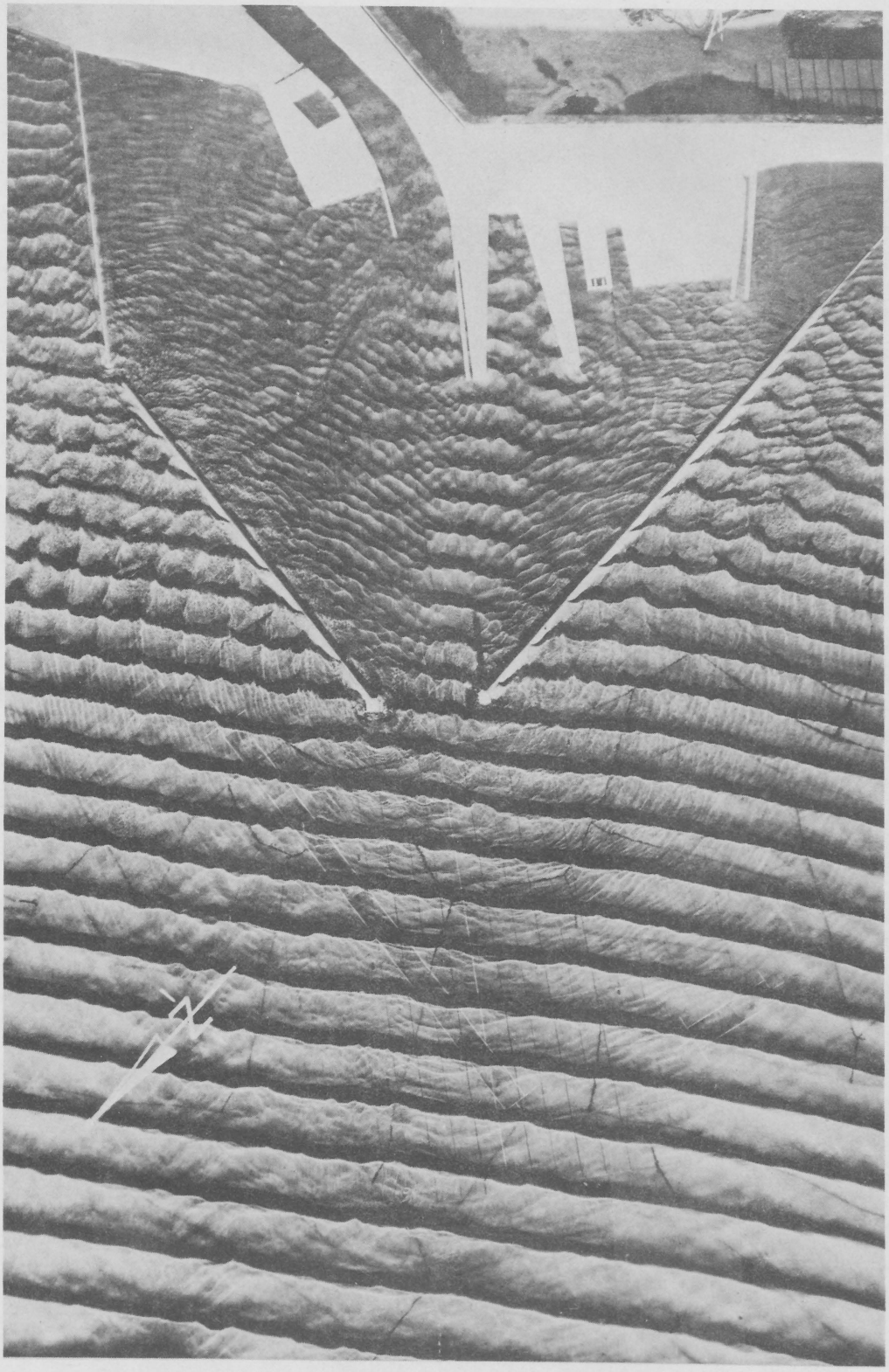

Figure 4-8. Wave patterns and base test conditions, Lorain Harbor model (Wilson, Hudson, and Housley, 1963).

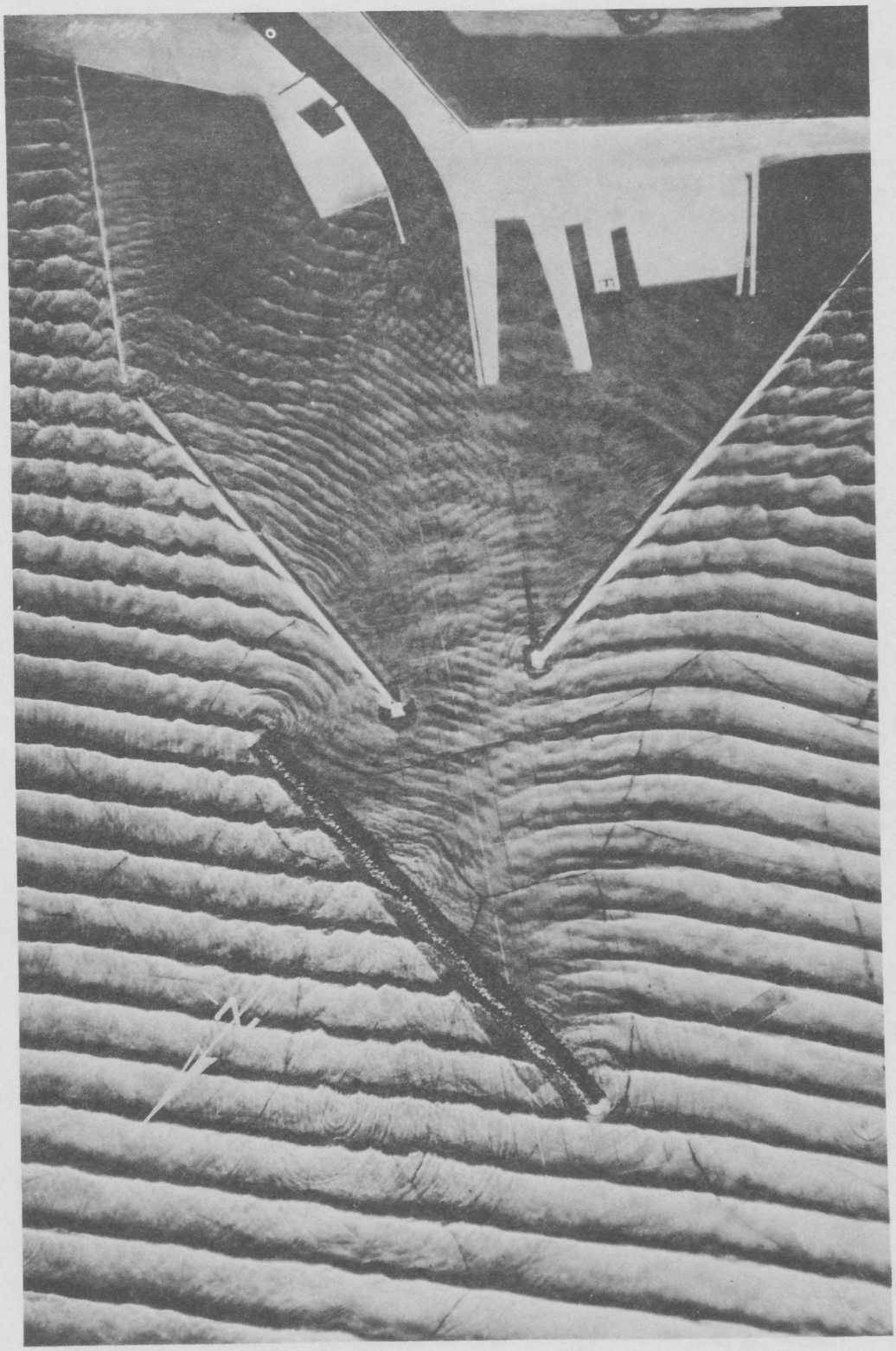

Figure 4-9. Wave patterns and proposed plan, Lorain Harbor model (Wilson, Hudson, and Housley, 1963).

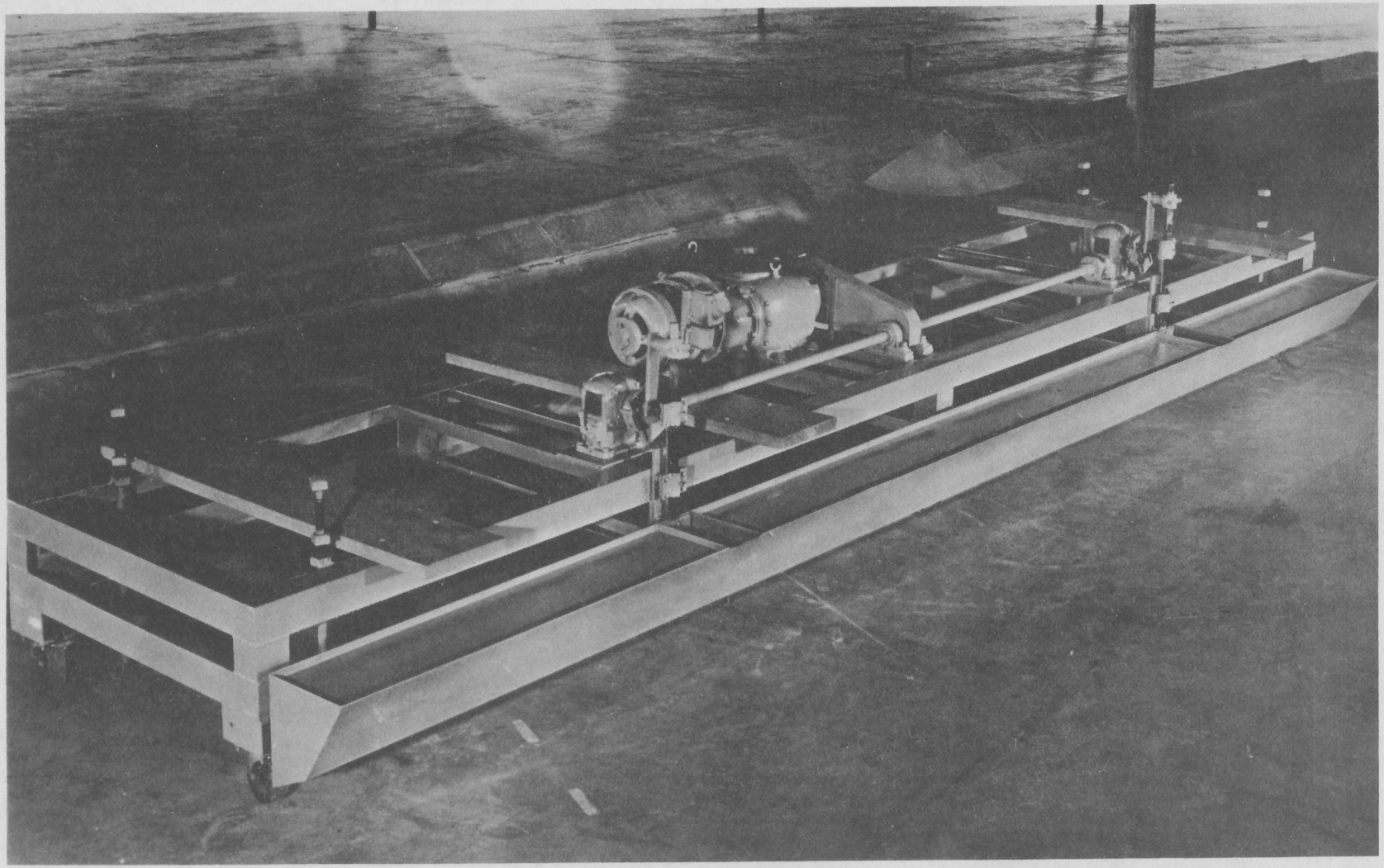

Figure 4-10. Wave generator with a trapezoidal plunger.

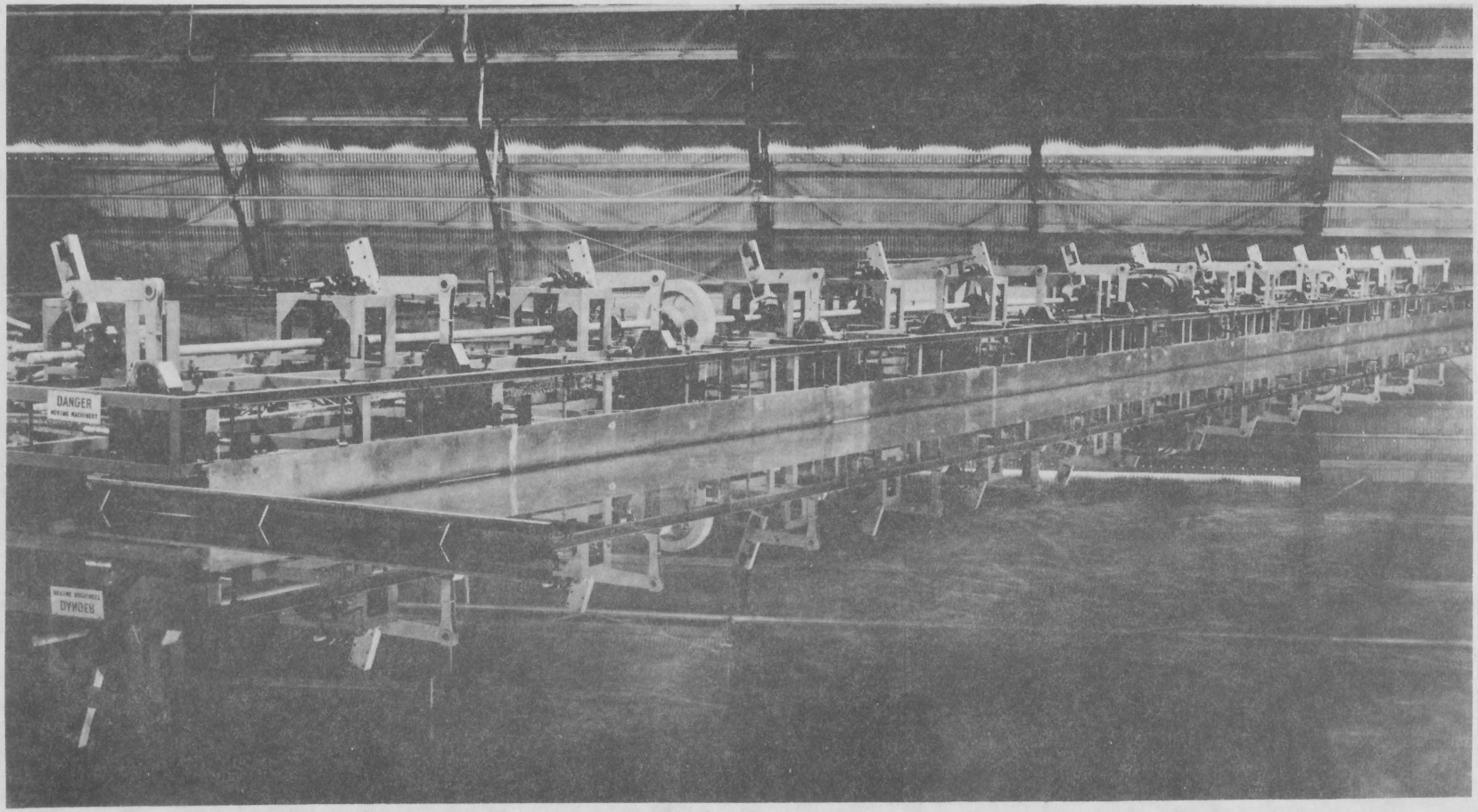

Figure 4-11. Vertical-bulkhead wave generator.

(e) Problem. Marina del Rey, a small-craft harbor designed to provide mooring for about 6,500 vessels, is located in Santa Monica Bay about 15 miles southwest of downtown Los Angeles (Fig. 4-12). The harbor is exposed to wind waves generated from all deepwater directions between west-northwest and south-southwest. After construction of the harbor, waves entering the 1,000-foot-wide entrance channel were observed to reflect off the vertical, concrete perimeter walls of the harbor, resulting in intolerable wave conditions in several of the harbor basins.

(f) Purpose of Model Study. The model study was conducted to investigate the existing wave conditions within the marina, and to determine the optimum plan for reducing the wave heights in the harbor basins to an acceptable level (less than 2 feet).

(g) The Model. The tests were conducted in a three-dimensional, undistorted-scale, geometrically similar replica of the existing harbor basins and jetties with enough area seaward and on either side of the navigation opening to allow proper reproduction of the incident waves (Fig. 4-13). The area of the model was approximately 15,000 square feet, equivalent to about 3 square miles in the prototype. The model was constructed of cement mortar to a linear scale of 1:75 (Fig. 4-14). Scale selection was based on the depths of water required in the model to prevent excessive bottom friction effects, the absolute size of the model waves, the capability of the existing wave generators as compared with those required as a function of model scale, the cost of model construction, efficiency of model operation, and the dimensions of the available shelters. After selection of the linear scale, the model was designed and operated in accordance with Froude's law. Model waves were generated by a 40-foot-long wave generator with a trapezoidal-shaped, vertical-motion plunger. Regular, monochromatic waves were used in the tests. Wave heights at selected locations in the model, measured by electrical wave height gages, were recorded on chart paper by a six-channel oscillograph.

(h) Test Procedures. From tide level data for the Los Angeles area, the average of the highest tides during each month of a 4-year period (1958-1961) was +6.5 feet mean lower low water (MLLW) (U.S. Coast and Geodetic Survey, 1958-61). This value was used in the model tests to minimize the effects of bottom friction. Available deepwater wave data (National Marine Consultants, 1960; Marine Advisers, 1961) prepared from hindcasting techniques were used, in conjunction with information from the preparation of refraction diagrams, to obtain the characteristics of shallow-water waves for use at the position of the wave generator in the model. Because of the urgency of the project (wave action in the harbor was preventing use of large areas of the wave basins and was causing damage to some of the perimeter walls), preliminary refraction diagrams were used to position the wave machines during initial stages of model operation. After completion of the refraction study, the previously selected wave directions were found to correspond closely to those calculated; therefore, they were used throughout the remainder of the testing program to avoid repetition of that part of the testing

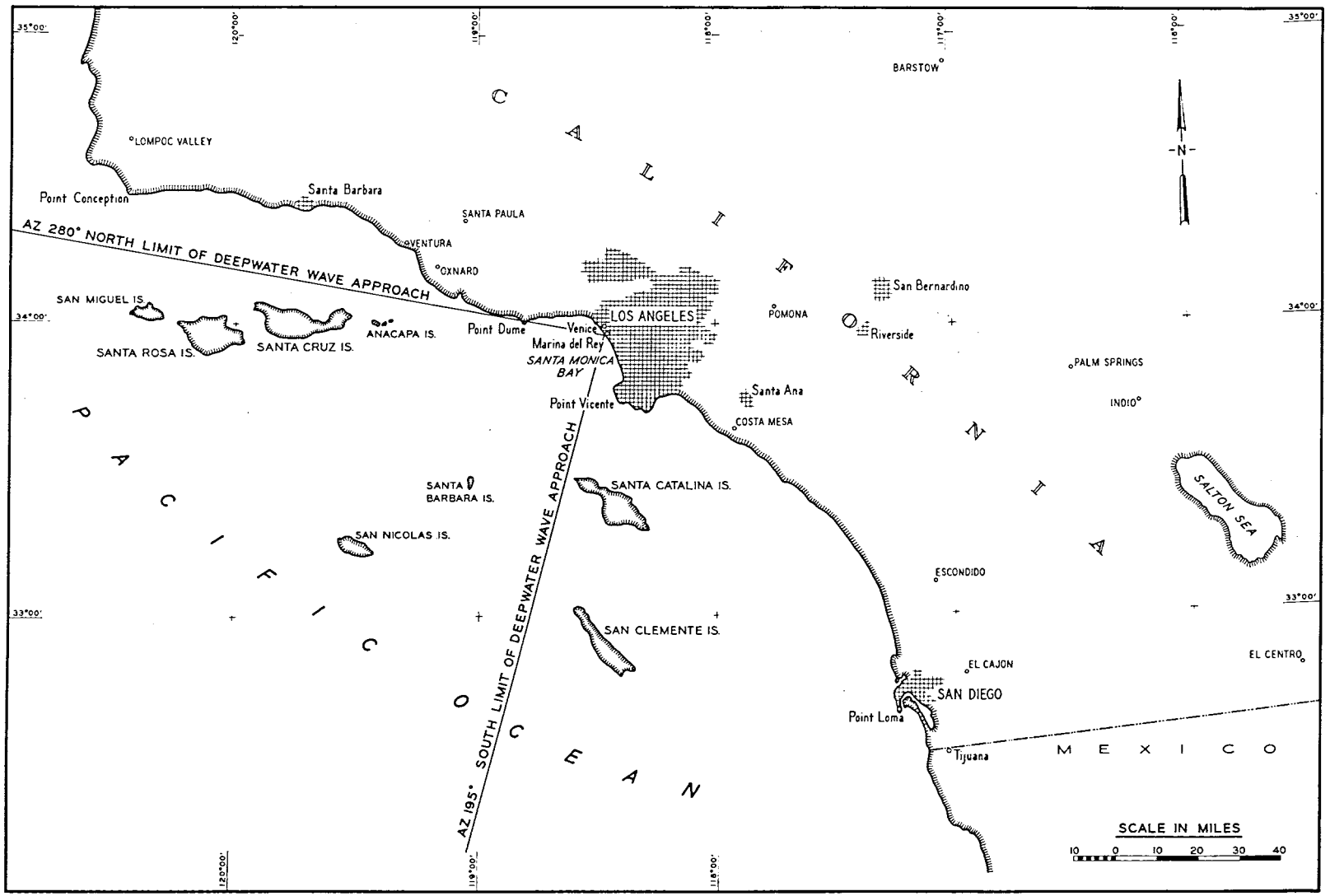

Figure 4-12. Location map, Marina del Rey, California (Brasfeild, 1965).

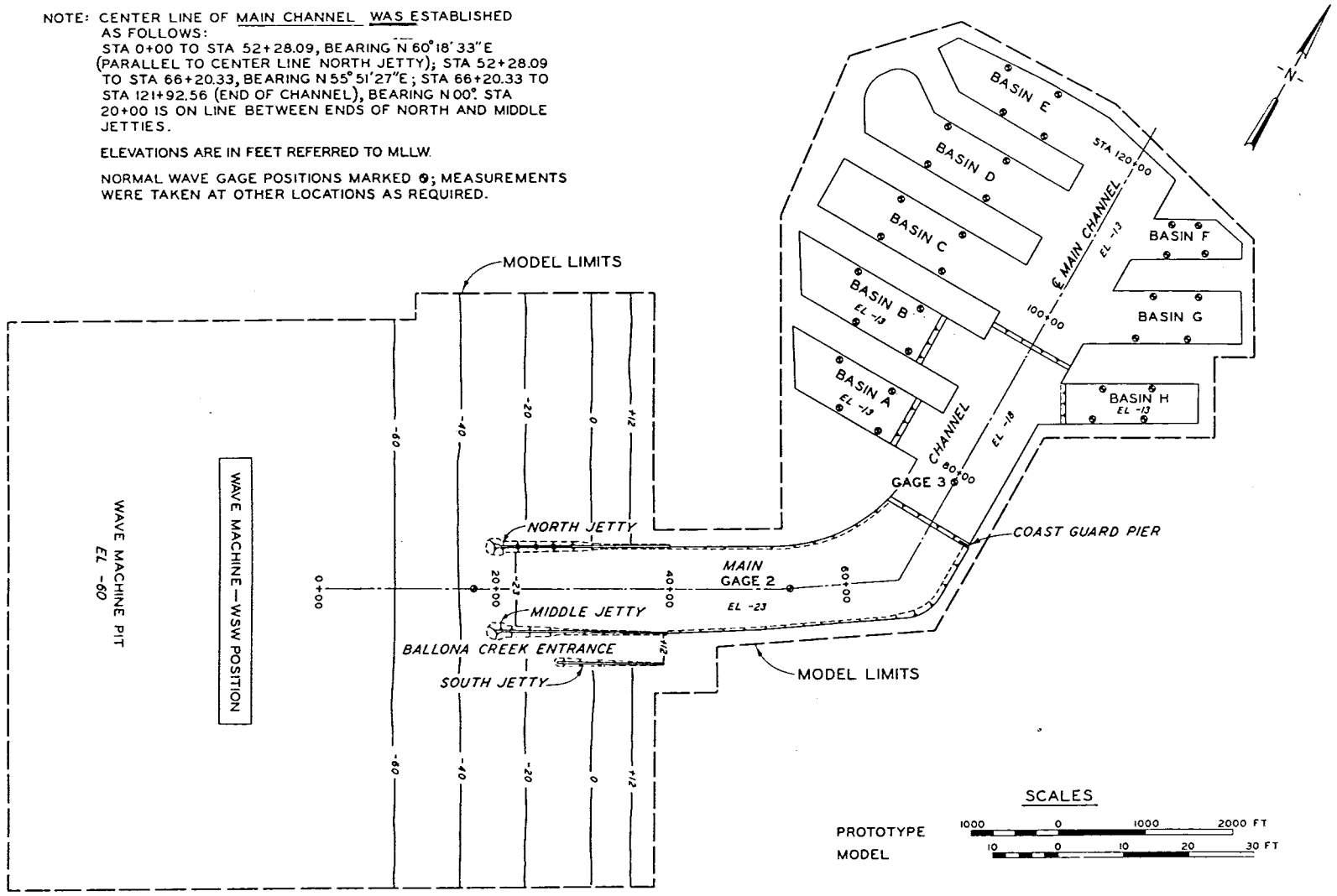

Figure 4-13. Marina del Rey model limits (Brasfeild, 1965).

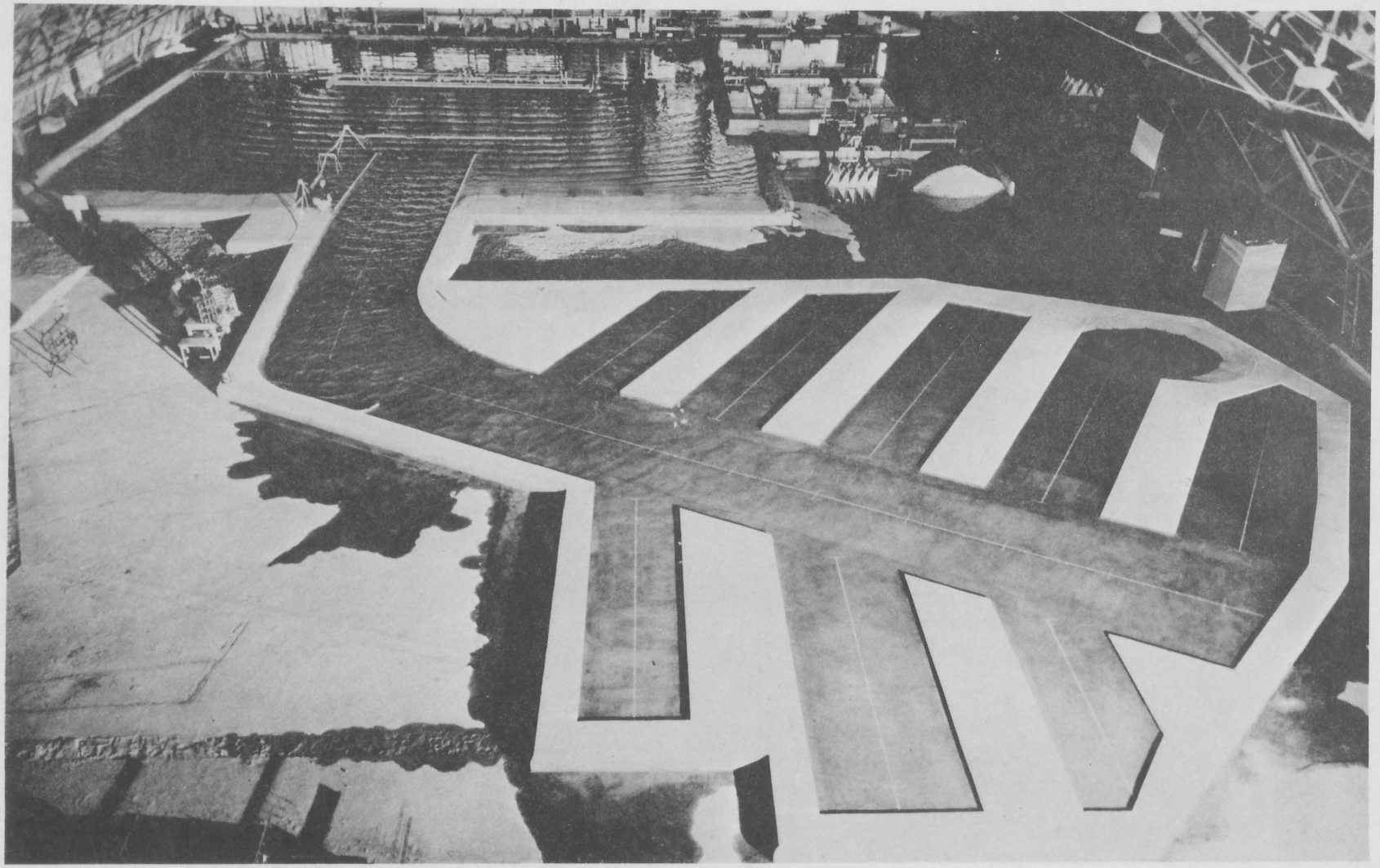

Figure 4-14. Marina del Rey model after construction (Brasfeild, 1965).

program. Table 4-6 shows the deepwater wave directions, the corresponding shallow-water directions, the actual wave generator directions used in the tests, and the wave periods and wave heights selected for the various wave directions. The procedures to evaluate the various plans tested included: (a) comparison of average maximum wave heights recorded at selected locations in the main channel and individual basins, (b) extension of these data into tables of estimated durations of wave heights at the selected locations, and (c) visual observations. Data were obtained for base test (existing) conditions and with various improvement plans installed in the model. Wave height data were adjusted to compensate for the greater rate of wave height attenuation in the model, as compared with the prototype, by the application of Keulegan's (1950b) equation. In recording wave heights in the individual basins in the model, two gages were positioned along each sidewall (Fig. 4-15) and were moved along the middle one-third of the wall length as necessary to coincide with the loop points of the standing wave patterns. This technique ensured that the maximum wave heights in the area of each gage would be recorded. In the analysis of test results, the maximum sustained wave heights recorded at each gage location (main channel and individual basins) were selected for the computations which, in effect, resulted in conservative results from the analysis. In the case of the main channel gages, the maximum wave heights for each gage were averaged from three or more similar tests; for the basins, the wave height data utilized were the averages of the maximum wave heights recorded at the four gages in each basin.

Table 4-6. Selected test wave conditions, Marina del Rey model.

Direction	Wave conditions			Shallow-water test waves (prototype dimensions)	
	Deep water	Shallow water	Wave machine	Period (s)	Height (ft)
W.N.W.	292°30′	267°15′	264°19′	8	13
W.N.W.	292°30′	267°15′	264°19′	12	9
W.N.W.	292°30′	267°15′	264°19′	16	9
W.	270°00′	258°30′	255°19′	8	11
W.	270°00′	258°30′	255°19′	12	9
W.	270°00′	258°30′	255°19′	16	9
W.S.W.	247°30′	243°15′	240°19′[1]	8	9
W.S.W.	247°30′	243°15′	240°19′[1]	12	8
W.S.W.	247°30′	243°15′	240°19′[1]	16	9
S.W.	225°00′	228°40′	225°19′	12	8
S.W.	225°00′	228°40′	225°19′	16	8
S.S.W.	202°30′	210°45′	210°19′	8	8
S.S.W.	202°30′	210°45′	210°19′	12	8
S.S.W.	202°30′	210°45′	210°19′	16	8

[1] Azimuth of centerline of entrance to the main channel.

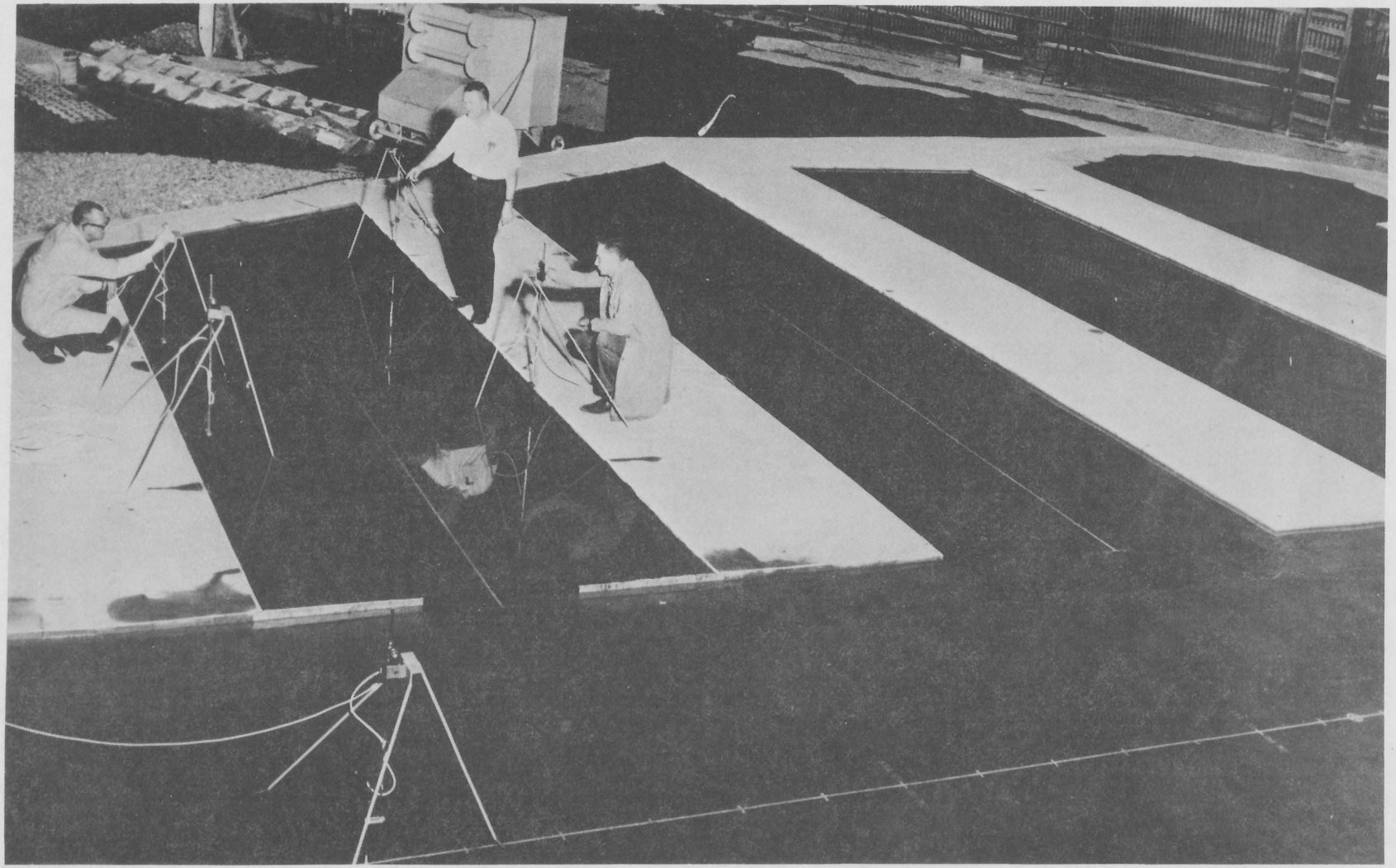

Figure 4-15. Positioning wave gages, Marina del Rey model (Brasfeild, 1965).

(i) Plans Tested. Before testing the various improvement plans, base test data were obtained in the main channel and each basin as previously described and as shown in Figure 4-15. The term "base test" is used to denote a test performed with existing prototype conditions installed in the model. These test results are used to judge the efficacy of proposed improvement plans by comparing the results of tests with improvement plans installed in the model with comparable base test data. Tests were first conducted using eight different offshore, detached, rubble-mound breakwater plans located either 500 or 700 feet from the seaward ends of the existing jetties. These breakwaters were straight structures, placed perpendicular to the centerline of the main channel, with a crown elevation of +22 feet MLLW (nonovertopping) and varying in length from 1,000 to 2,200 feet. The elements of a typical straight breakwater plan are shown in Figure 4-16. Tests were also conducted using a straight breakwater reach with angled wings of various lengths and angles on each end. The structures ranged from 1,800 to 2,325 feet in length including the wings. The center sections were either 640 or 700 feet seaward of the jetty ends and were perpendicular to the centerline of the main channel. The wings angled shoreward with deflection angles of from 10° to 30°. The crown elevation of the wings varied from +13 to +22 feet MLLW, and the crest of the center sections was either +20 or +22 feet MLLW. The elements of the best wing-type breakwater tested are shown in Figure 4-17. Several combinations of berm width and length of a rubble-mound wave absorber, placed along the east side of the main channel north and south of the Coast Guard pier, were also tested to determine the optimum dimensions of such a structure for reducing wave action in the harbor basins. The elements of these plans are shown in Figure 4-18.

(j) Summary of Test Results. The wing-type breakwater was found to be better than the other types tested; the best type is shown in Figures 4-17 and 4-19. Test results showed that this plan would provide the desired reduction of wave action at the entrance, in the main channel, and in the individual harbor basins by preventing about 95 percent of the short-period wave energy from entering the harbor. Construction of this plan was recommended.

(2) Vermilion Harbor, Ohio.

(a) Project. Improvement in wave conditions at the Vermilion Harbor entrance and river channel leading to the mooring areas in lagoons.

(b) Reference. Brasfeild (1970).

(c) Laboratory. WES.

(d) Test Period. August 1968 to July 1969.

(e) Problem. Vermilion Harbor is located on the south shore of Lake Erie at the mouth of the Vermilion River, about 37 miles

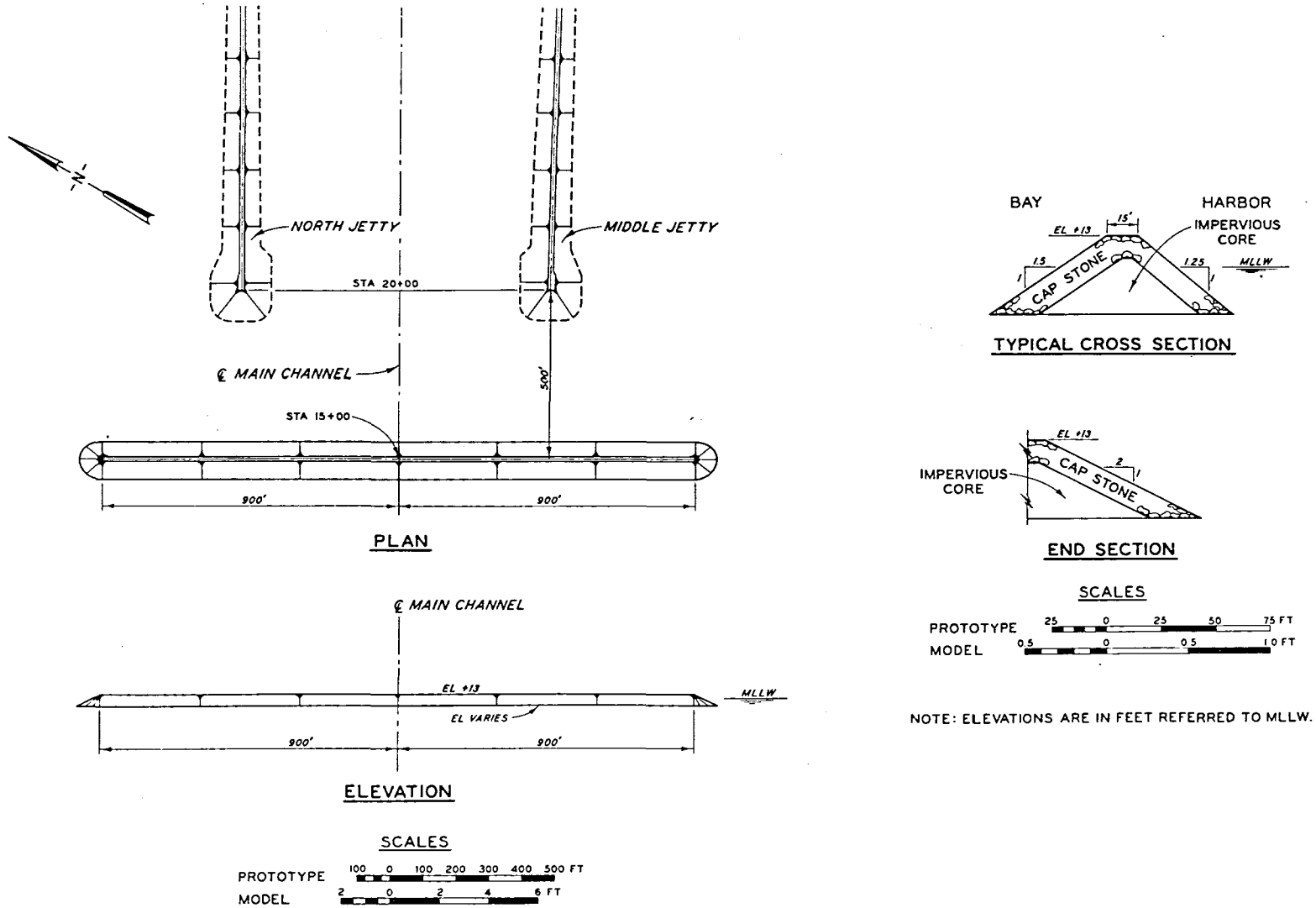

Figure 4-16. Elements of straight breakwaters, Marina del Rey model (Brasfeild, 1965).

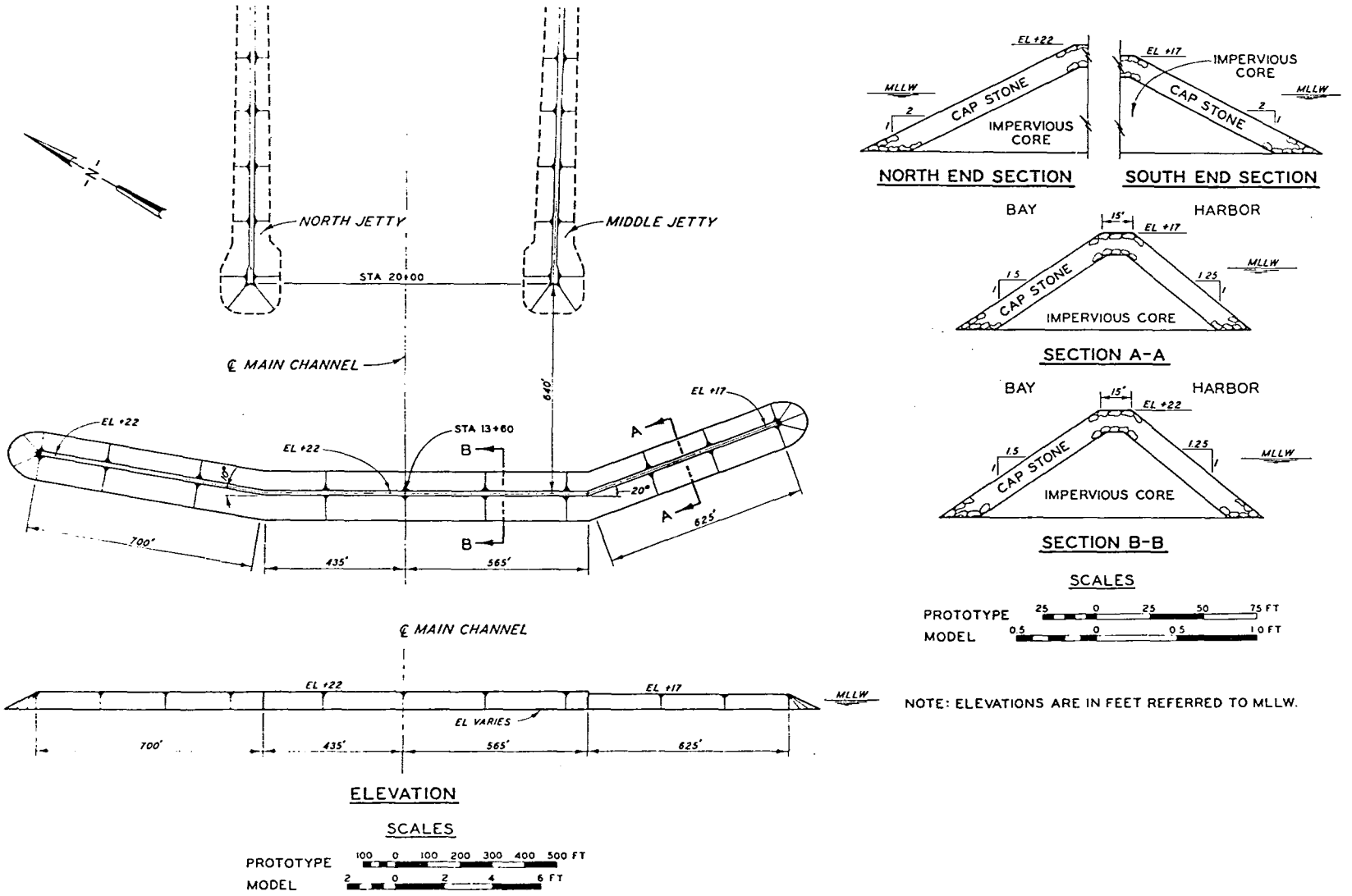

Figure 4-17. Elements of wing-type breakwater, Marina del Rey model (Brasfeild, 1965).

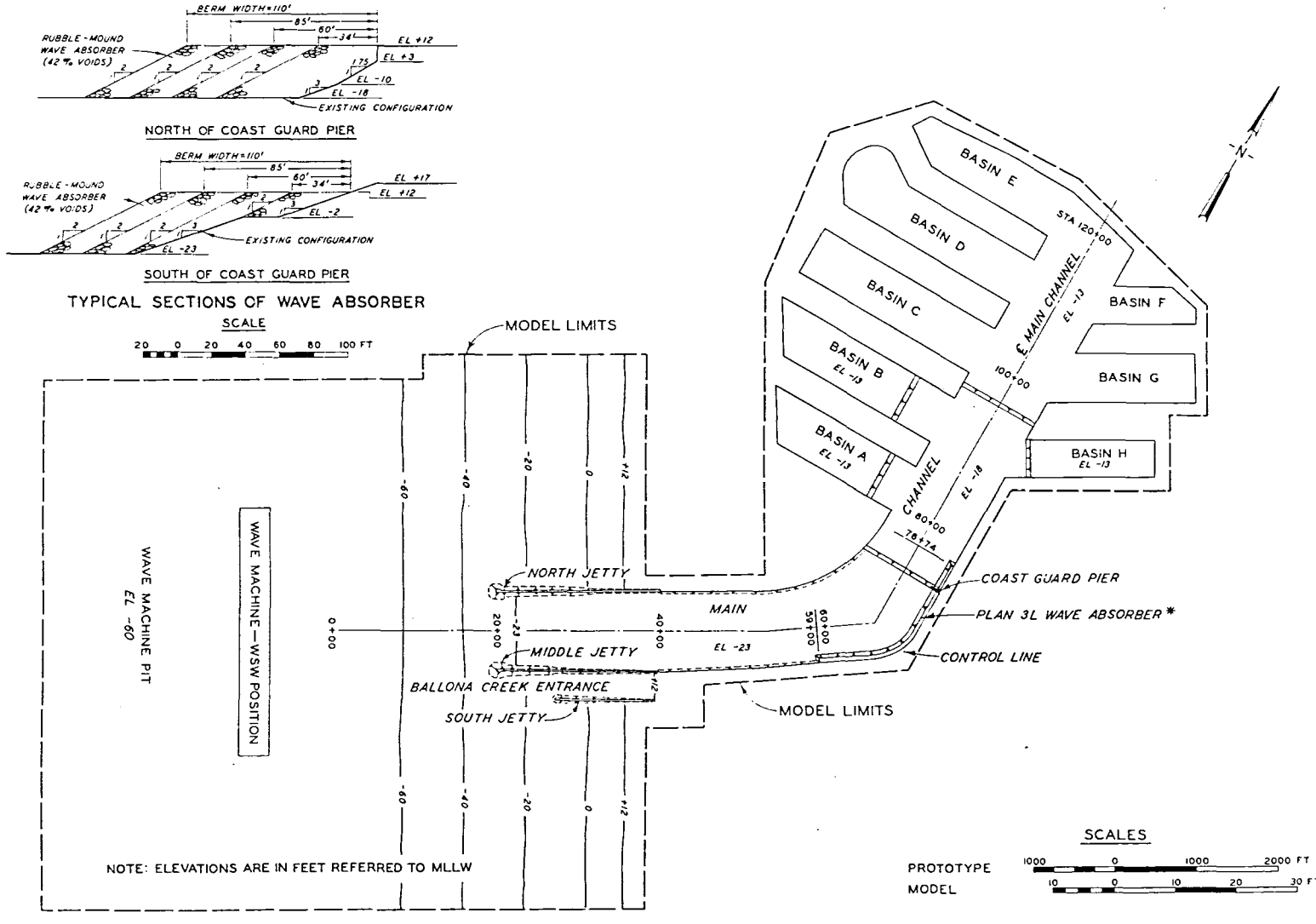

Figure 4-18. Elements of wave-absorber plan, Marina del Rey model (Brasfeild, 1965).

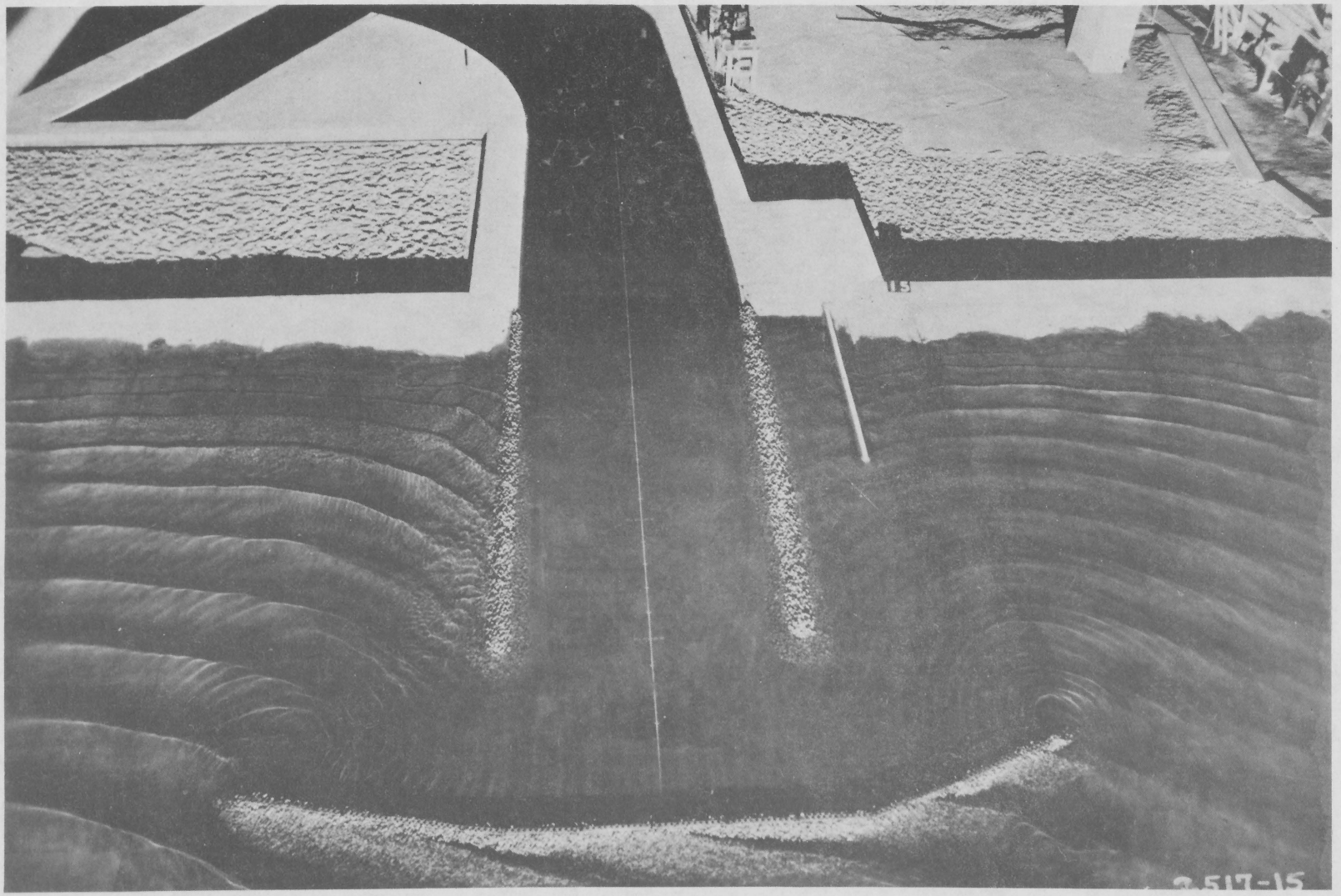

Figure 4-19. Wave patterns with recommended plan installed, Marina del Rey model (Brasfeild, 1965).

west of Cleveland, Ohio, and 21 miles east of Sandusky, Ohio (Fig. 4-20). The harbor includes the lower 3,600 feet of the Vermilion River, numerous artificial lagoons, and a channel of approach from the lake. Local interests requested improvements to Vermilion Harbor that included (a) construction of protective structures to provide a safe entrance to the harbor under moderate to fresh gale conditions, and (b) dredging of the river channel above the existing Federal project limit to provide adequate depths for navigation. The entrance to Vermilion Harbor is exposed in varying degrees to storms generating waves from directions ranging clockwise from west to northeast. The storm waves break in the relatively shallow water inside and immediately outside the entrance piers, making navigation difficult and dangerous during moderate storms and preventing use of the harbor as a harbor of refuge.

(f) Purpose of Model Study. The model study was conducted to (a) determine the extent of wave action in the harbor for existing conditions and after installation of the proposed revisions, (b) test and develop other remedial plans for alleviation of undesirable wave action at the harbor entrance and in the channel approaching the lagoons, and (c) determine whether modifications could be made to the proposed plans that would result in significant reduction in construction costs and still provide adequate protection from wave action in the problem area.

(g) The Model. The Vermilion Harbor model was designed in accordance with Froude's law and was constructed geometrically similar to the prototype at a linear scale of 1:75. The model, molded in cement mortar, reproduced approximately 1 mile of the Lake Erie shoreline, the harbor and lagoons to a point about 3,000 feet upstream in the Vermilion River, and sufficient underwater contoured area to permit generation of waves and wave-front patterns from all significant directions of wave approach to the harbor. Vertical control in model construction and operation was based on the low water datum for Lake Erie, which is 568.6 feet above mean water level at Father Point, Quebec (International Great Lakes Datum, 1955). Horizontal control was referenced to coordinates of the State of Ohio Lambert Projection, North Zone, U.S. Geological Survey. Lake bottom contours were reproduced to an approximate prototype depth of 22 feet. A sloped transition extended downward from the contoured area to the wave generator pit, which was at an elevation of -60 feet. The entire area of the model was about 8,800 square feet, representing nearly 1.8 square miles in the prototype (Fig. 4-20). Model waves were generated to scale by a bulkhead-type wave generator 52 feet in length. The waves were produced by the displacement of water incident to the horizontal periodic motion of the vertical bulkhead. The bulkhead speed and displacement were infinitely variable within sufficient ranges to generate waves of the periods and heights found in Lake Erie when reduced by the length and time scales of the model. The wave generator was also mounted on retractable casters that enabled the generator to be positioned to propagate waves from the required directions. Wave heights in the model were measured by electrical, printed-circuit staff gages and were recorded electrically with a multichannel oscillograph. Photography was also used to record comparative wave patterns that were obtained for individual test conditions.

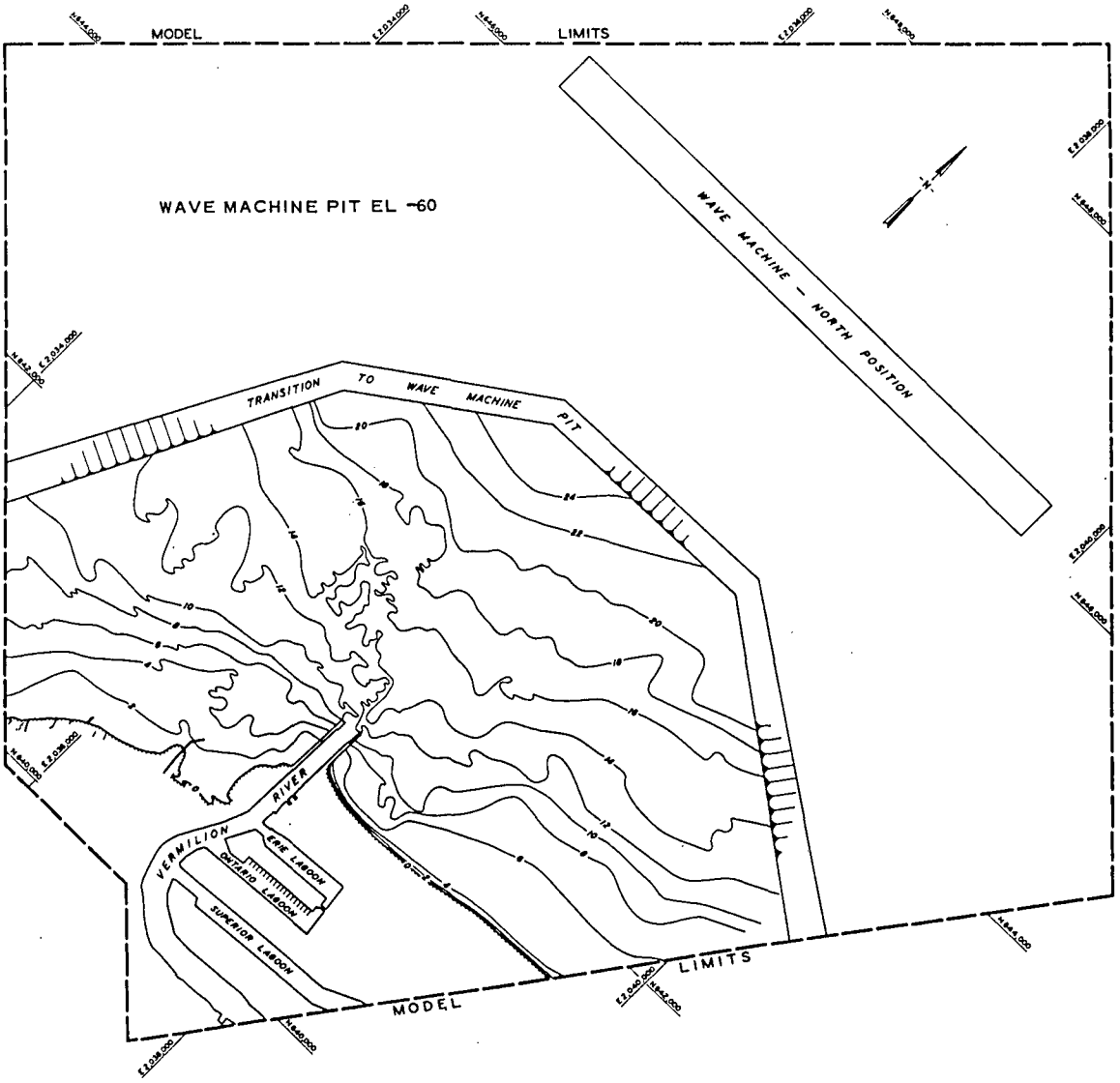

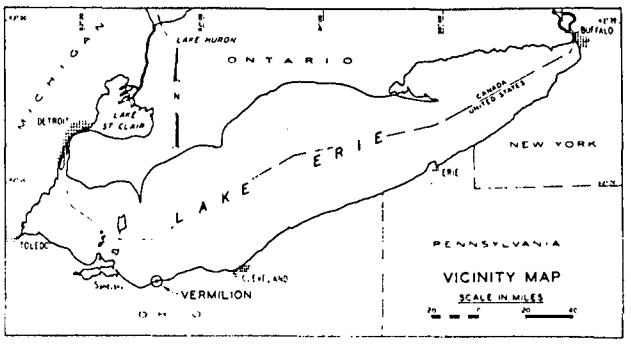

NOTE: DEPTH CONTOURS ARE IN FEET REFERRED TO LOW WATER DATUM FOR LAKE ERIE, ELEVATION 568.6 FEET ABOVE MEAN WATER LEVEL AT FATHER POINT, QUEBEC (IGLD 1955).

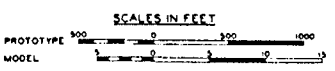

Figure 4-20. Vicinity map and layout, Vermilion Harbor model (Brasfeild, 1970).

(h) Test Procedures. A model stillwater level should be selected that closely approximates the higher water stages that normally prevail during severe storms in the prototype. This requires the study of water level records in the prototype locality, with proper attention given to the higher levels experienced in the area in the past. Water levels in Vermilion Harbor are determined by the water surface elevation of Lake Erie, which can vary monthly and also yearly. These seasonal and annual variations in the water level are related to volumetric changes in the lake, which are principally caused by precipitation, evaporation, and runoff. The usual pattern of seasonal variation of water levels in the Great Lakes consists of highs in summer and lows in late winter. The highest monthly average level is usually recorded in June and the lowest in February, though seasonal fluctuations have occasionally caused noticeable departures from this pattern (U.S. Army Engineer District, Lake Survey, 1952). Wind setup and seiches, which can cause the water level at a particular locality to vary daily and also hourly, are relatively short-period fluctuations superimposed on the longer variations in lake levels. These short-period oscillations are due to a tilting of the lake surface generally caused by wind and possibly by differentials in barometric pressure. Large short-period rises in local water level are associated with the most severe storms which generally occur in the winter months when the lake level is usually low; thus, the probability of a high lake level and a large wind setup or seiche occurring simultaneously is relatively small. A stillwater level of +3.0 low water datum (LWD) was selected for use in the model study. This value was determined by combining the average water level of Lake Erie during the ice-free period (+2.1 feet LWD) with an assumed 0.9-foot short-period rise in local water level due to wind setup. The entrance to Vermilion Harbor is exposed in varying degrees to storm waves from directions ranging clockwise from west to northeast. The most severe wave action at the harbor entrance is caused by storms from the north and northeast. Measured wave data on which to base a comprehensive statistical analysis of wave conditions were not available for the Vermilion area; however, records were available from which statistical wave hindcast data could be compiled. These records were U.S. Coast Guard wind data for a 6-year period (1946-1951) at Lorain Harbor, Ohio (11 miles east of Vermilion Harbor), and it was assumed that winds with similar characteristics could be expected to occur at Vermilion. The frequency of occurrence of winds of varying velocities from the different directions of storm approach has been compiled for the normal navigation season on Lake Erie (April to November). The characteristics of waves that could be expected to approach Vermilion Harbor were determined by applying these wind data and the fetch lengths corresponding to each direction to the theory of wave hindcasting. The deepwater wave characteristics were converted to shallow-water values, at the position of the model wave generator, by wave refraction techniques. Wave height, period, and direction characteristics used in the model tests (selected from the wave data obtained as previously discussed) are presented in Table 4-7. The data obtained during the testing program included (a) wave height measurements at several selected locations throughout the harbor area and the river channel, (b) photos of wave patterns, and (c) visual observations of wave action in the model. Wave heights measured in the model

Table 4-7. Selected test wave conditions, Vermilion Harbor model.

Wave period	Deepwater waves		Shallow-water test waves	
(s)	Direction	Height (ft)	Direction	Height (ft)
5	W.	6	N. 70°15′ W.	4
6	W.	8	N. 70°15′ W.	4
6	N.W.	6, 8	N. 38°30′ W.	6, 8
7	N.W.	7, 9, 11	N. 38°30′ W.	6, 8, 10
7	N.	7, 9	N. 01°00′ E.	6, 8
8	N.	7, 9, 11	N. 01°00′ E.	7, 9, 11
7	N.E.	6, 8	N. 30°00′ E.	6, 8
8	N.E.	7, 9, 11	N. 30°00′ E.	6, 8, 10

were corrected to compensate for the increased rate at which bottom friction attenuates waves in the model as compared with the prototype. Keulegan's (1950b) attenuation equation was used to calculate coefficients for this procedure.

(i) Plans Tested. Base tests were performed with existing prototype conditions installed in the model. The plans for improvement tested in the model consisted of variations in the number, length, and orientation of cellular sheet steel pile breakwater structures that would prevent excessive wave energy from reaching the entrance to the harbor. Brief descriptions of the various plans tested are given below; dimensional details are shown in the referenced figures.

1 Plan 1. This plan consisted of two structures with an aggregate length of 948 feet, set in an arrowhead pattern to form a 200-foot navigation entrance about 500 feet lakeward from the ends of the existing channel piers (Fig. 4-21).

2 Plans 2, 3, and 4. These plans involved variations in the elements of plan 1. For plan 2, a 115-foot extension was added to the north end of the west breakwater, angled to protect the navigation entrance from north to northeast waves. One circular cell and connecting section were added to this configuration at the south end of the east breakwater for plan 3; an additional cell and connecting section were added for plan 4. (Fig. 4-22.)

3 Plan 5. This plan consisted of one 608-foot-long structure located approximately perpendicular to the entrance channel centerline and 300 feet lakeward from the outer end of the east channel pier (Fig. 4-23).

4 Plans 6, 6A, and 6B. These plans involved variations in the elements of plan 5. For plan 6, one breakwater cell was added to the east end of the plan 5 structure. For plan 6A, quarrystone

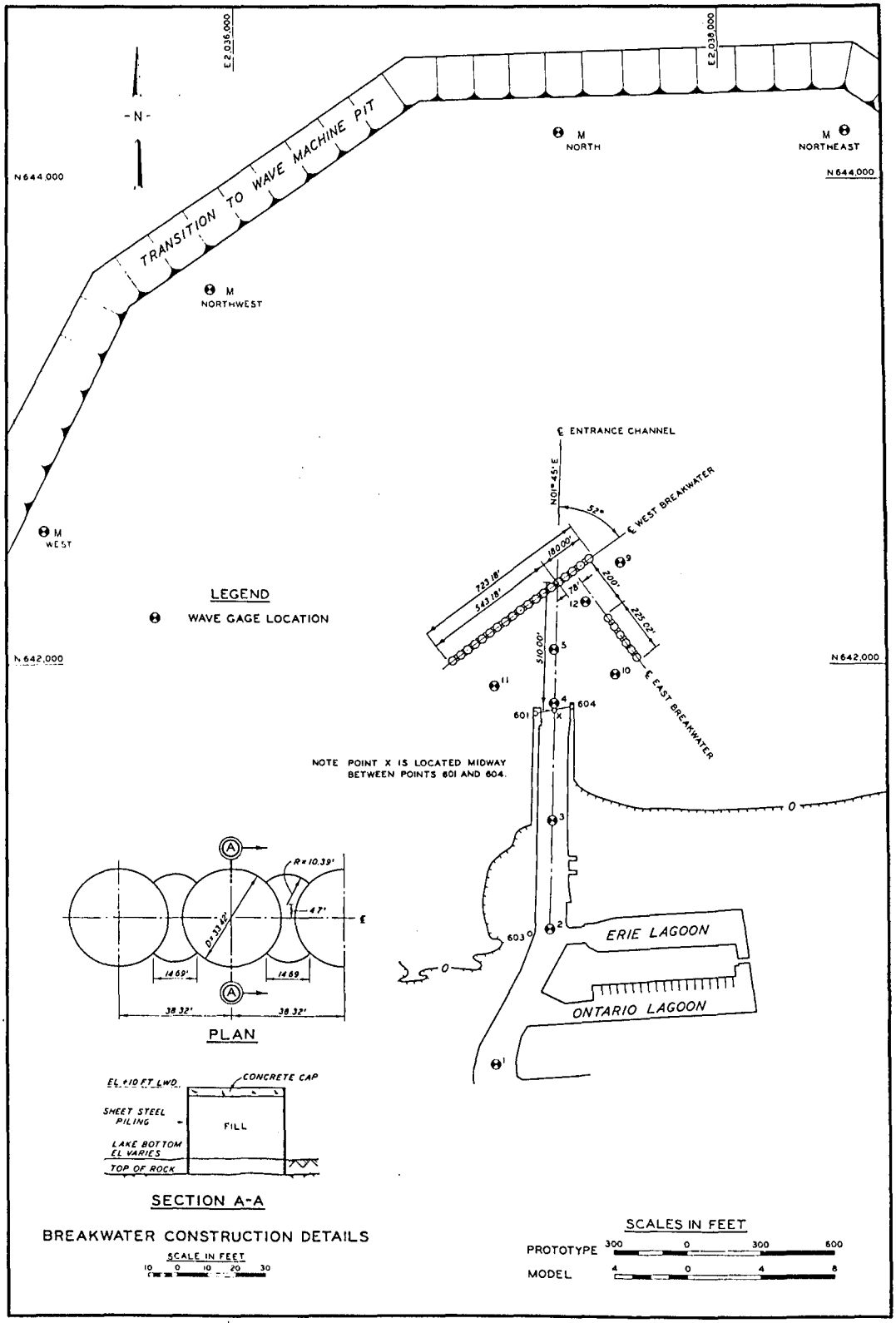

Figure 4-21. Elements of plan 1, Vermilion Harbor model (Brasfeild, 1970).

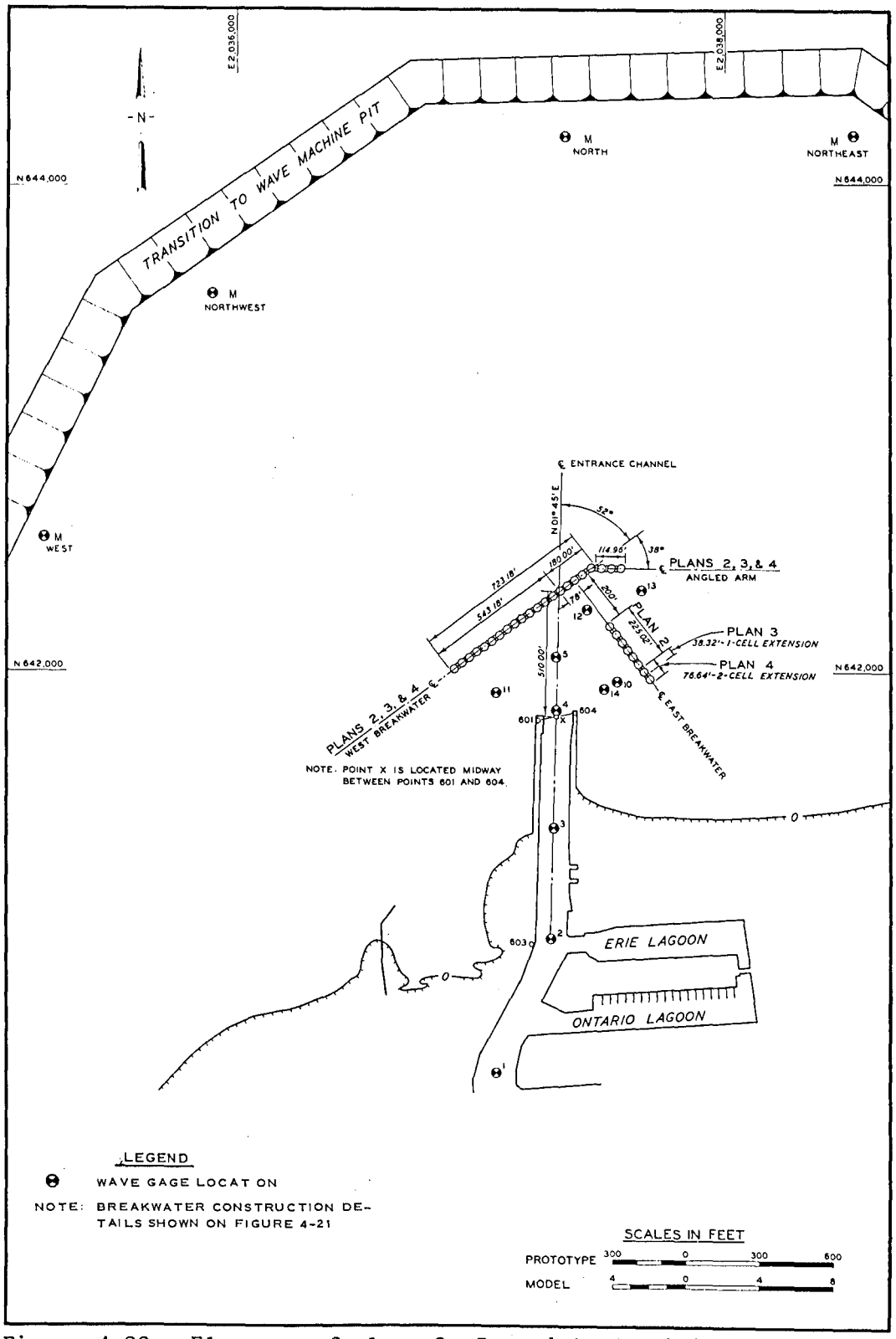

Figure 4-22. Elements of plans 2, 3, and 4, Vermilion Harbor model (Brasfeild, 1970).

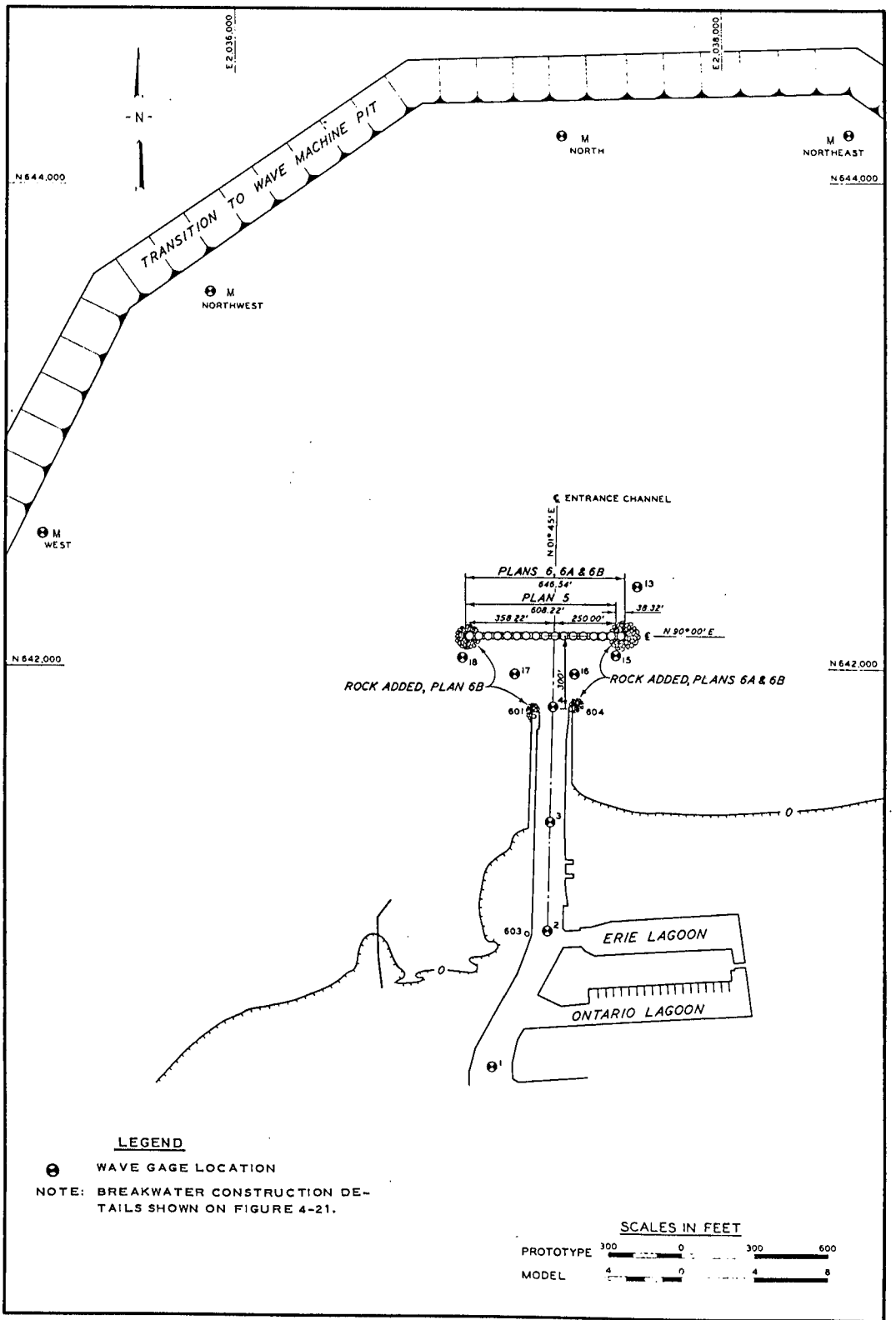

Figure 4-23. Elements of plans 5, 6, 6A, and 6B, Vermilion Harbor model (Brasfeild, 1970).

was placed around the east end of the plan 6 breakwater and around the end of the east channel pier to break up reflecting and diffracting waves around those structures. Additional stones were placed around the west end of the breakwater and around the end of the west channel pier for plan 6B. (Fig. 4-23.)

5 Plan 7. This plan consisted of one 608-foot-long breakwater located approximately perpendicular to the entrance channel centerline and 200 feet lakeward from the outer end of the east channel pier (Fig. 4-24).

6 Plans 7A and 7B. These plans involved variations in the elements of plan 7. For plan 7A, three breakwater cells and connecting sections were added to the west end of the plan 7 structure. For plan 7B, one of these cells was removed, and the other two were angled 30° toward the south. (Fig. 4-24.)

(j) Summary of Test Results.

1 Under existing conditions, Vermilion Harbor is exposed to severe wave attack from all directions clockwise from west to northeast. Resulting wave heights in the harbor area are of such magnitude as to severely restrict the use of the harbor and boat-mooring lagoons.

2 The most severe wave conditions in the harbor area are caused by storm waves approaching from the north to northeast directions.

3 The proposed plan of improvement (plan 1) will not provide sufficient protection for full use of the harbor.

4 Either plan 7A or 7B will provide the protection desired from wave action at the entrance to the river channel, up the channel, and in the entrances to the boat-mooring lagoons; however, since plan 7B uses one less cellular unit it should be more economical to construct.

b. Harbor Wave and Surge Action Studies; Intermediate- and Long-Period Waves; and Undistorted- and Distorted-Scale Models. (Since the need for model studies concerning tsunamis is rare and little is known about the methods of modeling this complicated phenomenon, the description of a tsunami model is omitted. However, seiche and tsunami models are discussed in the following references: Knapp and Vanoni, 1945; Hudson, 1947 and 1949; Hudson and Wilson, 1949; Palmer, Mulvihill, and Funasaki, 1967; Chatham, 1968.)

Monterey Harbor, California.

(a) Project. Enlargement of existing harbor at Monterey, California, by construction of additional breakwaters to provide safe

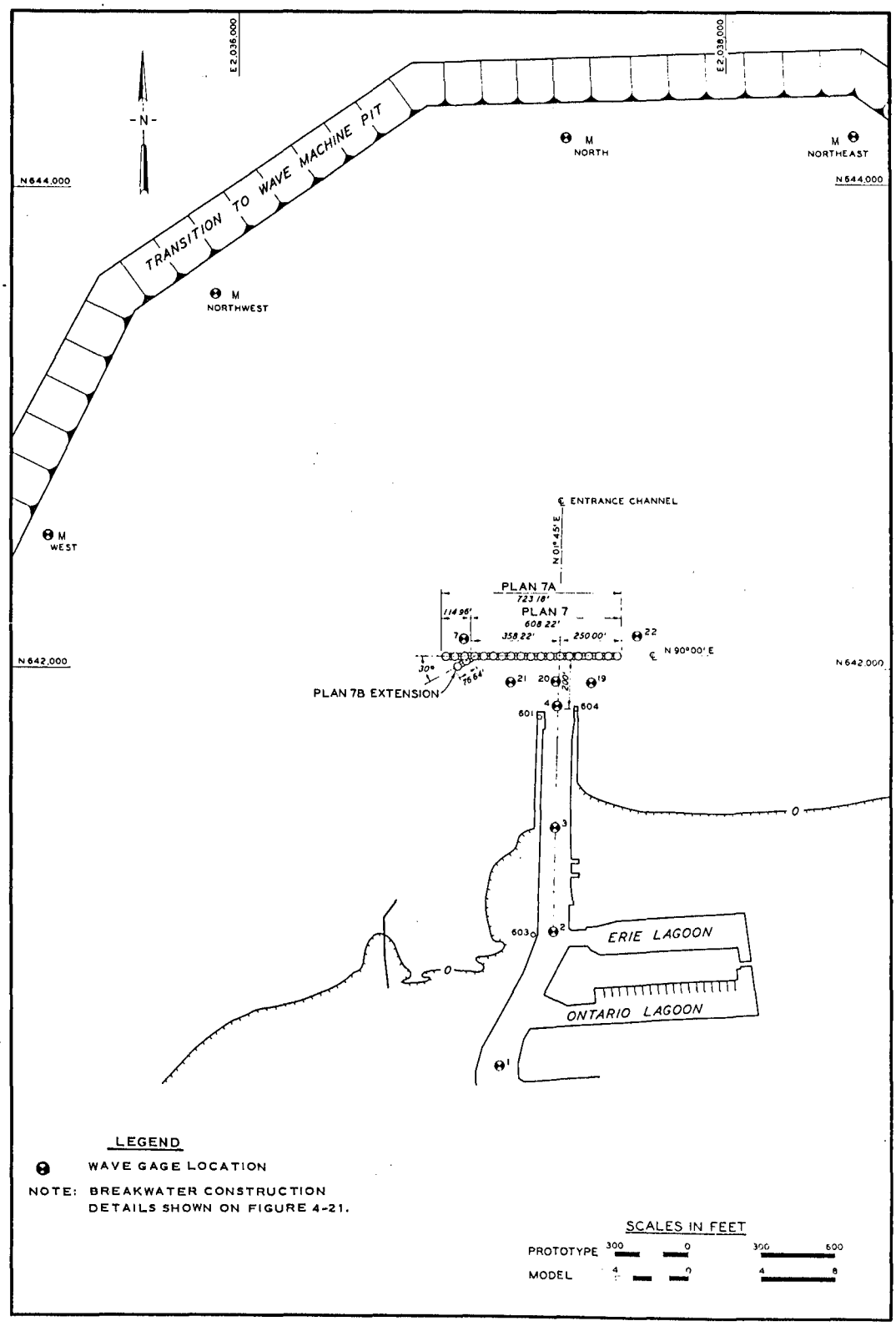

Figure 4-24. Elements of plans 7, 7A, and 7B, Vermilion Harbor model (Brasfeild, 1970).

anchorage for the commercial fishing fleet and additional facilities for pleasure craft. Development of the inner harbor area by construction of several moles to provide additional shelter for small-craft berthing facilities and land areas suitable for resort motels, restaurants, and related commercial activities.

(b) Reference. Chatham (1968).

(c) Laboratory. WES.

(d) Test Period. May 1966 to November 1967.

(e) Problem. Monterey Harbor is located at the southern end of Monterey Bay about 100 miles south of San Francisco, and is exposed to short-period, distant storm waves from the deepwater directions clockwise between west and northwest and local storm waves from the north direction (Fig. 4-25). Occasionally, these waves are of sufficient magnitude to damage fishing boats and harbor facilities and to cause mooring difficulties for small craft in exposed areas of the harbor. Intermediate- and long-period waves of considerable magnitude also occur in Monterey Bay, and such waves are capable, under certain circumstances, of a substantial increase in amplitude in some harbor areas due to resonance phenomena. Thus the proposed breakwaters and inner harbor structures should be designed to provide the maximum protection from short-period waves at minimum cost; further, the proposed construction should not amplify the intermediate- and long-period surge waves that occur in the harbor. Since the accurate prediction of the behavior of waves in a harbor is not possible by analytical methods, the need for a hydraulic model investigation was indicated. A field study was necessary to determine the wave conditions that occur in the harbor area (Marine Advisers, 1964); an analytical study was also conducted to determine the feasibility of a model study to resolve the intermediate- and long-period surge problems. The model study was determined feasible (Wilson, Hendrickson, and Kilmer, 1965).

(f) Purpose of Model Study. The model study was conducted to determine whether the proposed harbor revisions would provide adequate protection from intermediate-, long-, and short-period wave and surge action. It was desired that the intermediate- and long-period waves that occur in the harbor area not be amplified by resonance to such an extent that the resulting wave heights and currents in the navigation openings and inner harbor basins would constitute a hazard to small craft. Another objective of the model investigation was to determine whether suitable design modifications of the proposed plans could be made that would reduce construction costs significantly and still provide adequate protection from wave action. Presently (1976), no established criteria are available from which satisfactory conditions in a small-craft harbor can be assured for waves with periods greater than about 25 seconds. However, observations in the small-craft harbor at Santa Cruz, California (Magoon and Sarlin, 1970), indicate that waves with periods of 80 seconds to 10 minutes with heights of about 1.0 to over 4.0 feet occur frequently in

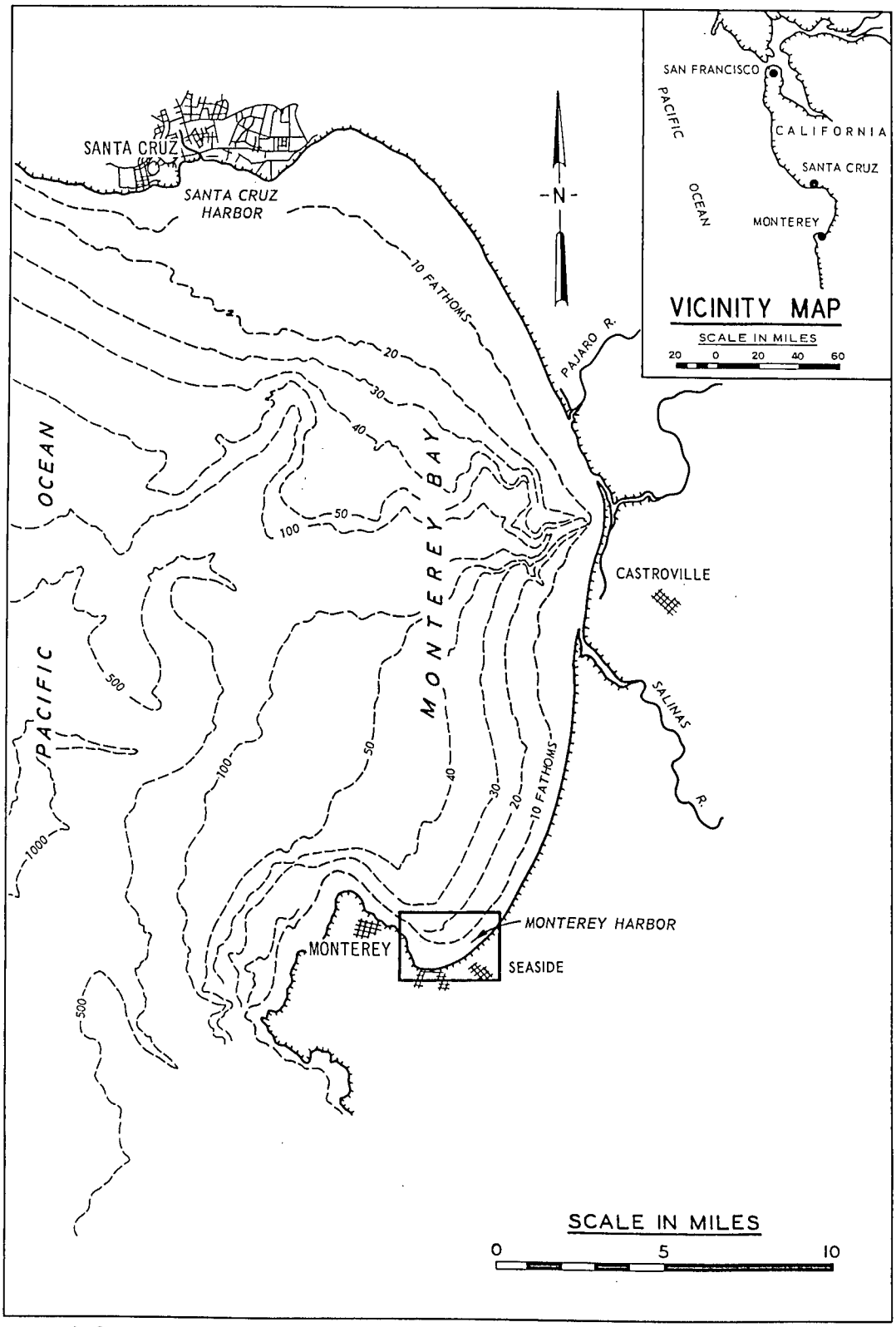

Figure 4-25. Location map, Monterey Harbor, California (Chatham, 1968).

that area, but that mooring conditions are considered satisfactory. Further, although difficulties resulting from surge currents have been reported in the entrance to the existing marina in Monterey Harbor, navigation and mooring conditions in the marina are generally considered to be acceptable. Thus, for this investigation, surge conditions in the existing marina and in the proposed additional small-craft basins in Monterey Harbor were assumed to be satisfactory if intermediate- and long-period wave heights and resulting currents in the existing and proposed basins and entrances do not exceed those that presently occur in the existing marina. Adequate criteria have not yet been developed to ensure satisfactory navigation and mooring conditions in small-craft harbors for short-period waves (waves with periods from about 5 to 20 seconds). However, when resonant surge conditions occur for small craft moored in present-day marinas, small wave heights can result in the breaking of mooring lines when the craft are incorrectly moored. In this study, satisfactory conditions are assumed if short-period wave heights do not exceed 1.5 feet in the inner basins and 4.0 feet at the basin entrances and in the fairway.

(g) The Model. Results of a feasibility study (Wilson, Hendrickson, and Kilmer, 1965), showed that the wave periods of concern were likely to be less than 3 minutes and certainly less than 7 minutes. Therefore, the vicinity of Mussel Point (about halfway between Point Pinos and Monterey; Fig. 4-26) was selected as the seaward limit of the model. Further, the intermediate- and long-period wave energy moving across the rim of the deep submerged canyon on the northern edge of the Continental Shelf (for the southern part of the bay) was concluded to be insignificant and the generation of intermediate- and long-period waves from this direction would be unnecessary. Thus, a side boundary for the model, normal to the coast from near the inlet to Laguna del Rey, would not seriously interfere with the oscillating regime, provided that enough wave-filter material was installed along the wall to prevent wave reflection. For the same reason, it was recommended that wave-filter material be placed in front of the wave generator. The recommended limits for a surge action model of Monterey Harbor were established as shown in Figure 4-26, with two wave-generator units to reproduce the correct directions of approach of the intermediate- and long-period waves south of Mussel Point. On the basis that the prototype harbor area to be modeled was about 10^4 by 10^4 feet, a horizontal linear scale of 1:200 was suggested for a convenient model size of 50 by 50 feet. A vertical scale of 1:120 was also suggested, which would give a distortion factor of 1.67 for the model. The maximum water depth in the marina (about 16 feet) would then be about 0.13 foot in the model, which is considered an adequate working depth in the inner basin. Wilson, Hendrickson, and Kilmer (1965) considered the 1.67 distortion factor as satisfactory for reliable reproduction of long-period waves down to about 30 seconds. However, because the model would also be used to study the effects of short-period waves (in the range of 5 to 20 seconds), and because these waves can best be investigated in undistorted models, a 1:120 linear scale was used for both the horizontal and vertical dimensions. The design and operation of the model were based on the recommendations in

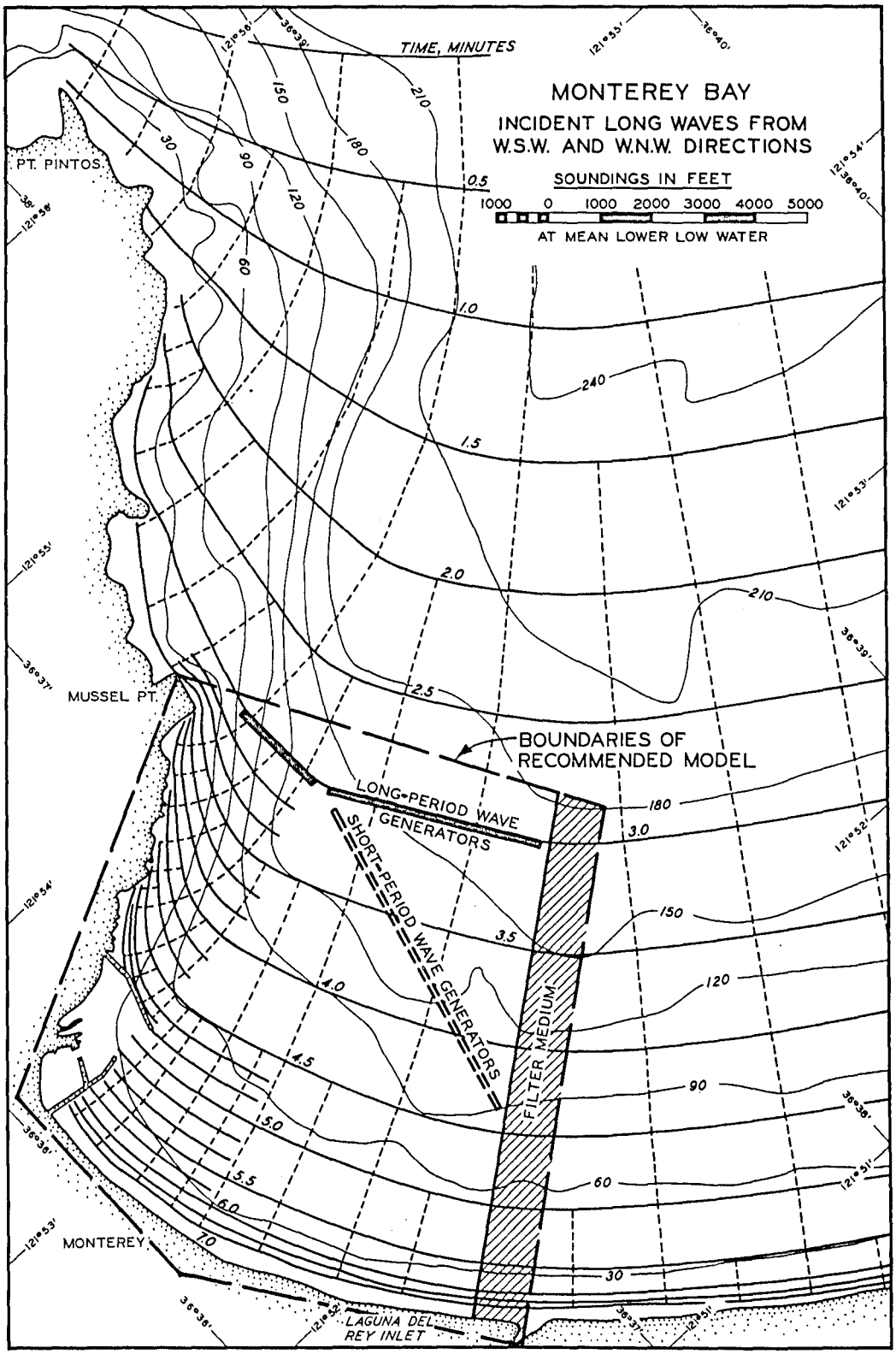

Figure 4-26. Recommended boundaries, Monterey Harbor model (Wilson, Hendrickson, and Kilmer, 1965).

the feasibility report and were in accordance with Froude's model law (Raichlen, 1968); the scale relations are given in Table 4-8.

Table 4-8. Monterey Harbor model scale relations.

Characteristic	Dimension[1]	Model-to-prototype scale
Length	L	$L_r = 1{:}120$
Area	L^2	$A_r = L_r^2 = 1{:}14{,}400$
Volume	L^3	$\bar{V}_r = L_r^3 = 1{:}1{,}728{,}000$
Time	T	$T_r = L_r^{1/2} = 1{:}10.95$
Velocity	L/T	$V_r = L_r^{1/2} = 1{:}10.95$

[1] Dimensions are in terms of length (L) and time (T).

Scale effects due to wave transmission through the rubble-mound breakwaters were reduced by increasing the quarrystone sizes in the model by a factor of two, compared to the sizes obtained by application of the linear scale (see Sec. IV,3,c). Wave heights measured in the model were corrected due to the effects of bottom friction by use of Keulegan's (1950b) equation. The model was molded in cement mortar and reproduced the entire harbor area and underwater contours to an offshore depth of 160 feet; enough of the offshore area was included to permit generation of both long- and short-period test waves from the selected model directions of wave approach. The total area reproduced in the model was approximately 7,800 square feet, representing about 4 square miles in the prototype. Several layers of wave-absorber material were placed around the seaward boundaries of the model and in front of the vertical-faced wave generator to reduce the effects of wave reflection on model test results. The intermediate- and long-period model waves were generated to scale by two sections of a vertical-bulkhead wave generator. The two sections had a total length of 56 feet and were positioned to reproduce the average curvature of a long-period wave front bent by refraction as it traveled through shallow water to the harbor area (Fig. 4-27). The generator, by use of universal couplings between sections, operated from a single power source. The horizontal movement of the vertical bulkhead caused a periodic displacement of water incident to this motion. The bulkhead speed and displacement were infinitely variable over the range necessary to permit generation of model test waves. For the short-period phase of the investigation, the two wave generator sections were combined into one straight 56-foot generator mounted on retractable casters to enable the generator to be positioned to generate waves from more than one test direction. To provide room for the wave generator to generate test waves from the north (azimuth 360°) direction, the outer reaches of the molded area were modified so that underwater contours were reproduced only to an offshore depth of 120 feet (Fig. 4-28).

(h) Test Procedures. The mean diurnal range of the astronomical tide at Carmel, California, near Point Pinos and adjacent to Monterey Harbor, is 5.2 feet; the maximum range is 9.7 feet. Mean higher

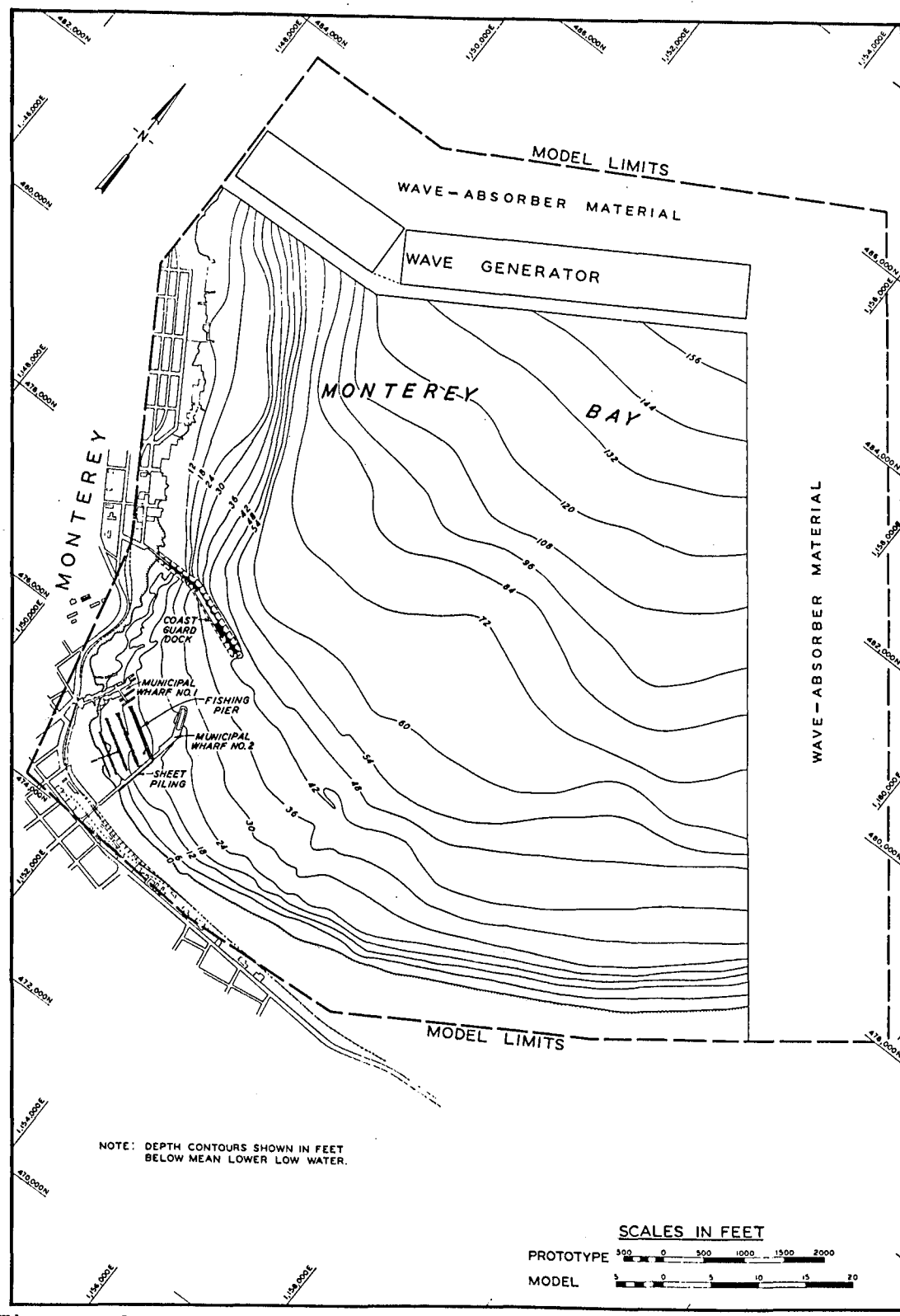

Figure 4-27. Layout for long-period wave tests, Monterey Harbor model (Chatham, 1968).

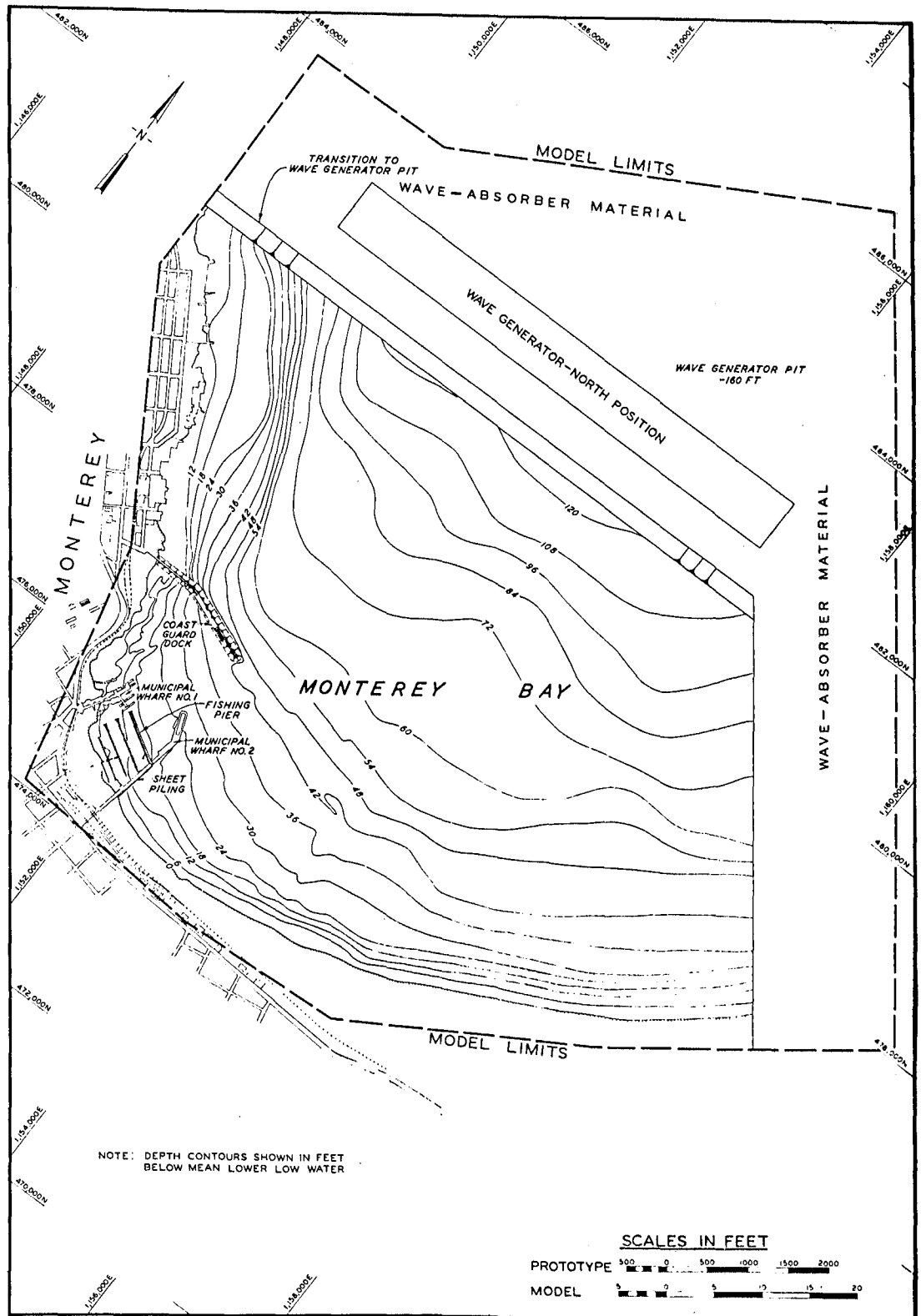

Figure 4-28. Layout for short-period wave tests, Monterey Harbor mode (Chatham, 1968).

high water (MHHW) is 5.2 feet above MLLW. Because of the low probability that an extreme wind tide, a high astronomical tide, and extreme storm waves would occur simultaneously, the selection of a stillwater level somewhat less than the maximum recorded tide appeared reasonable. Accordingly, the MHHW stage of +5.2 feet was selected as representative of conditions normally expected to occur during a severe storm, and this stillwater level was used for all tests conducted in the model. Since Monterey Harbor is subject to the action of intermediate-, long-, and short-period waves, it was necessary to incorporate these wave types into the testing program. Little is known about the basic causes of surging in Monterey Bay. Wave-refraction diagrams that were drawn for incident waves from south-southwest clockwise to west-northwest indicated that regardless of the deepwater direction all long-period waves reach Monterey Harbor from practically the same direction. An analytical study of the intermediate- and long-period oscillations was conducted in the Monterey Bay area for the possibility of related response in Monterey Harbor. Based on these results, the prototype wave periods selected for the intermediate- and long-period phases of the model study were T = 35, 38, 41, 44, 47, 51, 55, 60, 66, 72, 80, 88, 97, 100.2, 114, 124, 132, 138, 144, 158, 172, 185, 205, 225, 234, 257, 280, 305, 330, and 360 seconds. The short-period waves (Table 4-9) were selected from National Marine Consultants (1960) and a refraction diagram study. In evaluating the various design plans tested, corresponding model data (i.e., test results using similar input test conditions with different plans installed) were compared to determine the relative effectiveness of each individual plan. The long-period wave phase of the study included the comparison of: (a) Both maximum and average wave heights recorded in the individual harbor basins; (b) current velocities in the harbor basins and entrances; (c) modes of oscillation in the bay area; (d) frequency-response data for the various basins; and (e) time-exposure photos of float movement in critical areas. Visual observations during model testing and test notes aided in the analysis. In the short-period wave phase of the study, the relative merits of the various plans tested were evaluated by (a) comparison of wave heights at selected locations in the harbor, and (b) extension of the wave height data into tables showing the estimated duration of waves of various magnitudes that can be predicted at the selected locations. Visual observations, photos of wave crest patterns, and test notes were also used in the short-period wave test analysis. In the wave height data analysis, the average height of the highest one-third of the waves recorded at each gage location was selected for the computations. The direction and magnitude of surface currents in the model were measured by taking time-exposure photos of surface floats from camera positions directly above the model harbor area. From these photos, the progress of the floats over one wave cycle was measured relative to a horizontal grid system painted on the model floor, and the corresponding velocities were computed. Wave heights at selected locations in the model were recorded on chart paper by an electrically operated oscillograph. The input to the oscillograph was the output of electrical wave height gages that measured the changes in the water surface elevation with respect to time. The electrical output of each wave height gage was directly proportional to the submergence of the gage in the water.

Table 4-9. Selected short-period test wave conditions, Monterey Harbor model.[1]

Wave period T (s)	Deepwater waves		Selected shallow-water test waves	
	Direction	Height (ft)	Direction	Height (ft)
7	W.N.W.	11	N. 35° W.	7
	N.W.	9	N. 35° W.	7
9	N.W.	13	N. 35° W.	9
11	W.	19	N. 35° W.	7
	W.N.W.	15	N. 35° W.	7
	N.W.	9	N. 35° W.	7
	N.W.	17	N. 35° W.	13
13	W.	21	N. 35° W.	7
	W.N.W.	17	N. 35° W.	7
	N.W.	9	N. 35° W.	7
	N.W.	19	N. 35° W.	13
15	W.	25	N. 35° W.	7
	W.N.W.	11	N. 35° W.	7
	N.W.	9	N. 35° W.	7
	N.W.	17	N. 35° W.	13
17	W.	25	N. 35° W.	7
	W.N.W.	11	N. 35° W.	7
	W.N.W.	21	N. 35° W.	13
	N.W.	9	N. 35° W.	7
8	N.	9	N.	9
	N.	12	N.	12

[1] Prototype dimensions.

(i) Plans Tested. Tests were first performed with existing prototype conditions installed in the model (Fig. 4-29). Before tests of the various improvement plans, comprehensive base test data were obtained in the harbor and bay area and then used as a base to determine the relative efficacy of the various improvement plans. Model tests were conducted using two basic harbor configurations: double entrance (plan 1, Fig. 4-30) and single entrance (plan 2, Fig. 4-31). Typical sections of the various breakwater and revetment structures are shown in Figure 4-32; breakwater, mole, and basic designations are shown in Figure 4-33.

(j) Description of Tests. For the long-period wave phase of the investigation, the wave generator was calibrated using the Marine Advisers' (1964) data for sensor No. 1. In each individual wave period, the wave generator stroke was adjusted until the required wave height was recorded at the location of sensor No. 1 (gage 37 in the model). The corresponding input wave at the wave generator was then used for all subsequent base tests and tests of the two improvement plans. Preliminary mode of oscillation tests was conducted in which wave heights were measured over the entire bay area of the model for base test and plan 1

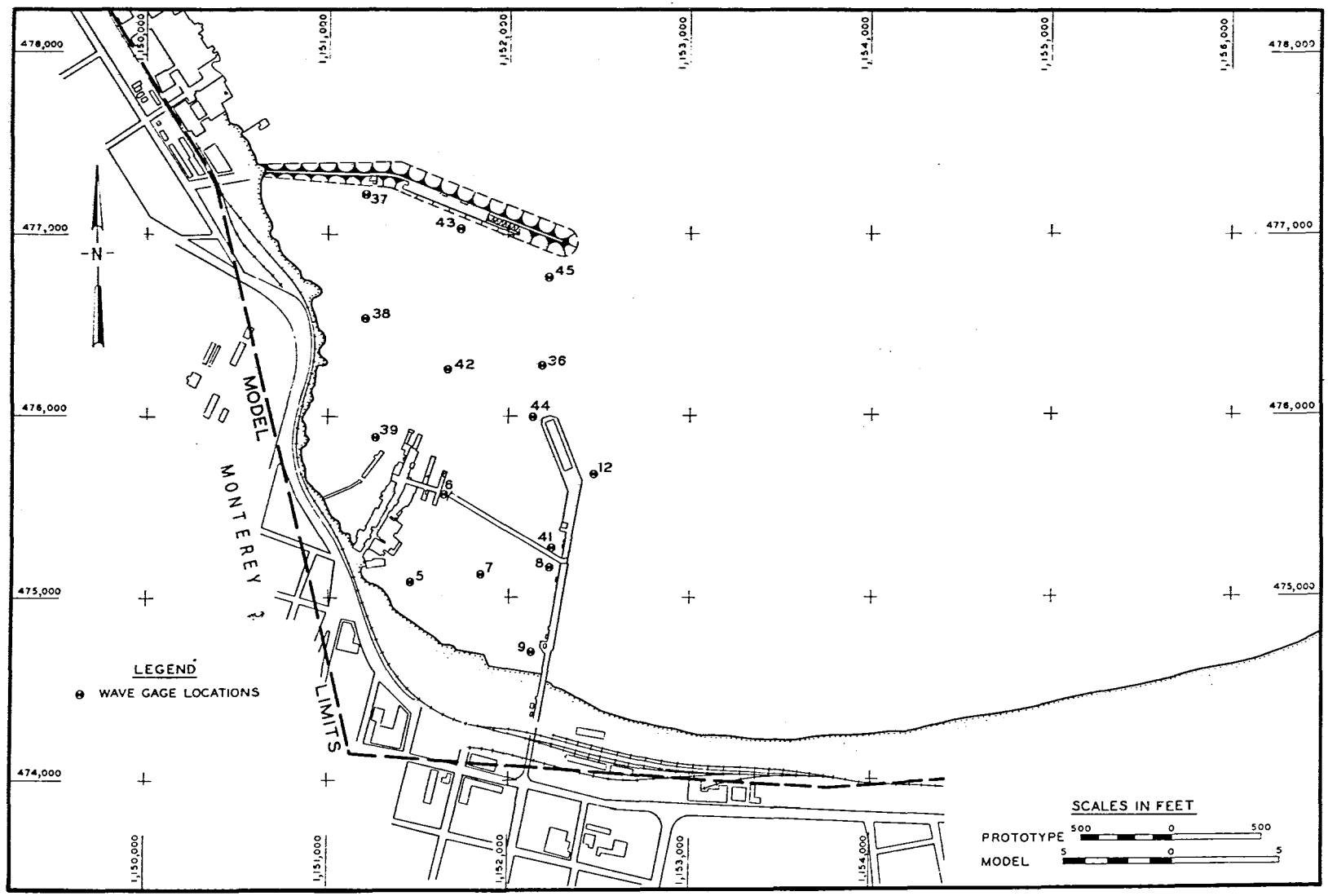

Figure 4-29. Elements of base tests, Monterey Harbor model (Chatham, 1968).

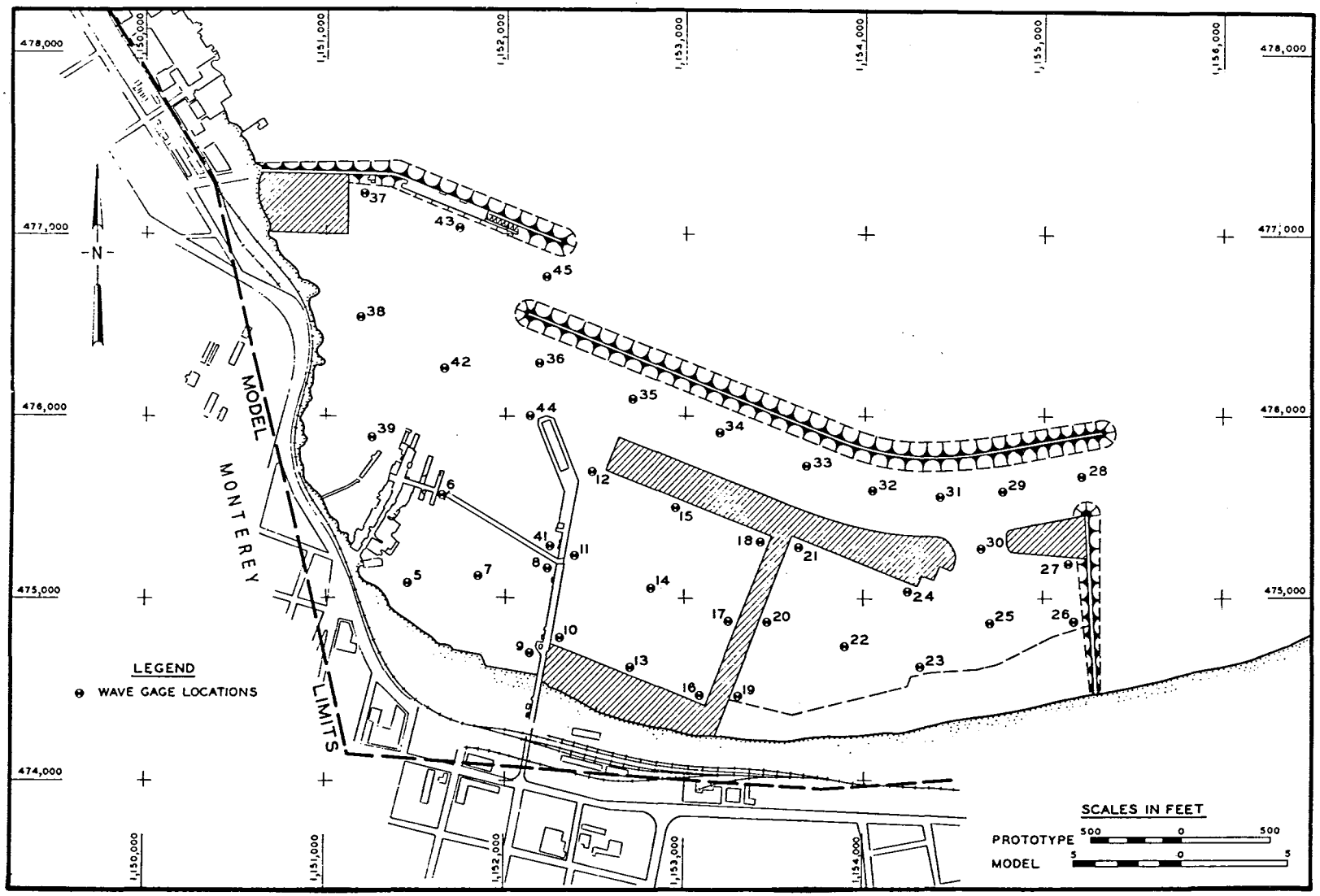

Figure 4-30. Elements of plan 1, Monterey Harbor model (Chatham, 1968).

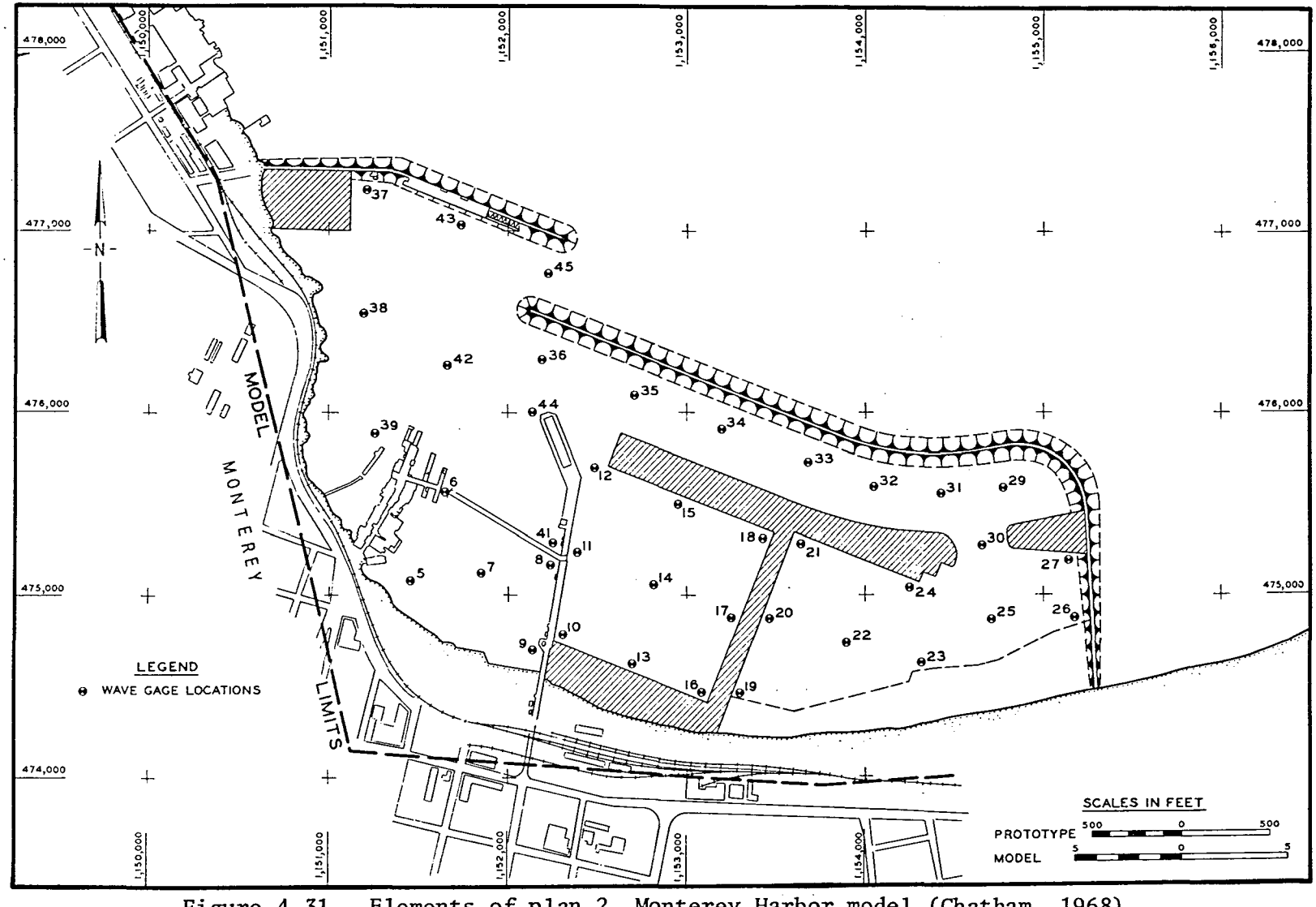

Figure 4-31. Elements of plan 2, Monterey Harbor model (Chatham, 1968).

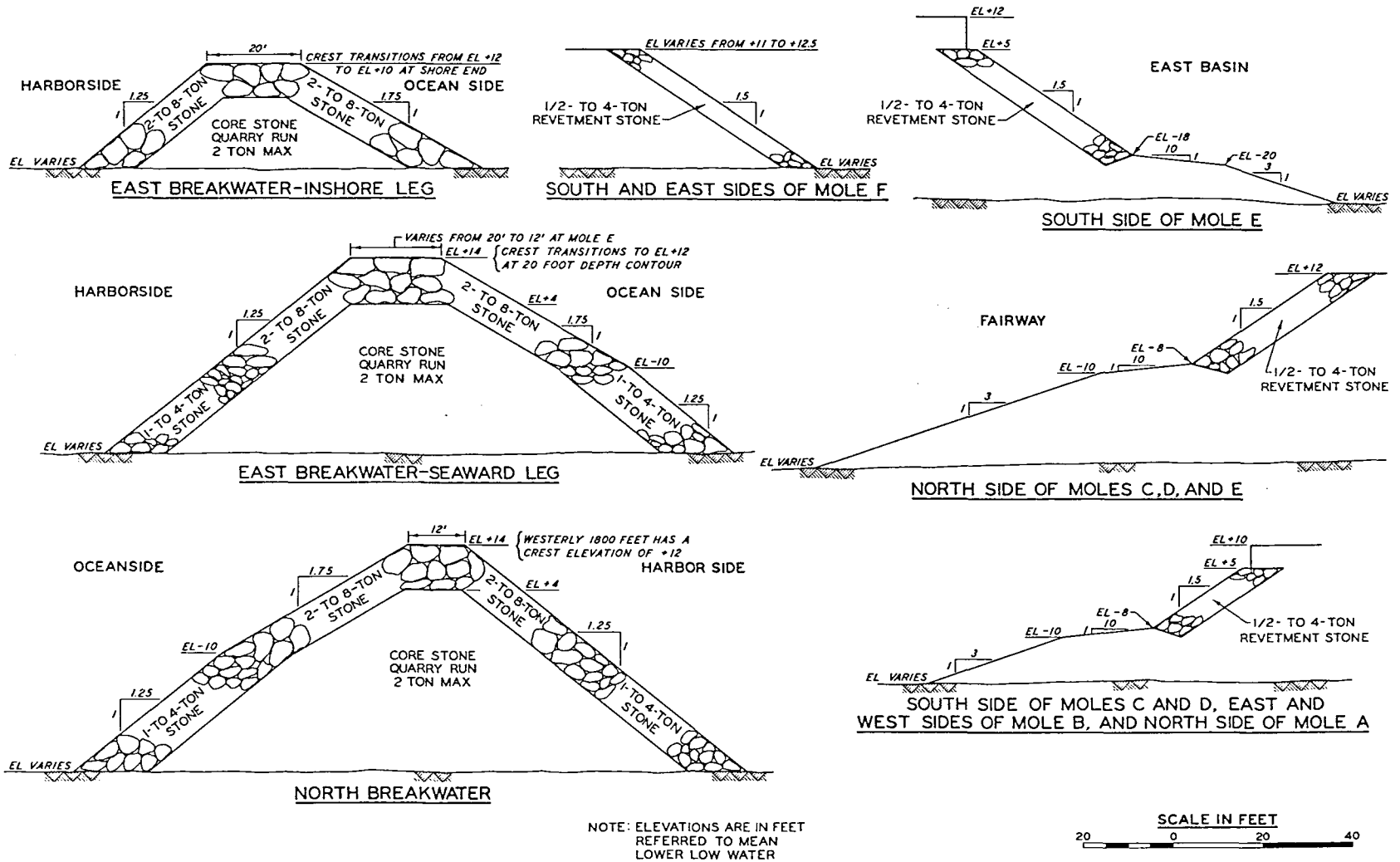

Figure 4-32. Typical sections of proposed structures, Monterey Harbor model (Chatham, 1968).

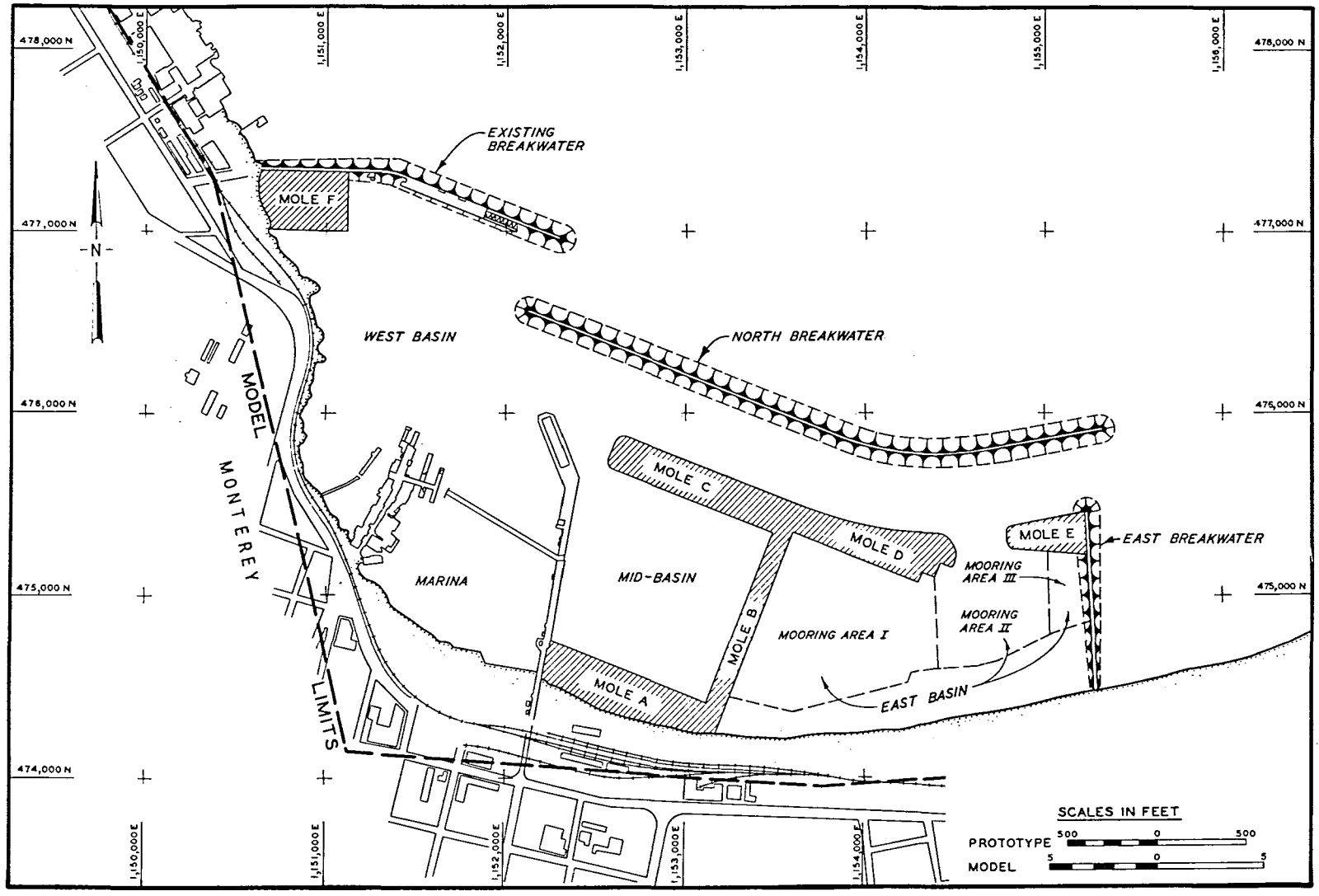

Figure 4-33. Breakwater, mole, and basin designations, Monterey Harbor model (Chatham, 1968).

conditions to determine if installation of the plan would cause any significant changes in the modes of oscillation in the model bay area. Measurements were made over a horizontal grid system, and contours of equal wave heights were drawn so that the various loop and node points could be distinguished. These tests used prototype wave periods of 35, 45, 55, 120, 130, 170, 180, 200, 230, and 255 seconds. Wave heights and surface currents were measured in the harbor basins and entrances for base test, plan 1, and plan 2 over the entire range of wave periods from 35 to 360 seconds. During each test where surface currents were measured, several hundred surface floats (approximately 1 inch square and 1/8 inch thick) were distributed throughout the harbor area, and time-exposure photos were taken of current movement over one wave cycle (one wave period). Frequency response tests were conducted to determine if any of the harbor basins responded to specific wave periods. In these tests, comprehensive wave height measurements were made in each of the basins for the entire range of wave periods (35 to 360 seconds). Time-exposure photos were also used to determine the degree of response of the harbor basins for the various wave periods. Short-period wave tests were conducted with base test conditions and plans 1 and 2 installed in the model for the entire range of test waves listed in Table 4-9. Wave height measurements were made in all of the harbor basins and basin entrances.

(k) Summary of Test Results.

1 The modes of oscillation in the bay area for base test conditions and with the proposed plan 1 installed were generally similar; the wave input into the harbor was reproduced with sufficient accuracy.

2 Intermediate- and long-period wave and current conditions in the harbor were approximately the same for either plan 1 or plan 2, and either plan offered a slight improvement over conditions in the existing harbor.

3 Intermediate- and long-period wave and current conditions in the newly formed basins of plans 1 and 2 compared favorably with those in the existing marina, indicating that, to the extent that present conditions in the existing marina are considered acceptable, conditions in the proposed additional basins were also satisfactory.

4 The harbor basins responded to some extent to several of the intermediate- and long-period waves tested; however, no serious resonance was noted.

5 For short-period wave heights, both plans (1 and 2) offered an improvement over existing conditions and neither plan appeared significantly better than the other.

6 Short-period wave heights in the marina, west basin, midbasin, and mooring area I of the east basin were considered acceptable for either plan 1 or plan 2.

7 During periods of attack by exceptionally high short-period storm waves, wave heights in mooring areas II and III of the east basin and in the fairway should exceed those generally accepted as safe for the navigation and the anchorage of small boats.

8 Reducing the length of the detached north breakwater by amounts up to 300 feet had little effect on wave heights in the east basin. However, wave heights in the east entrance to the harbor increased considerably, and serious overtopping of mole E occurred for all reductions in length greater than about 50 feet.

6. Cost and Time Estimates.

a. Harbor Wave Action Models, Short-Period Waves. In the conduct of short-period, harbor wave action models, the sponsoring agency usually furnishes the required field data at the outset of the study. These data include deepwater wave statistics, refraction diagrams from which the deepwater data can be converted into shallow-water wave data at the positions of the wave generator, tidal data, wind setup information, topographic and underwater contour data, and detailed plans of all existing and proposed harbor structures. Since the laboratory usually has the necessary wave generator on hand and adequate shelter space, the cost of these items and the costs of obtaining the necessary field data (listed above), are not included in the laboratory cost and time estimates for short-period, wave action models. Most harbor wave action model studies in which short-period waves are the primary problem involve the following work items:

(1) Preliminary model design and cost estimate, and necessary travel, conferences, and correspondence before authorization to conduct the model study.

(2) Final model design.

(3) Model construction.

(4) Calibration and adjustment of wave generator and wave-measuring apparatus for the selected test conditions.

(5) Conduct of model tests, including modifications of the model in accordance with the different plans, computer time, drafting and photography as required, preparation of monthly progress reports, and model demonstrations and conferences with representatives of the sponsoring agency (obtaining and processing of motion picture film showing wave action conditions in a harbor are sometimes requested as a special item; however, these costs are not included in the cost estimates).

(6) Analysis of test results after testing has been completed; preparation for and hosting of a final conference at which time the test results are presented and discussed.

(7) Preparation of the first draft of final report (usually sent to the sponsoring agency for review and comment).

(8) Preparation, publication, and distribution of the final report.

(9) Return remaining funds to the sponsor after completion of the study.

The cost of performing harbor model studies in which short-period waves are the cause of concern varies from about $50,000 to $180,000 depending on the size of the model and the number of plans investigated. Two typical studies completed at WES (September and November 1975) cost $117,000 and $84,000. The model areas were 16,000 and 14,000 square feet, respectively; operation times (after model construction) were 8 and 5 months, respectively. The total costs of performing the Vermilion Harbor model study, conducted during August 1968 to July 1969, was $70,000. The model area was 8,800 square feet and the operation time was 6 months. The costs of operation and construction have increased considerably since 1969. The estimated costs of the Vermilion Harbor model study in 1976 are given in Table 4-10. Although the costs of performing harbor wave action model studies have increased, the time required to operate such models has decreased since an automated data acquisition and control system has become available.

Table 4-10. Estimated cost (1976) of Vermilion Harbor model study.

Item	Estimated time	Estimated cost
Preliminary model design, etc.	2.0 wk	$ 2,100
Model design (final)	1.0 mo	4,200
Model construction	2.0 mo	46,200
Calibration of wave machine and wave gages	1.0 wk	1,600
Model operation	5.0 mo	31,400
Analysis of data and conference	3.0 wk	4,700
Report (preparation and publication)	6.0 mo	6,300
Total	15.4 mo	$96,500

b. Harbor Wave Action Models, Intermediate- and Long-Period Waves. The costs of conducting seiche-type model studies are greater than those for short-period waves because:

(a) Collection of the necessary prototype wave data is more difficult and time consuming;

(b) analysis of the prototype data (in a form that can be used to design and operate the model and analyze the test results) is more difficult and will normally require the use of a computer;

(c) a theoretical study where the modes of oscillation and resonant periods of the bodies of water (bay and shelf resonance) surrounding the problem area are determined, is usually required before the model can be designed;

(d) the longer wavelengths require a larger area of the surrounding ocean waters to be included within the model boundaries;

(e) a large volume of low-reflection, wave absorber-filter material must be used around the ocean boundaries of the model; and

(f) the testing program is usually very tedious and time consuming because of the large number of wave conditions that must be investigated.

The Monterey Harbor wave and surge action model study, which involved short-, intermediate, and long-period wave investigations, cost about $121,000. The area of the model was 7,800 square feet and the operating time was 7 months. The investigation was performed in 1966-67. The cost of such a study in 1976 would be about $170,000, exclusive of the costs of collecting the necessary prototype data and the performing of a theoretical study to ensure a sound basis of designing and operating the model.

LITERATURE CITED

AMERICAN SOCIETY OF CIVIL ENGINEERS, "Report on Small Craft Harbors," Task Committee on Small-Craft Harbors, No. 50, *ASCE Manuals and Reports on Engineering Practice*, New York, 1969.

BIESEL, F., and LE MEHAUTE, B., "Notes on the Similitude of Small-Scale Models for Studying Seiches in Harbors," *La Houille Blanche*, Vol. 10, No. 3, 1955 (translation available at U.S. Army Engineer Waterways Experiment Station, Vicksburg, Miss.).

BRASFEILD, C.W., "Selection of Optimum Plan for Reduction of Wave Action in Marina del Rey, Venice, California; Hydraulic Model Investigation," Technical Report No. 2-671, U.S. Army Engineer Waterways Experiment Station, Vicksburg, Miss., Jan. 1965.

BRASFEILD, C.W., "Wave Action and Breakwater Location, Vermilion Harbor, Ohio; Hydraulic Model Investigation," Technical Report H-70-5, U.S. Army Engineer Waterways Experiment Station, Vicksburg, Miss., May 1970.

CAHNERS PUBLISHING CO., INC., "The Boating Business," *Boating Industry*, Vol. 40, No. 1, Cahners Publishing Co., Inc., New York, Jan. 1977.

CHATHAM, C.E., "Wave and Surge Conditions After Proposed Expansion of Monterey Harbor, Monterey, California; Hydraulic Model Investigation," Technical Report H-68-9, U.S. Army Engineer Waterways Experiment Station, Vicksburg, Miss., Sept. 1968.

COX, D.C., "Tsunami Height-Frequency Relationship at Hilo," Hawaii Institute of Geophysics, University of Hawaii, Honolulu, Hawaii, Nov. 1964.

DUNHAM, J.W., and FINN, A.A., "Small-Craft Harbors: Design, Construction, and Operation," SR-2, U.S. Army Corps of Engineers, Coastal Engineering Research Center, Fort Belvoir, Va., Dec. 1974.

EAGLESON, P.S., "Model Laws," Chapter Q, *Estuary and Coastline Hydrodynamics*, Hydrodynamics Laboratory, Department of Civil and Sanitary Engineering, Massachusetts Institute of Technology, Cambridge, Mass., 1960.

EAGLESON, P.S., and DEAN, R.G., "Small Amplitude Wave Theory," *Estuary and Coastline Hydrodynamics*, A.T. Ippen, ed., Ch. 1, McGraw-Hill, New York, 1966, pp. 1-92.

GODA, Y., and IPPEN, A.T., "Theoretical and Experimental Investigation of Wave Energy Dissipators Composed of Wire Mesh Screens," Report No. 60, Hydrodynamics Laboratory, Massachusetts Institute of Technology, Cambridge, Mass., Aug. 1963.

HUDSON, R.Y., "Model Study of Wave and Surge Action, Naval Operating Base, Terminal Island, San Pedro, California," Technical Memorandum No. 2-237, U.S. Army Engineer Waterways Experiment Station, Vicksburg, Miss., Sept, 1947.

HUDSON, R.Y., "Wave and Surge Action, Long Beach Harbor, Long Beach, California; Model Investigation," Technical Memorandum No. 2-265, U.S. Army Engineer Waterways Experiment Station, Vicksburg, Miss., Sept. 1949.

HUDSON, R.Y., and WILSON, H.B., "Wave and Surge Action, Monterey Harbor, Monterey, California; Model Investigation," Technical Memorandum No. 2-301, U.S. Army Engineer Waterways Experiment Station, Vicksburg, Miss., Sept. 1949.

IPPEN, A.T., and GODA, Y., "Wave Induced Oscillations in Harbors: The Solution for a Rectangular Harbor Connected to the Open Sea," Report No. 59, Hydrodynamics Laboratory, Massachusetts Institute of Technology, Cambridge, Mass., July 1963.

IPPEN, A.T. and RAICHLEN, F., "Wave Induced Oscillations in Harbors: The Problem of Coupling of Highly Reflective Basins," Report No. 49, Hydrodynamics Laboratory, Massachusetts Institute of Technology, Cambridge, Mass., May 1962.

KEULEGAN, G.H., "Wave Motion," *Engineering Hydraulics*, H. Rouse, ed., Ch. XI, Wiley, New York, 1950a, pp. 711-768.

KEULEGAN, G.H., "The Gradual Damping of a Progressive Oscillatory Wave with Distance in a Prismatic Rectangular Channel," National Bureau of Standards, Washington, D.C., unpublished, May 1950b.

KEULEGAN, G.H., "Wave Damping Effects of Screens; Hydraulic Model Investigation," Research Report No. 2-12, U.S. Army Engineer Waterways Experiment Station, Vicksburg, Miss., Mar. 1968.

KEULEGAN, G.H., "Wave Transmission Through Rock Structures; Hydraulic Model Investigation," Research Report H-73-1, U.S. Army Engineer Waterways Experiment Station, Vicksburg, Miss., June 1969.

KEULEGAN, G.H., HARRISON, J., and MATHEWS, M.J., "Theoretics in Design of the Proposed Crescent City Harbor Tsunami Model," Technical Report H-69-9, U.S. Army Engineer Waterways Experiment Station, Vicksburg, Miss., June 1969.

KNAPP, R.T., and VANONI, V.A., "Wave and Surge Study for the Naval Operating Base, Terminal Island, California," Hydraulics Structures Laboratory, California Institute of Technology, Pasadena, Calif., Jan. 1945.

LEE, J.J., and RAICHLEN, F., "Wave Induced Oscillations in Harbors with Connected Basins," Report No. KH-R-26, California Institute of Technology, Pasadena, Calif., Aug. 1971.

LE MEHAUTE, B., "Wave Absorbers in Harbors," Contract Report No. 2-122, U.S. Army Engineer Waterways Experiment Station, Vicksburg, Miss., June 1965.

MAGOON, O.T., and SARLIN, W.O., "Effect of Long-Period Waves on Hydrographic Surveys," *Proceedings of the 12th Coastal Engineering Conference*, American Society of Civil Engineers, Vol. 3, 1970 (also Reprint 8-71, U.S. Army, Corps of Engineers, Coastal Engineering Research Center, Fort Belvoir, Va., NTIS AD 754 869).

MARINE ADVISERS, "A Statistical Survey of Ocean Wave Characteristics in Southern California Waters," La Jolla, Calif., Jan. 1961.

MARINE ADVISERS, "A Broad-Frequency-Band Wave Study at Monterey Harbor, California," La Jolla, Calif., July 1964.

NATIONAL MARINE CONSULTANTS, "Wave Statistics for Seven Deep Water Stations Along the California Coast," Santa Barbara, Calif., Dec. 1960.

PALMER, R.Q., MULVIHILL, M.E., and FUNASAKI, G.T., "Study of Proposed Barrier Plans for the Protection of the City of Hilo and Hilo Harbor, Hawaii," Technical Report No. 1, U.S. Army Engineer Division, Pacific Ocean, Honolulu, Hawaii, Nov. 1967.

RAICHLEN, F., "Motions of Small Boats Moored in Standing Waves," Contract Report H-68-2, U.S. Army Engineer Waterways Experiment Station, Vicksburg, Miss., Aug. 1968.

U.S. ARMY ENGINEER DISTRICT, LAKE SURVEY, "Variations in Great Lakes Levels, 1952," Detroit, Mich., 1952.

U.S. COAST AND GEODETIC SURVEY, "Tide Tables, West Coast, North and South America, 1958-1961," U.S. Government Printing Office, Washington, D.C., 1958-61.

WIEGEL, R.L., "Protection of Crescent City, California, from Tsunami Waves," Redevelopment Agency of the City of Crescent City, Calif., Mar. 1965.

WILSON, B.W., "The Threshold of Surge Damage for Moored Ships," *Proceedings of the Institution of Civil Engineers*, Vol. 38, Paper 7018, 1967, pp. 107-134.

WILSON, B.W., HENDRICKSON, J.A., and KILMER, R.E., "Feasibility Study for a Surge-Action Model of Monterey Harbor, California," Contract Report No. 2-136, U.S. Army Engineer Waterways Experiment Station, Vicksburg, Miss., Oct. 1965.

WILSON, H.B., HUDSON, R.Y., and HOUSLEY, J.G., "Detached Breakwater and Improved Navigation Entrance, Lorain Harbor, Lorain, Ohio; Hydraulic Model Investigation," Technical Report No. 2-628, U.S. Army Engineer Waterways Experiment Station, Vicksburg, Miss., June 1963.

V. COASTAL EROSION

by
Robert W. Whalin and C.E. Chatham, Jr.

1. Introduction.

This section discusses hydraulic models of coastal erosion. A model study of this type is a three-dimensional investigation which involves littoral transport, onshore-offshore transport, and possibly scour or erosion around structures. The discussion is limited to coastal erosion problems not involving tidal inlets; thus, the major forcing function of concern is that due to wind-wave action. A movable-bed model study is needed to investigate the effect of coastal or offshore structures on shoreline evolution, the stability of beach modifications (e.g., the construction of perched beaches; Chatham, 1972; Chatham, Davidson, and Whalin, 1973), and the design of functional structures for preventing coastal erosion. Shoreline dynamics and engineering problems resulting from coastal erosion are well documented (Bagnold, 1940; Krumbein, 1944; Keulegan, 1945; Brown, 1950; Bascom, 1951; Beach Erosion Board, 1954; Shinohara, 1958; Le Mehaute and Brebner, 1961; Eagleson, Glenne, and Dracup, 1961, 1963; Eagleson, 1965; Inman, 1965; Inman and Frautschy, 1965; Caldwell, 1966; Ippen, 1966; Johnson, 1919, 1956, 1957, 1959, 1966; Inman, Komar, and Bowen, 1968; Bijker and Svasek, 1969; Saville, 1969; Einstein, 1948, 1971; Yalin, 1972; and Silvester, 1959, 1974).

A completely quantitative movable-bed model investigation of coastal erosion appears to be impractical within the present state-of-the-art. However, movable-bed scale-model investigations of several types of coastal erosion problems are feasible and can be conducted in such a way that useful, and sufficiently accurate, information can be obtained for design purposes. If adequate prototype data are available, and verification procedures in the model are successful, an investigator should have confidence in the results of coastal erosion models (e.g., as in the movable-bed river models investigation by Vernon-Harcourt).

A satisfactory movable-bed scale-model investigation is perhaps the most difficult type of model study to perform. Some examples of laboratory movable-bed model studies include: U.S. Army Engineer Waterways Experiment Station (1943); Bagnold (1947); Saville (1950); Rector (1954); Watts (1954); Shinohara (1959); Shinohara and Tsubaki (1959); Iwagaki and Noda (1962); Savage (1959, 1962); Inman (1963); Sitarz (1963); Kalkanis (1964); Bonnefille and Pernecker (1965); and Nayak, 1970. A study of the physical processes involved in beach erosion by wave action (Manohar, 1955; Eagleson and Dean, 1961; Collins, 1963; Vanoni, 1964; Eagleson, 1957, 1959, 1965; and Galvin, 1967) would lead to an appreciation of these difficulties. There is a transition from one basic regime of boundary flow to another as sediment motion outside the surf zone is compared to sediment motion in the surf zone; thus, exact dynamic similitude of the dominant physical processes in both regimes simultaneously (using the

same model fluid and the same model laws for reproducing the waves, currents, and bottom material for both regimes) is impossible. Other effects, such as edge waves, rip currents, the directional spectrum, the long-wave environment, and the prototype sediment-size distribution and amount of sorting (Longuet-Higgins, 1953), must all be considered at least to the point of showing that they are unimportant at the particular location being studied. Other questions also arise concerning both scale effects (Bijker, Stapel, and de Vries, 1957; Diephius, 1957; Saville, 1957) and operational techniques that should be used in the model.

An alternative to a completely movable-bed model is the fixed-bed model using relatively small quantities of tracer material to qualitatively indicate shoaling patterns. Such model studies are less expensive to conduct and, depending on the problem studied, may be only slightly less useful than completely movable-bed models. Tracer studies can be particularly well adapted to existing fixed-bed models (perhaps originally constructed for another type of study) where shoaling information is desired.

At the present time, movable-bed scale modeling of coastal sediment transport should be considered an art rather than a science. Although the development of this art is difficult, it can be useful when fully understood and appreciated. Le Mehaute (1962) expresses some interesting and informative thoughts on this subject and Simmons (1950) discusses the contribution of hydraulic models to coastal sedimentation studies. As discussed below in the similitude for movable-bed models, a number of similitude relations have been developed, each containing its own particular assumptions and constraints. The derivation of these scaling relations varies from completely empirical to completely mathematical. Hence, the investigator is immediately at the crossroads, because many choices are available and probably one of several will suffice provided the correct art is applied to model operation. The objective of additional applied research on coastal erosion should not be to develop the artist's techniques but to further the science. Several areas where additional study is necessary are delineated in this section; however, this does not mean that sufficiently accurate model studies cannot now be performed, but rather it indicates that comprehensive planning and serious thought are required to conduct such studies. More importantly, it means that the conduct of this type of model should not be rushed. Adequate time and funds must be allocated to assure that accurate model results are obtained.

2. Similitude Relations.

The similitude relations for movable-bed models are discussed in numerous sources; some of the more detailed discussions include Allen (1947); Sedov (1959); Goddet and Jaffry (1960); Valembois (1960); Langhaar (1962); Bijker (1967), Fan and Le Mehaute (1969); Le Mehaute (1970); Yalin (1962, 1963, 1971); Kamphius (1972); and Noda (1972). Only the main points relative to similitude relations, rather than complete discussions of the subject, are presented in this section. This

discussion of model scales is based on Noda (1972) and Le Mehaute (1970); two tables and a figure taken directly from Noda and Le Mehaute contain their symbols which were not converted to conform with the other sections of this report. (Symbols used only in this section are specifically identified in the Symbols and Definitions of the Appendix.)

The basic philosophy for movable-bed scale-model investigations is founded on the physical laws responsible for the dynamic processes involved and the understanding of these phenomena to ensure that the relative magnitudes of all dominant processes are the same in model and prototype. This is an impossible task for movable-bed scale models, since most of the fluid processes involved are complicated by nonlinear fluid behavior, turbulence, and complex boundary conditions. Thus, the complicated combination of forces that occur in the prototype cannot always be reproduced exactly in the model. In such instances, an attempt is made to reproduce the dominant processes with the anticipation that other forces are small. In attempting to develop similitude relations, the idea of reproducing the dominant physical processes may be abandoned and attention turned to an attempt to maintain similitude of the beach profiles and longshore transport rates.

This section discusses some of the pertinent coastal processes and important parameters in deriving similitude relations. The first of these is the beach profile where considerable effort has been expended in explaining the existence of summer and winter beach profiles. Motion of the water itself is important in determining the beach profile. Sediment characteristics are acutely important in determining the motion induced by wave action. Accurate modeling of cohesive sediments is assumed to be beyond the present state-of-the-art; therefore, attention is focused on noncohesive sediments. A sediment is described by its median diameter, D_{50}, and the specific weight, γ. The relative specific weight γ' of a material is defined by $\gamma' = (\gamma_s - \gamma_f)/\gamma_f$, where γ_s is the specific weight of the sediment and γ_f the specific weight of the fluid. Hydrodynamic properties of the sediment are usually represented by the fall velocity which is related to the drag coefficient, fluid density, particle volume, and projected area of the particle normal to its direction of motion. Initiation of sediment motion is extremely important in modeling sediment transport. For steady-flow conditions, the classical Shields criterion is the required similitude relation; however, it is questionable whether the Shields criterion is valid for initiation of sediment motion in the coastal zone since the processes are much more complicated than that of steady uniform flow.

Four basic parameters must be chosen in the construction of a movable-bed scale-model law: the horizontal scale λ; the vertical scale μ; the sediment size, D_{50} (median diameter); and the specific weight of the sediment γ_s. The functional relationships among these four parameters, which result in identical model and prototype beach profiles, changes in beach profiles, and longshore transport rates for identical spatial and temporal wave and tide conditions, are the desired model laws. Numerous model laws can be postulated from various assumptions regarding the physical processes governing sediment motion.

Possible model laws prepared by Noda (1972) are presented in Table 5-1; several of the possible scale-model laws are derived from various combinations of seven derived similitude conditions.

The table shows several uncertainties. Noda includes a column for assumed conditions to clear up any discrepancies resulting from uncertainties in the basic seven conditions of similitude. An interesting column in Table 5-1 is for $n_\gamma = n_D = n_w = 1$ which gives the scale-model relations when a prototype material is used. Noda uses this table to guide his experimental testing program where he first concludes that condition four is the proper one and then proceeds to derive a completely empirical model law based on similitude of equilibrium beach profiles in the breaker zone. Several proposed model laws are shown in Table 5-2. A considerable number of uncertainties obviously exist relative to the proper similitude laws for movable-bed models. The inherent basic problems are discussed further in Section V,6.

3. Model Design.

a. Prototype Data Required. An important step in conducting a movable-bed scale model of coastal sediment transport is to obtain the essential prototype data, and to assure that the data quality is sufficient for use as a basis of model verification. Data of the quantity and quality considered necessary for exact model verification have never been obtained; however, the acquisition and analysis of such data and the use of the data for model verification are within the present state-of-the-art. Collection of the following prototype data is considered essential:

(1) A detailed sediment-size distribution over the entire area of interest (both offshore, beyond the breaking zone for the largest waves considered important, and alongshore).

(2) A computational estimate of yearly and monthly net longshore transport. Wave statistics should be used to perform this computation along with refraction, shoaling, and breaking criteria. The selection of a suitable formula for the longshore velocity must be largely subjective at the present time, and the use of two or three formulas may be warranted to obtain the best possible selection. These computations serve to (a) illustrate which part of the wave climate is responsible for the majority of the longshore transport (even if the accuracy of the total computation is incorrect, the relative contribution of each component of the wave climate should be approximately correct); (b) indicate the months during which the majority of sediment is transported; (c) indicate the relative importance of the long wave climate (which may be more important on the west coast than the east and gulf coasts); (d) allow an appreciation of the large quantities of material that can be transported in each direction even though the net transport may be quite small; and (e) indicate the relative importance of major storms and

Table 5-1. Possible coastal movable-bed model laws (Noda, 1972).

Case No.	Similitude conditions: Condition 1 $n_F = 1 \therefore n_u = \mu^{1/2}$, $n_T = \mu^{1/2}$, $n_L = \mu$	Condition 2 $n_{F_*} = 1 \therefore n_{\gamma'} n_D = n_{u_*}^2$	Condition 3 $n_{R_*} = 1 \therefore n_{u_*} n_D = 1$	Condition 4 Turbulent flow $n_{u_*} = \mu^{1/2} n_f^{1/2}$	Condition 5 Friction factor $n_f = \frac{\mu}{\lambda}$	Condition 6 $\frac{n_u}{n_w} = \frac{\lambda}{\mu} \therefore n_w = \frac{\mu^{3/2}}{\lambda}$	Condition 7 Stokes velocity $Re \leq 1$ $n_w = n_D^2 n_{\gamma'}$	Assumed condition	Result when $n_{\gamma'} = n_D = 1$, $n_w = 1$	Coastal movable-bed model laws
1	×	×	×	×	×				$\lambda = \mu^2$ $(\mu \propto \lambda^{1/2})$	$n_D = \frac{\lambda^{1/2}}{\mu}$, $n_{\gamma'} = \frac{\mu^3}{\lambda^{3/2}}$, $n_{\gamma'} n_D^3 = 1$, $n_{u_*} = \frac{\mu}{\lambda^{1/2}}$ Proposed by Fan and Le Mehaute (1969)
2	×	×	×	×				$n_f = \frac{\mu^m}{\lambda^n}$	$\lambda = \mu^{\frac{1+m}{n}}$	$n_D = \lambda^{n/2} \mu^{-(1+m)/2}$, $n_{\gamma'} = \mu^{3(1+m)/2\lambda - 3n/2}$ $n_{\gamma'} n_D^3 = 1$, $n_{u_*} = \mu^{(1+m)/2\lambda - n/2}$
3	×	×	×					$n_{u_*} = \mu^{p\lambda - q}$	$\lambda = \mu^{p/q}$	$n_D = \frac{\lambda^q}{\mu^p}$, $n_{\gamma'} = \left(\frac{\mu^p}{\lambda^q}\right)^3$, $n_{\gamma'} n_D^3 = 1$, $n_{u_*} = \frac{\mu^p}{\lambda^q}$
4	×	×		×	×	×	×		$\lambda \equiv 1$, $\mu \equiv 1 \therefore$ using prototype materials, a model is not valid	$n_D = \frac{1}{\mu^{1/2}}$, $n_{\gamma'} = \frac{\mu^{5/2}}{\lambda}$, $n_{u_*} = \frac{\mu}{\lambda^{1/2}}$
5	×	×		×		×	×	$n_f = \frac{\mu^m}{\lambda^n}$	$\lambda = \mu^{3/2}$ $m = 1$ $n = 2$	$n_D = \frac{\lambda}{\mu^{1/2}}$, $n_{\gamma'} = \frac{\mu^{5/2}}{\lambda^3}$, $n_f = \frac{\mu}{\lambda^2}$, $n_{\gamma'} n_D^3 = \mu$, $n_{u_*} = \frac{\mu^{3/2}}{\lambda}$
6	×	×				×	×	$n_{u_*} = \frac{\mu^p}{\lambda^q}$	$\lambda = \mu^{3/2}$ $p = 3$ $q = 2$	$n_D = \lambda^3 \mu^{-9/2}$, $n_{\gamma'} = \mu^{21/2\lambda - 7}$, $n_{\gamma'} n_D^{7/3} = 1$, $n_{u_*} = \frac{\mu^3}{\lambda^2}$, $\lambda = n_D^{1/3} \mu^{3/2}$
7	×	×	×			×	×		$\lambda = \mu^{3/2}$	$n_D = \frac{\lambda}{\mu^{3/2}}$, $n_{\gamma'} = \frac{\mu^{9/2}}{\lambda^3}$, $n_{u_*} = \frac{\mu^{3/2}}{\lambda}$, $n_{\gamma'} n_D^3 = 1$
8	×	×	×	×		×	×		$\lambda = \mu^{3/2}$	$n_D = \frac{\lambda}{\mu^{3/2}}$, $n_{\gamma'} = \frac{\mu^{9/2}}{\lambda^3}$, $n_{\gamma'} n_D^3 = 1$, $n_{u_*} = \frac{\mu^{3/2}}{\lambda}$, $n_f = \left(\frac{\mu}{\lambda}\right)^2$

Table 5-2. Comparison of various approaches for determination of basic scale ratios of a coastal movable-bed model.

Source	Basic relations	Method of derivation
Goddet and Jaffry (1960)	$n_D = \mu^{17/20}\Omega^{8/5}$ $n_{\gamma'} = \mu^{3/20}\Omega^{-3/5}$	Sediment motion due to combined action of waves and currents
Valembois (1960)	$\Omega = n_{\gamma'}^{-1}$ $n_{\gamma'}n_D^3 = 1$ $\mu = n_{\gamma'}^3 n_D\left(\frac{n_H}{\mu}\right)^4$	Kinematics of motion of suspended sediments Similitude of D_* Modified relation of initiation of sediment motion: $D_* = KR_*^{8/9}$
Yalin (1963)	$n_D = \mu^{3/4}\lambda^{1/2}$ $n_{\gamma'}n_D^3 = 1$	Dimensional analysis
Bijker (1967)	$n_{\gamma'}n_D\Omega^{-1} = \mu n_{\mu r}$ $\Omega \leftarrow$ equilibrium beach profiles	Similitude of F_* SEE NOTE:
Fan and Le Mehaute (1969)	$n_{\gamma'}n_D^3 = 1$ $n_{\gamma'} = \mu^3\lambda^{-3/2}$ or $n_D = \lambda^{1/2}\mu^{-1}$ $\Omega \leftarrow$ equilibrium beach profiles	Similitude of sediment transport characteristics, i.e., F_* and R_*
Noda (1971)	$n_D n_{\gamma'}^{1.84} = \mu^{0.55}$ $\lambda = \mu^{1.32}n_{\gamma'}^{-0.386}$ $\Omega \leftarrow$ equilibrium beach profiles	Similitude of sediment transport characteristics; i.e., F_* and R_*

Note: Although this basic relation was noted to be in error, it was not corrected.

hurricanes. Under certain circumstances, the major shoreline evolution is likely the result of infrequent but disastrous events such as hurricanes.

(3) All available survey data (profiles) and aerial photos of the shoreline to help understand the existing problems, or to anticipate the problems in construction of a proposed structure or topographic modification.

(4) Accurate simultaneous measurements of the wave environment and sediment transport (both onshore-offshore and alongshore). These measurements are the integral parts of the data necessary for model verification. Measurements of the accuracy and extent desirable for model verification have never been obtained; however, it is realistic to obtain such data. The length of time of the measurements must extend over an erosion and accretion period and hopefully over a period of both high and low littoral transport. Thus, the longshore transport computation described is also used to select the optimum time of year for the prototype data acquisition effort to have the desired erosion and accretion periods occur within the shortest possible time interval. A reasonable estimate of the time required for acquisition of the desired data is 1 to 3 months. The wave measurements must be accurate and must include the directional spectrum. Although both the planning and analysis are difficult, it is definitely within present capabilities. One reason that past attempts at measuring the directional spectrum have been of limited success is the lack of sufficient redundancy in the number of wave sensors to validate the statistics and to prevent the results from becoming questionable when one or two sensors develop problems. These measurements should be made just outside the breaking zone for the largest waves anticipated. A system similar, or one identical to that used by the U.S. Army Engineer Waterways Experiment Station (WES) in the Los Angeles-Long Beach Harbors study (Pickett, Durham, and McAnally, 1975) is recommended. The WES system consisted of pressure transducers with ranges of 25 and 50 pounds per square inch, and with a very accurate response. A minimum of problems occurred during a year's use, and all data were recorded in digital form on magnetic tape. One tape contained approximately 5 days of data for 15 sensors at a sample rate of one sample per second. The sample rate was flexible and could either be increased or decreased as the situation required. Careful planning of the sensor spacing is required to ensure both the desired accuracy and resolution; measurement of atmospheric pressure is also required. All data should be analyzed during periods of rapid erosion, accretion, and littoral transport. Segments of data should be analyzed at least every 6 hours during the entire test program. These data would be used for input to the wave generator during model verification. In addition to the wave sensor data, photos should be taken periodically each day to show the wave breaking angle and

location (used as backup data to determine whether the analysis techniques are yielding the desired results). Note that the measurement system recommended includes the measuring of tidal heights. Since the sensors do not filter, all filtering is accomplished analytically during the data analysis.

The measurement of sediment transport, onshore-offshore and alongshore, is probably the most difficult problem in obtaining adequate prototype data required for model verification. Although the accuracy of sediment transport measurements (or the most practical way to make them), is difficult to determine, a carefully planned measurement program is considered to result in sufficient accuracy for model verification. Some type of tracer measurement will probably yield the best data; however, the program must be more extensive than any conducted to date. Profiling of the beach and offshore area beyond the breaker zone is required at as close an interval as possible (once a day is desirable). The planning of a detailed sediment transport measurement program is difficult, and the best method is not as obvious as in the case of wave measurements. However, rapid advances are being made in the area of oceanographic and estuarine surveying and mapping.

b. Selection of Model Scales and Materials. As discussed previously, the complete similitude of all dynamic processes involved in the movement of coastal sediment is impractical. The modeling of cohesive bottom sediments is not discussed in this section because it is considered beyond the present state-of-the-art. Modeling of the motion of noncohesive sediments (sands and cobbles) presents a formidable task in itself. As shown previously, similitude of certain dynamic processes fixes the relation between model and prototype linear dimensions, material characteristics, and other factors. Therefore, no particular set of scale-model laws for coastal sediment models is recommended at the present time. Each of the scale-model laws in Table 5-1 is believed to have its own special area of application, and the selection of the appropriate set of equations (model laws) for a particular problem largely depends on the experience and expertise gained by a particular group of laboratory personnel in performing movable-bed scale-model tests.

In arriving at a set of scale-model laws to be applied for a given problem at a specific location, the following items must be analyzed:

(1) Existing prototype wave environment.. This includes monthly wave statistics (numerical wave hindcasts are preferable), the incidence of severe storms on the west coast of the United States and the Great Lakes, and the incidence of hurricanes on the east and gulf coasts of the United States.

(2) Computation of the prototype longshore transport (possibly using several different approaches).

(3) Size of the prototype area to be studied.

(4) Type and size distribution of prototype bottom material.

(5) Size and capabilities of model test facilities.

(6) Model test materials either available or readily procured.

(7) Accuracy to which model test results are desired.

(8) Funds available to conduct the study.

(9) Time available to conduct the study.

(10) Qualified personnel available for assignment to the study.

The above items are not necessarily compatible; i.e., funds or time available to conduct the study may not be commensurate with the desired accuracy of the experimental results. However, after full consideration of the above items, a set of wave-flume experiments is recommended before final selection of the scale-model laws. These tests would be two-dimensional beach profile tests where it would be attempted to reproduce the dominant existing beach characteristics (relative to onshore-offshore transport) using several different scaling relations and beach materials. After a particular set of scale-model laws (and consequently linear scales and bottom material) is selected, it is recommended that the same law be applied using a larger model (and consequently a different model material) and that wave-flume tests be conducted to ensure reproducibility of results and establish confidence in the selected scaling relations (at least for onshore-offshore transport).

At this point in the investigation, a set of scaling relations has been tentatively selected and the recommended prototype data have been obtained (to the best possible extent). A bottom material and tentative model scales (for the three-dimensional, movable-bed model) have also been selected. Before proceeding further, one more step in assuring the accuracy of model results is necessary. An average bottom profile should be used to construct a test section of straight parallel bottom contours. Tests should be conducted with waves at an angle to this test section and measurements made of the longshore transport and the evolution of the model bottom topography. Model test results should then be compared with either those predicted or those measured during the prototype data acquisition phase of the study. After confirmation of the longshore transport, the investigator is ready to proceed to the model operation phase of the study and in particular to model verification.

4. Model Operation.

a. Verification of the Model. The first and most important step in conducting a quantitative, movable-bed scale-model investigation of coastal erosion or coastal sediment transport is model verification.

Enough data should be obtained during prototype data acquisition to verify that the hydraulic model accurately reproduces the prototype features of interest. Thus, it is essential that the prototype data of bottom evolution (erosion, accretion, and littoral transport) are accurate and that the corresponding incident wave conditions (height, period, and direction) are known.

Initial verification efforts should be directed toward reproducing the most severe short-term prototype erosion. Hopefully, this would comprise a storm period of perhaps 1 to 2 days where the wave direction remained relatively constant and only a slow variation in height and period occurred. If adequate prototype data were acquired on the erosion rate and littoral transport rates, then attempts can be made to verify the short-term erosion properties of the hydraulic model. However, numerous problems will arise and the sensitivity of the erosion response of the model must be correlated with changes in incident wave characteristics (height, period, and direction). The model response must not vary significantly within the accuracy of prototype measurements of wave height and bottom evolution. If significant model variations are recorded within the accuracy of the verification data, then either the prototype data quality must be improved or the model is too sensitive, and different scales and model materials are probably required.

After verification of short-term, large-scale erosion characteristics, verification of shoreline accretion is necessary. This is usually a longer term process and may be interrupted by changes in wave direction and possibly by either small or large storms causing additional erosion. An effort should be made to precisely reproduce the prototype wave and tide characteristics during this period. Successful verification of the accretion phase of the prototype measurement period is a major step. Littoral transports are also measured and correlated with the prototype data taken during these periods.

The next phase of the model verification is to ascertain if correct littoral transport rates are occurring. There will be some periods during the prototype data acquisition phase where waves are at an extreme angle to the shoreline. If the wave heights are significant, then a rapid longshore transport of material will take place.

Finally, verification of the prototype beach behavior for the entire measurement period should be attempted. If this is accomplished, the investigator can then be confident of the hydraulic model results.

Although this brief discussion of model verification does not include the numerous problems involved, it is considered adequate for the present state-of-the-art.

b. Operational Constraints of the Model. Any scale-model investigation has its limitations and operational problems; however, a completely movable-bed scale-model study contains more than its share of operational problems. Some of these problems and constraints are:

(1) Model Boundaries. Any model must have some artificial boundaries; however, this presents several problems in a movable-bed model. Sediment must be injected artificially at the proper rate and at the proper location (relative to the shoreline) along one lateral boundary and the sediment must be removed at the other boundary. The other alternative (usually impractical) is to make the model area large enough to study the area of interest before the model walls introduce any undesirable model effects. Lateral model boundaries are also responsible for introducing a model circulation (due to interruption of the longshore current and transport). This circulation can be compensated for by providing sufficiently effective energy absorbers at the model boundaries or perhaps by allowing a return channel for water to flow from one model boundary to the other. Injecting and removing water at the model boundaries through the application of a type of manifold system has been postulated by some investigators as a method of solving this problem; however, the method usually introduces more problems than it solves.

The seaward boundary of the model may also provide a possible source of undesirable model effects. If the wave generator produces a wave behind it, this energy must be effectively absorbed. If there is a nonnegligible reflection coefficient from the model beach and underwater topography, then rereflection of this energy by the wave generator must be avoided. In most cases this can be accomplished by using wave filters in front of the wave generator.

Since the linear scales of the model will be distorted, reflection coefficients from the shoreline will be exaggerated. The grain size of the model material will also be too large, and the permeability of the model sediment is expected to be too large. Thus, the model bed will dissipate too much wave energy. Therefore, these two scale effects tend to compensate each other.

Another possible model boundary effect is the reinforcement of model edge waves due to the lateral boundaries. Edge wave reinforcement tends to increase model rip currents. The effect of linear-scale distortion on rip currents should be further investigated, as well as the effects of artificial bottom material on rip current velocities.

(2) Wave Generator Characteristics. In practice, all wave generators have certain inherent limitations. Waves can be generated over a definite range in wave periods without gear changes or modifications, and there is a finite limit to a generator stroke, which limits the wave height that can be generated. Wave generators designed to produce monochromatic waves usually tend to generate more energy at harmonics of the fundamental frequency as the stroke increases. Spectral wave generators have the same

limitations in addition to other problems which deal only with the generation of spectral waves; however, they are more difficult to define.

(3) Remolding of bottom topography. After completion of a test, one operational constraint is remolding of the bottom topography. Since the topography may have changed, the entire model area must be checked and remolded. During testing, segregation by size frequently occurs if the model material is not uniformly sized, necessitating remixing before remolding.

c. Selection of Test Conditions. Selection of test conditions is a relatively straightforward procedure. The first task is to obtain wave hindcast data for the area of interest. Secondly, the littoral transport rates should be computed for each segment of the wave climate. These computations are not expected to be extremely accurate, but they should yield an accurate picture of the relative importance of each part of the wave climate concerning the transport of bed material. The above data, along with those analyzed during the prototype data acquisition study, should be adequate to allow an intelligent selection of test conditions. The normal wave climate should be tested with particular emphasis on each segment which produces a significant contribution to the yearly transport rates in each direction.

Depending on the prototype data acquired, it may be necessary to either produce a wave spectrum in the model or to generate monochromatic waves from more than one direction.

d. Model Measurements. The primary model process of interest is bottom evolution as a function of incident wave conditions, tide level, and duration of wave conditions. Therefore, measurement of erosion and accretion rates, bottom profiles, and longshore transport rates are desirable. Accurate measurements of incident wave heights and tidal heights (especially during model verification) are necessary. Model measurements of wave heights and currents in shallow water and inside the surf zone may also be necessary.

Profiling of the model topography is extremely important and tedious if not performed automatically. Several devices (acoustic and laser) are well suited for this task. All data should be recorded on magnetic tape for automatic data processing.

Model measurements of onshore-offshore and littoral transport are certainly as difficult as they are in the prototype. Either fluorescent or radioactive tracers could be used satisfactorily in conjunction with an automatic counter operating in much the same manner as the profiler. If a device of this nature does not prove feasible, model sediment traps may have to be devised. An excellent measure of the total longshore transport rate can be ascertained from the amount of sand injected at one boundary and then removed at the other boundary after equilibrium conditions are established.

e. Analysis and Interpretation of Results. Although many questions remain unanswered relative to the conduct of satisfactory movable-bed scale models of coastal sediment transport, such investigations are considered feasible. The degree of confidence for such studies is largely dependent, for each individual case, on the success of the prototype data acquisition program, flume tests required for scale selection, and the model verification phase.

5. Fixed-Bed Tracer Models.

Fixed-bed hydraulic models have long been recognized as an extremely valuable tool in studying the effects of coastal construction projects on wave, tide, and current conditions. In recent years, the use of relatively small quantities of sediment tracer material in fixed-bed models has generally been accepted as the most reliable and least expensive method of studying sediment transport due to wave and tidal action. In practically all cases, the results of such studies are considered qualitative rather than quantitative.

In general, movable-bed model laws require distorted scales unless the sediment in the model is the same as in the prototype (i.e., sand). However, these laws can be adapted to undistorted-scale fixed-bed models for the selection of tracer materials, and the scaling relations of Noda (1972) are used as an example.

Noda indicates a relationship or model law among the four basic scale ratios: the horizontal scale, λ; the vertical scale, μ; the sediment-size ratio, n_D; and the relative specific weight ratio, n_γ, (see Fig. 5-1). These relationships were determined experimentally from a wide range of wave conditions and beach materials and are valid mainly for the breaker zone. Therefore, if there is an interest in longshore and onshore-offshore sediment transport (which occurs mostly in and around the breaker zone), this appears to be a most appropriate scale relation.

Tracer material is selected for undistorted-scale models by the following procedure. Using the characteristics of the prototype sediment (grain-size distribution, specific weight, etc.), the vertical model scale is assumed correct and, for a specified material, the median grain size and horizontal scale are computed. Next, the horizontal scale is assumed correct and, for the same material, the median grain size and vertical scale are computed. This procedure is repeated for several materials and results in a range of median grain sizes for each material. Preliminary model tests are conducted with the different sizes and based on these test results, judgment, past experience, and knowledge of sediment movement in the prototype, the most realistic tracer material is selected (i.e., the engineer is practicing art rather than science). This procedure has proven effective in evaluating the movement and subsequent deposits of sediment in several three-dimensional models at WES; typical case histories are described below.

Examples of Model Studies Conducted.

(1) Port Orford Harbor, Oregon.

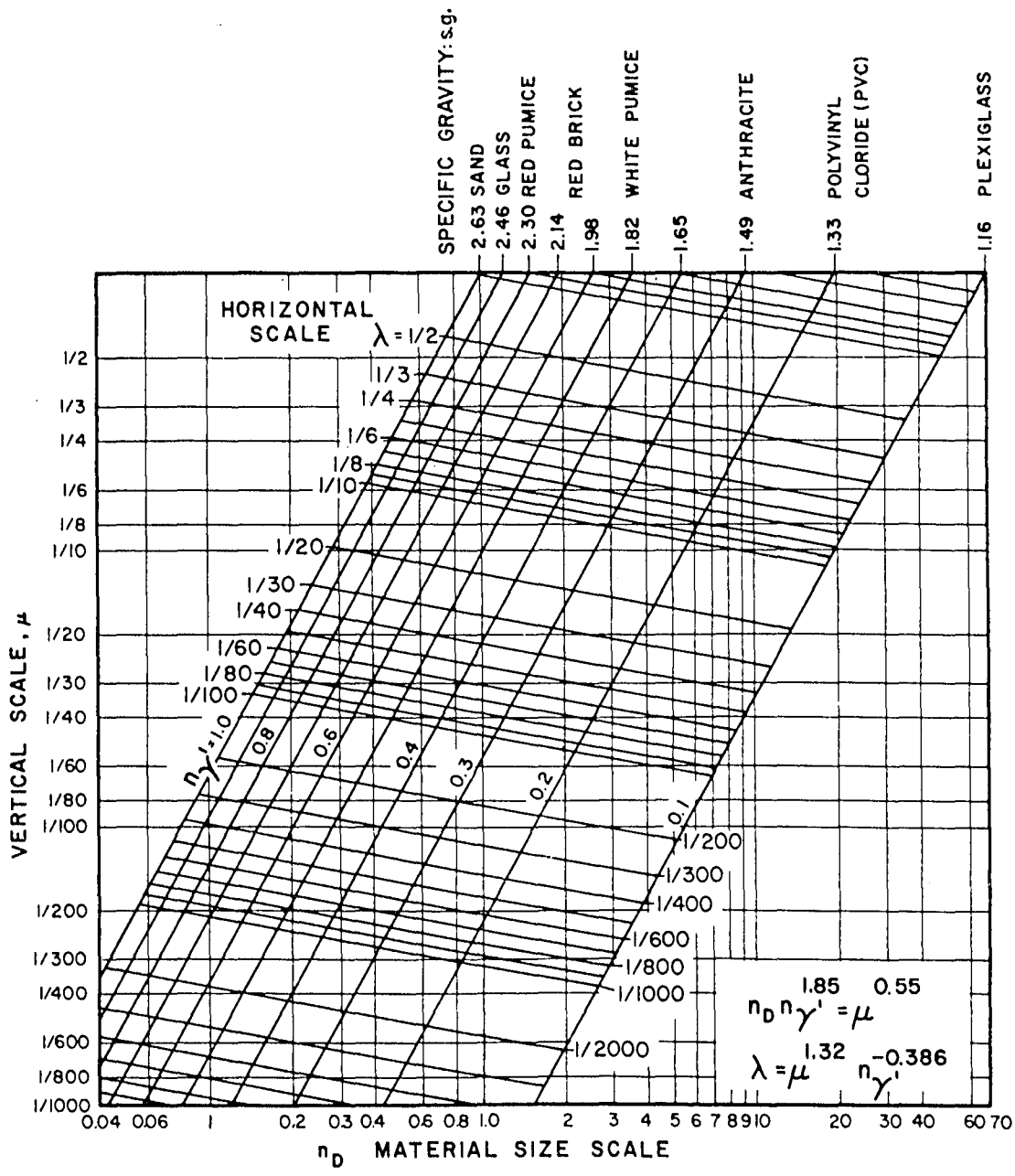

Figure 5-1. Graphic representation of model law (Noda 1972).

(a) Project. Breakwaters for wave protection and prevention of shoaling.

(b) Reference. Giles and Chatham (1974).

(c) Laboratory. WES.

(d) Test Period. July 1972 to October 1973.

(e) Problem. Severe shoaling of Port Orford Harbor began shortly after construction of a 600-foot-long breakwater in 1968. This breakwater (built to provide wave protection for the existing pier) intercepts and traps the south-to-north littoral transport when waves are from the south and alters current patterns when waves are from the north so that the north-to-south littoral currents cannot move sediment out of the harbor. Extensive maintenance dredging has been required.

(f) Purpose of Model Study. The model study was conducted to (a) compare prebreakwater and existing breakwater conditions to determine the causes and sources of harbor shoaling, and (b) develop cost-effective remedial plans to eliminate shoaling at the pier without significantly increasing wave action.

(g) The Model. The undistorted, 1:100-scale hydraulic model reproduced the entire harbor area, approximately 3 miles of shoreline, and underwater contours to an offshore depth of -60 feet (Fig. 5-2). The total area reproduced in the model was approximately 10,300 square feet, representing about 3.7 square miles in nature.

(h) Test Procedures. Tests consisted of measuring wave heights and wave-generated currents, obtaining photos of wave, current, and shoaling patterns, and visual observations. Using the procedures discussed previously for the scaling relations of Noda (1972), crushed coal (median diameter, 0.55 millimeter; specific gravity, 1.30) and nylon (median diameter, 3.0 millimeters; specific gravity, 1.14) were selected as tracer materials to simulate the prototype sand (median diameter, 0.21 millimeter; specific gravity, 2.65).

(i) Plans Tested. Initial tests were conducted for prebreakwater and existing breakwater conditions to determine the causes and sources of harbor shoaling. Improvement plans consisted of modifications to the existing breakwater (removing sections, lengthening, realinement, etc.) and installation of new breakwaters near Fort Point and Battle Rock.

(j) Summary of Test Results. Test results indicated that (a) the source of sediment was the area seaward and to the east of Battle Rock; (b) the modification of the existing breakwater was not a viable alternative; and (c) a new 1,100-foot-long breakwater extending from Fort Point would be required to completely prevent harbor shoaling. Shoaling patterns for existing conditions and the recommended plan are shown in Figures 5-3 and 5-4.

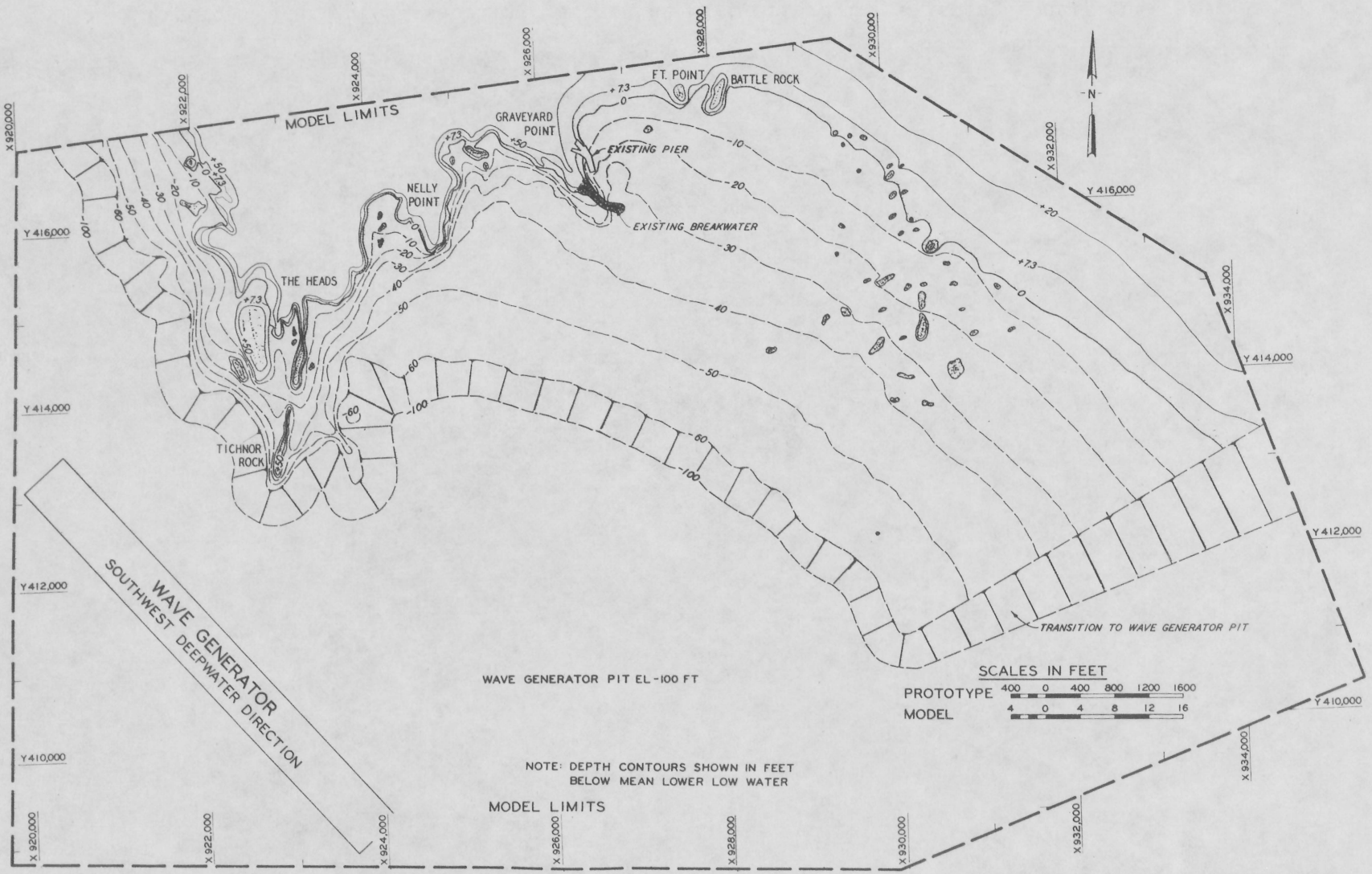

Figure 5-2. Port Orford Harbor, Oregon, model layout.

Figure 5-3. Typical shoaling pattern at Port Orford for existing conditions.

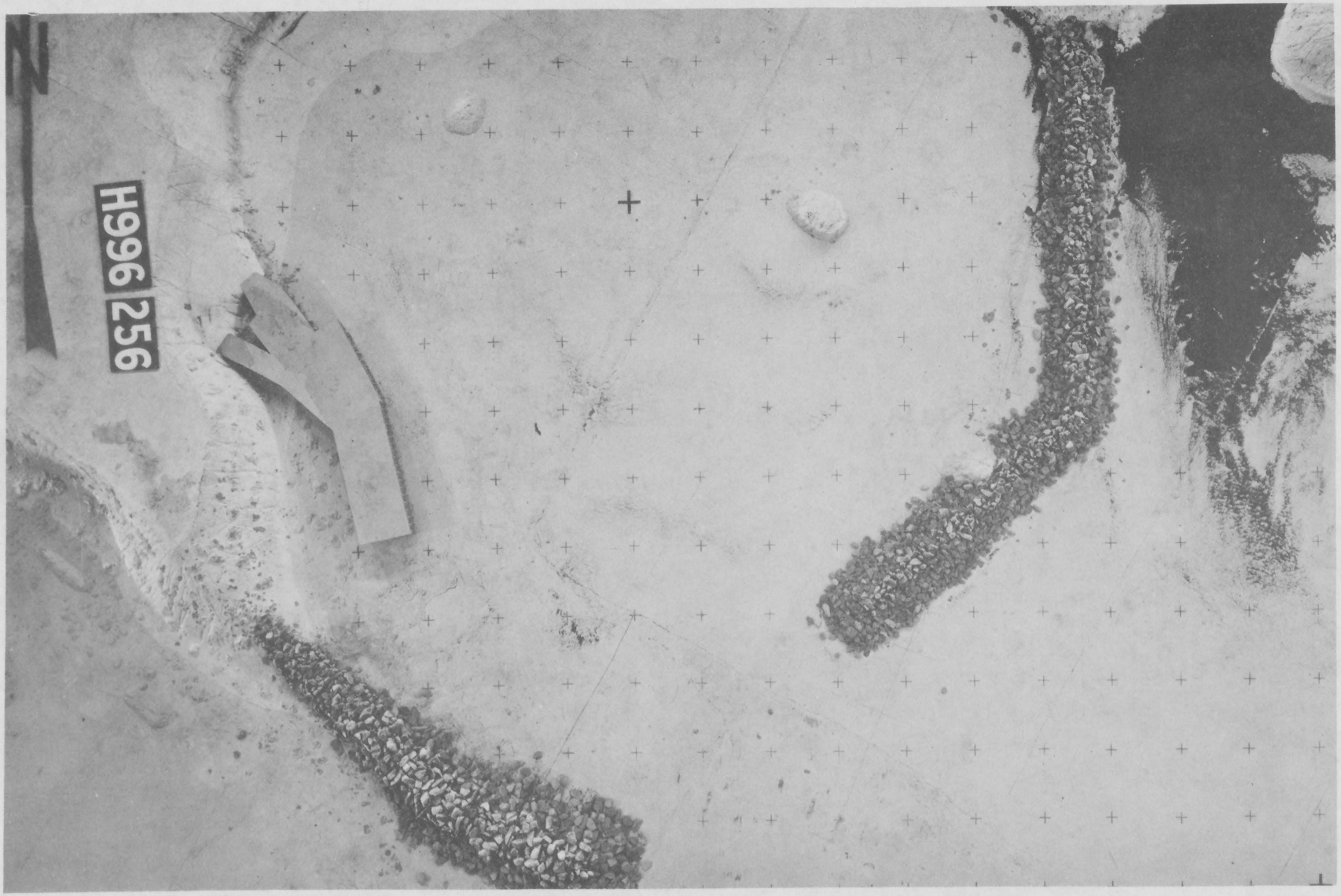

Figure 5-4. Typical shoaling pattern at Port Orford for recommended plan of improvement.

(2) Cattaraugus Creek Harbor, New York.

(a) Project. Jetties for wave protection, passage of floodflows and ice, and prevention of shoaling.

(b) Reference. Bottin and Chatham (1975).

(c) Laboratory. WES.

(d) Test Period. May 1974 to April 1975.

(e) Problem. Stream discharges on Cattaraugus Creek move sediment (sand and gravel) downstream where it is deposited on a delta at the creek mouth. Wave action from Lake Erie rearranges this material to form a bar across the creek mouth. This bar restricts navigation and provides a natural barrier, resulting in the formation of ice jams and flooding of the low-lying surrounding area.

(f) Purpose of Model Study. The model study was conducted to develop the most cost-effective jetty arrangement at the creek mouth which would prevent shoaling, provide wave protection, and allow the passage of floodflows and ice.

(g) The Model. The undistorted, 1:75-scale hydraulic model reproduced the lower 5,400 feet of the creek channel and underwater contours in Lake Erie to offshore depths ranging from -38 feet on the north to -18 feet on the south (Fig. 5-5). The total area reproduced in the model was approximately 16,380 square feet, representing about 3.3 square miles in the prototype.

(h) Test Procedures. Tests consisted of measuring wave heights, wave- and stream-generated currents, and water surface profiles for various stream discharges; obtaining photos of wave, current, and shoaling patterns; and qualitative investigations of ice-jamming tendencies using a low-density polyethylene material to simulate ice fragments. Using the procedures discussed previously for the scaling relations of Noda (1972), crushed coal and granulated nylon were selected as tracer materials to simulate the prototype sand (median diameter, 0.25 millimeter; specific gravity, 2.65). Initial model tests indicated that relative deposits for these two materials were almost identical. The main difference was that the larger nylon particles were more sensitive to wave action and, in general, did not deposit on the beach or form bars as readily as coal. Considering the behavior of the two materials and field observations of shoaling at the existing harbor, it was decided that the crushed coal more reliably reproduced the prototype shoaling patterns and coal was used for all subsequent tests.

(i) Plans Tested. Tests were conducted for one jetty arrangement with the entrance oriented to the southwest and for several modifications of length, orientation, type (sheet pile or rubble mound), etc. of a jetty arrangement with the entrance oriented to the north.

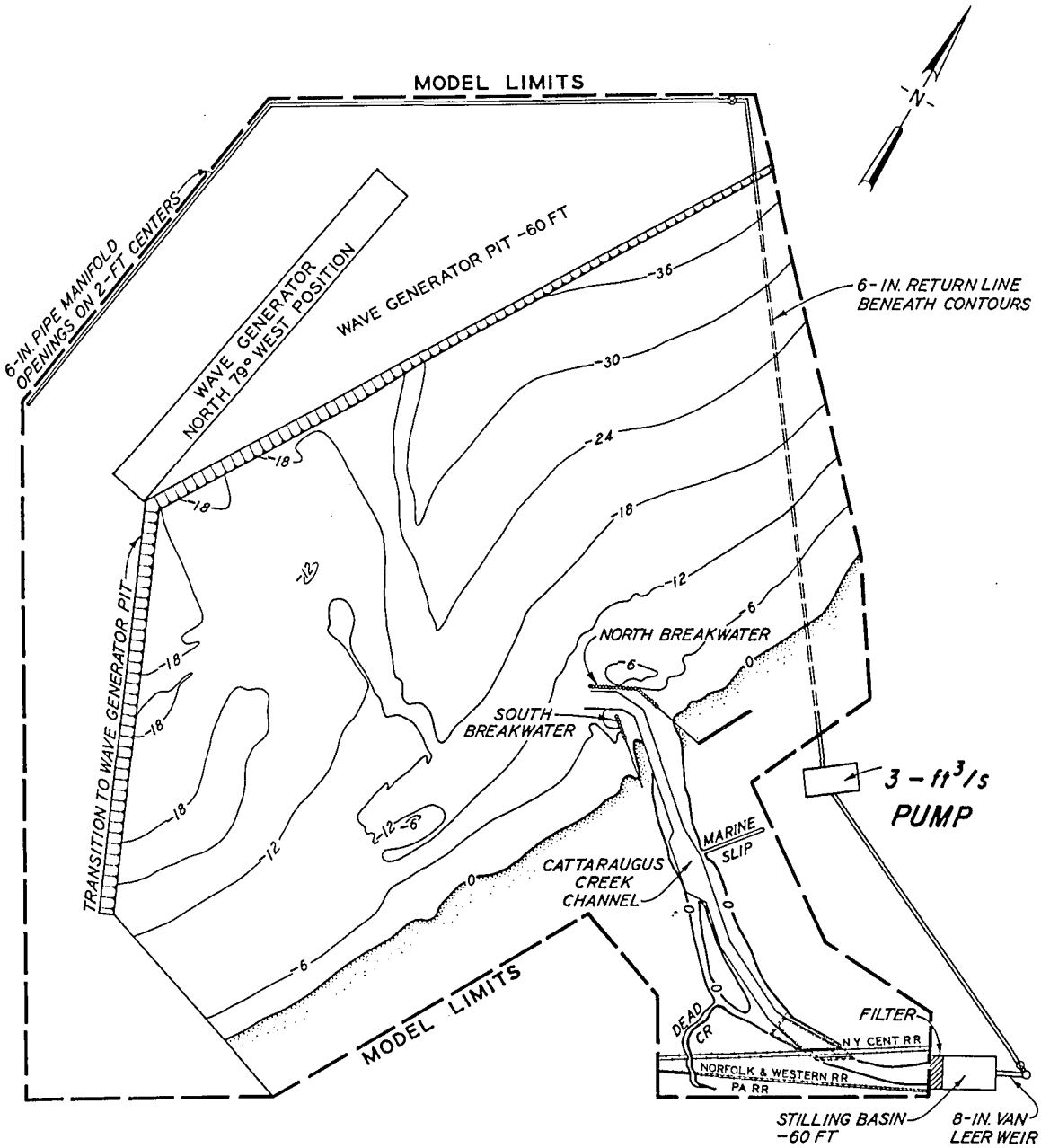

NOTE: CONTOURS AND ELEVATIONS SHOWN IN FEET REFERRED TO LOW WATER DATUM(LWD) ELEVATION 568.6 FEET ABOVE MEAN WATER LEVEL AT FATHER POINT, QUEBEC (IGLD 1955)

SCALES IN FEET

PROTOTYPE 375 0 375 750 1125 1200 1575

MODEL 5 0 5 10 15 20 25

Figure 5-5. Cattaraugus Creek Harbor, New York, model layout.

(j) Summary of Test Results. The model accurately reproduced existing shoaling patterns (i.e., a bar across the entrance) as shown in Figure 5-6. The originally proposed jetty arrangement with the entrance oriented to the southwest resulted in shoaling in the harbor entrance. The best jetty configuration tested (shown in Fig. 5-7) prevented shoaling, provided adequate wave protection, and allowed the passage of floodflows and ice.

6. Recommendations for Further Research.

Considerable work is obviously required before the design and operation of quantitative movable-bed scale-model investigations of coastal sediment transport become routine. However, considerable optimism regarding the success of such an endeavor is apparently justified. Because of the pressing national need for shoreline protection and preservation, as well as the need to acquire a reliable assessment of the effects of coastal and offshore construction (such as deepwater superports, offshore airports, or offshore nuclear powerplants) on shoreline evolution, it is imperative that satisfactory accuracy in modeling capability be developed to the fullest extent possible. A few specific areas requiring further research are:

(a) Determine the effect of model sediment-size distribution on equilibrium beach profiles and longshore sediment transport. Since the median diameter of model sediments is important, the immediate questions are whether the model sediment can be of uniform size, must the sediment have precisely the same particle-size distribution as the prototype, or is some scaling relation required other than merely that involving the mean particle diameter.

(b) Perform a comprehensive and thorough experimental and analytical investigation of the scale-model laws proposed by Noda (1972). These laws show promise in some areas but are lacking in others; however, the approach appears to have merit and should be pursued further.

(c) Perform additional experimental and analytical tests (after completion of (a) and (b) above) to derive a recommended scale-model law based on similitude of equilibrium beach profiles and, if possible, on longshore transport rates.

(d) Perform the required prototype data acquisition and analysis effort for a suitable site.

(e) Attempt to verify the laws developed in (c) above with the data obtained in (d).

(f) Investigate the effects of model linear-scale distortion and bottom material on edge wave development and rip current intensity, and attempt to ascertain when (if at all) their reproduction in the model is necessary.

Figure 5-6. Typical shoaling pattern at Cattaraugus Creek for existing conditions.

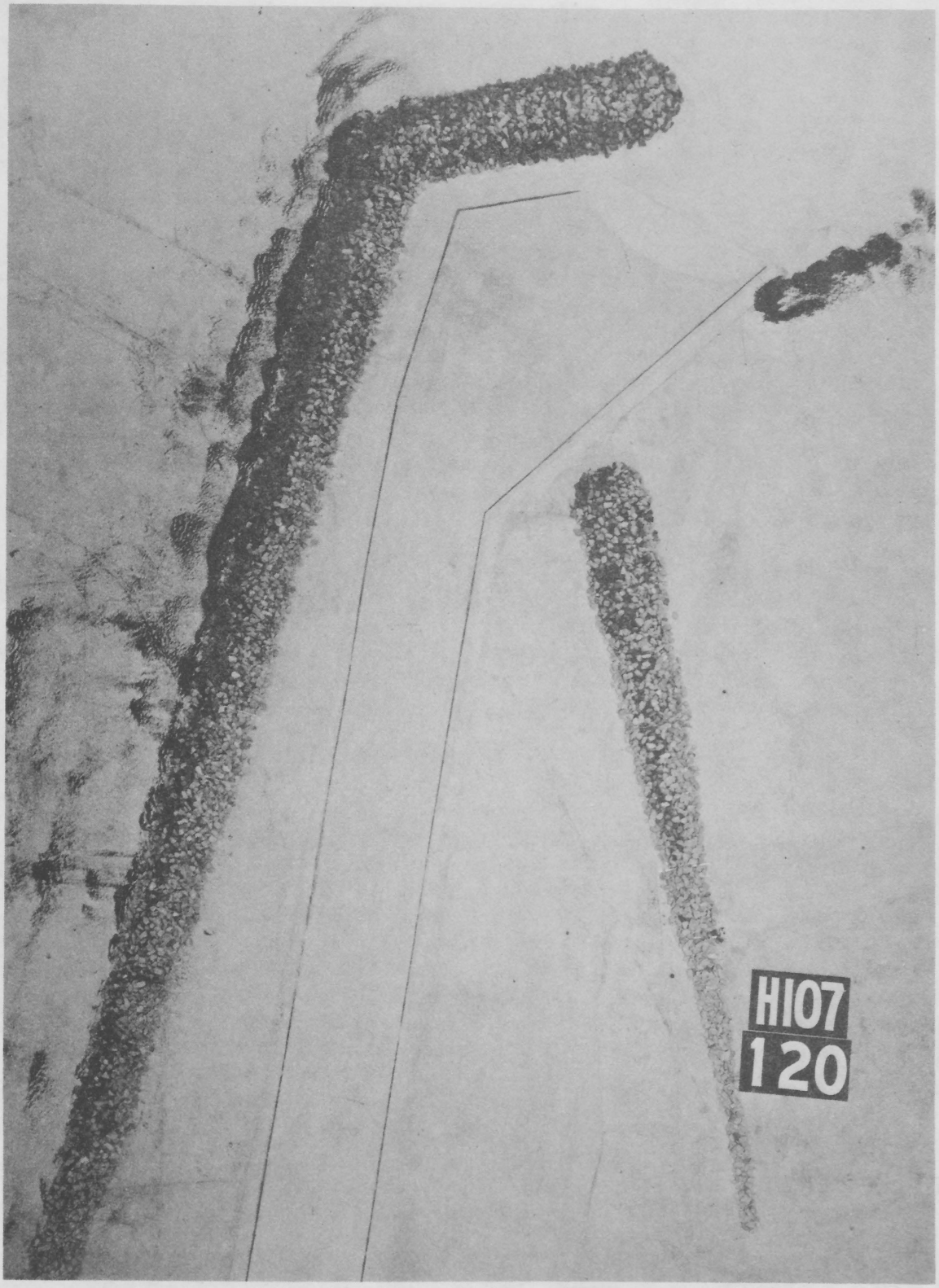

Figure 5-7. Typical shoaling pattern at Cattaraugus Creek for recommended plan of improvement.

(g) Investigate the model effects of using monochromatic waves or a wave spectrum to obtain equilibrium beach profiles and longshore transport rates.

(h) Evaluate the importance of the long-wave components of the spectrum in the transport of bottom sediment.

(i) Complete a comprehensive three-dimensional, movable-bed scale-model study based on the research areas above. Hopefully, this will establish the necessary scale-model laws, confidence in scale-model results, and procedures for subsequent efforts.

(j) Conduct a postconstruction verification study of the scale-model results. This requires extensive prototype measurements, and perhaps fairly extensive additional scale-model tests.

7. Summary.

Movable-bed scale-model investigations of coastal erosion and coastal sediment transport phenomena are probably the most difficult hydraulic models to conduct. However, such model studies are feasible in certain circumstances; careful planning is required, and the acquisition of extensive and accurate prototype data is necessary. Numerous scale-model laws can be derived by making various assumptions regarding the physical processes governing sediment motion.

The most important phase in this type of scale-model study is to obtain the quantity and quality of prototype data required for model verification. Some of the many problems that must be dealt with in model operation are model circulation, type of bottom sediment, model size, and rapid measurements and remolding of bottom topography. Although nearly quantitative movable-bed scale-model investigations of some coastal erosion and coastal sediment transport problems are considered feasible, a considerable amount of additional applied research is necessary before such studies become routine.

LITERATURE CITED

ALLEN, J., *Scale Models in Hydraulic Engineering*, Longmans, Green and Co., London, 1947.

BAGNOLD, R.A., "Beach Formation by Waves; Some Model Experiments in a Wave Tank," *Journal of the Institution of Civil Engineers*, Vol. 15, Nov. 1940, pp. 27-52.

BAGNOLD, R.A., "Sand Movement by Waves--Some Small Scale Experiments with Sand of Very Low Density," *Journal of the Institution of Civil Engineers*, Vol. 27, No. 4, Feb. 1947, pp. 447-469.

BASCOM, W.N., "The Relationship Between Sand Size and Beach-Face Slope," *Transactions of the American Geophysical Union*, American Geophysical Union, Vol. 32, 1951, pp. 866-874.

BEACH EROSION BOARD, "Coast Erosion and the Development of Beach Profiles," TM-44, U.S. Army, Corps of Engineers, Washington, D.C., June 1954.

BIJKER, E.W., "Some Considerations about Scales for Coastal Models with Movable Bed," No. 50, Delft Hydrographic Laboratories, Delft, The Netherlands, Nov. 1967.

BIJKER, E.W., and SVASEK, J.N., "Two Methods for Determination of Morphological Changes Induced by Coastal Structures," *Proceedings of the 22d International Navigation Congress*, Permanent International Association Navigation Congress, Vol. 2, 1969, pp. 181-202.

BIJKER, E.W., STAPEL, D.R.A., and DE VRIES, M., "Some Scale Effects in Models with Bed Load Transportation," *Proceedings of the Seventh Congress of International Association for Hydraulic Research*, Vol. 1, 1957, pp. A1-1--A1-16.

BONNEFILLE, R., and PERNECKER, L., "Etude Bibliographique et Experimentale Sur Le Charriage Des Sediments Par La Houle," National Hydraulic Laboratories, Chatou Research and Experiment Center, France, 1965., 67 pp.

BOTTIN, R.R., Jr., and CHATHAM, C.E., Jr., "Design for Wave Protection, Flood Control, and Prevention of Shoaling, Cattaraugus Creek Harbor, New York; Hydraulic Model Investigation," Technical Report H-75-18, U.S. Army Engineer Waterways Experiment Station, Vicksburg, Miss., Nov. 1975.

BROWN, C., "Sediment Transportation," Ch. XII, *Engineering Hydraulics*, H. Rouse, ed., 1950.

CALDWELL, J.M., "Coastal Processes and Beach Erosion," *Journal of the Boston Society of Civil Engineers*, Vol. 53, No. 2, Apr. 1966, pp.142-157.

CHATHAM, C.E., "Movable-Bed Model Studies of Perched Beach Concept," *Proceedings of the 13th International Conference on Coastal Engineering*, American Society of Civil Engineers, Vol. 2, 1972, pp. 1197-1216.

CHATHAM, C.E., DAVIDSON, D.D., and WHALIN, R.W., "Study of Beach Widening by the Perched Beach Concept, Santa Monica Bay, California, Hydraulic Model Investigation," Technical Report H-73-8, U.S. Army Engineer Waterways Experiment Station, Vicksburg, Miss., June 1973.

COLLINS, J.I., "Inception of Turbulence at the Bed Under Periodic Gravity Waves," *Journal of Geophysical Research*, Vol. 68, No. 21, Nov. 1963, pp. 6007-6014.

DIEPHUIS, J.G.H.R., "Scale Effects Involving the Breaking of Waves," *Proceedings of the Sixth Conference on Coastal Engineering*, American Society of Civil Engineers, Vol. 1, Dec. 1957, pp. 194-201.

EAGLESON, P.S., "The Mechanics of the Motion of Discrete Spherical Bottom Sediment Particles Due to Shoaling Waves," TM-104, U.S. Army, Corps of Engineers, Beach Erosion Board, Washington, D.C., 1957.

EAGLESON, P.S., "Growth of Longshore Currents Downstream of a Surf Zone Barrier," *Proceedings of a Specialty Conference on Coastal Engineering in Santa Barbara*, American Society of Civil Engineers, Oct. 1965, pp. 487-507.

EAGLESON, P.S., "Wave Induced Motion of Discrete Bottom Sediment Particles," *Journal of the Hydraulic Division*, Vol. 85, No. HY10, Oct 1959, pp. 53-80.

EAGLESON, P.S., "Theoretical Study of Longshore Currents in a Plane Beach," Report No. 82, Hydrodynamics Laboratory, Department of Civil Engineering, Massachusetts Institute of Technology, Cambridge, Mass., Dec. 1965.

EAGLESON, P.S., and DEAN, R.G., "Wave-Induced Motion of Bottom Sediment Particles, *Transactions of the American Society of Civil Engineers*, American Society of Civil Engineers, Vol. 126, 1961, pp. 1162-1189.

EAGLESON, P.S., GLENNE, B., and DRACUP, J.A., "Equilibrium Characteristics of Sand Beaches in the Offshore Zone," Technical Report No. 41, Hydrodynamics Laboratory, Massachusetts Institute of Technology, Cambridge, Mass., Jan. 1961.

EAGLESON, P.S., GLENNE, B., and DRACUP, J.A., "Equilibrium Characteristics of Sand Beaches," *Journal of the Hydraulics Division*, Vol. 89, No. HY1, Jan. 1963, pp. 35-58.

EINSTEIN, H.A., "Movement of Beach Sands by Water Waves," *Transactions of the American Geophysical Union*, American Geophysical Union, Vol. 29, 1948, pp. 653-655.

EINSTEIN, H.A., "A Basic Description of Sediment Transport on Beaches," Technical Report HEL 2-34, Hydraulic Engineering Laboratory, University of California, Berkeley, Calif., Aug. 1971.

FAN, LOH-NIEN, and LE MEHAUTE, B., "Coastal Movable Bed Scale Model Technology," Tetra Tech Report TC-131, Tetra Tech, Inc., Pasadena, Calif., June 1969.

GALVIN, C.J., Jr., "Longshore Current Velocity: A Review of Theory and Data," *Reviews of Geophysics*, Vol. 5, No. 3, Aug. 1967, pp. 287-304.

GILES, M.L., and CHATHAM, C.E., Jr., "Remedial Plans for Prevention of Harbor Shoaling Port Orford, Oregon; Hydraulic Model Investigation," Technical Report H-74-4, U.S. Army Engineer Waterways Experiment Station, Vicksburg, Miss., June 1974.

GODDET, J., and JAFFRY, P., "Similitude Laws for Sediment Transport Under the Simultaneous Action of Waves and Currents," *La Houille Blanche*, Grenoble, France, Vol. 15, No. 2, Apr. 1960, pp. 136-147.

INMAN, D.L., "Flume Experiments on Sand Transport by Waves and Currents," *Proceedings of the Eighth Conference on Coastal Engineering*, American Society of Civil Engineers, Ch. 11, 1963, pp. 137-150.

INMAN, D.L., and FRAUTSCHY, J.D., "Littoral Processes and the Development of Shorelines," *Proceedings of the Coastal Engineering Santa Barbara Specialty Conference*, Ch. 22, 1965, pp. 511-536.

INMAN, D.L., KOMAR, P.D., and BOWEN, A.J., "Longshore Transport of Sand," *Proceedings of the Coastal Engineering Conference*, American Society of Civil Engineers, Vol. 1, 1968, pp. 298-306.

IPPEN, A.T., *Estuary and Coastline Hydrodynamics*, McGraw-Hill, New York, 1966, 744 pp.

IWAGAKI, Y., and NODA, H., "Laboratory Study of Scale Effects in Two-Dimensional Beach Processes," *Proceedings of the Eighth Conference on Coastal Engineering*, American Society of Civil Engineers, Ch. 14, 1962, pp. 194-210.

JOHNSON, D.W., *Shore Processes and Shoreline Development*, Wiley, New York, 1919.

JOHNSON, J.W., "Dynamics of Nearshore Sediment Movement," *Bulletin of the American Association of Petroleum Geologists*, Vol. 40, No. 9, Sept. 1956, pp. 2211-2232.

JOHNSON, J.W., "The Littoral Drift Problem at Shore-Line Harbors," *Journal of the Waterways and Harbors Division*, Vol. 83, No. WW1, Apr. 1957, pp. 1211-1--1211-37.

JOHNSON, J.W., "The Supply and Loss of Sand to the Coast," *Journal of the Waterways and Harbors Division*, Vol. 85, No. WW3, Sept. 1959, pp. 227-251.

JOHNSON, J.W., "Estimating the Importance of Nearshore Sediment Movement in Engineering Problems," *Proceedings of the Golden Jubilee Symposium*, Central Water and Power Research Station, Vol. 2, 1966, pp. 43-50.

KALKANIS, G., "Transportation of Bed Material due to Wave Action," Technical Report HEL 2-4, Hydraulic Engineering Laboratory, University of California, Berkeley, Calif., Feb. 1963; also TM-2, U.S. Army, Corps of Engineers, Coastal Engineering Research Center, Washington, D.C., Feb. 1964.

KAMPHUIS, J.W., "Scale Selection for Wave Models," Research Report No. 71, Department of Civil Engineering, Queen's University, Kingston, Ontario, Feb. 1972.

KEULEGAN, G.H., "Depths of Offshore Bars," TM-8, U.S. Army, Corps of Engineers, Beach Erosion Board, Washington, D.C., July 1945.

KRUMBEIN, W.C., "Shore Processes and Beach Characteristics," TM-3, U.S. Army, Corps of Engineers, Beach Erosion Board, Washington, D.C., May 1944.

LANGHAAR, H.L., *Dimensional Analysis and Theory of Models*, Wiley, New York, 1962, pp. 166.

LE MEHAUTE, B., "Philosophy of Hydraulics," *Journal of the Hydraulics Division*, Vol. 88, No. HY1, Jan. 1962, pp. 45-66.

LE MEHAUTE, B., "A Comparison of Fluvial and Coastal Similitude," *Proceedings of the 12th Conference on Coastal Engineering*, American Society of Civil Engineers, Vol. 2, 1970, pp. 1077-1096.

LE MEHAUTE, B., and BREBNER, A., "An Introduction to Coastal Morphology and Littoral Processes," Report No. 14, Queen's University, Kingston, Ontario, Jan. 1961.

LONGUET-HIGGINS, M.S., "Mass Transport in Water Waves," *Philosophical Transactions of the Royal Society of London*, Series, A, Mathematical and Physical Sciences, Vol. 245, 1953, pp. 535-581.

MANOHAR, M., "Mechanics of Bottom Sediment Movement Due to Wave Action," TM-75, U.S. Army, Corps of Engineers, Beach Erosion Board, Washington, D.C., June 1955.

NAYAK, I.V., "Equilibrium Profiles of Model Beaches," Technical Report HEL-2-25, Hydraulic Engineering Laboratory, College of Engineering, University of California, Berkeley, Calif., May 1970.

NODA, E.K., "Equilibrium Beach Profile Scale-Model Relationship," *Journal of the Waterways, Harbors, and Coastal Engineering Division*, Vol. 98, No. WW4, Nov. 1972, pp. 511-528.

PICKETT, E.B., DURHAM, D.L., and McANALLY, W.H., "Los Angeles and Long Beach Harbors Model Study; Prototype Data Acquisition and Observations," Technical Report H-75-4, U.S. Army Engineer Waterways Experiment Station, Vicksburg, Miss., June 1975.

RECTOR, R.L., "Laboratory Study of Equilibrium Profiles of Beaches," TM-41, U.S. Army, Corps of Engineers, Beach Erosion Board, Washington, D.C., Aug. 1954.

SAVAGE, R.P., "Laboratory Study of the Effect of Groins on the Rate of Littoral Transport; Equipment Development and Initial Tests," TM-114, U.S. Army, Corps of Engineers, Beach Erosion Board, Washington, D.C., June 1959.

SAVAGE, R.P., "Laboratory Determination of Littoral Transport Rates," *Journal of the Waterways and Harbors Division*, Vol. 88, No. WW2, May 1962, pp. 69-92.

SAVILLE, T., Jr., "Model Study of Sand Transport Along an Infinitely Long Straight Beach," *Transactions of the American Geophysical Union*, American Geophysical Union, Vol. 31, 1950, pp. 555-565.

SAVILLE, T., Jr., "Scale Effects in Two-Dimensional Beach Studies," *Proceedings of the Seventh Congress of the International Association for Hydraulic Research*, Vol. 1, 1957, pp. A3-1--A3-8.

SAVILLE, T., Jr., "Present Status of Littoral Transport," *Proceedings of the 22d International Navigation Congress*, Permanent International Association of Navigation Congresses, 1969, pp. 249-271.

SEDOV, L.J., *Similarity and Dimensional Methods in Mechanics*, Academic Press, New York, 1959.

SHINOHARA, K., "Sand Transport Along a Model Sandy Beach by Wave Action," *Coastal Engineering in Japan*, Tokyo, Japan, Vol. 1, Oct. 1958, pp. 111-130.

SHINOHARA, K., and TSUBAKI, T., "Laboratory Study of Sand Movement and Equilibrium Profiles of Beaches," *Coastal Engineering in Japan*, Tokyo, Japan, Vol. 2, Nov. 1959, pp. 29-34.

SILVESTER, R., "Engineering Aspects of Coastal Sediment Movement," *Journal of the Waterways and Harbors Division*, Vol. 85, No. WW3, Sept. 1959, pp. 11-39.

SILVESTER, R., *Coastal Engineering*, Vols. 1 and 2, Elsevier Scientific Publishing Co., Amsterdam, London and New York, 1974.

SIMMONS, H.B., "Contribution of Hydraulic Models to Coastal Sedimentation Studies," *Proceedings of the First Conference on Coastal Engineering*, American Society of Civil Engineers, 1950, pp. 161-168.

SITARZ, J.A., "Contribution a 1'Etude de L'evolution des Plates a Partir de la Connaissance des Profiles D'equilibre," *Travaus du Center de Recherches et d'Etudes Oceanographiques*, Paris, France, Vol. 5, Sept. 1963, 199 pp.

U.S. ARMY ENGINEER WATERWAYS EXPERIMENT STATION, "Model Study of Plans for Elimination of Shoaling in Absecon Inlet, New Jersey," Technical Memorandum No. 204-1, Vicksburg, Miss., Sept. 1943.

VALEMBOIS, J., "Etude Sur Modele Du Transport Littoral Conditions De Similitude," *Proceedings of the Seventh Conference on Coastal Engineering*, American Society of Civil Engineers, Vol. 1, 1960, pp. 307-317. (Translation No. 65-7 available at U.S. Army Engineer Waterways Experiment Station, Vicksburg, Miss.)

VANONI, V.A., "Measurements of Critical Shear Stress for Entraining Fine Sediments in a Boundary Layer," Technical Report KH-R-7, W.M. Keck Laboratory of Hydraulics and Water Resources, California Institute of Technology, Pasadena, Calif., May 1964.

WATTS, G.M., "Laboratory Study of the Effect of Tidal Action on Wave Formed Beach Profiles," TM-52, U.S. Army, Corps of Engineers, Beach Erosion Board, Washington, D.C., Dec. 1954.

YALIN, M.S., *Mechanics of Sediment Transport*, 1st ed., Pergamon Press, Oxford, New York, 1972.

YALIN, S., "Method for Selecting Scales for Models with Movable Bed Involving Wave Motion and Tidal Currents," *Proceedings of the 10th Congress of the International Association for Hydraulic Research*, Vol. 1, 1963, pp. 221-229.

YALIN, S., *Theory of Hydraulic Models*, The MacMillan Co., London, 1971, 266 pp.

YALIN, S., and RUSSELL, R.C.H., "Similarity in Sediment Transport Due to Waves," *Proceedings of the Eighth Conference on Coastal Engineering*, American Society of Civil Engineers, 1962, pp. 151-167.

VI. STABILITY OF COASTAL STRUCTURES

by
R.Y. Hudson

1. Introduction.

The economic design of a stable coastal structure is a difficult problem involving the complex interaction of waves and structure. Waves may be of the short-period type generated by storm winds with periods from about 1 to 25 seconds and heights from about 1 to 40 feet or more; or waves may be of seismic origin (tsunamis), which are long waves with periods ranging from about 5 to 35 minutes and heights nearshore up to 30 feet or more. The magnitude and distribution of wave pressures on coastal structures vary with the type and geometry of the structure, the depth of water and bottom configuration immediately seaward of the structure, the stage of tide relative to the crest of the structure at the time the wave action occurs, and the wave dimensions. Since accurate determination of wave forces on other than structures of simple shape in relatively deep water cannot be calculated, hydraulic models are commonly used to obtain sufficiently accurate data from which to make engineering decisions.

This section discusses the design, operation, accuracy, utilization of test data, and costs of hydraulic models, the results of which are used for optimum designs of coastal structures concerning their stability under wave attack. The types of structures considered are (a) rubble-mound breakwaters, jetties, and wave absorbers; (b) vertical-wall breakwaters and jetties; (c) composite breakwaters; (d) seawalls; and (e) floating, pneumatic, and hydraulic breakwaters.

Rubble-mound breakwaters, jetties, and wave absorbers are used extensively where the depths are not prohibitive and suitable quarrystone is available locally or within transporting distance at competitive prices. These structures are also used if the foundation materials are such that the stability of a vertical-wall structure would be endangered. Rubble-mound structures can be constructed in stages if the natural foundation material is incapable of supporting the weight of the completed structure without considerable settlement, with enough lapse of time between the stages to allow settlement to take place. Rubble-mound wave absorbers may be used inside harbors to reduce the wave action to acceptable levels. Rubble wave absorbers are similar in construction to rubble breakwaters except that they may have flatter slopes, a thicker cover layer with a maximum of voids, and they are usually backed by a vertical, impervious bulkhead.

Vertical-wall breakwaters and jetties may be more economical when the foundation material is firm, homogeneous, and not easily scoured. Vertical-wall breakwaters may also be used as additional pier facilities if enough top width is provided and overtopping can be prevented. The foundation is seldom such that a vertical-wall, gravity-type structure

can be placed directly on the bottom without special preparation of the foundation material. Thus, the bottom material may be prepared by placing riprap in layers until adequate bearing pressures are obtained. When the water depths are appreciable, and when the economics and purpose of the structure permit, a rubble-mound base for the vertical wall may be placed on the bottom to an elevation that comprises a considerable part of the water depth. This rubble mound with the vertical wall which surmounts the rubble is called a composite breakwater. Breakwaters protect mooring areas from wave action, whereas jetties are structures extending from shore to prevent shoaling of channels by littoral material, or constructed at the mouth of a river or tidal inlet to confine the flow and deepen and stabilize the entrance channel. Jetties as breakwaters may be either a rubble-mound, vertical-wall, or composite-type of structure.

Seawalls are structures that separate land and water areas; in harbors they are frequently bulkheads on the landside and breakwaters on the seaside. Seawalls may also be either vertical-wall, rubble-mound, or composite-type structures.

Floating breakwaters, as the name implies, are floating structures (usually fixed in place by mooring cables) designed to prevent passage of all but a minimum, allowable percentage of the wave energy. The structures must extend deep enough into the water to be effective, and must have a natural period of oscillation that is large relative to the period of the selected design waves to prevent large oscillations and the consequent generation of waves by the structure itself. Floating breakwaters are not widely used because they are usually not efficient wave reducers except for the conditions of relatively deepwater and short-period waves. However, these breakwaters offer several advantages, compared to fixed structures, such as mobility, ease of installation, elimination of littoral drift and scour problems that are sometimes caused by the construction of fixed impervious structures, freedom from foundation problems, and relatively small initial and maintenance costs.

The pneumatic breakwater consists of a bubble screen that is generated by compressed air passing through a submerged perforated pipe, and rises to the surface in the form of air bubbles. While rising to the surface, the air bubbles induce a vertical current which, in turn, produces horizontal currents away from the bubble screen on the surface in both the upstream and downstream directions and toward the screen near the bottom. The surface current moving against the direction of wave propagation produces some attenuation of the waves.

The hydraulic breakwater is similar in principle to the pneumatic breakwater, except that the surface currents are generated by forcing water through a perforated pipe or nozzle system. Pneumatic and hydraulic breakwaters, like the floating breakwater, are only effective for relative deepwater and short-period waves.

The erosive action due to waves and currents of beach material in the toe areas of rubble-mound and vertical-wall breakwaters and jetties,

and in front of seawalls, is not discussed in this section. However, scour is sometimes a problem in the stability of coastal structures, and when model studies (conducted in accordance with the scale-model techniques and transference equations discussed in Section V) or field experience indicate that scour due to wave action is likely to endanger the stability of these structures, the area of scour may be covered with a riprap blanket. The stability of the blankets can be determined by model studies of the type used to test the stability of rubble breakwaters, jetties, and wave absorbers.

2. Similitude Relations.

a. Rubble-Mound Structures. When a rubble-mound breakwater, jetty, or wave absorber with a given geometry (crest width, crest height above or below the stillwater level, number of layers and size of stones in the underlayer system, height of the impervious core material above or below the stillwater level, and the depth below stillwater level to which the armor units in the protective cover layer extend) are subjected to the attack of gravity water waves, the stability of the armor units is a function of the following variables:

d = depth of water in which the structure is situated, measured at the seaside toe

D = percent damage to the cover layer caused by waves of a given height, as measured by the number of armor units displaced compared with the total number of armor units in the cover layer

g = acceleration due to gravity

H = height of waves that attack the structure

$(\ell_c)_a$ = characteristic linear dimension of the armor units

V_w = velocity of water that impinges on and flows around individual armor units in the area where damage to the cover layer occurs

α = angle of seaside slope, measured from the horizontal

β = angle of incidence of wave attack

Δ = shape of armor units

θ = angle of bottom slope seaward of the structure, measured from the horizontal

λ = wavelength

μ = dynamic viscosity of water in which the structure is situated

$(\xi_c)_a$ = characteristic linear dimension of the surface roughness of armor units

ρ_a = mass density of armor units

ρ_w = mass density of water in which the structure is situated

Thus, by the π theorem (see Sec. II),

$$f\left[V_w, g, \rho_a, \rho_w, \mu, H, \lambda, d, (\ell_c)_a, (\xi_c)_a, \alpha, \beta, \Delta, \theta, D\right] = 0 \qquad (6\text{-}1a)$$

and

$$f'\left[\frac{V_w}{g^{1/2}(\ell_c)_a^{1/2}}, \frac{V_w(\ell_c)_a}{\mu/\rho_w}, \frac{\rho_w}{\rho_a}, \frac{(\ell_c)_a}{d}, \frac{H}{\lambda}, \frac{d}{\lambda}, \frac{(\xi_c)_a}{(\ell_c)_a}, \alpha, \beta, \Delta, \theta, D\right] = 0\,. \qquad (6\text{-}1b)$$

The forces imposed on individual armor units by the flow of water caused by wave action are inertia, form drag, and surface drag (viscous shear). The inertia forces result from the pressure gradient in the water (Allen and Russel, 1958). Since gravity forces are also involved, and are predominant for this type of phenomenon, stability models of rubble-mound structures are designed based on Froude's law. For such models the inertia forces, relative to gravity forces, scale down correctly; the form drag forces, relative to gravity forces, scale down nearly correctly, depending on the form of armor unit, its weight, and the size of wave; and viscous forces scale down incorrectly. For the armor units, the viscous forces can be made negligible if the linear scale is selected so that the Reynolds number, R_n, is not too small. However, for the smaller underlayer rock, it is difficult at times (depending on the height of the design wave) to select a scale so that the viscous forces in the underlayers are negligible.

In equation (6-1b) the Froude number and the density ratio can be combined, since the stability of the armor units is determined to a considerable extent by the relative magnitudes of the form drag and submerged weight of the armor units. Since it can be shown that equation (6-1b) has been solved for the combined terms,

$$\frac{V_w}{g^{1/2}(\ell_c)_a^{1/2}} \frac{(\rho_w)^{1/2}}{(\rho_a - \rho_w)^{1/2}} = f''\left[\frac{V_w(\ell_c)_a}{\mu/\rho_w}, \frac{(\ell_c)_a}{d}, \frac{H}{\lambda}, \frac{d}{\lambda}, \frac{(\xi_c)_a}{(\ell_c)_a}, \alpha, \beta, \Delta, \theta, D\right]. \qquad (6\text{-}1c)$$

Equation (6-1c) is the basis for design and operation of stability models for use in general testing of rubble-mound breakwaters, wave absorbers, and jetties exposed to wave action.

The desired relationships, model-to-prototype, for similarity of stability of the armor units, $D_m = D_p$, will be obtained if each π term

in equation (6-1c) has the same value in both the model and the prototype for a particular form of breakwater section and a particular set of wave conditions; i.e.,

$$\left[\frac{V_w}{(\ell_c)_a^{1/2} g^{1/2}}\right]_m = \left[\frac{V_w}{(\ell_c)_a^{1/2} g^{1/2}}\right]_p \tag{6-2a}$$

$$\left(\frac{\rho_w}{\rho_a - \rho_w}\right)_m = \left(\frac{\rho_w}{\rho_a - \rho_w}\right)_p \tag{6-2b}$$

$$\left[\frac{V_w(\ell_c)_a}{\mu/\rho_w}\right]_m = \left[\frac{V_w(\ell_c)_a}{\mu/\rho_w}\right]_p \tag{6-2c}$$

$$\left[\frac{(\ell_c)_a}{d}\right]_m = \left[\frac{(\ell_c)_a}{d}\right]_p \tag{6-2d}$$

$$\left(\frac{H}{\lambda}\right)_m = \left(\frac{H}{\lambda}\right)_p \tag{6-2e}$$

$$\left(\frac{d}{\lambda}\right)_m = \left(\frac{d}{\lambda}\right)_p \tag{6-2f}$$

$$\left[\frac{(\xi_c)_a}{(\ell_c)_a}\right]_m = \left[\frac{(\xi_c)_a}{(\ell_c)_a}\right]_p \tag{6-2g}$$

$$\alpha_m = \alpha_p \tag{6-2h}$$

$$\beta_m = \beta_p \tag{6-2i}$$

$$\Delta_m = \Delta_p \tag{6-2j}$$

and

$$\theta_m = \theta_p \tag{6-2k}$$

Since stability models of rubble-mound breakwaters are designed based on Froude's law and are constructed geometrically similar with undistorted linear scales, all the above-listed relationships can be satisfied for a particular set of test conditions except for those indicated by equation (6-2c) (Reynolds number) and equation (6-2g) (surface roughness of individual armor units). The effects of surface roughness of the ordinary quarrystone and concrete armor units are negligible in full-scale prototype structures, and they can be made negligible in the model by use of relatively smooth-surfaced armor units. For stability models with linear scales, L_m/L_p, where the model velocities and armor-unit sizes are too small, the viscous effects are accentuated and the scale effects may no longer be negligible. Tests to determine the scale effects in the

stability of armor units, as a function of Reynolds number, have been conducted (see Sec. VI,3,c). In tests where the reflection of waves from, and the transmission of waves through, rubble-mound structures are studied, the scale effects also vary with Reynolds number. Studies to determine model design procedures to minimize the scale effects have been discussed by Le Mehaute (1965); the results of tests concerning this aspect of model design were also reported by Keulegan (1973).

Since the velocity, V_w, of the waves or of the water particles that impinge on armor units during wave attack are not easily measured during the conduct of breakwater stability tests, V_w can be conveniently eliminated from equation (6-1c) by the relation $V_w = f(gH)^{1/2}$. Other helpful substitutions are $\nu = \mu/\rho_w$, $\gamma_a = \rho_a g$, and $(\ell_c)_a = k_v(W_a/\gamma_a)^{1/3}$,

where

ν = kinematic viscosity

γ_a = specific weight

W_a = weight of the armor unit

k_v = shape coefficient such that $W_a = k_v^{-3}\gamma_a(\ell_c)_a^3$.

After making these substitutions, equation (6-1c) becomes

$$\frac{\gamma_a^{1/3}H}{(\gamma_a/\gamma_w - 1)W_a^{1/3}} = f'''\left[\frac{g^{1/2}H^{1/2}}{\nu}, \frac{(\ell_c)_a}{d}, \frac{H}{\lambda}, \frac{d}{\lambda}, \frac{(\xi_c)_a}{(\ell_c)_a}, \alpha, \beta, \Delta, \theta, D\right] . \quad (6\text{-}3a)$$

Considering that the model structures would be constructed geometrically similar to hypothetical or proposed prototype structures; assuming that the model structure and wave dimensions are such that the Reynolds number is large enough to render the viscous forces negligible, and that the surface texture of the model armor units are sufficiently smooth, relative to that of the prototype units; and then recognizing that the shape of armor unit, Δ, and the manner in which armor units are placed in the cover layer of the structure (placing technique, P_t) are important parts of the condition of geometrical similarity (relatively small variations in placing technique can cause relatively large variations in the stability of armor units), and that the seaward slope of the breakwater, wave absorber, or jetty face, α, is an important variable in both the stability and cost of the structure, the basic equation used for guidance in the testing of specific or hypothetical structures reduces to

$$\frac{\gamma_a^{1/3}H}{(\gamma_a/\gamma_w - 1)W_a^{1/3}} = f''''\left(\frac{H}{\lambda}, \frac{d}{\lambda}, \alpha, \Delta, \theta, P_t, D\right). \quad (6\text{-}3b)$$

This relation is the same as that used by Hudson (1958) in a general testing program to determine the function f'''' for an idealized breakwater

trunk section situated in relatively deep water with no overtopping of the structure, for nonbreaking waves approaching the breakwater with an angle of incidence, β, of 90°, for random placement of stone armor units, and for various values of H/λ, d/λ, α, and D. The term on the left side of the equality sign, which was derived using a combination of the dynamic and dimensional analysis methods, was designated the stability number, N_s. It was found that, for the selected test conditions,

$$N_s = (K \cot \alpha)^{1/3} \tag{6-4a}$$

from which

$$W_a = \frac{\gamma_a H^3}{K\left(\gamma_a/\gamma_w - 1\right)^3 \cot \alpha} \tag{6-4b}$$

and, $K = F(\Delta, P_t, D)$. Tests in which $\beta = 90°$ and both partially breaking waves and waves breaking directly onto the breakwater slope are used should show in accordance with equation (6-3b), that

$$K = f\left(\frac{H}{\lambda}, \frac{d}{\lambda}, \Delta, P_t, D\right). \tag{6-5}$$

Information obtained from the generalized tests is used primarily for purposes of preliminary design. In the final design of a proposed structure where the geometry of the structure section is planned according to local conditions and the purpose of the structure, scale model studies are often necessary to ensure that the structure will provide the desired protection at a minimum of cost.

b. Vertical-Wall (Impervious) Breakwaters and Jetties. When vertical-wall, gravity-type breakwaters or jetties are situated in depths of water (relative to the wave dimensions) such that the waves do not break on the face of the structure, when the height of the structure is such that all but minor overtopping is prevented, and when the angle of wave approach β is 90°, the pressure intensity as a function of elevation (in the vertical plane of the structure face) can then be calculated by using either the equations of Sainflou (Sainflou, 1928; Hudson, 1953) (first order of approximation) or of Miche (Miche, 1944a; Kamel, 1968a) (second order of approximation) for the "clapotis" (a French term that refers to the phenomenon in which a series of progressive waves is reflected by a vertical surface perpendicular to the advancing waves and produces standing waves seaward of the structure). Sainflou's equations give conservative results and his pressure curve, modified to simplify calculations, is considered adequate for design in most instances. However, if the geometry of the breakwater is more complex (e.g., with the upper part of the seaward face sloping, as suggested by Van de Kreeke and Paape (1964) and Lundgren (1962) to reduce the effects of wave forces on the stability of the structure), the angle of wave attack is less than 90°, or if there is considerable overtopping, model tests are necessary for an accurate determination of the wave forces on the structure. Such models are designed and operated by Froude's law.

When vertical-wall breakwaters of the type discussed above are situated where the bottom slopes seaward and in depths only slightly greater than the wave heights, the waves are no longer completely reflected but are partially destroyed orbitally and can break on the structure with resulting shock pressures that are much higher in intensity and much shorter in duration than those caused by the clapotis-type of wave motion. In this case the phenomena are so complex that an adequate analytical solution has not been possible, and it is necessary to rely on scale-model tests. The magnitude of shock pressures formed by breaking waves varies greatly with the form of the waves as they make contact with the breakwater. The following factors are of primary importance in determining the magnitude, duration, and disposition of the pressures formed by breaking waves on impervious breakwater surfaces:

(a) The wave dimensions, angle of wave approach, water depth at the toe of the structure, the bottom slope seaward, and the reflective characteristics of the structure determine the waveform when contact is made with the structure face.

(b) The concentration of entrained air in the water as the wave impinges on the structure face and the pressures in the bubbles of entrained air.

(c) The pressures in air pockets that may be trapped between the structure face and the wave front when contact is made with the structure face.

(d) The pressures in air cushions formed by wave fronts and the wall to allow the escape of air upward or laterally.

Thus, flow phenomena can be assumed a function of

d = depth of water in which the structure is situated, measured at the seaside toe

E_w = modulus of elasticity of the water

E'_{bm} = bulk modulus of the breakwater material

g = acceleration due to gravity

H = height of wave that breaks on the structure

k = adiabatic constant of air

p = pressure intensity on the vertical wall

p_{at} = atmospheric pressure

T = wave period

β = angle of incident wave attack

θ = angle of bottom slope seaward of the structure, measured from the horizontal

λ = wavelength measured in depth d + Δd corresponding to the breaking depth

μ = dynamic viscosity of the water

ρ_{bm} = mass density of the breakwater material

ρ_w = mass density of the water in which the structure is situated

σ = surface tension of the water

Thus, in accordance with the π theorem

$$f(d, g, H, T, \theta, \beta, \mu, \sigma, \rho_w, E_w, E'_{bm}, \rho_{bm}, p, p_{at}, k) = 0 \tag{6-6a}$$

$$\frac{p - p_{at}}{p_{at}} = f'(d, g, H, T, \theta, \beta, \mu, \sigma, \rho_w, E_w, E'_{bm}, \rho_{bm}, k) = 0 \tag{6-6b}$$

and

$$\frac{p - p_{at}}{p_{at}} = f''\left[\frac{H}{d}, \theta, \beta, \frac{(gH)^{1/2}T}{d}, \frac{dH}{T\mu/\rho_w}, \frac{\sigma T^2}{\rho_w H d^2}, k, \left(\frac{E_w}{\rho_w}\right)^{1/2}\frac{T}{d}, \left(\frac{E'_{bm}}{\rho_{bm}}\right)^{1/2}\frac{T}{d}, \frac{\rho_w}{\rho_{bm}}\right]. \tag{6-6c}$$

With geometrical similarity and similar test conditions, model-to-prototype, and considering that viscous shear forces are negligible with respect to gravity, inertia, pressure, and elastic forces, the functional relation for use in guiding the testing program and correlating test data is

$$\frac{p - p_{at}}{p_{at}} = f'''\left[\frac{H}{d}, \frac{(gH)^{1/2}T}{d}, \frac{\sigma T^2}{\rho_w H d^2}, k, \left(\frac{E_w}{\rho_w}\right)^{1/2}\frac{T}{d}, \left(\frac{E'_{bm}}{\rho_{bm}}\right)^{1/2}\frac{T}{d}, \frac{\rho_w}{\rho_{bm}}\right]. \tag{6-6d}$$

The above discussion and functional relations show that the extremely complex interactions of the water, compressed air, and capillary forces cause difficulty in determining approximate equations for correcting model results to minimize errors in transferring the results to prototype quantities. However, it is believed that the model should be designed and operated based on Froude's law and the test data transferred to prototype terms using approximate methods of reducing the resulting scale effects to a minimum. The method suggested by Lundgren (1969) is adopted. According to Lundgren the three breaking waveforms that cause shock-type pressures with intensities greater than those of the clapotis are generally similar to the ventilated, compression, and hammer types of shock pressures shown in Figure 6-1.

(1) Ventilated Shock. If the wave front approaches the vertical wall so that the air between the wave front and the wall is able to escape

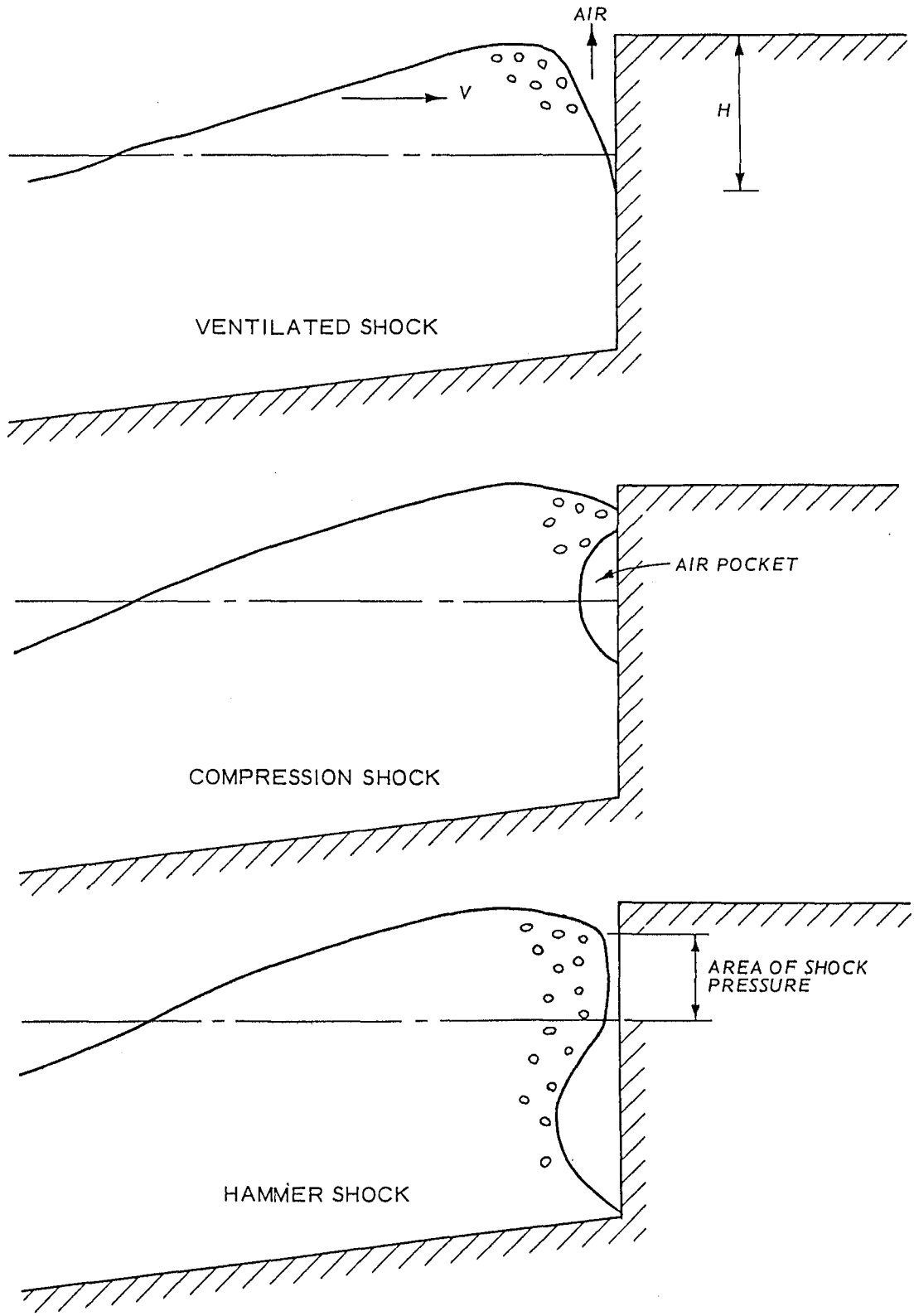

Figure 6-1. Types of shock pressures on vertical-wall breakwaters (after Lundgren, 1969).

entrapment, the ventilated type of shock pressure occurs. Although some scale effects are involved because the acoustical velocity E_w/ρ_w was assumed infinite (actually a function of the concentration of bubbles in the water), the primary forces in the ventilated shock phenomenon are inertial and gravitational. Thus, the impulses and the pressures can be transferred from the model to the prototype with enough accuracy on the basis of Froude's law.

(2) Compression Shock. If the wave front approaching the wall is concave in shape, the crest part of the front can reach the wall first, trapping an air pocket and producing a compression shock. This phenomenon involves a very complicated process and only the impulses can be transferred from model-to-prototype on the basis of Froude's law. Lundgren (1969) recommends the use of an equation derived by Mitsuyasu (1966), who used the water-piston model of Bagnold (1939), as a "compression model law" for the interpretation of model-test results when the compression type of pressure curve with respect to time is obtained. This equation is

$$\left(\frac{p_{max}}{p_{at}}\right)^{2/7} + 0.4\left(\frac{p_{max}}{p_{at}}\right)^{-5/7} - 1.4 = K\frac{\rho_w g H}{p_{at}} \qquad (6\text{-}7)$$

where p_{max} is the maximum pressure developed on the vertical wall by the compression shock phenomenon, and K is a dimensionless constant equal in model and prototype. A convenient method of using equation (6-7) in the interpretation of model results, as recommended by Lundgren, is to:

(a) Plot a curve calculated from equation (6-7) with values of $(p_{max} - p_{at})/p_{at}$ on one axis and values of $\rho_w g H/p_{at}$, a dimensionless wave height, on the other axis;

(b) use the model test data, enter the curve with the value of $(p_{max})_m$ and determine the corresponding value of the model dimensionless wave height $(H_{dim})_m$;

(c) multiply $(H_{dim})_m$ by L_p/L_m to obtain the dimensionless value of the prototype wave $(H_{dim})_p$; and

(d) enter the curve with the value of $(H_{dim})_p$ and determine the corresponding value of the prototype pressures $[(p_{max} - p_{at})/p_{at}]_p$, from which $(p_{max})_p$ is calculated.

(3) Hammer Shock. In the discussion of compression shock pressure, the phenomenon was such that the maximum pressures which are possible to obtain when a plane wave front impinges on a plane breakwater surface could not be generated because of the cushioning effects of the trapped air pocket. However, in rare instances the wave front may be so plain that a real water hammer occurs. In this case, the theoretical maximum pressure that occurs is a function of the elasticity of the

breakwater material and the compressibility of the water. In this theory the effects of the air that is usually trapped are ignored. According to Kamel (1968b) the maximum shock pressure that can occur is given by the relation

$$p_t = \frac{\rho_{bm} C_{bm}}{\rho_w C_w + \rho_{bm} C_{bm}} \rho_w C_w V_w \qquad (6\text{-}8)$$

where

p_t = theoretical maximum pressure

ρ_{bm} and ρ_w = mass densities of the breakwater material and the water (respectively)

C_{bm} and C_w = acoustical velocities of the shock front in the material and the water (respectively)

V_w = velocity of the water (wave front) impinging on the structure

Kamel performed special tests where plates of different types of metal were dropped on both glassy and disturbed water surfaces, and the resulting pressures were recorded electrically. His results showed that, because all the air could not be evacuated from the area between the plate and the water surface at the instant of impact, the recorded pressures were never more than about 50 percent of the theoretical. Considering that a prototype breakwater surface will never be as smooth and regular as the test plates, that a storm wave front will never be as plane as the glassy water surface used in the tests, and that a prototype wave at the instant of breaking will contain large amounts of trapped air in the form of bubbles, pressures more than $0.5p_t$ are believed unlikely to occur for a full-scale structure. Therefore, model studies for determining the maximum shock pressures on breakwaters are considered unnecessary. However, such tests, designed and operated by Froude's law, can give valuable information as to the relative magnitude of water-hammer shock pressures for different geometric shapes of the breakwater.

(4) Shape of Pressure Curves and Model Design. The above discussions showed that the method of model design and interpreting the results varied with the type of phenomena causing the wave pressures (ventilated shock, compression shock, and hammer shock). The type of phenomena involved in a particular model study can be determined by observing the shapes of the recorded pressure curves. The pressure curves for the ventilated and compression shock are similar in shape, varying in the rate of pressure rise and the maximum pressure. The water-hammer shock curve has a very fast rising front and a very high maximum pressure compared with the ventilated and compression shocks. Figure 6-2 shows the shapes of the compression- and hammer-shock pressure curves as recorded in wave-flume tests by Hayashi and Hattori (1958).

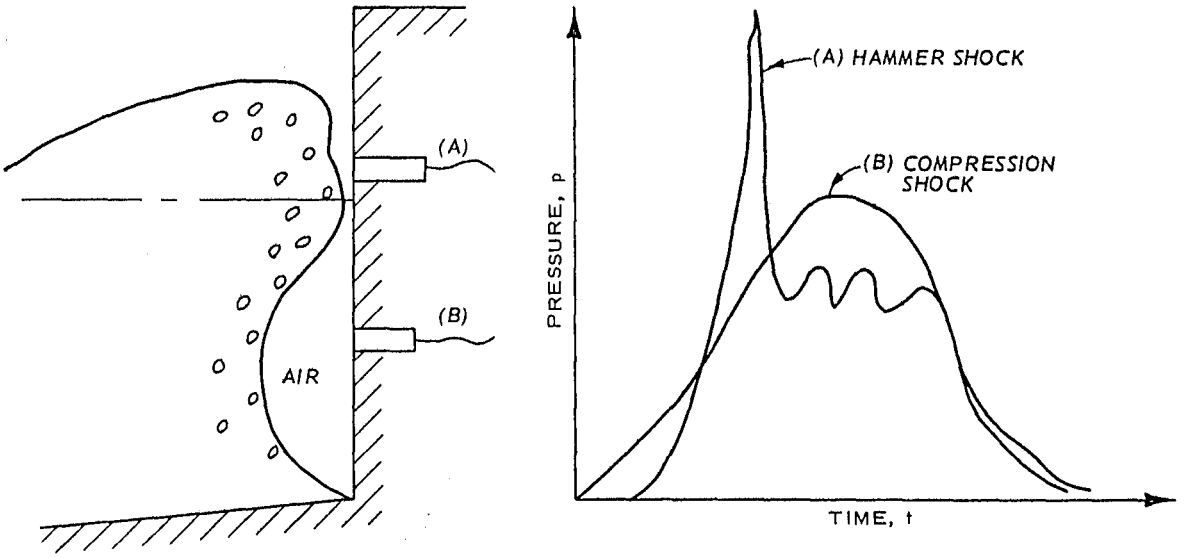

Figure 6-2. Compression- and hammer-shock pressure curves (after Lundgren, 1969).

c. Composite Breakwaters and Jetties. For the composite type of breakwater or jetty where the rubble base is of considerable height relative to the depth of water (Fig. 6-3), the rubble base absorbs a larger part of the incident wave energy than the vertical wall absorbs, when situated only on a filter blanket, and a larger percent of the waves can break on the vertical-wall part of the structure. However, the same types of pressure curves can be formed as for the simple vertical-wall type. Therefore, for a composite structure, the model should be designed in the same manner as for the vertical wall, except that the rubble-mound base part would be designed according to Froude's law, with scale-effect corrections for the viscous shear in a manner similar to that for stability tests of rubble-mound breakwaters (see Sec. VI,2,a and 3,c).

d. Seawalls. Since seawalls may be either rubble mound, vertical wall, or composite structures (or constructed similar to vertical-wall structures except that their seaside face is in the form of steps or is concaved seaward), the forms of the attacking waves can be any of those discussed previously (clapotis, ventilated shock, etc.). Thus, for the composite breakwater or jetty the model design procedures would be the same as those discussed in Section VI,2 and VI,3.

e. Floating Breakwaters. The methods by which floating breakwaters reduce incident wave heights to provide a measure of protection to the harbor area are reflection, forced instability, out-of-phase damping, destruction of orbital motion, and viscous damping (Bulson, 1964). Except for rare occasions (e.g., the formation of portable harbors for military use), the use of floating breakwaters of any type is not very practical unless the wave environment consists of short-period waves of moderate height and water depths that are deep relative to wavelength. For such a wave environment, a practical type of breakwater structure is one that

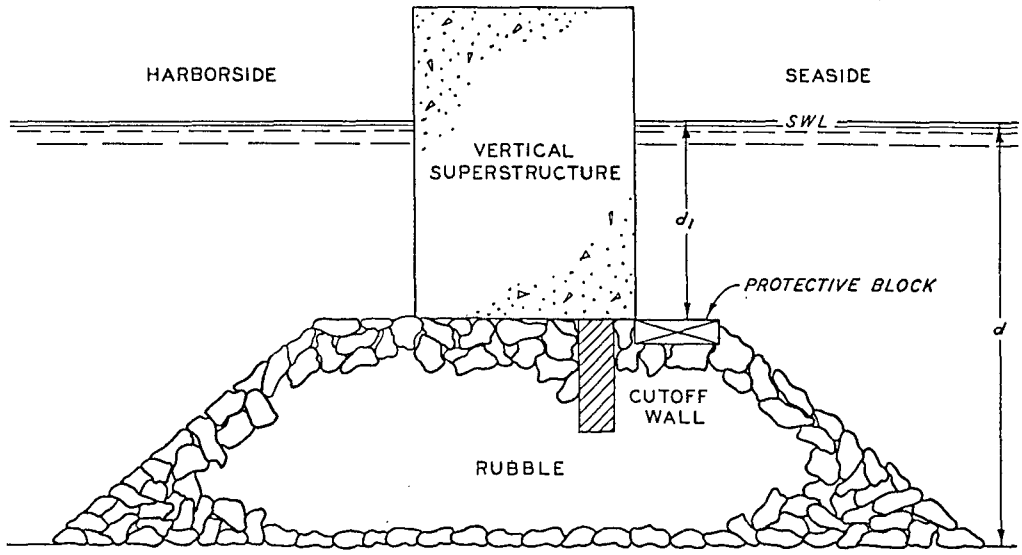

Figure 6-3. Example of composite-type breakwater.

reflects a part of the incident wave energy and reduces the transmitted wave heights further by out-of-phase damping. Some of the incident wave energy is converted into heat by turbulence, primarily by waves breaking onto the top of the structure. For the structures to be effective, cross sections must be designed so as to combine a large mass, with as large a mass moment of inertia as possible, and a relatively small restoring force, to obtain large periods of roll, pitch, and heave relative to the periods of the incident waves. These factors, and the necessity of reducing mooring-line forces to a minimum, make it difficult to design the structures to meet local conditions. Three floating breakwaters of the out-of-phase damping type (shown schematically in Fig. 6-4) are: the rectangular box, the cross or Bombardon (used during the invasion of France in World War II), and the A-frame tested by Brebner and Ofuya (1968). The A-frame floating breakwater is an example of the type of cross section designed to obtain a relatively large mass moment of inertia with a minimum of mass.

Although gravity, inertia, elastic, surface tension, and viscous shear forces exist in a moored floating breakwater assembly, it is not possible or necessary to design the model to be dynamically similar for all of these forces. The waves and breakwater structure are modeled according to Froude's law. The structure is constructed geometrically similar to its prototype, and with the correct weight and mass distribution so that the correct buoyancy and mass moments of inertia are modeled correctly. The linear scale is selected so that the waves and model breakwater (thus Reynolds number) are as large as possible, and the scale effects due to nonsimulation of the surface tension and viscous forces are assumed negligible. Thus, the time and velocity scales are

$$\frac{T_m}{T_p} = \frac{V_m}{V_p} = \left(\frac{L_m}{L_p}\right)^{1/2} . \qquad (6\text{-}9)$$

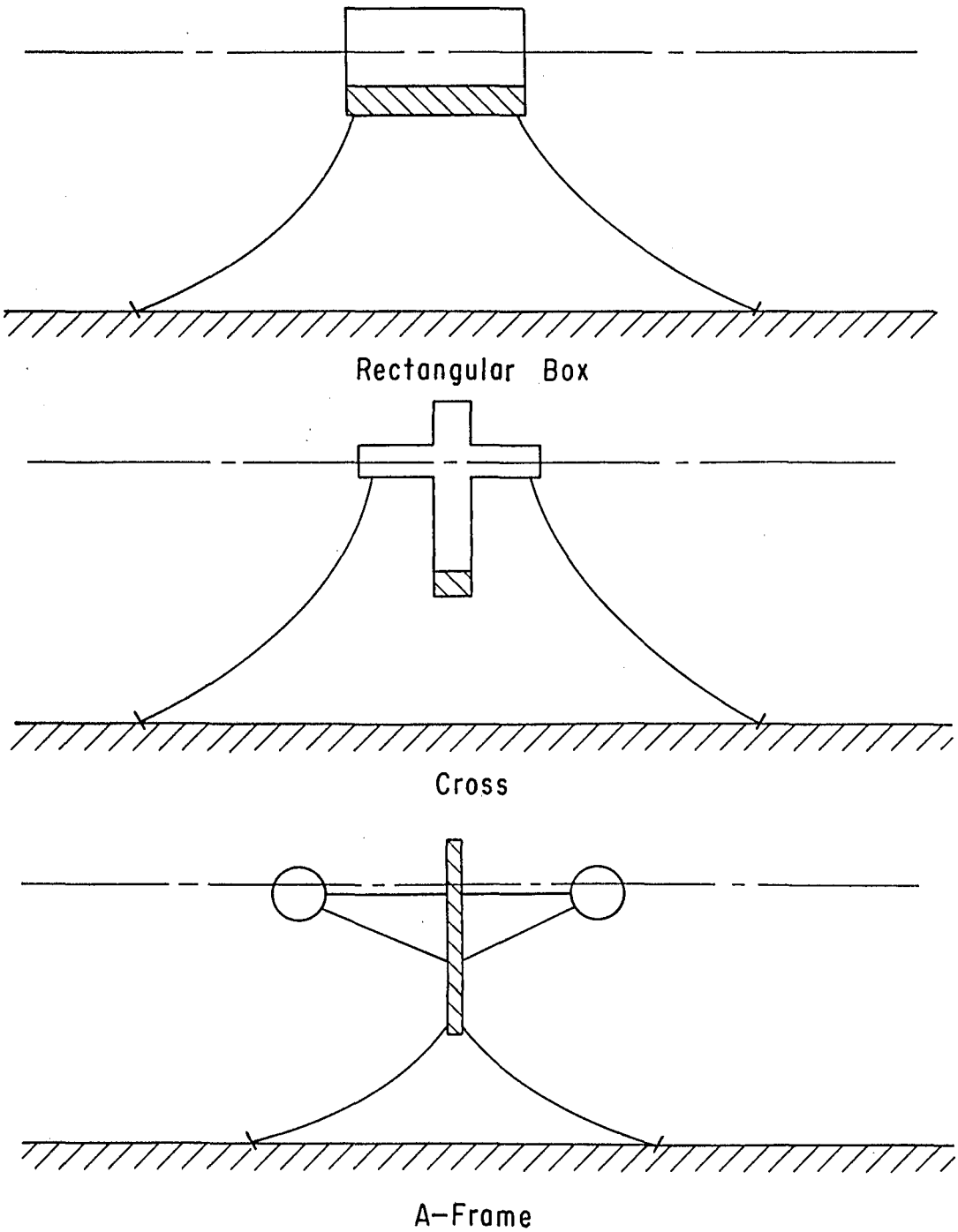

Figure 6-4. Examples of out-of-phase damping types of floating breakwaters.

The scales for wave forces, and the weights of the structure and of the mooring cables, when modeled by Froude's law, are

$$\frac{F_m}{F_p} = \frac{W_m}{W_p} = \frac{(\gamma_w)_m}{(\gamma_w)_p}\left(\frac{L_m}{L_p}\right)^3 . \tag{6-10}$$

The elastic properties of the mooring cables are modeled by the Mach-Cauchy law; i.e., for elongation,

$$\frac{F_m}{(EA)_m} = \frac{F_p}{(EA)_p} \tag{6-11a}$$

where A is the cross-sectional area of the cable and E is the modulus of elasticity of the cable. Thus,

$$\frac{F_m}{F_p} = \frac{(EA)_m}{(EA)_p} = \frac{(\gamma_w)_m}{(\gamma_w)_p}\left(\frac{L_m}{L_p}\right)^3 . \tag{6-11b}$$

In equation (6-11b), it was assumed that both the weight and the elasticity of the cable are important variables. However, if the cables were heavy steel chain links, then the elastic effects would be negligible, but flexibility of the linkages and the weight per unit length of the chain must be scaled correctly. The flexibility would be modeled by using small chain links as in the prototype, and the weight of the chain mooring line would be modeled by equation (6-10). However, if the prototype mooring cable were a relatively lightweight elastic rope, the weight scale would only be approximated, and the elastic, elongation properties would be modeled by equation (6-11b). If a relatively heavy, stiff steel cable were used as mooring line, the weight and bending forces could be appreciable. In this case the weight of the cable would be scaled by equation (6-10), and the bending properties would be scaled from the force scale (eq. 6-10), and the deflection formula

$$\Delta = \frac{kFL^3}{EI} \tag{6-12}$$

where I is the area moment of inertia of the cable cross section, and k is a constant that depends on the end restraints and the distribution of loading forces along the cable length, which distribution is assumed to be equal in model and prototype. Based on these considerations, and that $\Delta_m/\Delta_p = L_m/L_p$, since the model is geometrically similar to the prototype, the transference equation for cable bending is

$$\frac{E_m I_m}{E_p I_p} = \frac{(\gamma_w)_m}{(\gamma_w)_p}\left(\frac{L_m}{L_p}\right)^5 . \tag{6-13}$$

f. Pneumatic Breakwaters. Pneumatic breakwaters reduce incident wave heights by generating horizontal surface currents, a part of which flows counter to the orbital velocities of the oncoming waves. The horizontal surface currents are generated by the action of vertically rising air bubbles discharged from a pipe manifold system placed on or near the bottom. The waves from which protection is desired are propagated by the restoring force of gravity and are, therefore, modeled from Froude's law. However, since the generation of the counter surface currents, on which the reduction of wave action depends, is the result of rising air bubbles, viscous shear and surface tension forces must be considered. According to Kurihara (1956), the viscous forces in the turbulent area where the surface currents encounter the orbital velocities of the waves are also involved to some extent in the reduction of wave heights. Thus, pneumatic breakwater models must be designed and operated based on model laws that consider the forces of inertia, gravity, viscous shear, and surface tension. Pressure forces are also involved in the bubble formation.

When waves pass through a bubble screen, with the manifold located on the bottom, the reduction in wave heights may be assumed a function of the following variables:

$$H_i,\ H_t,\ \lambda,\ d,\ g,\ Q_{air},\ \rho_{air},\ \rho_w,\ p_{at},\ \mu,\ \text{and}\ \sigma,$$

where

H_i = incident wave height

H_t = transmitted wave height

λ = incident wavelength

d = depth of water

g = acceleration of gravity

Q_{air} = quantity of air emerging per second per foot from the orifices of the manifold; the quantity of free air delivered by the compressor to the manifold system per foot of manifold is

$$(Q_{air})_{at} = Q_{air} \frac{(p_{at} + \rho_w g d)}{p_{at}}$$

ρ_{air} = mass density of air

ρ_w = mass density of the water

p_{at} = atmospheric pressure

μ = dynamic viscosity of the water

σ = surface tension of the water

from which, by dimensional analysis,

$$f(H_i, H_t, \lambda, d, g, Q_{air}, \rho_{air}, \rho_w, p_{at}, \mu, \sigma) = 0 \qquad (6\text{-}14a)$$

and

$$\frac{H_t}{H_i} = f'\left(\frac{H_i}{\lambda}, \frac{d}{\lambda}, \frac{\rho_{air}}{\rho_w}, \frac{\rho_w g d}{p_{at}}, \frac{g^{1/3} d}{Q_{air}^{2/3}}, \frac{Q_{air}}{\nu}, \frac{\sigma d}{\rho_w Q_{air}^2}\right). \qquad (6\text{-}14b)$$

If a model study could be conducted in which (for individual test conditions) all the π terms within f' were held constant, then

$$\left(\frac{H_t}{H_i}\right)_m = \left(\frac{H_t}{H_i}\right)_p . \qquad (6\text{-}15)$$

However, only the first five π terms in f' can be held constant, simultaneously; therefore, before accurate transference equations can be determined for use in a model study, special scale-effect tests must be conducted over a wide range of values of the last two π terms to determine

$$\left(\frac{H_t}{H_i}\right)_r = f''\left[\left(\frac{Q_{air}}{\nu}\right)_r, \left(\frac{\sigma d}{\rho_w Q_{air}^2}\right)_r\right] \qquad (6\text{-}16)$$

where the subscripts refer to model-to-prototype ratios. The reduction ratio should be determined as a function of the two π terms in f'' for a range of values of H_i/λ and d/λ that occur in the prototype.

Each value of d used in the scale-effect tests would correspond to another model; therefore, the linear scales of the models, one to another, would be

$$\frac{L_m}{L_p} = \frac{d_m}{d_p} \qquad (6\text{-}17)$$

in both the vertical and horizontal directions. Thus, the tests would correspond to model studies using undistorted linear scales. This ensures that H_i/λ and d/λ would be constant, model-to-prototype, for the same selected prototype test conditions. The third π term, ρ_{air}/ρ_w, would be held constant during scale-effect tests by using air and water as the two fluids for all tests. For the fourth π term to be constant

$$\left(\frac{\rho_w g d}{p_{at}}\right)_m = \left(\frac{\rho_w g d}{p_{at}}\right)_p \qquad (6\text{-}18a)$$

since $(\rho_w)_m = (\rho_w)_p$ and $g_m = g_p$,

$$\frac{(p_{at})_m}{(p_{at})_p} = \frac{d_m}{d_p} = \frac{L_m}{L_p} . \qquad (6\text{-}18b)$$

This required condition can be attained by installation of an airtight cover on the test flume so that the air pressure above the water surface can be adjusted in accordance with the linear scale. In addition, for the fifth π term,

$$\left(\frac{g^{1/3}d}{Q_{air}^{2/3}}\right)_m = \left(\frac{g^{1/3}d}{Q_{air}^{2/3}}\right)_p \tag{6-19a}$$

from which

$$\frac{(Q_{air})_m}{(Q_{air})_p} = \left(\frac{d_m}{d_p}\right)^{2/3} = \left(\frac{L_m}{L_p}\right)^{2/3} . \tag{6-19b}$$

Other model-to-prototype ratios derived from the above relations are equation (6-9),

$$\frac{T_m}{T_p} = \frac{V_m}{V_p} = \left(\frac{L_m}{L_p}\right)^{1/2}$$

and

$$\frac{(p_w)_m}{(p_w)_p} = \frac{(p_{at})_m + (\gamma z)_m}{(p_{at})_p + (\gamma z)_p} \tag{6-20}$$

where

T = time

V = velocity

γ = $\rho_w g$

p_w = pressure at any depth z below the water surface

g. Hydraulic Breakwaters. Hydraulic breakwaters reduce wave heights in the same manner as pneumatic breakwaters, except that the horizontal surface currents are generated by water jets formed by forcing water through a series of nozzles in a pipe situated at or near the mean still-water level, and alined so that the currents generated are opposite in direction to the incident wave velocities. Thus, the important forces that must be modeled are inertia, gravity, and viscosity; the variables are presumed to be H_i, H_t, λ, d, g, Q_w, ρ_w, and μ, where Q_w is the quantity of water emerging from the orifices per second per foot of manifold (cubic feet per second per foot). From dimensional analysis,

$$f(H_i, H_t, \lambda, d, g, Q_w, \rho_w, \mu) = 0 \tag{6-21a}$$

and

$$\frac{H_t}{H_i} = f'\left(\frac{H_i}{\lambda}, \frac{d}{\lambda}, \frac{g^{1/3}d}{Q_w^{2/3}}, \frac{Q_w}{\nu}\right) . \tag{6-21b}$$

Since only three of the four π terms in f' can be held constant, model-to-prototype, special scale-effect tests must be conducted over a wide range of values of the Reynolds number term, Q_w/ν, to determine

$$\left(\frac{H_t}{H_i}\right)_r = f''\left(\frac{Q_w}{\nu}\right)_r . \qquad (6\text{-}21c)$$

As in the pneumatic breakwater tests, each depth d would correspond to another model, and from equation (6-17),

$$\frac{L_m}{L_p} = \frac{d_m}{d_p}$$

which would ensure that, for the same selected prototype conditions, H_i/λ and d/λ would remain constant during the scale-effect tests. Also (eqs. 6-19a and 6-19b)

$$\left(\frac{g^{1/3}d}{Q_w^{2/3}}\right)_m = \left(\frac{g^{1/3}d}{Q_w^{2/3}}\right)_p$$

from which

$$\frac{(Q_w)_m}{(Q_w)_p} = \left(\frac{d_m}{d_p}\right)^{2/3} = \left(\frac{L_m}{L_p}\right)^{2/3} .$$

Other ratios that can be derived from the above relations are, as in the pneumatic breakwater tests (eqs. 6-9 and 6-20),

$$\frac{T_m}{T_p} = \frac{V_m}{V_p} = \left(\frac{L_m}{L_p}\right)^{1/2}$$

and

$$\frac{(p_w)_m}{(p_w)_p} \equiv \frac{(p_{at})_m + (p_w gz)_m}{(p_{at})_p + (p_w gz)_p} .$$

For these tests, $(p_a)_m = (p_a)_p$ and water would be used for the test fluid.

3. Model Design.

a. Field Data Required. In the design of hydraulic models, it is important that adequate information is available about the prototype so that major problems confronting the field design engineer are clearly understood by the laboratory engineer. The purpose and scope of model studies should be determined to the extent possible at the outset. Model design and the testing program can then be better directed toward solution of those parts of the overall problem that are the most critical and are best suited for investigation by a hydraulic model. In addition to general information about the design problems (to determine the purpose and

scope of the model investigation), the design, construction, and operation of stability models of coastal structures exposed to wave action require (a) detailed information on the geometry of the structure and materials of which the structure will be composed, (b) information concerning the bottom materials upon which the structure will be situated (except for floating, pneumatic, and hydraulic breakwaters which require no foundation), (c) the bottom contours along the alinement of the structure and seaward of the structure to a water depth of nearly one-half the maximum wavelength, and (d) statistical data to determine the frequency of occurrence of waves with different heights and periods at the structure site.

Although accurate wave data are required to ensure that stability of a structure is obtained by a safe and efficient design, adequate wave records at the site are seldom available. However, when wave records are available, or if recorders are installed especially for a particular project from which the needed statistics can be prepared, the methods of analysis and presentation of the data as proposed by Draper (1966) are suggested. In the absence of wave records near the site of a proposed structure, the necessary statistical wave climate data can be determined by the forecasting and hindcasting techniques for deepwater stations offshore of the structure site (see Bretschneider, 1966 and U.S. Army, Corps of Engineers, Coastal Engineering Research Center, 1977). The deepwater wave data must then be transferred to the site of the proposed structure, which is usually located in shallow water relative to wavelength (except for floating, pneumatic, and hydraulic breakwaters), taking into consideration the effects of refraction, diffraction, reflection, and bottom friction phenomena. This can be done analytically either by graphical or computer methods (Bretschneider and Reid, 1953; Johnson, 1953; Dobson, 1967; Whalin, 1971; U.S. Army, Corps of Engineers, Coastal Engineering Research Center, 1977). The results of these studies will provide wave heights, wavelengths, and directions of approach at the site of the structure (or at the outer ocean limits of the model if a three-dimensional model study is conducted) as a function of the corresponding deepwater wave conditions. In most model studies concerned with the stability of coastal structures, the wave statistics can be presented in the form of frequency of occurrence data for the significant wave heights and wave periods ($H_{1/3}$, $T_{1/3}$). However, for some studies the effects on the structure of irregular wave trains which more closely represent the characteristics of actual prototype wind-generated waves must be determined. Prototype wave-spectra data are necessary for tests of this type. The maximum waves that can attack a coastal structure is dependent on the wave steepness, H/λ, relative depth, d/λ, slope of the bottom seaward of the structure, and the geometry and percent voids of the structure (Miche, 1944b; Danel, 1952; Kishi, 1959; Jackson, 1968; Weggel, 1973; U.S. Army, Corps of Engineers, Coastal Engineering Research Center, 1977).

Floating, pneumatic, and hydraulic breakwaters are generally impractical except for conditions where the water depths are large compared with wavelength. Thus, detailed bottom contour data (used for wave refraction

studies) are seldom required for model studies of these structures. Statistics of the wave dimensions, directions, and frequency of occurrence of local, wind-generated waves are the type of wave data needed for these studies. Some floating breakwater studies may require wave spectra data. However, wave data of significant wave dimensions should be adequate for most studies of pneumatic and hydraulic breakwaters. Information concerning the densities and weight distribution of the materials used to construct the breakwater, together with details of the geometry and dimensions of the structure is needed for calculation of the mass moments of inertia for both the transverse and longitudinal axes. Data are also needed concerning the mooring cables (length, diameter, mass density, and modulus of elasticity) and the cable assembly (number of cables and the positions of attachment to the structure).

The conduct of stability models of rubble-mound breakwaters, jetties, wave absorbers, seawalls, and the rubble-mound bases of composite breakwaters requires details of the structures' overall geometery and the characteristics of the armor units, underlayer rock, and core material. For some studies, it can be determined before the model study whether quarrystones of sufficient size and density to withstand the attack of the largest expected waves are available at competitive prices. Model tests are necessary in other studies to determine whether quarrystones are adequate as armor units, or whether concrete armor units of special shape are required. For quarrystone armor units, the expected shapes, the densities, and the estimated percentages of different size stone that will be obtained from the quarrying of selected rock formations within shipping or hauling distances of the prototype site are required; for concrete armor units, the shape of unit and density of concrete are required. Information is also needed as to the extent and frequency of damage that the structure can tolerate, and the economical and social consequences if damage were to occur to the point of failure. The latter information can affect the selection of design waves, and indicate the desirability of conducting tests in which the wave height is correlated with the amount of damage to the structure. The cost of repair versus the cost of constructing a breakwater or seawall that is not expected to be damaged can then be estimated from the test results, the construction and repair costs, and the interest rates during the economic life of the structure.

The normal water depths at the structure site and the range of water surface elevations about the selected stillwater level are important variables in the design of coastal structures (especially rubble-mound, composite, and vertical-wall structures), selection of design waves, and selection of model test conditions. Thus, statistical data of tidal ranges, wind setup, or storm surge are necessary for the design and efficient operation of stability models for all types of coastal structures.

b. Selection of Linear Scale. In the design of coastal structure models, it is desirable to obtain dynamic similarity with an accuracy sufficient for the needs of the design engineer, at the least possible cost of construction, operation, and analysis of test results. The

linear scale affects appreciably both the cost and the accuracy of test results, and should be selected, to the extent possible, so that viscous and surface tension forces are negligible compared with gravity forces. Economy dictates that the models be as small as possible; however, if a model is too small it may be difficult to adjust the test data analytically so that the results are of sufficient accuracy.

(1) Rubble-Mound Breakwaters, Jetties, Wave Absorbers, and Seawalls. Rubble-mound stability models are designed and operated based on Froude's law, and the scale effects are minimized as much as possible by selecting the largest practical size of model, relative to the prototype size. Within the limits prescribed by the need for accurate results, selection of scale is based on such practical considerations as the size of model armor unit available (compared with the estimated size of prototype armor unit required for stability), depths of the available wave flumes (compared with the prototype depths), and the capability of available wave generators (compared with the prototype wave dimensions). Insofar as possible, it is better to err on the conservative side. The linear scales that have been used with considerable success in the past, and can be used as a guide, range from about 1:5 to 1:70, model-to-prototype, depending primarily on the prototype water depths and wave dimensions relative to the dimensions of available wave flumes and the wave generator capacity. With the large wave flume (15 feet wide, 20 feet deep, and 635 feet long) at CERC, which has a wave generator capable of generating waves up to 6 feet in height, it is possible to conduct stability tests on rubble-mound structures using linear scales from about 1:5 to 1:10, depending on the prototype water depths and wave dimensions. These tests are expensive, however, and this facility is used mostly for basic research and for the solution of special problems. Tests in the large wave flume have also been useful in establishing the bases for determining correction coefficients for scale effects (obtained for similar models of smaller size). A large number of rubble-mound stability tests and model studies have been conducted at WES during the past 30 years, most of which were conducted in a wave flume 5 feet wide, 4 feet deep, and 119 feet long with a wave generator capable of generating waves up to nearly 1 foot in height. The linear scales of the model studies ranged from 1:30 to 1:68, with most of the studies conducted at scales from 1:40 to 1:50.

(2) Vertical-Wall and Composite Structures. Model studies are seldom necessary for vertical-wall breakwaters or jetties that will be situated in water depths sufficient to prevent the breaking of waves on the structure face, if the waves approach with an angle of incidence of 90°, or nearly so, and if there is no appreciable overtopping of the structure. For these conditions the theories of Sainflou (1928) (also Hudson, 1953; and Kamel, 1968a) and Miche (1944a) (also Kamel, 1968a) are adequate for determination of wave forces. In conditions where breaking waves occur, where the face of the structure is irregular, or where appreciable overtopping occurs, model studies usually determine the disposition and intensity of pressure over the face of the structure and the quantity of overtopping water.

The selection of linear scales for vertical-wall stability models is based partly on practical considerations, such as size and capability of available wave flume and wave-generating facilities. Another factor in scale selection is the size, sensitivity, response characteristics, and range of pressures over which available pressure transducers will operate with sufficient accuracy for purposes of the model study. When pressure transducers are used, the intensity of pressure must be measured simultaneously at different locations over the structure face so that the maximum total force can be calculated. Another method is the use of strain gages to measure the overturning moment and the vertical and horizontal force components, from which the stability of the structure in overturning and sliding can be calculated (Leendertse, 1962). Several research studies have been conducted which determined the magnitude of breaking wave pressures and impulses on vertical-wall surfaces (Bagnold, 1939; Mitsuyasu, 1966; Garcia, 1968; Kamel, 1968b). A few model studies have also been conducted concerning the measurement of wave forces due to breaking waves (Lundgren, 1962; Jackson, 1966; Nagai, 1968). The linear scales of these models ranged from about 1:20 to 1:50.

(3) Floating Breakwaters. The selection of linear scales for floating breakwater studies is, at times, based on the structure size, water depth, and wave dimensions in the prototype, versus the size of available wave flume and wave generator capability. However, prototype floating breakwaters are usually impractical except for relatively deep water and short wavelengths (in this respect the floating breakwater is similar to the pneumatic and hydraulic breakwaters), and the structures are not unusually large in cross section. Thus, if the structures were freely floating, the models could be of considerable size, relative to their prototype. However, the structures must be moored, in most instances with elastic cables, and the selected model scale may also be based on the similarity requirements of the mooring-line assembly. Most of the model studies conducted have used linear scales between 1:6 and 1:27 (Jackson, 1964; Davidson, 1971a).

(4) Pneumatic Breakwaters. A patent for a device to protect coastal areas and structures from water waves by a controlled flow of compressed air from a submerged pipeline was obtained by Philip Brasher in 1907 (U.S. Patent No. 843926); the device was installed at Crotch Island, Maine, in 1908 (Laurie, 1952). Other installations were made in Maine and Massachusetts in 1908, 1911, and 1912, and in El Segundo, California, in 1915 (Scientific American, 1916). These installations were credited with various degrees of success, but the estimates of wave height reductions were mostly subjective. Full-scale tests have been made in England (Evans, 1955; Heath, 1959; Bulson, 1961), Japan (Kurihara, 1955, 1956), Russia (Bogolepoff, 1937; Teplov, 1958; Radionov, 1960), and the United States (Sherk, 1960); experimental and theoretical investigations have been conducted in several countries (Schiff, 1943; Carr, 1950; Wetzel, 1955; Taylor, 1955; Bulson, 1968) in which the effectiveness of pneumatic breakwaters was studied in wave flumes using water depths of less than 1 foot to about 35 feet. However, a comprehensive series of controlled tests to determine the quantity of compressed air required to

provide desired percentage reductions in wave height, for various wave height, wavelength, and water depth combinations as a function of the Reynolds and Weber numbers, has not been performed. As a result, accurate transference equations to determine the horsepower requirements for proposed full-scale installations are not available, and there is a considerable divergence of opinion as to the effectiveness and feasibility of full-scale pneumatic breakwaters.

The nature of the compressed air-bubble screen phenomena and the types of facilities required to assemble a pneumatic breakwater are such that it is not necessary to perform model studies for other than the most complex prototype installations. However, additional laboratory tests should be conducted, using a wide range of test conditions and small, medium, and large wave flumes, to determine transference equations and scale-effect data that can be used by the design engineer for application to particular prototype situations. The test results would also indicate the linear scales to be used for model studies that may be deemed necessary for particular, complex, prototype installations. For each series of tests in the proposed investigation, values of the wave height reduction coefficient, H_t/H_i, should be obtained for values of d/λ from about 0.05 to 0.5 and for values of H_i/λ from about 0.01 to 0.10. The tests should be conducted by the procedures outlined in Section VI,2,f based on equations (6-14) to (6-20). To prevent exaggeration of the effectiveness of the pneumatic breakwaters, the transmitted wave height, H_t, should be measured a distance landward of the bubble screen where the horizontal current generated by the bubble screen is essentially zero.

(5) Hydraulic Breakwaters. Although the pneumatic breakwater was invented in 1907, the mechanism by which the reduction of wave heights is achieved was apparently not understood until Thijsse performed a few tests at Delft, Netherlands, in 1936 (Evans, 1955) and suggested that the wave reduction was caused by water currents generated by the rising air bubbles. In 1942, Taylor showed mathematically that a current directed against oncoming waves should stop all waves shorter than those of a certain critical length (Taylor, 1955), and White investigated the problem experimentally in 1943, using both air bubbles and water jets to generate the horizontal water currents (Evans, 1955). Carr (1950) conducted tests at the University of California in 1950 to investigate wave reduction by horizontal water currents generated by both the pneumatic and water-jet methods. Since 1950 several hydraulic breakwater investigations have been conducted, mostly in the United States. These tests were performed in wave flumes using water depths ranging from about 0.3 to 4.5 feet (Wetzel, 1955; Herbich, Ziegler, and Bowers, 1956; Williams, 1960; Williams and Wiegel, 1961; Nece, Richey, and Rao, 1968). However, no known full-scale hydraulic breakwater tests have been made. Several experimental investigations have been conducted to determine the ability of the hydraulic breakwater to reduce wave heights, and a few tests have been made to determine the effects of linear scale on the required discharge from the jet manifold to obtain specified reductions in wave height. However, more information is needed to obtain transference equations for the design engineers to accurately determine the horsepower requirements

for proposed prototype installations. The range of wave dimensions and water depths, and the wave gage position for measuring the transmitted wave heights, should be the same as those suggested for the pneumatic breakwater tests (Sec. VI,3,b). The test procedures should be according to equation (6-21) (Sec. VI,2,g).

c. Scale Effects. For complete dynamic similarity between model and prototype, the ratio of inertia forces of the two systems must be equal to the ratio of the resultant of all forces acting on the two systems (eq. 2-6), the ratio of the inertia forces of the two systems must be equal to the ratio of individual component forces (eq. 2-7), and the two systems must be geometrically similar. These conditions of similitude cannot be met completely as explained below and in Section II. The deviations of model test results from corresponding prototype behavior, caused by the lack of complete dynamic similarity, are known as scale effects. For coastal structure models the predominant force involved is usually gravity, and the models are designed and operated based on Froude's law. Thus, the scale effects to be considered when the test results are analyzed and transferred to prototype values are caused by the lack of similarity, model-to-prototype, of the other forces involved; i.e., viscous, surface tension, and elastic forces.

The conditions for similitude discussed above are imposed on the laboratory engineer by the laws of fluid dynamics. Other factors that influence the accuracy of model test results (and must be considered in addition to those due to scale effects) in model design and operation are:

(a) Type of wave generator and the distance between the generator and the test structure.

(b) Distance between the test structure and the wave absorber used in the shoreward end of the wave flume.

(c) Reflection coefficient of the wave absorber.

(d) Type, magnitude, and duration of attack of the test waves.

(e) Stillwater level selected for testing.

(f) Manner of determining the amount of damage to the test section when it is a rubble-mound structure.

(g) Accuracy with which the wave dimensions are measured.

(h) Other test conditions that must be selected by the laboratory engineer based on available prototype data and experience with similar model studies previously conducted.

Fan and Le Mehaute (1969) refer to the similitude relations dictated by the laws of mechanics as conditions of similitude, and conditions that can be specified by the laboratory engineer as criteria of similitude.

(1) Rubble-Mound Structures. Surface tension and elastic forces do not affect the stability of full-scale, rubble-mound structures in the field, and they are also negligible in hydraulic models of such structures. Viscous forces are also negligible for full-scale structures, but they become important in the model if the model is too small. For practical reasons, all rubble-mound stability models cannot be made of sufficient size to eliminate scale effects due to the lack of similarity of the viscous forces. Therefore, special tests have been necessary to determine the effects of linear scale and obtain scale-effect correction coefficients for the prediction or transference equations derived based on Froude's law. One such series of tests was conducted by Hudson and Jackson (1953) where a rubble-mound breakwater similar in cross section to that of an existing breakwater in San Pedro Bay, California (Fig. 6-5), was modeled and tested by the Froude law using linear scales of 1:30, 1:45, and 1:60. The test results are compared one to the other, and with storm damage to the San Pedro breakwater (Figs. 6-6 and 6-7). These results indicate that for the linear scales, prototype wave dimensions, and breakwater armor units used in these tests, the Froude law is sufficiently accurate for use in the design of such models. Other tests, the results of which can be used to determine the scale effects and corrective coefficients, were conducted by Dai and Kamel (1969). Their data, plotted to show the relation between N_S and R_n, are given in Figure 6-8; the data points that are in the range of values of R_n between 5.0×10^5 and 1.0×10^6 were obtained from tests conducted in the large wave flume at CERC, using waves up to 4 feet in height and armor units weighing up to 162 pounds. The averge value of the stability number as determined by the CERC data can be used as prototype values to obtain approximate corrective coefficients $(N_S)_p/(N_S)_m$. However, more data points are considered necessary for Reynolds numbers from about 3.0×10^4 to 1.0×10^6 to ensure that accurate values of the ratio $(N_S)_p/(N_S)_m$ are obtained.

A few investigations have been conducted from which the effects on test results of some of the "criteria of similitude" can be estimated; however, little quantitative information is available concerning these effects, and more data of this type are needed. There is also a need to standardize the model design and test procedures so that the differences in the test results for similar model studies obtained in different laboratories can be reduced to a minimum.

(2) Vertical-Wall Structures. When nonbreaking waves attack a vertical-wall impervious structure, the phenomena can be modeled with negligible scale effects. Since accurate pressure measuring and recording apparatus are available, and with the use of modern wave flume and wave-generating facilities, wave pressures can be determined with enough accuracy for design purposes when such model studies are necessary. When the attacking waves break directly on vertical-wall structures, shock pressures occur and cause scale effects that are difficult to define and measure. The magnitude and duration of shock pressures can be measured with enough accuracy using presently available pressure cells and

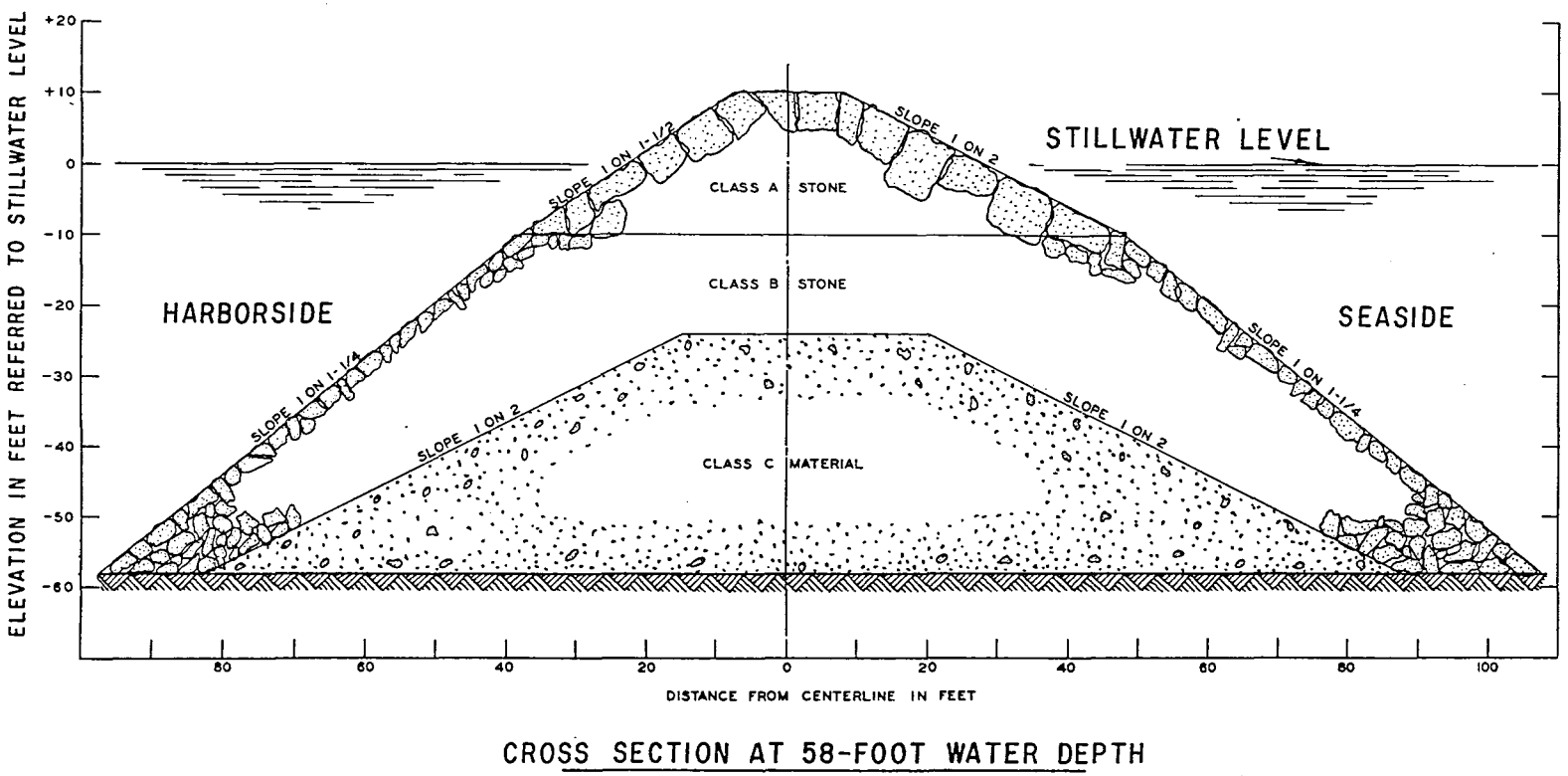

CROSS SECTION AT 58-FOOT WATER DEPTH

NOTE: CLASS A STONE IS SELECTED FROM QUARRY. NO PIECES LESS THAN 1 TON AND AT LEAST 75 PERCENT (BY WEIGHT) WEIGHING 10 TONS OR MORE EACH.
CLASS B STONE IS QUARRY RUN. NOT MORE THAN 25 PERCENT BY WEIGHT IN PIECES LESS THAN 20 LB, AND NOT LESS THAN 40 PERCENT IN PIECES OF 1 TON OR MORE EACH.
CLASS C MATERIAL IS A RESIDUUM FROM QUARRY OPERATIONS OR A DREDGED MATERIAL.

Figure 6-5. Prototype breakwater, similar to the existing breakwater at San Pedro Bay, California (Hudson and Jackson, 1953).

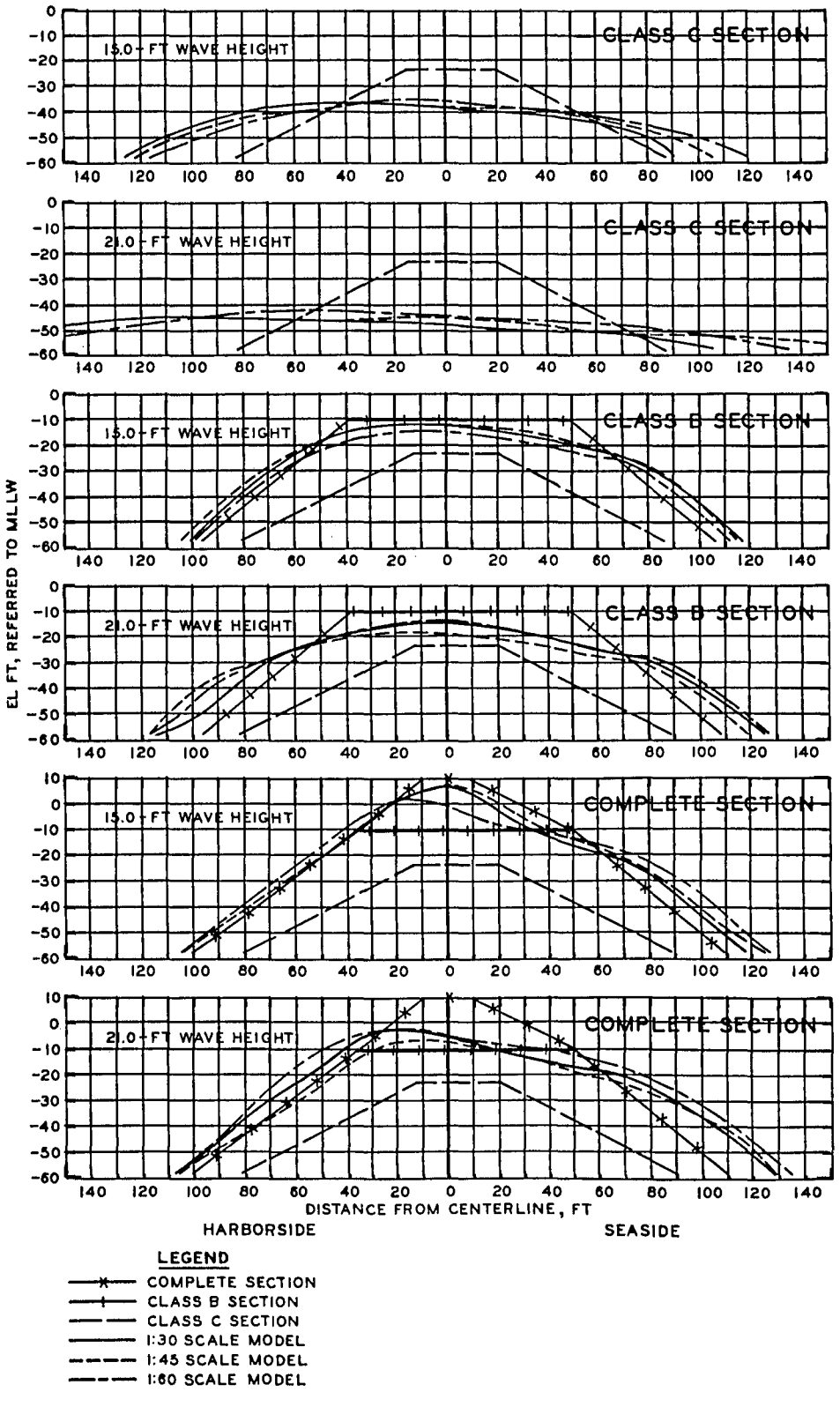

Figure 6-6. Scale-effect tests; comparison of sections after stabilization (Hudson and Jackson, 1953).

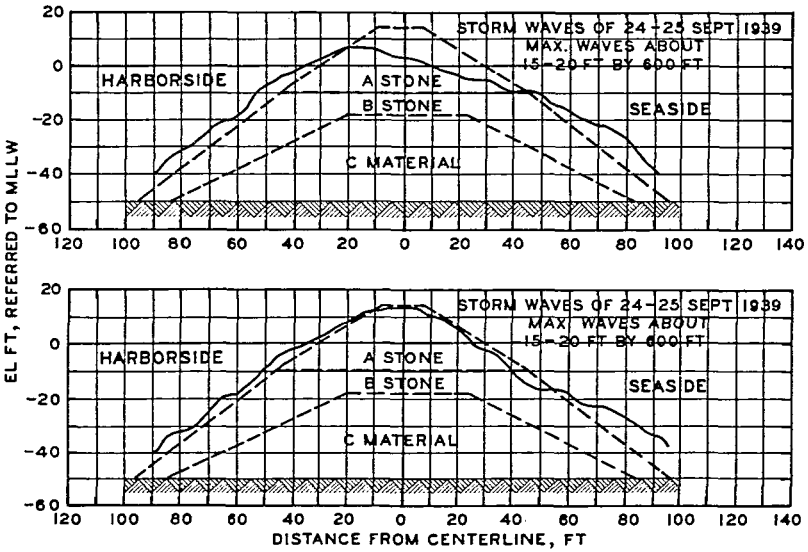

MAXIMUM AND MINIMUM STORM DAMAGE TO DETACHED BREAKWATER, SAN PEDRO BAY, CALIFORNIA

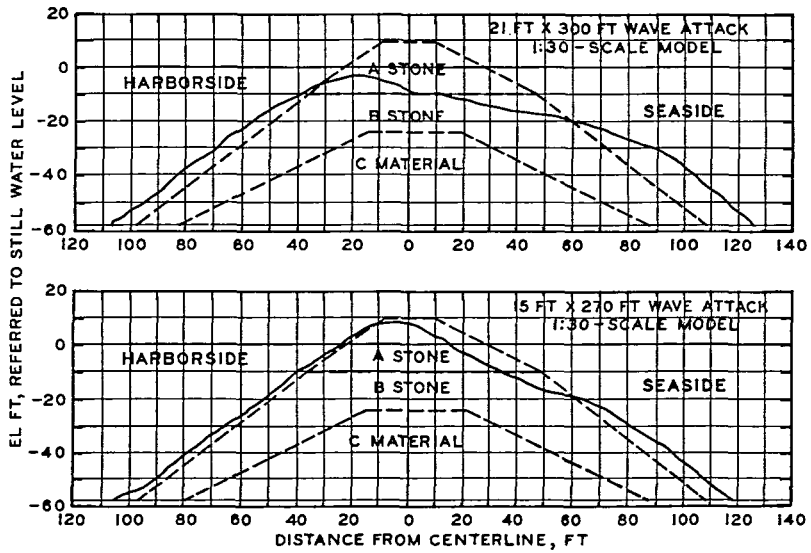

DAMAGE TO MODEL BREAKWATER WITH WAVE ATTACK UNTIL MOVEMENT CEASED

SPECIFICATIONS OF BREAKWATER MATERIALS

SAN PEDRO BREAKWATER

CLASS A STONE. QUARRY RUN, WEIGHING NOT LESS THAN 160 LBS PER CU FT (SOLID DRY), IN PIECES OF NOT LESS THAN ONE TON, OF WHICH NOT LESS THAN 50 PER CENT BY WEIGHT TO BE IN PIECES OF TEN TONS OR MORE EACH.

CLASS B STONE. QUARRY RUN, WEIGHING NOT LESS THAN 120 LBS PER CU FT (SOLID DRY), OF WHICH NOT MORE THAN 25 PER CENT BY WEIGHT TO BE IN PIECES OF LESS THAN 20 LBS EACH, AND AT LEAST 40 PER CENT BY WEIGHT TO BE IN PIECES OF ONE TON OR MORE EACH.

CLASS C MATERIAL. A MOUND OF DREDGED SAND SURMOUNTED BY A MOUND OF DREDGED CLAY.

MODEL BREAKWATER

CLASS A STONE. SELECTED STONE FROM QUARRY (STONE FROM QUARRY UNDER CONSIDERATION WEIGHS 165-170 LBS PER CU FT). NO PIECE TO WEIGH LESS THAN ONE TON, AND AT LEAST 75 PER CENT BY WEIGHT TO BE IN PIECES WEIGHING TEN TONS OR MORE EACH.

CLASS B STONE. QUARRY RUN, OF WHICH NOT MORE THAN 25 PER CENT BY WEIGHT TO BE IN PIECES OF LESS THAN 20 LBS, AND NOT LESS THAN 40 PER CENT BY WEIGHT TO BE IN PIECES OF ONE TON OR MORE EACH.

CLASS C MATERIAL. ALL RESIDUAL MATERIAL FROM QUARRY OPERATIONS, SIMILAR MATERIAL OBTAINED IN THE VICINITY OF THE QUARRY, OR DREDGED MATERIAL.

Figure 6-7. Comparison of known breakwater damage with result of model stability tests (Hudson and Jackson, 1953).

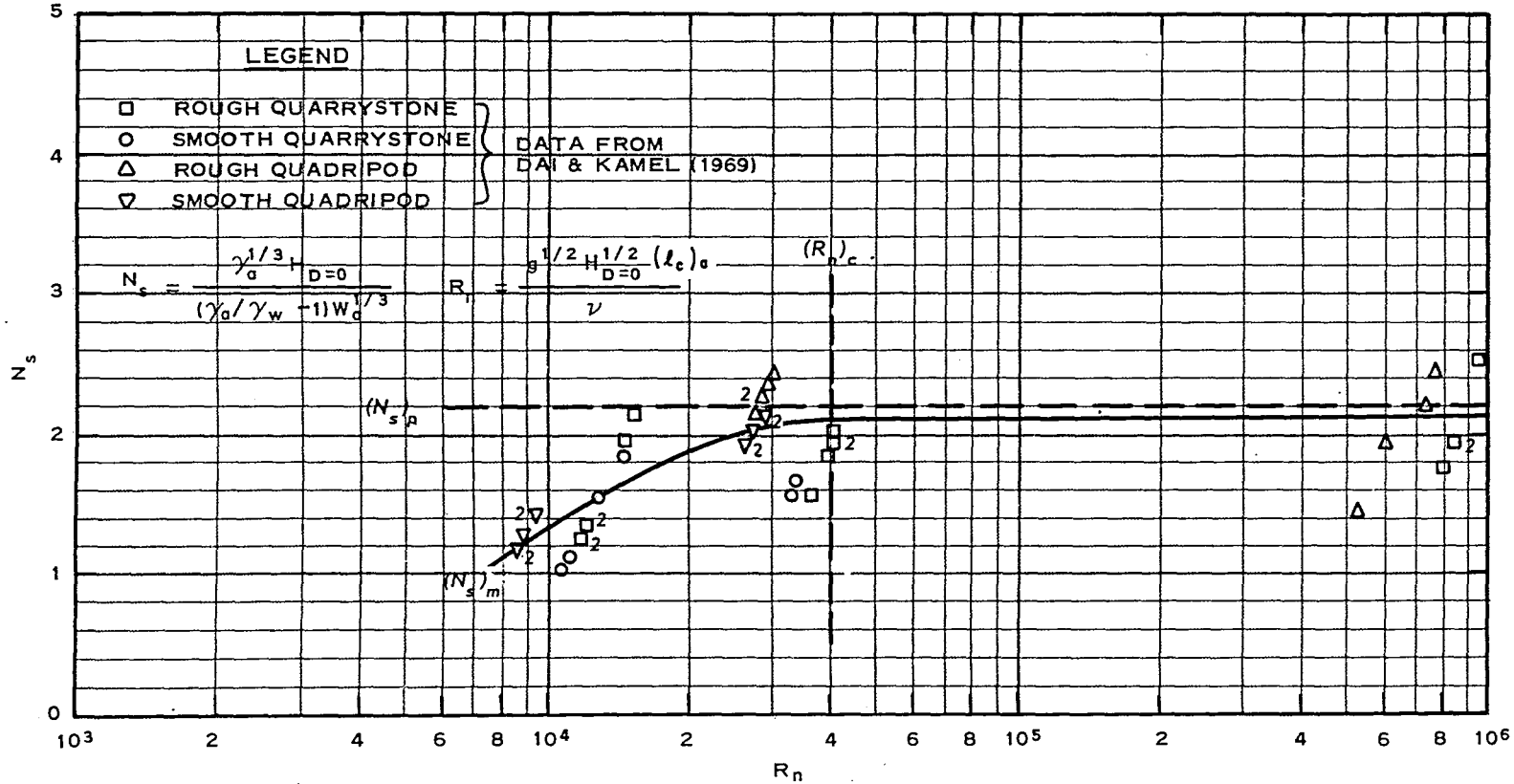

Figure 6-8. Scale effects of rubble-mound stability models (after Dai and Kamel, 1969).

electric recorders; however, the scale effects due to variations in the concentration of entrained air in model waves, compared to prototype waves and the difficulties of generating model waveforms that correspond to the complex wave spectra of prototype waves, cause large variations in individual pressure measurements that are difficult to interpret as prototype shock pressure impulses. Research is needed to accurately determine the effects of model scale and operating procedures on the model-to-prototype transference equations for breaking wave pressures.

(3) Floating Breakwaters. Scale effects in the oscillating characteristics of floating structures are negligible if care is taken to construct the breakwater geometrically and dynamically similar. The elastic and weight properties of the mooring lines can be modeled with enough accuracy in most cases. The largest errors that occur in this type of model study are those obtained by using monochromatic waves and the necessity of using two-dimensional rather than three-dimensional model structures. Most tests of floating structures are conducted in this manner for economic necessity. Studies are needed to determine the variations in test results for floating breakwaters with and without mooring restraints, for the conditions of two-dimensional, monochromatic waves compared with those using selected wave spectra and three-dimensional floating structures.

(4) Pneumatic Breakwaters. A considerable number of model and prototype studies have been done to determine the efficacy of pneumatic breakwaters. However, the prototype tests were not performed over a sufficient range of the primary variables, and the model studies have not been conducted so that accurate transference equations with known scale effects can be determined. Additional research is urgently needed to determine scale effects with sufficient accuracy that the design engineer can calculate, for a proposed installation, the quantity of free air that must be delivered by a compressor to the manifold system to obtain the required reduction in wave height to ensure satisfactory mooring conditions. These scale-effect tests should be performed under the suggested program of tests outlined in Section VI,2,f.

(5) Hydraulic Breakwaters. Hydraulic breakwaters are similar to pneumatic breakwaters in that the mechanism that effects a reduction in wave height is a system of horizontal currents. Scale-effect tests are needed to obtain accurate data concerning the discharge of water from the orifices of the manifold system required for the required reduction of wave heights. However, the tests required are not as numerous or as complicated as those needed for pneumatic breakwaters. The scale-effect tests for hydraulic breakwaters should follow the suggestions given in Section VI,2,g.

4. Model Operation.

a. Selection of Test Conditions. In general, test conditions selected for model studies concerning the stability of coastal structures are determined by the type of structure under consideration, the purpose and scope

of the model study, the available statistical data describing the wave environment, and other factors that influence the severity of wave attack. The need for a model study, the type of structure required for optimum performance, and the purpose and scope of the model study are usually determined at the time preliminary designs are made, based on theoretical and experimental information available in the literature and field data already available or obtained especially for the particular investigation. If, during preliminary design, it is not possible to decide which type of structure will best serve the purpose for which the structure is to be constructed, the purpose and scope of the model study could be enlarged to include tests to determine comparable designs of two or more types of structures so that the most economical structure could be selected. A typical testing program will include tests of the structures as originally envisioned by the design engineer, and tests of any modifications in design developed during the course of the investigation.

Test conditions for model studies must be selected based on considerations of all the variables that affect the structure's ability to perform an intended function at a minimum cost and with a minimum risk factor. For the types of structures under consideration, the important variables generally include (a) the shape and size of the structure, (b) the materials used in construction, (c) the shape, size, and density of the armor units (if a rubble-mound structure), (d) the stillwater depth at the seaward toe of the structure, (e) the bottom slope seaward from the structure toe, (f) the range of astronomical tide, and (g) the largest wind setup or storm surge (or setdown) expected to occur with sufficient frequency that it should be added to the high tide (and subtracted from the low tide) conditions selected for the testing program. For floating breakwaters the testing program will usually include tests with different types of mooring conditions. In the case of floating, pneumatic, and hydraulic breakwaters (which are usually ineffective for conditions other than deepwater and short-period waves), the tidal range, magnitude of wind setup or storm surge, and the bottom slope seaward of the structure are not important variables for the proper functioning of the structure or the selection of test conditions. In the selection of test waves for rubble-mound, vertical-wall, composite, and seawall types of coastal structures, the possibility that the design engineer might recommend a structure that would not be completely stable for the maximum storm wave condition should be considered. This could occur if it is judged less expensive to repair the structure after the occurrence of severe storms than to select a design wave to keep the structure from being damaged during its economic life.

The largest and most destructive wave that can attack a rubble-mound or vertical-wall structure is a function of the wave dimensions in deep water, the bottom contours between deep water and the structure site, water depth at the structure toe, bottom slope seaward of the structure toe, and the seaside slope, crest height, and porosity of the structure. Experiments to determine the limiting heights of both breaking and nonbreaking waves that can attack typical rubble-mound breakwater sections have been conducted by Jackson (1968) and Weggel (1973). Similar tests

for vertical-wall breakwaters and nonbreaking waves were conducted by Danel (1952). However, for model studies of some structures where the maximum wave that can attack has not been determined and estimates of the maximum waves based on depth limitation ($H_{max} = 0.78d$) are not adequate for use as design waves, special tests must be performed to determine the maximum waves that can attack the test structures. Such waves should be determined for both high and low design water levels, using selected wave periods within the range of periods that occur in the prototype wave environment. Tests by Danel (1952) and Jackson (1968) were conducted using simple, monochromatic wave trains of constant height. Model tests of proposed structures to determine the maximum wave that can reach the structure, and stability tests to determine the optimum design of such structures using the maximum breaking waves, have also been conducted using simple wave trains of regular height and period. Tests of this type using irregular wave trains would be difficult to conduct in such a way as to ensure that the selected test-wave spectra included the wave height-wave period combination that corresponds to the maximum wave that could attack the structure, unless the maximum wave had been determined previously using the simple type of wave train.

b. Generation of Test Waves.

(1) Short-Period Wave Generators. In stability models of coastal structures where the major forces are due to short-period, wind-generated waves, the test waves are generated by the periodic displacement of water in a wave flume. Water is displaced by a vertical plunger, a horizontal bulkhead motion, or a rigid plate hinged at the bottom and driven by a crank and rod attached near the top of the plate. The latter is referred to as a flap generator. Most other types of mechanical generators incorporate the characteristics of one or more of the above-listed generators. The pneumatic-type wave generator, in which the periodic displacement of water is accomplished by the variation of pressure above a body of water in a confined pneumatic chamber, has also been used to generate short-period waves; however, this type is probably better suited for the generation of long waves, such as seiches, surges, tides, and tsunamis. Wave generators may be used to produce simple wave trains of nearly constant height and period, or they can be programed to generate irregular waves of variable height and frequency. Irregular waves can also be generated in a wind-tunnel type of wave flume by the action of wind blowing over the water surface, or by the combined action of wind and a mechanical or pneumatic generator.

Equations for determining the wave heights generated by the various wave machines are useful in designing new generators, in selecting linear scales for proposed models using existing generators, and in reducing the work required to calibrate existing generators for use in model tests. Equations based on the complete linear wave generator theory have been derived for the piston and flap generators (Ross and Bowers, 1953), but these equations do not apply to the plunger type and are not strictly applicable for waves of large steepness (experiments by Ursell, Dean, and Yu (1958) showed that the measured wave heights generated by a piston

generator were about 10 percent less than indicated by small-amplitude theory for wave steepnesses between 0.045 and 0.048; for steepnesses between 0.002 and 0.03 the experimental values were only 3.4 percent less than the theoretical). The wave height that a generator produces can also be estimated with sufficient accuracy, for the purposes mentioned above, by using an equation based on a simple wave generator theory. This equation, derived by equating the volume displaced by the wave generator in one-half of a wave period to the elevated volume in one-half a wavelength of a sinusoidal wave, is

$$H = \frac{2\pi}{\lambda} \overline{V}_w \tag{6-22}$$

where λ is wavelength and $\overline{V}_W$ is the volume of water, displaced per foot length of generator in one-half the wave period, that is used in the generating of that part of the wave train that travels toward the test section (some generators displace water in both directions depending on the type and shape of the generator, and all have some leakage between the generator and the flume walls and bottom). Since $\overline{V}_W = S(\ell_c)_G - \Delta\overline{V}_W$, where S is the generator stroke, $(\ell_c)_G$ is a characteristic linear dimension of the generator, and $\Delta\overline{V}_W$ is the leakage volume,

$$H = \frac{2\pi}{\lambda} \left[S(\ell_c)_G - \Delta\overline{V}_w \right] . \tag{6-23}$$

With proper care $\Delta\overline{V}_W$ can be reduced to such an extent that, for the purposes discussed above, it can be ignored. For the shapes of generators shown in Figure 6-9, Galvin (1964) gives the following values for $(\ell_c)_G$:

Generator	$(\ell_c)_G$ (ft)
Piston	d
Flap	d
Cylindrical plunger	r
Prismatic plunger	b + h tan α

The terms S, d, r, b, h, and α are as shown in Figure 6-9. Galvin's experiment showed that observed values of wave height were in good agreement with those calculated from equation (6-23), except for the flap-type generator. Ursell, Dean, and Yu (1958), state that the equation for the flap generator (derived on the basis of the complete linear wave generator theory and which agrees with the equation derived on the basis of the simple theory for values of $2\pi d/\lambda < 1$) should be as applicable as the equation derived for the piston-type generator. The lack of verification of the theory for the flap generator was considered the result of effects not accounted for in the theory, such as leakage around the edges of the generator, motion of the generator which was not simple harmonic, or other effects. Additional research is needed to determine whether the flap generator theory is as accurate as the theories for the other generators and to determine the effects of leakage and other factors on the generated wave heights.

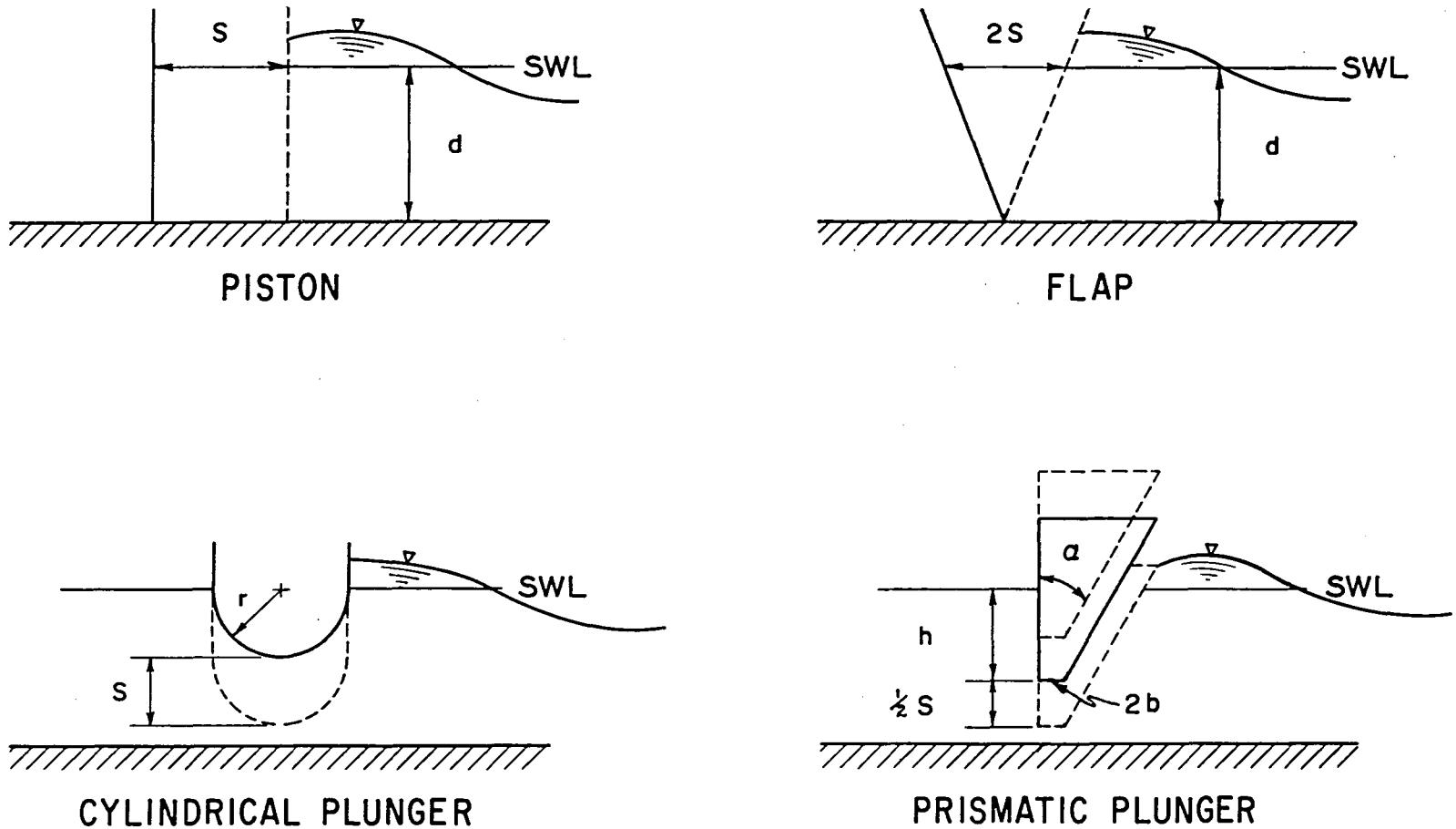

Figure 6-9. Types of wave generators (Galvin, 1964).

The above discussions of wave generators show that, except for the flap generator, even the simple theory is accurate enough for determining wave heights for the design of new generators, in selecting linear scales for proposed models, and as a basis for correlating test results to reduce the work required to calibrate a generator. However, for model studies of coastal structures, the wave generator should be calibrated as accurately as possible, over the ranges of the variables used in the testing program, and under the conditions that exist in the wave flume. The calibration curves obtained should be checked at regular intervals.

The horsepower required to operate a wave generator must be sufficient to supply the power necessary for generation of the waves, including the waves generated in the rear of the generator, leakage around the edges of the generator, and the inertia and friction forces of the generator assembly. The required wave power as determined from wave theory is

$$\text{Wave power} = \frac{\text{Group Velocity} \times \text{Wave Energy}}{\text{Wavelength}}$$

from which the wave horesepower per foot of generator is

$$\text{WHP} = \frac{k}{550}\,\frac{1}{16}\,\gamma_w H^2 V\left(1 + \frac{\frac{4\pi d}{\lambda}}{\sinh\frac{4\pi d}{\lambda}}\right) \tag{6-24}$$

where γ_w is specific weight of water, V is the wave velocity

$$V = \left(\frac{g\lambda}{2\pi}\tanh\frac{2\pi d}{\lambda}\right)^{1/2} \tag{6-25}$$

and k is a coefficient that is a function of the generator shape. $k = 2$ for the piston, flap, and cylindrical plunger, less than 2 for the prismatic plunger, depending on the value of b, and can be made less than about 1.5 by inclining the bottom part b of the plunger toward the wave direction, and placing a fixed vertical plate within about 0.5 inch of the rear face of the plunger. Experiments conducted at CERC (Madsen, 1970) indicate that leakage around the edges of a generator can cause a considerable reduction in wave height if care is not taken to reduce leakage to a minimum. However, if the use of zero-linkage gaskets are attempted, the friction factor may increase the horsepower requirements appreciably. Thus, an acceptable compromise must be determined. The horsepower required to operate the wave generator, excluding that required for the wave power alone (eq. 6-24), is difficult to calculate accurately, varies considerably with the type of generator, and is usually estimated from previous experience. The ratio of the motor horsepower (mhp) to the wave horsepower (whp) varies with the inertia of the generator, wave period, friction, leakage, and ability of the machine to generate a pure sinusoidal wave. The peak power required can be reduced considerably by an inertia (fly) wheel. Typical

values of the mhp to whp ratio for wave generators in use at different laboratories (using values of k in equation 6-24 of 1.5 and 2.0 for plunger and flap generators, respectively) are presented in Table 6-1.

(2) Tsunami Generators. Tsunamis are seismic sea waves caused by submarine earthquakes and volcanic eruptions of the ocean floor. The explosion of an atomic bomb underwater can also generate a tsunami. An active seismic belt extends around a major part of the Pacific Ocean with all bordering coastal zones subject to the attack of tsunamis. These disturbances travel in a series of waves of long lengths and periods, at the speed of

$$V = (gd)^{1/2} . \qquad (6\text{-}26)$$

Tsunamis in the open ocean have lengths as much as 100 miles or more, and can travel at speeds in excess of 600 miles per hour, depending on the depth of water; their heights in the open ocean are unknown, but probably do not exceed 1 or 2 feet. As tsunamis approach shore, shoaling effects cause a decrease in speed and wavelength and an increase in height. The heights of tsunamis can be greatly increased in bays if the bay's configuration and bottom contours are such that resonance is obtained between the period of the incident waves and the natural period, or one of the harmonics of the water mass in the bay. Tsunami wave periods from 5 to 60 minutes are common, and wave heights on the Pacific coast were as high as about 20 feet at Crescent City, California, in 1964 (Keulegan, Harrison, and Mathews, 1969), and about 35 feet at Hilo Harbor, Hawaii, in 1960 (Eaton, Richter, and Ault, 1961). Heights of nearly 100 feet have been reported in Japan (Ichiye, 1958). When tsunamis approach shore, in the water depths where coastal structures are located, two types of phenomena may occur, depending on the steepness of the wave front. If the steepness is large the front advances in the form of a wall of water, or bore, and breaks in the manner of surf where the water depth is approximately equal to the bore height. For smaller steepnesses the tsunami appears as a rise in sea level, and will simply overflow the land area if the rise above mean sea level is of sufficient height relative to the elevation of the coastal areas. Thus, coastal structures should be designed to withstand the frontal attack of bores with steep fronts and the overtopping of these structures due to either type of tsunamis where the height is sufficient to cause overtopping.

Theoretical and experimental investigations of three types of bore generators (piston, gate, and pneumatic) were made by Shen (1965); a theoretical study of pneumatic wave generators was made by Keulegan (1966). Based on these studies, the pneumatic generator is considered the most practical for use in wave flumes to determine the stability of coastal structures that will be subjected to the attack of tsunamis. This type of generator consists of a pneumatic tank similar to that shown in Figure 6-10. The upper part of the tank has a constant cross section, and the lower part transforms gradually into a horizontal nozzle. The angle of expansion of the nozzle is small enough to prevent separation of flow. Water is drawn into the tank with a vacuum pump to the height

Table 6-1. Values of mhp/whp for various wave generators.

Laboratory	d (ft)	H_{max} (ft)	T [1] (s)	mhp/whp
Piston generator				
CERC	14.50	6.00	14.0	2.5
CERC	1.20	0.67	3.5	13.6
University of California	2.10	0.50	1.0	41.6
University of California	5.20	1.00	2.0	11.4
University of California	4.40	0.80	1.4	14.1
University of California	0.70	0.25	0.6	34.7
Flap generator				
C.H.L., France	3.94	0.98	3.5	3.5[2]
MIT	2.50	0.80	3.0	4.4
N.H.L., Chatou	4.93	1.48	2.0	7.4
N.H.L., Chatou	8.21	1.64	3.0	5.4
Osaka University	6.60	1.60	3.0	9.2
Osaka University	2.60	0.70	1.5	2.0
Osaka University	4.30	1.30	3.0	6.0[3]
Queen's University	4.25	0.83	2.0	14.2
Queen's University	4.25	0.83	2.0	21.2
Queen's University	3.28	0.50	1.4	20.4[2]
Technical University of Denmark	2.62	0.92	1.2	9.7
University of California	0.90	0.60	1.3	4.3
University of Minnesota	4.50	1.67	1.9	12.6
WES	3.00	1.00	3.0	5.4
Piston-flap combination				
C.H.L., France	3.28	0.98	3.5	10.4[2]
MIT	1.50	0.60	2.0	10.4
N.H.L., Chatou	5.57	1.64	5.0	12.0
N.R.C., Canada	3.00	1.50	2.3	10.3
N.R.C., Canada	3.00	1.65	2.3	7.7
Plunger generator				
MIT	1.00	0.21	1.5	29.6
University of Hawaii	6.00	3.00	3.0	2.9
University of Minnesota	1.00	0.27	0.6	4.3
WES	3.00	0.75	1.0	21.9
WES	3.00	0.75	1.0	32.7

[1] Wave period corresponding to the maximum wave height that can be generated in water depth, d.

[2] Irregular waves.

[3] Waves generated with wind blower.

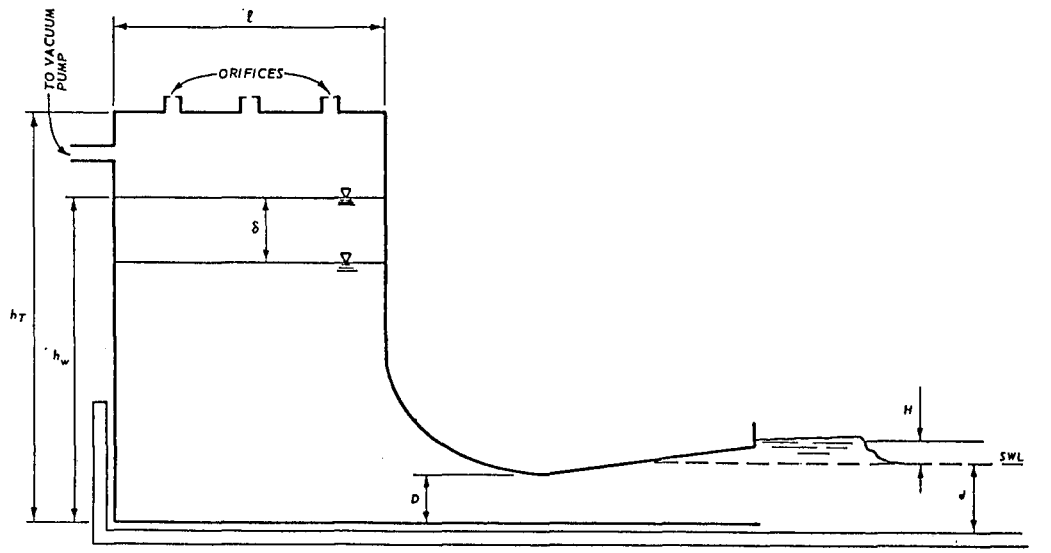

Figure 6-10. Pneumatic bore generator.

necessary for generation of the model tsunami. The pressure in the air chamber above the raised water is then below atmospheric. To generate the wave, the water in the tank is discharged by allowing air to enter the chamber through several ports, the areas of which may be varied as required by removable circular-orifice plates. Each port is fitted with valves actuated by microswitches to control the rate of air entering the pneumatic chamber by programing a sequence of opening and closing each port. This results in a variation of the port area as a function of time so that, with proper calibration, reproduction of the selected bore height, shape, and duration of overtopping of the test structure can be obtained. Design of the tank height and length with enough head and water volume available to generate the maximum wave can be accomplished by the equations derived by Keulegan (1966),

$$\frac{H}{d} = \left(\frac{h_w}{d} - 1\right)\left(1 - \frac{1}{4}\frac{H}{d}\right)\frac{k_1}{1+f} \tag{6-27}$$

$$2k_2 = \frac{H}{d}\frac{(gd)^{1/2}}{(h_w - d)}\left(1 - \frac{3}{4}\frac{H}{d}\right)\frac{d}{\ell} \tag{6-28}$$

$$\frac{2k_2}{k_1} = \frac{(gd)^{1/2}}{(1+f)\ell}\left(1 + \frac{1}{2}\frac{H}{d}\right) \tag{6-29}$$

$$\frac{\Delta p}{\Delta p_o} = 1 - k_1 - 2k_2 t \text{ ; and } \frac{\Delta p_o - \Delta p_i}{\Delta p_o} = k_1 \tag{6-30}$$

$$\Delta p_o = \rho g\left(h_w - d\right) \tag{6-31}$$

$$2k_2 = \frac{KC_d A}{1 + \gamma\left(\frac{h_w - d}{h_T - h_w}\right)\frac{p}{\Delta p_o}} \tag{6-32}$$

$$K = \frac{c_o \gamma^{1/2}}{\left(\overline{V}_{air}\right)_o}\left(\frac{p_{at}}{\Delta p_o}\right)^{1/2}, \text{ and } C_d = 1 \tag{6-33}$$

$$u_2 = (gd)^{1/2}\frac{H}{d}\left(1 - \frac{1}{4}\frac{H}{d}\right) \tag{6-34}$$

$$V = (gd)^{1/2}\left(1 + \frac{3}{4}\frac{H}{d}\right) \tag{6-35}$$

$$\delta\ell = VtH \tag{6-36}$$

$$f = 0.83\left(\frac{d}{D}\right)^2 \frac{H}{d} \tag{6-37}$$

The terms in the above equations are defined as follows:

A = area of ports prorated per foot of chamber width, ft^2

C_d = coefficient of discharge for orifice

c_{at} = velocity of sound for outside air, ft/s; $c_{at} = 49.1(\theta)^{1/2}$, where θ temperature in degrees Rankin = 460 + °F.

D = depth of narrowest part of the nozzle, ft

d = undisturbed depth of water at nozzle mouth, ft

f = friction factor of nozzle

g = acceleration of gravity, ft/s^2

H = wave height at nozzle mouth, ft

h_T = elevation of pneumatic chamber ceiling (height of tank), ft

h_w = elevation of water in the pneumatic chamber at the start of the wave, ft

ℓ = width of pneumatic chamber in horizontal direction, ft

p = pressure in pneumatic chamber, measured relative to atmospheric pressure, lb/ft^2

p_o = atmospheric pressure outside of pneumatic chamber, lb/ft^2

u_2 = wave particle velocity at nozzle mouth, ft/s

V = wave velocity, ft/s

$(\overline{V}_{air})_o$ = initial volume of air in pneumatic chamber per foot of chamber length = $\ell(h_T - h_w) \times 1.0$, ft^3

γ = ratio of specific heats, for air $\gamma = 1.40$

Δp = suction pressure in pneumatic chamber during the subsequent wave motion, lb/ft^2

Δp_i = suction pressure in pneumatic chamber at the beginning of wave motion, $poundals/ft^2$

Δp_o = initial suction pressure in pneumatic chamber to raise water to height h_w, lb/ft^2 (Δp_o is a positive quantity)

δ = fall of water surface in pneumatic chamber, ft

ρ = density of water, lb/ft^3

Application of the above equations to the design of a pneumatic generator for use in a three-dimensional tsunami model of Hilo Bay, Hawaii, is discussed by Keulegan (1966). The generator actually used in the Hilo Bay model study is described by Palmer, Mulvihill, and Funasaki (1967). The use of equations (6-25) to (6-37) in the design of the pneumatic generator for a two-dimensional, wave flume study concerning the stability of a proposed rubble-mound tsunami barrier for the protection of Hilo Harbor (with details on the use and calibration of the generator and wave flume) is presented by Kamel (1967).

c. Construction of Model Structures.

(1) Rubble-Mound Structures. Rubble-mound breakwaters, jetties, seawalls, and wave absorbers in nature are usually constructed with a core material consisting of quarry-run stones, two outer layers of selected armor stones and enough intermediate underlayers to provide protection to the core material, and good bedding for the armor stones. The armor stones are of sufficient weight to withstand the forces of the selected design wave, the first underlayer stones are slightly larger than that required to prevent leaching of the underlayer material through the voids in the armor stones (usually about one-tenth the weight of the armor stones), and the quarry-run core material is composed of that part of the blasted rock not used in the underlayers or for armor stones. Quarry-run stones usually vary from 10 pounds or less to about 4 tons, depending on the type of rock, method of blasting, and the design wave

height. According to Quinn (1972), a quarry consisting of fine-grained basalt may break into relatively small pieces in sizes only about 6 percent heavier than 8 tons; however, a quarry composed of hard anorthosite (a type of diorite), by special drilling patterns has produced relatively large pieces, as much as about 12 percent in sizes between 8 to 15 tons and about 15 percent larger than 15 tons. Twenty-ton stones are about the largest size that can be quarried economically in enough quantities for armor stones. When the design wave height requires a size of armor stone that cannot be quarried economically near the proposed structure, it becomes necessary to use one of the several available types of molded concrete armor units for which accurate stability coefficients have been determined.

There are several methods of constructing rubble-mound structures in the field, depending on the type of structure, the size of the armor units, the depth of water, the degree of wave protection during construction, and the equipment available for placing the material. When water depths permit, the core and underlayer materials that are underwater are usually dumped from scows, the armor units are usually placed individually from a floating plant by crane using a sling, and the underlayer stones upon which the armor units rest can be placed from a scow (if the stones are not too large) or from a floating plant by crane using an orange-peel type of grapple. Special techniques may be used in the placing of stone armor units to increase the stability of the cover layers against wave action, such as placing all long-axis stones with the longer axis perpendicular to the face slope, and using special care in the nesting of each armor rock; however, it is usually too expensive to ensure that such placing will be accomplished satisfactorily in the prototype except for that part of the structure that is above water. Thus, most rubble-mound structures are designed and constructed using a random or pell-mell type of placement technique. Certain shapes of concrete armor units can be placed in a regular pattern to greatly increase the stability coefficient, but the required placing techniques for these units are also expensive, and such methods are not presently in common use. The required placing techniques for some of the concrete armor units have been, or can be developed in the laboratory, and as marine contractors accept these special placing techniques, their use should become more frequent. Therefore, the construction of small-scale, rubble-mound structures for use in hydraulic model investigations duplicates as closely as possible the techniques used in the field.

Scale models of rubble-mound structures are constructed in a wave flume on a sand base. The core material, underlayer stones, and armor units are placed with the flume dewatered (Fig. 6-11). The core material, which usually consists of crushed basalt or limestone, sized and graded to represent the material that will be used in the field using the proper scale relationships, is saturated with a hose and then compacted with a hand trowel to simulate natural compaction resulting from wave action during construction of the full-scale structure. The underlayer material is placed by shovel and smoothed to grade by hand without compaction or the rearranging of individual stones. The armor units are placed by hand

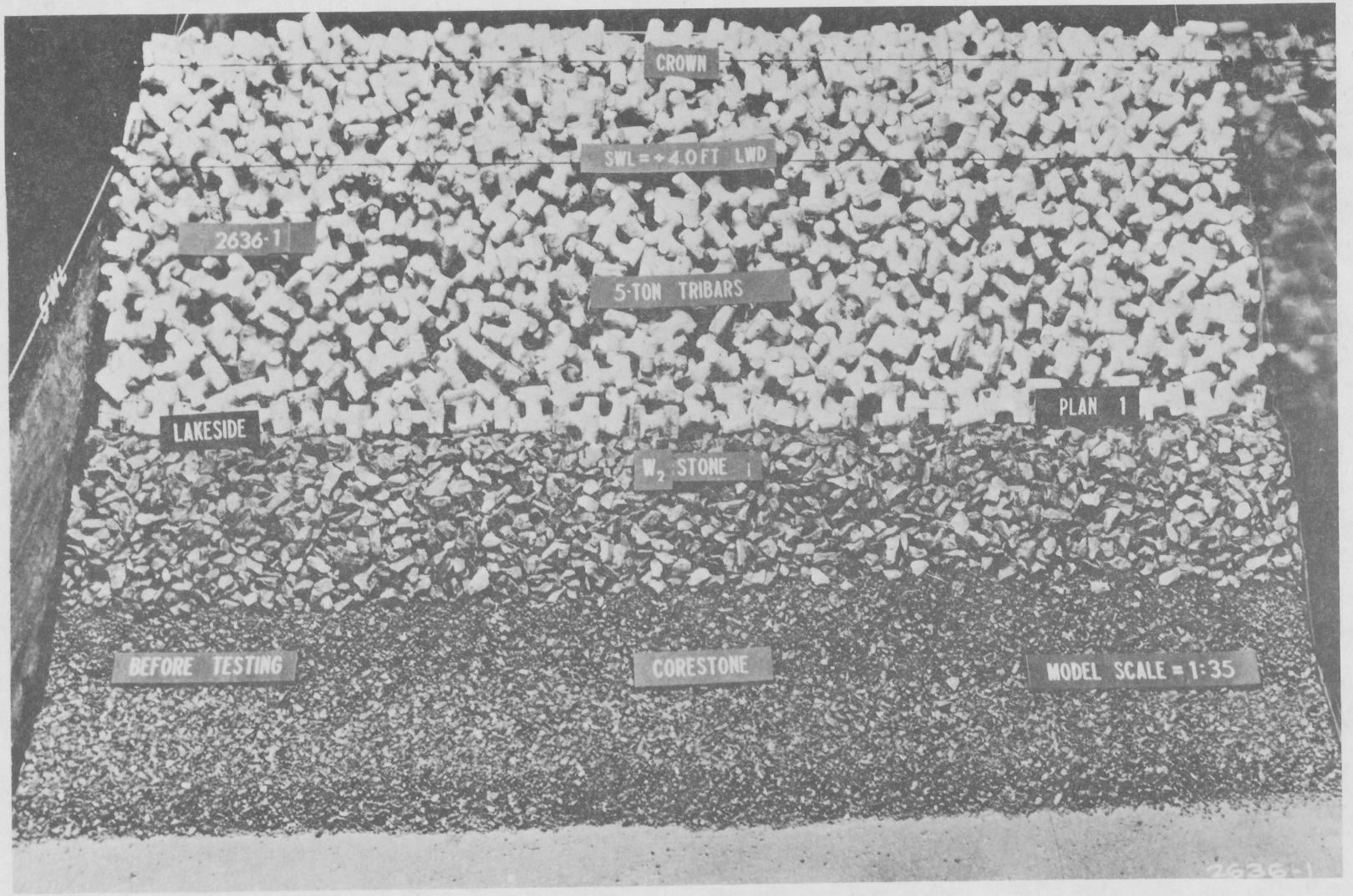

Figure 6-11. Rubble-mound breakwater section before wave attack (tribar armor units are randomly placed) (Jackson, 1967).

to simulate the type of placing technique used in construction of the prototype structure. Most armor units are randomly placed without attempting to obtain an interlocking action between units. Before each series of tests, each newly constructed test section is subjected to a few waves of sufficient height to provide a slight shaking down and consolidation of the armor units and underlayer material. This is done under the assumption that a prototype structure will be subjected to waves of progressively greater height at the outset of a given storm, and that it will be unusual for the design storm wave or one of greater height to occur immediately after construction has been completed.

The preparation of the material for construction of scale models of rubble-mound structures, except for the core material, is tedious, time consuming, and because of the labor involved, expensive. After the core material has been crushed, it is sized by a power-shaker type of seive assembly. Some of the smaller sizes of the underlayer material are also sized by the power shaker, with the unusually long pieces removed by hand. Model armor units that simulate full-scale quarrystone armor units are usually crushed basalt or limestone and handpicked and sized with a chipping hammer and weighed on a torsion balance with a sensitivity of one-tenth of a gram. Model armor units that simulate full-scale concrete armor units of special shape (tetrapods, tribars, dolosse, etc.) are molded of aluminum-magnesium alloy, zinc-magnesium alloy, polyester fiberglass premix material, or a mixture composed of sulfur, silicon, and barite or sand. A typical mixture is composed of 90 percent Cylcap (a commercial name for a sulfur-silicon compound) and 10 percent barite, or 78 percent Cylcap and 23 percent Ottawa sand. Units molded with this mixture have a specific weight of about 140 pounds per cubic foot. This mixture must be heated to a temperature between 110° and 116° Celsuis (230° and 240° Fahrenheit), and special precautions must be taken to prevent the breathing of fumes if overheating of the mixture occurs. Because of the difficulty and expense of obtaining and sizing stone armor units and the molding of special armor-unit shapes, all the units prepared for model studies and research projects are retained for future use. The sizes and weights of the units on hand at a particular time, together with the sizes and weights of prototype units estimated to be required for a proposed project, determine to a considerable extent the model scale selected for a proposed model study.

(2) Vertical Wall Structures. Vertical-wall structures in the model may be constructed of wood, with a special section for pressure cells and wave rods constructed of steel (Fig. 6-12); the structures may also be constructed partly of wood and filled with gravel with a cap molded of concrete (Fig. 6-13), or of transparent plastic. Because the structures are usually simple in cross section, fabrication is not difficult unless they are relatively small and do not provide enough space for the required instrumentation. This situation can result in the use of larger models.

(3) Floating Breakwaters. Full-scale floating breakwaters may be formed of log rafts, steel A-frame with steel pontoon outriggers, rectangular pontoons constructed of wood, steel, or concrete, steel or concrete

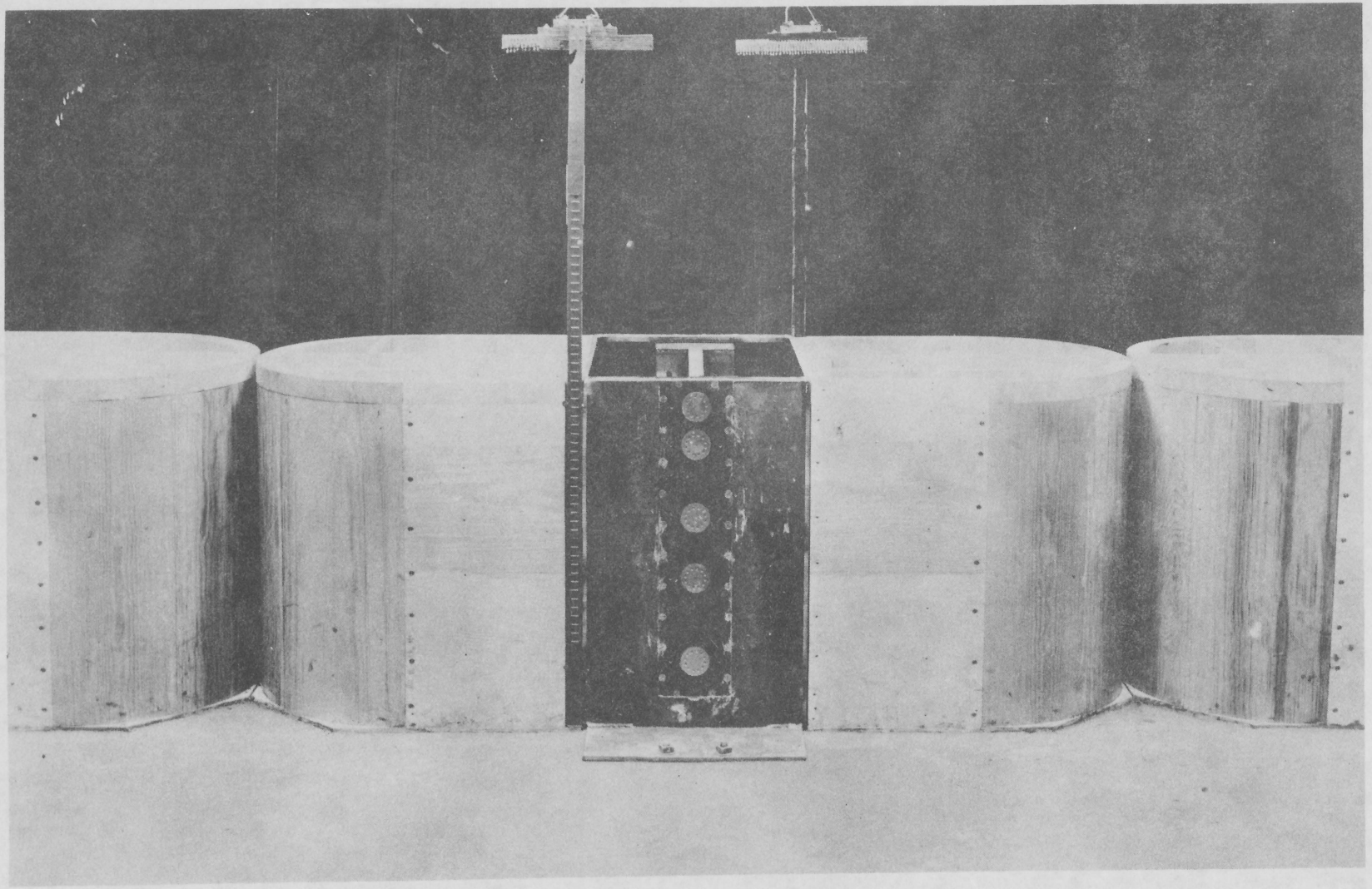

Figure 6-12. Vertical-wall breakwater section constructed of wood; pressure-cell section constructed of steel (Hudson, 1945).

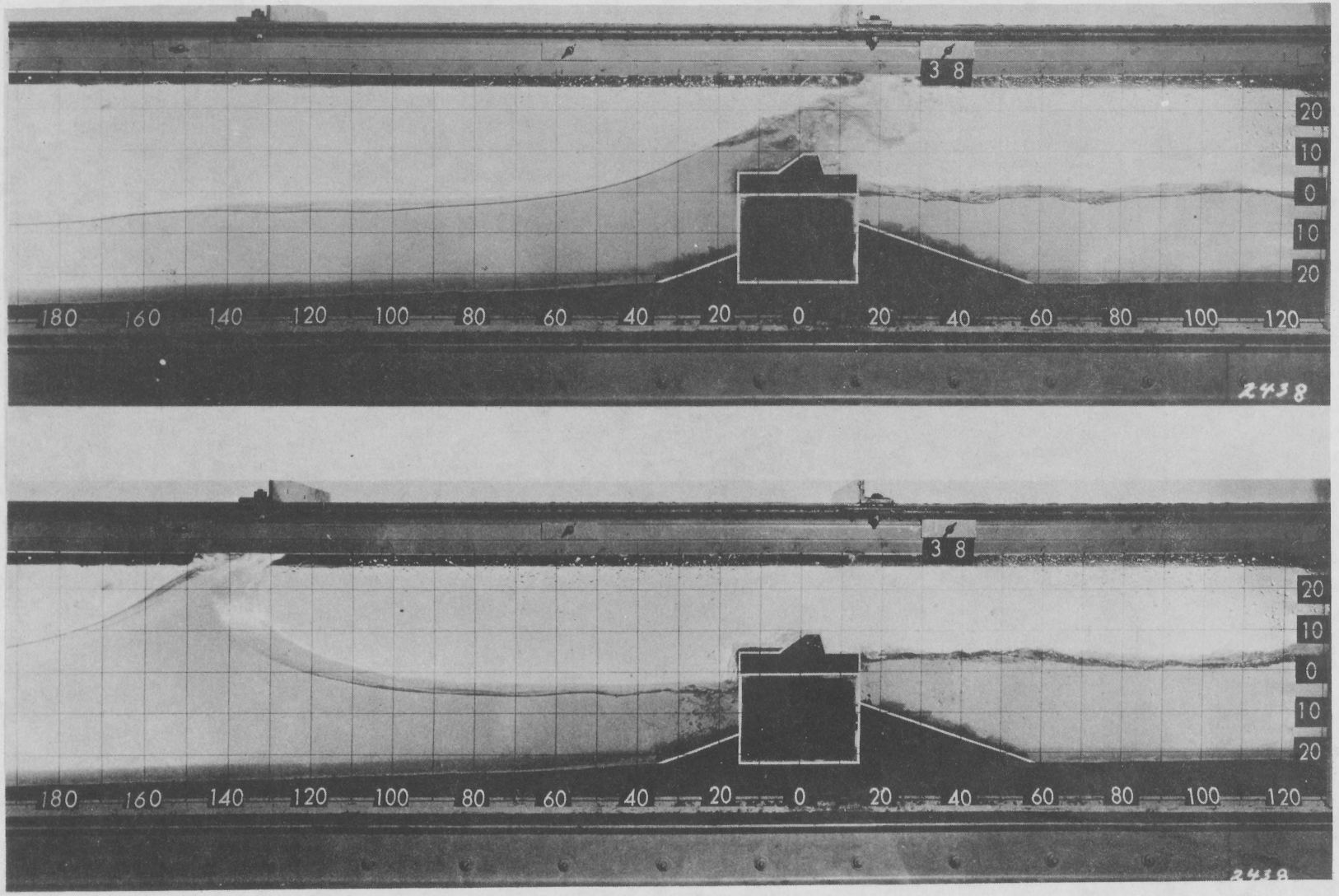

Figure 6-13. Vertical-wall breakwater section constructed of wood, filled with stones, and with a molded concrete cap (Wilson and Hudson, 1965).

pipes lashed together, or an assembly of auto tires, rubber spheres, or other material. Some of these structures require built-in flotation chambers which may be filled with polystyrene. Model structures are at times fabricated from the same materials used for the prototype, but most model materials are different from the prototype. However, in all cases the outside geometry and total weight of the prototype structure must be reproduced from the length and weight scales, and the moments of inertia about the different axes must be reproduced properly. Thus, any variations between model and prototype values caused by the use of model material different from the corresponding prototype material must be considered in the calculations involving geometric, kinematic, and dynamic reproduction of the prototype structure in the model. Figure 6-14 shows cross sections of a floating breakwater proposed for a prototype installation at Oak Harbor, Washington, together with the corresponding cross section used in the model (Davidson, 1971a).

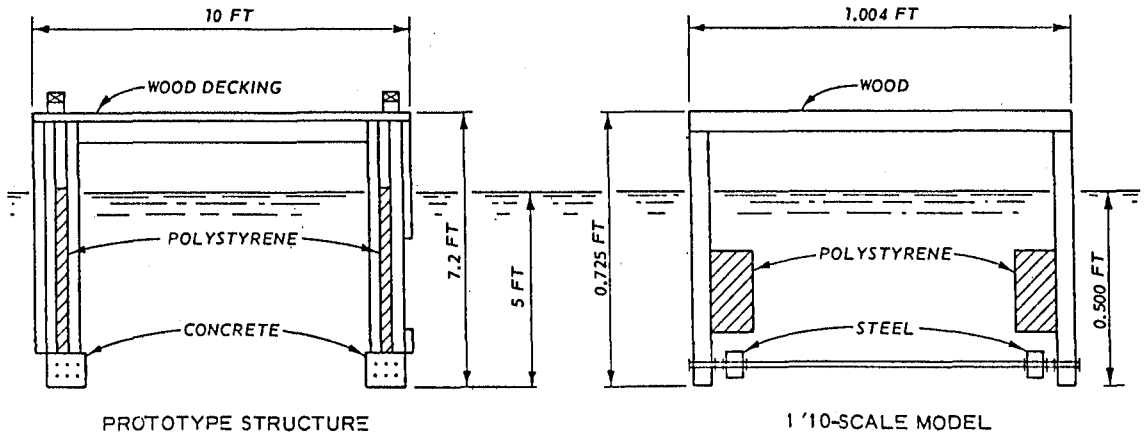

Figure 6-14. Model reproduction of a proposed floating breakwater (after Davidson, 1971a).

d. Measurement of Waves and Wave Forces.

(1) Measurement of Wave Characteristics. The wave height and wave period are usually required measurements in model studies concerning the stability of coastal structures. With a known wave period and depth of water, it is more convenient and usually more accurate to determine wavelength using the equation

$$\lambda = \frac{gT^2}{2\pi} \tanh \frac{2\pi d}{\lambda} \qquad (6\text{-}38)$$

which is based on the linear theory for progressive waves. Although wave heights may be measured approximately by eye with a graduated scale, they are usually determined with electronic wave gage apparatus and recorded on an oscillograph or magnetic tape. The wave period may be determined by a stopwatch, or by a photoelectric counting device if more accuracy is required. If the waveform is also desired in some model studies, it can

be determined satisfactorily in some instances by the electronic wave gage apparatus and the oscillograph. In other studies, if determination of waveforms are desired when breaking on a structure, high-speed photography may be used. The direct measurement of particle velocity is seldom necessary in model studies of coastal structures. However, in research studies of wave-induced sediment motion (which may affect the stability of coastal structures by erosion at the toe of the structures) or in basic studies of wave forces on the structures, the kinematics of the water particles are of fundamental importance. Orbital velocities in progressive waves have been measured by introducing neutrally buoyant particles in the waves and photographing their motion by a high-speed movie camera (Marlow, 1957). This method was determined fairly accurate, but it was not considered completely satisfactory because the points of measurement could not be controlled; the effort in obtaining photos and the reduction and analysis of data were difficult and required considerable time and effort. As a result, other methods of measuring orbital velocities have been investigated, including the hot-wire anemometer, the thermistor, and the hot-film sensor (Eagleson and Van de Watering, 1964; Kolpak and Eagleson, 1969).

Wave height measuring devices for model use consist of a wave gage, a power supply, an amplifier and control system, and an oscillograph (Fig. 6-15). This apparatus measures changes in water surface elevation with respect to time by measuring and recording the corresponding variations in current flow with respect to time by resistance or capacitance wave gages. The first wave gages used at WES were the step-resistor type, but most laboratories now use the two-wire or printed-circuit resistor gages or the one-wire capacitance gages. The capacitance wave gage has been described by Killen (1952), Campbell (1953), Tucker and Charnook (1954), Ippen and Eagleson (1955), and Moore (1964). The development of the printed-circuit gage was described by Hanes (1957), who listed the following advantages and disadvantages of the four types of wave gages.

(a) Step-Resistor Gage. Advantages are good linearity, rugged construction, and simplicity of operation. Disadvantages are high cost of construction and of auxiliary equipment, distortion of wave shape, obstruction of wave fronts, difficulties in maintaining waterproofness, and relatively poor accuracy.

(b) Two-Wire Electrode Gage. Advantages are low cost of wave gage construction, minor obstruction of wave fronts, good linearity and accuracy over small ranges of wave height, and long service life. Disadvantages are high cost of auxiliary equipment, distortion of wave shape due to finite distance between elements, and small ranges of linearity.

(c) Capacitance Wave Gage. Advantages are good linearity and dynamic response, minor obstruction to wave fronts, and low cost of wave gage construction. Disadvantages are high cost of auxiliary equipment and the requirement of a bridge network of capacitors and resistors (which must be accurately matched), that is sensitive to temperature variations.

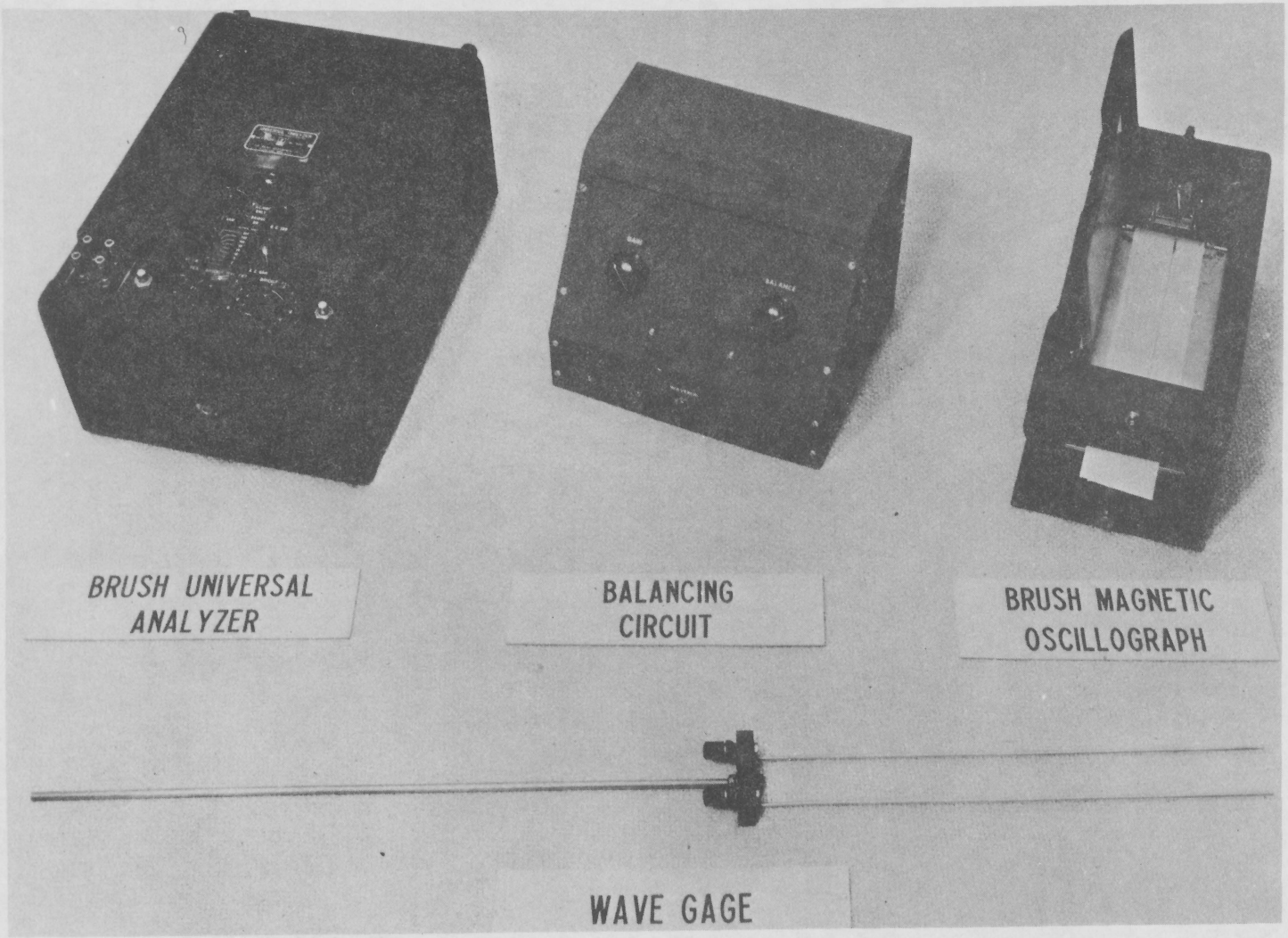

Figure 6-15. Wave gage assembly (Hudson and Jackson, 1955).

(d) Printed-Circuit Gage. Advantages are low cost of wave gage construction (constructed of printed-circuit board on Formica grade FF-91, selected because of a low moisture absorption characteristic), good linearity and dynamic response, and negligible obstruction to wave fronts. Disadvantages are the necessity to electroplate the surface of the rod with silver and the difficulty of maintaining clean surfaces during operation. Deposits on the rods cause a shift in the null point of the bridge and a distortion of the calibration curve.

The above characteristics of wave height measuring assemblies reflect the experience of instrumentation engineering during the period 1952 to 1964. Since that time, many improvements have been made in electronic circuits and the use of different materials. Thus, the design of wave gage instruments has changed considerably in recent years; the best method of obtaining up-to-date information concerning the best designs of the instruments is to contact the electronic design and development engineers in the different laboratories that use the devices, such as CERC, WES, Massachusetts Institute of Technology (MIT), University of Iowa, National Research Council, Ottawa, Canada, and the manufacturers of commercial instrumentation.

The prototype wave data needed for the basis of model design and operation, and the analysis of test results, are obtained by hindcasting techniques and the direct measurement of the wave heights and periods. CERC has used wave gages since 1948 to obtain prototype wave data. Two basic types of gages are used in the field: the step-resistance staff gage and the underwater pressure-sensitive gage. Three step-resistance gages that have been developed are a series type for use in freshwater, a parallel type for use in saltwater, and a relay type for use in water where wide ranges of salinity occur. The pressure gage can be used in water of any salinity. Details of these gages, including theory of operation, techniques of fabrication, calibration, installation, and maintenance, are discussed by Williams (1969).

(2) Measurement of Wave Forces. Breakwaters and other coastal structures were designed and constructed long before reliable information was available concerning the magnitude and distribution of the forces that occur on the structures due to wave action. However, the tremendous forces exerted on coastal structures by storm wave action was recognized by early designers, as evidenced by descriptions in the literature of damages that occurred and by attempts to measure the magnitude of the wave forces on structures. According to Gaillard (1904), Thomas Stevenson was the first to measure wave forces in 1842 and continued the measurements for many years. The first wave pressures measured at WES were for a model study to determine pressures on a vertical-wall breakwater subjected to nonbreaking waves (Hudson, 1942).

Measurement of the pressures exerted on coastal structures by breaking waves requires pressure transducers with characteristics matched to the characteristics of wave pressure phenomena. The extremely short duration

of the peak pressure pulse requires a transducer with a frequency response exceeding about 1,000 cycles per second (1 kilohertz). The transducer must have a good transient response and an amplitude range matched to the wave dimensions used in the tests. This may require a capability of measuring from 100 to 1,000 pounds per square inch, although the model waves are only a few inches in height. Another important factor in transducer selection is the need to avoid distortion of the pressure pulse by changes in the shape or stiffness of the test structure that result from the installation of the transducer in the face of the test structure. Experiments at WES during the period 1963 to 1968 used two types of pressure transducers in model tests of breaking wave pressure--the miniature flush diaphragm strain gage and the miniature piezoelectric pressure transducers. The transducers were selected on the basis of physical size and frequency response characteristics, and because of the experience with similar transducers in a large number of experiments where pressures due to water shock were measured. The flush diaphragm cells used were commercially available CEC Model 4-312 units. The piezoelectric cells were fabricated at WES from zirconate ceramic elements. Details of the experimental procedure and the equipment used in the tests to determine pressures on vertical-wall structures due to breaking waves were reported by Ross (1955), Garcia (1968), and Kamel (1968b).

Pressure measurements are useful in understanding the nature of wave action on structures. For nonbreaking waves when sufficient simultaneous measurements will allow determination of the shape of the pressure curve in the vertical, the total force per unit length of the structure can be estimated with enough accuracy for design purposes. However, pressure measurements alone, which provide time-pressure histories on relatively small areas of the breakwater face, are not sufficient for determining the force time histories needed to design structures to withstand the forces of breaking waves. These forces have been measured in the laboratory by Carr (1953, 1954a, 1954b) and by Leendertse (1962) using a three-component wave force balance. The measured quantities were the horizontal component of force, the vertical component of force, and the total moment about an arbitrary horizontal reference axis. Forces on vertical, inclined, and stepped barriers were investigated by Carr. The geometry of the force balance is shown in Figure 6-16, where R is the resultant force on the barrier; T is the horizontal component of the resultant force; L is the vertical component of the resultant force; M_p is the moment of the resultant force about the fixed balance pivot; x and y are the horizontal and vertical distances of the pivot from the toe of barrier; M is the moment of the resultant force about the barrier toe ($M = M_p + Ty + Lx$); θ is the angle of inclination of the resultant force from the horizontal; and c.p. is the center of pressure distance (i.e., the perpendicular distance from the barrier toe to the line of action of the resultant). The vertical and horizontal forces and the moment about the fixed balance pivot were measured by shop-fabricated force-sensing cells of 1,000-pound capacity. The cells consisted of heat-treated stainless-steel bars with a milled flat gage section (about 0.375 inch wide and 0.08 inch thick) bonded by four Baldwin Type AB-7 gages. Two gages were bonded on each side, one parallel and one transverse to

the gage axis. By using matched gages, and by connecting all four gages in a bridge circuit, cancellation of the bending strain and temperature drift was obtained.

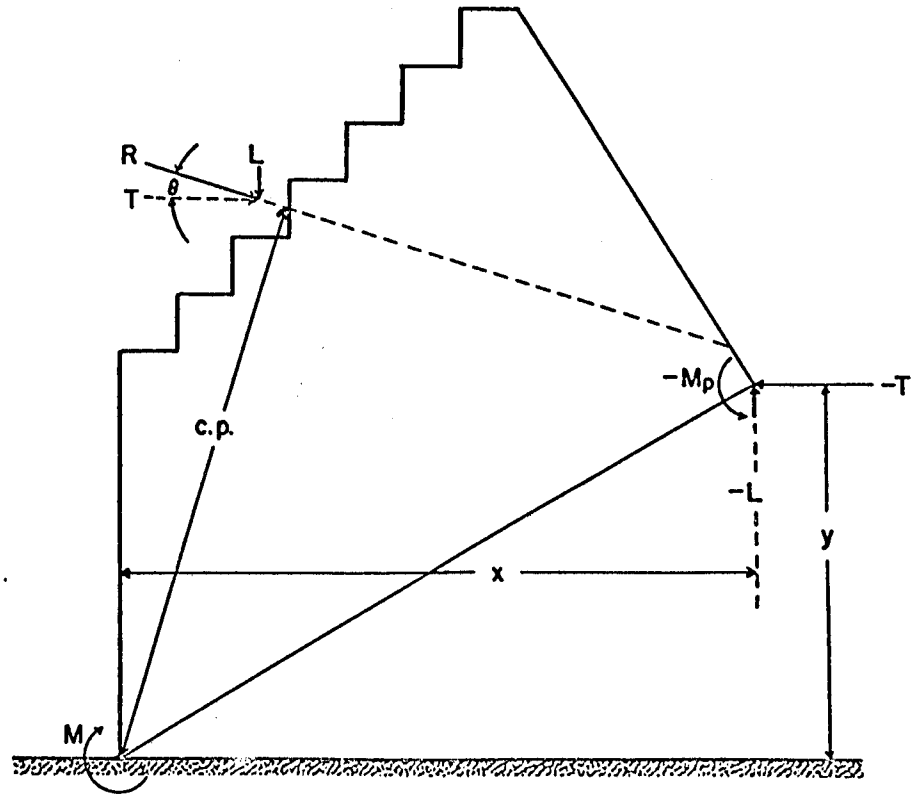

Figure 6-16. Geometry of a wave force balance (Carr, 1954a).

e. Analysis and Interpretation of Results. It is important that the analysis and interpretation of test results are carried out concurrently during the test program. This procedure allows the changing of test conditions and the general thrust of the program as may be indicated by the results of tests as they are performed. The field design engineer should be kept informed of the test results during the tests so that necessary revisions in structure design can be made and tested. In this way the number of tests to obtain the best overall design can be reduced to a minimum. The required coordination between the field design engineer and the laboratory engineer can be accomplished by telephone, conferences, and those data included in progress reports. The end product of all model studies is a report that presents the test data and the analysis and interpretation of the test results. Thus, preparation of the testing program, conduct of the tests, and the analysis of test results should be done based on the requirements of a good technical report (Smart, 1967).

The use of dimensional analysis in the design of hydraulic models and in the preparation of testing programs was discussed in Section II,2 and Section VI,2. Dimensional analysis is also useful in the correlation,

analysis, interpretation, and the presentation of experimental data. The most important advantage gained in dimensional analysis techniques is the reduction of the number of variables in a problem. If only two variables are involved in a problem, a single curve can be used to describe the functional relationship; if three variables are involved, a family of curves relating two of the variables with constant values of the third variable (the varying parameter) is required. As the number of variables increase further, the number of families of curves also increases. Thus, without dimensional analysis to group the variables into a smaller number of dimensionless terms (the values can be used to plot curves for analysis and presentation of the data in a more precise form), it would be impossible in many cases to perform model tests economically or to present experimental data in a way that would allow easy interpretation. The application of functional relationships can also facilitate the detection of random errors in test data, as contrasted to the less likely situation where a complete set of data may be erroneous because of faulty recording apparatus or the use of an incorrect datum.

The correct interpretation of a set of measurements from an engineering or scientific experiment is often more difficult than performing the tests and obtaining the observations. The accuracy of the measurements depends on the precision of the instruments used and on the observers dependability and skill. "Precision" refers to the degree of mutual agreement among independent measurements of a single quantity when measurements are repeated; "accuracy" refers to the agreement of the measurements with the absolute or true value. When a large number of observations are made of quantities that are supposedly identical, such as the still-water depth in a wave flume, these data can be plotted as a frequency graph (number of observations versus the measured value of water depth), to derive a normal distribution curve from which, with certain necessary assumptions, the standard deviation from the mean and the probable error can be calculated (Murphy, 1950). The curves and indexes of precision can be obtained, for example, for the weight and specific weight of armor units in rubble-mound stability tests, and the heights and periods of test waves. However, the wave height can vary considerably with respect to time and from test to test due to transverse oscillations, circulation due to mass transport, reflected waves from the test structure, and differences in starting positions of the wave machine plunger. In wave pressure measurements, the pressures due to nonbreaking waves can also vary considerably because of variations of wave height with respect to time and variations in the reflection coefficients due to variations in overtopping. The variations in pressures caused by breaking waves can be large because of the nature of the phenomena itself, as well as the variations of the wave heights with respect to time as noted above. Therefore, the interpretation of these data must consider the precision of the instruments used in the observations, and the degree to which the variations are inherent in the prototype phenomena.

The interpretation of test results from rubble-mound stability models is difficult even when care is taken in the construction of the test sections and the measurements of the wave conditions. The construction of

test sections is costly both in terms of time and money, and to repeat the tests a sufficient number of times to obtain data that can be analyzed on a statistical basis is usually not feasible. Unfortunately, the shape of the armor units, the placement of the armor units, and the waveforms which impinge on the structure slope are also important variables in stability of the structure. The waveform is a function of the wave height and period and the phase relations between the incident and reflected waves. Thus, large variations in stability often occur between successive tests when there are no discernable differences in the test conditions. When differences in stability occur, there is no recourse but to repeat the test. The question then arises, because a large number of repeat tests may not be feasible, as to which set of test results is the most representative of the conditions that will occur in the prototype considering the difficulties of reproducing the prototype wave trains in the model and duplicating the placing techniques to be used by the contractor in constructing the prototype breakwater. These and perhaps other factors result in a situation where more than 100 percent variation has occurred in the stability coefficient for a particular type of armor unit and breakwater section; i.e., K in equation (6-4b), obtained by two different laboratories with comparable facilities and personnel.

5. Utilization of Hydraulic Models.

a. Problems Susceptible to Model Analysis. Hydraulic models should be used only if the phenomena involved are too complicated and not understood sufficiently to allow solution of the problems by theoretical study, or have not been solved by systematic experiments already conducted. However, a large number of problems in hydraulic engineering cannot be solved satisfactorily without the aid of scale models. Most physical systems can be studied by scale models if valid scaling laws are available. Scaling laws for problems involving the stability of coastal structures (derived in Section VI,2) have shown that the stability of structures subjected to the forces of wave action can be investigated successfully if the scale effects, resulting from the incorrect reproduction of viscous forces, can be made negligible by use of relatively large models. Because of the high cost of providing a shelter and constructing and operating the model, smaller models can also be used when enough experimental data are available for wave forces on the structure as a function of Reynolds number. As indicated in Section VI,2, adequate scale-effect data are not presently available for all types of coastal structures. However, nearly all of the major problems concerning the stability of coastal structures are believed to be susceptible to scale-model analysis after experimental data become available.

b. Advantages and Disadvantages of Hydraulic Models. The engineer uses scale models for more reliable solutions to design problems than can be derived by mathematical analysis. When an existing structure is not performing satisfactorily, or when a proposed structure cannot be designed adequately by analytical means, together with information in the literature, the use of a scale model may be indicated. Generally, scale models can be regarded as a type of analog for solving differential equations of

fluid motion with a given set of rather complicated boundary conditions. In many instances the models help the designer to better understand the nature of the problem to be solved. Model studies are usually expensive compared to the costs of conducting theoretical investigations and should not be used when purely analytical methods will give reliable solutions. However, the cost of scale-model studies is often low compared with the cost of the prototype structure, including the consequences of structure damage or failure that may occur as the result of underestimating the wave forces imposed on the structure. Thus, because the justification of many model studies is mostly an economic one, it is usually easier to justify a model study if the project is large and important. Conversely, smaller projects may not afford the cost of a scale model, although the project may concern extremely complex phenomena that defy analysis by theoretical means alone. A disadvantage of some model studies is the cost and time necessary to conduct the tests. However, the importance of conducting model studies of coastal structures cannot be overstated. In many instances the studies are more than just a good investment; they can prevent disastrous errors in prejudging the performance of the prototype structure, and they usually result in considerable savings in design and construction.

This section has emphasized the importance of model studies in determining the forces imposed on coastal structures so that they can be designed to successfully withstand those forces. Model studies can also be performed so that the optimum construction methods and schedules can be selected. The results of stability tests on scale models can be used, in conjunction with applicable economic factors, such as the economic life of the structure, frequency of occurrence of the selected design wave, initial cost of construction, subsequent repair costs, and the interest rate, to obtain the optimum design for the structure. The results of such a comprehensive study can be negative, indicating that construction of the proposed structure would not accomplish the intended purpose, unless the structure was enlarged or strengthened to increase construction costs appreciably.

The scope of usefulness of scale models as discussed in this section is very broad, and the advantages are considerable both from the technical and economical viewpoints. It should be emphasized that although most stability models can be designed, constructed, and operated with the results interpreted to provide sufficiently accurate results for the purpose of the investigation, the laboratory engineer conducting the investigations must have considerable experience, familiarity with basic wave mechanics, and engineering judgment.

c. Examples of Model Studies Conducted. Many model studies have been conducted in laboratories worldwide on the stability, wave transmission, and overtopping characterisitics of coastal structures (rubble-mound, vertical-wall, composite, and floating types). A smaller number of full-scale model studies, theoretical investigations, and flume experiments have been conducted to determine the horsepower required per

foot of structure and the efficacy of pneumatic and hydraulic breakwaters in preventing the transmission of wave energy into areas where protection was desired from storm wave action.

Selected examples of such investigations are discussed below. Reports on a few model studies and experimental investigations pertaining to the stability and wave-transmission characteristics of coastal structures are referenced in the examples.

(1) Rubble-Mound Breakwater Trunk; Nonbreaking Waves.

(a) Example of a Typical Study.

1 Project. Proposed rubble-mound breakwater, Burns Waterway Harbor, Indiana.

2 Reference. Jackson (1967).

3 Laboratory. WES.

4 Test Period. April to July 1966.

5 Problem. Burns Waterway Harbor was proposed for construction on the south shoreline of Lake Michigan, 15 miles east of Indiana Harbor, Indiana, to consist of north and west breakwaters, east and west outer bulkheads, inner bulkheads, and an outer harbor area with east and west inner harbor mooring areas (Fig. 6-17). The harbor would be exposed to storm waves from the northerly directions with heights to about 13 feet and periods to about 11 seconds. The maximum water depth along the toe of the breakwater was about 43 feet referred to low water datum (LWD) for Lake Michigan and the selected high water level for testing was +4 feet LWD.

6 Purpose of Model Study. The model study was conducted to determine the stability of the proposed breakwater designs, to develop alternate designs if necessary, and to investigate the effectiveness of the proposed breakwater in reducing transmitted wave energy. Two basic designs were investigated, one with tribar armor units and the other with generally rectangular limestone blocks from quarries near Bedford and Bloomington, Indiana. Since the majority of the proposed designs involved a protective cover layer of the limestone blocks, determining whether this type of stone (in the sizes and shapes available) could provide the required stability using the random-placing technique was desired.

7 The Model. Stability and wave transmission tests were conducted with section models of the proposed structures in a wave flume 119 feet long, 5 feet wide, and 4 feet deep. A plunger-type wave generator was used and wave heights were recorded using two-wire resistor rods, an amplifier and control system, and an oscillograph similar to the one shown in Figure 6-15. The model was designed and operated based on Froude's law. The linear scale of the model was 1:35, model-to-prototype.

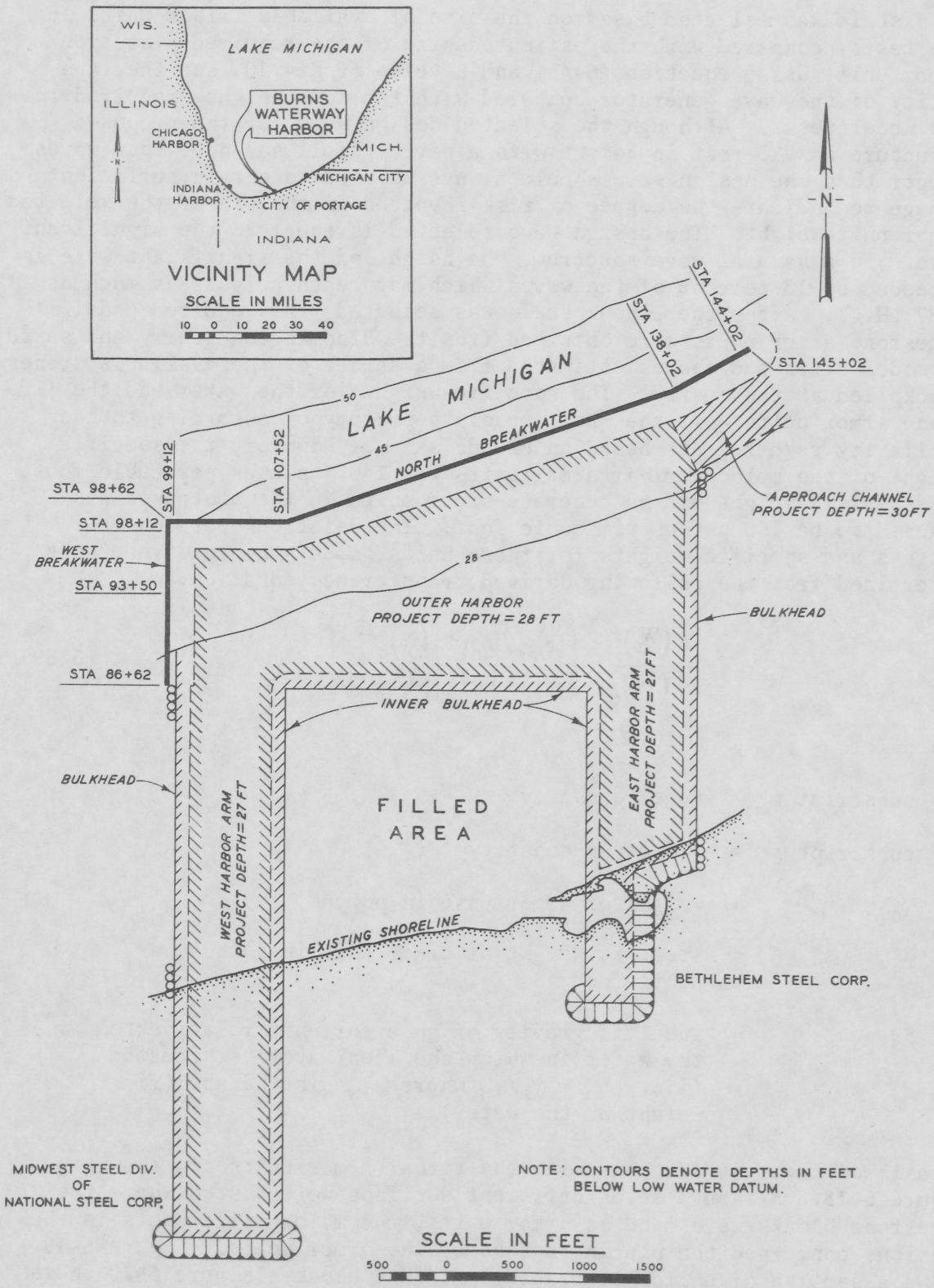

Figure 6-17. Location map and details of proposed Burns Waterway Harbor, Indiana (Jackson, 1967).

This scale was selected based on the size of available tribar units for the tests, compared with the estimated size of the required prototype armor unit, using equation (6-4b) and a value of K = 10, and the capability of the wave generator compared with the wave heights required in the model tests. Although the selected design wave for the proposed structure was 13 feet in height with a period of 11 seconds, test waves larger than the design wave should always be used to obtain sufficient damage to indicate the degree of risk involved in the use of the selected armor unit weight. The design wave selected is equal to the significant wave. In a natural wave spectrum, the height of the significant wave is exceeded by 13 percent of the waves which may reach heights as much as 1.87 ($H_{1/3}$). After the linear scale was selected, the required model limestone armor units were obtained from the Bloomington quarry and sawed to model sizes and shapes estimated from a survey of the available stones stockpiled at the quarry. The specific weights of the water and the limestone armor units were the same, model-to-prototype, according to the similarity requirements based on Froude's law. However, the specific weight of the molded tribar armor units was 140.4 pounds per cubic foot; the specific weight of the concrete armor units in the prototype was assumed to be 150 pounds per cubic foot. The relations between the weights and specific weights for these units, model-to-prototype, were determined from the following derived transference equation:

$$\frac{(W_a)_m}{(W_a)_p} = \frac{(\gamma_a)_m}{(\gamma_a)_p}\left(\frac{L_m}{L_p}\right)^3\left[\frac{(S_a)_p - 1}{(S_a)_m - 1}\right]^3 \qquad (6\text{-}39)$$

where

subscript m = model quantity

subscript p = prototype quantity

W_a = weight of armor unit in pounds

γ_a = specific weight of armor unit in pounds per cubic foot

S_a = specific gravity of an armor unit relative to the water in which the breakwater is situated (i.e., $S_a = \gamma_a/\gamma_W$ where γ_W is the specific weight of the water)

Details of the test section using the tribar armor units are shown in Figure 6-18. Although seven different sections were tested where the limestone blocks were used as armor units, the major differences in the sections concerned the placing method of the armor units. Figure 6-19 shows a section of uniformly placed limestone blocks; Figure 6-20 shows a section of randomly placed limestone armor units. Table 6-2 gives the weights of the tribar and limestone armor units, the underlayer units, and the core stone.

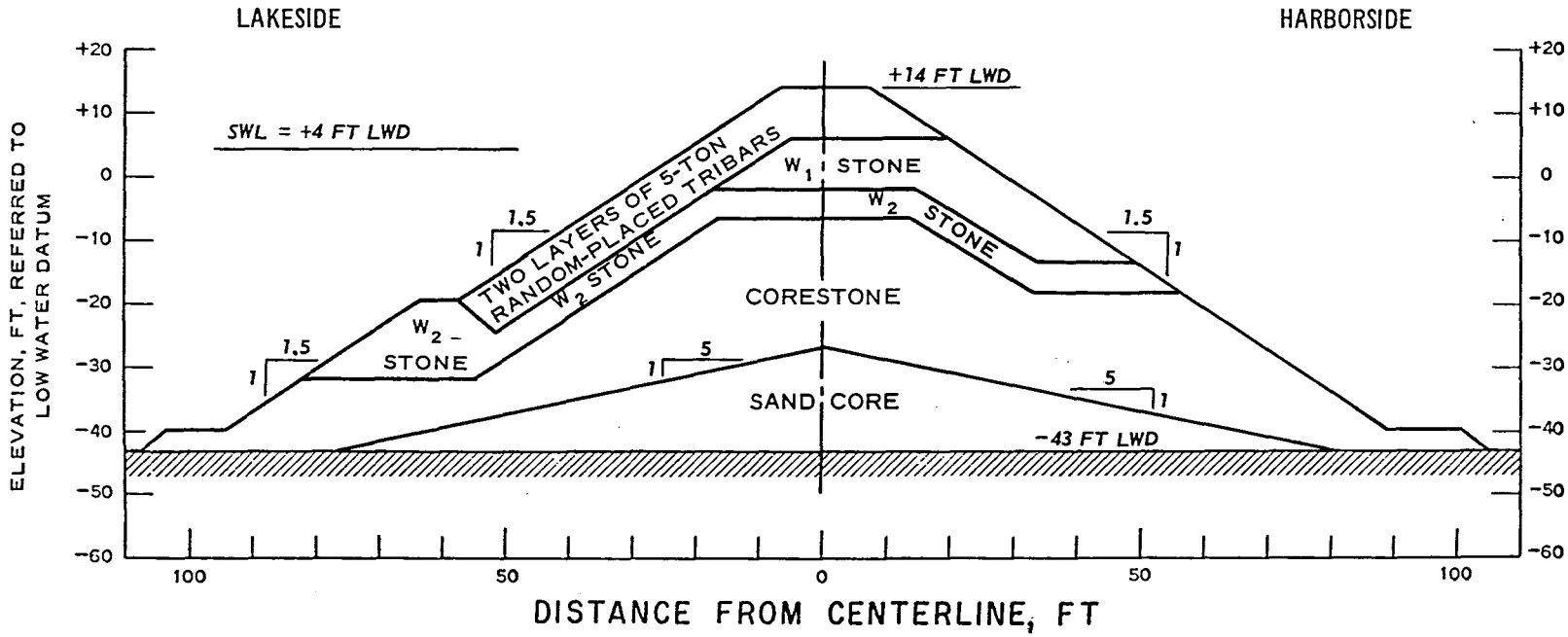

TYPE OF BREAKWATER MATERIAL	PROTOTYPE WEIGHT LB	TON
TRIBAR		5
W_1 STONE*		3 TO 10
W_2 STONE*	1000 TO 1500	
CORESTONE	5 TO 90	

* CRUSHED LIMESTONE USED IN LIEU OF LIMESTONE BLOCKS.

Figure 6-18. Elements of test section with tribar armor units randomly placed in Burns Waterway Harbor model (Jackson, 1967).

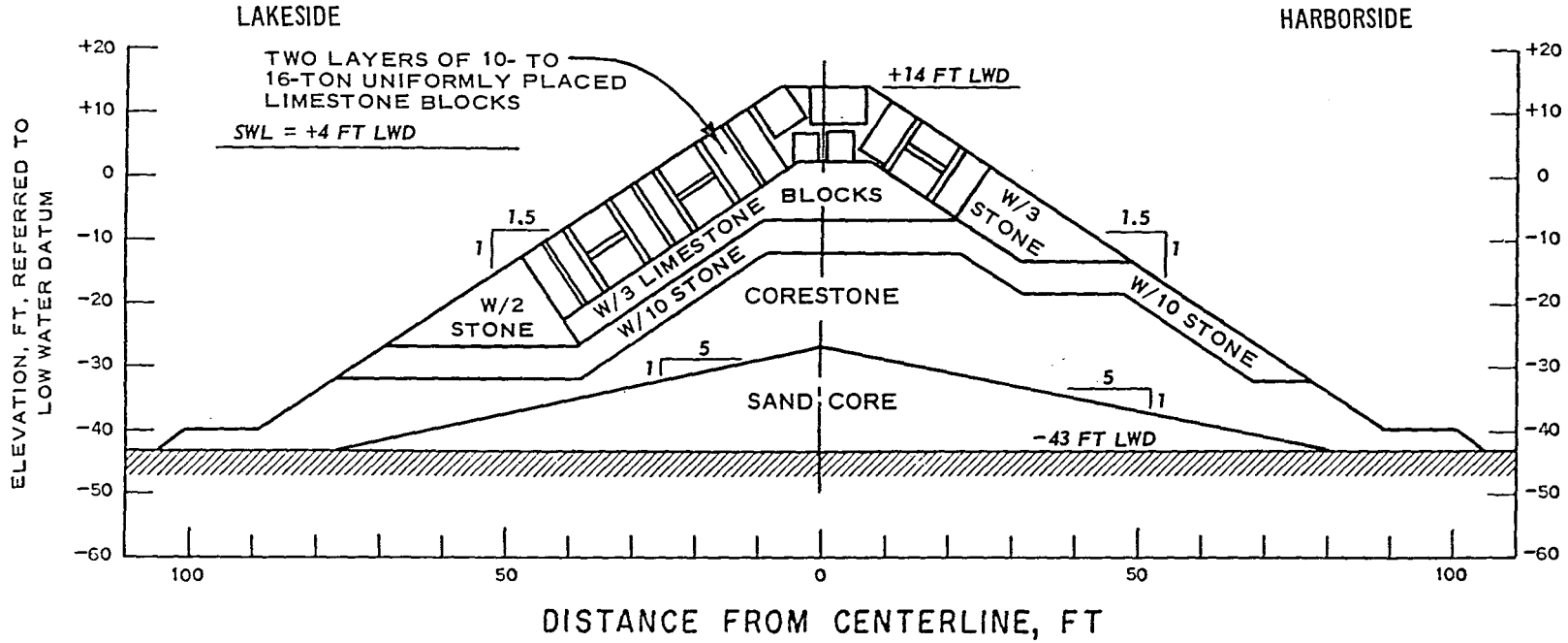

TYPE OF BREAKWATER MATERIAL	PROTOTYPE WEIGHT LB	PROTOTYPE WEIGHT TON
W STONE*		10 TO 16
W/2 STONE*		5 TO 10
W/3 STONE*		3 TO 10
W/10 STONE	1500 TO 3000	
CORESTONE	5 TO 90	

* LIMESTONE BLOCKS.

Figure 6-19. Elements of test section with limestone blocks uniformly placed in Burns Waterway Harbor model (Jackson, 1967).

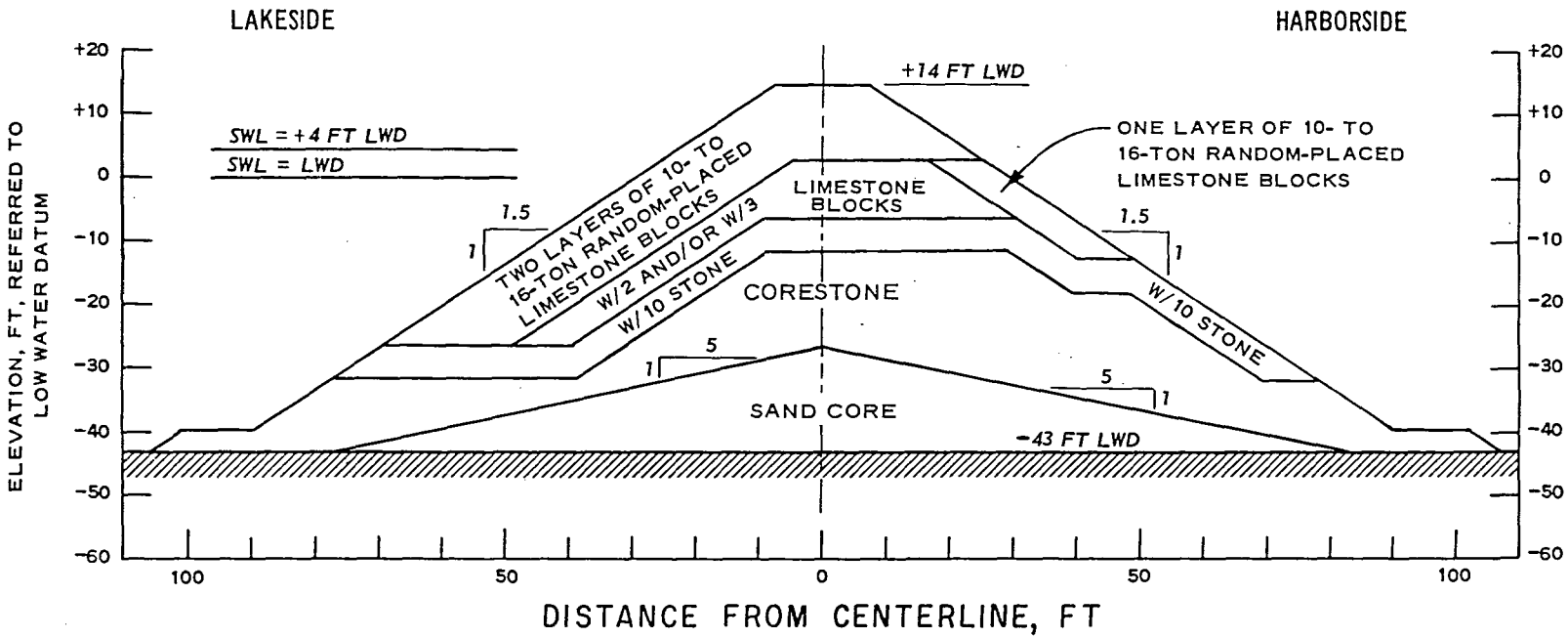

TYPE OF BREAKWATER MATERIAL	PROTOTYPE WEIGHT LB	PROTOTYPE WEIGHT TON
W STONE*		10 TO 16
W/2 STONE*		5 TO 10
W/3 STONE*		3 TO 10
W/10 STONE	1500 TO 3000	
CORESTONE	5 TO 90	

* LIMESTONE BLOCKS.

Figure 6-20. Elements of test section with limestone blocks randomly placed in Burns Waterway Harbor model (Jackson, 1967).

Table 6-2. Model and prototype breakwater material.

Breakwater material	Weight of tribar and stone		
	Model (lb)	Prototype (lb)	Prototype (ton)
W (tribar)	0.30		5
W (stone)	0.47 to 0.75		10 to 16
W/2 (stone)[1]	0.23 to 0.46		5 to 10
W/3 (stone)	0.14 to 0.46		3 to 10
W/10 (stone)	0.04 to 0.07	1,500 to 3,000	
W/2 (stone)[2]	0.02 to 0.04	1,000 to 1,500	
Core stone	12×10^{-5} to 21×10^{-4}	5 to 90	

[1] Used under the limestone armor units.

[2] Used under the tribar armor units.

Table 6-3 gives the gradations of the limestone blocks used in the model tests for the armor units and underlayers, based on estimates of the available stockpiled units for the prototype structure.

Table 6-3. Prototype stone gradation.

Type of stone	Prototype weight (ton)	Pct. by weight
W	10	30
	12	30
	14	30
	16	10
W/2	5	33
	8	33
	10	34
W/3	3	25
	5	25
	8	25
	10	25

8 Test Procedures. The stability of each breakwater test section was determined by constructing the section in the wave flume and subjecting it to the attack of test waves, varying in period from 7 to 11 seconds and in height from 5 to 20 feet (prototype dimensions), for durations varying from a few minutes to about 6 hours prototype time. Tests were made using stillwater levels of +4.0 and 0.0 feet LWD, corresponding to water depths at the lakeside toe of the structure of 47 and 43 feet, respectively. The behavior of the test section and the extent of damage were determined by visual observation. Design waves for the

no-damage criterion (i.e., the largest waves that did not remove nested armor units from the test sections) were also determined in this manner. Waves slightly smaller than the selected design waves did, at times, remove a few loose armor units without endangering the stability of the structure. Photos were made of most wave conditions and breakwater sections were tested. The wave heights generated on the harborside of the breakwater by wave energy transmitted through and over the breakwater were measured at two positions from the structure, one at a distance of $\lambda/2$ and another at a distance of one wavelength, measured from the centerline of the structure. Breakwater design requires, in addition to accurate data concerning the stability of the armor units, quantitative data concerning the thickness and percent voids of the armor-unit layers. Measurements were made on the model sections to determine the percentage of voids in the armor layers tested. The thickness of each armor layer was determined from soundings made before and after placing of the armor units; the total weight of the armor units was determined by weighing the total number of armor units used. The total square feet of surface area of the armor-unit part of the test section was also determined. The shape and placing coefficient and the porosity in the cover layers were then determined from the equations

$$t = nk_{\Delta P}\left(\frac{W_a}{\gamma_a}\right)^{1/3} \tag{6-40}$$

and

$$P = \left(1 - \frac{\overline{W}_a}{A\gamma_a t}\right) \tag{6-41}$$

where

t = the thickness (ft) of n layers of stones of weight W_a (lb) and specific weight γ_a (lb/ft^3)

$k_{\Delta P}$ = the shape-placing coefficient

P = the porosity ($P < 1.0$)

$\overline{W}_a$ = the total weight (lb) of armor units in a cover layer of thickness t required for a given surface area A (sq ft)

The experimental values of $k_{\Delta P}$ and P for the limestone blocks, randomly placed with $n = 2$, were 1 and 0.41, respectively. Corresponding values of $k_{\Delta P}$ and P for tribar armor units (randomly placed with $n = 2$), obtained from previous tests, were 1 and 0.54, respectively.

9 Summary of Test Results. Stability tests of the tribar armor-unit section (Fig. 6-18) using a stillwater level of +4 feet LWD showed that the armor-unit part of the section would be stable for waves to about 16 feet in height; however, for waves 14 feet in height some of the W/2 stones were displaced. It was decided that the W/2 stone

should be increased in weight by about 50 percent. A model design wave height of 16 feet was selected for the test structure, which corresponded to a value of 14.9 for K in equation (6-4b). The results of the wave transmission tests are shown in Figure 6-21. The figure also shows that the transmission coefficient, H_t/H_i, varies with the wave period, increasing as the wave period increases. The maximum transmitted wave height of 3 feet for the selected prototype design wave height, based on the prototype wave climate of 13 feet, was considered satisfactory for the type of ships that would use the harbor. The stability tests of the breakwater section using uniformly placed limestone blocks (Fig. 6-19) showed that the largest waves tested (18 feet in height) did not remove any of the armor units from the structure; however, damage to the W/2 stone section began at the 11-foot height, and several of the W/3 stones on the harborside were displaced by 12-foot waves. Also, because of the smooth surface and lack of voids in the armor-unit section, the runup and overtopping increased and the waves generated on the harborside increased to about 4.5 feet for the 13-foot prototype design wave. Thus, for these reasons, and because it was not considered practical in the prototype to place the armor units below the water level in the same manner as in the model, this plan was not considered suitable for use in constructing the full-scale structure. After testing several breakwater sections with limestone armor units randomly placed, it was decided that the section shown in Figure 6-20, in which randomly placed limestone blocks were used, would be satisfactory at Burns Harbor. This structure was considered stable for waves as high as 18 feet when tested with a stillwater level of +4 feet LWD. This corresponds to a value of K of 14.0 in equation (6-4b), using an assumed effective value of W_a of 13 tons. When tested using a stillwater level of 0.0 foot LWD, the structure was stable for a maximum wave of 15 feet in height, which corresponds to a K of 8.1. The rather high values of K for the tribars and the limestone armor units were caused by the large amounts of overtopping for the high stillwater level and the larger wave heights tested. The transmitted wave heights for the most stable section tested (Fig. 6-20) are shown in Figure 6-22 for both the +4 and the +0.0 stillwater levels. The transmitted wave heights corresponding to the 13-foot prototype design wave were 3 and 2 feet for stillwater levels of +4.0 and 0.0 feet, respectively.

(b) Example of a Minimum Study.

1 Project. Proposed expansion of Monterey Harbor, Monterey, California.

2 References. Davidson (1969) and Chatham (1968).

3 Laboratory. WES.

4 Test Period. September 1969.

5 Problem. Monterey Harbor is located at the southern end of Monterey Bay about 100 miles south of San Francisco, and is exposed

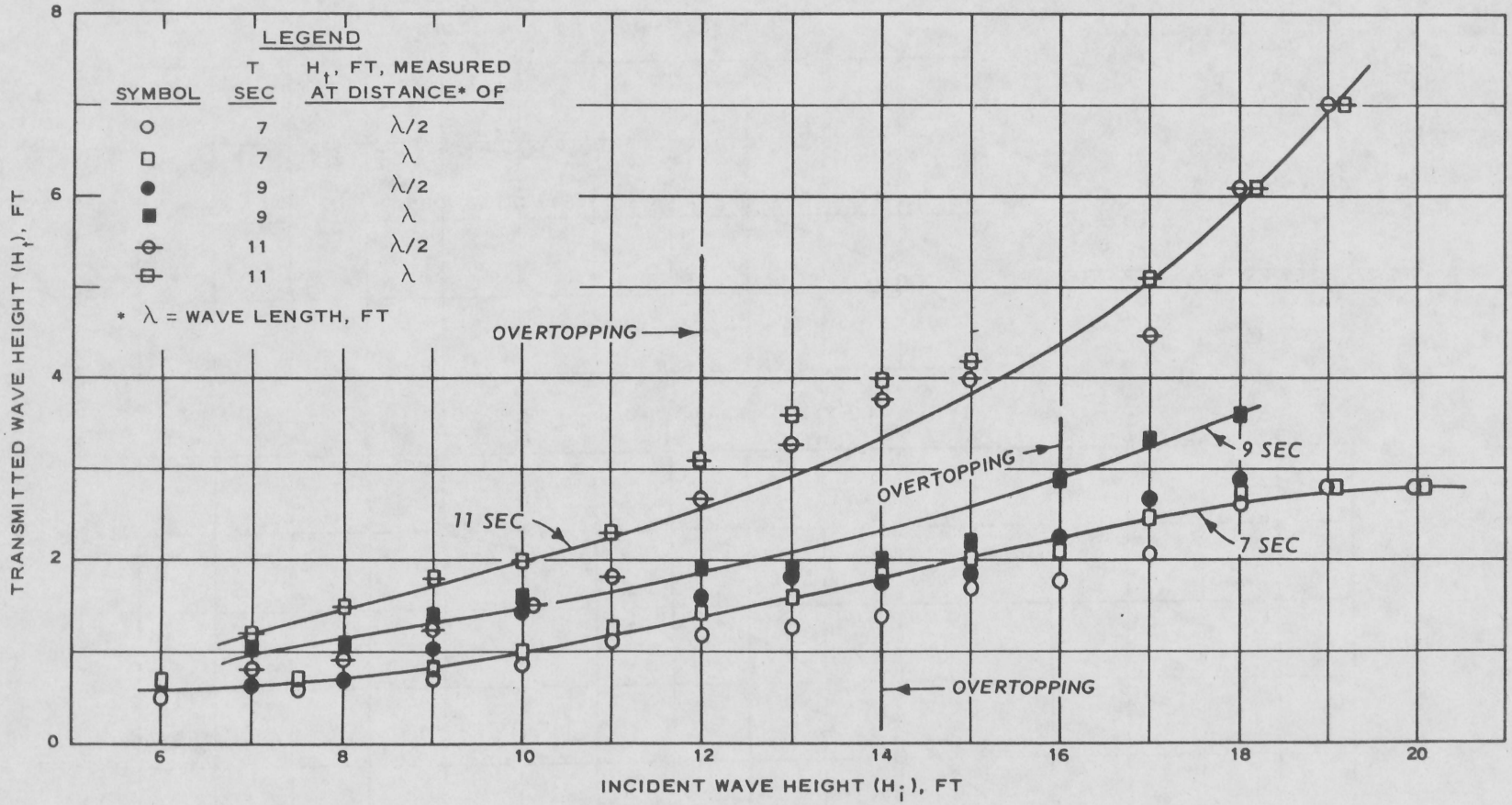

Figure 6-21. Transmitted wave heights for breakwater section with tribars randomly placed in Burns Waterway Harbor model (Jackson, 1967).

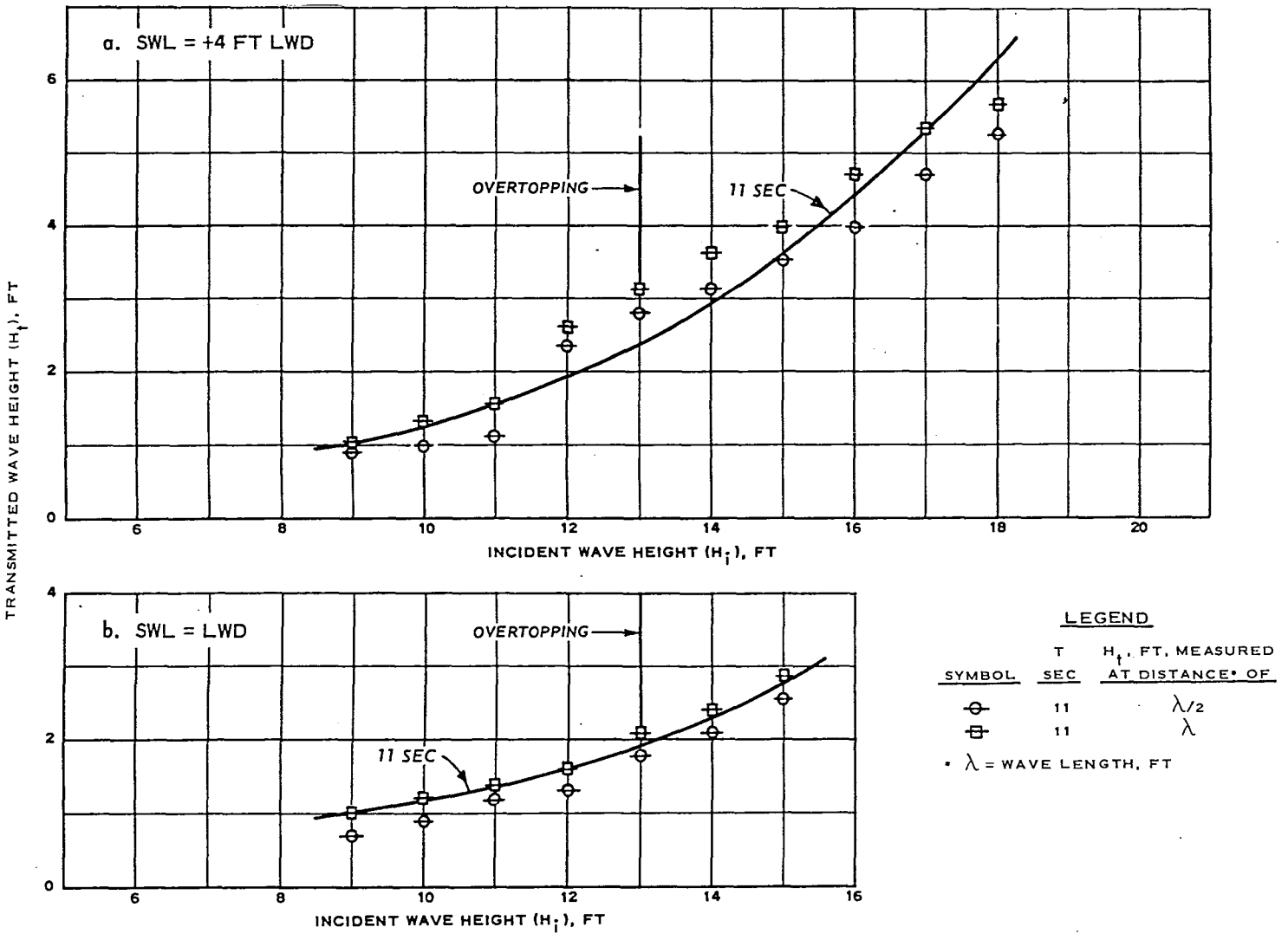

Figure 6-22. Transmitted wave heights for breakwater section with limestone blocks randomly placed in Burns Waterway Harbor model (Jackson, 1967).

to short-period, distant storm waves from the deepwater directions clockwise between west and northwest, and local storm waves from the north (Fig. 6-23). The magnitude of these waves is sometimes sufficient to damage fishing boats and harbor facilities, causing mooring difficulties for small craft in exposed areas of the harbor. It was proposed to enlarge the existing harbor by constructing one or more additional breakwaters to provide safe anchorage within the harbor. The problem of concern in this study was the design of a tribar cover layer for a part of the proposed north breakwater. It had been considered that a concrete cap on the crown of a breakwater was needed if molded concrete armor units were to be used for structures where overtopping was expected. However, tests conducted in 1966 in connection with a proposed rubble-mound breakwater at Nassau Harbor, Bahamas (Hudson and Jackson, 1966), indicated that tribar armor units do not necessarily require a concrete cap to ensure that the overtopping waves do not damage the breakwater crown. Therefore, a model study was considered necessary to check the stability of the proposed Monterey Harbor breakwater since the crest elevation, intensity of wave action, and the size of the armor units at Monterey Harbor were not the same as those at Nassau Harbor.

6 Purpose of Model Study. This investigation was conducted to determine the stability of the proposed cover layer and heights of waves transmitted through and over the east end of the proposed north breakwater at Monterey Harbor (Fig. 6-24). It was desired to determine the stability of the structure using the selected design wave in the prototype studies (15-second wave, 18 feet in height), and the heights of transmitted waves for the design wave conditions and for 17-second waves up to 16 feet in height.

7 The Model. Stability and wave transmission tests were conducted on a 1:40-scale model of the proposed prototype section in a flume 119 feet long, 5 feet wide, and 4 feet deep. The model was designed and operated by Froude's law, and the linear scale was selected on the basis of the size of armor units available compared with those proposed for the prototype section (12 tons), the water depth in which the prototype structure would be placed (36 feet MLLW), and the capability of the wave generator. The stillwater level used for testing (MHHW), which is +5.2 feet MLLW, was selected as being representative of conditions normally expected to occur during severe storms. Both the damage to the crest of a structure of the type being tested, and the heights of waves generated on the harborside of the structure due to wave transmission and overtopping, are larger for the higher stillwater levels. The maximum waves that can attack such a structure also increase as the water depth increases. A plunger-type wave generator was used and wave heights were measured using electrical wave gages and a recording oscillograph.

8 Test Procedures. The test section (Fig. 6-25) was subjected to waves, measured without the structure in place, of 15-second period ranging in height from 2 to 21 feet and 17-second waves ranging from 2 to 18 feet in height. During construction of the test section,

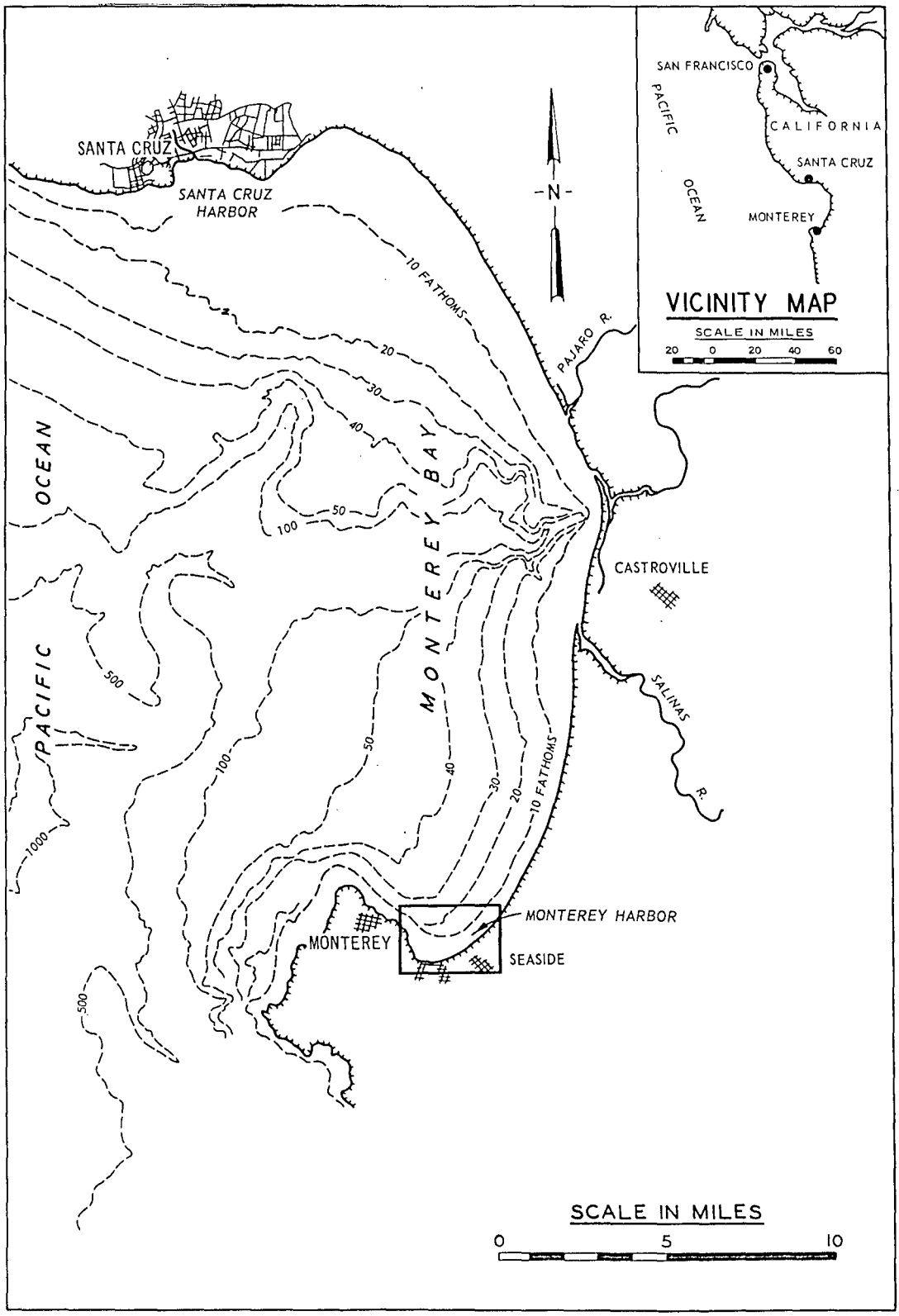

Figure 6-23. Location map, Monterey Harbor, California (Chatham, 1968).

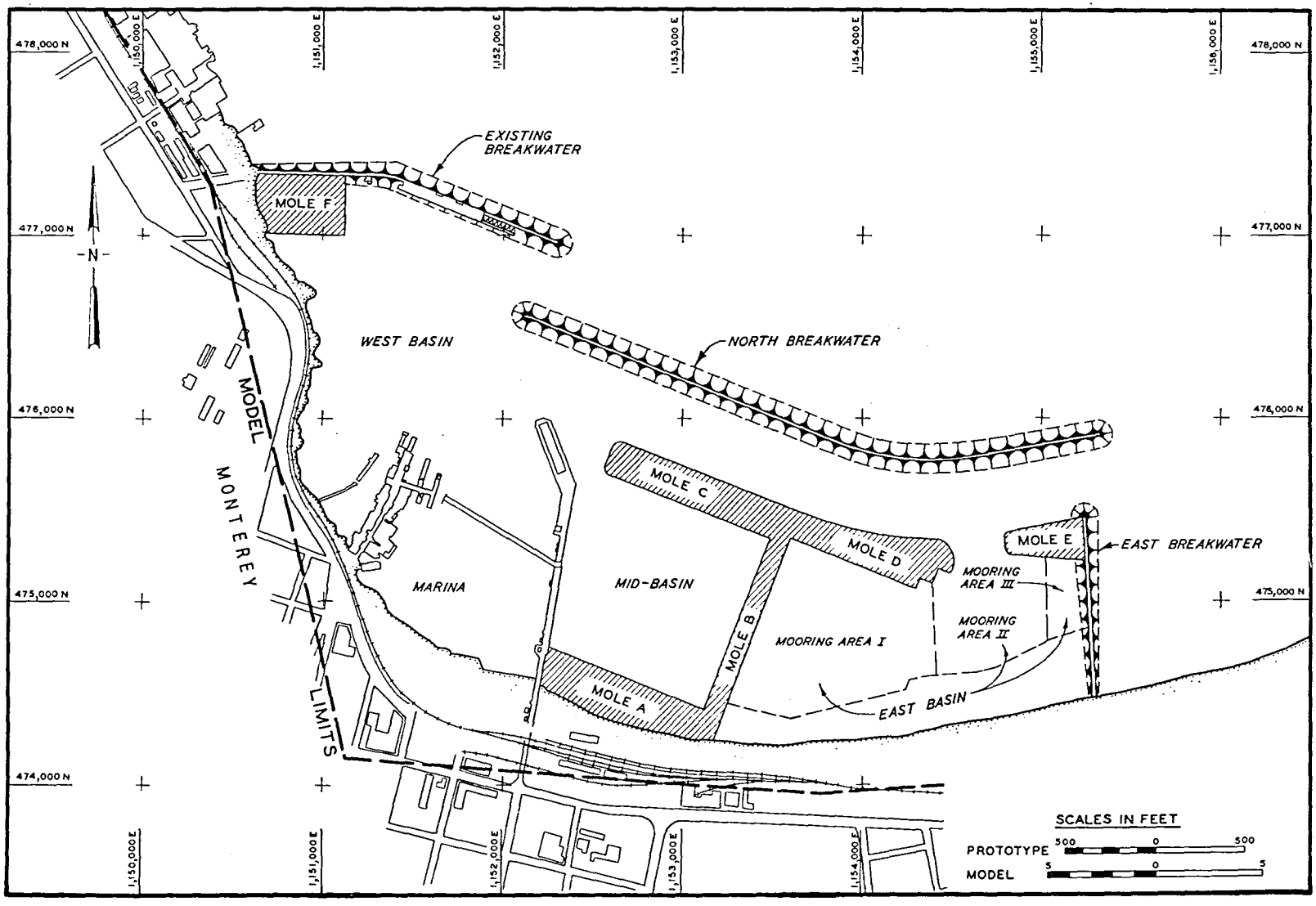

Figure 6-24. Breakwater, mole, and basin designations, Monterey Harbor model (Chatham, 1968).

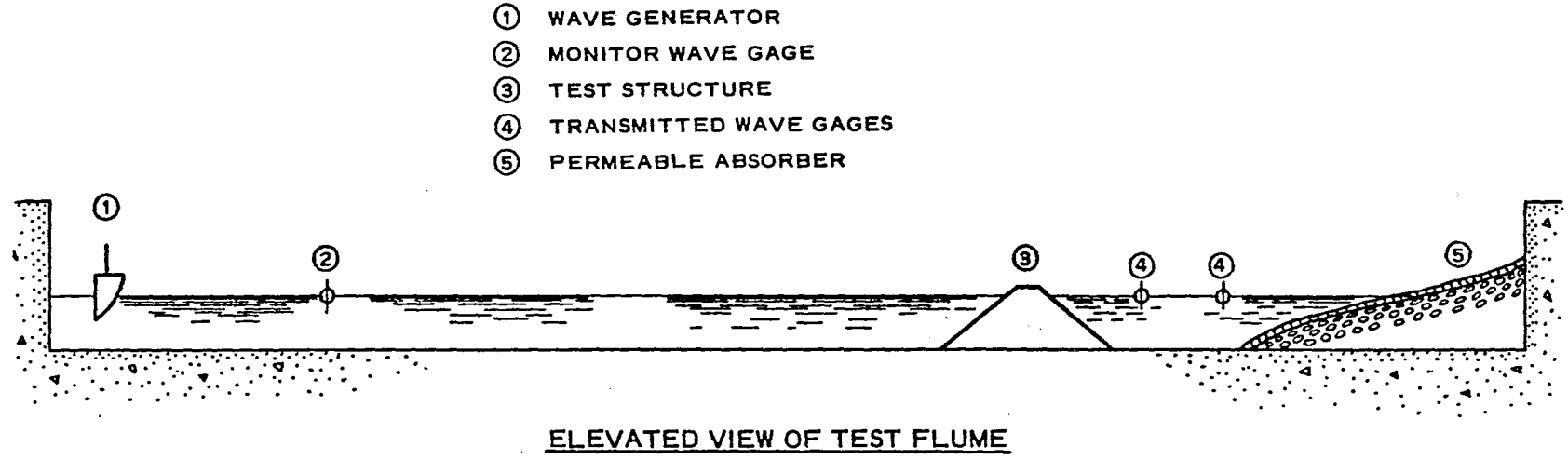

Figure 6-25. Layout of test flume and details of breakwater test section, breakwater stability and transmission tests, Monterey Harbor, California (Davidson, 1969).

all the armor units were carefully placed at random so that each armor unit within the trench formed by the A-3 rocks at MLLW on the harborside of the structure was placed in such a way as to be nested with a firm support. This procedure had previously been necessary to obtain stability of breakwaters with armor units randomly placed over the top and down the back side of the crest of structures and subjected to appreciable wave overtopping. The stability of the armor units was observed visually, and the wave heights on the harborside, generated by wave transmission and overtopping, were measured at distances of one-quarter and one-half the wavelength, measured from the centerline of the test section.

9 Summary of Test Results. During the stability tests no damage occurred to the test section for any of the 17-second waves. The selected prototype design wave (15-second, 18-foot waves) caused one tribar armor unit to be displaced from its nested position on the breakwater crown and deposited on the harborside slope. The 15-second, 21-foot waves caused three additional tribars to be displaced in a similar manner. No damage occurred to the oceanside of the structure during any of the stability tests. The test structure was reconstructed twice and repeat tests were conducted. Results of the repeat tests verified the results of the original tests. The results of the transmission tests (see Fig. 6-26) show that the transmitted wave heights are from about 25 to 40 percent of the incident wave heights for waves that do not overtop the structure and about 40 to 52 percent of the incident wave heights for waves that overtop the structure.

(2) Rubble-Mound Jetty Head; Breaking Waves (Example of an Unusual and Extensive Study).

(a) Project. Proposed jetty-head repair, Humboldt Bay, California.

(b) Reference. Davidson (1971b).

(c) Laboratory. WES.

(d) Test Period. June 1968 to December 1970.

(e) Problem. Humboldt Bay is located on the California coast about 280 miles north of San Francisco. The harbor elements concerned in this model study were the seaward ends (heads) of the 7,500-foot-long north jetty and the 9,000-foot-long south jetty at the entrance to the bay (Fig. 6-27). Design of the repair sections was difficult because of the extremely large breaking waves that attack the structures, the nearly continuous rough seas, and the necessity of using the existing underwater rubble-mound slope of about 1 on 5 (remains of previous jetty heads that had been severely damaged by storm wave action) as the base of the design repair sections. The 1 on 5 slope made it impractical to carry the protective cover layer of armor units down to the ocean bottom to obtain a firm toe condition for the armor-unit section because of the

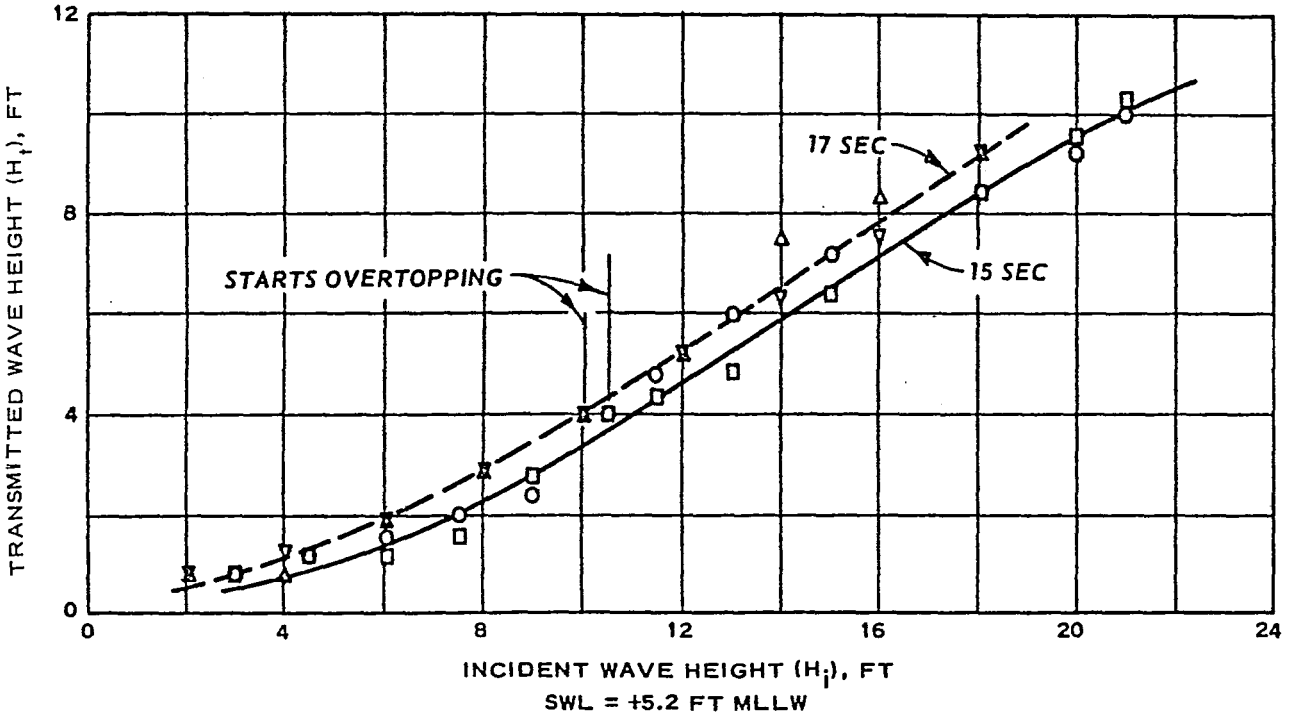

LEGEND

SYMBOL	T SEC	H_t, FT, MEASURED AT DISTANCE* OF
○	15	λ/4
□	15	λ/2
△	17	λ/4
▽	17	λ/2

* λ = WAVE LENGTH, FT

Figure 6-26. Transmitted wave heights for proposed breakwater using tribar armor units in the breakwater stability and transmission test, Monterey Harbor, California (Davidson, 1969).

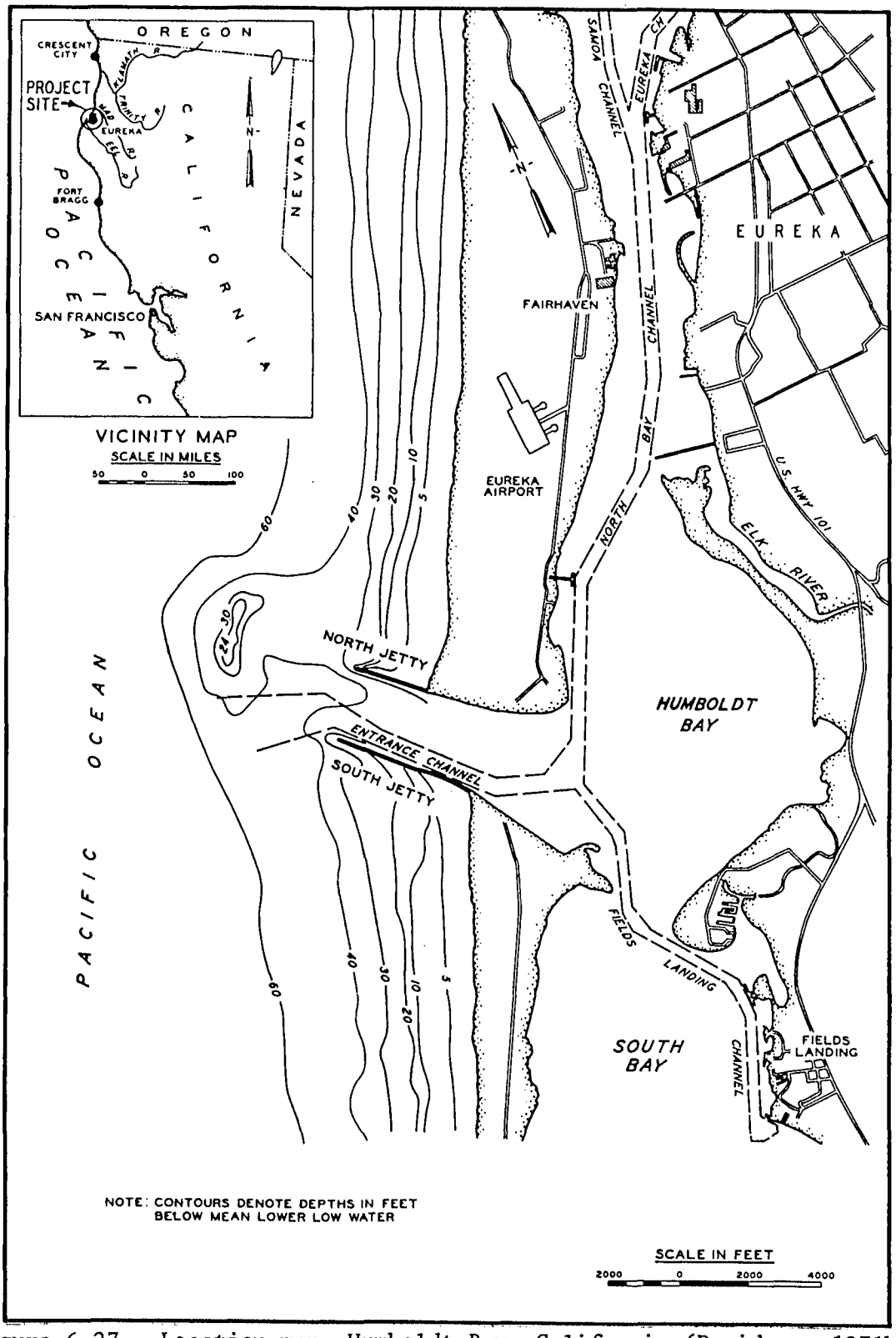

Figure 6-27. Location map, Humboldt Bay, California (Davidson, 1971b).

limited lifting capacity and horizontal reach of available land-based cranes. Floating plant equipment could not be used to place the toe parts of the repair section because of the intensity of daily wave action and the frequency of storm wave conditions. In the initial phase of the jetty repair a new monolith cap was to be constructed at the jetty head. This cap would then be used as a platform from which armor units, of such size and shape to protect the jetty head from wave action, could be either launched or placed by crane. The initial construction plan was to launch 100-ton concrete cubes either as single units or in clusters of units linked with 4-inch nylon rope. The jetty heads are exposed to storm waves from the deepwater directions (clockwise) between south-southwest and north. The maximum hindcasted deepwater wave was a 13-second period wave estimated to be 34 feet in height. The results of a wave refraction study showed that the maximum waves that could attack the jetty heads were considerably larger than the maximum deepwater wave height. Thus, the selected design wave for the structures would be limited by the bottom slopes near the structures, the water depths at the toe of the structures at the time of the storm, and the structure characteristics.

(f) Purpose of Model Study. The study was conducted to determine the adequacy of the proposed jetty repair plans and, if necessary, develop alternate designs from which the optimum plan for stability, construction techniques, and economy could be determined. It was desired to determine (1) the largest waves that could attack the structures within the limits of the wave dimensions that occur in the prototype area and refract onto the structures, (2) the best method of launching 100-ton cubes from the crest of the monolith, (3) the stability of the launched, 100-ton cube section with and without the linking of units, (4) whether the 4-inch nylon rope would be an adequate means of linking the units, (5) the best shape and minimum size of armor unit, with and without the use of a linking medium, and (6) the best shape of armor-unit section, considering the restraints imposed by the necessity of placing the protective cover layer section of armor units on the existing slope of rubble around the head of the structures. Although this investigation was concerned with the design of repair sections for both the north and south jetty heads, testing was restricted to the north jetty since the results would be generally applicable to the repair of both structures.

(g) The Model. Tests to determine the largest critically breaking waves that can attack the north jetty head, and stability tests of the different proposed plans, were conducted in an L-shaped, diffraction-type wave flume 250 feet long, and 4.5 feet deep, 50 and 80 feet wide at the wave generator and test section ends of the flume, respectively (Fig. 6-28). A flap-type wave generator was used and the wave heights were recorded by printed-circuit rods and a CEC oscillograph. The linear scale of the model was 1 to 50. This scale was selected based on the prototype waves, water depths, and length of structure shoreward of the jetty head (which required reproduction) compared with the dimensions of the wave flume and the capability of the wave generators. Although some of the armor units already available were used in the tests, it was necessary to mold additional sizes of tribars, fabricate new forms and mold an adequate

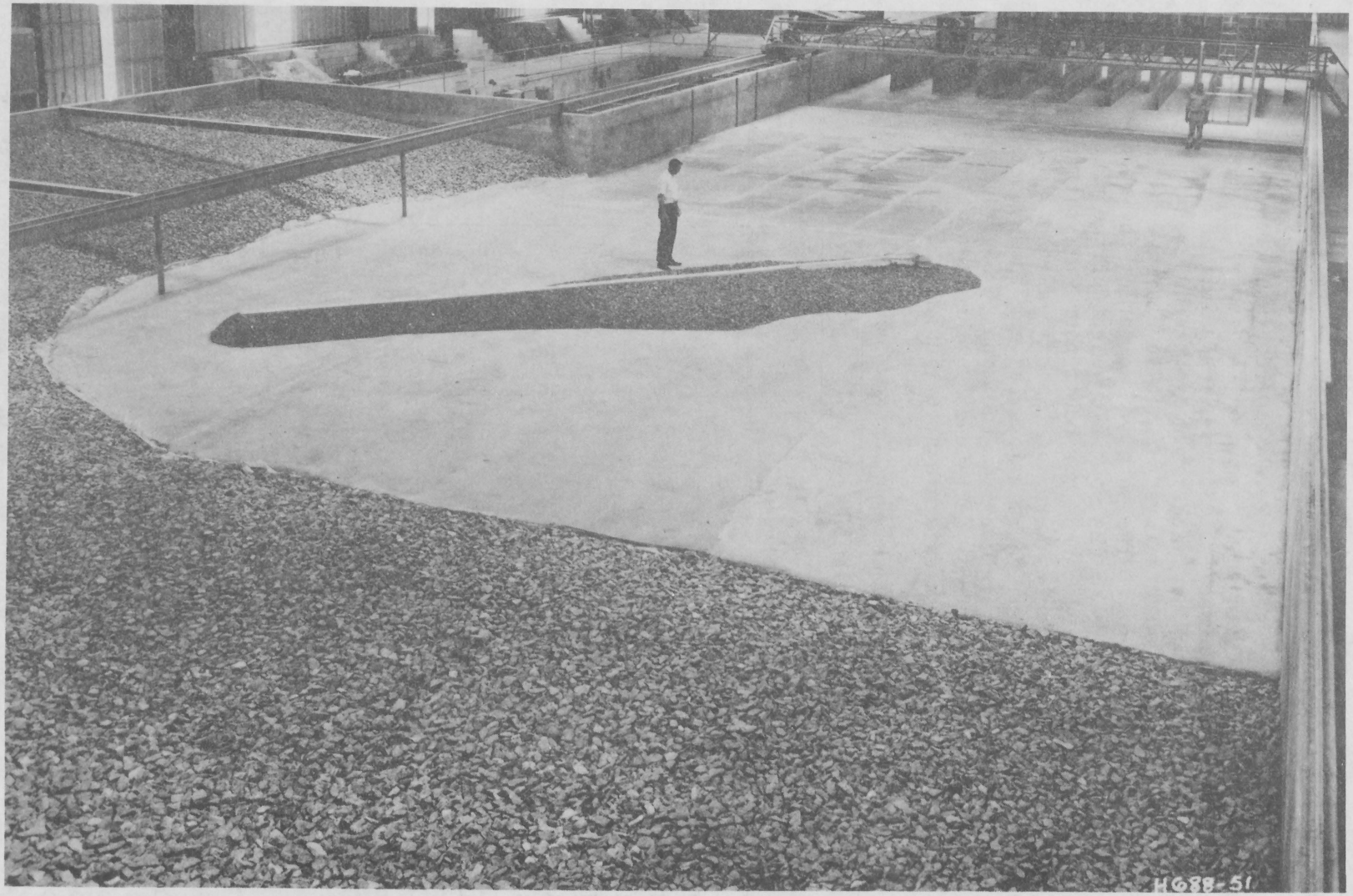

Figure 6-28. L-shaped wave flume 250 feet long, 80-foot-maximum and 50-foot-minimum width, and 4.5 feet deep (Davidson, 1971b).

supply of dolosse and trilongs, and saw limestone units to simulate the proposed 100-ton cubes. The jetty head and about 300 feet of the adjacent trunk section were reproduced, as accurately as possible, to scale. An additional 1,000-foot reach of the shoreward trunk section was reproduced to ensure that the wave environment on the outer reaches of the structure was reproduced properly. Since the stability of the 1,000-foot reach was not in question, the reach was reproduced correctly only with respect to its geometery and its wave reflective characteristics were reproduced only approximately. The specific weight of the model water was 62.4 pounds per cubic foot; the specific weight of the prototype seawater was assumed to be 64 pounds per cubic foot. Also, the specific weights of the model armor units were not the same as those of the proposed prototype armor units. The relations between these variables, model-to-prototype, were determined from equation (6-39). The weights and specific weights of the armor units used in the model tests and the corresponding prototype equivalents are given in Table 6-4.

Table 6-4. Weights of armor units in model and prototype.

Armor unit[1]	Model		Prototype	
	W_a (lb)	γ_a (lb/ft^3)	W_a (ton)	γ_a (lb/ft^3)
Cube	1.62	145.0	100	150
Trilong	0.50	142.0	28	150
Tetrapod	0.49	141.6	28	150
Tribar	0.43	140.4	23	150
Tribar	0.62	140.1	33	150
Tribar	0.80	141.0	44	150
Tribar	1.13	142.2	65	150
Dolos	0.58	140.4	32	150
Dolos	0.90	142.2	51	150
Dolos	0.90	142.2	45	155
Dolos	1.00	141.4	56	150
Dolos	1.00	141.4	43	160

[1] Details of the various types of armor units are described in Hudson (1974).

The values of $k_{\Delta p}$ and P in equations (6-40) and (6-41), as determined during the testing program, are shown in Table 6-5.

(h) Test Procedures. The test sections were installed in the flume so that the waves, which approached the structure with an angle of incidence of about 45°, reflected from the test section and were dissipated on the rubble wave absorber along the perimeter walls of the diffraction basin. Average bottom slopes were used seaward of the jetty head to approximate the prototype bottom contours. A stillwater level of +7 feet MLLW was used in all high water test conditions. This level was selected based on MHHW level of +6.4 MLLW and a superimposed wind setup of 0.6 foot. A stillwater level of 0.0 foot MLLW was also used in

Table 6-5. Shape-placing coefficient and porosity of armor units.

Armor unit	Placement method	n	Shape-placing coefficient $k_{\Delta p}$	Porosity P
Tribar	Random	2	1.02	0.54
Tetrapod	Random	2	1.04	0.50
Trilong	Random	2	0.94	0.40
Dolos	Random	2	0.81	0.56
Cube	Launched	(-------- Not applicable ----------)		

a large percentage of the tests to determine the effects of storm waves at low tide on the stability of the toe part of the repair section of armor units. The water depth at the toe of the existing rubble-mound part of the jetty head was 36 feet MLLW. Since the bottom slope seaward of the toe in the immediate vicinity of the structure was about 1 on 10, the critically breaking waves that could attack the structure correspond to breaking depths somewhat greater than the depth at the toe. The statistical deepwater data and the results of the refraction study indicated that the design waves for the structure at each water depth would be critically breaking waves (the largest wave that can attack a particular structure for a given depth and wave period without forming a cushion of water between the impinging jet of water and the structure slope). The magnitude of such waves must be determined by use of scale models. Preliminary tests with several of the different types of repair sections under consideration were conducted to determine the critically breaking waves, since the waves would be used both in the testing program and in the designing of the prototype repair section. This procedure is in contrast to the situation where the structure under design is a rubble-mound breakwater trunk. In this case the design waves can be selected from available statistical deepwater wave data and refraction studies, and from available experimental data relating the largest waves that can attack the structure as a function of the breakwater slope, bottom slope seaward of the toe, the depth of water at the toe, and the wave characteristics (Jackson, 1968). The results of the preliminary tests showed that a 16-second, 40-foot-high wave was the largest and most damaging that would break on the repair sections with a stillwater level of +7 feet MLLW. The corresponding wave for the 0.0-foot stillwater level was a 16-second wave with a height of 31 feet. Larger waves are believed to have occurred according to the available statistical data and refraction study; however, such waves would break before reaching the structure. In an attempt in 1963 to protect the toe of the concrete monolith on the south jetty, 100-ton unlinked concrete cubes were cast on the edge of the monolith and launched by jacking up the rear side of the bottom form and applying air pressure to initiate movement of the cube from the form bottom. This method and other approaches to the launching problem, such as sliding the cubes down an inclined plane, were tested in the model. It was found that either of the launching methods tested would be satisfactory. Since the original proposal called for repairs to the jetty heads by linking clusters of

100-ton cubes with 4-inch-diameter nylon rope, determining by model tests whether the rope would withstand the forces induced during construction and by wave action after construction was desired. To obtain elastic similarity between model and prototype linking media, the ratio between elastic and gravity forces must be equal in model and prototype (eq. 6-11b). If it is assumed that $(\gamma_w)_m = (\gamma_w)_p$, which is accurate enough for this study, equation (6-11b) reduces to

$$\frac{(E_N A)_m}{(E_N A)_p} = \left(\frac{L_m}{L_p}\right)^3 \tag{6-11c}$$

and, since for this model study $(L_m/L_p)^3 = (1/50)^3$,

$$(E_N A)_m = \frac{(E_N A)_p}{125{,}000} \tag{6-11d}$$

where E_N is the modulus of elasticity of nylon in pounds per square inch and A the cross-sectional area of the rope in square feet. A 4-inch nylon rope has a breaking strength of about 360,000 pounds, and the working load was assumed to be about 100,000 pounds with the elongation about 33 percent. To reproduce an equivalent model linkage at a linear scale of 1:50, the medium should elongate 33 percent at a load of about 1.5 pounds and break at a load of about 3 pounds. Tests of different material found that the only material to have the required elongation and breaking characteristics (a combination of neoprene and rubber-rayon cords) was too stiff; i.e., the bending qualities were not adequate. Because the breaking characteristics were the most important for these tests, a size 000 silk surgical thread with a breaking strength of 3 pounds and an elongation of 3 percent was selected for the linkage tests. Preliminary launching tests were made for several clusters of 100-ton model cubes with the surgical thread as the linkage medium, and each time a cluster was launched several of the lines were broken. Since the 4-inch nylon rope proposed for use in the prototype was inadequate, it was decided to perform all linkage tests with No. 15 nylon twine which had a breaking strength of 41 pounds and was sufficiently flexible. In this way the advantages of using a linking medium for different types of repair sections could be evaluated, although the rope strength required to prevent breaking could not be determined.

(i) Summary of Tests and Results. The existing rock mound and the broken monolithic head of the north jetty were reproduced in the model down to the -36-foot contour (MLLW), and the proposed rehabilitated concrete monolith was constructed around the existing part of the monolith from the plans furnished by the U.S. Army Engineer District, San Francisco (Fig. 6-29). The crest elevation of the monolith was +25 feet MLLW and the radius was 55 feet. The protective cover layer for each plan for repair tested was placed on the existing rubble slope (about 1 on 5) around the rehabilitated monolith and as far shoreward and seaward as was considered necessary to provide the required stability of the armor units and protection of the monolithic head. A series of 10 tests was

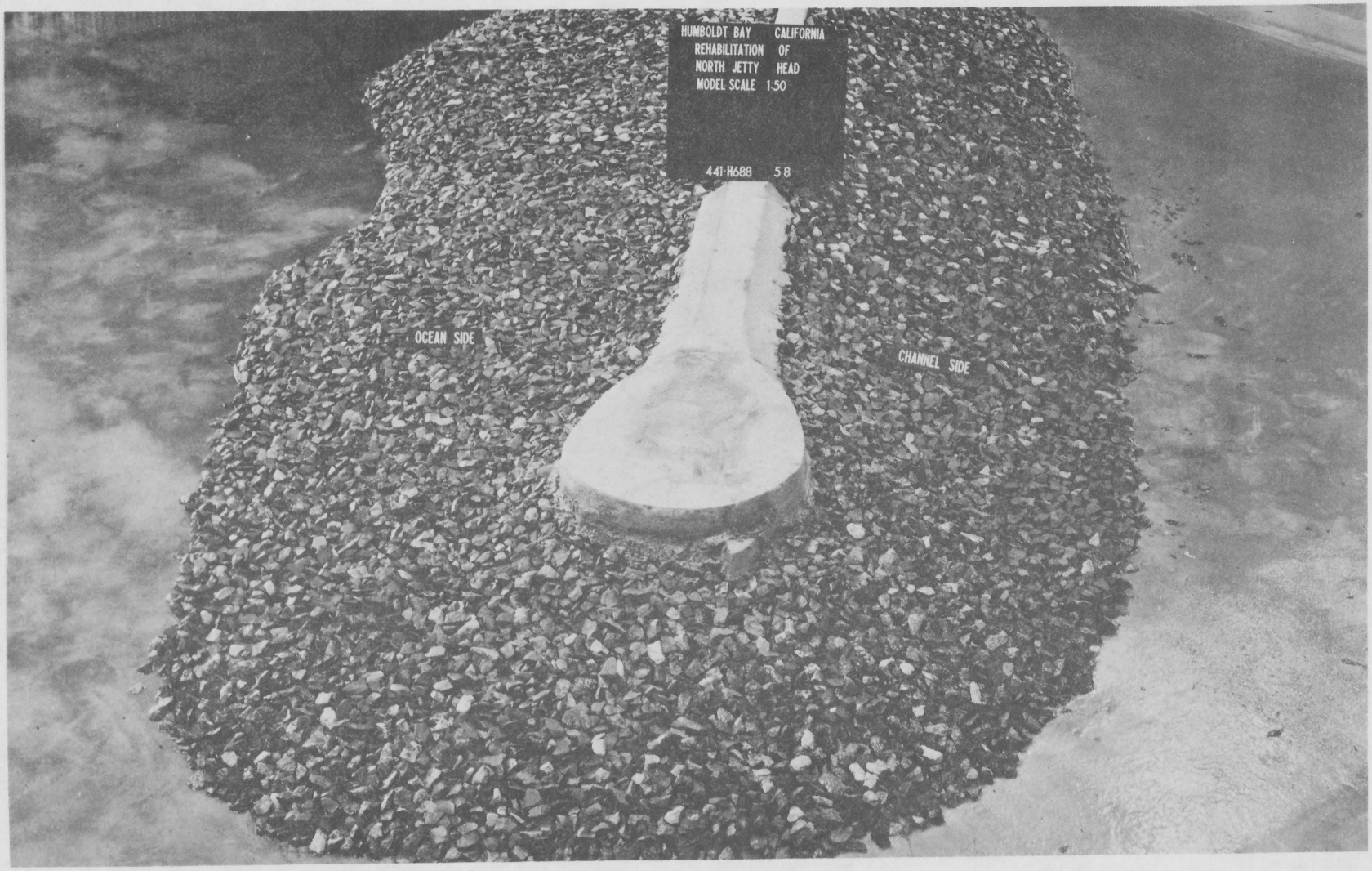

Figure 6-29. Rehabilitated concrete monolith head proposed for the north jetty, Humboldt Bay jetty model (Davidson, 1971b).

conducted (with the type of plan and tests conducted based on the results of the preceding tests); the purpose and summary of results for each test series are given below.

1 Test 1. Purpose: To determine the relative stability of unlinked armor-unit repair sections using cubes, tetrapods, and tribars. (A supply of dolos armor units was not available at test time, and the trilong unit was devised later.)

Results: The stability of the armor units for the conditions tested (i.e., cot α = 5, nonbreaking waves, and an SWL = +7 feet MLLW) in terms of K in the stability equation, was:

Armor unit	Weight (ton)	$H_{D=o}$ [1] (ft)	K
Cube	100	22	0.7
Tetrapod	28	23	2.7
Tribar	23	29	6.6

[1] $H_{D=o}$ is the model selected design wave height for the no-damage criterion.

Based on these results, further testing of cubes was limited to determining whether the linking medium would make the use of cubes feasible (test 2), and no further tests of tetrapods were made.

2 Test 2. Purpose: To determine the feasibility of linking 100-ton cubes in clusters and the effects of armor-unit linking on the stability of the repair sections using cubes.

Results: Tests showed that the free-fall launching of cubes would not result in an armor toe distance seaward of the monolith sufficient to ensure a stable cover layer, and that stability of the section was not increased by using more than three units in a cluster when the units are launched by the free-fall method (Fig. 6-30).

3 Test 3. Purpose: To determine the best arrangement of tribar armor units with and without linking lines. The largest tribar armor unit available at test time (23-ton unit) was used.

Results: Tests showed that 23-ton tribars, when properly linked, could provide the desired protection to the structure head. However, considerable rocking movement of the nested armor units began at a wave height of about 34 feet. Thus, the possibility of abrasion failure of the linking medium, and the problems in placing the units in the field in the manner used in the model, made this plan unacceptable.

4 Test 4. Purpose: To determine the stability characteristics of the trilong armor unit (for both the linked and unlinked conditions) used to form the protective cover layer of the rehabilitated jetty head. Units of 28 tons were used in the tests.

Results: The maximum wave height for which two layers of the 28-ton (150 pounds per cubic foot) trilong armor units, randomly placed, were stable on the 1:5 slope was 21 feet, corresponding to a K of 2.1.

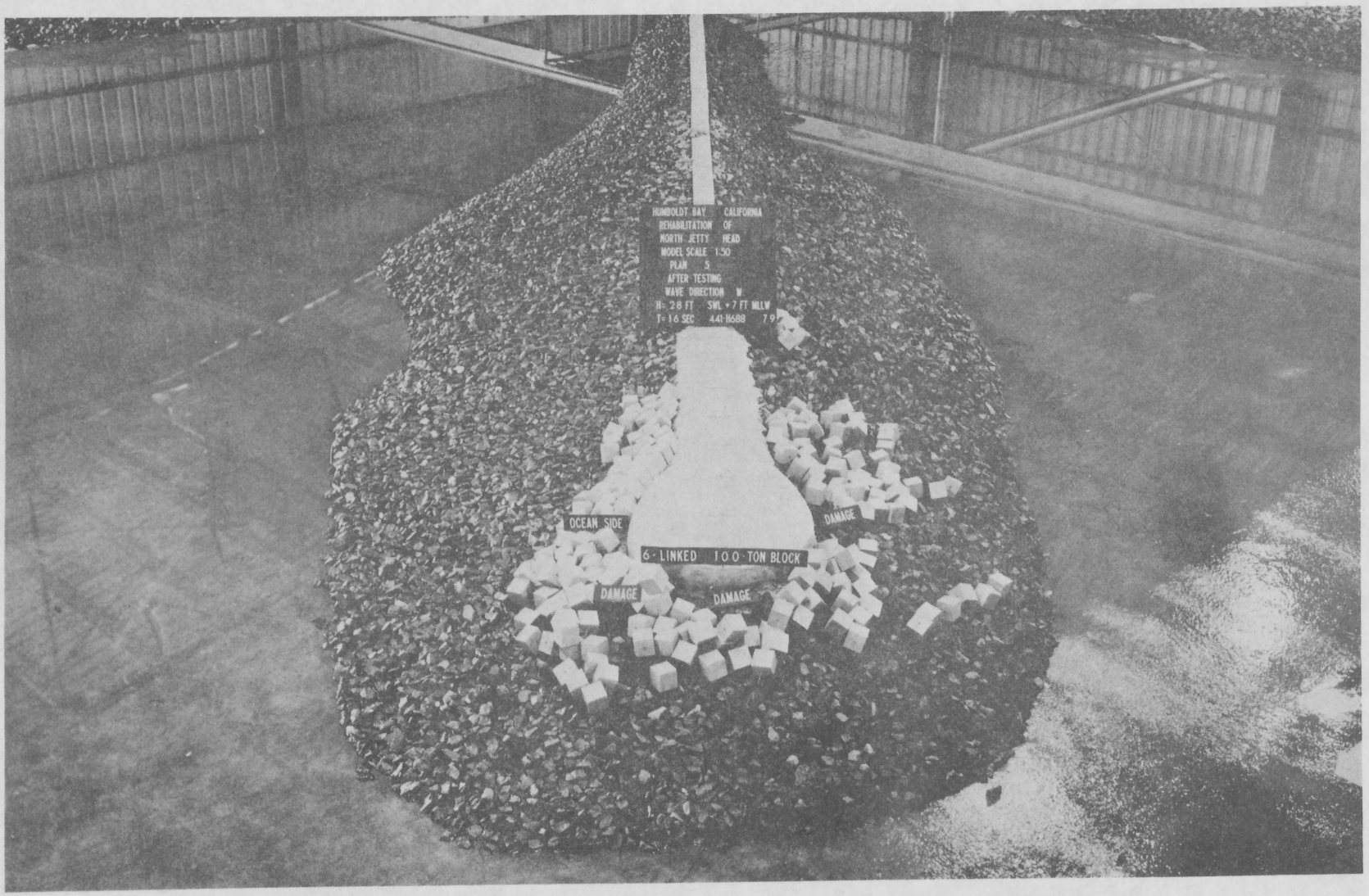

Figure 6-30. Jetty plan after attack by 16-second, 28-foot waves (cubes of 100 tons were linked in clusters of six), Humboldt Bay jetty model (Davidson, 1971b).

Linking the units increased stability; however, they began rocking in their nested positions at a wave height of about 30 feet. Thus, the units were considered unacceptable, and no further stability tests were conducted.

5 Test 5. Purpose: To determine the stability of 33- and 44-ton tribar armor units (with and without the use of a linking medium) for protection of the rehabilitated jetty head.

Results: The linked 33- and 44-ton tribar armor units were stable for the 40-foot design wave, but failure occurred when the linking medium was cut to simulate breakage by abrasion. Considerable damage occurred when the 44-ton units were tested unlinked using 40-foot waves. Therefore, it was decided to design a tribar section stable for 40-foot waves when the units were unlinked. Tribars of 65 tons were selected for these tests (test 8).

6 Test 6. Purpose: Previous tests indicated that it was difficult to obtain stability of the armor units at the shoreward end area of the repair section, and that the repair section usually failed in this area before the no-damage wave for the head section was determined. Thus, this series of tests was conducted to determine the most practical method of obtaining stability of both areas of the repair section for the same no-damage wave height.

Results: The use of a linking medium and either 33- or 44-ton tribars would provide the shoreward end area with stability comparable to that of the head section, provided the linking lines do not fail by abrasion. It was found that migration of 44-ton tribar units could be prevented by the use of concrete or pile barriers if practical methods of constructing these barriers in the prototype could be devised (Fig. 6-31).

7 Test 7. Purpose: To determine the stability of the toe part of the test sections for the low water (SWL = 0.0 foot MLLW) condition. Since the slope of the repair section was about 1:5, and the design waves for the high water and low water conditions were 40 and 31 feet in height, respectively, the toe distance from the edge of the monolith was critical because of the difficulty and expense of providing a crane with adequate reach and lift capacity.

Results: Tests showed that the stability of the toe armor units around the jetty head at low tide was critical with respect to the design of the repair section.

8 Test 8. Purpose: To develop a stable repair section with 65-ton (150 pounds per cubic foot) tribars using the selected design waves of 40 feet at the +7 foot MLLW level and 31 feet at the 0.0-foot MLLW level. The tribar weight of 65 tons was selected based on the results of previous tests, using 33- and 44-ton units, and the stability equation (eq. 6-4b).

Results: A repair section of unlinked 65-ton (150 pounds per cubic foot) tribars was found to be stable for the 40-foot design wave at +7 feet MLLW (stillwater level), and for the 31-foot design wave at the 0.0 foot MLLW (stillwater level).

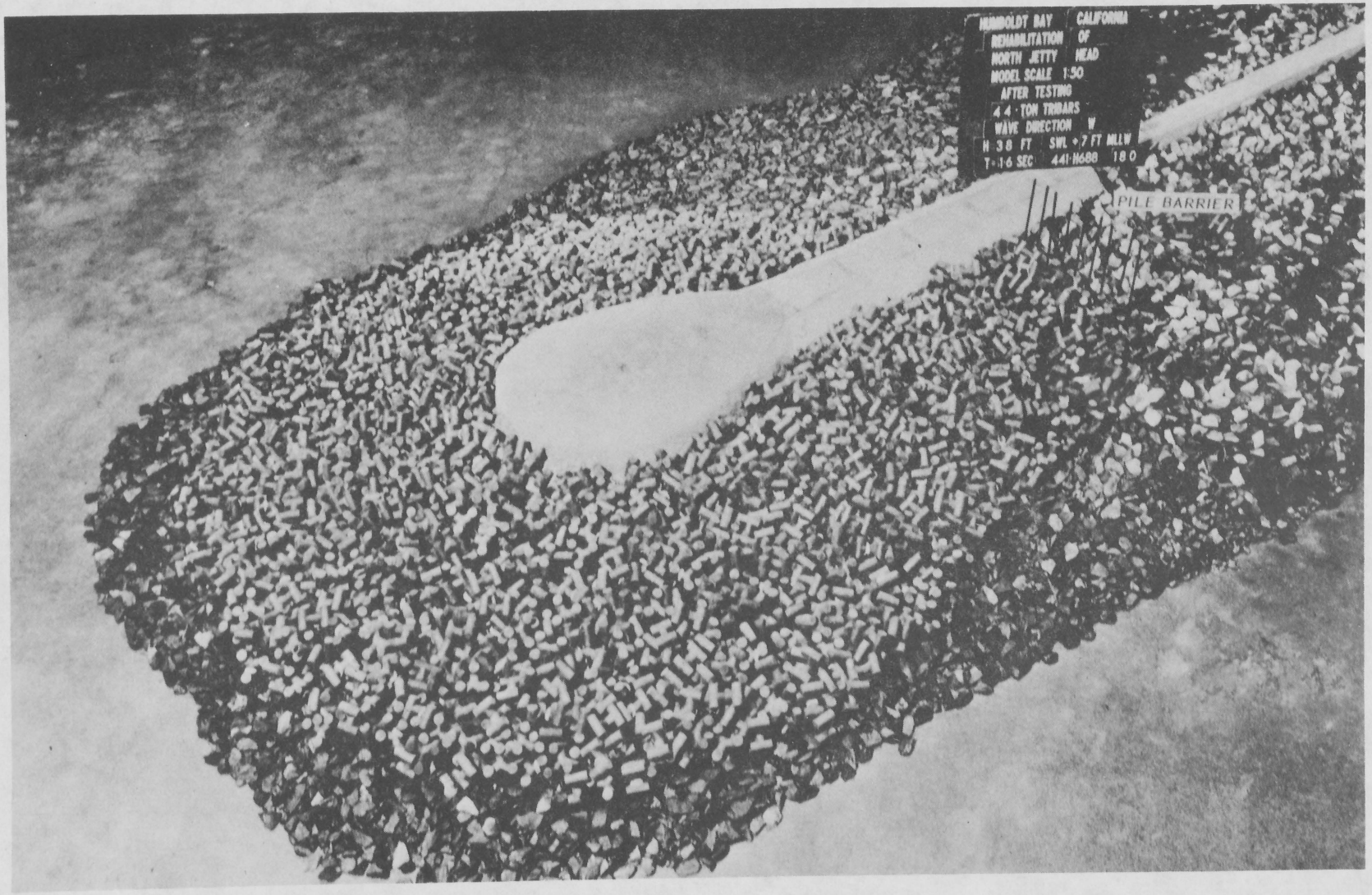

Figure 6-31. Jetty plan with pile barrier at station 71 + 50 after attack by 16-second, 38-foot waves (unlinked 40-ton tribars), Humboldt Bay jetty model (Davidson, 1971b).

9 Test 9. Purpose: To determine the stability of 32-ton dolos armor units (this unit weight became available at test time from another study under investigation). The results of these tests would then be used, in conjunction with the stability equation, to estimate the required weight of dolos required for stability.

Results: Tests of 32-ton dolosse showed that the maximum no-damage waves for this unit were 36 feet in height for the +7 foot stillwater level and 30 feet in height for the 0.0-foot stillwater level. It was estimated that 48-ton (150 pounds per cubic foot) dolos armor units would be stable for both high tide and low tide design wave conditions.

10 Test 10. Purpose: On the basis of the series 9 test results, a prototype repair section using 48-ton (150 pounds per cubic foot) dolos was indicated for the north jetty head section. Because a modest increase of specific weight would allow a comparatively large decrease in armor-unit weight, for the same armor-unit stability, a repair section using 42-ton (155 pounds per cubic foot) dolos on the shoreward end area of the structures was proposed. The lighter weight units, both using the same forms for molding, would allow a smaller toe distance from the monolith. Thus, the use of a lighter weight unit and a shorter toe distance would decrease the required lifting and reaching capability of the crane. The series 10 tests were conducted to check the stability of this revised design section.

Results: This test series concluded that 43-ton (160 pounds per cubic foot) dolos armor units would be satisfactory if a minimum toe distance of 215 feet from the radius point of the monolith is used (Fig. 6-32).

(3) Composite Breakwater Trunk; Nonbreaking Waves (Example of Combined Model and Analytical Design).

(a) Project. Proposed construction of a vertical-wall parapet on an existing rubble breakwater, Indiana Harbor, Indiana.

(b) Reference. Hudson and Wilson (1953).

(c) Laboratory. WES.

(d) Test Period. October 1952 to January 1953.

(e) Problem. Indiana Harbor is located on the south shore of Lake Michigan about 5 miles from the southeast limits of Chicago, and is exposed to waves from the northerly directions. Previous tests on a 1:150-scale model of Indiana Harbor indicated that the crest of the rubble-mound east-west breakwater (Fig. 6-33) should be raised to an elevation of about +15 feet LWD for adequate protection from wave overtopping to allow construction of a proposed inner-harbor pier expansion. A vertical-wall parapet situated on top of the existing east-west breakwater was proposed for this purpose.

(f) Purpose of Model Study. The combined scale model and analytical investigation was conducted to determine the wave forces on the proposed vertical-wall parapet, and the weight of parapet necessary to ensure its stability against overturning and sliding.

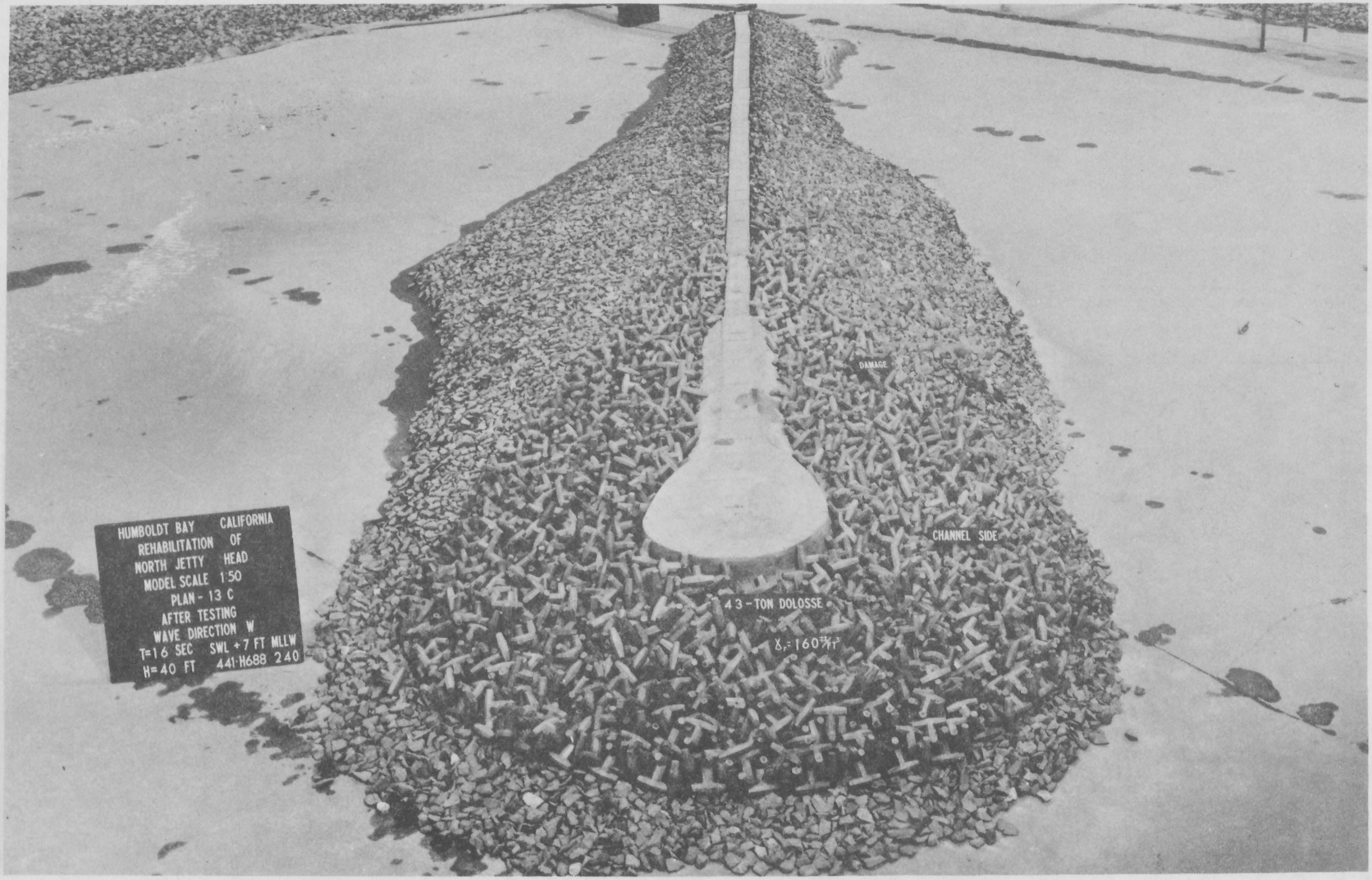

Figure 6-32. Jetty plan after attack of 16-second, 40-foot waves with stillwater level of +7 feet (unlinked 43-ton dolosse), Humboldt Bay Jetty model (Davidson, 1971b).

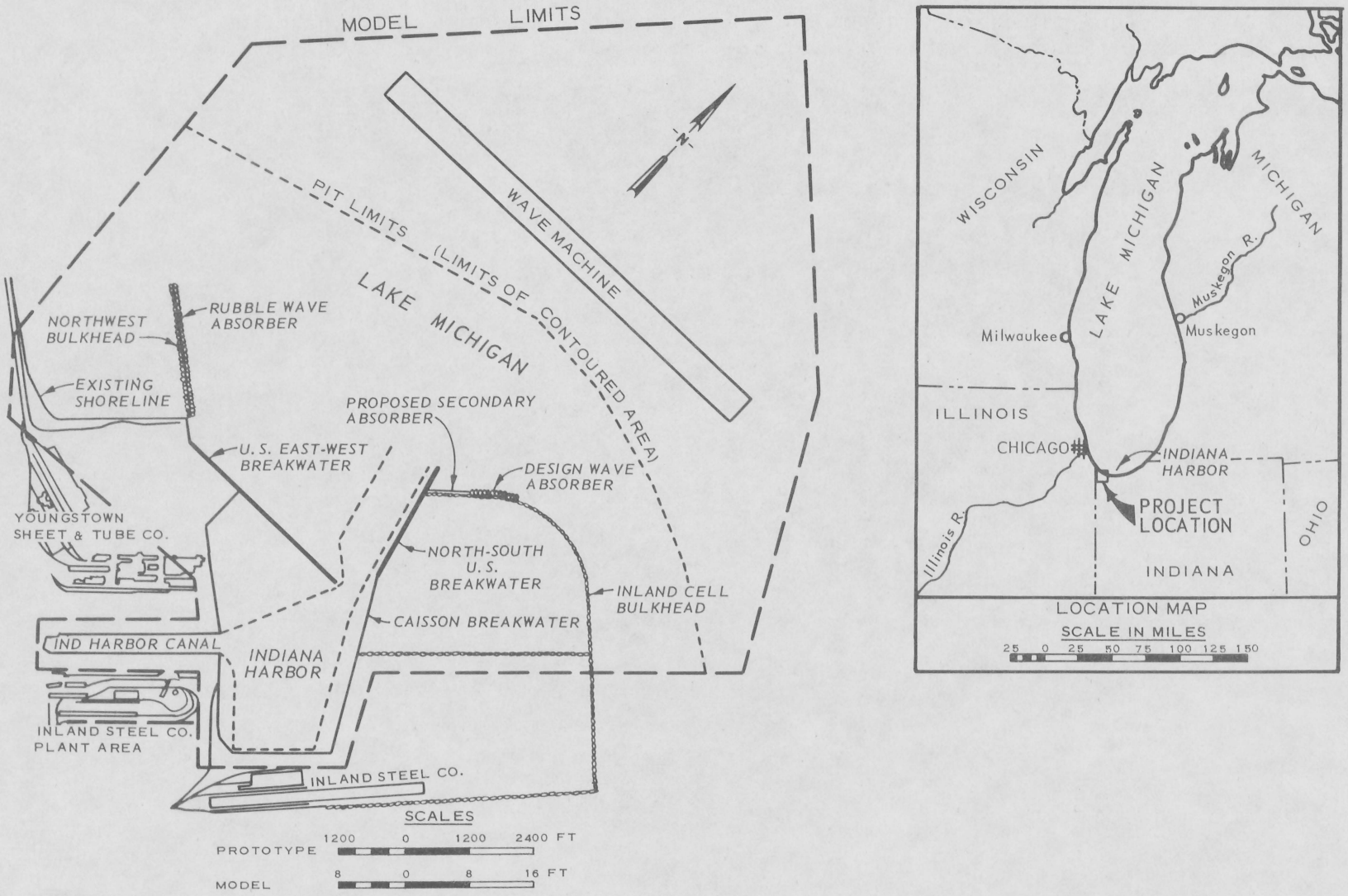

Figure 6-33. Location map and limits of 1:150-scale harbor model, Indiana Harbor, Indiana (Straub and Hudson, 1953).

(g) The Models. Tests on 1;50- and 1:55-scale models, designed and operated by Froude's law, were conducted in a wave flume 1.0 foot wide, 1.5 feet deep, and 76.0 feet long. The test sections were placed at one end of the flume and test waves were generated at the other end by a combination flap-piston wave generator. Wave heights were measured with electrical gages and recorded on an oscillograph. Horizontal wave forces on the parapet were measured on the 1:50-scale model with a Statham force gage mounted on the harborside of a hinged gate in a fixed parapet (Figs. 6-34 and 6-35). Force-time curves were recorded on a Brush oscillograph. The hinged gate was 0.5 foot wide (model dimension) and was mounted on an aluminum part of the test section. Lakeward of the parapet, the existing rubble breakwater was modeled of molded concrete blocks and crushed limestone. In the 1:55-scale model, the test section of the existing rubble breakwater was simulated throughout with concrete blocks and crushed stone. The model parapet was molded in concrete (Fig. 6-36). The bases of the parapet test sections were ground smooth to conform to the curvature of the breakwater crest. The breakwater cap rocks were also smoothed and placed to provide a uniform bearing surface for the parapet. For these tests the parapet was placed on the breakwater crest without restraints.

(h) Test Procedures. The dimensions of the proposed parapet are shown in Figure 6-37. The testing procedure was such that the wave forces on the parapet, caused by the design wave, could be evaluated and a stable parapet could be developed. Storm waves that attack the east-west breakwater vary in period from about 5 to 10 seconds and in height to about 15 feet. However, since the selected stillwater level was +3 feet LWD, and the proposed crest elevation of the parapet was +15 feet, preliminary tests showed that the maximum wave force on the structures would be caused by waves smaller than 15 feet in height. Based on the preliminary tests, a design wave with a 10-second period and a 10.5-foot height was selected. The objectives of this study were to determine the total horizontal force, F, and the uplift force, U, acting per foot length of parapet. It was assumed that the horizontal force diagram was triangular (Fig. 6-38). The maximum force, P, determined with respect to time with the force gage (Fig. 6-39) and the maximum instantaneous force on the force-time curve (with the assumed horizontal force diagram) were used to derive the total horizontal force, F. The horizontal force-time curve was also used, with the torque-acceleration equation of motion for a rigid body rotating about a fixed axis (eq. 6-42) to determine the tendency of the parapet to overturn (Fig. 6-40).

$$\theta = \frac{a}{I_M} \int_o^t \int_o^t P dt dt - \frac{Wbt^2}{2 I_M} + \frac{Uct^2}{2 I_M} . \qquad (6\text{-}42)$$

The uplift forces on the parapet were estimated by tests in which the weight of the parapet was reduced by small decrements until the waves caused failure by sliding. This parapet section was designated the maximum failing parapet (dimensions are shown in Fig. 6-41). Figure 6-42

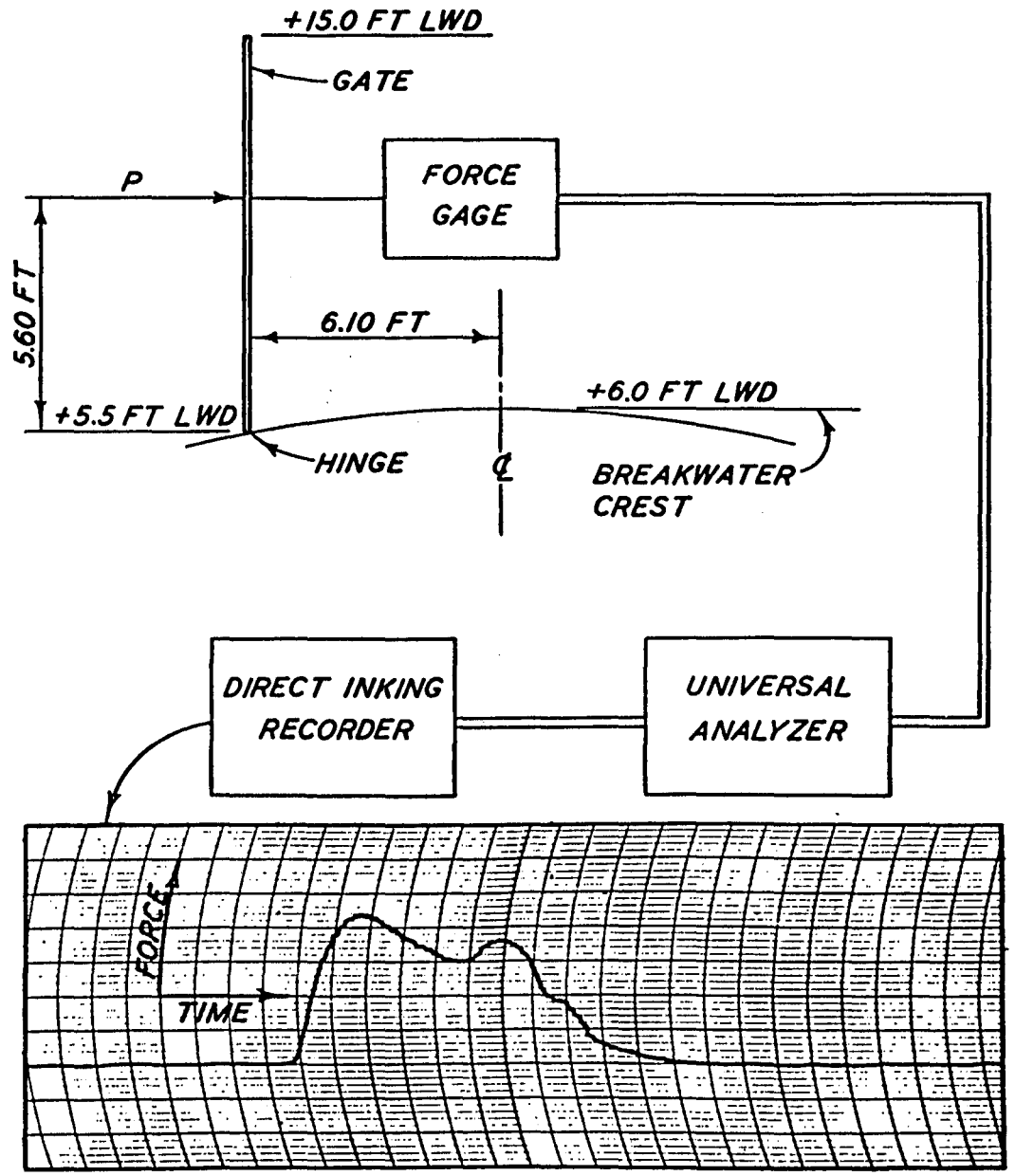

Figure 6-34. Apparatus used to measure wave forces, Indiana Harbor breakwater model (Hudson and Wilson, 1953).

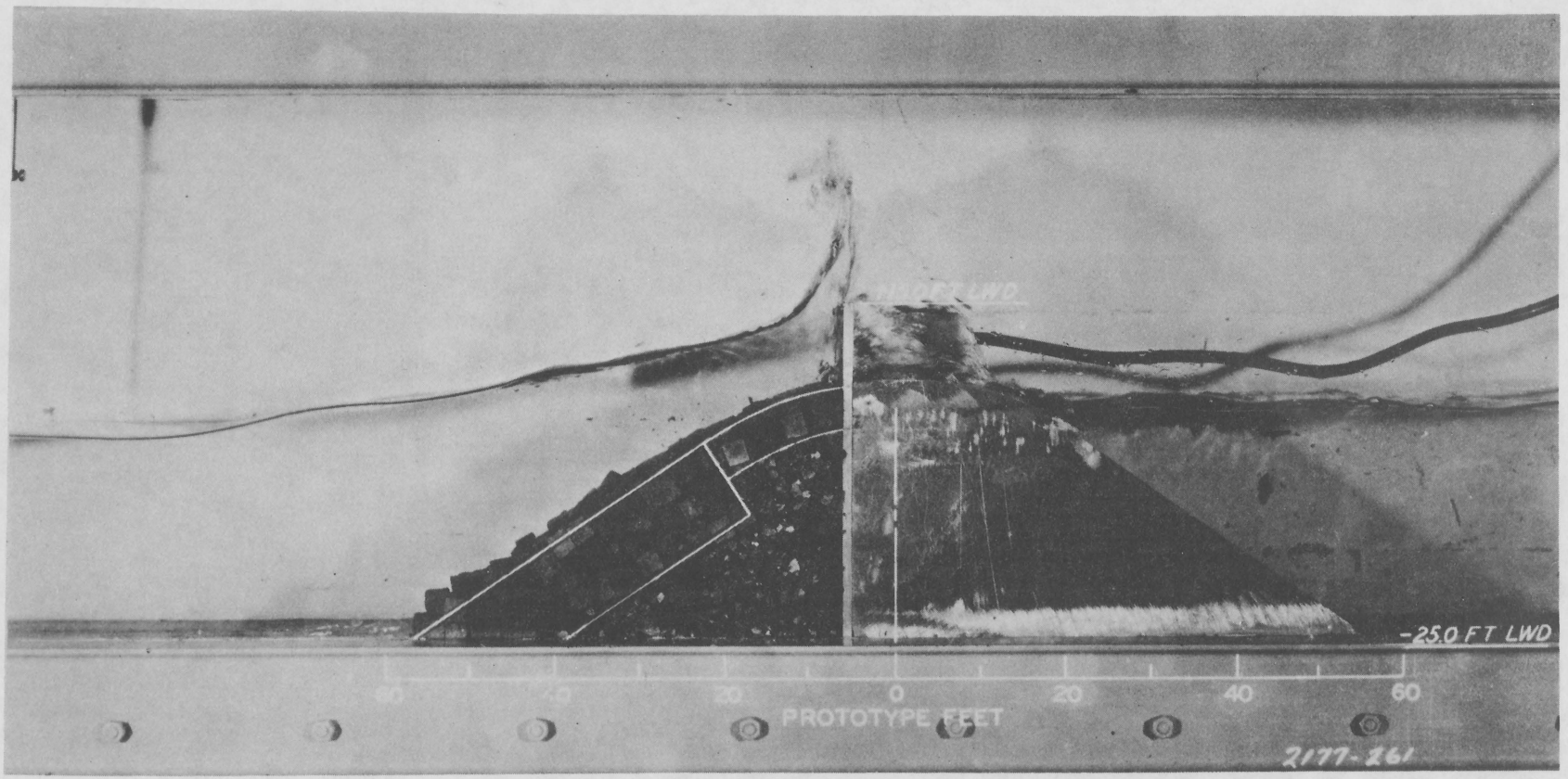

Figure 6-35. 1:50-scale test section (10-second, 10.5-foot waves), Indiana Harbor breakwater model (Hudson and Wilson, 1953).

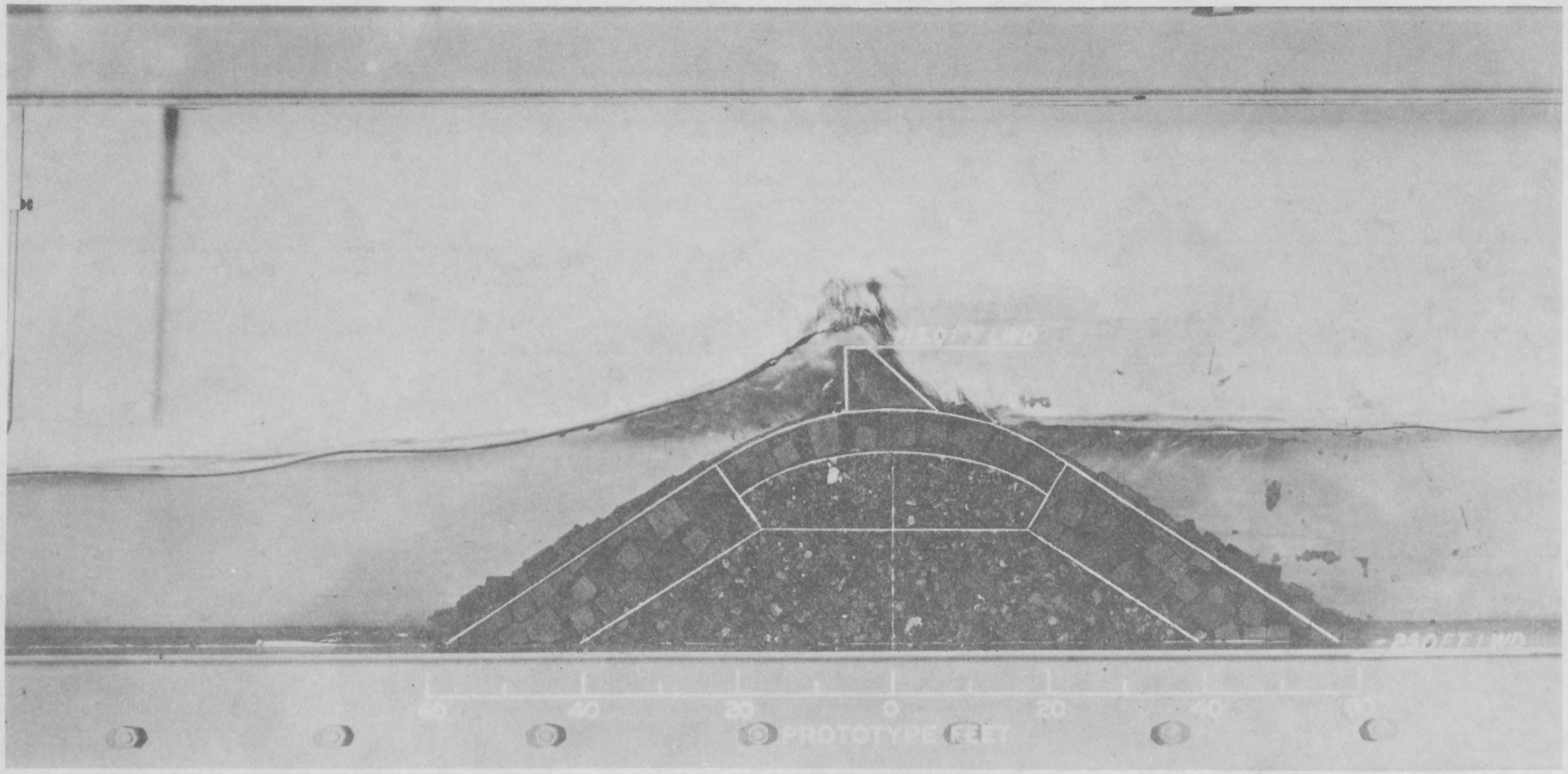

Figure 6-36. 1:55-scale east-west breakwater and proposed parapet (10-second, 10.5-foot waves), Indiana Harbor breakwater model (Hudson and Wilson, 1953).

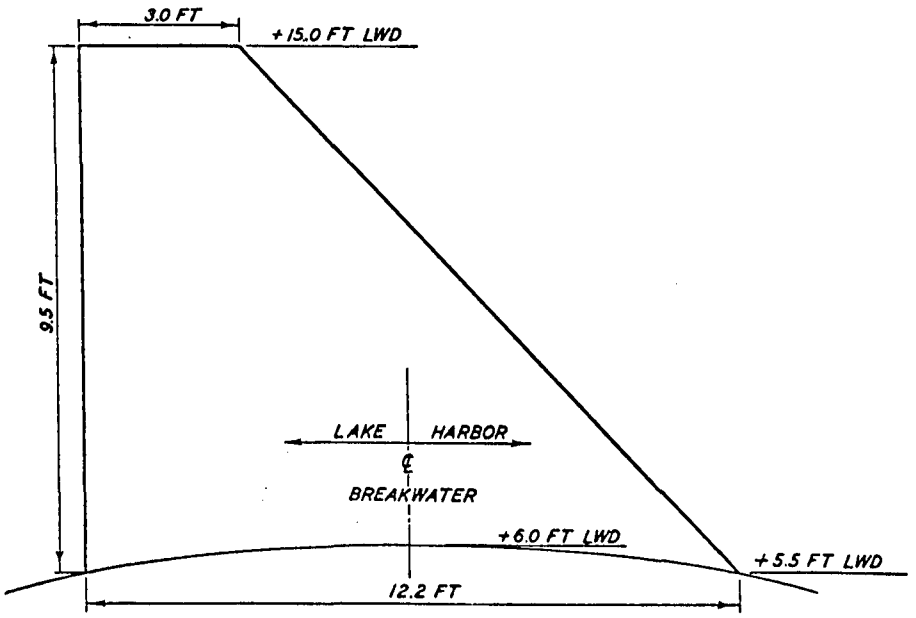

Figure 6-37. Dimensions of proposed parapet, Indiana Harbor breakwater model (Hudson and Wilson, 1953).

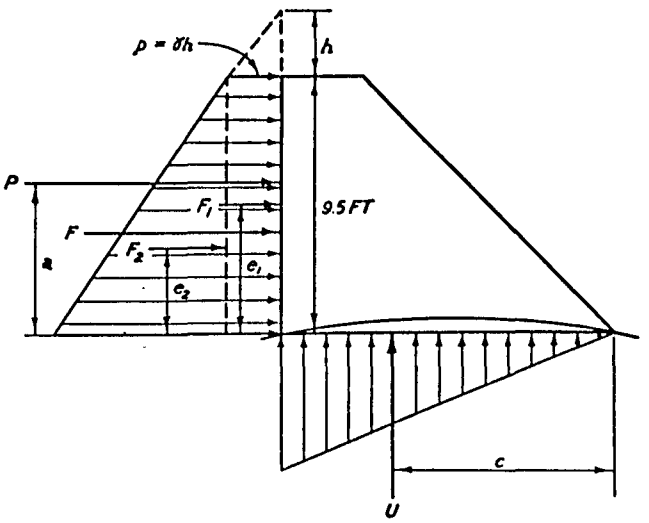

$F_1 = 9.5\,\gamma h$

$F_2 = \frac{P_a - F_1 e_1}{e_2}$

$F = F_1 + F_2$

$a = 5.60$ FT
$c = 8.13$ FT
$e_1 = 4.75$ FT
$e_2 = 3.17$ FT
$h = 2.50$ FT
$\gamma = 62.4$ LB/FT^3

Figure 6-38. Assumed wave-force distribution and equations for maximum force, Indiana Harbor breakwater model (Hudson and Wilson, 1953).

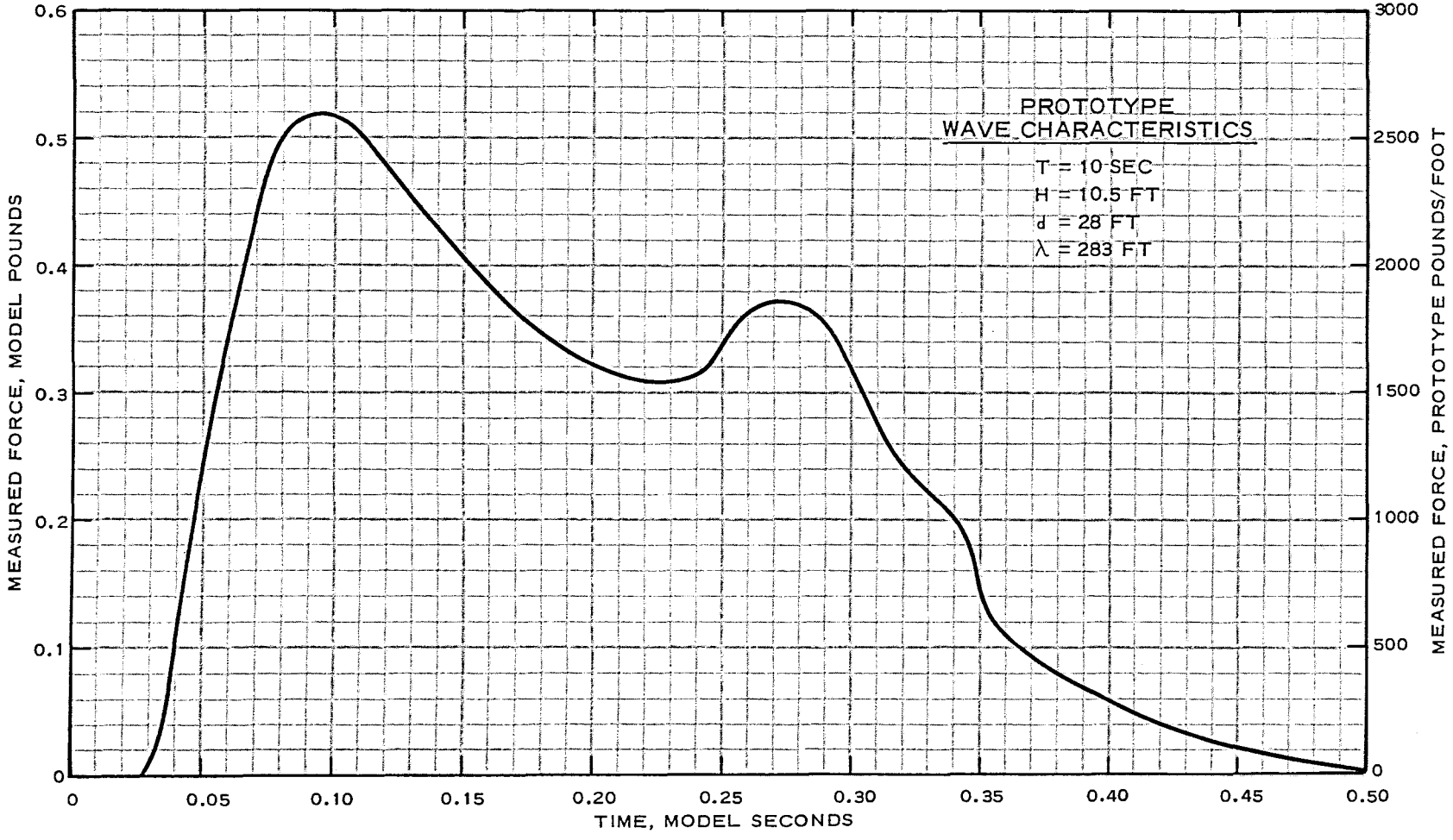

Figure 6-39. Force-time curve, 1:50-scale Indiana Harbor breakwater model (Hudson and Wilson, 1953).

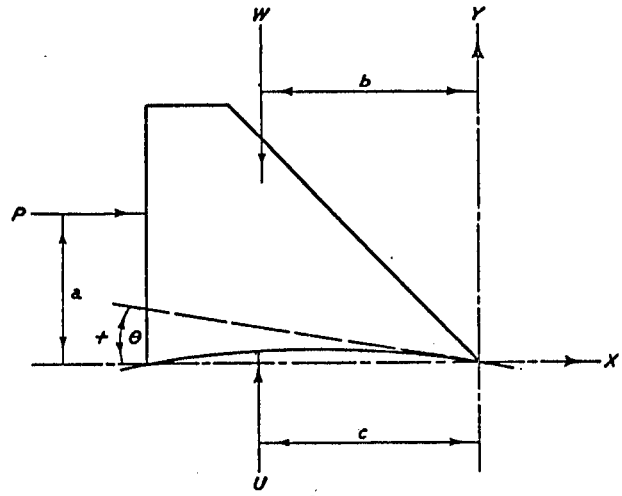

$$I_M \alpha = \Sigma T_0 \qquad \alpha = \frac{d\omega}{dt} = \frac{d^2\theta}{dt^2}$$

$$I_M \frac{d^2\theta}{dt^2} = Pa - Wb + Uc$$

$$\theta = \frac{a}{I_M}\int_0^t\int_0^t P\,dt\,dt - \frac{Wb}{I_M}\int_0^t\int_0^t dt\,dt + \frac{Uc}{I_M}\int_0^t\int_0^t dt\,dt$$

$$\theta = \frac{a}{I_M}\int_0^t\int_0^t P\,dt\,dt - \frac{Wbt^2}{2I_M} + \frac{Uct^2}{2I_M}$$

IF θ IS POSITIVE, SECTION WILL FAIL BY OVERTURNING

Figure 6-40. Overturning equation for parapet, Indiana Harbor breakwater model (Hudson and Wilson, 1953).

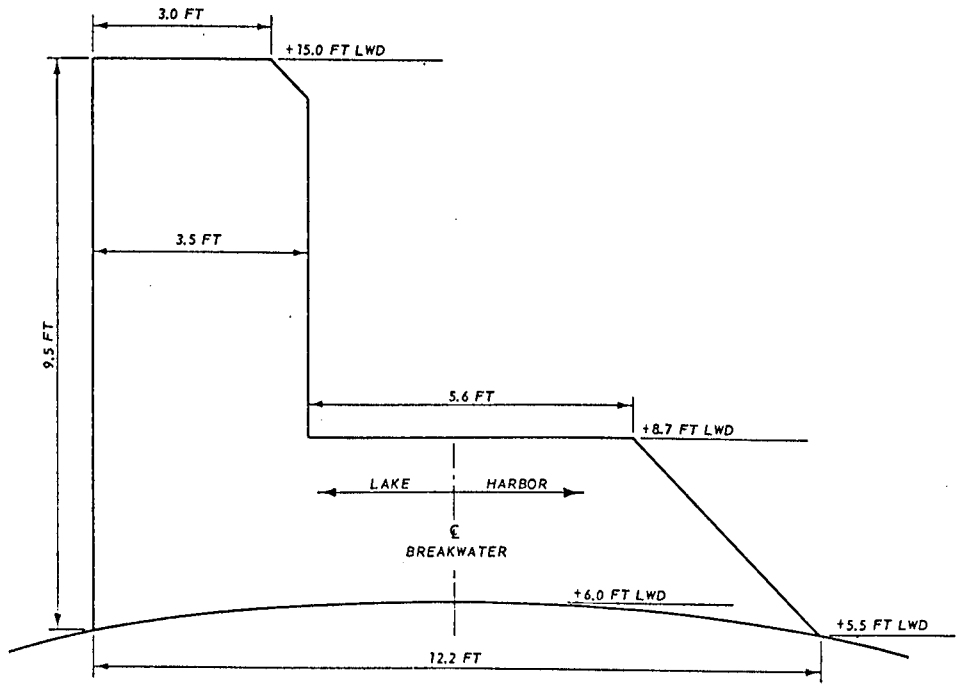

Figure 6-41. Maximum failing parapet, Indiana Harbor breakwater model (Hudson, and Wilson, 1953).

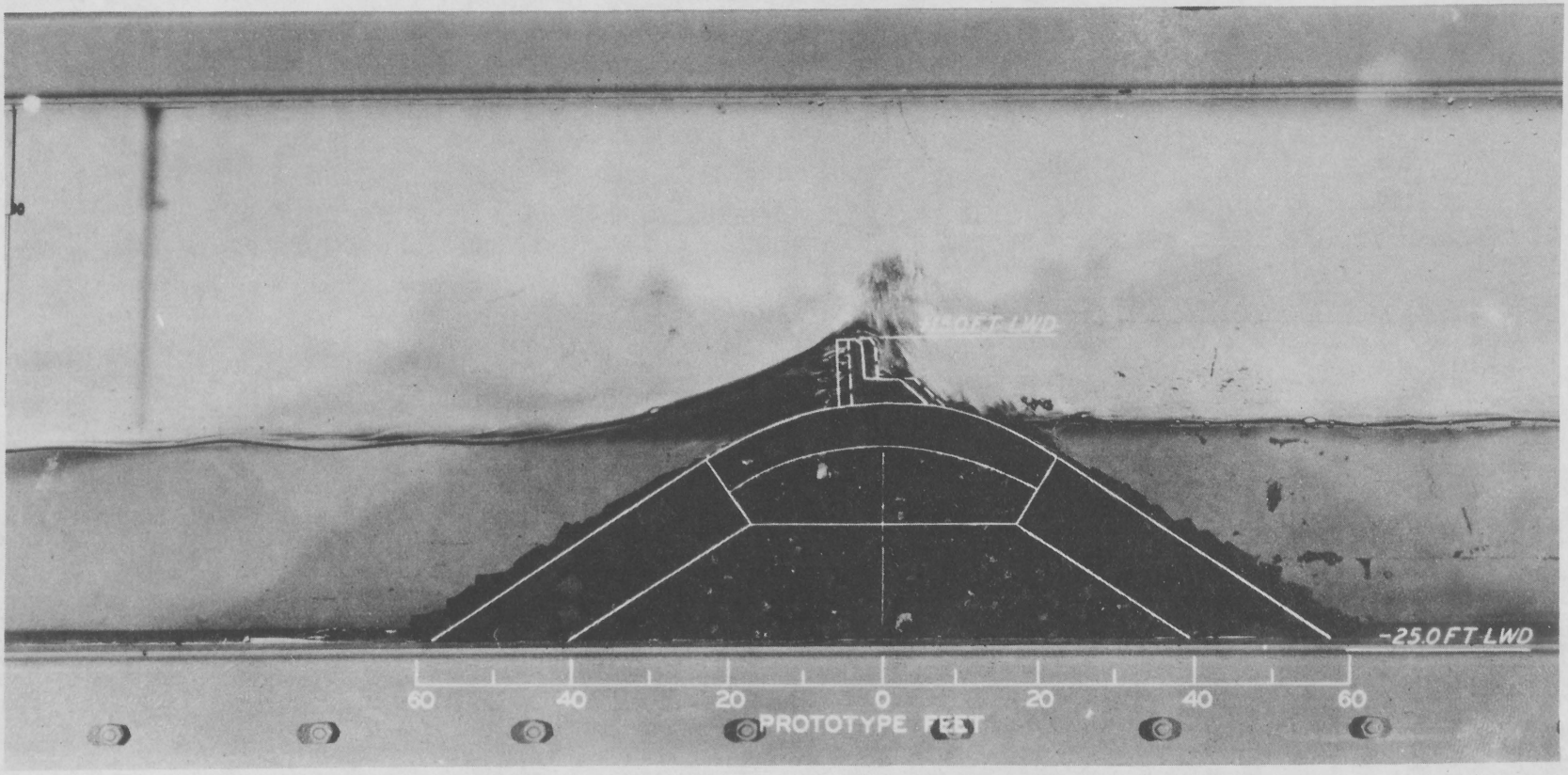

Figure 6-42. 1:55-scale test section with maximum failing parapet (10-second, 10.5-foot waves), Indiana Harbor breakwater model (Hudson and Wilson, 1953).

shows the selected design waves attacking the maximum failing parapet and the resulting failure by sliding. The specific weight of the model concrete was 133.4 pounds per cubic foot. The friction coefficient, f, between the model parapet and rubble breakwater was determined independently, with no wave action, by measuring the horizontal force on the parapet required to induce sliding. This force, F_f was obtained by a small spring-type force indicator and the friction coefficient was calculated from the relation $f = F_f/Wp$. The uplift force, U, was then calculated from the relation

$$F = F_f = f(W_p - U) \tag{6-43}$$

where F is the total calculated wave force, F_f the frictional resistance between the parapet and the rubble mound (assuming that the maximum wave force and the corresponding uplift force occur simultaneously), and W_p the dry weight of the maximum failing parapet.

(i) Summary of Test Results. The maximum measured force, P, on the parapet corresponded to a prototype force of 2,600 pounds per foot. The parapet was overtopped by 2.5 feet of solid water. Using these values, the equations and the assumed force distributions shown in Figure 6-38, a total maximum force, F, of 3,860 pounds per foot was obtained. The weight W_p of the maximum failing parapet was 7,070 pounds, the bottom area of the parapet was 53 square feet, and the friction coefficient averaged 0.76. The uplift force, calculated from equation (6-43) $U = W_p - F/f$, was 1,990 pounds per foot. A safety factor of 3 for overturning of the parapet was determined by: the equation for rotation (Fig. 6-40); a prototype concrete of 144 pounds per cubic foot; a parapet face area of 69.2 square feet; a duration of wave force t, (obtained from the force-time curve) of 3.4 seconds; a prototype weight W_p of 9,960 pounds per foot for the proposed parapet section shown in Figure 6-37; values of a, b, c, and I_M of 5.6, 8.0, and 8.1 feet, and 30,300 pounds per foot seconds squared per foot, respectively; and by graphical integration of the force-time curve. The safety factor for sliding was 1.6. Thus, sliding of the parapet is the critical condition and, considering the simplifying assumptions made in the analysis, it was concluded that the weight of the parapet should be increased by 25 percent without increasing the face area, and that structural methods be used; e.g., anchoring the parapet to the cap stones of the breakwater with dowel bars to increase the effective friction coefficient.

(4) Seawalls (Rubble-Mound and Vertical-Wall Types); Breaking and Nonbreaking Waves.

(a) Project. Proposed seawalls, Texas City, Texas.

(b) Reference. Jackson (1966).

(c) Laboratory. WES.

(d) Test Period. October 1963 to August 1964.

(e) Problem. Texas City, Texas, is located on the southwest shore of Galveston Bay about 9 miles northwest of Galveston and about 9 miles from the Gulf of Mexico. The Texas City ship channel connects the Texas City Harbor with the gulf (Fig. 6-43). Most of the city's developed area occupies an east-west ridge through the central part of the city. The ridge slopes from an elevation of +15 feet MSL to about + 5 feet MSL. Hurricane surges can raise the water levels at Texas City to an elevation of about +15 feet MSL with significant waves of 6-second period and 8-foot height in the unsheltered areas and of 3.5-second period and 3-foot height in the sheltered areas. The corresponding maximum waves in the wave trains are about 15 feet and 5.6 feet in height, respectively. A seawall is proposed to protect Texas City and vicinity from hurricane surges. This flood protection project consists of new and enlarged levees and seawalls (approximately 16 and 1.3 miles in length, respectively), together with the necessary drainage and stop-log structures, a navigation opening, and pumping plants.

(f) Purpose of Model Study. The model study was conducted to derive design data of cover layers for (1) a rubble-mound structure with an impermeable wall standing vertically at the centerline of the structure, (2) an earth levee with the bayside protected by rubble layers, (3) a vertical-faced seawall with a rubble mound protecting the natural ground on the bayside, and (4) a vertical-faced structure with no rubble mound on either the bayside or the landside. Data on the quantities of overtopping water and the forces exerted on the vertical-faced seawall by both breaking and nonbreaking waves were also desired.

(g) The Model. Tests were conducted using section models of the proposed structures in a wave flume 119 feet long, 5 feet wide, and 4 feet deep. The model was designed by Froude's law. A linear scale of 1:35 was selected on the basis of the estimated size of armor units required for stability, the capabilities of the available wave generator, and the water depths at the toe of the proposed seawall. A plunger-type wave generator was used and the wave heights were recorded by printed-circuit rods and a CEC oscillograph. The protective cover layer for a considerable part of the proposed seawall would consist of quarrystone armor units; granite was the only natural stone available within economic hauling distance. When quarried by blasting, the armor stones were nearly rectangular with moderately rough surfaces and rather sharp corners and edges. Since model stones of this type were not available, and the process of hand-shaping and hand-sizing model stones similar to the prototype stones was tedious and costly, concrete blocks with four smooth faces and two slightly roughened faces were cast for this study. The weights and specific weights of the different sizes of armor stones with the 50-percent sizes and specific weights of the core stone, blanket stone, crushed stone, riprap, A-rock underlayer, and toe stone used in the model tests are given in Table 6-6. The model weights were determined from equation (6-39), considering that the specific weights of the water in model and prototype were 62.4 and 64 pounds per cubic foot, respectively, and that the linear scale was 1:35.

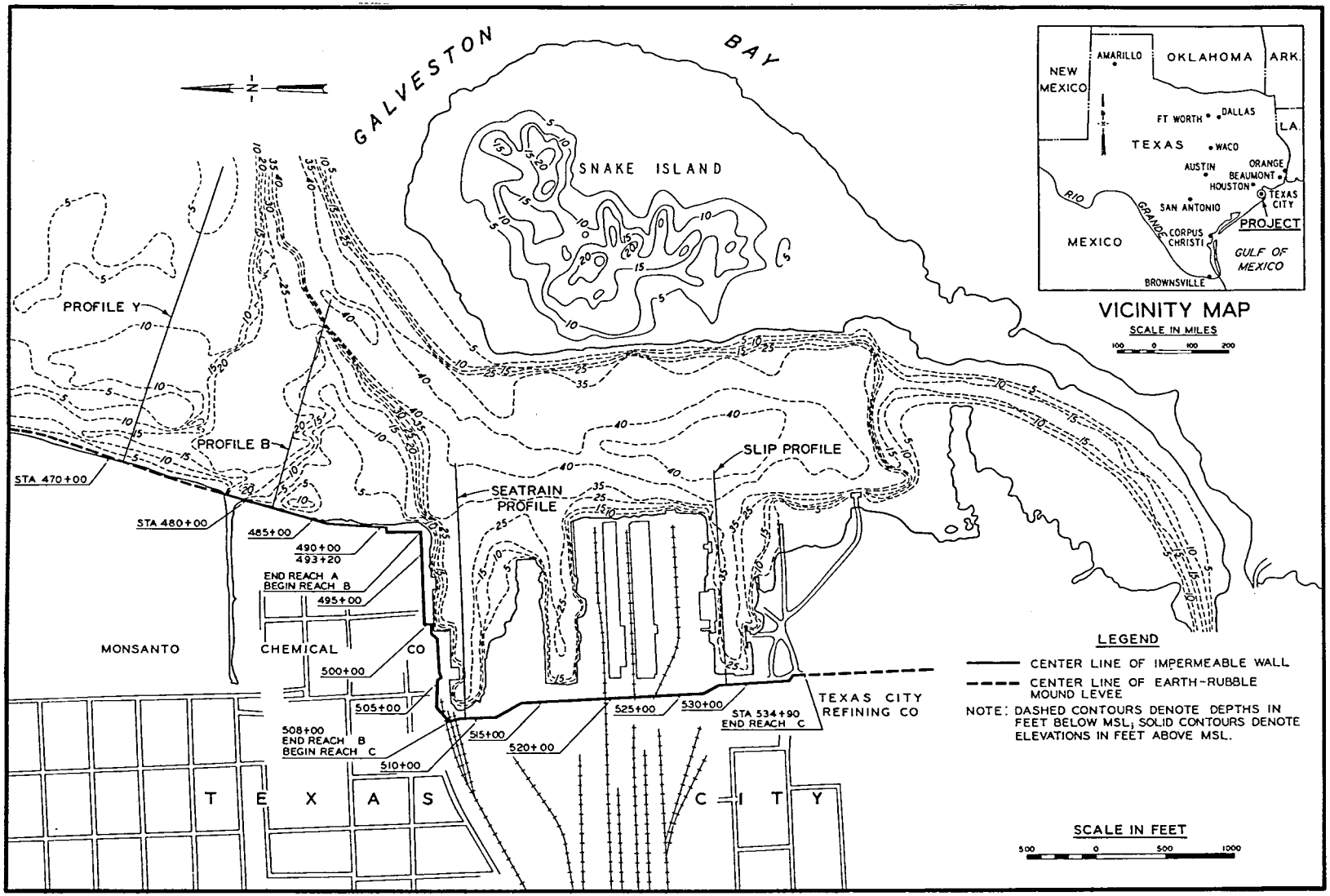

Figure 6-43. Location map of proposed seawalls, Texas City, Texas (Jackson, 1966).

Table 6-6. Model-prototype quarrystone relationship for Texas City, Texas.

Type of quarrystone	Model			Prototype		
	W_a (lb)	W_{50} (lb)	γ (lb/ft^3)	W (ton)	W_{50} (lb)	γ (lb/ft^3)
Armor units	0.60		141	8.0		162
Armor units	0.46		139	6.0		162
Armor units	0.27		142	3.3		162
Crushed stone		1.45×10^{-5}	165		0.75	162
Blanket stone		6.17×10^{-4}	165		32	162
Riprap		1.05×10^{-3}	176		70	162
Core stone		6.77×10^{-3}	176		450	162
A-rock underlayer		9.40×10^{-3}	176		625	162
Toe stone		4.82×10^{-2}	165		2,500	162

The gradations of these materials were based on the different sizes of stones obtained economically from quarries near Texas City. The sizes of the various underlayer stones were also selected to prevent the leaching of smaller material through the voids of the upper layers.

(h) Test Procedures. Model sections, simulating each type of seawall proposed for Texas City, were tested with a 90° angle of wave incidence. Concrete bottoms in the flume reproduced the natural groundline profiles shown in Figure 6-43. Photos were taken of most wave conditions and seawall sections tested. Visual observations were made to determine the behavior of the test structures under wave attack and to select the no-damage wave heights; i.e., the largest waves that would not damage the seawall sections. The volume of overtopping water was measured (in all tests where overtopping occurred) by a calibrated tank located immediately behind the test section. The amount of overtopping water was measured in cubic feet per second per foot of wave crest; i.e., the volume of overtopping water per foot of crest divided by the wave period. Wave forces were measured at various increments on the vertical face of the seawalls tested with a vertical wall. These measurements were made using a 1-foot-wide part of the 5-foot-wide test section. The bottom of a weighted block was placed on a plane horizontal surface with its vertical face in the plane of the vertical-wall part of the test section. A plastic sheet prevented uplift pressures from acting on the bottom of the block. Weights were removed from the block in small decrements until the wave forces caused a slight movement of the block. The force required to move the block was then measured by a spring balance with an accuracy of ±0.1 pound. The seawall sections with parts composed of underlayers protected by quarrystone armor units were constructed by hand-placing the armor units in a manner corresponding to placement by crane in the prototype. The water levels used in stability models of coastal structures are selected so that the effects of water depth on the breaking characteristics of the waves that attack the prototype structure are reproduced as accurately as possible. Based on a study of storm-surge frequency in the Texas City area, water depths for the different test sections were selected using a storm-surge elevation

of +15 feet MSL. On this basis, tests were conducted with depths at the toe of the seawall of 17, 32, 35, and 40 feet referred to a stillwater level of +15 feet MSL. Wave periods of 3.5, 6.0, 8.0, 8.5, and 9.0 seconds were used; wave heights varied from 2.5 to 16 feet. Stability tests to determine the largest waves that will not displace armor units from the test sections, based on the no-damage criterion, require the use of test waves slightly greater in height than the selected prototype design wave. With profile Y (see Fig. 6-43) installed in the model and a stillwater level of +15 feet MSL, the water depth at the toe of the test sections was 17 feet. Preliminary tests showed that the largest 6-second wave that could be generated in this water depth by the available plunger-type wave generator was 10 feet. Therefore, because the selected prototype design wave was 15 feet in height, the stillwater level and the test structure were raised to obtain a depth at the structure toe of 40 feet referred to +15 feet MSL. This was the smallest depth found sufficient to ensure that waves reaching the test sections were large enough to damage the protective cover layers. In developing plans for the proposed seawalls, the best design was desired for each type of structure required for the various reaches of the bay shoreline. Four series of tests were conducted and two or more seawall plans were investigated in each test series. Stability tests of the armor-unit cover layers were conducted for each plan in test series 1, 2, and 3. Overtopping data were obtained for at least one plan in each of the test series. Wave forces were determined on incremental sections of one plan in test series 3 and three plans in test series 4. The conditions for which breaking waves would attack the test sections were determined for all plans in test series 4.

(i) Summary of Test Results. Test series 1 consisted of plans for seawalls in the area of profile B (Fig. 6-43) and concerned a simple rubble-mound structure with a vertical, impermeable wall at the centerline. This reach of shoreline would be subjected to the largest waves (6-second period, 15-foot height) likely to attack any section of the proposed seawall. The protective cover layer on the bayside would consist of one layer of the rectangular-shaped, quarried armor stones weighing 8 tons each on a slope of 1:2. Toe units consisted of 3.3-ton stones. Preliminary tests showed that the toe stones were moved downslope by waves only 8 feet high. The toe section was then redesigned using 6-ton stones and the toe section was extended farther downslope (Fig. 6-44). This plan was found to be stable for the selected design wave; however, because of the lack of space between the shoreline and the existing industrial and commercial developments along parts of this reach of seawall, the plan was judged unacceptable. Another seawall section consisting of a vertical concrete wall with a rubble mound on the bayside to protect the natural ground was then tested. Initial tests showed that the toe needed added protection. The modified section that was found stable for the selected design wave is shown in Figure 6-45. Overtopping tests showed that a maximum of 3.7 cubic feet per second of overtopping water would occur per foot of seawall for the 6-second period and 15-foot height design wave. Wave forces were also measured on the vertical-wall part of the structure. The measured wave forces resulting

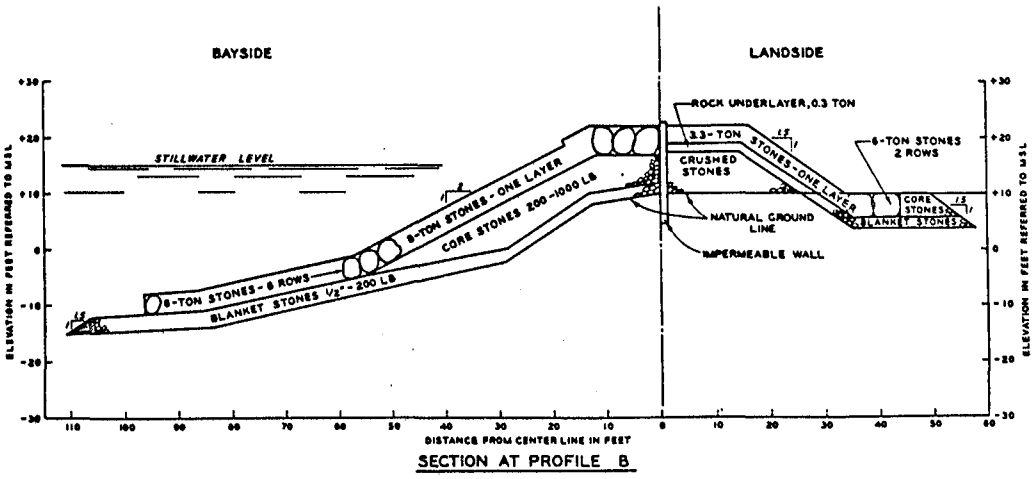

Figure 6-44. Elements of test section (plan 2), Texas City seawall model (Jackson, 1966).

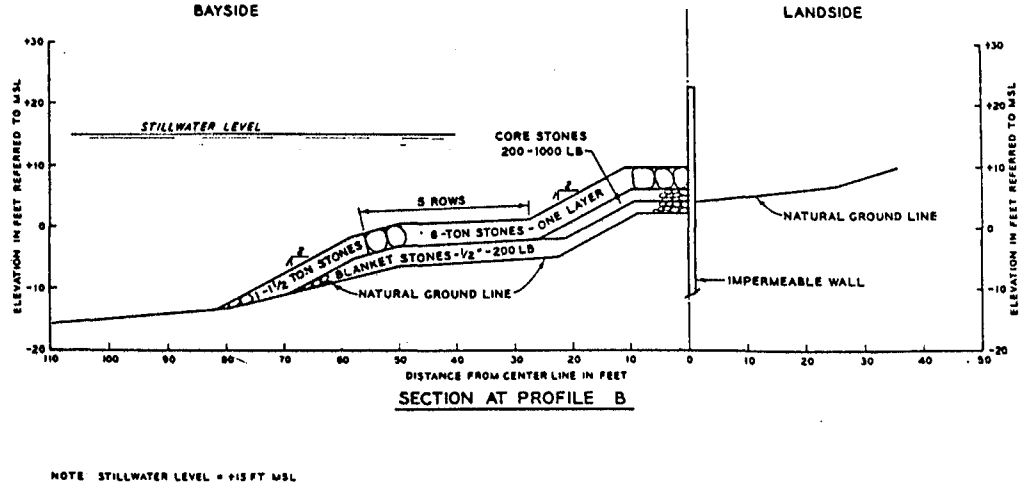

Figure 6-45. Elements of test section (plan 5B), Texas City seawall model (Jackson, 1966).

from the attack of the selected design wave and corresponding to average pressure intensities over the different vertical increments of the vertical-wall parapet are:

Vertical increment MSL (ft)	Pressure (lb/ft^2)
0 to 5	1,550
5 to 10	1,790
10 to 15	2,130
15 to 20	1,200
20 to 23	695

These pressures are about three times those obtained from Sainflou's (1928) equation, and are about one-sixth the pressures from Minikin's (1963) equation. The type of structure developed for profile Y is shown in Figure 6-46. Overtopping tests showed 7.3 cubic feet per second of overtopping water per foot of seawall. Vertical-wall seawalls were tested for the slip profile and the sea train profile; profile locations are shown in Figure 6-43. The elements of the test sections are shown in Figures 6-47 and 6-48. The breaking and nonbreaking wave tests determined that breaking waves would not occur on these structures for wave periods less than about 6 seconds. Since the sheltering effects of Snake Island protect the reaches from the longer-period waves, it was concluded that these structures could be designed from Sainflou's equation (for nonbreaking waves only), using waves of 3.5-second period and wave heights from 2.5 to 6 feet, depending on the depths of water bayward of the reaches corresponding to the slip and sea train profiles (Fig. 6-43).

(5) Floating Breakwaters; Nonbreaking Waves.

(a) Project. Proposed floating breakwaters, Oak Harbor, Washington.

(b) Reference. Davidson (1971a).

(c) Laboratory. WES.

(d) Test Period. September 1969 to March 1970.

(e) Problem. A floating breakwater in combination with a timber-pile and rubble-mound breakwater is proposed for protection of a small-craft harbor at Oak Harbor, Washington. Oak Harbor is located on Whidbey Island in Puget Sound about 50 miles north of Seattle, Washington (Figs. 6-49 and 6-50). Water depths along the breakwaters range from about 10 to 15 feet MLLW on the south side of the harbor and from about 0 to 15 feet MLLW on the east side. The maximum tide elevation is +14.5 feet MLLW. The proposed small-craft harbor is exposed to short-period wind waves from east clockwise to west. The maximum waves range to about a 3.5-second period and a 2.0-foot height; wave heights in the mooring areas of the harbor basin were not to exceed 0.5 feet. The floating

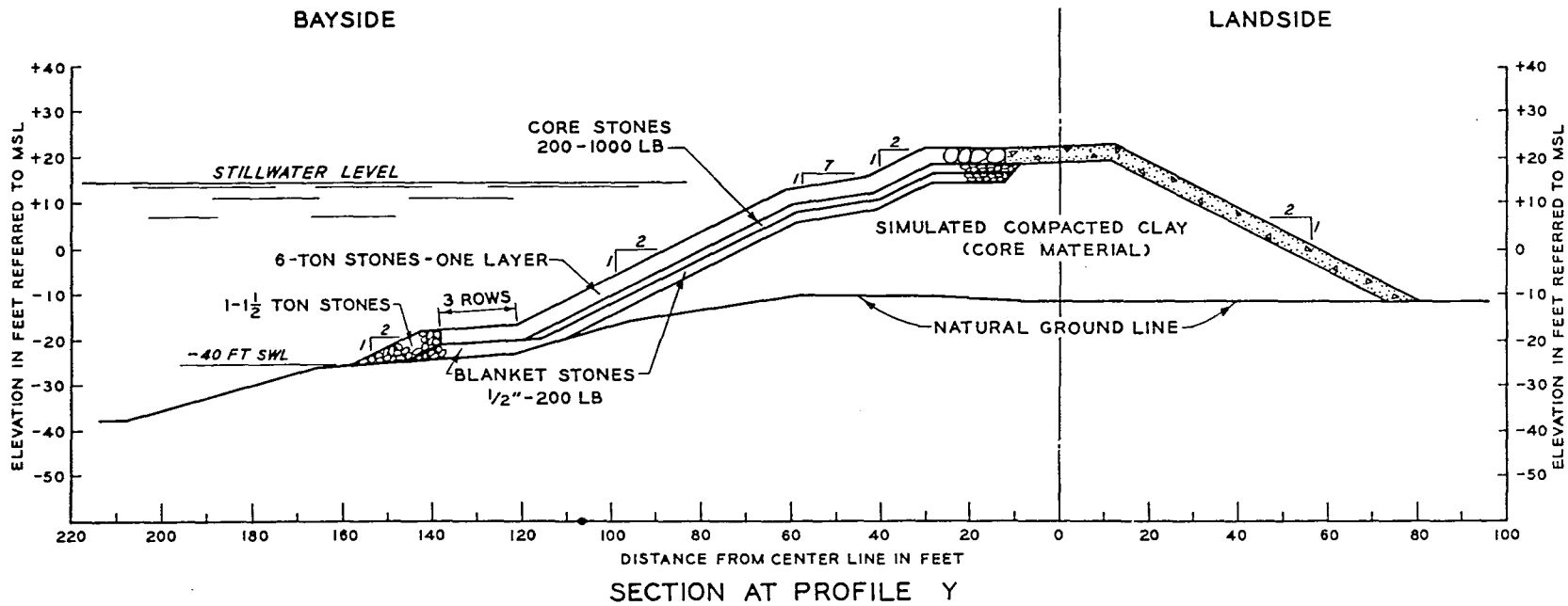

SECTION AT PROFILE Y

NOTE: STILLWATER LEVEL = +15 FT MSL.

Figure 6-46. Elements of test section (plan 3B), Texas City seawall model (Jackson, 1966).

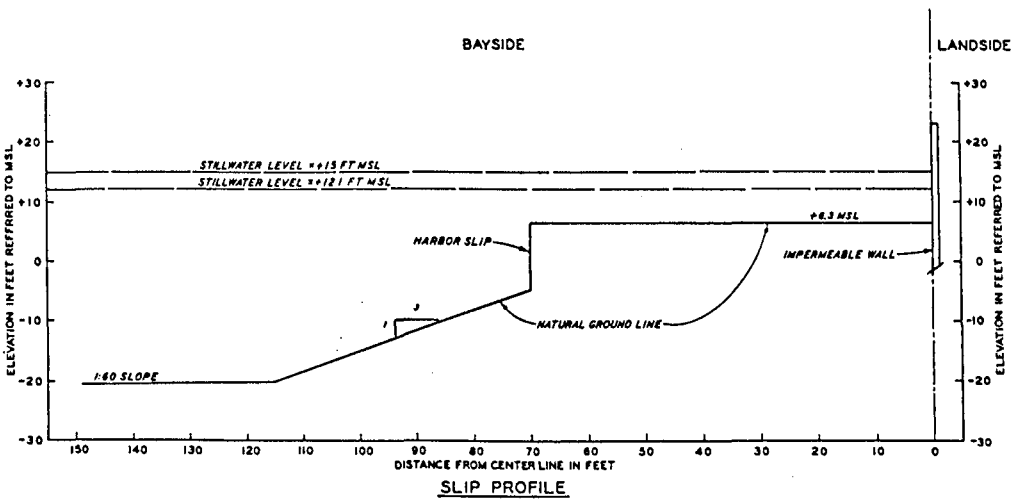

Figure 6-47. Elements of test section (plan 6), Texas City seawall model (Jackson, 1966).

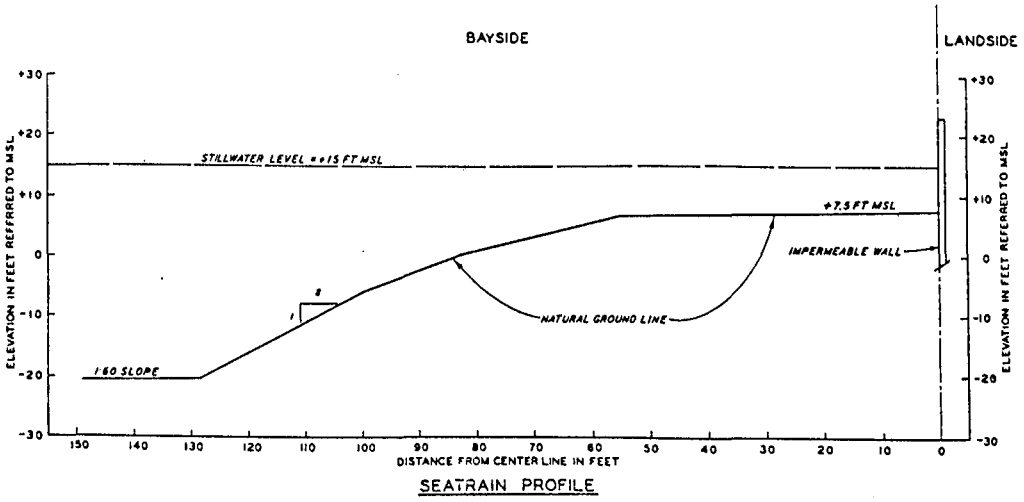

Figure 6-48. Elements of test section (plan 7), Texas City seawall model (Jackson, 1966).

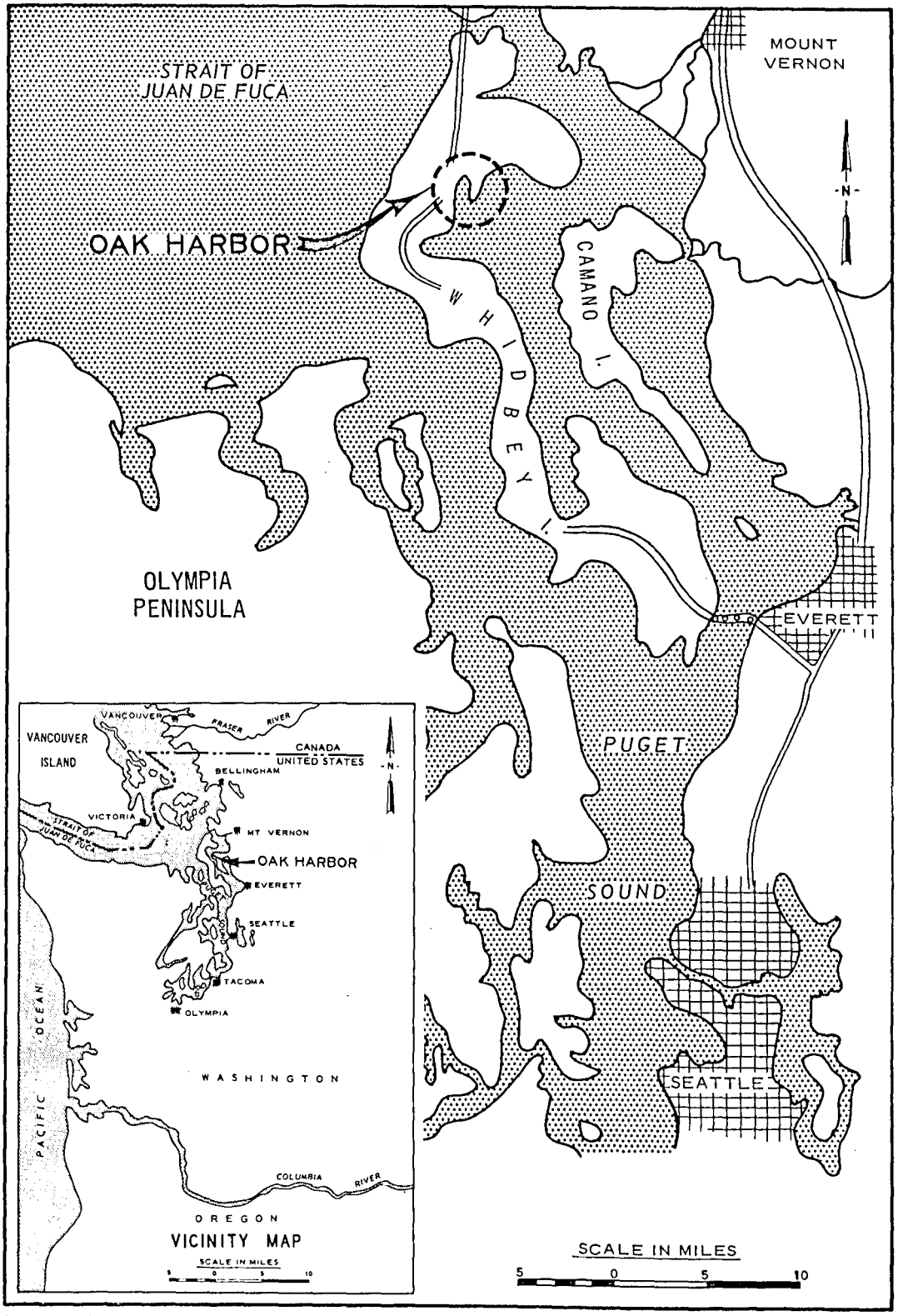

Figure 6-49. Location map, Oak Harbor, Washington (Davidson, 1971a).

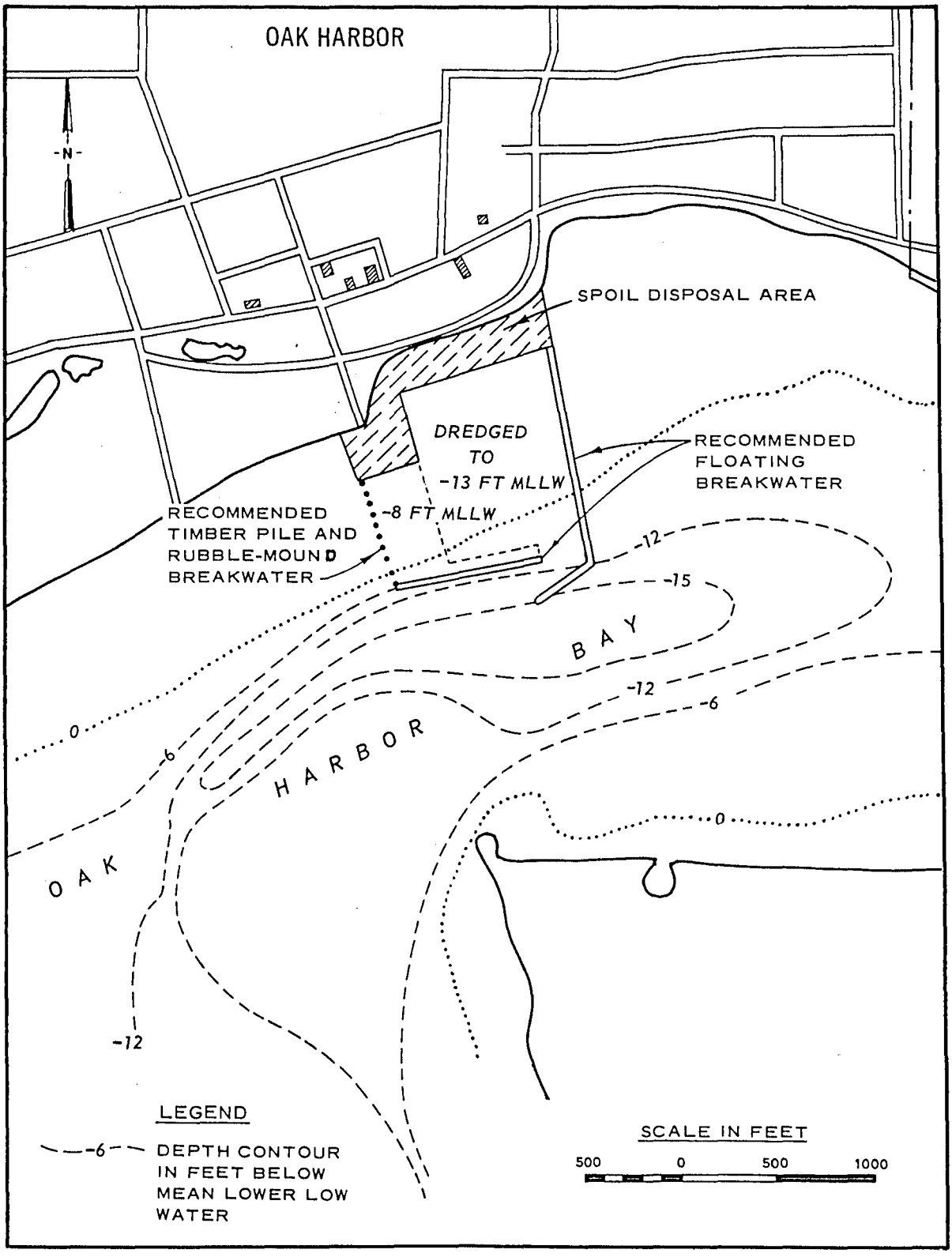

Figure 6-50. Proposed improvements and revisions, Oak Harbor breakwater model (Davidson, 1971a).

breakwater part of the protective structures was proposed because of poor foundation conditions and the relatively large tidal range. The floating breakwater would consist of rectangular wooden modules fastened together to obtain the required breakwater length. Each module would be 42.5 feet long, 10 feet wide, and 7.2 feet deep and consist of a wooden framework covered with wood decking on the top and sides, concrete beams for ballast, and polystyrene for flotation (Fig. 6-51). The mooring systems would consist of either chains fastened to concrete anchors (both seaward and shoreward of the breakwater) or piles placed between the breakwater modules. The preliminary design of the floating breakwater was based on available wave transmission and reflection data for restrained floating structures. However, actual wave attenuation, mooring forces, and response characteristics of floating structures vary with the shape, dimensions and specific weights of the modules, wave characteristics, water depths, and the mass moments of inertia of the modules. Thus, data to determine the effectiveness of the structures and the magnitude of the forces in the mooring lines were desired.

(f) Purpose of Model Study. The model study was conducted to determine (1) the effectiveness of the proposed floating breakwater in preventing the transmission of wave heights larger than the acceptable value, (2) the mooring forces for both chain and pile mooring systems, (3) whether resonant oscillations of the proposed structure would increase mooring forces appreciably, and (4) the natural period of oscillation of the proposed module unrestrained in still water.

(g) The Model. One module of the proposed floating breakwater was reproduced to a linear scale of 1:10 and installed for testing in a wave flume 119 feet long, 5 feet wide, and 4 feet deep. The scale was determined by the dimensions of the prototype structure, the depths of water at the breakwater site, the capability of the wave generator, and the dimensions of the waves selected for testing. The model was designed and operated based on Froude's law. The specific weight of the water (γ_m) in the model was 62.4 pounds per cubic foot and that of seawater in the prototype was 64 pounds per cubic foot. The specific weights of the material $(\gamma_{bm})_m$ used in constructing the model module were different than the weights in the prototype. These variations between model and prototype values were considered in the calculations to obtain geometric, kinematic, and dynamic similarity between the model and prototype structure, $(\gamma_w)_m/(\gamma_w)_p = (\gamma_{bm})_m/(\gamma_{bm})_p$. Dynamic similarity also required that the model structure accurately reproduce the mass, moments of inertia, radius of gyration, depth of flotation, and general geometric dimensions of the prototype structure. The chain mooring lines on the model, designed from equation (6-11b), were fastened to strain-gage measuring blocks on the floor of the wave flume to determine the forces in the mooring lines. The seaside and harborside measuring blocks were positioned at horizontal distances of 195.5 and 86.0 feet (prototype) from the front and rear edges of the floating structure, respectively. The initial tension in each mooring line was 2,200 and 0.0 pounds (prototype) for tests in water depths of 29.5- and 10-foot depths, respectively. The lengths of the seaside and harborside chains were 200 and 90 feet, respectively (Fig. 6-52). The

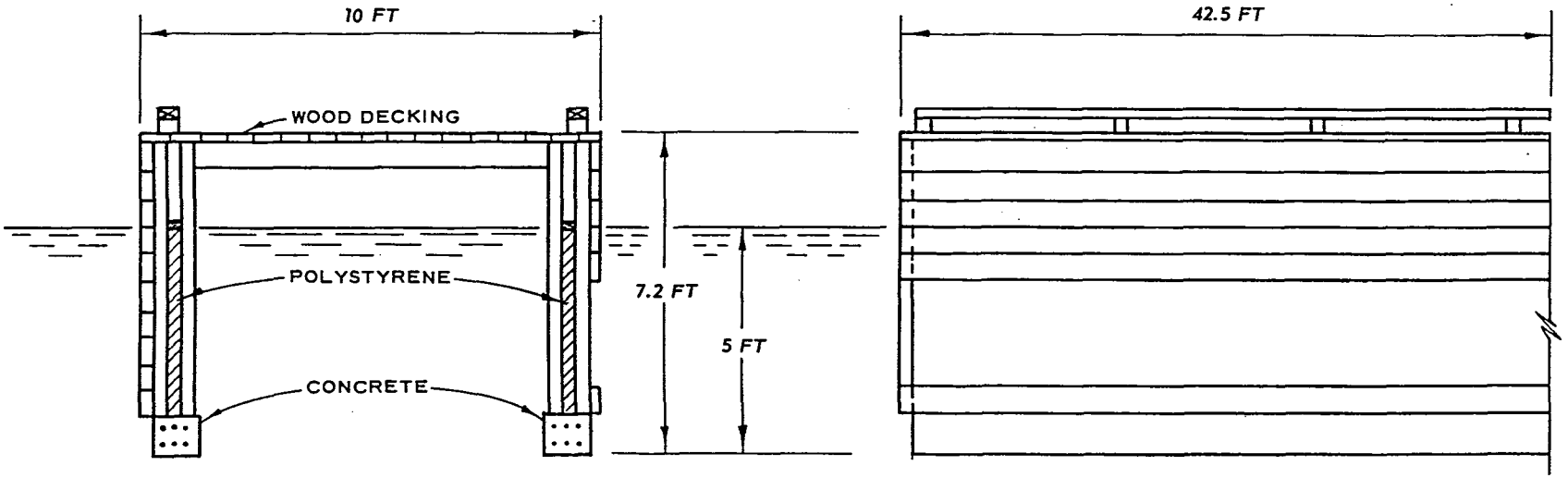

Figure 6-51. Proposed floating breakwater module, Oak Harbor breakwater model (Davidson, 1971a).

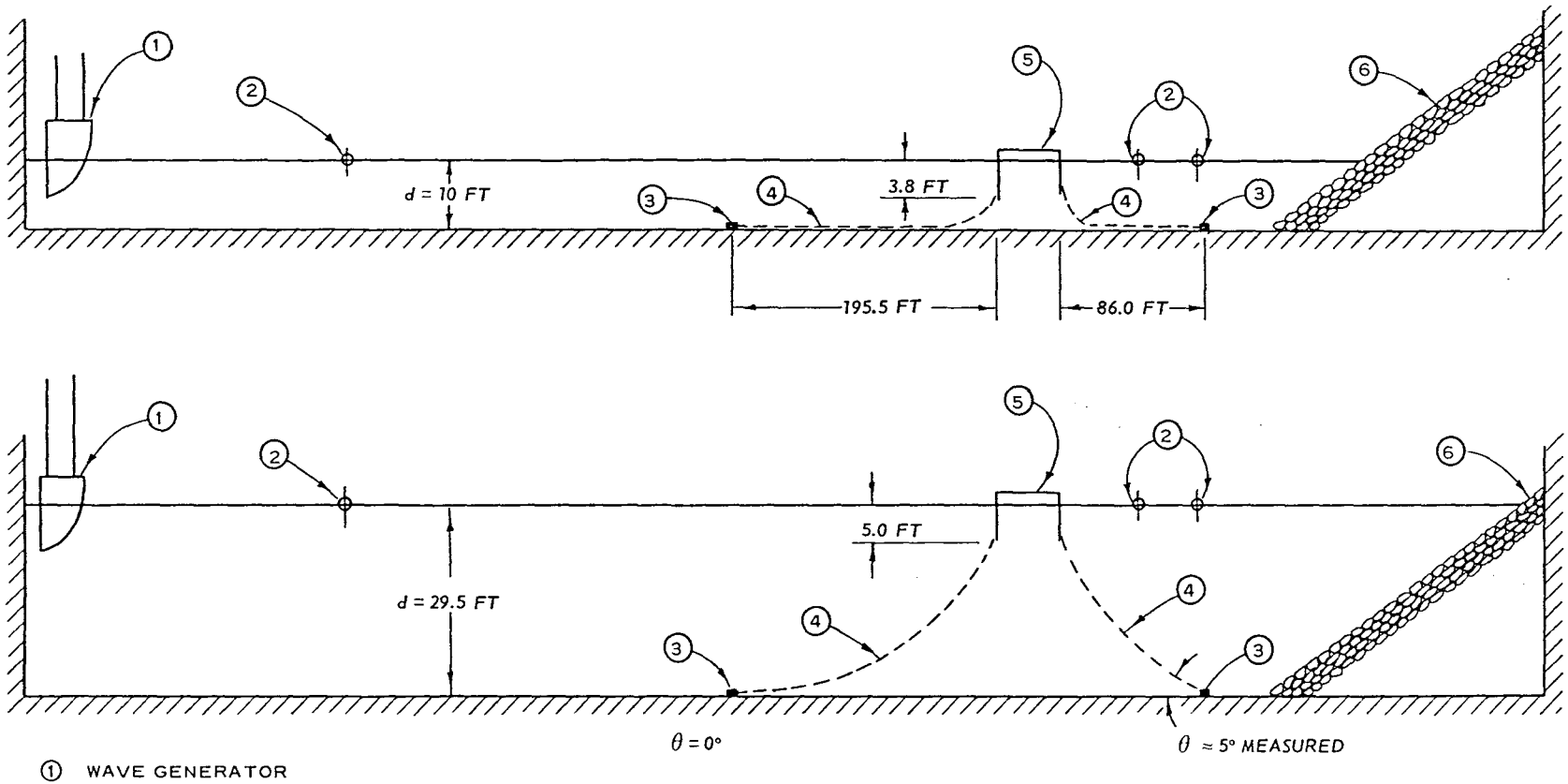

① WAVE GENERATOR
② WAVE GAGE
③ ANCHOR FORCE GAGE
④ ANCHOR CHAIN
⑤ FLOATING BREAKWATER
⑥ WAVE ABSORBER

NOTE: DIMENSIONS ARE IN PROTOTYPE FEET

Figure 6-52. Typical test setup using chain mooring system, Oak Harbor breakwater model (Davidson, 1971a).

pile mooring system in the model consisted of a pile on each end of the module, with each pile fitted with a strain gage at the bottom of the flume and calibrated to measure the seaside and harborside forces in the direction of wave travel (Fig. 6-53).

(h) Test Procedures. The unrestrained natural period of oscillation of the breakwater was determined by applying a torque to the structure in still water and measuring (by a stopwatch) the time required for the module to oscillate from one extreme position to the other extreme and back to the first position. An attempt to determine the period of oscillation of the module while it was restrained by the chain-mooring system was not successful because the module would not oscillate in the restrained condition sufficiently to allow determination of a complete period of oscillation. The effectiveness of the proposed floating breakwater in attenuating wave action was determined by measuring the heights of incident and transmitted waves. The incident waves were measured at the position of the module before it was placed in the wave flume. The transmitted waves were measured during a test with the module placed in the restrained conditions, at distances of 1 and 1.5 wavelengths shoreward of the structure. Wave heights were measured by printed-circuit gages and a CEC oscillograph; photos were also made of several wave conditions (Fig. 6-54). Mooring forces were measured for most waves used in the transmission tests. Chain anchor-force data were obtained from the strain-gage measuring blocks mounted on each anchor chain; pile anchor-force data were obtained by strain-gaged piles in conjunction with the amplifier-oscillograph assembly. Observations were made during all the tests to determine whether the module and mooring system were in resonance with any of the wave conditions tested. Stillwater levels for this type of model study are selected so that the effectiveness of the proposed floating structures can be obtained over the range of depths corresponding to the local tide conditions. The tide elevations at Oak Harbor range from an estimated maximum of +14.5 to -4.5 feet MLLW (MHHW is + 11.4 feet MLLW). Since most of the proposed breakwater length would be located in depths from 10 to 15 feet MLLW, depths of 10 feet and 29.4 feet (corresponding to tide elevations of 0.0 and +14.5 feet MLLW and bottom elevations of -10 and -15 feet MLLW, respectively) were selected for low tide and high tide conditions, respectively. Hindcast data for the Oak Harbor vicinity indicated that the maximum incident wave conditions would be a period of about 3.5 seconds and a height of about 2.0 feet. Model tests used wave periods from 2.0 to 3.5 seconds and wave heights to 5.0 feet. Wave heights larger than 2.0 feet were tested so that the effectiveness of the proposed structure (as determined in the Oak Harbor model study) could be used in determining the feasibility of using similar floating structures at locations with more severe wave conditions.

(i) Summary of Test Results. The natural period of the proposed breakwater unrestrained was 7.1 seconds (prototype). The wave transmission data (Figs. 6-55 and 6-56) show that the proposed breakwater, either a chain or pile mooring, will adequately attenuate waves as large as 2.0 feet in height with a period of 2.5 seconds. The seaside chain anchor forces for the 10-foot depth conditions are shown in Figure 6-57.

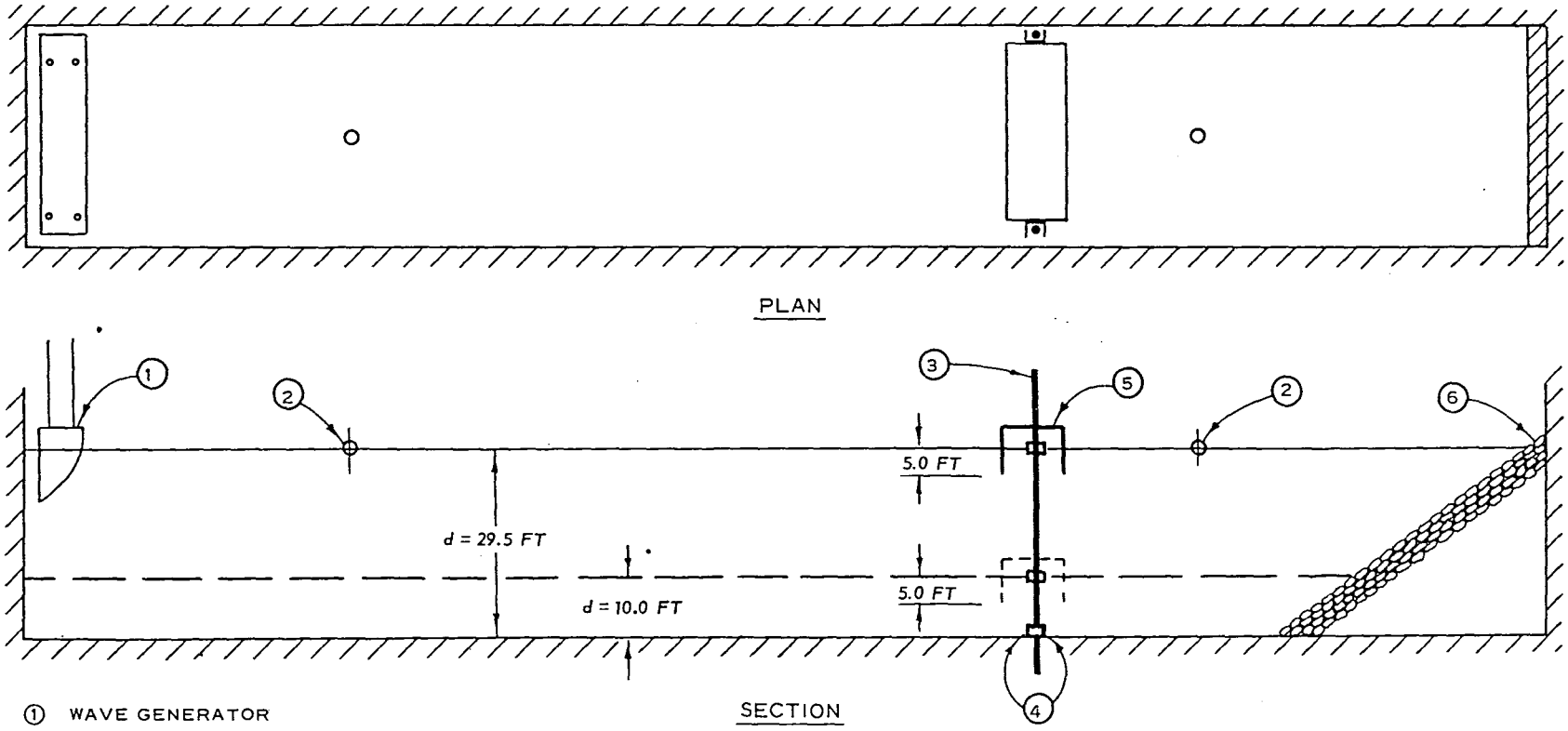

Figure 6-53. Typical test setup using pile mooring system, Oak Harbor breakwater model (Davidson, 1971a).

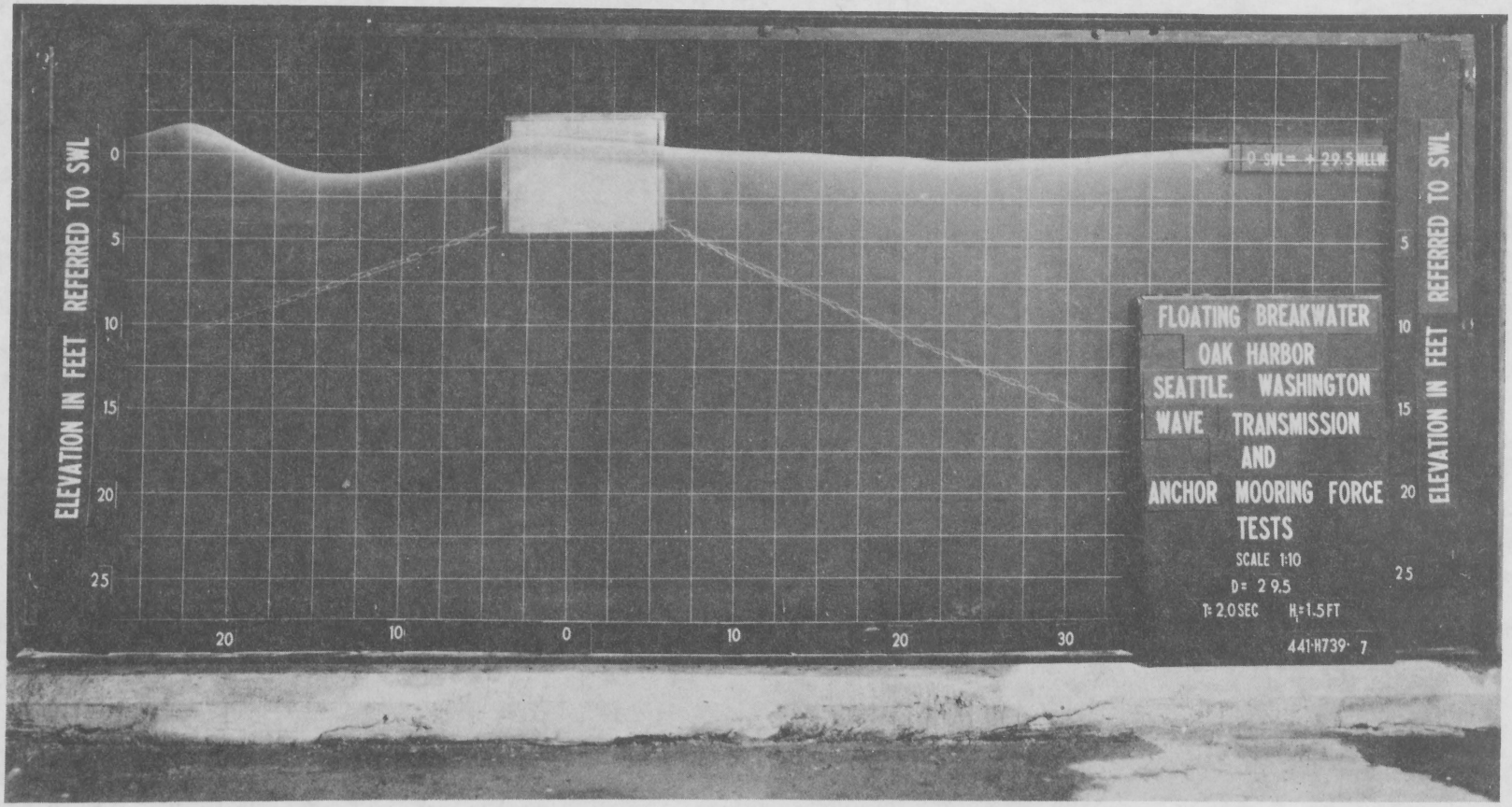

Figure 6-54. Test module with chain mooring system during attack of 2.0-second, 1.5-foot waves, Oak Harbor breakwater model (Davidson, 1971a).

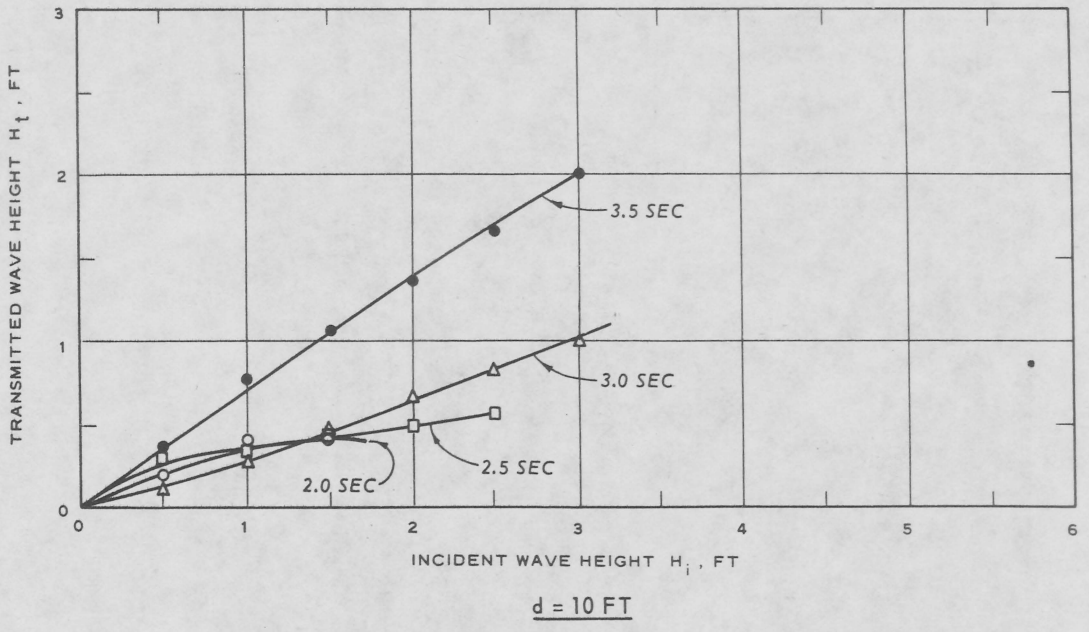

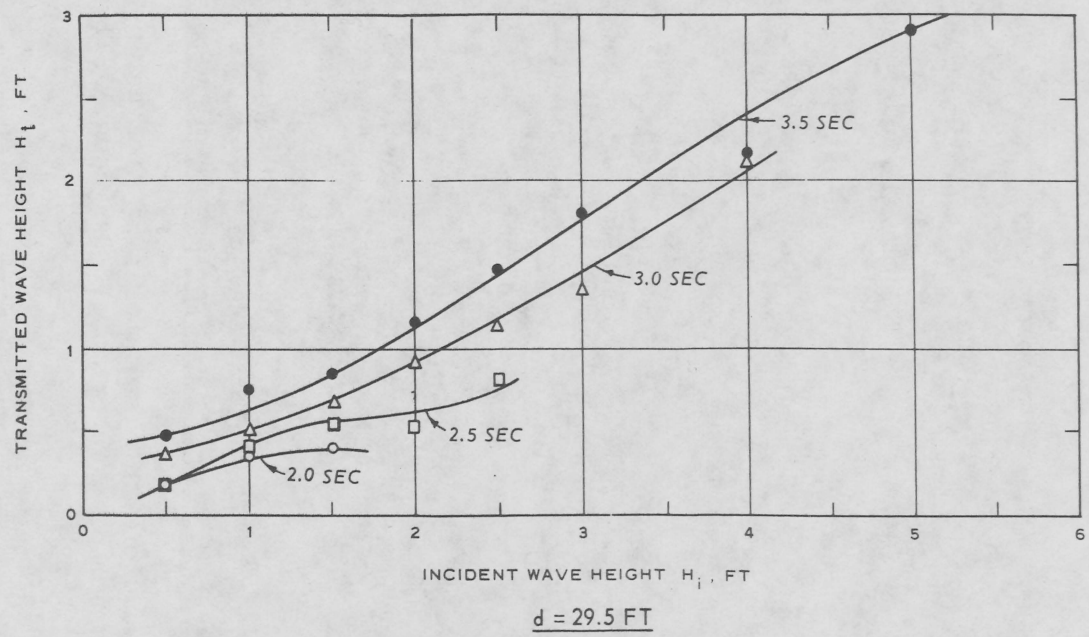

LEGEND

SYMBOL	T SEC
○	2.0
□	2.5
△	3.0
●	3.5

Figure 6-55. Transmitted wave heights with chain mooring system, Oak Harbor breakwater model (Davidson, 1971a).

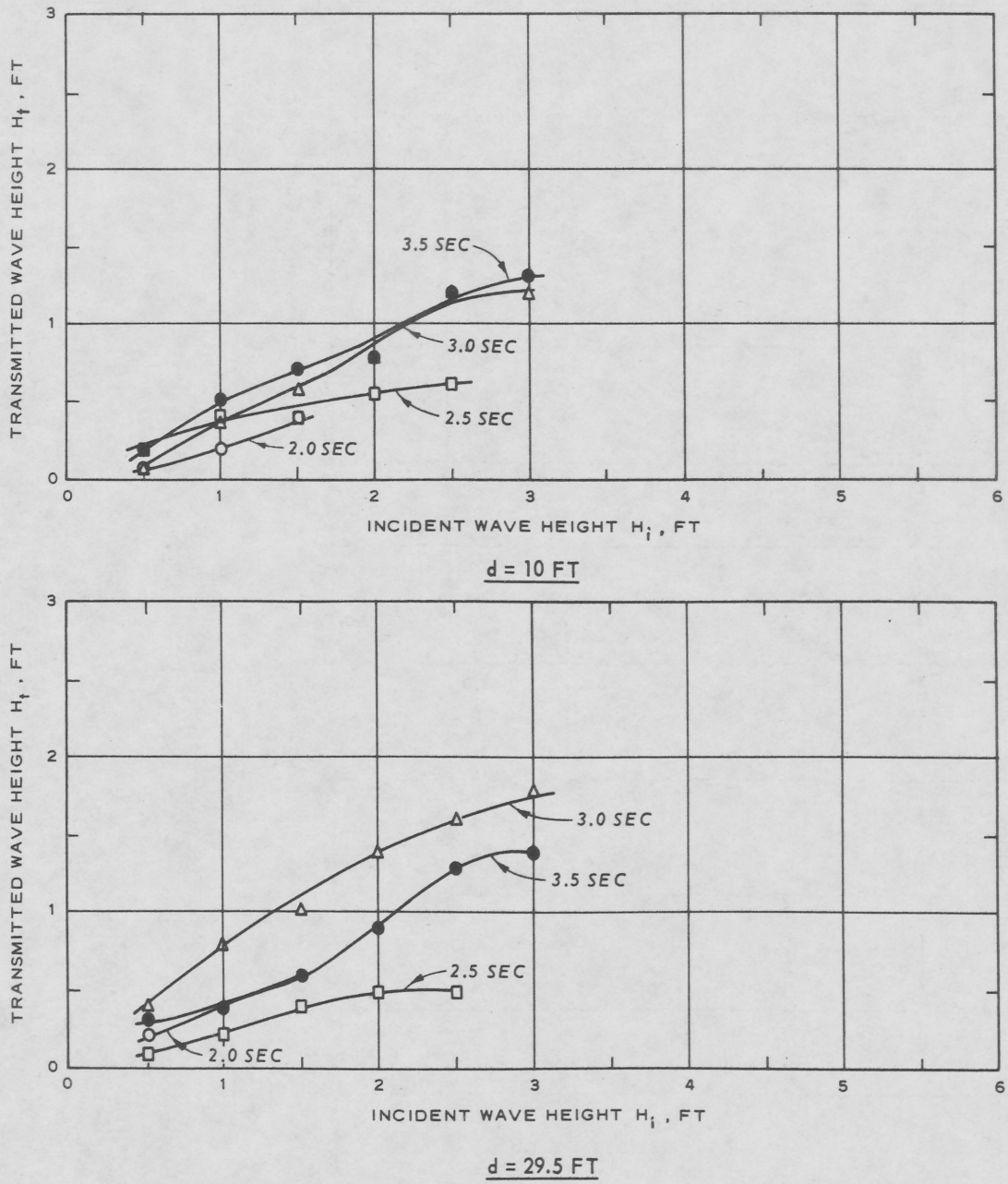

Figure 6-56. Transmitted wave heights with pile mooring system, Oak Harbor breakwater model (Davidson, 1971a).

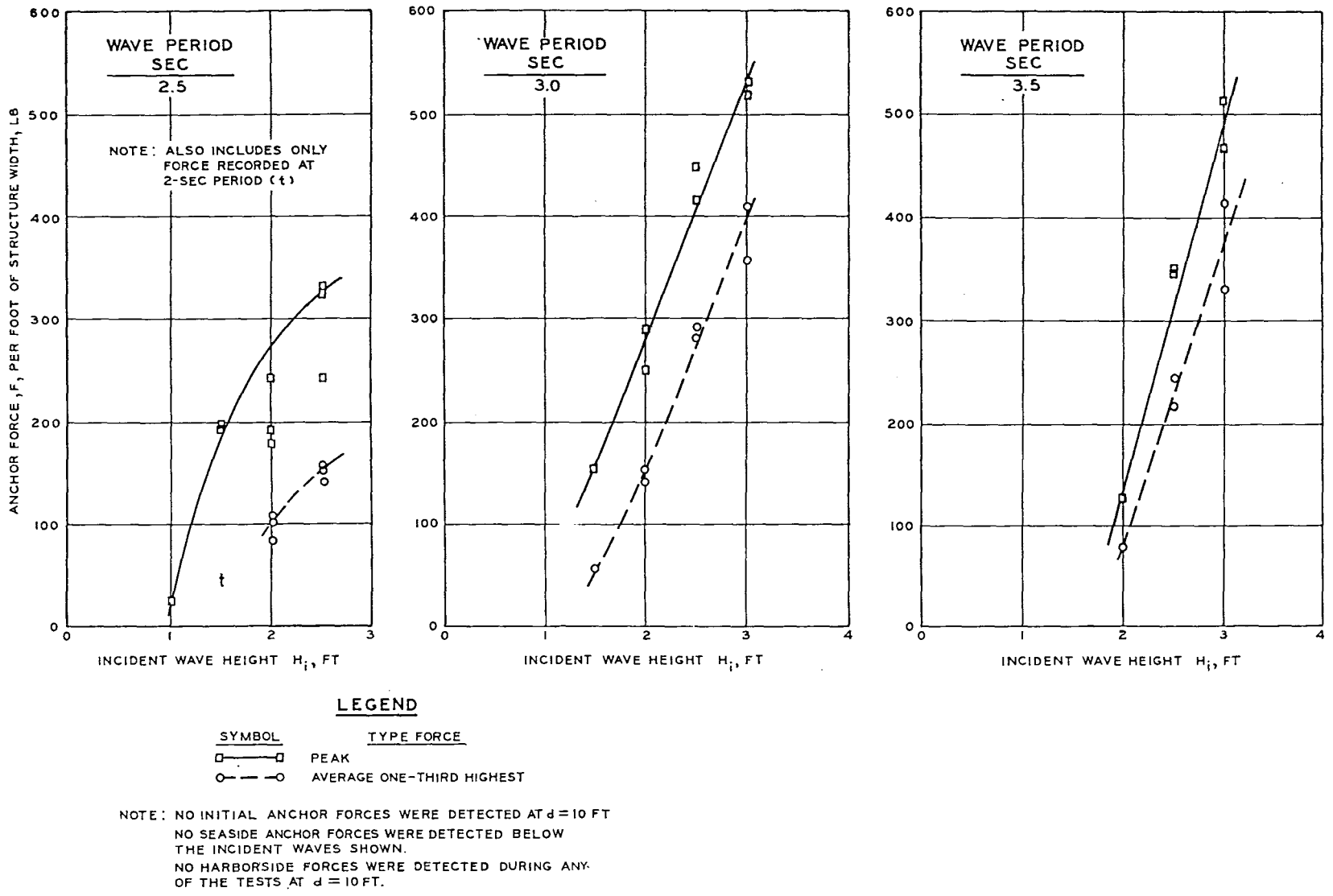

Figure 6-57. Chain anchor forces on seaside of structure (d = 10 feet), Oak Harbor breakwater model (Davidson, 1971a).

No harborside anchor forces were detectable during any of the chain anchor tests with a 10-foot depth. The seaside and harborside chain anchor forces for tests with a water depth of 29.5 feet are shown in Figures 6-58 and 6-59. The results of the pile mooring force tests are shown in Figures 6-60 through 6-63. The type of model mooring system used to obtain the pile force data should be noted, and the model data should be adjusted by the deflection and absorption characteristics of the selected prototype piles before pile mooring data are used for prototype design.

(6) Pneumatic Breakwaters.

(a) Project. Application of pneumatic breakwaters to Transportation Corps, Department of the Army, problems of offshore discharge.

(b) Reference. Sherk (1960).

(c) Laboratory. CERC.

(d) Test Period. August to September 1959.

(e) Problem. The development of a new series of amphibians required an examination of the problems involved in the transfer of cargo from conventional ships to amphibians in offshore discharge operations. The main problem is that amphibians used for offshore discharge are severely curtailed when wave heights exceed 2 feet; the degree of curtailment increases with wave height with nearly 100-percent loss of discharge capability when wave heights exceed 8 feet. If relatively calm water could be produced around ships at anchor and if a relatively calm track of water could be produced through the surf zone, the capability of moving supplies ashore would be increased considerably and moderate sea conditions would not reduce over-the-beach supply to a mere trickle.

(f) Purpose of Study. The investigation was conducted primarily to determine the practicability of using pneumatic breakwaters (i.e., a screen of rising air bubbles) to reduce wave heights sufficiently to allow offshore discharge operations during moderate wave conditions. Because of scale effects, with respect to the quantity of air required for adequate wave height reduction, full-scale tests were necessary to obtain more conclusive evidence of the feasibility of using the pneumatic breakwater for the protection of offshore discharge operations.

(g) Test Facilities. After investigation of several wave flumes, the Transportation Corps selected the large wave-flume facility available at CERC (then called the Beach Erosion Board) at its Washington, D.C. location. This was the only wave flume where tests could be conducted for conditions approaching full scale. The concrete flume is 635 feet long, 20 feet deep, and 15 feet wide. The wave generator was a piston-type powered by a 510-horsepower, constant-speed motor capable of generating waves with periods from 2.6 to 16.0 seconds and wave heights

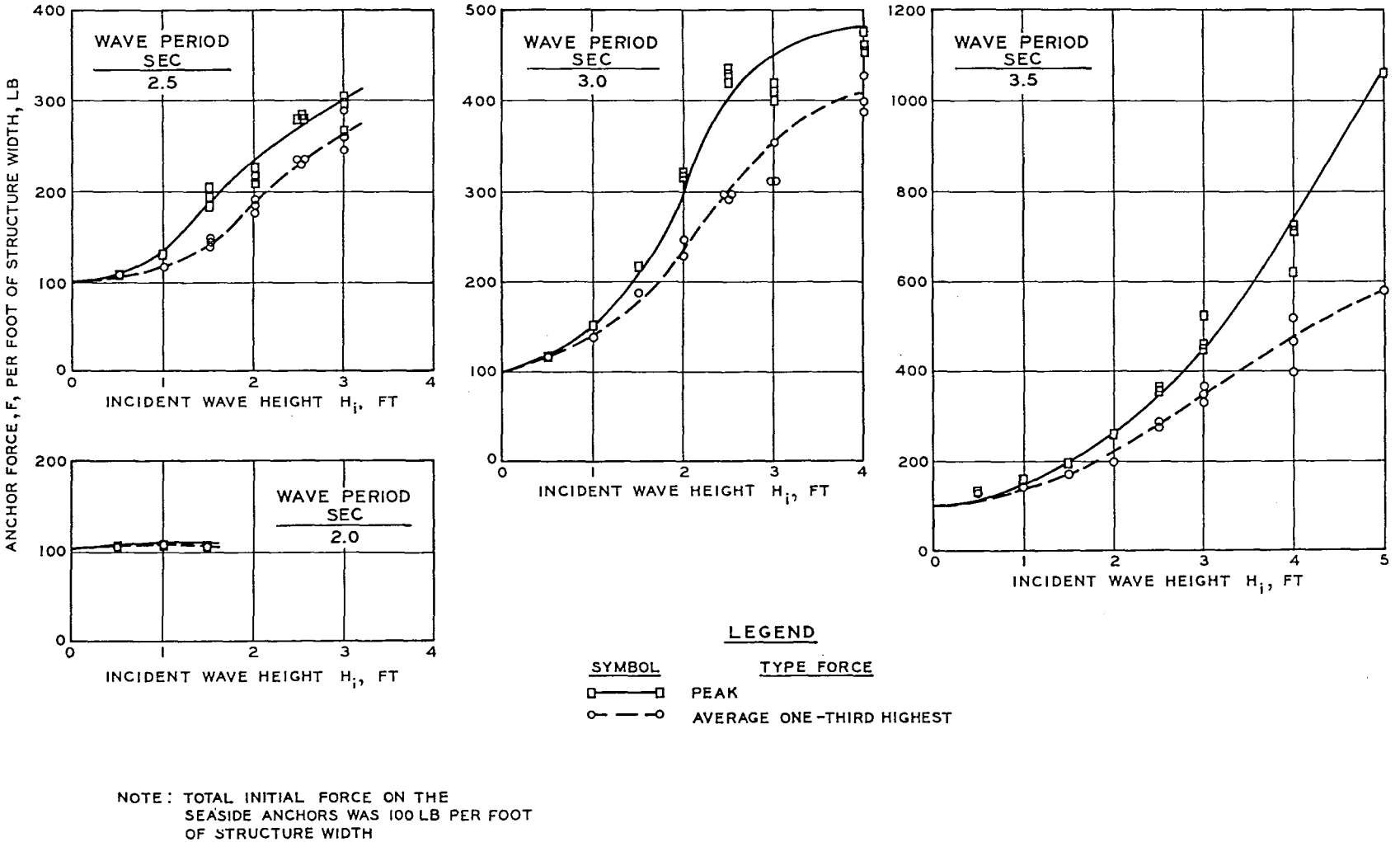

Figure 6-58. Chain anchor forces on seaside of structure (d = 29.5 feet), Oak Harbor breakwater model (Davidson, 1971a).

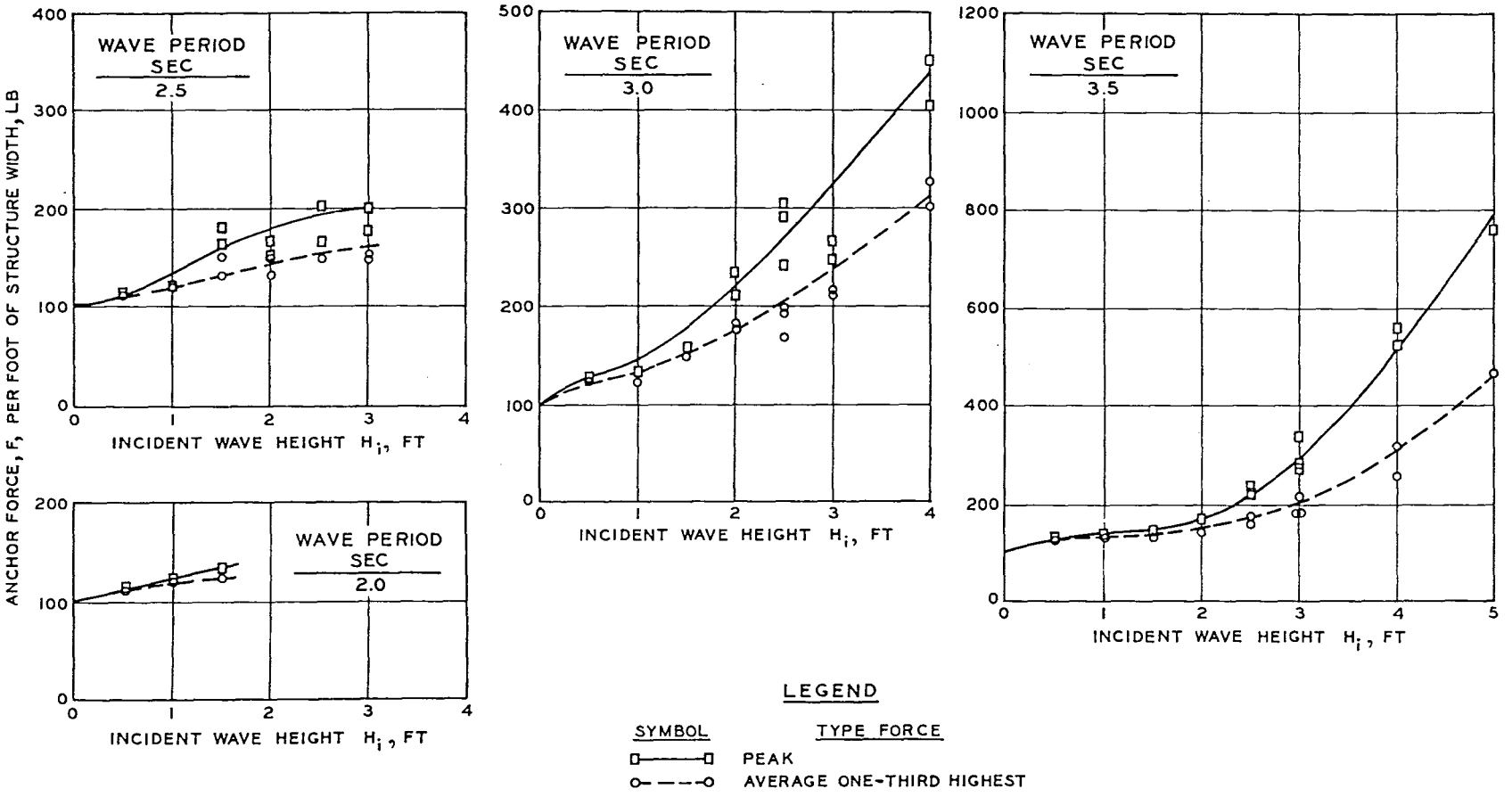

NOTE: TOTAL INITIAL FORCE ON THE HARBORSIDE ANCHORS WAS 100 LB PER FOOT OF STRUCTURE WIDTH.

Figure 6-59. Chain anchor forces on harborside of structure (d = 29.5 feet), Oak Harbor breakwater model (Davidson, 1971a).

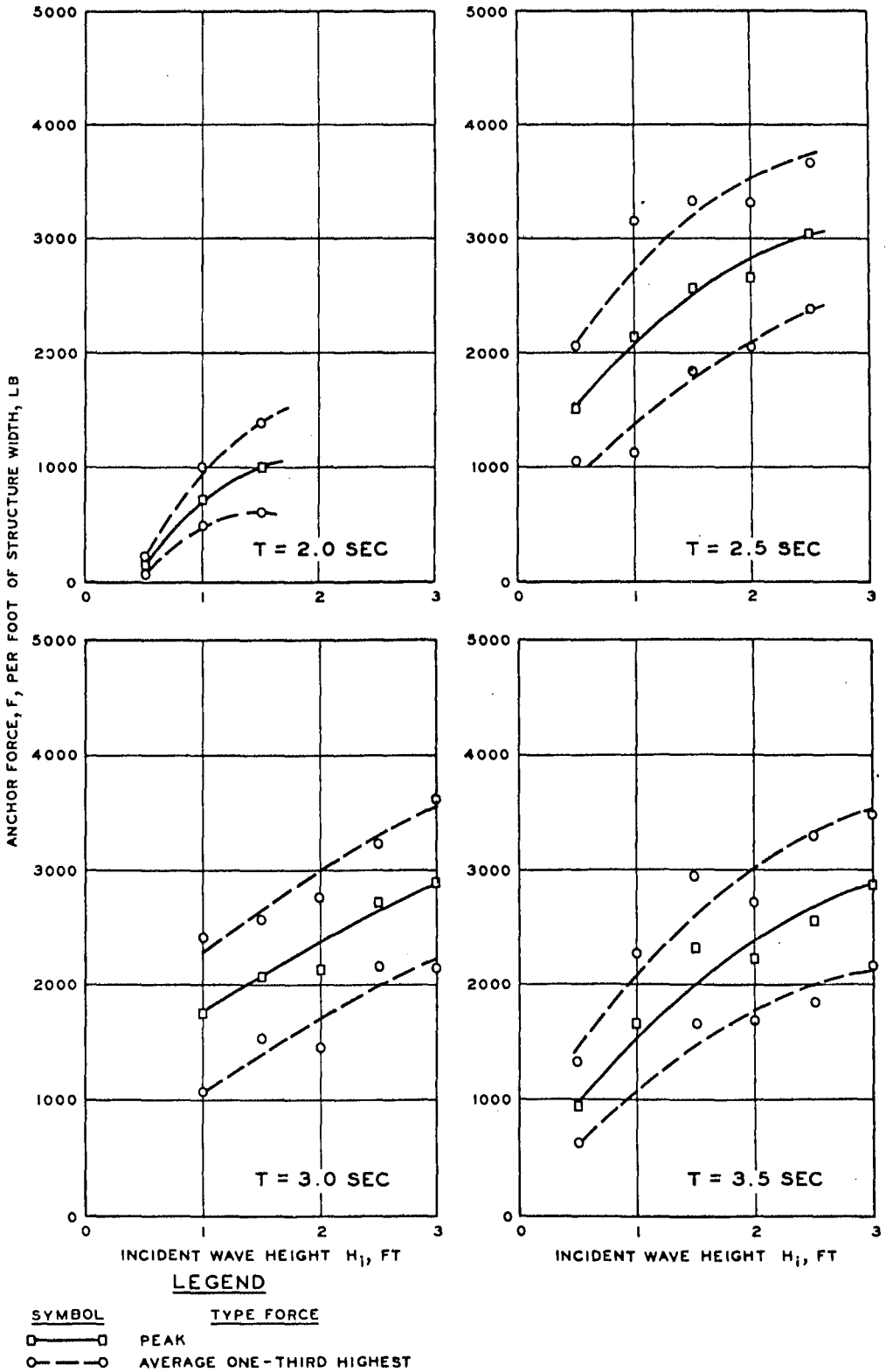

Figure 6-60. Forces on seaside of pile (d = 10 feet), Oak Harbor breakwater model (Davidson, 1971a).

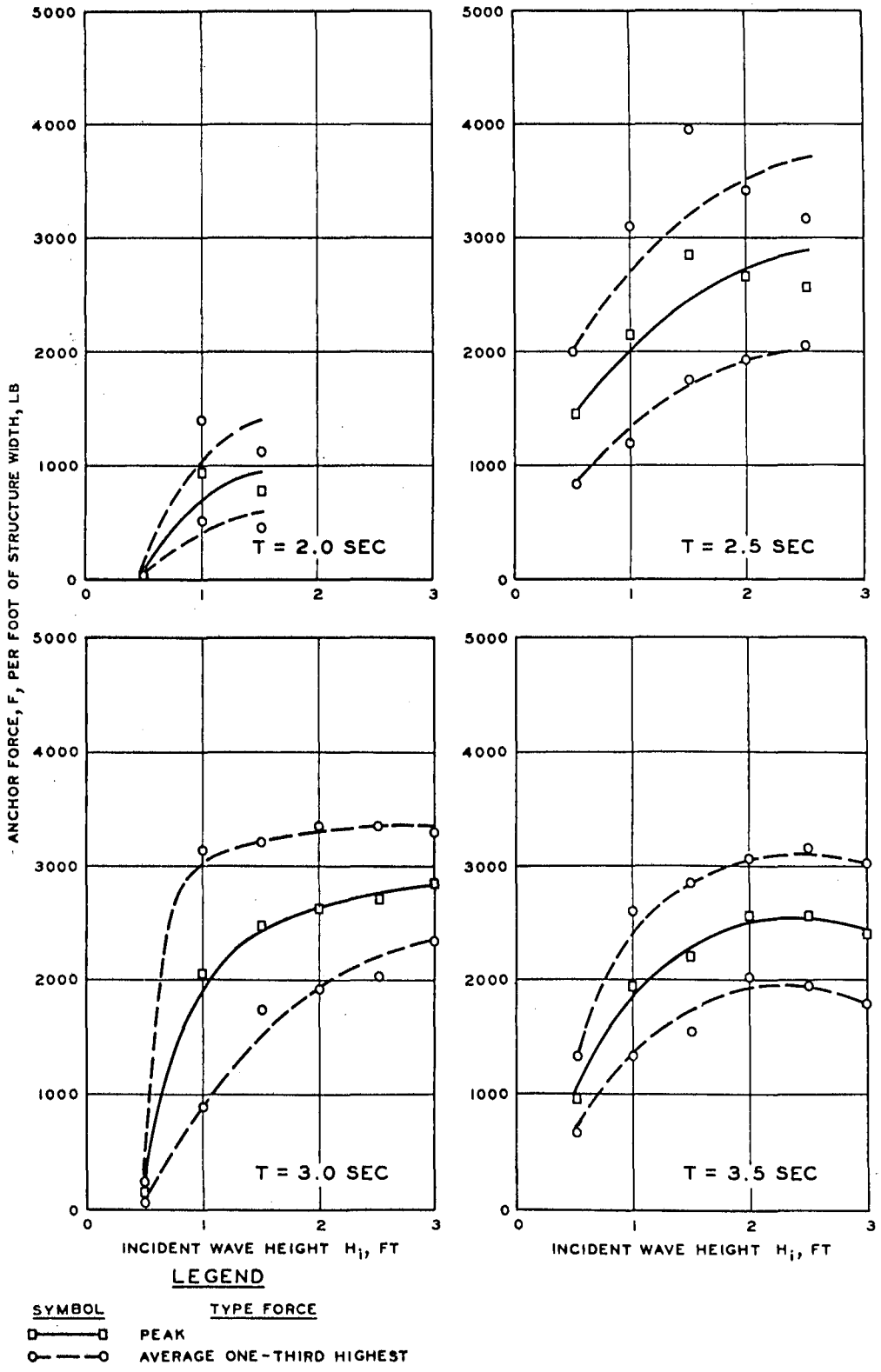

Figure 6-61. Forces on harborside of pile (d = 10 feet), Oak Harbor breakwater model (Davidson, 1971a).

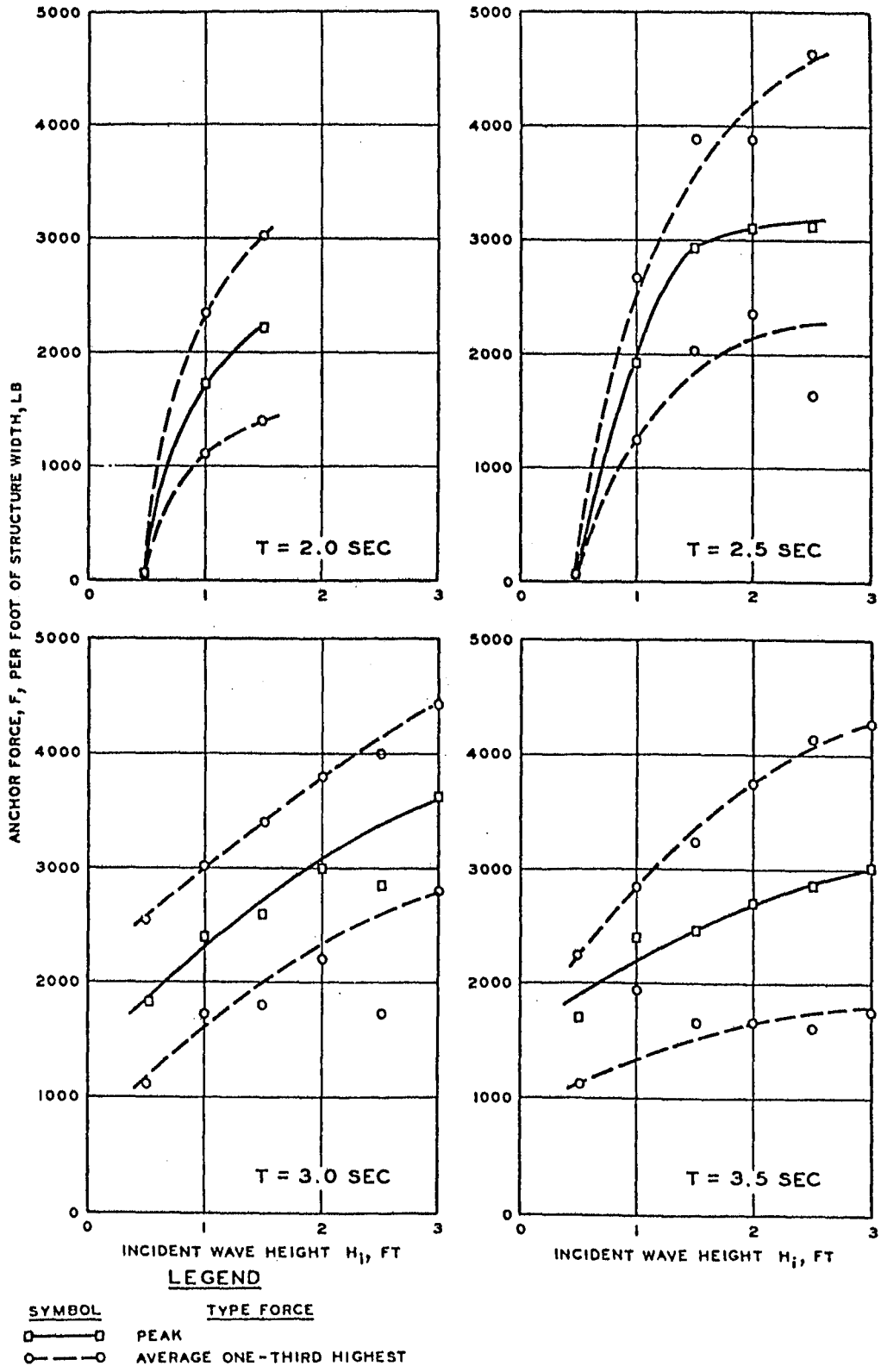

Figure 6-62. Forces on seaside of pile (d = 29.5 feet), Oak Harbor breakwater model (Davidson, 1971a).

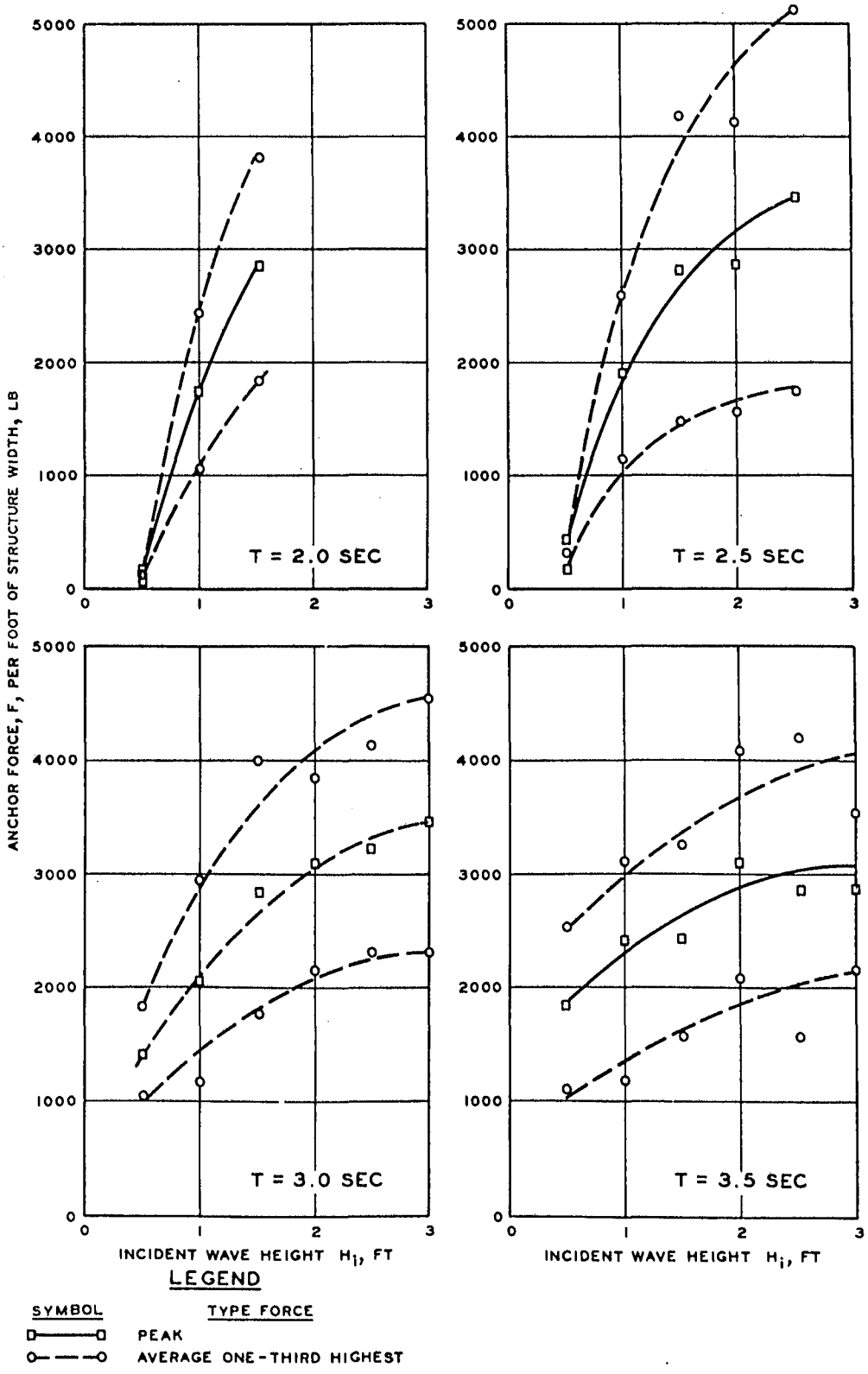

Figure 6-63. Forces on harborside of pile (d = 29.5 feet), Oak Harbor breakwater model (Davidson, 1971a).

to about 6.5 feet. Wave heights were recorded by step-resistance gages in conjunction with a Brush oscillograph. The gage consisted of a vertical plastic staff with equally spaced plugs interconnected by appropriate resistances providing a linear relationship between plug distance and wave height. Both incident and attenuated wave heights, were measured at distances between 187 and 396 feet from the wave generator position. Air temperature was measured by a commercial, single well-type thermometer with a range of 30° to 240°. A submerged rubble-mound wave absorber was constructed in the wave flume 465 feet from the wave generator piston. When waves impinged and broke over the absorber, a rise in water level or setup occurred that extended back toward the wave measuring area. Since it was necessary to monitor the water level in the area of the wave height measurement, a water level gage was installed near the wave absorber. A rotary meter of the cone anemometer-type was used for the water current measurements. A signal was transmitted to the Brush recorder tape for each revolution of the current meter shaft. Four air compressors were used, each with a capacity of 500 cubic feet per minute (the piping arrangement is shown in Figure 6-64a). The test rig consisted of that part of the equipment from the outlet of the flow-metering apparatus up to and including the discharge tubes (Fig. 6-64b). Three discharge manifolds were used, each 3 inches in diameter and 15 feet in length with 26 discharge holes (evenly spaced) approximately 1/4 inch (6 millimeters) in diameter. The most important and accurate measurement needed to determine the effectiveness of pneumatic wave attenuation is the volume of air discharged per foot length of breakwater. The pipe arrangement, pressure gages, flow-meter, and thermometer are shown in Figure 6-65. Flow calibration charts were prepared for the flowmeter from data of pressure and percentage flow, correcting for temperature and pressure. By knowing the pressure used for a particular test, the charts can be used to determine the air discharge volume.

(h) Test Procedures. Tests were conducted using water depths from 13.4 to 16.75 feet; manifold depths from 7.0 to 16.75 feet; single, double, and triple manifolds; wave periods from 2.6 to 16.0 seconds; wave heights from 3.06 to 6.40 feet; wavelengths from 35 to 347 feet; and air discharges from about 9 to 105 cubic feet per minute at 21° Celsius (70° Fahrenheit) and 14.7 pounds per square inch absolute pressure. The procedure for a typical test was as follows:

(1) The four compressors were started and allowed to reach normal running temperature;

(2) the Brush recorders were adjusted and the wave gages were positioned according to the water depth while the compressors were warming up;

(3) the wave generator was then started;

(4) the recorders were started when the waves reached a steady-state condition;

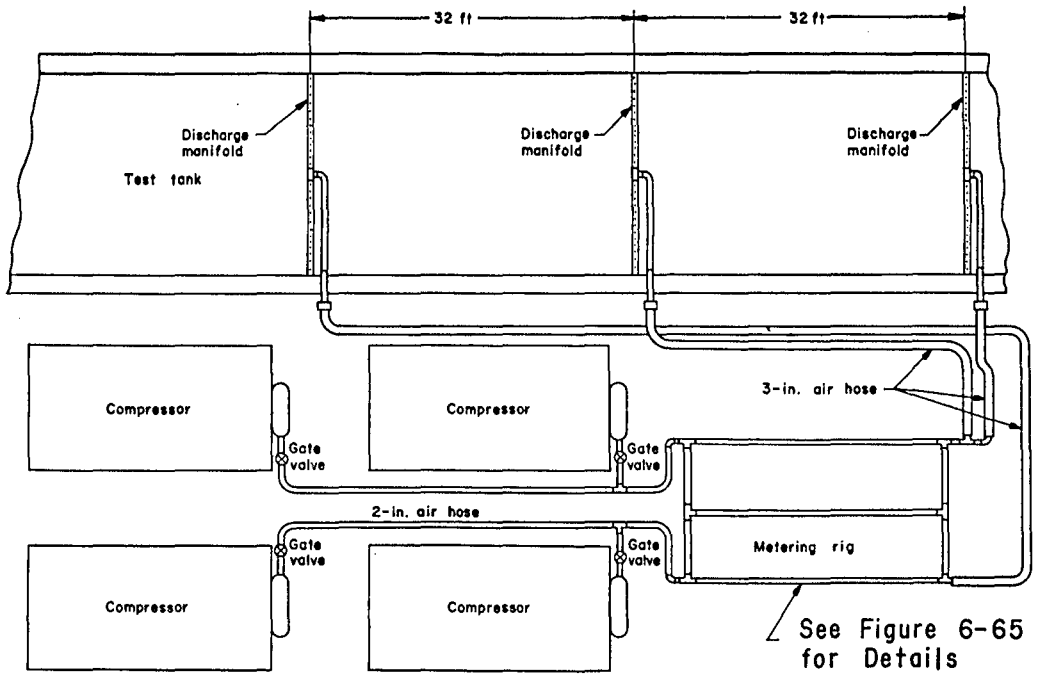

a. AIR COMPRESSOR ARRANGEMENT

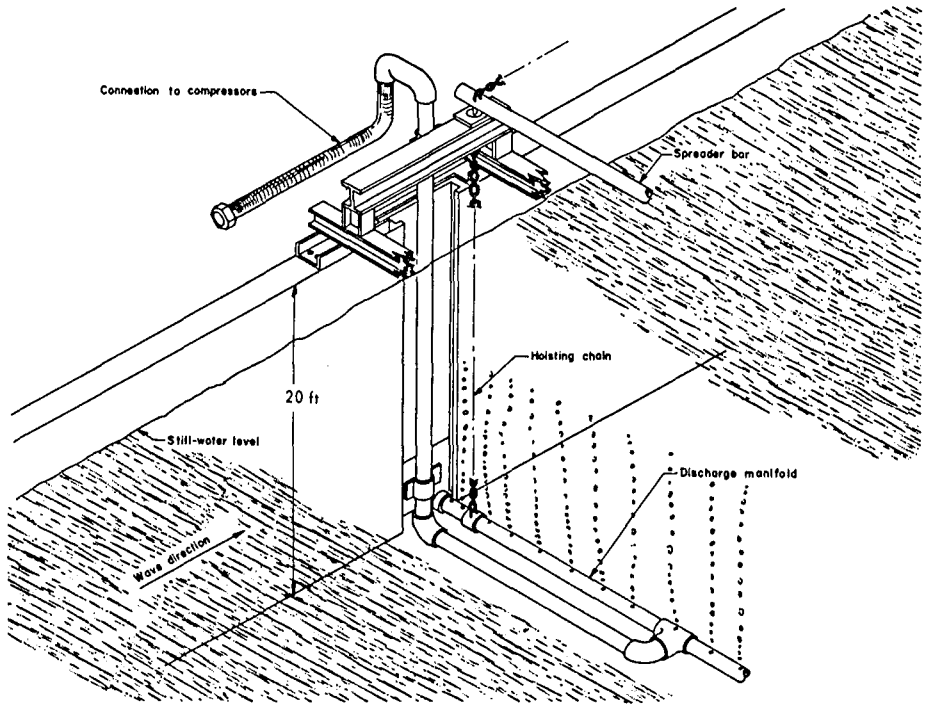

b. TEST RIG CONFIGURATION

Figure 6-64. Pneumatic breakwater test arrangement (Sherk, 1960).

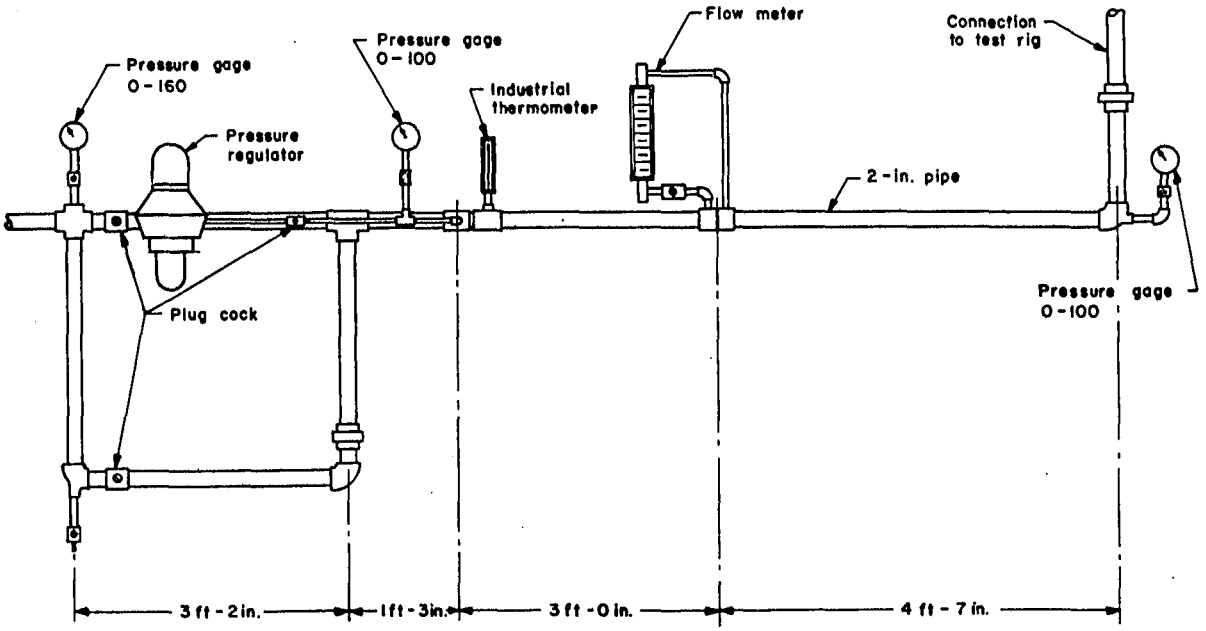

INITIAL METERING ARRANGEMENT

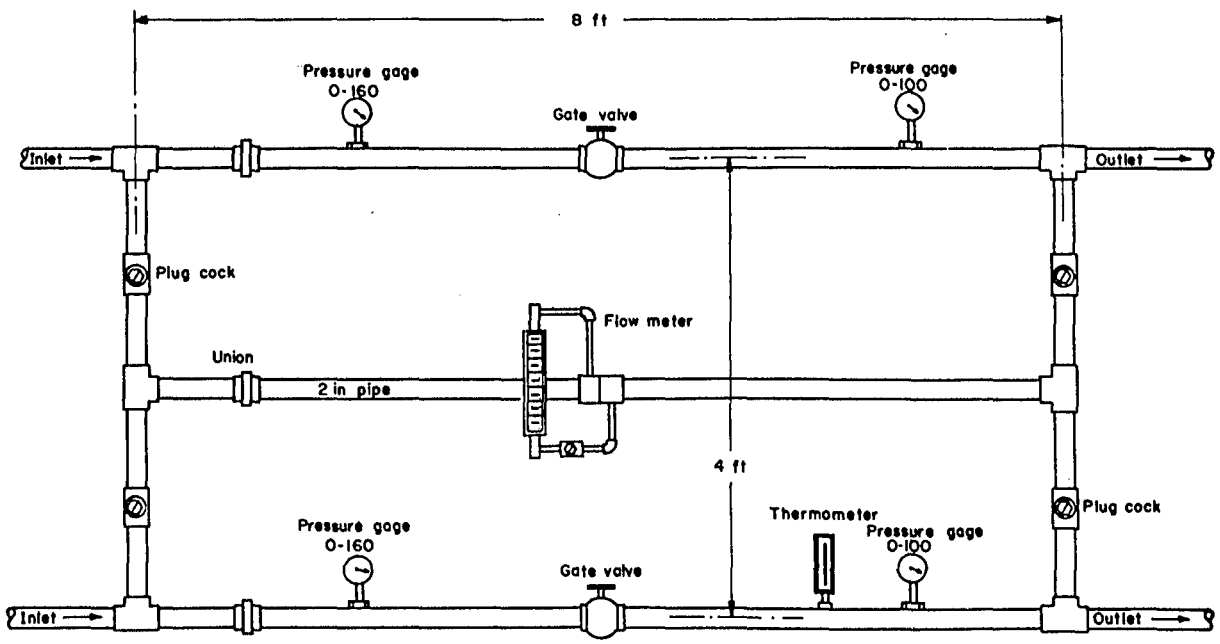

FINAL METERING ARRANGEMENT

Figure 6-65. Pneumatic breakwater metering arrangement (Sherk, 1960).

(5) the air was then turned on for a period of 5 minutes;

(6) temperature, pressure, and flow readings were recorded at the start and finish of the 5-minute period;

(7) the air was turned off;

(8) the wave recorders were allowed to run until the waves were again in a steady-state condition; and

(9) the wave recorder and the wave generator were turned off.

(i) Summary of Test Results. Unfortunately, the tests were not extensive enough to furnish data that could be analyzed and then transferred to prototype situations other than those used in the tests. However, the tests used values of the primary variables of considerable magnitude and the data reflect (more accurately than small-scale models) the quantity of air required for substantial reductions of incident wave heights (the requirements for pneumatic breakwater tests so that the results can be applied to prototype structures are given by eqs. 6-14a to 6-20). Some important conclusions from these tests are:

(1) The use of pneumatic breakwaters in limited Transportation Corps problem areas is feasible, although the air requirements are rather high;

(2) the tests (nearly full scale insofar as the offshore discharge problems of the Transportation Corps are concerned) indicate that about one-sixth less air horsepower is required than was predicted by the results of previous small-scale tests, transferred to prototype values based on the Froude law scaling relations;

(3) wave attenuation by pneumatic breakwaters is primarily a function of the wave dimensions, water depth, manifold submergence, and the quantity of air discharged by the manifold system; and

(4) the major part of the attenuation was the result of the horizontal surface currents (generated by the air bubbles) opposing the incident waves.

(7) Hydraulic Breakwaters.

(a) Project. Experimental and analytical studies in the mechanics of selected methods of wave absorption.

(b) Reference. Herbich, Ziegler, and Bowers (1956).

(c) Laboratory. St. Anthony Falls.

(d) Test Period. April 1955 to April 1956.

(e) Problem. Previous theoretical and experimental investigations have shown that a rising curtain of air bubbles can provide adequate protection to boats from waves with relatively small dimensions in deep water, and that the wave attenuation is accomplished by the horizontal water currents generated by the rising air bubbles. This problem concerns the practicality of generating the horizontal currents by water jets directed horizontally toward the oncoming waves.

(f) Purpose of Study. This investigation was conducted to determine the relationship between wave attenuation and the incident wave characteristics as a function of water depth, jet submergence, jet diameter, horizontal and vertical jet spacing, angle between wave direction and jet direction, and jet discharge. The tests used two wave flumes, one considerably larger than the other to obtain some information on scale effects.

(g) Test Facilities. The smaller of the two wave flumes was 50 feet long, 2 feet wide, and 1.25 feet deep, and was equipped with a pendulum-type wave generator. This generator is essentially a form of the piston generator, in which the piston is suspended by two movable arms connected above to a fixed beam. The movable part (piston and arms) is oscillated by a connecting rod attached to a drive wheel. By shifting the upper pivot points of the arms, the piston path is deviated from the horizontal during each cycle of the drive wheel. The result is a motion of the piston similar to the orbital motion of water particles in generated waves. The generator, powered by an alternating current, 0.5-horsepower (1,724 revolutions per minute), electric motor, could produce waves with a maximum height of 0.25 and 10 feet in length. The larger wave flume was 253 feet long, 9 feet wide, and 6 feet deep, and was equipped with a flap-type wave generator capable of producing waves with a maximum height of 1.5 and 18 feet in length. Both channels were equipped with wave absorbers on the test structure end of the facility. Wave heights were measured with a capacitive-type gage and recorded on an oscillograph. Water was supplied to the manifolds by a 3-horsepower pump in the small channel and a 25-horsepower pump in the larger channel. Suction lines for the pumps were located near the wave absorbers; thus, the currents in the flumes formed a closed system. Discharges into the manifolds were measured by Venturi meters (Fig. 6-66).

(h) Test Procedures. The test procedure consisted essentially of measuring incident and transmitted wave heights for various water discharges, jet spacings, jet diameters, jet directions relative to wave direction, depths of water, wave heights, and wavelengths. The tests were in two wave flumes; the larger flume had linear dimensions 4.5 times those in the smaller flume.

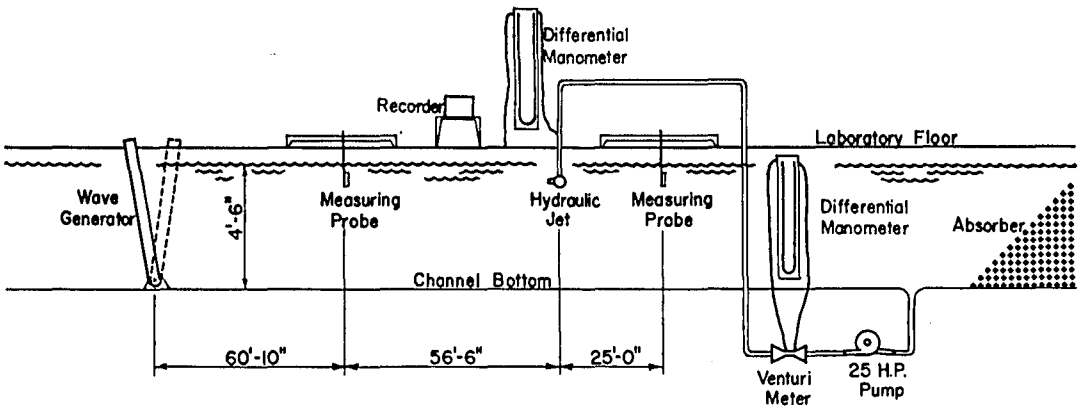

Figure 6-66. Sketch of test setup in the large channel, hydraulic breakwater tests (Herbich, Ziegler, and Bowers, 1956).

(i) Summary of Test Results. Conclusions from the tests are:

(1) Water discharge and horsepower requirements for the hydraulic breakwater are dependent on the d/λ and H/λ ratios, the manifold jet characteristics, and the submergence of the nozzles;

(2) a single manifold system is effective for deep-water waves, but its effectiveness decreases with decreasing values of d/λ;

(3) power requirements increase with wave steepness for high attenuation values; however, the efficiency of the system, which is based on the ratio of the difference between incident and transmitted wave energy to the jet energy, is higher for the steep waves than for the flat waves;

(4) zero submergence of the nozzles (nozzle located at the stillwater level) is the most efficient for the range of wave conditions tested;

(5) the power requirement at the nozzles decreases and the discharge increases as the jet area (jet diameter and number of jets per foot of manifold) increases; however, since the energy losses in the pumping and supply systems are dependent on the discharge, these systems must be analyzed along with the manifold jet system to determine the optimum jet area; and

(6) comparative data for the hydraulic breakwaters tested in the small and large wave flumes (scale ratio of 1:4.5) agree quite well when compared on the basis of Froude's law for d/λ values between 0.56 and 0.82.

d. Cost and Time Estimates. Cost and time estimates for the conduct of stability models of coastal engineering structures vary with many factors, and providing information to derive even approximate estimates for specific problems is difficult. However, examples of actual costs and times previously expended to perform model studies, with estimates of times and costs for conducting the same studies in 1976, may be helpful. The following work items are involved in the conduct of stability models for those structures discussed in this section, and may serve as a guide in the preparation of estimates for such studies:

(1) Preliminary model design and cost estimate, and necessary travel, conferences, and correspondence before authorization to conduct the model study.

(2) Final model design.

(3) Model construction.

(4) Calibration of wave generator and wave measuring apparatus for the selected test conditions.

(5) Conduct of model tests, including necessary modifications of model, computer time, required drafting and photography, preparation of monthly progress reports and model demonstrations, and conferences with representatives of the sponsoring agency.

(6) Analysis of test results after testing has been completed; the preparation for and the hosting of a final conference to present and discuss the test results.

(7) Preparation of first draft of the final report, which is usually sent to the sponsoring agency for review and comment.

(8) Preparation, publication, and distribution of the final report.

(9) Any authorized funds remaining in the job account after completion of the study are returned to the sponsoring agency.

The total costs for conducting the model studies, and the approximate times and costs for the different items listed above, are given in Table 6-7 for five of the example model studies.

The study concerning the stability of a vertical-wall parapet on rubble-mound breakwater at Indiana Harbor, Indiana, was conducted in 1952; no cost records are available. However, it is estimated that about $34,000 would be required to conduct the same study in 1976. The detailed costs given for the five example model studies are the costs accrued at the time each study was conducted; i.e., during the period 1963 to 1971. The estimated costs of these studies in 1976 are presented in Table 6-8; the actual time and costs from Table 6-7 are shown for comparison.

Table 6-7. Time and cost estimates for five example model studies.

Item	Burns Harbor breakwater		Monterey Harbor breakwater		Humboldt Bay jetty		Texas City seawall		Oak Harbor breakwater	
	Time (mo)	Cost	Time (mo)	Cost	Time (mo)	Cost	Time (mo)	Cost	Time (mo)	Cost
Preliminary model design, cost estimate, and necessary travel, conferences, and correspondence.	0.25	$ 300	1.00	$ 400	5.00	$ 10,000	1.00	$ 1,000	1.00	$ 3,000
Model design.	0.25	300								
Model construction.	0.50	400					1.00	1,000	1.00	500
Calibration of wave generator and wave gages. Conduct of model tests, including modifications of model, photography, and drafting, etc., necessary for preparation of progress reports.	3.00	11,000	1.00	1,500	28.00[1]	82,500	10.00	39,000	6.00	17,500
Analysis of test results (after testing has been completed); preparation for and costs of final conference.	0.50	1,000								
Preparation of first draft of final report.	2.50	3,000	2.00	100	4.00	7,000	4.00	3,500	4.00	3,000
Preparation and publication of report.	5.00	3,000			8.00	3,000	17.00[2]	2,500	9.00	2,000
Totals	12.00	$19,000	4.00	$2,000	45.00	$102,500	33.00	$47,000	21.00	$26,000

[1]Part-time work; most of the testing program was completed during a 14-month period.

[2]Part-time work; most reports are completed and published within 6 to 8 months after review of first draft.

Table 6-8. Time and costs of example model studies.

Model study	Actual		Estimated in 1976	
	Time (mo)	Costs	Time (mo)	Costs
Burns Harbor breakwater	12.0	$ 19,000	11.0	$ 36,000
Monterey Harbor breakwater	4.0	2,000	3.5	6,000
Humboldt Bay jetty	45.0[1]	102,500	24.0	140,000
Indiana Harbor breakwater	3.0	----------[2]	3.0	34,000
Texas City seawall	33.0[1]	47,000	18.0	88,000
Oak Harbor breakwater	21.0	26,000	12.0	43,000

[1] Part-time work.

[2] Costs not available.

Many factors can determine the cost of model studies, including the complexity of the phenomena involved; the availability of prototype data for selecting design conditions and designing the model; the availability of wave flumes, wave generators, electrical recording equipment, adequate shelter space, and armor units of the required shape and weight; the size of the prototype compared with the available equipment; the extent of the testing program required, and the technical abilities of the engineers involved in the study. However, the largest item of expense is usually the cost of conducting the testing program.

LITERATURE CITED

ALLEN, F.H., and RUSSELL, R.C.H., "Discourse on Hydraulic Models as an Aid to Solving River, Estuary and Harbour Problems," The Institution of Civil Engineering, London, England, June 1958.

BAGNOLD, R.A., "Interim Report on Wave Pressure Research," *Journal of the Institution of Civil Engineers*, London, England, Vol. 12, No. 7, June 1939, pp. 201-226.

BOGOLEPOFF, I.A., "The Compressed Air Breakwater," *Bulletin of the Permanent International Association of Navigation Congresses*, Brussels, Belgium, Vol. 12, No. 23, Jan. 1937, pp. 101-125.

BREBNER, A., and OFUYA, A.O., "Floating Breakwaters," *Proceedings of the 11th Conference on Coastal Engineering*, American Society of Civil Engineers, Vol. 2, 1968, pp. 1055-1094.

BRETSCHNEIDER, C.L., "Wave Generation by Wind, Deep and Shallow Water," *Estuary and Coastline Hydrodynamics*, A.T. Ippen, ed., McGraw-Hill, New York, 1966, pp. 133-196.

BRETSCHNEIDER, C.L., and REID, R.O., "Change in Wave Height Due to Bottom Friction, Percolation and Refraction," *Proceedings of the 34th Annual Meeting of the American Geophysical Union*, unpublished, 1953.

BULSON, P.S., "Currents Produced by an Air Curtain in Deep Water," *Dock and Harbour Authority*, London, England, Vol. 42, No. 487, May 1961, pp. 15-22.

BULSON, P.S., "Transportable Breakwaters--A Feasibility Study," Research Report 42.1/4, Military Engineering Experimental Establishment, Christchurch, Hampshire, England, Apr. 1964.

BULSON, P.S., "The Theory and Design of Bubble Breakwaters," *Proceedings of the 11th Conference on Coastal Engineering*, American Society of Civil Engineers, Vol. 2, 1968, pp. 995-1015.

CAMPBELL, W.S., "An Electronic Wave-Height Measuring Apparatus," Report No. 859, David Taylor Model Basin, U.S. Navy, Washington, D.C., Oct. 1953.

CARR, J.H., "Mobile Breakwater Studies," Report No. N-64.2, California Institute of Technology, Hydrodynamics Laboratory, Pasadena, Calif., Dec. 1950.

CARR, J.H., "Wave Forces on Plane Barriers," Report No. E-11.1, California Institute of Technology, Hydrodynamics Laboratory, Pasadena, Calif., Oct. 1953.

CARR, J.H., "Wave Forces on Curved and Stepped Barriers," Report No. E-11.2, California Institute of Technology, Hydrodynamics Laboratory, Pasadena, Calif., June 1954a.

CARR, J.H., "Breaking Wave Forces on Plane Barriers," Report No. E-11.3, California Institute of Technology, Hydrodynamics Laboratory, Pasadena, Calif., Nov. 1954b.

CHATHAM, C.E., "Wave and Surge Conditions After Proposed Expansion of Monterey Harbor, Monterey, California; Hydraulic Model Investigation," Technical Report H-68-9, U.S. Army Engineer Waterways Experiment Station, Vicksburg, Miss., Sept. 1968.

DAI, Y.B., and KAMEL, A.M., "Scale Effect Tests for Rubble-Mound Breakwaters; Hydraulic Model Investigation," Research Report H-69-2, U.S. Army Engineer Waterways Experiment Station, Vicksburg, Miss., Dec. 1969.

DANEL, P., "On the Limiting Clapotis," *Gravity Waves*, Circular No. 521, National Bureau of Standards, Washington, D.C., 1952.

DAVIDSON, D.D., "Stability and Transmission Tests of Tribar Breakwater Section Proposed for Monterey Harbor, California," Miscellaneous Paper H-69-11, U.S. Army Engineer Waterways Experiment Station, Vicksburg, Miss., Sept. 1969.

DAVIDSON, D.D., "Wave Transmission and Mooring Force, Tests of Floating Breakwater, Oak Harbor, Washington; Hydraulic Model Investigation," Technical Report H-71-3, U.S. Army Engineer Waterways Experiment Station, Vicksburg, Miss., Apr. 1971a.

DAVIDSON, D.D., "Proposed Jetty-Head Repair Sections, Humboldt Bay, California; Hydraulic Model Investigation," Technical Report H-71-8, U.S. Army Engineer Waterways Experiment Station, Vicksburg, Miss., Nov. 1971b.

DOBSON, R.S., "Some Applications of a Digital Computer to Hydraulic Engineering Problems," M.S. Thesis, Stanford University, Stanford, Calif., unpublished, 1967.

DRAPER, L., "The Analysis and Presentation of Wave Data--A Plea for Uniformity," *Proceedings of the 10th Conference on Coastal Engineering*, American Society of Civil Engineers, Vol. 1, 1966, pp. 1-11.

EAGLESON, P.S., and VAN DE WATERING, W.P.M., "A Thermistor Probe for Measuring Particle Orbital Speed in Water Waves," TM-3, U.S. Army, Coastal Engineering Research Center, Washington, D.C., Mar. 1964.

EATON, J.P., RICHTER, D.H. and AULT, W.V., "The Tsunami of May 23, 1960, on the Island of Hawaii," *Bulletin of the Seismological Society of America*, Berkeley, Calif., Vol. 51, No. 2, Apr. 1961, pp. 135-157.

EVANS, J.T., "Pneumatic and Similar Breakwaters," *Proceedings of the Royal Society*, Series A, Mathematical and Physical Sciences, Vol. 231, 1955, pp. 457-466.

FAN, LOH-NIEN, and LE MEHAUTE, B., "Coastal Movable Bed Scale Model Technology," TC-131, Tetra Tech, Inc., Pasadena, Calif., June 1969.

GAILLARD, D.D., "Wave Action in Relation to Engineering Structures," The Engineer School, Fort Belvoir, Va., 1935.

GALVIN, C.J., Jr., "Wave-Height Prediction for Wave Generators in Shallow Water," TM-4, U.S. Army, Coastal Engineering Research Center, Washington, D.C., Mar. 1964.

GARCIA, W.J., Jr., "An Experimental Study of Breaking Wave Pressures," Research Report H-68-1, U.S. Army Engineer Waterways Experiment Station, Vicksburg, Miss., Sept. 1968.

HANES, F.P., "Development of Wave-Height Measuring Device," Miscellaneous Paper No. 5-231, U.S. Army Engineer Waterways Experiment Station, Vicksburg, Miss., June 1957.

HAYASHI, T., and HATTORI, M., "Pressure of the Breaker Against a Vertical Wall," *Coastal Engineering in Japan*, Tokyo, Japan, Vol. 1, Oct. 1958, pp. 25-38.

HEATH, W.A., "Pneumatic Breakwater Development in England," *The Military Engineer*, Washington, D.C., Vol. 51, No. 340, Apr. 1959. pp. 104-106.

HERBICH, J.B., ZIEGLER, J., and BOWERS, C.E., "Experimental Studies of Hydraulic Breakwaters," Project Report No. 51, St. Anthony Falls Hydraulic Laboratory, University of Minnesota, Minneapolis, Minn., June 1956.

HUDSON, R.Y., "Model Study of Wave Force Against Breakwaters; Interim Report," U.S. Army Engineer Waterways Experiment Station, Vicksburg, Miss., Mar. 1942.

HUDSON, R.Y., "Model Tests of Portable Breakwaters for D-Day Invasion Harbors," *Civil Engineering*, Vol. 15, No. 9, Sept. 1945, pp. 405-408.

HUDSON, R.Y., "Wave Forces on Breakwaters," *Transactions of the American Society of Civil Engineers*, Vol. 118, 1953, pp. 653-685.

HUDSON, R.Y., "Design of Quarry-Stone Cover Layers for Rubble-Mound Breakwaters; Hydraulic Laboratory Investigation," Research Report No. 2-2, U.S. Army Engineer Waterways Experiment Station, Vicksburg, Miss., July 1958.

HUDSON, R.Y., ed., "Concrete Armor Units for Protection Against Wave Attack; Report of Ad Hoc Committee on Artificial Armor Units for Coastal Structure," Miscellaneous Paper H-74-2, U.S. Army Engineer Waterways Experiment Station, Vicksburg, Miss., Jan. 1974.

HUDSON, R.Y., and JACKSON, R.A., "Stability of Rubble-Mound Breakwaters; Hydraulic Model Investigation," Technical Memorandum No. 2-365, U.S. Army Engineer Waterways Experiment Station, Vicksburg, Miss., June 1953.

HUDSON, R.Y., and JACKSON, R.A., "Design of Tetrapod Cover Layer for a Rubble-Mound Breakwater, Crescent City Harbor, Crescent City, California," Technical Memorandum No. 2-413, U.S. Army Engineer Waterways Experiment Station, Vicksburg, Miss., June 1955.

HUDSON, R.Y., and JACKSON, R.A., "Stability Tests of Proposed Rubble-Mound Breakwaters, Nassau Harbor, Bahamas; Hydraulic Model Investigation," Miscellaneous Paper No. 2-799, U.S. Army Engineer Waterways Experiment Station, Vicksburg, Miss., Mar. 1966.

HUDSON, R.Y., and WILSON, H.B., "Stability of East-West Breakwater Parapet, Indiana Harbor, Indiana," Fifth Interim Report, U.S. Army Engineer Waterways Experiment Station, Vicksburg, Miss., unpublished, Feb. 1953.

ICHIYE, T., "Tsunami Waves," *Collected Reprints*, Contribution No. 952, Woods Hole Oceanographic Institution, Woods Hole, Mass., 1958.

IPPEN, A.T., and EAGLESON, P.S., "A Study of Sediment Sorting by Waves Shoaling on a Plane Beach," TM-63, U.S. Army, Beach Erosion Board, Washington, D.C., Sept. 1955.

JACKSON, R.A., "Twin-Log Floating Breakwater, Small-Boat Basin No. 2, Juneau, Alaska," Miscellaneous Paper No. 2-648, U.S. Army Engineer Waterways Experiment Station, Vicksburg, Miss., May 1964.

JACKSON, R.A., "Stability of Seawall, Texas City, Texas; Hydraulic Model Investigation," Technical Report No. 2-728, U.S. Army Engineer Waterways Experiment Station, Vicksburg, Miss., May 1966.

JACKSON, R.A., "Stability of Proposed Breakwater, Burns Waterway Harbor, Indiana; Hydraulic Model Investigation," Technical Report No. 2-766, U.S. Army Engineer Waterways Experiment Station, Vicksburg, Miss., Mar. 1967.

JACKSON, R.A., "Limiting Heights of Breaking and Nonbreaking Waves on Rubble-Mound Breakwaters; Hydraulic Model Investigation," Technical Report H-68-3, U.S. Army Engineer Waterways Experiment Station, Vicksburg, Miss., June 1968.

JOHNSON, J.W., "Engineering Aspects of Diffraction and Refraction," *Transactions of the American Society of Civil Engineers*, Vol. 118, 1953, pp. 617-652.

KAMEL, A.M., "Stability of Rubble-Mound Tsunami Barrier, Hilo Harbor, Hawaii; Hydraulic Model Investigation," Technical Report No. 2-792, U.S. Army Engineer Waterways Experiment Station, Vicksburg, Miss., Aug. 1967.

KAMEL, A.M., "Water Wave Pressures on Seawalls and Breakwaters," Research Report No. 2-10, U.S. Army Engineer Waterways Experiment Station, Vicksburg, Miss., Feb. 1968a.

KAMEL, A.M., "Shock Pressures Caused by Waves Breaking Against Coastal Structures," Research Report H-68-2, U.S. Army Engineer Waterways Experiment Station, Vicksburg, Miss., Sept. 1968b.

KEULEGAN, G.H., "The Approximate Theories of Pneumatic Wave Generators; Hydraulic Laboratory Investigation," Research Report No. 2-7, U.S. Army Engineer Waterways Experiment Station, Vicksburg, Miss., Apr. 1966.

KEULEGAN, G.H., "Wave Transmission Through Rock Structures; Hydraulic Model Investigation," Research Report H-73-1, U.S. Army Engineer Waterways Experiment Station, Vicksburg, Miss., Feb. 1973.

KEULEGAN, G.H., HARRISON, J., and MATHEWS, M.J., "Theoretics in Design of the Proposed Crescent City Harbor Tsunami Model," Technical Report H-69-9, U.S. Army Engineer Waterways Experiment Station, Vicksburg, Miss., June 1969.

KILLEN, J.M., "A Capacitive Type Wave Recorder," Technical Paper No. 11, Series B, St. Anthony Falls Hydraulic Laboratory, University of Minnesota, Minneapolis, Minn., Oct. 1952.

KISHI, T., "The Possible Highest Gravity Waves on Shallow Water," *Coastal Engineering in Japan*, Tokyo, Japan, Vol. 2, Nov. 1959, pp. 9-16.

KOLPAK, M.M., and EAGLESON, P.S., "The Utility of a Hot-Film Sensor and a Direction-Vane in the Laboratory Measurement of Velocity Fields in Water Waves," Laboratory Report No. 118, Hydrodynamics Laboratory, Department of Civil and Sanitary Engineering, Massachusetts Institute of Technology, Cambridge, Mass., Dec. 1969.

KURIHARA, M., "Pneumatic Breakwater (II)--Field Test at Iwo-Jima Island," *Proceedings of the Second Conference on Coastal Engineering in Japan* (in Japanese--translation by K. Horikawa, TR Series 104, Issue 5, Aug. 1958, Institute of Engineering Research, Wave Research Laboratory, University of California, Berkeley, Calif.), 1955, pp. 71-77.

KURIHARA, M., "Pneumatic Breakwater (III)--Field Test at Ha-Jima," *Proceedings of the Third Conference on Coastal Engineering in Japan* (in Japanese--translated by K. Horikawa, TR Series 104, Issue 6, Nov. 1958, Institute of Engineering Research, Wave Research Laboratory, University of California, Berkeley, Calif.), 1956, pp. 139-149.

LAURIE, A.H., "Pneumatic Breakwaters," *The Dock and Harbour Authority*, London, England, Vol. 33, No. 379, May 1952, pp. 11-13.

LEENDERTSE, J.J., "Forces Induced by Breaking Waves on a Vertical Wall," U.S. Naval Civil Engineering Laboratory, Port Hueneme, Calif., Jan. 1962.

LE MEHAUTE, B., "Wave Absorbers in Harbors," Contract Report No. 2-122, U.S. Army Engineer Waterways Experiment Station, Vicksburg, Miss., June 1965.

LUNDGREN, H., "A New Type of Breakwater for Exposed Positions," *The Dock and Harbour Authority*, London, England, Vol. 43, No. 505, Nov. 1962, pp. 228-231.

LUNDGREN, H., "Wave Shock Forces: An Analysis of Deformations and Forces in the Wave and in the Foundation," *Proceedings of the Symposium on Research on Wave Action*, Delft Hydraulics Laboratory, Vol. 11, Paper 4, 1969, 20 pp.

MADSEN, O.S., "Waves Generated by a Piston-Type Wavemaker," *Proceedings of the 12th Conference on Coastal Engineering*, American Society of Civil Engineers, Vol. 1, 1970, pp. 589-607.

MARLOW, T.A., "An Experimental Determination of Particle Velocities in the Oscillatory Water Wave," M.S. Thesis, Massachusetts Institute of Technology, Department of Civil and Sanitary Engineering, Cambridge, Mass., unpublished, 1957.

MICHE, R., "Mouvements Ondulatoires de la Mer en Profondeur Croissante ou Décroissante," *Annales des Ponts et Chaussees*, Paris, France, 1944a.

MICHE, R., "Mouvements Ondulatoires des Mers en Profondeur Constante au Décroissante," *Annales des Ponts et Chaussees*, Paris, France, 1944b.

MINIKIN, R.R., *Winds, Waves, and Maritime Structures*, 2d rev. ed., Charles Griffin and Co., Ltd, London, England, 1963, 294 pp.

MITSUYASU, H., "Shock Pressure of Breaking Wave," *Proceedings of the 10th Conference on Coastal Engineering*, American Society of Civil Engineers, Vol. 1, 1966, pp. 268-283.

MOORE, J.B., "A Water Wave Recording Instrument for Use in Hydraulic Models," *Journal of Scientific Instruments*, Bristol, England, Vol. 41, No. 5, May 1964, pp. 321-323.

MURPHY, G., *Similitude in Engineering*, The Ronald Press, New York, 1950, 302 pp.

NAGAI, S., "Pressures by Breaking Waves on Composite-Type Breakwaters," *Proceedings of the 11th Conference on Coastal Engineering*, American Society of Civil Engineers, Vol. 2, 1968, pp. 920-923.

NECE, R.E., RICHEY, E.P., and RAO, V.S., "Dissipation of Deep Water Waves by Hydraulic Breakwaters," *Proceedings of the 11th Conference on Coastal Engineering*, American Society of Civil Engineers, Vol. 2, 1968, pp. 1032-1048.

PALMER, R.Q., MULVIHILL, M.E., and FUNASAKI, G.T., "Study of Proposed Barrier Plans for the Protection of the City of Hilo and Hilo Harbor, Hawaii," Technical Report No. 1, U.S. Army Engineer Division, Pacific Ocean, Ft. Shafter, Hawaii, Nov. 1967.

QUINN, A.D., *Design and Construction of Ports and Marine Structures*, 2d ed., McGraw-Hill, New York, 1972, 611 pp.

RADIONOV, S.I., "Wave Dissipation by Compressed Air" (in Russian--Translated by H. Arnesen, TR Series 104, Issue 9, Apr. 1960, Institute of Engineering Research, Wave Research Laboratory, University of California, Berkeley, Calif.), 1958.

ROSS, C.W., "Laboratory Study of Shock Pressures of Breaking Waves," TM-59, U.S. Army, Beach Erosion Board, Washington, D.C., Feb. 1955.

ROSS, J., and BOWERS, C.E., "Laboratory Surface Wave Equipment; A Summary of Literature," Project Report No. 38, St. Anthony Falls Hydraulic Laboratory, University of Minnesota, Minneapolis, Minn., Nov. 1953.

SAINFLOU, M., "Essai sur les Digues Maritimes Verticales," *Annales des Ponts et Chaussées*, Paris, France, Vol. 2, No. 4, 1928, 51 pp.

SCHIJF, J.B., "Breaking Up Waves by Air Injection" (in Dutch--Translated by H.B. Edwards, Translation No. 43-2, Nov. 1943, U.S. Army Engineer Waterways Experiment Station, Vicksburg, Miss.), Oct. 1940.

SCIENTIFIC AMERICAN, "The Air Breakwater Put to Severe Test," New York, Apr. 1916.

SHEN, C.C., "Selection and Design of a Bore Generator for the Hilo Harbor Tsunami Model; Hydraulic Model Investigation," Research Report No. 2-5, U.S. Army Engineer Waterways Experiment Station, Vicksburg, Miss., June 1965.

SHERK, S.N., "Offshore Discharge (Pneumatic Wave Attenuation Full-Scale Tank Tests)," TR No. 60-26, U.S. Army Transportation Research Command, Fort Eustis, Va., Dec. 1960.

SMART, R.T., "Guide for Preparation of Waterways Experiment Station Technical-Information Reports," Instruction Report No. 9, U.S. Army Engineer Waterways Experiment Station, Vicksburg, Miss., Sept. 1967.

STRAUB, L.G., and HUDSON, R.Y., "Hydraulic Model Tests for Indiana Harbor Development," *Proceedings of the Fourth Conference on Coastal Engineering*, Council on Wave Research, 1953, pp. 371-383.

TAYLOR, G., "The Action of a Surface Current Used as a Breakwater," *Proceedings of the Royal Society of London*, Series A, Mathematical and Physical Sciences, Vol. 231, 1955, pp. 466-478.

TEPLOV, A.P., "The Scientific Principles for the Use of Pneumatic Breakwaters" (in Russian--translated and issued Dec. 1958 by Technical Information and Library Services, Ministry of Supply, Great Britain), 1954.

TUCKER, M.J., and CHARNOOK, H., "A Capacitance-Wire Recorder for Small Waves," *Proceedings of the Fifth Conference on Coastal Engineering*, Council on Wave Research, 1954, pp. 177-188.

URSELL, F., DEAN, R.G., and YU, Y.S., "Forced Small-Amplitude Water Waves; A Comparison of Theory and Experiment," Technical Report No. 29, Massachusetts Institute of Technology, Department of Civil and Sanitary Engineering, Cambridge, Mass., July 1958.

U.S. ARMY, CORPS OF ENGINEERS, COASTAL ENGINEERING RESEARCH CENTER, *Shore Protection Manual*, 3d ed., Vols. I, II, and III, Stock No. 008-022-00113-1, U.S. Government Printing Office, Washington, D.C., 1977, 1,262 pp.

VAN DE KREEKE, J., and PAAPE, A., "On Optimum Breakwater Design," *Proceedings of the Ninth Conference on Coastal Engineering*, American Society of Civil Engineers, 1964, pp. 532-552.

WEGGEL, J.R., "Maximum Breaker Height for Design," *Proceedings of the 13th Conference on Coastal Engineering*, American Society of Civil Engineers, Vol. 1, 1973, pp. 419-432.

WETZEL, J.M., "Experimental Studies of Pneumatic and Hydraulic Breakwaters," Project Report No. 46, St. Anthony Falls Hydraulic Laboratory, University of Minnesota, Minneapolis, Minn., May 1955.

WHALIN, R.W., "The Limit of Applicability of Linear Wave Refraction Theory in a Convergence Zone," Research Report H-71-3, U.S. Army Engineer Waterways Experiment Station, Vicksburg, Miss., Dec. 1971.

WILLIAMS, J.A., "Verification of the Froude Modeling Law for Hydraulic Breakwaters," TR Series 104, Issue 11, Institute of Engineering Research, Wave Research Laboratory, University of California, Berkeley, Calif., Aug. 1960.

WILLIAMS, J.A., and WIEGEL, R.L., "Final Report on the Hydraulic Breakwater; Attenuation of Wind Waves by a Hydraulic Breakwater," TR Series 104, Issue 12, Institute of Engineering Research, Wave Research Laboratory, University of California, Berkeley, Calif., Dec. 1961.

WILLIAMS, L.C., "CERC Wave Gages," TM-30, U.S. Army, Corps of Engineers, Coastal Engineering Research Center, Washington, D.C., Dec. 1969.

WILSON, H.B., and HUDSON, R.Y., "Stability Determination and Design of Outer Breakwater Revision, Gary Harbor, Indiana," Miscellaneous Paper No. 2-755, U.S. Army Engineer Waterways Experiment Station, Vicksburg, Miss., Nov. 1965.

VII. INLETS

by
Richard A. Sager and Lyndell Z. Hales

1. Introduction.

The coastal inlet is a complex part of the coastal environment. The three primary forces of importance to the coastal inlet are lunar-dominated ocean tides, winds, and freshwater inflow. These forces interact in the ocean, bay, and inlet proper to produce many phenomena that affect the inlet. Among these phenomena are: (a) tidal currents, (b) littoral currents, (c) wind waves, (d) density currents, (e) changes in water levels due to lunar tides, (f) wind wave runup, (g) currents generated by wind-water surface interaction, (h) littoral transport of material to the inlet, (i) wind transport of material to the inlet, and (j) freshwater transport of material to the inlet. A true physical model requires the accurate simulation of all of these phenomena active at a particular inlet. This simulation is not only beyond the capability of present physical modeling, but beyond the capabilities of any known simulation technique. The physical model does, however, provide a means of investigating the effects of a significant number of these phenomena. For many cases, this will allow an effective understanding of what does or could occur at a tidal inlet.

Although any one of these phenomena could be particularly important for understanding conditions at an inlet, this section discusses only the more critical phenomena affecting an inlet; i.e., physical modeling of tidal oscillations, tidal currents, tidal current-wind wave interaction, and the movement and deposition of material within the inlet complex by hydraulic forces. The physical modeling of wind-transported material and the effects of density currents (sometimes vital to the understanding of coastal inlets where large freshwater sources can act on an inlet) are not discussed in this section. Physical modeling of density current phenomena is discussed in Section III; modeling of the littoral transport of material approaching the inlet is discussed both in this section and in Section V. Many aspects of wind wave modeling particularly important to physical modeling of tidal inlets are briefly covered in this section; details of physical modeling of wind waves are discussed in Sections II, IV, and VI.

Studies in tidal inlet models are generally directed to development of methods for maintaining an effective navigation channel through the inlet, but often other aspects must also be investigated. Problems that can be investigated by physical inlet models are:

(a) Stabilization of navigation channel dimensions and location.

(b) Structural dimensions of jetties, etc., and location and configuration.

(c) Sand-bypassing techniques.

(d) Shoaling and scouring trends to approach beach, inlet, and bay.

(e) Tidal prism changes.

(f) Navigation conditions.

(g) Salinity effects.

Modification of the inlet by a proposed plan of improvement could result in changes to the tidal prism; i.e., the magnitude of flow into and out of the bay system, or changes to current patterns and the location of predominant currents within the bay system. Effective analysis of a potential plan of improvement dictates consideration of these aspects. Although prototype data can be analyzed, the most effective procedure is to conduct model studies to provide the information desired. Depending on the problem being investigated, mathematical or physical models can be used. (Mathematical modeling capabilities are not discussed in this report.) The effectiveness of various types of physical models is summarized in Table 7-1, which indicates that the most effective model to provide guidance on all aspects (with the exception of shoaling and scouring) is a fixed-bed, undistorted-scale model of the complete area of interest; i.e., ocean approach to the inlet, inlet proper, and entire tidal prism. Table 7-1 also shows that this is the most expensive type of model from which results can be obtained. The high cost is basically a result of the need to maintain a reasonable vertical scale. The maximum scale to obtain accurate results should not exceed a scale ratio of 1:100. If no distortion of scales is required for the particular problem being investigated, the 1:100-scale ratio for the plan area of interest results in an excessively large model with resulting high costs.

Further, Table 7-1 shows that generally very good results can be derived from a fixed-bed, distorted-scale model of the complete area of interest. In some cases, a different vertical and horizontal scale will result in a better model. Careful consideration is necessary in the simulation of short-period waves. Although the cost of this model remains relatively high, a considerable reduction in cost is possible due to the ability of reducing the plan area of the model by distortion of the horizontal scales. This type of model is most commonly used for the study of tidal inlets.

Both types of fixed-bed section models (undistorted- and distorted-scale) are relatively special-purpose models. A section model is defined as a model with only the inlet and a small part of the ocean and bay reproduced by the model. Studies conducted in these models can provide valuable information on the hydraulic characteristics of the inlet; however, because the bay is not reproduced in the model, the effects of the tidal prism on the hydraulics of the inlet and the effects of changes to the inlet on the tidal prism cannot be defined. Where applicable, the

Table 7-1. Capabilities of various types of inlet or inlet-bay physical hydraulic models.

Phenomena	Fixed-bed, undistorted scale		Fixed-bed, distorted scale		Movable-bed, distorted scale	
	Sectional model	Complete model	Sectional model	Complete model	Sectional model	Complete model
Tidal currents						
In inlet	Very good	Very good	Good	Good	Varied	Varied
In bay	----------	Very good	----------	Good	----------	Varied
Circulation patterns						
In inlet	Good	Very good	Good	Very good	Varied	Varied
In bay	----------	Very good	----------	Very good	----------	Varied
Tidal heights						
In inlet	Very good	Excellent	Good	Excellent	Varied	Varied
In bay	----------	Excellent	----------	Excellent	----------	Varied
Wave effects						
In inlet	Very good	Excellent	Limited	Limited	Limited	Limited
In bay	----------	Excellent	----------	Limited	----------	Limited
Bed movement						
In inlet	Good[1]	Good[1]	Good[1]	Good[1]	Good	Good
In bay	----------	Good	----------	Good	Very poor	Good
Cost[2]	$100,000 to $300,000	$400,000 to $500,000	$100,000 to $300,000	$300,000 to $400,000	$400,000 to $500,000	> $500,000

[1]Using tracer techniques.

[2]In 1977 dollars.

relatively low cost (about 20 to 60 percent of the cost of a complete model) of each of these models can lead to a desirable approach for specific information.

The uses of specific types of physical hydraulic models for inlet studies are summarized below.

a. Fixed-Bed, Undistorted-Scale, Sectional Model. This model may be used for investigations when little or no hydrographic information is available from the prototype. Although effective use of this model requires that bed forms and general inlet configurations be assumed before initiation of studies, the effects of these forms on the resulting hydraulics of the inlet can be obtained with a relatively high degree of confidence. Specifically, the fixed-bed, undistorted-scale, sectional model can be used to define the hydraulic characteristics of a proposed new inlet where prototype information cannot be obtained. The results from the model can then be used in a distorted-scale model to define the effects of the inlet on the ocean-inlet-bay system. The model can also be used to investigate the interaction of tidal flow and wind waves which may affect bed movement, flow through the inlet, and navigation conditions in the inlet.

b. Fixed-Bed, Undistorted-Scale, Complete Model. This model will provide the most accurate results on hydraulic conditions in the inlet-bay system; however, the costs are extremely high. Studies in this type of model for an inlet-bay complex have never been conducted at WES, since no study to date has sufficiently justified the high costs compared to costs for obtaining results by other models or other means; therefore, only estimates on the improvement of accuracy of results can be made.

c. Fixed-Bed, Distorted-Scale, Sectional Model. If a problem concerns the evaluation of effects of changes to an inlet on the inlet hydraulics or shoaling, this model can be effective. The major disadvantage is that the model does not provide specific information on the interaction with the bay; therefore, estimates of conditions at the boundaries of the model must be made.

d. Fixed-Bed, Distorted-Scale, Complete Model. This is the model most commonly used to investigate general hydraulic conditions in an inlet-bay system. The model can provide reasonably accurate data without excessive costs. The major limitations to the model are that for inlet or bay conditions where both wave refraction and diffraction are important, extreme care must be taken in selection of the model scales as true similitude for both wave refraction and diffraction cannot be achieved.

e. Movable-Bed, Distorted-Scale, Sectional Model. This model has the potential of being the most effective type of model to investigate shoaling and scouring trends within the inlet. Because of the methods required to conduct movable-bed studies, the capability to control the flow at both the bay and ocean ends of the inlet enhances the operation of the model (discussed later in this section).

f. Movable-Bed Distorted-Scale, Complete Model. This model is essentially as effective as the movable-bed sectional model for investigations of shoaling and scouring in the inlet, except that the sectional model is more adaptable to operational requirements. The model allows investigation of bed movement within the bay; however, techniques do not presently exist to allow investigations of shoaling and scouring trends from approximately the throat of the inlet oceanward at the same time as shoaling and scouring trends in the bay. Different model operating procedures and usually different movable-bed model materials are required for these two areas of investigation. Both movable-bed models require extensive prototype data collected over a period of several years to obtain an adequate verification of the model.

2. Planning for a Model Study.

The most important point concerning an effective model study is that the results can only be as accurate as the prototype data on which the model study was based. This requires that prototype information be available at critical times during the course of the model study. Unfortunately, the normal model study must be undertaken without this information, with resulting adverse effects on time and costs unless proper planning is maintained to obtain information during the study. The need for proper planning as well as the effect of prototype data input to a model study can be demonstrated by two modified critical path charts shown in Figures 7-1 and 7-2 for studies of tidal inlets. The times shown in the charts are only estimates which can vary considerably for specific inlet studies; however, the time frames are sufficiently accurate for demonstration.

In the example charts, the assumption is made that the study will be directed toward defining, in detail, conditions in or near the throat of the inlet and that definition of effects outside this area will be limited to gross tidal prism changes only. Specifically, the example model will be used to evaluate the effectiveness of plans to stabilize the navigation channel through the inlet, define the hydraulic conditions for existing or proposed conditions, evaluate the effectiveness of sand-bypassing systems, and define the effects of the proposed improvement works on the tidal prism in terms of total flow through the inlet. Similar charts can be prepared based on specific purposes of model studies.

The tasks represented by each block in Figures 7-1 and 7-2 are discussed below.

a. Block 1. This is the designated starting time based on a decision to conduct the model study. At this time, all preliminaries have been completed; the purpose and scope of the model study have been defined, and the need for the model investigation confirmed.

b. Block 2. Model studies of this type require both shelter space and associated plant equipment, such as tide generators, wave generators, movable-bed sounding systems, water level recorders, and velocity recorders.

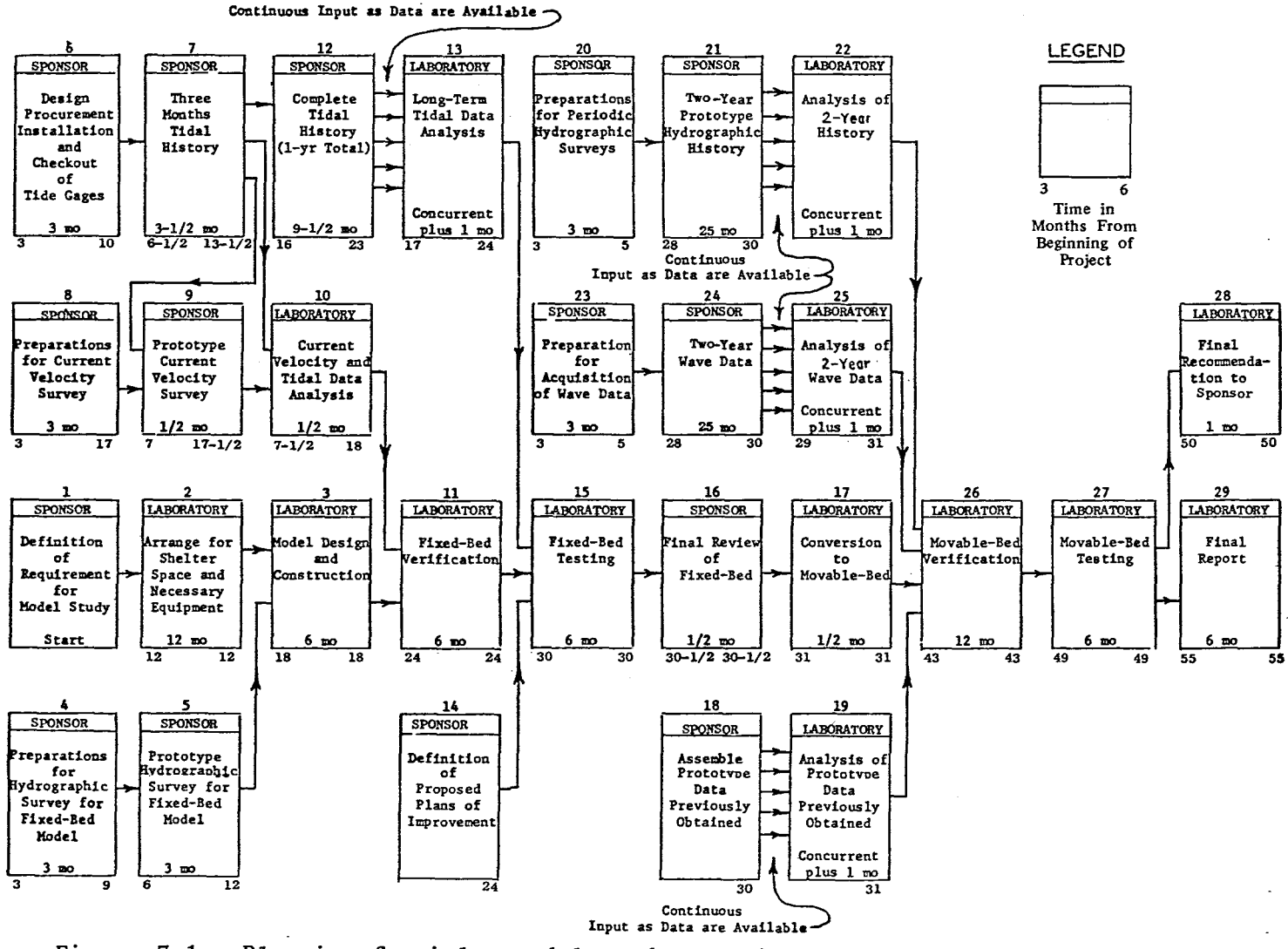

Figure 7-1. Planning for inlet model study assuming 2 years of prototype data.

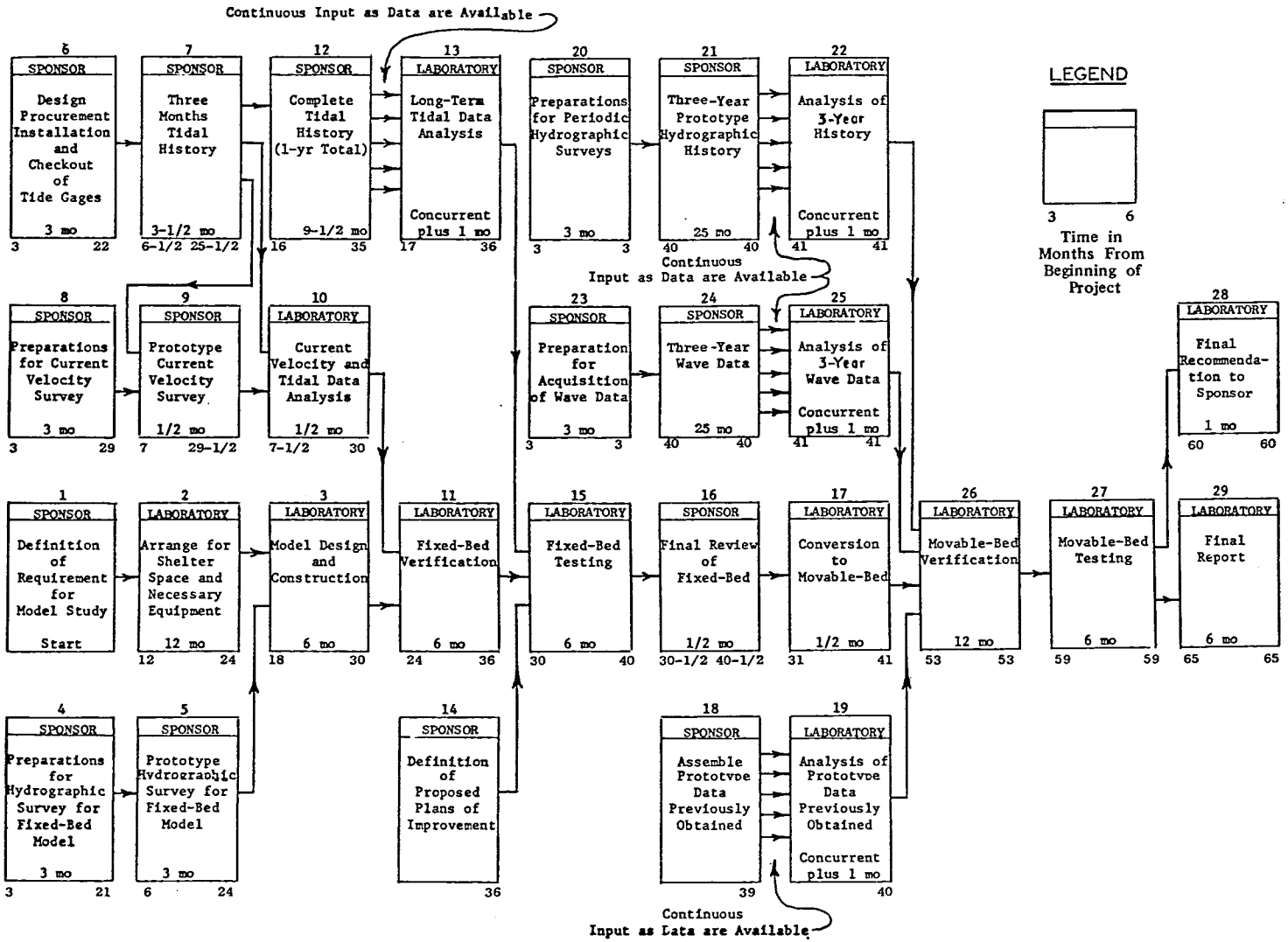

Figure 7-2. Planning for inlet model study assuming 3 years of prototype data.

Since the time required for procurement or construction of this equipment varies considerably (depending on workload, availability of plant funds, and availability of shelter space), an orderly procedure usually requires approximately 2 years leadtime (notification to the laboratory by the sponsor that a model study will be authorized); however, experience indicates that arrangements can be made in as short a time as 12 months. A longer leadtime increases the probability that proper space and equipment would be available at the desired time.

c. Block 3. This task requires the detailed design of all parts of the model (e.g., piping systems, pump locations, tide generator locations, model layout, anticipated future changes, control templates, etc.) and actual construction of the fixed-bed model.

d. Block 4. After determining the specific requirements of the model investigation, necessary hydrographic information for the model can be defined and arrangements made to obtain the data.

e. Block 5. This task requires obtaining and then providing the prototype hydrographic information to the laboratory. The final time estimate for this task should be noted to include the time necessary to prepare and transmit the information to the laboratory.

f. Blocks 6 and 8. As in the case of hydrographic survey requirements, after the study objectives have been established, accurate determination can be made of the tidal and current velocity requirements.

g. Block 7. Analysis of the hydraulic conditions for the inlets is dependent on knowledge of the long-term tidal conditions of the bay and ocean. Therefore, the tide gages should be in operation approximately 3 months (minimum) before conducting the current velocity survey to allow the velocity data to be evaluated properly. The time estimate for this task should include the time required for preparing and transmitting the information to the laboratory.

h. Block 9. This effort includes obtaining and transmitting current velocity data to the laboratory.

i. Block 10. The laboratory analyzes and prepares the tidal and velocity data for verification of the model.

j. Block 11. The laboratory adjusts the tide-generating mechanism, the model roughness, and possibly the size and shape of the part of the model which is beyond the limits of the area reproduced in detail to assure accurate reproduction of prototype tides and velocities.

k. Blocks 12 and 13. A 1-year history of tides is necessary to establish possible tide conditions for the inlet. If analysis of these data indicates that extreme conditions occur a small percentage of the time, limited or possibly no testing of such conditions would be scheduled. The studies are based on the assumption that hurricane-surge conditions will not be investigated.

l. Block 14. A definition of the scope and details of the proposed plans of improvement are required before initiation of the fixed-bed testing. Initial development of these plans is normally accomplished by the sponsor. The laboratory offers additional suggestions before testing is begun.

m. Block 15. The time and cost for fixed-bed testing are highly dependent on the number and extent of possible plans for improvement to be investigated.

n. Block 16. Close contact is maintained between the sponsor and laboratory during all aspects of the study, and all output data from the model are supplied by the laboratory to the sponsor; however, a meeting should be held after the scheduled fixed-bed testing is completed to assure that all laboratory and sponsor recommendations and plans have been considered and evaluated. This review will determine if all desired hydraulic data have been obtained and conversion of the model to a movable-bed, if required, could be initiated.

o. Block 17. Conversion of the model to a movable-bed model is completed.

p. Blocks 18 and 19. Before initiation of the verification of the movable-bed model, analysis of available field data is necessary to assure effective verification. Specifically, information on wave climate, littoral transport, prior hydrographic changes to the inlet, stability of the inlet, and any other information applicable to changes that have occurred at the inlet should be defined.

q. Blocks 20, 21, and 22. Planning, acquisition, and analysis of prototype hydrographic data are completed. Seasonal surveys and post-storm surveys are necessary.

r. Blocks 23, 24, and 25. Simulation of the forces acting on the inlet is also dependent on a long-term knowledge of the wave climate affecting the inlet. Concurrent with the hydrographic survey, a definition of wave conditions is necessary. Data following storms are important.

s. Block 26. Verification of the movable-bed model consists of a series of "trial-and-error" tests in the model to establish the combination of wave climate and tide conditions required for a reproduction of a known shoal and scour history in the prototype. This is accomplished by initially establishing the long-term distribution of wave energy approaching the inlet and reproducing the distribution in the model. A test is conducted with the wave and spring tide conditions with the movement of material documented. A comparison is made between the movement of material in the model and the prototype, and if the trends of the prototype are not reproduced, modifications to the wave or tidal conditions are made based on an analysis of the results. Although the magnitude of tidal flow may not duplicate the scaled prototype values, gross distribution of prototype flow patterns is maintained. Verification tests are

continued until shoaling and scouring histories of the prototype are reproduced in the model.

t. Block 27. Movable-bed tests repeating the fixed-bed testing will establish the effect of a plan on material movement. If necessary, additional tests are conducted until an effective plan of movement is defined. It may then be necessary to convert the model back to fixed-bed conditions to determine the hydraulic conditions for the best plan using the inlet hydrography predicted by the movable-bed tests.

u. Block 28. Test results are transmitted to and discussed with the sponsor as the results become available. When the final recommended plan is defined, this information is also immediately transmitted to the sponsor. At this time the sponsor is aware of all significant results from the investigation.

v. Block 29. A final report is published including all significant results of the investigation.

Figures 7-1 and 7-2 show that (depending on requirements imposed on the inlet study) the total time to complete the model study cannot be determined without considering the time to accomplish tasks by both the laboratory conducting the model study and the sponsoring organization (field office). Figure 7-1 shows that if the movable-bed verification is based on a 2-year (minimum) prototype history, assuming that a major change in hydrography has occurred, the only effort the sponsor must complete as scheduled without delaying the overall study is the review of the fixed-bed results. If the study is based on a 3-year prototype history, however, the prototype hydrographic survey becomes more critical to the overall schedule than the fixed-bed model testing (Fig. 7-2). If the laboratory completes specific tasks in the estimated times after start of the project without delays between tasks, the verification of the movable-bed model could not be efficiently initiated until the prototype hydrographic information is available and analysis completed. Because of these possible differences, proper advanced planning must be based on a full definition of prototype data available, prototype data required (with proper consideration of accuracy of the model results required), and extent of testing required in the model.

3. Physical Modeling of Tidal Inlets.

Because the fluid-flow problems associated with tidal inlet studies usually involve a large number of variables, many of the problems are not readily amenable to mathematical analysis. Therefore, recourse is often taken to the operation of physical hydraulic models to determine the significant kinematic and dynamic features of the prototype.

In any hydraulic model study, the physical phenomena observed in the model should represent those phenomena occurring in the prototype, so that the prototype action can be predicted by operating the model. A model is then, by definition, a device which is so related to a physical

system that observations on the model may be used to accurately predict the performance of the physical system.

a. Similitude. The general theory of model design is based on the fundamental principle that a functional relationship exists among all the variables associated with the system. Further the number of variables can be significantly reduced by forming a complete set of dimensionless variables for which a new function expressing the relationship between the dimensionless terms exists. If the model is designed so that each of the dimensionless terms of the complete set is the same in the model as in the prototype, then the nature of the unknown function is identical for the model and the prototype. If all these conditions are satisfied, the model is considered a "true" model which provides accurate information concerning the behavior of the prototype.

Although space limitations for the construction of the model may sometimes dictate that the model be distorted, a physical model can usually be operated with the same linear scale in all three dimensions (i.e., an undistorted-scale model). This dictates that geometric similarity exists, as the ratios of all homologous dimensions on the model and prototype are equal.

In addition to geometric similarity, a true undistorted-scale model requires that kinematic similarity and dynamic similarity also exist. Kinematic similarity exists when the ratios of all homologous velocities and accelerations are equal in the model and prototype. Dynamic similarity requires that the ratios of all homologous forces be the same in the model and prototype. Since force is related to the product of mass and acceleration, dynamic similarity implies the existence of kinematic similarity which, in turn, implies the existence of geometric similarity.

For an inlet model, the forces influencing the physical phenomena include pressure, gravity, viscosity, surface tension, and Coriolis (to a lesser extent). The Coriolis force has a significant effect on wind-driven and tide circulations and water surface elevations in large tidal estuaries, bays, and lakes; however, for a localized system such as a tidal inlet, Coriolis force is truly insignificant. Elasticity is negligible in either case.

Each force is related to the geometry and motion of the flow. In Newton's second law of motion, the inertial force, F_i, equivalent to the product of mass and acceleration, is equal to the sum of all external forces applied to a body. This inertial force can be considered as the vector sum of all the others, or

$$F_i = F_{pr} + F_g + F_\mu + F_{st} \quad , \tag{7-1}$$

where F_{pr}, F_g, F_μ, and F_{st} are the forces due to pressure, gravity, viscosity, and surface tension respectively. These forces usually suffice to describe hydraulic phenomena.

For dynamic similarity the ratio of the inertial force between model and prototype must be the same as the ratio of the individual force components between the model and prototype. The ratios of the inertial force to the other component forces must also be the same between model and prototype. These ratios have developed a reference to specific names, such as the ratio of the inertial force to the pressure force as

$$E_n = \frac{F_i}{F_{pr}} = \frac{p}{\rho V^2} \quad \text{(Euler No.)}$$

$$F_n = \frac{F_i}{F_g} = \frac{V}{(gL)^{1/2}} \quad \text{(Froude No.)} \tag{7-2}$$

$$R_n = \frac{F_i}{F_\mu} = \frac{VL\rho}{\mu} \quad \text{(Reynolds No.)}$$

and

$$W_n = \frac{F_i}{F_{st}} = \frac{\sigma}{\rho V^2 L} \quad \text{(Weber No.)} \ .$$

Since only three of these equations are independent, the Euler number will automatically be equal in the model and prototype if the other numbers are equal.

From the remaining three equations,

$$\left(\frac{V}{(gL)^{1/2}}\right)_r = \left(\frac{VL\rho}{\mu}\right)_r = \left(\frac{\sigma}{\rho V^2 L}\right)_r = 1 \ . \tag{7-3}$$

It can be demonstrated that no single model fluid will permit all of these equations to be satisfied at once; therefore, true dynamic and kinematic similarity apparently cannot be achieved between a model and the prototype.

However, one or more of the specific forces is often found to be negligible and the number of equations to be satisfied can be reduced accordingly. In fact, the phenomena in a particular instance often involve the effect of only one force ratio and the others are negligible.

The use of water as a model fluid is usually necessary in coastal engineering models. Surface tension, the least important term if the depths of the fluid are not excessively small, will have a negligible effect on the flow of water more than 0.25 foot deep, or on waves with lengths exceeding about 1.0 foot in the same water depth. By ensuring that the flow and waves exceed these limiting values, the effect of surface tension can be neglected.

When both viscous and gravity forces are important, as in open channel flow on mild slopes, the Froude and Reynolds numbers should both be

satisfied simultaneously. This requirement can only be met by choosing a special model fluid. Since water is the only practical model fluid, an approximate similarity requirement may be used, based on empirical relationships which include the major effects of frictional forces (such as Manning's equation). This approach is used in studying inlet problems. Another approach is to attempt to correct both model and prototype measurements for the forces due to friction during operation of the model by Froude law.

Since fairly high Reynolds numbers are usually associated with tidal flow through an inlet, the shear stresses are primarily determined by form drag. When Manning's formula is used in an undistorted-scale model, and assuming similarity for velocity,

$$V_r = \frac{L_r^{2/3}}{n_r} \quad \text{and} \quad n_r = L_r^{1/6} \ , \tag{7-4}$$

where n is Manning's roughness coefficient.

The use of Manning's formula as a similarity criterion requires that the flow be fully rough turbulence in both the model and the prototype. When a bulk Reynolds number defined as Vd/ν is greater than about 1,400 (where d is the depth of flow and ν is the kinematic viscosity), fully rough turbulence will normally exist.

A surface gravity wave is essentially a gravitational phenomenon; therefore, the controlling criterion of similitude is the Froude number, and waves may be represented correctly in undistorted-scale models.

Based on the Froude criterion of scaling, and considering an undistorted-scale, fixed-bed model, the geometric, kinematic, and dynamic scaling ratios may be expressed in terms of the model-prototype length ratio used for scaling, L_r, when the same fluid is used in the model and the prototype (see Table 7-2).

There are several physical interpretations that may be given the Froude number, but fundamentally it is the ratio of inertial to gravitational forces acting on a particle of fluid. It can be shown that this ratio reduces to $V/(gL)^{1/2}$, where V is a characteristic velocity, and L is a representative length. Here the velocity is taken to be a horizontal length divided by the time parameter. However, any representative velocity and any representative length can be used in the Froude number as long as dynamic similarity is maintained and corresponding regions are considered in the model and prototype. For an undistorted-scale model, the scaling ratios in Table 7-2 are appropriate; here the time and velocity ratios are equal to the square root of the linear scale ratios, where the horizontal and vertical linear scale ratios are identical. The Froude number, defined as $V/(gd)^{1/2}$, is related to the

Table 7-2. Froude criteria scaling relationships.

	Undistorted-scale model	Distorted-scale model
Geometric similarity		
Length	L_r	
(horizontal)		$(L_h)_r$
(vertical)		$(L_v)_r$
Area	L_r^2	
(horizontal)		$(L_h)_r^2$
(vertical)		$(L_h)_r(L_v)_r$
Volume	L_r^3	$(L_h)_r^2(L_v)_r$
Kinematic similarity		
Time	$L_r^{1/2}$	$(L_h)_r/(L_v)_r^{1/2}$
Velocity	$L_r^{1/2}$	$(L_v)_r^{1/2}$
Acceleration	1	1
Discharge	$L_r^{5/2}$	$(L_h)_r(L_v)_r^{3/2}$
Kinematic viscosity	$L_r^{3/2}$	$(L_v)_r^{3/2}$
Dynamic similarity		
Mass	L_r^3	$(L_h)_r^2(L_v)_r$
Force	L_r^3	
(horizontal)		$(L_h)_r^3$
(vertical)		$(L_h)_r^2(L_v)_r$
Dynamic viscosity	$L_r^{3/2}$	$(L_v)_r^{3/2}$
Surface tension	L_r^2	$(L_h)_r^2$
Pressure intensity	L_r	$(L_v)_r$
Impulse and momentum	$L_r^{7/2}$	$(L_h)_r^2(L_v)_r^{3/2}$
Energy and work	L_r^4	$(L_h)_r^2(L_v)_r^2$
Power	$L_r^{7/2}$	$(L_h)_r(L_v)_r^{5/2}$

vertical scale (depth) so that the velocity ratios are equal to the square root of the depth ratios; consequently, for a distorted-scale model the time ratios are equal to the horizontal length ratios divided by the vertical length ratio. Symbolically, for a distorted-scale model

$$V_r = (L_v)_r^{1/2} \quad \text{and} \quad T_r = \frac{(L_h)_r}{(L_v)_r^{1/2}} \tag{7-5}$$

which shows the significance of distortion. These and other pertinent ratios required for geometric, kinematic, and dynamic similarity are easily developed (see Table 7-2).

b. Model Design. After the purpose of the model study has been defined, the actual design of the model can proceed. The significant steps are: (1) acquisition of prototype data to assure model accuracy, (2) establishment of model limits, and (3) definition and acquisition of model appurtenances.

The importance of accurate prototype data cannot be overemphasized in model operation. The accuracy of the model is dependent on the use of proper field data. Although the similitude of fixed-bed, undistorted-scale models indicates that good approximation of bed-form losses can be derived in the model, assurance of accurate model results can only be achieved through a comparison of model and prototype results. To assure that the model is a geometric reproduction of the prototype, hydrographic and topographic surveys must include the inlet and pertinent ocean and bay approaches that influence the inlet. The complete model requires a detailed definition of the entire bay; whereas, the section model only requires definition of that part of the bay directly influencing the inlet. A critical need is topographic information for land flooding by the highest expected water levels, particularly when investigating storm surge conditions. Section III,2e of this report discusses the type and method of field data collection.

Because bed form plays an important role in boundary losses of an inlet, attention must be given to this feature. Although more research is needed on the effect of bed form on energy losses through an inlet, the present knowledge can guide the successful design of a physical model. With the physical characteristics of the prototype known and similitude as a guide, the required bed form of the model can be estimated.

The final proof of model effectiveness is a comparison of current velocities and water surface elevations in both the model and the prototype. The requirements for a particular inlet model can vary extensively; however, a limited number of critically placed tide gages and wave gages, along with carefully located velocity stations, can provide enough information for confidence in the model operation.

The appurtenances required for an effective model study include:

(a) a tide reproducing system for the ocean,

(b) a tide reproducing system for the bay if the bay is not completely modeled,

(c) wave generator or generators,

(d) tidal height measuring and recording system,

(e) velocity measuring and recording system,

(f) wave measuring and recording system, and

(g) photographic capabilities.

Each of these systems requires proper planning in designing the model as construction of the model depends on advanced knowledge of the specific requirements of each system.

c. Model Construction. The construction of the model requires the proper planning and sequencing of:

(1) Basic site preparation;

(2) installation of buried features (i.e., pipelines, required bases for instrumentation support systems, etc.);

(3) installation of control templates;

(4) installation of base material;

(5) placement of material (normally concrete) forming the model;

(6) finishing the model for the desired surface texture;

(7) fabrication and installation of tide-generating capabilities; and

(8) installation of wave generators, velocity recording systems, tide recording systems, wave recording systems, and photographic capabilities.

Among the details that must be planned in model construction are the various inlet changes to be evaluated during the model study. If the effects of dredging a feature are evaluated, the construction of the model should be based on this information. The templates prepared from detailed hydrographic and topographic maps to assure the model is a true representation of the prototype should be modified to include the deepest possible navigation channel, deposition basin, turning basin, etc. This would allow the study of these features in later stages of the model testing program. A second set of templates can then be installed in the molded model to allow features of lesser depth to be incorporated into the model.

Tests can then be conducted with the conditions of lesser depth in the model; when tests are completed, conversion of the model to evaluate a proposed change to the inlet can be easily accomplished.

4. Fixed-Bed, Undistorted-Scale Models.

For coastal studies not concerned with the movement of bed material, fixed-bed models can often be easily developed to provide kinematic and dynamic responses indicative of the prototype conditions. Specifically, fixed-bed models reveal information regarding velocities, discharges, flow patterns, water surface elevations, and energy losses between points in the prototype. In the superposition of surface gravity waves on the fixed-bed flow conditions, an undistorted-scale model ideally provides greater insight at less effort into the refraction and diffraction phenomena associated with the wave passing the underwater topography and around coastal features. Accordingly, the fixed-bed, undistorted-scale model can be effectively used for the analysis of kinematic and dynamic conditions associated with waves, current intensities and patterns, discharges, and forces existing along coasts and in inlets.

A fixed-bed model (although not its primary purpose) may also be useful in studying shoaling of entrance and interior inlet channels. Saltwater intrusion and the effects thereon of proposed changes in the physical or hydraulic regimes of the system can be effectively studied by fixed-bed models. The diffusion, dispersion, and the flushing of wastes discharged into inlets and the hydraulics of the inlet as related to the location and design of channels suitable for navigation can be expediently studied. Tidal flooding by hurricane surges or other unusual tidal phenomena can also be readily analyzed.

a. Model Verification. The verification of a fixed-bed, undistorted-scale model consists basically of conducting sufficient tests in the model to reproduce model boundary conditions (i.e., ocean tides, ocean waves, bay tides, and current velocities). The model data are then compared with prototype data for duplicate locations in the model and prototype to define the accuracy with which the model reproduces the prototype. If reproduction of the prototype is not achieved, the differences are evaluated for possible sources of error. Frequently, the differences are a result of either incorrect location of roughness in the model or improper magnitude of model roughness. If the comparison shows isolated stations to differ, the differences are usually caused by incorrect model results or erroneous prototype data collection. Repeating the model test will clearly indicate which of these causes produced the difference between the model and prototype information. If it is concluded that the model data were in error, then new model data can be quickly obtained.

Model verification can also include definition of the model operating characteristics required to achieve reproduction of shoaling patterns throughout the inlet. This consists of a trial-and-error operation until the model operating conditions required to reproduce known changes in prototype shoaling are developed.

b. Model Verification for Tidal Constituents. Installation and operation of an automated model data acquisition and control system (ADACS) will increase accuracy and reduce time required for verification of tidal inlet (or estuary) hydraulic models, either fixed-bed, undistorted-scale or fixed-bed, distorted-scale. The flexible sampling rate (usually about 200 samples per model tidal cycle for each gage) and digital recording of the data by an ADACS allow harmonic analysis and comparison with prototype data defining the coefficients and phase for each tidal constituent at various key locations within a tidal lagoon and at an open-ocean station removed from the immediate influence of the tidal inlet.

The ADACS can also rapidly and efficiently operate the model and collect required data. Its principal functions are to provide automated acquisition of wave and tide data in a format compatible for digital reduction and analysis, and automated control of model sensor calibration and of wave and tide generators.

The concept used is to force the model with the M_2 tidal constituent with the amplitude being correct at the ocean tide gage. A harmonic analysis is performed at all other gage locations corresponding to the prototype measurements, and the amplitude and phase (relative to the ocean tide gage) are calculated and compared with the prototype data. Investigation of the relative phases between various gages shows the areas that require either more or less model roughness. All phases for the M_2 constituent are expected to be verified within 1°. In most cases, tidal elevations are expected to be verified to within a maximum of ±0.1 foot (prototype) in both tidal height and mean tide level. After verification of the M_2 constituent, to ensure that the proper channel roughness is obtained, a progressive tide can be constructed; an attempt should then be made to verify a 14.765-day (synoptic period for M_2 and S_2 components) progressive tide (at U.S. east coast locations) using the prototype measurements of tidal velocities for the final verification data. If additional roughness is necessary, it will mostly be on mudflats or marsh areas. Computations have shown that energy transfer occurs from the M_2 constituent to higher order harmonics as the wave propagates from the ocean to the back of the estuary, and that this energy transfer is, at worst, the same order of magnitude in both the model and prototype.

The principal information required in the verification process is tidal elevation data. Various types of tidal height sensors are used; one particular type is a "bubbler system" or gage which measures small hydrostatic pressure changes associated with changes in model tidal elevations. The bubbler system consists of a high precision pressure transducer, a scani-valve device for sequencing input ports, and multiple pressure inputs. Wave gages can also be installed in the model but may not be essential for the verification process. Velocities of tidal currents may be measured with miniature Price-type current meters or with electromagnetic velocity meters. Electromagnetic current meters appear quite promising for future model use.

c. Model Tests. Tests in undistorted-scale, fixed-bed models can provide useful information on not only the hydrodynamics of an inlet, but the expected changes to the hydrodynamics due to changes in the inlet. An effective model test program should include initially a complete set of tests to define the conditions that exist in the model for hydrographic, topographic, and hydraulic conditions for which the model was verified. These data then form the base conditions to which all future tests can be compared to evaluate the effects of changes to the inlet.

The data obtained from the model for the base conditions should include (a) detailed current velocities at critical locations throughout the model for a complete tidal cycle, (b) detailed surface current patterns of the entire area of interest at incremental times throughout the tidal cycle, (c) detailed wave characteristics throughout the inlet for an array of expected prototype conditions, and (d) a complete documentation of tidal elevations throughout the area of interest. The evaluation of a particular proposed change to an inlet can then be accomplished by installing the proposed change in the model, duplicating the procedure followed in obtaining a base set of data, and comparing the results of each set of data.

5. Fixed-Bed, Distorted-Scale Models.

Tidal inlet models are frequently distorted for various reasons. Many tidal inlets are large and the flood and ebb tidal deltas are quite shallow, leading to large model energy attenuation and viscous friction scale effects on waves. These effects can be minimized through distortion and at the same time decrease model costs. Reproduction of the entire tidal estuary in the model is often desirable, since inclusion of the tidal estuary results in the flexibility to study the effects of proposed improvements on the tidal prism, tidal circulation, tidal flushing, and salinity of the estuary. Inclusion also results in the correct nonlinear energy transfer from various tidal constituents to higher order harmonics. Deletion of a major part of the estuary leaves reproduction of this phenomenon more uncertain, although its importance is not yet well established.

Distorted-scale models for use in the study of inlets have generally been universally accepted. The horizontal scale ratio is often dictated by the size of the facility in which the inlet is placed or the construction cost. The vertical scale ratio need not be larger than the ratio of model measurement accuracy to prototype measurement accuracy. The accuracy of laboratory measurements of water surface is generally on the order of 0.001 foot; the accuracy of prototype measurements varies with equipment and field conditions, but is generally within 0.1 foot. Thus, a vertical scale ratio, model-to-prototype, of 1:100 will fully utilize the capabilities of the model in simulating the prototype. Models of larger vertical scale are often used to simplify operational techniques and to assure model depths large enough that surface tension does not affect flow.

A second factor to be considered in the selection of scales is the "distortion." Distortion is the ratio of the horizontal scale to the

vertical scale, and its value relates the order all slopes of the prototype are steepened in the model. In the study of tidal inlets, particularly with movable-bed models, efforts are made to design models with distortion values of five or less. Otherwise, the slopes required in the movable-bed model for accurate reproduction of the prototype may be steeper than the angle of repose of the model material, thus creating a difficult scale effect to overcome. This point is introduced in this section because inlets are often modeled with both a fixed bed and a movable bed and with a distorted scale. Vertical scale ratios, model-to-prototype, are generally in the order of 1:40 to 1:100; horizontal scale ratios are generally in the order of 1:100 to 1:500.

Distorted-scale inlet models are frequently constructed for multiple purposes; e.g., an investigation of an inlet may be necessary where a jetty is to be installed. A prediction will be required of the effects of the jetty on tidal currents and water levels near the inlet and also the degree to which the jetty interrupts the littoral drift and affects deposition patterns near the inlet. In this case, a multipurpose model is needed. This model would first be built with a distorted-scale fixed-bed design and then adjusted and tested to determine the effects of the jetty on tidal heights and currents. A segment of the fixed part of the model surface would then be carefully removed and replaced with a movable material to evaluate the effects of the jetty on the littoral drift.

Model verification and testing in a distorted-scale, fixed-bed model follow essentially the same procedures discussed for an undistorted-scale, fixed-bed model. However, because of distortion effects the transference equations from the model to a prototype situation are, in general, completely different.

6. Movable-Bed Models.

a. Theoretical Aspects of Movable-Bed Material Modeling. The accepted practice at many hydraulic laboratories experienced in the art of movable-bed modeling is to construct the model to a manageable size based on space limitations and instrumentation ability, and to use a readily available material for construction (usually sand) which constitutes a model scale distortion. Next, the empirical process of verifying the model to reproduce prototype bed forms such as scour and deposition has led to the distortion of a second parameter. This is usually accomplished in the model by altering the wave climate, increasing or decreasing tidal flow, or by changing the time scale from that resulting from the hydrodynamic scaling relations to an empirically selected one which reproduces the sedimentology (referred to as the sedimentological time scale). These are empirical solutions based on the clever application of scale modeling and the experience of the researcher; however, the mechanism of most sedimentation phenomena is still not well understood. Several investigators have attempted to derive formal scaling laws resulting in many varying modeling formulas from which to choose, and, according to Kamphuis (1975), owing to the variety and magnitude of scale effects, modeling coastal movable-bed material continues to be an art rather than a science.

The movement of loose bed material is governed by the inertial forces of the particles and of the water against them, by the weight of the particles, and by the viscous forces acting between the water and the particles. Three physical laws have evolved from an analysis of these forces: Newton's law of inertia, the law of gravitation, and the viscous friction law of Newtonian fluids. These laws have provided two well-known dimensionless terms which must be equated between the model and the prototype for kinematic and dynamic similarity to prevail; i.e., the Reynolds number and the Froude number,

$$R_n = \frac{Vd}{\nu} \tag{7-6}$$

and

$$F_n = \frac{V}{(gd)^{1/2}} , \tag{7-7}$$

where the symbols have been previously defined.

The simultaneous conformation of the model and the prototype to both the Reynolds number and Froude number yields the familiar problem that the length-scale factor becomes a function of the scale factor of the kinematic viscosity. This determines that no readily available fluid possesses the kinematic viscosity to make a useful model fluid. Schuring (1977) reasons that, since the same fluid for model and prototype requires less than perfect similarity but probably must be used, design requirements can be relaxed if the inertial forces of the sediment are much smaller than the rest of the forces and therefore can be neglected. Then, Newton's law of inertia must only be applied to the fluid. A further simplification, without loss of generality, is achieved by restricting the law of gravitation to the weight difference of water and sediment. With these two modifications, a qualified Froude number evolves often referred to as a densimetric Froude number), and the length-scale factor is freed from its dependence on kinematic viscosity;

$$F_* = \frac{V}{\left[\left(\rho_s/\rho_w - 1\right)gd\right]^{1/2}} . \tag{7-8}$$

The penalty for this simplification is a restriction of the particles to a state of rolling or sliding with small or no inertial forces acting upon them. The model becomes invalid when the particles begin to leave the bed and are carried upward, such as in the surf zone or in relatively shallow water affected by surface gravity waves. Very good correlation between variables was achieved in flume experiments with unidirectional flow (Schuring, 1977).

A different approach, advanced by Gessler (1971), assumes that both the prototype sediment and the material used as model sediment are given, and the model geometric scales are determined to fit the requirements of these materials. In this approach, supplemental information should be used in the form of the Shields parameter regarding the critical tractive

force necessary to produce incipient motion. However, model scales based on the principles of unidirectional motion may not be strictly applicable to the case of oscillatory wave motion, but a first approximation is probably permissible. By setting a lower limit to the model Reynolds number and computing the prototype Reynolds number, the ratio of the prototype-to-model Reynolds number will determine the scale of the characteristic length used in the vertical direction of the model. In this procedure, it is assumed that the ratio of model-to-prototype velocity is a function only of the depth ratio, as determined by the Froude law.

If the model sediment material has not been selected beforehand, a revised approach can be developed (Gessler, 1971). To have similarity in incipient motion and bedload transport, the bed mobility in the model and prototype should be the same at homologous points. This mobility is determined by the ratio of the actual Shields parameter to the critical Shields parameter. The reason for this modification in approach is that the critical Shields parameter depends somewhat on the grain Reynolds number for values below about 150. For ordinary model materials (fine-grained sands), the grain Reynolds number is on the order of 5 to 10. The Shields diagram is poorly verified in this range, so the grain Reynolds number should not be smaller than about 15. This can be achieved by using a coarser bed material in the model than in the prototype but one that is less dense. The Shields parameter is

$$\tau_* = \frac{\gamma_w dS}{(\gamma_s - \gamma_w)D_s} , \qquad (7\text{-}9)$$

where S is the channel slope and D_s the particle size. By using this definition and evaluating the ratio of the prototype-to-model Shields parameters, a generalized criterion will evolve which can be solved for the specific weight (submerged) of the bed material to be used in the model. (The reason for using a lightweight material refers to the idea that the grain size is relatively too large in the model.) The final selection of the model material will depend on the materials available; however, a slight adjustment in the desired grain size may be necessary.

The analyses of Gessler (1971) are applicable only to unidirectional flow at one specific discharge; this means that highly unsteady flow processes like surface gravity waves cannot adequately be modeled by this process. Changes in discharge require that the time scale of the discharges be modeled according to the time scale associated with the sedimentation processes to obtain similarity in bed-forming processes. The considerable discrepancy between the hydrodynamic and sedimentological time scales means that the sedimentation processes are advancing too rapidly in the model. Gessler concludes that no matter how carefully the design is done, it remains absolutely essential for distorted-scale as well as undistorted-scale models to be verified against field data.

When studying problems of scour and deposition, it becomes necessary to add the critical shear stress and sublayer criteria to the gravity and frictional criteria, as developed by Graf (1971). Introducing the empirical relationship between the bed particle diameter and Manning's n value produces:

$$(d_r)^{1/6} = n_r = (R)_r^{2/3} \left(\frac{1}{L_{h_r}}\right)^{1/2} \qquad (7\text{-}10)$$

where d is the bed particle diameter and R the hydraulic radius. When model and prototype fluids are identical, four independent variables are found, and three equations provide a solution. The problem is determined if one of the four parameters is chosen, and the remaining three variables are found from the equation solutions. A distorted-scale model was assumed in this analysis. Various researchers have stated that some model laws can be relaxed with little harm to the overall investigation. Einstein (1954) suggested that the friction criterion, the Froude criterion, or the sublayer criterion might absorb further distortions. Under certain circumstances, small deviations from the exact similarity may be allowed, making it possible to arbitrarily select more than one single variable.

From the application to strictly coastal sediment modeling problems, Migniot, Orgeron, and Biesel (1975) have stated that, since all of the similitude conditions involved cannot be satisfied, the model scales, the material size and density, and the current exaggeration cannot be determined by straightforward computations but must be chosen to obtain the most favorable balance between all relevant phenomena. In many respects, this is more an art than a science, and a feeling of the problem, previous experience, and a perspective of the relative importance of each factor is of paramount value. The sedimentological time scale can be derived from general transport formulas, and when sand is simulated with a lightweight material such as plastic with a density of 1.4, the sedimentological time scale will be in the range of 1:1,000; this means that a year will correspond to some 8 hours of model time. Although it is disquieting to note that so much empirism prevails in the design of coastal movable-bed models, the model is only fit for predictive use when it has successfully reproduced past evolution. While the various similitude conditions may not all be satisfied, the conditions do not differ too much from each other, so fairly satisfactory compromises can usually be found. For instance, model material density required to satisfy these various prototype conditions may typically vary from 1.3 to 1.6, while size exaggeration may vary from 1.0 to 1.7.

The movable-bed coastal model by Kamphuis (1975) is a wave model incorporating coupled wave motion and sediment motion relationships which have been determined experimentally. The unidirectional flow phase is then added to the basic wave model and adjusted to yield correct results for different situations. This is a basically different philosophy from Le Mehaute (1970) who assumed that a coastal movable-bed model is a unidirectional flow model modified by waves. The difference in scale laws is quite evident when the results of their methods are compared.

According to Kamphuis (1975), the movable-bed phase of the model study is subjected to four relaxed basic scaling criteria: (a) The particle Reynolds number, (b) the densimetric Froude number, (c) the relative density, and (d) the relative length-scale relating water motion to sediment size. Ideally, all of these basic scaling criteria must be satisfied simultaneously, but this is impossible in practice. As more of these criteria are ignored, the model will perform successively less like the prototype, and scale effects (nonsimilarity between model and prototype) increase. Only a lightweight material can be used to keep the model and prototype particle Reynolds numbers identical. Any deviation from unity is rather small (in all cases) and is not considered to limit the model seriously. Similarity of the densimetric Froude number is considered to be the most important of the four modeling criteria. If the model densimetric Froude number is less than some critical value and the prototype number is greater than this critical value, the model is useless. The model and prototype densimetric Froude numbers should be equal, or incorrect scaling will result in considerable distortion of the sediment motion parameters with the exaggerated time scales for sediment motion, and the model will take longer to move the material than it theoretically should. This means that sediment motion will start later in the model (in shallower water), but in the area where material moves freely, the nonsimilarity of the densimetric Froude numbers will manifest itself in adjustment of the time scale for sediment motion. The time scale also varies with depth, and moreover, if initial motion and depositional patterns are important, it is necessary to model the densimetric Froude number correctly.

The nonsimilarity of the model and prototype ratios of sediment particle density to water density affects the process in two distinct ways. The acceleration of the particle is changed and the particle becomes relatively too heavy when no longer submerged. For a lightweight material, the individual particles are relatively heavier in the surf zone than if sand were used. Therefore, the beach material has a tendency to pile up immediately past the surf zone, and the particles will remain in this location because they become relatively heavier when not submerged. This results in a highly distorted version of sediment transport in the surf zone. It is very difficult to duplicate prototype conditions in the littoral zone using lightweight materials.

Coastal movable-bed models suffer from various scale effects when the particle sizes are not scaled down geometrically. Since this is the case for most models, the prediction of bed morphology time scales is virtually impossible. Thus, verification using historical survey data remains a necessary step. Because of the variety of scale effects, coastal movable-bed modeling continues to be as much an art as an exact science.

b. Prototype Data Requirements. Perhaps the most important aspect of the design phase of a movable-bed model study is to assure the adequacy of the prototype data. The model is constructed to conform to prototype surveys; adjustment of the model to accurately reproduce prototype hydraulics or sedimentation patterns is based on prototype measurements.

Any errors or insufficiencies in prototype information will result in inadequate and incorrect performance of the model.

Prototype information required for a movable-bed model study includes inlet geometry and sediment properties, bar configuration and sediment properties, adjacent beach configuration and sediment properties, bay geometry, wave measurements, littoral drift estimates, water surface time histories, and concurrent tidal currents in the ocean, inlet, and bay. Wind observations are also required to determine the resulting wind-driven setup or setdown of the water surface. If evaporation or precipitation appears to be important, or if freshwater inflows constitute a significant part of the flow through the inlet, these should also be observed. The occurrence of storms of low-return frequency should be noted in the history of the inlet, since large volumes of sand can be displaced during these activities. Hydrographic and wave observations should also be made frequently enough to detect seasonal and yearly fluctuations.

A longer data collection period is needed for a movable-bed study than for a fixed-bed model. The period length also varies with the data type; e.g., longer term wave data are needed than tide level and current data to calibrate a movable-bed model.

Prototype observations for several consecutive years before the model study will allow an evaluation of both short- and long-term tendencies of the inlet and the selection of a typical period on which to base the model verification. A 3-year documentation period is probably the minimum length, since major trends cannot usually be detected in shorter time periods.

If these data are not available, a program to collect sufficient information may have to be initiated before beginning the model study. Although such action at times may seem to unreasonably delay the model study, experience has shown the impracticality of attempting model studies without adequate prototype information.

The construction of a movable-bed model is usually straightforward. The charts containing the inlet hydrographic surveys are contoured, and the contours are transferred to a network of templates. The templates are suspended and the modeling material is carefully placed between them so that the templates just touch the surface. The templates are removed before the tests begin.

c. Model Verification. The verification phase of the model study is perhaps the most important. A well-accomplished verification will minimize or eliminate the effects of small errors in construction, and will allow the evaluation of the effects of poorly understood variables on the inlet system during the testing phase.

Verification requires the adjustment of model boundary conditions to re-create or correct conditions that were altered in the scaling process. Sedimentation verification is based on prototype observations and is accomplished by selecting an appropriate model sediment and developing

the necessary model operating technique to reproduce the observed scour and fill patterns. Thus, the accuracy and adequacy of prototype data are very important.

Verification of a movable-bed model is, theoretically, more difficult than for a fixed-bed model. The purpose of a movable-bed model is to simulate the evolution of the inlet bathymetry. This evolution takes place in response to many factors, but primarily to the sediment washed from adjacent beaches by wave action, to erosion of the inlet channel by tidal currents, and to trapment of material at the bars on the ocean and bay sides of the inlet. These same factors must be included in the model to simulate degree as well as type of bathymetry evolution.

Since a movable-bed model simulates shoaling and scouring patterns in and near the inlet, the requirement that the model also simulate the basic hydraulic quantities (tidal heights, tidal phases, velocities, etc.) is somewhat relaxed. In practice, and contrary to the above discussion, the verification of a movable-bed model is a little easier than for a fixed-bed model, since the experimenter has more variables available with which to work to achieve the desired verification.

The validity of tests of proposed improvement plans in a movable-bed model is based on the following premise: If model reproduction of the prototype forces known to affect movement and deposition of sediments (tides, tidal currents, waves, etc.) produces changes in model bed configuration similar to those observed in the prototype under similar conditions, then the effects of a proposed improvement plan on the movement and deposition of sediments will be substantially the same in both model and prototype.

Trends and magnitudes of prototype bed movement under existing conditions are determined primarily through detailed comparison of two or more periodic prototype surveys of the area under study. The time between the earliest and latest surveys used in this comparison becomes the verification period, and the movable-bed part of the model is molded to conform to the prototype survey at the beginning of the verification period. The model is then operated under conditions that existed in the prototype during the verification period until model bed configurations throughout the problem area are in conformance with those shown by the prototype survey at the end of the period. Model bed movement is then considered to be verified, or in proper adjustment, if changes in the model bed configurations during the verification period agree reasonably well with those that occurred in the prototype during the corresponding period. However, when a model is operated in this fashion, basic similitude rules are ignored and the model does not reproduce prototype forces. Only the sediment motion at a particular point during a particular time period is being modeled. Any major changes in hydrography may introduce errors into the results.

One very important reason for the verification of a movable-bed model is the establishment of the time scale with respect to bed movement. The

model-to-prototype time scale for bed movement cannot be computed from the linear scale relations because the interrelation of the various prototype forces affecting movement and deposition of sediments is too complicated for accurate definition, and consequently is much too intricate to permit establishment of mathematical scale relations for each component of force. The model-to-prototype time scale for bed movement is therefore determined empirically during the model verification; i.e., the actual time required for the model to reproduce certain changes that occurred in a given period of time in the prototype is used to determine the model time scale for bed movement.

d. Model Tests. The testing phase is the fruition of the efforts expended in the development of the model study, and is perhaps the easiest of all phases to accomplish. The model has been carefully designed and built based on measurements obtained from the prototype. The model has performed similarly to the prototype by responding to events to which it was subjected during verification in the same manner the prototype was observed to respond when similar events occurred in its history. The model may now be justifiably expected to respond as the prototype would respond to an event or sequence of events which has not yet occurred to the prototype at the particular point being investigated, for the same hydrography and operating conditions. This response of the model is termed the "predictive capability" of the model, since the behavior of the prototype under similar conditions can be inferred from that response.

The predictive capability of the model is quite important, but this capability has its limitations in time and in the relative magnitude of the events used in the testing program. The time limitation is imposed since many natural events (winds, waves, etc.) are random in nature and thus impart a probablistic pattern to the behavior of the prototype inlet which cannot be described or treated by the deterministic means involved in modeling. As the duration of the model prediction period is increased, this probabilistic part grows, and at a distant point in time the predictive capability of the model becomes questionable. Therefore, long-term shoal and scour projections with the model is undesirable unless long-term data are available for model verification. Attempts to change the values of variables by large amounts may also lead to a breakdown of the predictive capability of the model since the variables may exert a nonlinear effect on the behavior of the model inlet. For instance, the use of very high and steep storm-type waves in a model test may give misleading results unless assurance was made during verification that the model responds properly to waves of this type.

A model test series always involves at least two separate tests. The first test is a "base" test, which studies the existing inlet and provides a basis for comparison with later tests that have alterations to the inlet. The next test or tests in the series is the "plan" test, so called because the plan or plans for improving or stabilizing the inlet are installed in the model and tested. The plan tests are always conducted with model conditions identical to those of the base test. This test procedure allows straightforward interpretation of the test

results, as differences in results are attributable to the plan under investigation although some differences may occur because similitude criteria have not been completely satisfied.

The predictive capabilities of fixed-bed, distorted-scale models concerning the hydraulics of inlets are quite good where similitude criteria are satisfied. Accuracies of the order of a few tenths of a prototype foot can be expected for water surface elevations and within about 20 percent for current velocities. The predictive capabilities of movable-bed, distorted-scale models discussed above, concerning the depositional character of inlets, are not as reliable as for the fixed-bed hydraulics. Many more variables and opportunities for the introduction of errors and scale effects are present with movable-bed models. However, accuracies within the range of normal seasonal fluctuations are possible.

7. Postconstruction Verification.

The results of model-prototype confirmation studies are valuable to both field and laboratory engineers. Such studies provide the field engineer a measure of the degree of reliance that can be placed on model predictions, and thus a better basis for deciding whether or not to request model studies for similar or related problems. To the laboratory engineer, the results of confirmation studies may bring out certain significant discrepancies in model predictions and thus provide a sound basis for evaluating the reasons as well as serving as a guide in improving model techniques and procedures as required to increase the accuracy of model predictions in future studies.

Confirmation studies require followup studies in the field to determine the degree of accuracy with which predictions obtained from either physical or mathematical model, relative to the effects of a given improvement plan, are borne out after the plan is constructed in nature. Followup studies are not carried out after each model study in which an improvement plan was developed that was subsequently constructed in nature. Two principal reasons for this are: (a) If the plan developed and constructed resolves the problem satisfactorily, the field engineers then turn to other problems and are reluctant to expend time and funds on followup studies of an area that is no longer critical; (b) plans developed in a model study are often modified during construction in the field because of unexpected foundation conditions, fiscal limitations, or other reasons so that a direct comparison between model predictions and prototype performance cannot be made.

8. Examples of Model Studies Conducted.

The inlet model studies which have been performed by WES fall into one of four distinct catagories (fixed-bed, undistorted-scale; fixed-bed, distorted-scale; movable-bed, distorted-scale; and a combination of fixed- and movable-bed, distorted-scale). To show the applicability of these

distinctions, four inlet studies have been selected as examples which conform to the requirements of the unique situation associated with each inlet. Frequently, the inlet to be investigated is a component of a much larger bay or estuary model and therefore is probably distorted in scale. In other situations, the inlet may not presently exist as a prototype or may not be allied with an existing model; the opportunity then occurs for construction of an undistorted-scale model. The scales of movable-bed models are, in general, distorted.

The Shrewsbury Inlet model was selected as typical of fixed-bed, undistorted-scale models. This model study required an investigation of hydraulic phenomena in the vicinity of a proposed new inlet; therefore, the fixed-bed criterion prevailed. The size of the area to be reproduced permitted model construction to an undistorted scale.

A representative example of a fixed-bed, distorted-scale inlet model was the study of the Galveston Bay entrance. Hydraulic characteristics were required in this study to determine discharge coefficients to verify the results of surge routings by analytical means. Steady-state flows were established in the existing, comprehensive model of the Houston Ship Channel.

The Fire Island Inlet model study is a typical case where the primary problem was littoral drift trapped in the inlet; thus, sand movement along the beaches had to be simulated in the model. A distorted-scale, fixed-bed model was first constructed and all proposed alternatives were tested to determine their effects on hydraulic conditions in the inlet. After completion of the hydraulic tests, the problem area of the model was converted to a movable bed molded of sand.

Other problems occurred at Galveston Bay and it became necessary to study shoaling of the entrance channel. A movable-bed, distorted-scale model was appropriate for this study, but an analysis of the forces available to transport sediment indicated the movable bed should be molded of crushed coal. This study demonstrated the practicality of using material other than sand as the transport medium when the scaled forces involved dictated a size and density relationship as one which had to be of a manufactured variety. In this case, coal crushed to a desired size was appropriate.

a. New Inlet Construction and the Effects on Shoaling, Navigation and Water Quality--Shrewsbury Inlet, New Jersey.

(1) Project. Construction of a small boat channel across Sandy Hook Peninsula to connect the Atlantic Ocean with Sandy Hook Bay.

(2) References. McNair and Hill (1972); Section III,6,h of this report.

(3) Laboratory. WES.

(4) Test Period. January to December 1969.

(5) Problems. A new small boat channel across Sandy Hook Peninsula was needed to shorten the distance boats must traverse from the Shrewsbury River and Navesink River region to the Atlantic Ocean. Serious questions arose concerning the effect of this new inlet construction on water surface elevations at the Highlands shoreline during normal tides or during hurricane surges, current velocities and flow patterns, the influx of pollution into Sandy Hook Bay from sources in Raritan Bay and Upper New York Bay, and the transmission of wave energy through the inlet.

(6) Purpose of Model Study. The model study was conducted to determine the effects of the inlet on (a) water quality in Sandy Hook Bay and the Shrewsbury and Navesink Rivers from the viewpoints of public health, recreation, and fish and wildlife; (b) flooding within the areas as a result of normal tides and hurricane surges; (c) recreational boating and commercial navigation; (d) general shoaling characteristics and maintenance requirements in the inlet channel; (e) the optimum location and length of jetties at the ocean end of the proposed inlet; and (f) transmission of wave energy through the inlet into Sandy Hook Bay. Because of the complicated phenomena to be investigated, an existing comprehensive model of the New York Harbor area was used to study the effects of the inlet on water quality. Since many of these phenomena are in line with estuarine modeling procedures, testing in the New York Harbor model is discussed in Section III,b,h. Only parts of the study concerning the new inlet model are discussed here.

(7) The Model. A location map in Figure 7-3 shows part of the region reproduced by the New York Harbor model; the area reconstructed for the tests of the proposed new inlet (shown in Fig. 7-4), was a 1:100-scale, undistorted, fixed-bed model of the inlet and adjacent parts of the ocean and Sandy Hook Bay. This model was used to provide calibration data for the various inlet plans constructed in the New York Harbor model, to study flow patterns and velocity distribution for the various channel alinements and jetty locations, and to define the amount of wave energy reaching the Highlands Marina area from storm waves generated in the Atlantic Ocean and propagating through the inlet. Details of the new inlet model are shown in Figure 7-5.

Four plans were tested in the model. Plan 1 involved a channel with a bottom width of 200 feet, beginning at the -17.2-foot depth MSL in the Atlantic Ocean and continuing at that depth to the approximate centerline of Sandy Hook Peninsula; a 1 on 20 transition slope of the bottom to a depth of -11.2 feet MSL; and a bottom elevation of -11.2 feet MSL until the inlet channel intersected the existing Federal navigation channel from Sandy Hook Bay up Shrewsbury River. The channel sides had transition slopes of 1 on 3. The ocean end of the channel was flanked on each side by protection jetties, each about 600 feet long. The width and depth of the plan 2 inlet were the same as in plan 1; however, the alinement of the bay part of the plan 2 channel was straight from the ocean to the existing Shrewsbury River channel. The alinement of the plan 3 inlet was identical to plan 1; however, the depth of the plan 3

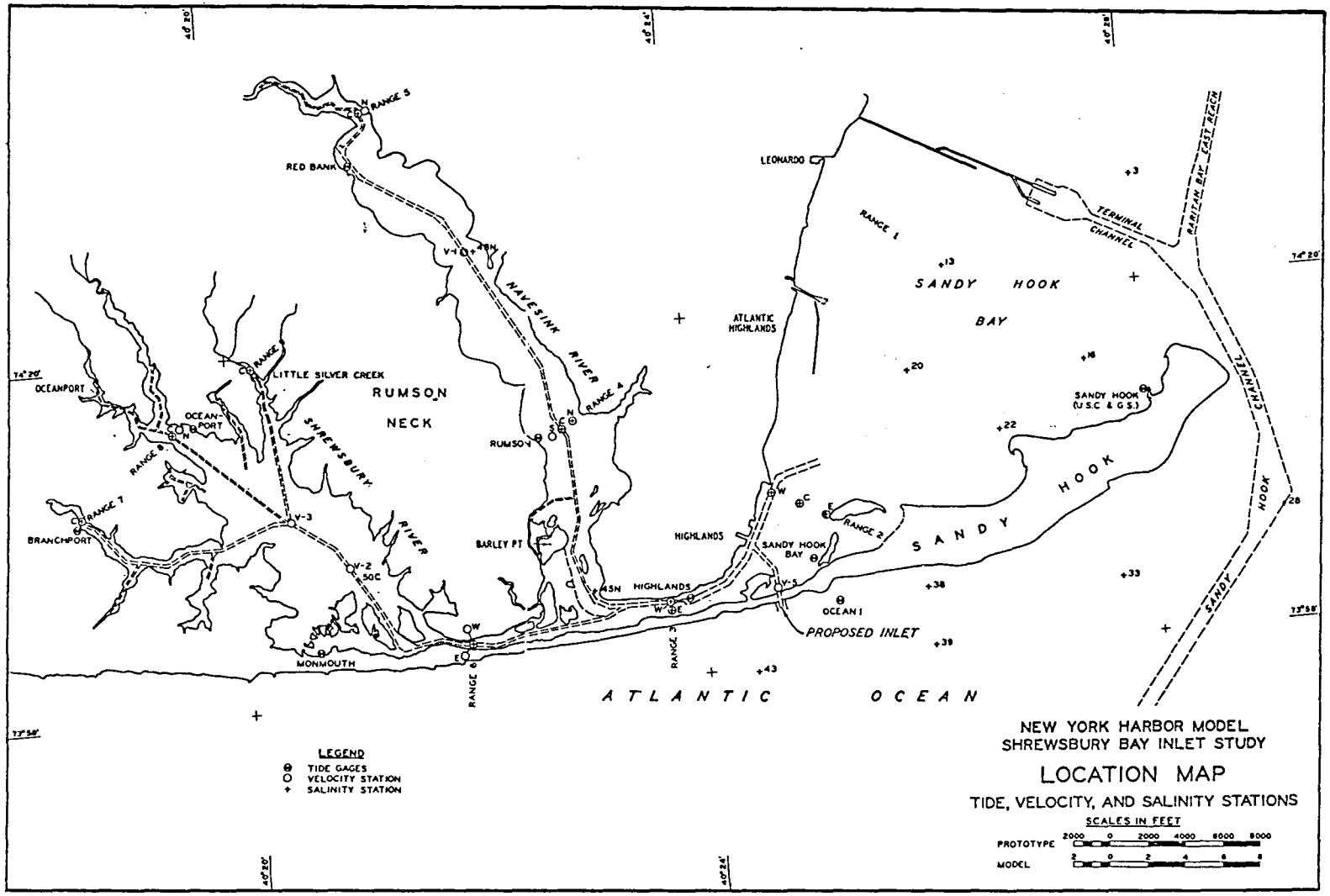

Figure 7-3. New York Harbor model limits.

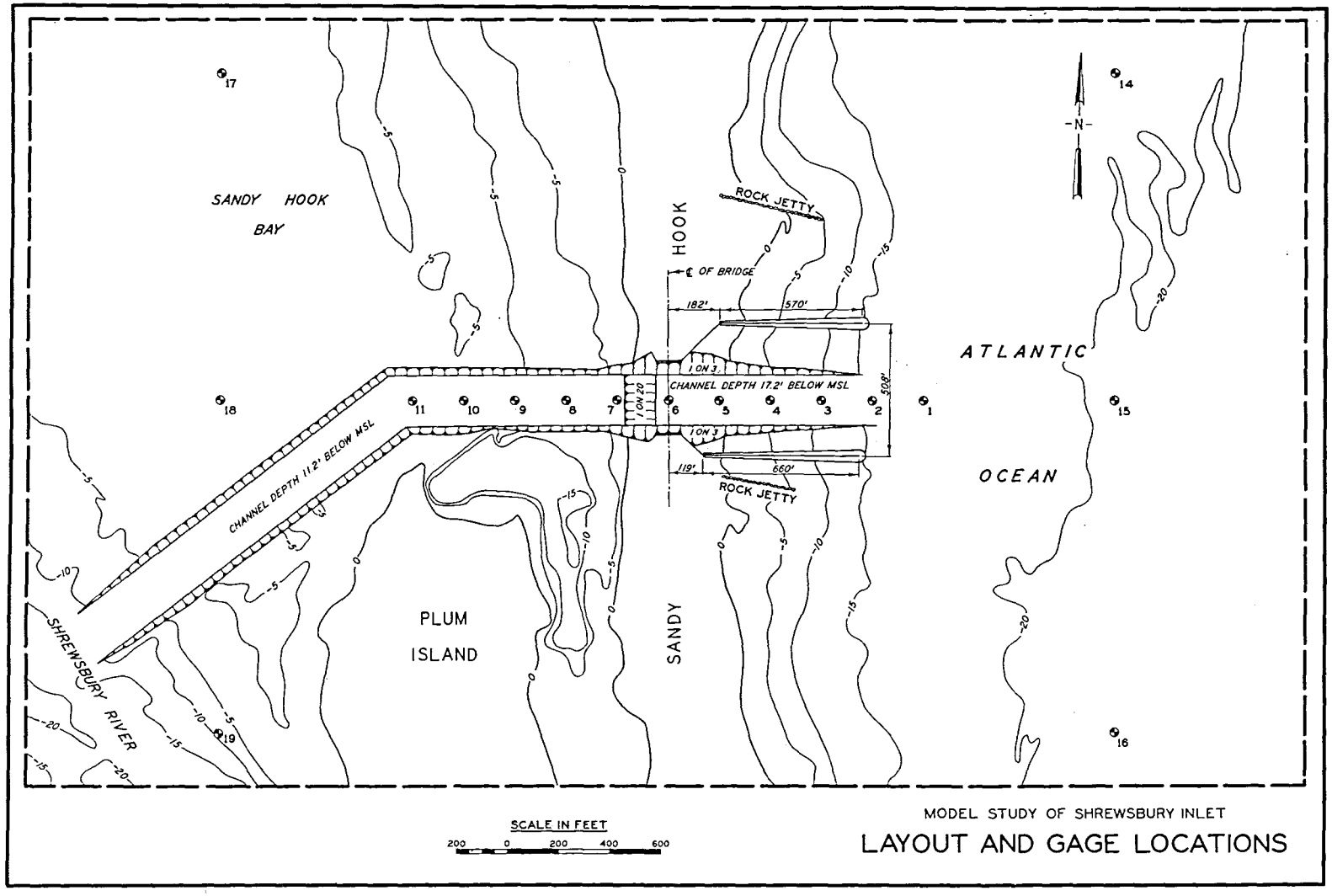

Figure 7-4. Shrewsbury Inlet and adjacent parts of Sandy Hook Bay.

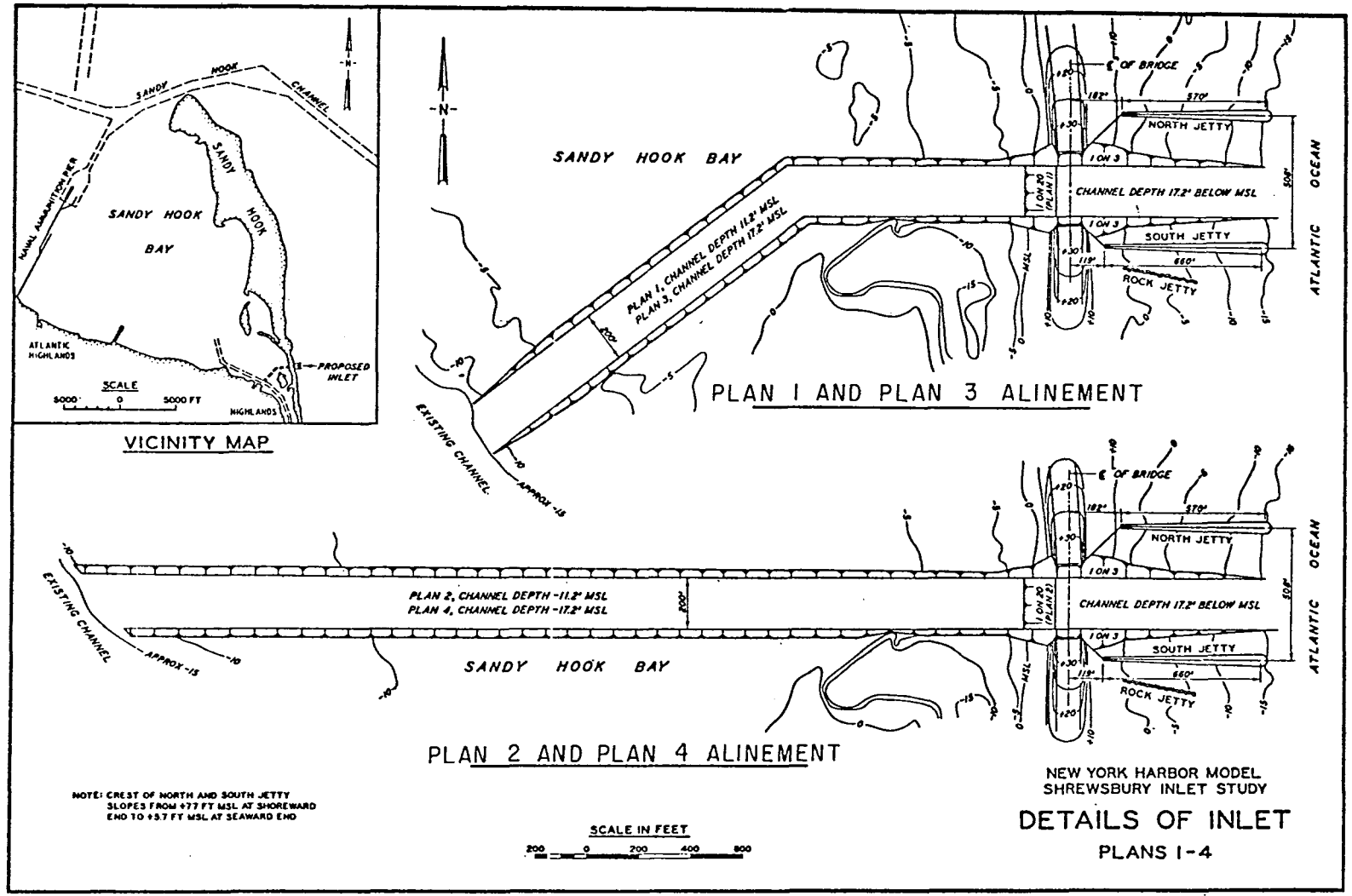

Figure 7-5. Details of plans of Shrewsbury Inlet physical model.

channel was -17.2 feet MSL for its entire length. The depth of the plan 4 inlet was also -17.2 feet MSL for its entire length, and the alinement was identical to that of plan 2.

(8) Test Procedures. The New York Harbor model is an estuarine model operated with saltwater. The new model of the proposed inlet was operated with freshwater because the required information was independent of salinity effects.

The plan 1 inlet (Fig. 7-5) described in the authorizing document, was first modeled to an undistorted scale of 1:100, and steady-state tests were made for both flood and ebb flows over the full range of head differentials and water surface elevations to be expected during later tests. From these test results, the discharge through the inlet as a function of head differential and water surface elevation was determined, and these data provided a basis for calibration of the inlet. The plan 1 inlet was then constructed in the distorted-scale New York Harbor model, and the calibration data described above were used to adjust the hydraulic resistance of the inlet so that both flood and ebb discharges were reproduced accurately over the full range of head differentials and water surface elevations to be encountered during actual tests.

Tests were conducted in the New York Harbor model to determine the effects of the plan 1 inlet on normal tides, tidal current directions and velocities, salinities, and the dispersion of dye tracers from simulated pollution sources in Raritan Bay, Upper New York Bay, and the Shrewsbury and Navesink Rivers (Fig. 7-5). The test results suggested that plan 1 should be modified in the interest of improving flow conditions at the bay end of the inlet, and possibly in improving shoaling characteristics. Consequently, plans 2, 3, and 4 were devised. Each plan was calibrated in the undistorted-scale model of the new inlet and then reproduced in the New York Harbor model. All four plans were subjected to the above-mentioned series of tests; plan 3 was selected as the optimum inlet plan on the basis of these tests.

Plan 3 was tested in the New York Harbor model to determine effects on the temperature regime of Sandy Hook Bay and the Shrewsbury and Navesink Rivers. Tests were also conducted to determine the effects on flooding for conditions of the November 1950 hurricane surge. Finally, tests were made with plan 3 in the undistorted-scale model to determine the optimum location of the jetties, the wave climate between and adjacent to the jetties during storm wave action in the ocean, and the transmission of wave action through the inlet and its effects on the Highlands Marina shoreline.

(9) Summary of Test Results. Three jetty plan locations were tested in the model of the new inlet (Fig. 7-6). Comparison of the test results shows that jetty plan C produces the most desirable tidal flow conditions. The high currents which attacked the end of the south jetty in jetty plan A are minimized in jetty plan C; eddies which developed

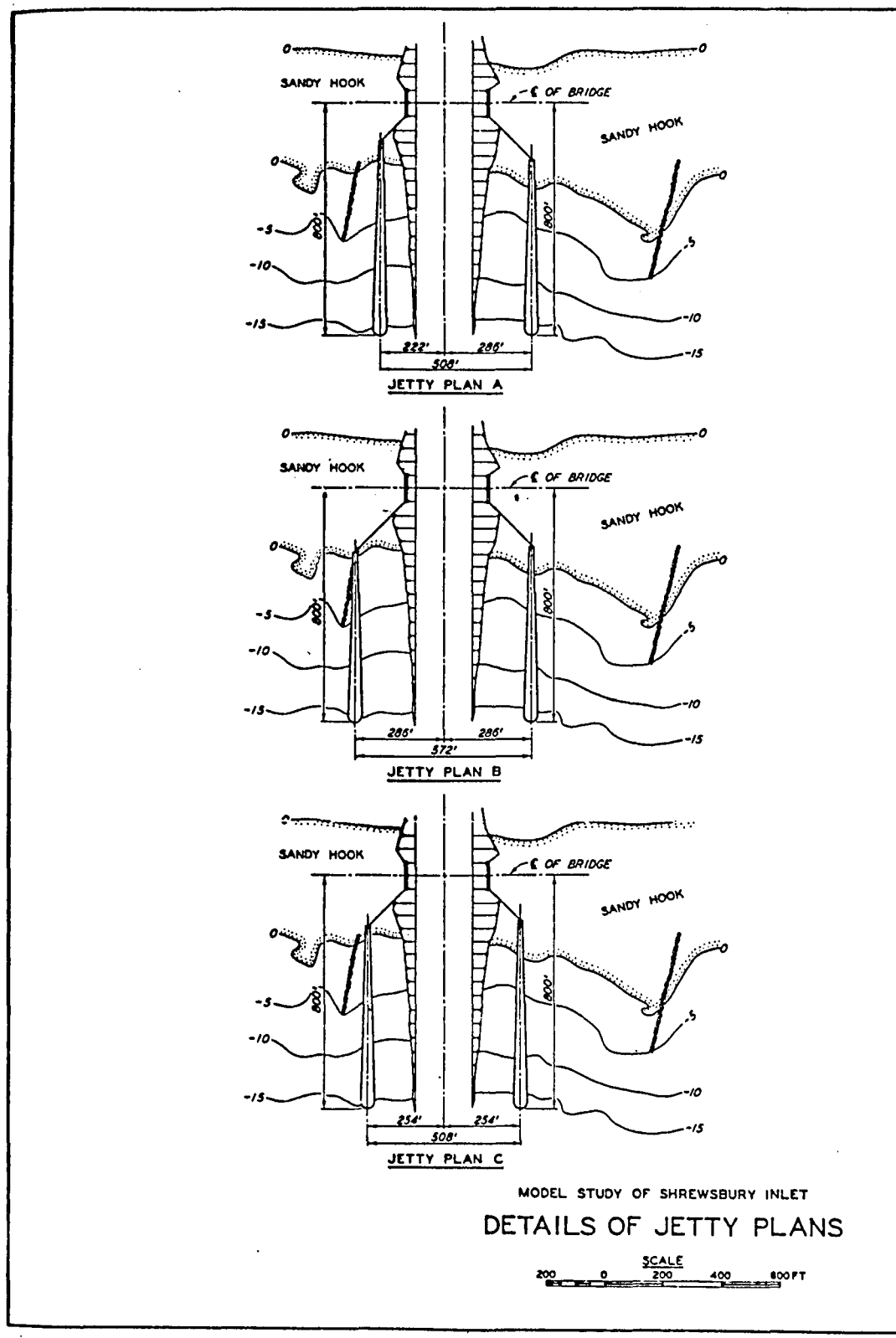

Figure 7-6. Details of jetty plans, Shrewsbury Inlet.

between the navigation channel and both jetties for jetty plan B did not occur with jetty plan C. Therefore it appears that the jetty alinements and spacings for jetty plan C would result in a satisfactory distribution of flow through the inlet.

The results of the tests to define wave conditions in the Highlands Marina area showed that waves generated in the Atlantic Ocean and propagated through the inlet are dissipated in Sandy Hook Bay to such an extent that essentially no wave energy reaches the Highlands Marina area. The maximum wave height recorded during these tests was 0.3 foot, well below wave heights resulting from waves generated within Sandy Hook Bay. Thus, it appears certain that energy passing through the inlet from waves generated in the Atlantic Ocean will not significantly affect wave conditions in the Highlands Marina area.

The results of tests to define wave conditions in and near the inlet showed that the maximum increase in wave height occurred with an ebb flow approximately 40 percent of the maximum spring tide ebb flow. Increases in wave heights of 60 to 70 percent, as compared to wave heights measured about 600 feet oceanward from the ends of the jetties, were observed just inside the ends of the jetties. Significant increases in wave heights between the jetties were not observed for tests with flood currents or for high water slack conditions. The alinement of the primary wave was generally perpendicular to the centerline of the navigation channel during all tests. Wave conditions within the inlet apparently would not cause significant navigation problems except possibly for certain ocean wave conditions combined with a critical ebb discharge in the inlet.

Conclusions based on test results in the undistorted-scale model and in the New York Harbor model, relative to Shrewsbury Inlet were:

(a) None of the plans tested would have significant effects on water surface elevations during normal tides or during hurricane surges.

(b) Current velocities and flow patterns would not change appreciably except in the immediate vicinity of the inlet.

(c) Current velocities in the new inlet for normal tides should not be excessive for safe navigation.

(d) None of the plans tested offered a unique advantage over the other plans in relation to the crosscurrents during certain periods of the tide phase; however, the alinement of plans 1 and 3 appeared to be better than that of plans 2 and 4.

(e) For pollution sources in Raritan Bay, the influx of pollution into Sandy Hook Bay, Shrewsbury River, and Navesink River would be reduced slightly.

(f) For pollution sources in Upper New York Bay, the influx of pollutants to Sandy Hook Bay and the Shrewsbury and Navesink Rivers would be increased.

(g) For pollution sources in Shrewsbury and Navesink Rivers, the flushing rate would be improved by construction of the inlet.

(h) Plan 3 would be less expensive to maintain than the other plans tested.

(i) Wave energy originating in the ocean and passing through the new inlet would have insignificant effects on wave heights along the Highlands Marina shoreline.

(j) The wave climate between the jetties should not be dificult to navigate except possibly under certain combinations of ocean wave conditions and critical ebb discharges in the inlet.

b. Hydraulic Characteristics of Inlet and Hurricane Surge Study--Galveston Bay Entrance Channel, Texas.

(1) Project. Design of barriers for protection of all or parts of Galveston Bay against inundation by hurricane surge.

(2) References. Brogdon (1969); Bobb and Boland (1970a, 1970b); Sager and McNair (1973a, 1973b); Section III,6,i of this report.

(3) Laboratory. WES.

(4) Test Period. Effects of barriers on hurricane surge heights, January 1965 to December 1967; effects of barriers on tides, currents, salinities, and dye dispersion for normal tide conditions, August 1967 to April 1970.

(5) Problems. The tremendous growth and development of the Texas coast have required an investigation for protection of this area from inundation resulting from storm surges. The design of barriers for protection of all or parts of the Galveston Bay region against flooding by hurricane storm surges required hydraulic model studies of the bay complex to verify the results of surge routings by analytical methods, and to determine the effects of all proposed structures on normal tides and hurricane surge heights upstream and downstream from barrier sites. Current velocities throughout the bay system, the salinity regime of the bay, and the rates of diffusion and flushing of pollutants discharging into the bay also required investigation.

(6) Purpose of Model Study. As part of the investigation for hurricane protection plans in the Galveston Bay area, a mathematical model was used to evaluate the effectiveness of the protection plans. Discharge coefficients were assigned to the Galveston Harbor Entrance to verify the mathematical model. These characteristics were obtained by subjecting a physical model of the entrance to a series of steady-state flows for several constant elevations of the water surface in the Gulf of Mexico. In this manner, the discharges moving through the entrance for the anticipated fluctuations of the levels of the gulf and the projected

range of head differentials between the gulf and the bay were defined. This information then formed the basis for definition of losses for the Galveston Harbor Entrance as input to the mathematical model. Only that part of the overall study concerned with the Galveston Bay inlet is discussed here.

(7) The Model. An existing, comprehensive, fixed-bed model of the Houston Ship Channel was used for the tests (Fig. 7-7). The model limits were altered to confine the surface area of the model and to reduce the stabilization time required for the individual tests. An artificial outflow channel equipped with an adjustable tailgate was also installed to facilitate the regulation of the water levels in the bay and to channel the water into a collection sump. The model limits and outflow channel, together with the locations of the water surface gages, are shown in Figure 7-8.

The model, including the harbor entrance, was molded to conform with soundings in the prototype during July to October 1962. The model was adjusted hydraulically soon after construction so that velocities and current patterns observed in the prototype for normal tidal ranges were accurately reproduced by the model (comparisons are shown in Fig. 7-9). This adjustment was also assumed to be reliable for surge conditions where water levels considerably exceed the high water level associated with normal tides, because the physical characteristics of all existing features were installed to scale and the correct overflow characteristics of the jetties were determined by independent tests in an undistorted-scale model.

The jetties protecting the entrance are not overtopped by tidal waters during normal tides, but during periods of hurricane surge flow will occur over the jetties and into the entrance. Therefore, it was necessary to install jetties in the model with the correct overflow characteristics; this was accomplished by construction of a 300-foot-long section of jetty to an undistorted scale of 1:100. Tests were then conducted in the undistorted-scale model to define the hydraulic characteristics of the jetty. Finally, with the desired properties known, a jetty shape which would duplicate these properties in the Houston Ship Channel model (distorted scale) was developed and molded into the model.

(8) Test Procedures. The test procedures consisted of stabilizing the flow in the model so that the water surface elevations of the Gulf of Mexico, West Bay, and Galveston Bay were at predetermined elevations of interest. The stabilized elevations of the water surface of West Bay and Galveston Bay were established essentially identical for any specific tests. The inflow to the Gulf of Mexico, the elevation of the tailgate located at the end of the outflow channel, and the cross-sectional area at the outflow channel in West Bay were adjusted until the desired elevations of the water surface were obtained. The discharge through the inlet was defined and all gages (see Fig. 7-8) were monitored for each test.

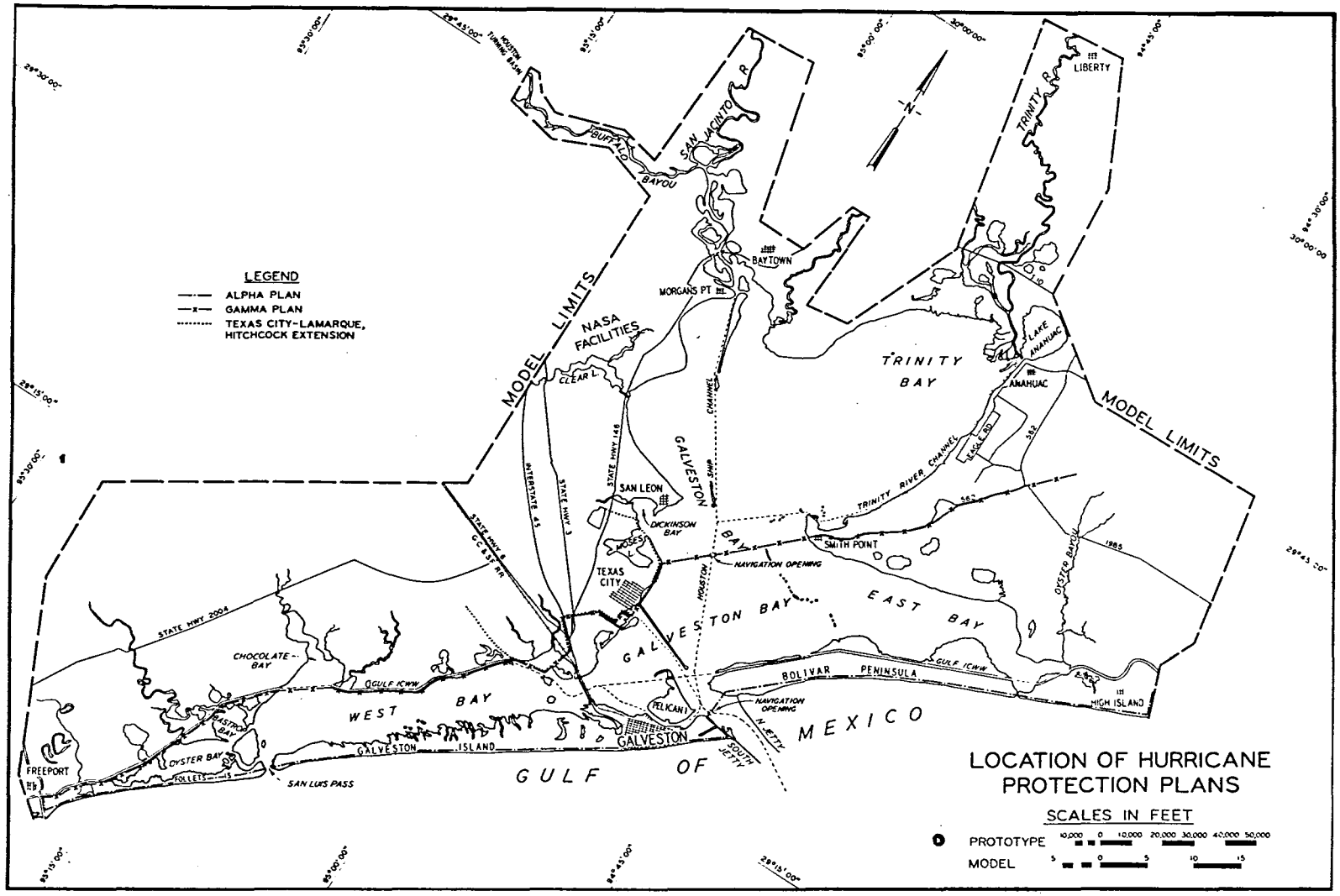

Figure 7-7. Houston ship channel model limits.

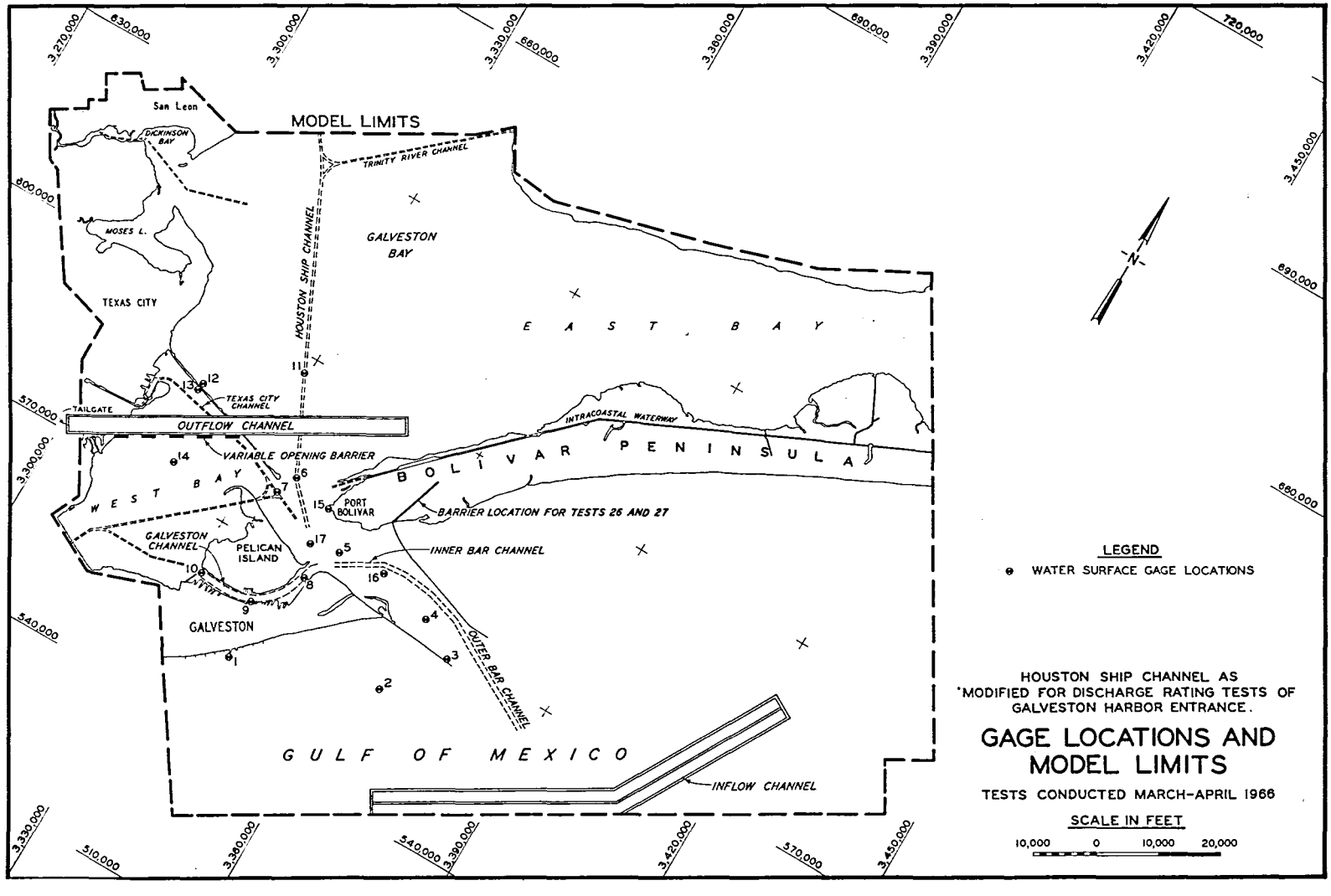

Figure 7-8. Houston ship channel model modified for Galveston Harbor and entrance channel discharge rating tests.

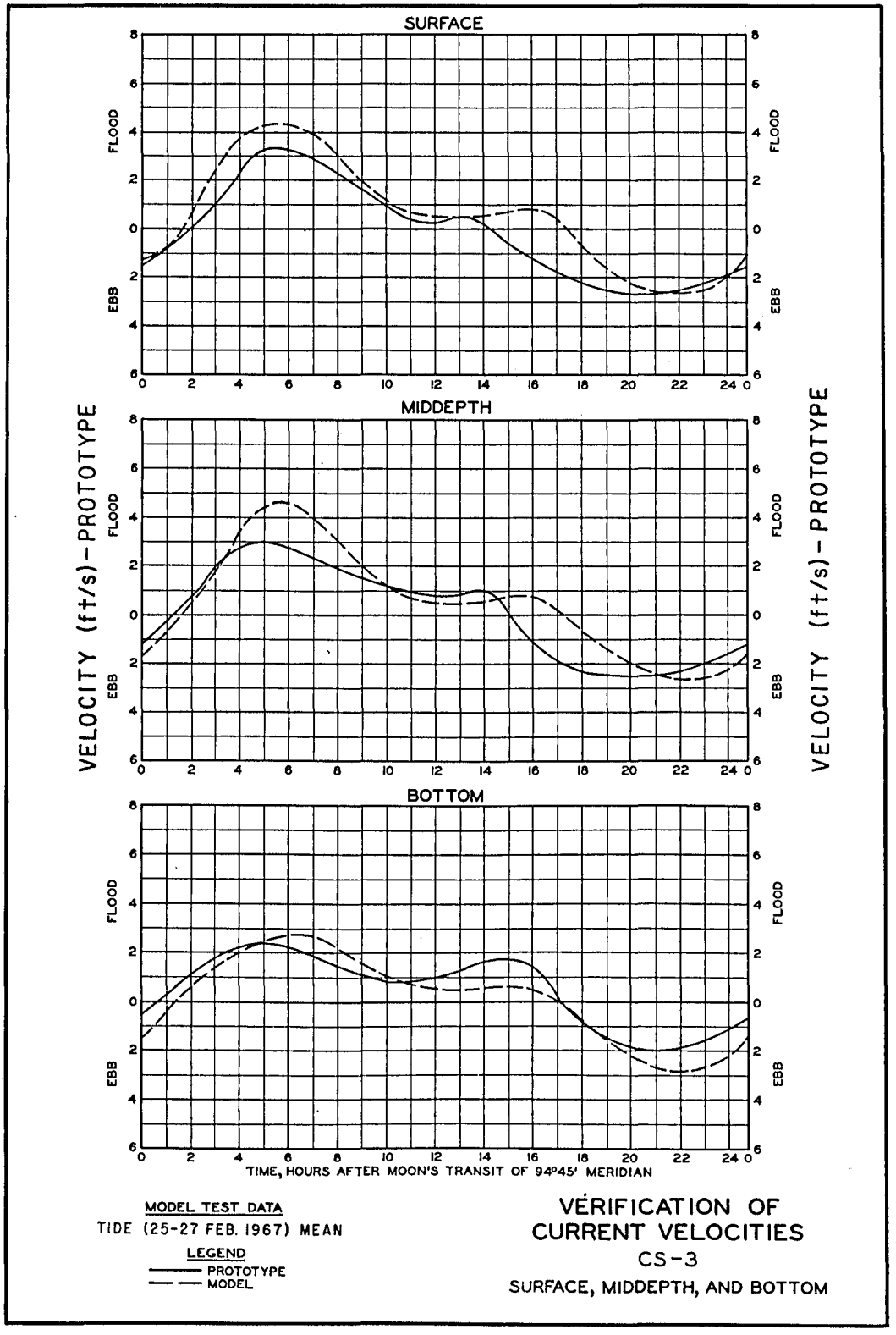

Figure 7-9. Verification of current velocities.

Two modifications to the model during the test program where: (a) the cross-sectional area through which water flowed from West Bay into the outflow channel was adjusted by changing the cross-sectional area between West Bay and the Outflow Channel; and (b) an artificial barrier was installed in the model from the inner end of the north jetty to approximately the +10.0-foot contour MSL on Bolivar Peninsula for tests 26 and 27 (see Fig. 7-8). The barrier was high enough to eliminate all flow over Bolivar Peninsula in that area. The only overtopping of Bolivar Peninsula or Galveston Island during any test was in the immediate vicinity of the Galveston Harbor Entrance.

(9) Summary of Test Results. The average discharge and water surface elevation at each gage location for each test was determined, and the tests were grouped according to the approximate elevation of the Gulf of Mexico; i.e., -1.5, +3.0, +4.5, +5.9, and +8.5 feet MSL. Discharge coefficients were defined for the inlet using the orifice equation:

$$Q = C_d A\sqrt{2g\Delta h} \quad (7\text{-}11)$$

where

Q = the discharge through the opening

C_d = the coefficient of discharge

A = the cross-sectional area of the entrance

g = the acceleration of gravity

Δh = the difference between the gulf water surface elevation (averaged data from gages 1 and 2 in Fig. 7-8) and the bay water surface elevation (averaged data from gages 11 and 14 in Fig. 7-8).

The results of the study of the discharge coefficients are shown in Figure 7-10. The coefficient varied from 0.3 to 0.6 with an average value of 0.47 for hurricane surge conditions. The area of the entrance was determined from a cross section taken at the position of gage 5 (see Fig. 7-8); the area varied with the appropriate water surface elevation measured at gage 5 for each flow condition.

The accuracy of these data apparently centered on four major limitations:

(a) The Houston Ship Channel model used for the tests is a distorted-scale model; therefore, the model was verified by adjustment of the roughness of the model until known prototype conditions were reproduced. Since adjustment was based on normal tidal conditions, the assumption was that the model roughness applied to conditions of the prototype where water surface above high tide exists. Although extensive tests in the model could

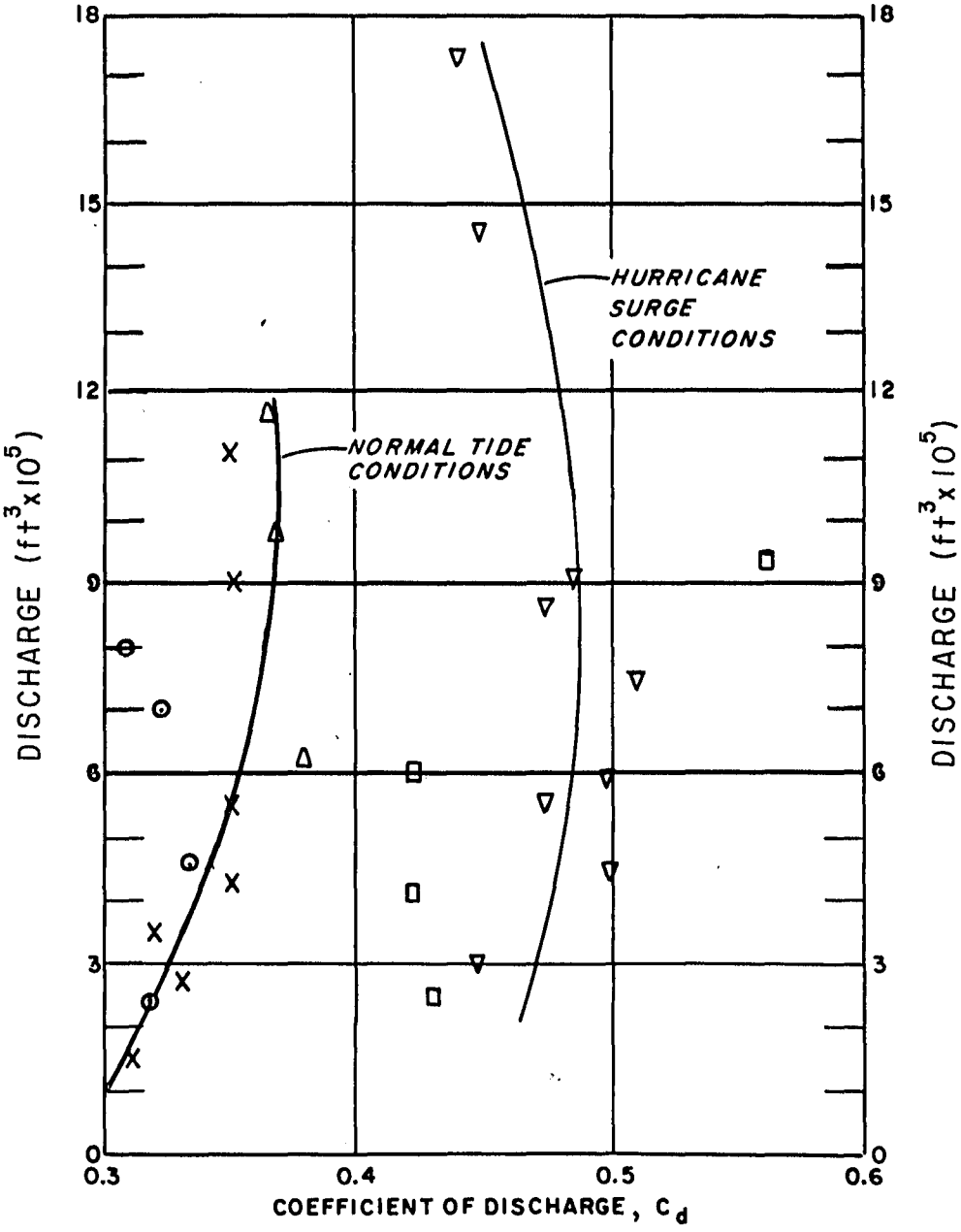

APPROXIMATE GULF ELEVATIONS (MSL)

O	−1.5
X	3.0
Δ	4.5
□	5.0
∇	8.4

DISCHARGE VERSUS
COEFFICIENT OF DISCHARGE
GALVESTON HARBOR ENTRANCE

Figure 7-10. Discharge coefficients for Galveston Harbor entrance channel.

have refined the accuracy of the model roughness, the anticipated refinement of the resultant data did not appear to be justified. In addition, major changes to model pumping control apparatus would have been required to simulate hurricane surges.

(b) A second potential refinement of accuracy was related to the overtopped jetties. The tests to develop a distorted-scale version of the jetties were all conducted with flow normal to the jetties. During the model tests, flow approached the jetties at varying angles. Again, additional tests could have investigated these conditions more extensively; however, the resultant improvement in accuracy did not appear to justify the tests.

(c) Both potential sources of error in test results could have been minimized further by testing in an undistorted-scale physical model of the Galveston Harbor Entrance at a considerably greater cost. Undistorted-scale model tests will certainly be beneficial as the program for protection of the Galveston Bay complex reaches the detailed design stage; however, the expense of undistorted-scale testing was not considered feasible at this stage of the study.

(d) The final significant limitation to the results is the basic bed-form changes (in shape and orientation) that would occur during a hurricane surge condition in the prototype. The tests were conducted in a model molded in concrete; therefore, no simulation of these effects was attempted. The basic changes in shape of the entrance during periods of high flow would not be considered significant enough to materially change the results. A more significant change might occur from the changes in bed form during the course of the varying flows expected during a hurricane surge. For this investigation, the subject was not examined in detail; however, care must be taken to assure that some consideration of this matter is included in a detailed hydraulic evaluation.

c. Stabilization of Navigation Channel and Sand Bypassing--Fire Island Inlet, New York.

(1) Project. Stabilization of the navigation channel and construction of a littoral drift trap and a rehandling basin in the inlet, a connecting channel for a loaded hopper dredge, and 1,000-foot extension to the Federal jetty.

(2) References. Bobb and Boland (1969).

(3) Laboratory. WES.

(4) Test Period. June 1965 to June 1968.

(5) Problems. Fire Island Inlet is located on the south shore of Long Island, and is the primary waterway for boat traffic between the Atlantic Ocean and Great South Bay (Fig. 7-11). The inlet is about 3,500 feet wide with depths to about 25 feet MLW. The western end of Fire Island migrated westerly a distance of over 4 miles between 1825 and 1940, when this migration was arrested by the construction of the 5,000-foot Federal jetty which extends generally southwest toward the ocean. The jetty trapped the littoral drift for about 10 years, then sand began by-passing the structure and filling the navigation channel. Corrective measures designed to alleviate channel deposition problems and supply sand for down-beach nourishment (completed in December 1959) consisted of (a) dredging an extensive area to -18.0 feet through the mouth of the inlet, (b) using a part of the material to construct a sand dike across the deep channel adjacent to Oak Beach, and (c) depositing an ample supply for down-beach nourishment in a feeder beach area. The sand dike was effective in diverting maximum currents from Oak Beach toward the center of the inlet; however, the entrance channel was not stabilized and continued to migrate as a result of accretion west of the Federal jetty.

(6) Purpose of Model Study. The Fire Island Inlet model study was conducted to:

(a) Investigate the proposed design of a combination sand bypassing and channel maintenance procedure, consisting of a littoral trap, a rehandling basin, an entrance channel connecting the two, and a training dike, as recommended by the U.S. Army Engineer District, New York, for Fire Island Inlet;

(b) investigate effects of changes in the dimensions and depths of the channel, trap, basin, and dikes through the physical model;

(c) determine the need for extending the Federal jetty (estimated cost about $2,650,000 for 1,000 feet in 1963);

(d) determine the need for additional dikes; and

(e) establish locations and dimensions of any additional improvements needed to increase the effectiveness of the plan and maintain a stable channel through the inlet.

Many alternatives and modifications of the original plan were tested during the study to ensure that all possibilities had been investigated for the best overall solution to the problems.

(7) The Model. The model reproduced a 60-square mile area that included all of Fire Island Inlet and the ocean beaches from Fire Island light on the east to beyond Gilgo on the west, along with a part of the Atlantic Ocean (Fig. 7-11). The Atlantic Ocean part of the model extended 5 miles to the east of and 7.5 miles to the west of the Federal

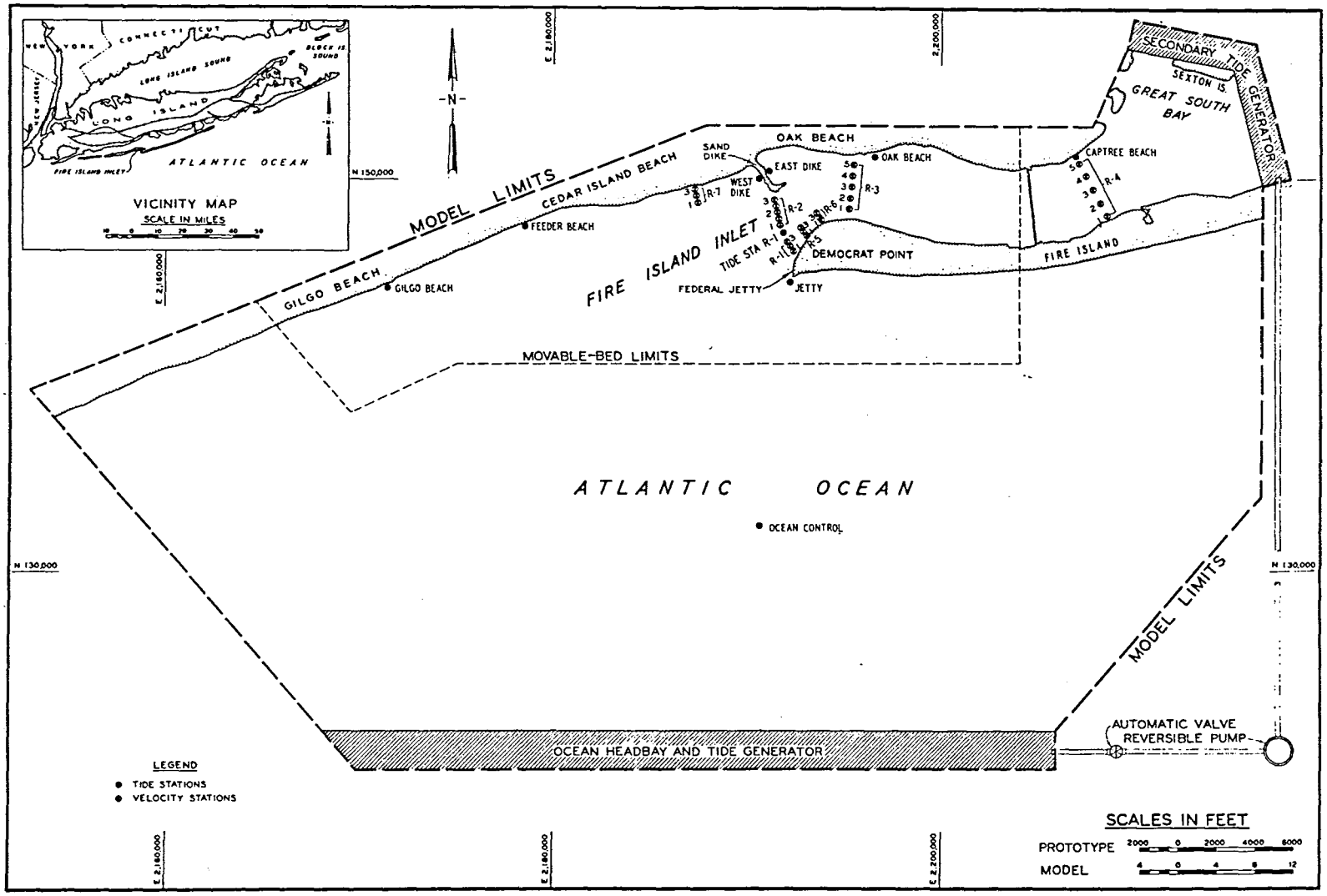

Figure 7-11. Fire Island Inlet model limits.

jetty and offshore to about the 60-foot depth. The Fire Island Inlet problem was caused primarily by littoral drift trapped in the inlet, thus starving the downdrift beaches and shoaling the navigation channel. Therefore, it was necessary that sand movement along the beaches be simulated in the model. The Fire Island Inlet model was first constructed as a fixed-bed model and all proposed improvement alternatives were tested quickly and economically to determine their effects on hydraulic conditions in the inlet. After completion of hydraulic tests, the problem area of the model was converted to a movable bed, and the most promising alternatives from the results of the fixed-bed studies were investigated further. In the fixed-bed studies, the entire model bed was molded of concrete; in the movable-bed studies, the part of the model outlined by a dashline in Figure 7-11 was molded of sand with a mean grain diameter of 0.25 millimeter and a specific gravity of about 2.65.

The model was constructed to linear scale relations, model-to-prototype, of 1:500 horizontally and 1:100 vertically with a resultant slope scale of 5:1. One prototype semidiurnal tidal cycle of 12 hours 25 minutes was reproduced in the model in 14.9 minutes. The computed time scale of 1:50 was applied only to reproduction of prototype hydraulic forces in the fixed-bed model and had no relation to time required in the movable-bed model to reproduce observed changes in prototype hydrographic conditions. The results of the movable-bed verification indicated that, using the operation schedule derived empirically, the time scale for bed movement in the model was approximately 36 tidal cycles (or 9.0 hours of model operation) to 1 year in the prototype. In the final verification test, a total of 1 million cubic yards of movable-bed material was introduced at the extreme east end of the model beach to replace the quantity of sand moved in a westerly direction by the model waves. This rate of movement, applied to the empirically determined time scale for bed movement, is in close agreement with the computed rate of prototype littoral drift along this reach of the south shore of Long Island.

(8) Test Procedures. Eleven different plans were investigated during the fixed-bed phase of the model study to determine plan effects on tides, current velocities, tidal discharges, current patterns, and flow distribution in the problem area. These plans involved (a) development of the best location and dimensions for the littoral reservoir and the rehandling basin (plans 2, 3, and 3A); (b) groins along Oak Beach to divert the stronger ebb currents away from the beach and into the navigation channel (plans 4 and 4B); (c) extension of the Federal jetty (plans 6 and 7); (d) dikes to partially or completely close the secondary channel off the end of the existing sand dike and thus divert more flow into the navigation channel (plans 8, 9, and 10); and (e) a deflector dike located on the west side of the navigation channel to deflect some ebb flow from the secondary channel into the navigation channel (plan 5).

In the movable-bed tests, the effects of plans on movement and deposition of bed material were determined by direct comparison of test results for existing conditions with those incorporating proposed improvements.

Base movable-bed tests were started with known model-bed configurations, the model tide and wave generators were operated through a predetermined schedule, and the model bed was surveyed periodically to record developments during the test. The movable-bed test for any plan was an exact duplicate of the base test except that the alternative plan was installed at the beginning of the test. The effects of the plan were determined by comparing the configuration of the model bed at the end of the plan test with the configuration of the model bed at the end of the base test.

(9) Summary of Test Results. The verification period selected for the Fire Island Inlet model was the 2 years immediately after construction of the navigation channel in November 1964. A careful study determined the following significant changes in prototype bed configurations that occurred during this period: (a) A scour area developed just north of the inner part of the navigation channel, (b) a shoal about 6 to 12 feet high developed in the inner part of the inlet channel, and (c) a shoal about 6 to 12 feet high developed along the eastern edge of the outer part of the navigation channel. After operating the model for 72 tidal cycles, it was found that the gross changes in bed configuration in the model were very similar to those indicated by comparison of the prototype surveys made 2 years apart. The bed movement during verification of a movable-bed model is not expected to duplicate exactly all changes in prototype bed configurations during the selected verification period because (a) the trends in bed movement in the prototype are not constant with time, although the model verification procedure constitutes an attempt to reproduce such movement on an average basis, and (b) certain observed changes in prototype bed configurations are mostly the result of storms or other extreme conditions, which the model verification (necessarily based on average conditions) cannot be expected to reproduce. Instead, the model-bed movement verification is an attempt to reproduce the gross changes that occurred in the prototype between the beginning and end of the verification period, and minor discrepancies of a local nature (or which are attributable to unusual prototype conditions) may be neglected. The deviations of the Fire Island Inlet model from the prototype conditions during a 2-year period are shown in Figure 7-12.

Conclusions based on the results of hydraulic and movable-bed model tests concerning proposed improvement plans for Fire Island Inlet were:

(a) Plan 3A, which required a littoral reservoir dredged to -34.0 feet, a deposition or rehandling basin to -28.0 feet when filled, and a 28-foot-deep connecting channel, will result in a safe and stabilized navigation channel with enough sand for bypassing to the downdrift beaches. Maintenance dredging of the littoral trap and connecting channel will be required about every 2 years; most of this dredging can be accomplished with conventional dredging plants. Since deposition in the littoral trap and connecting channel occurs in the form of a high bar, which builds from east to west, a sidecast dredge or similar equipment will probably be required to lower the bar crest enough for a hopper dredge to restore the basin depths.

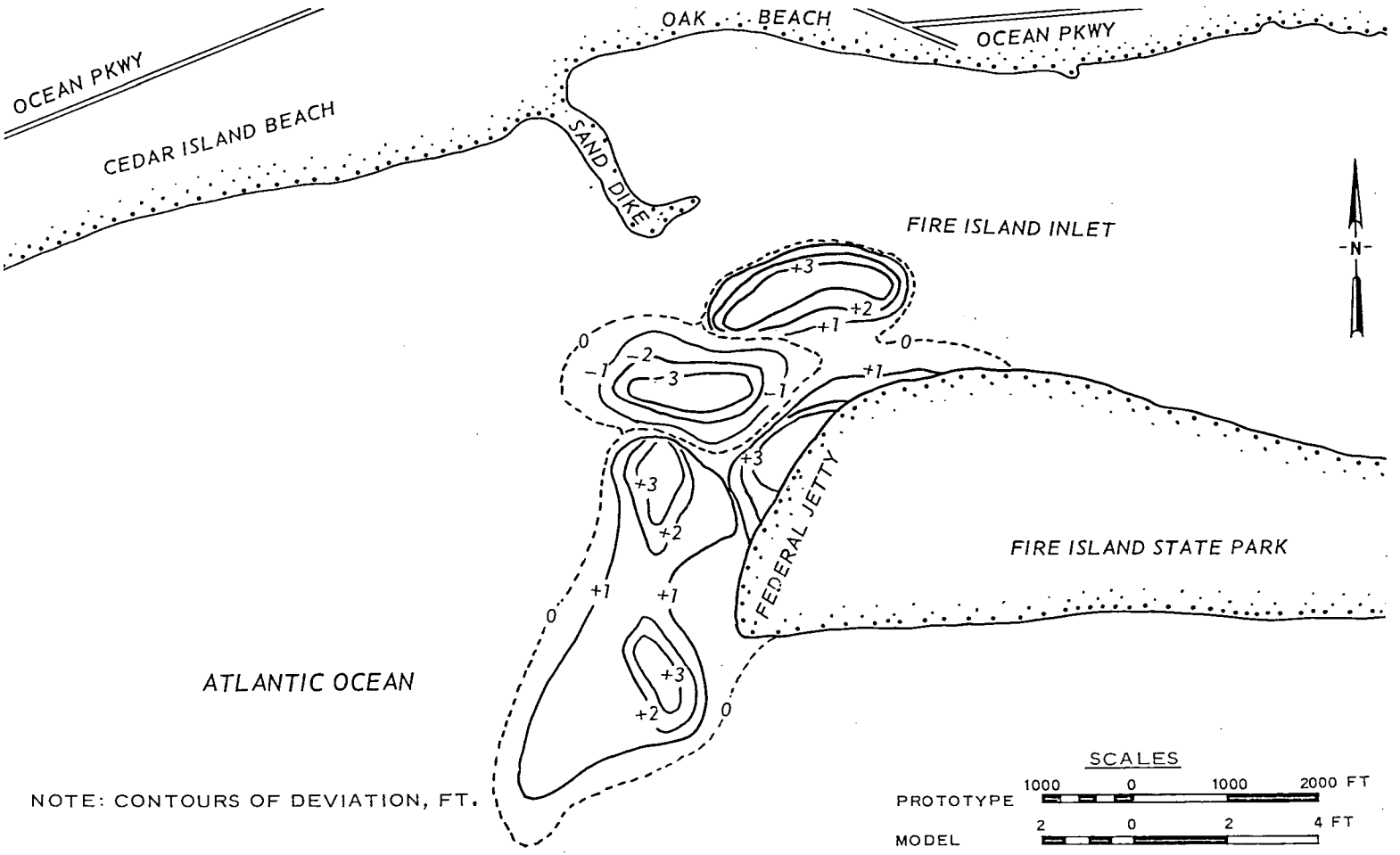

Figure 7-12. Fire Island Inlet prototype scour and fill during a 2-year period.

(b) The removal of large deposits of sand from Fire Island Inlet for beach restoration projects will not adversely affect the functioning of plan 3A.

(c) Extension to the existing sand dike will not improve the functioning of plan 3A in channel shoaling or deposition patterns. Likewise, construction of a dike at Cedar Island Beach would not improve the functioning of plan 3A.

(d) A deflector dike parallel to the entrance channel would not improve the functioning of plan 3A from either shoaling of the navigation channel or deposition patterns; further the dike would be extremely difficult to maintain.

(e) Extension of the Federal jetty would not reduce channel shoaling or improve deposition patterns observed for plan 3A. An extension to the jetty would reduce channel shoaling on a temporary basis while the impounding capacity of the extended jetty was being filled; shoaling rates and deposition patterns would then be the same as for plan 3A. Material impounded by a jetty extension would also be permanently lost as a source of beach nourishment.

(f) Extension of the Federal jetty, as a combination low weir inner section and high outer section, did not function as intended. Instead of moving readily over the low weir section, a large percentage of the littoral drift was trapped to the east of the jetty extension; it appeared that the weir section would be blocked and thus be rendered completely inoperative.

(g) An offshore breakwater and littoral trap would also satisfy all the necessary requirements of a plan for channel stabilization and sand bypassing at Fire Island Inlet.

Representative tidal elevations for plan 3A are shown in Figure 7-13; the effect of plan 3A on current velocities at typical locations is shown in Figure 7-14. A scour and fill map for plan 3A after 2 years of prototype operation is shown in Figure 7-15. Thus, it was determined that dredging must be performed approximately every 2 years.

d. Improvement of Navigation Channel--Galveston Bay and Harbor Entrance Channel, Texas.

(1) Projects. Stabilization of jetty channel; north jetty protection; investigation of shoaling characteristics between jetties; and location of anchorage area.

(2) References. Simmons and Boland (1969); Letter and McAnally (1977).

(3) Laboratory. WES.

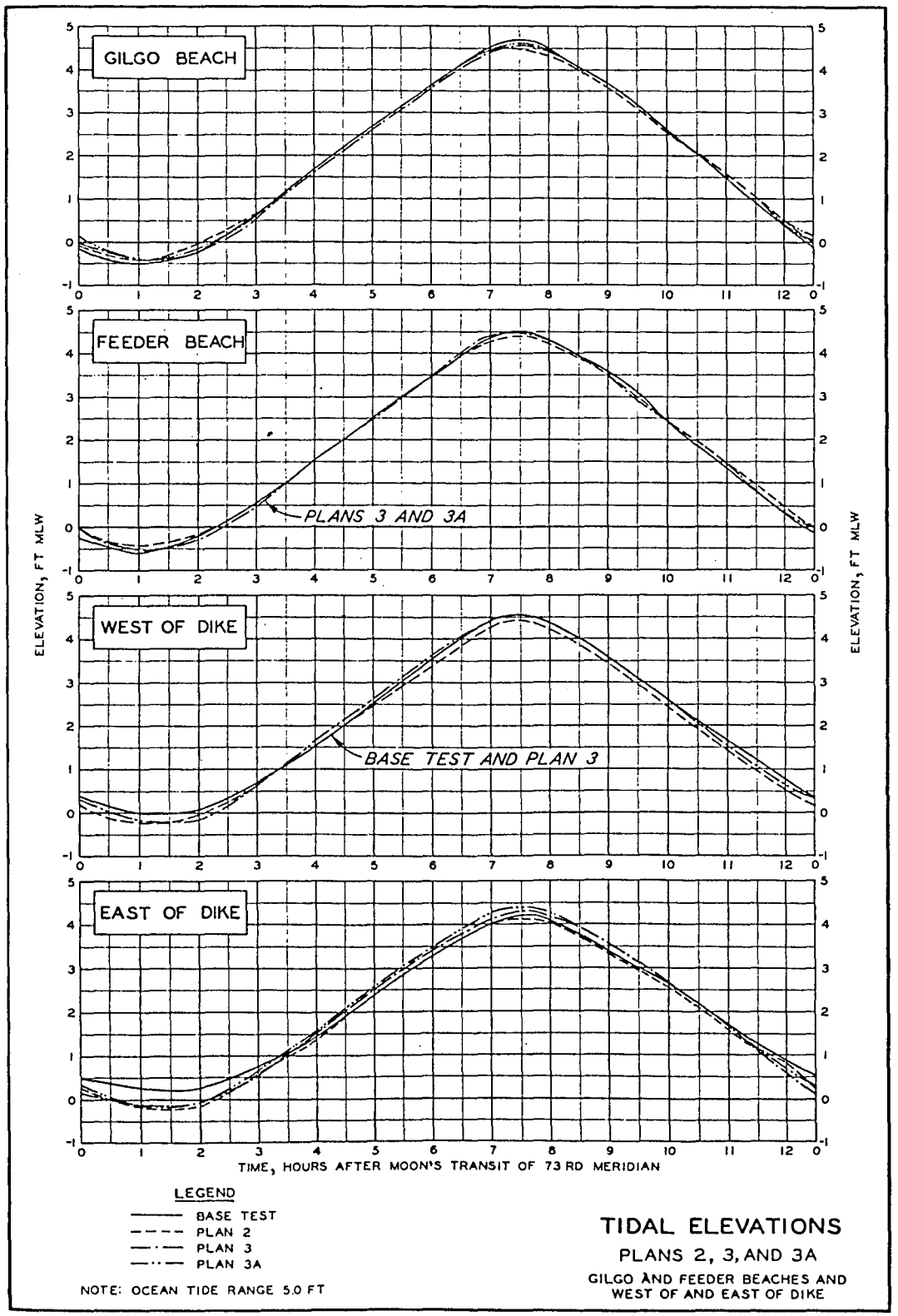

Figure 7-13. Representative tidal elevations from model tests, Fire Island Inlet.

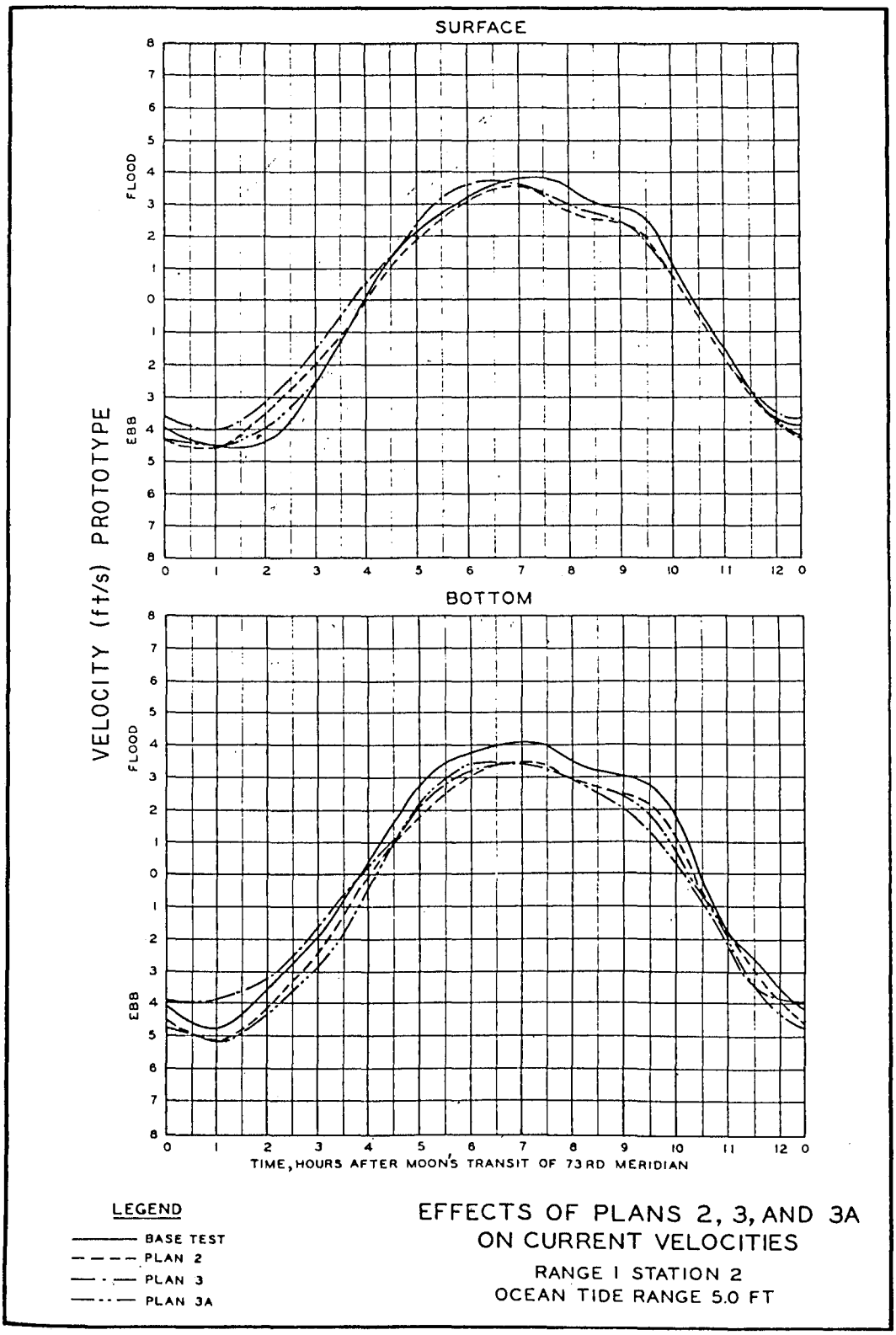

Figure 7-14. Effects of representative plans on current velocities, Fire Island Inlet.

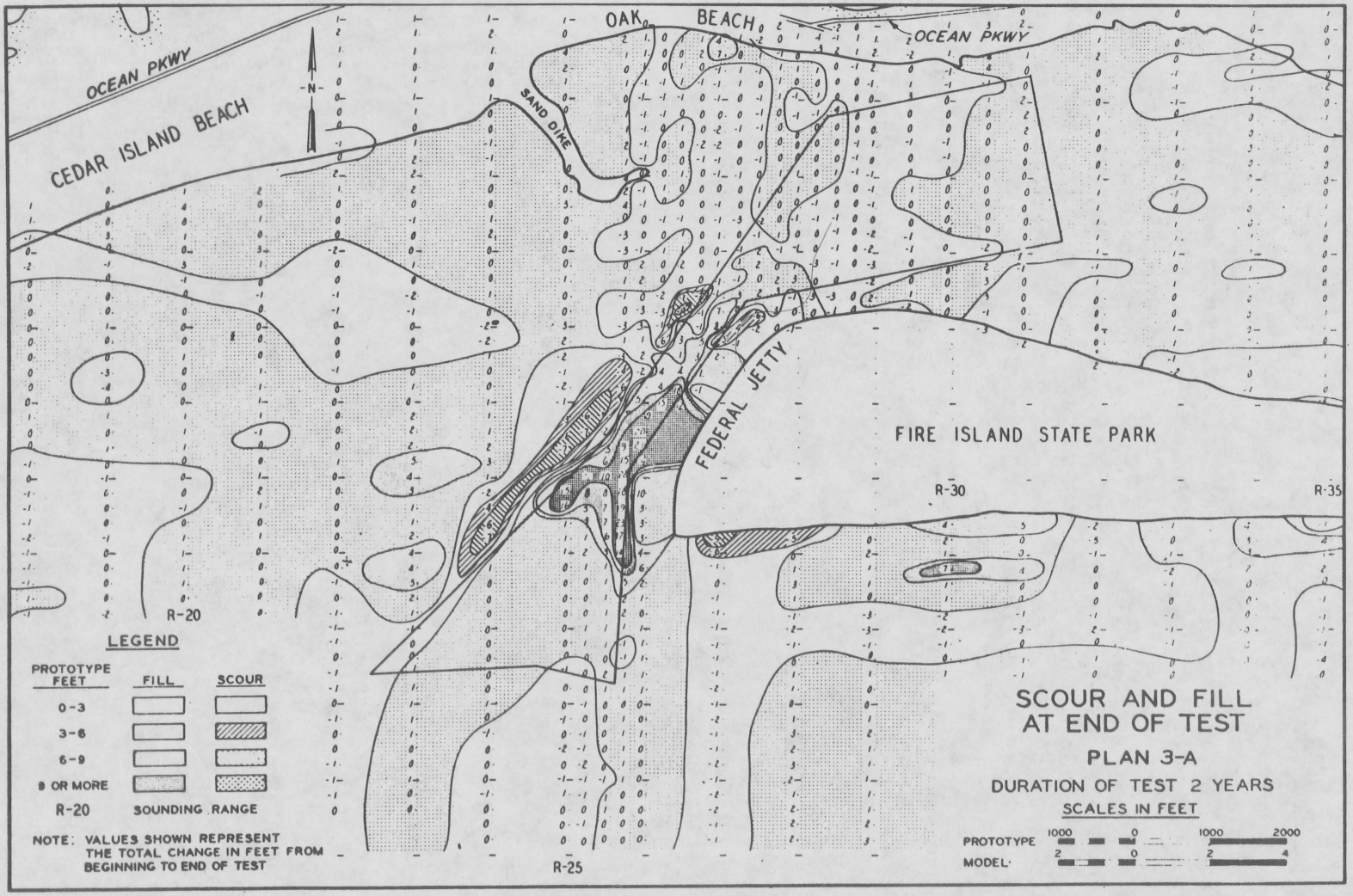

Figure 7-15. Model scour and fill tests for plan 3A at end of 2-year prototype period, Fire Island Inlet.

(4) Test Period. May 1960 to February 1966.

(5) Problems. At the time of the model study, the jetty channel at the entrance to Galveston Bay had three major problems: (a) the extremely sharp turn, located at approximately the inner end of the jetty channel which caused difficulty for larger ships, especially tankers, to negotiate at or near the strength of the tidal currents; (b) the extremely deep water immediately alongside the north jetty in the area where the navigation channel was close to the structure (the concern was that, during a severe storm, a section of the jetty might slough into the channel and block navigation); and (c) shoaling in the inner and outer bar parts of the navigation channel (for the depth of -38.0 feet of the inner bar and -40.0 feet of the outer bar, the average annual shoaling rates were 452,000 cubic yards and 731,000 cubic yards respectively). A location map of the problem area is shown in Figure 7-16.

As part of the improvement desired, it was anticipated that the depth throughout the entrance channel would be increased by 2 feet, and an increase of shoaling in both the inner and outer bars could logically be expected.

(6) Purpose of Model Study. The Galveston Bay and Harbor Entrance Channel model study was conducted to:

(a) Develop plans for relocation and stabilization of the jetty channel on an alinement and at a depth suitable for the safe passage of supertankers;

(b) determine means for protecting the north jetty from the undermining action of tidal currents;

(c) determine the shoaling characteristics of the relocated and deepened inner bar parts of the jetty channel, and develop plans for minimizing shoaling in the relocated channel;

(d) determine the shoaling characteristics of the deepened outer bar part of the jetty channel; and

(e) determine the best locations for additional anchorage areas within the jetty channel or in Bolivar Roads.

(7) The Model. The Galveston Harbor model was a scale reproduction of a 174.5-square mile area which included a small part of Galveston Bay and a much larger part of the Gulf of Mexico (Fig. 7-16). The Gulf of Mexico part extends 8 miles to the north of the north jetty, 6.5 miles to the south of the south jetty, and offshore to about the 50-foot depth.

A movable-bed model was used to reproduce the critical area under study. An analysis of the scaled-down forces available to move sediment in the model indicated that the movable bed should be molded of crushed coal. This material was of proper weight to permit movement and deposition in the model by the model hydraulic forces in a manner similar to

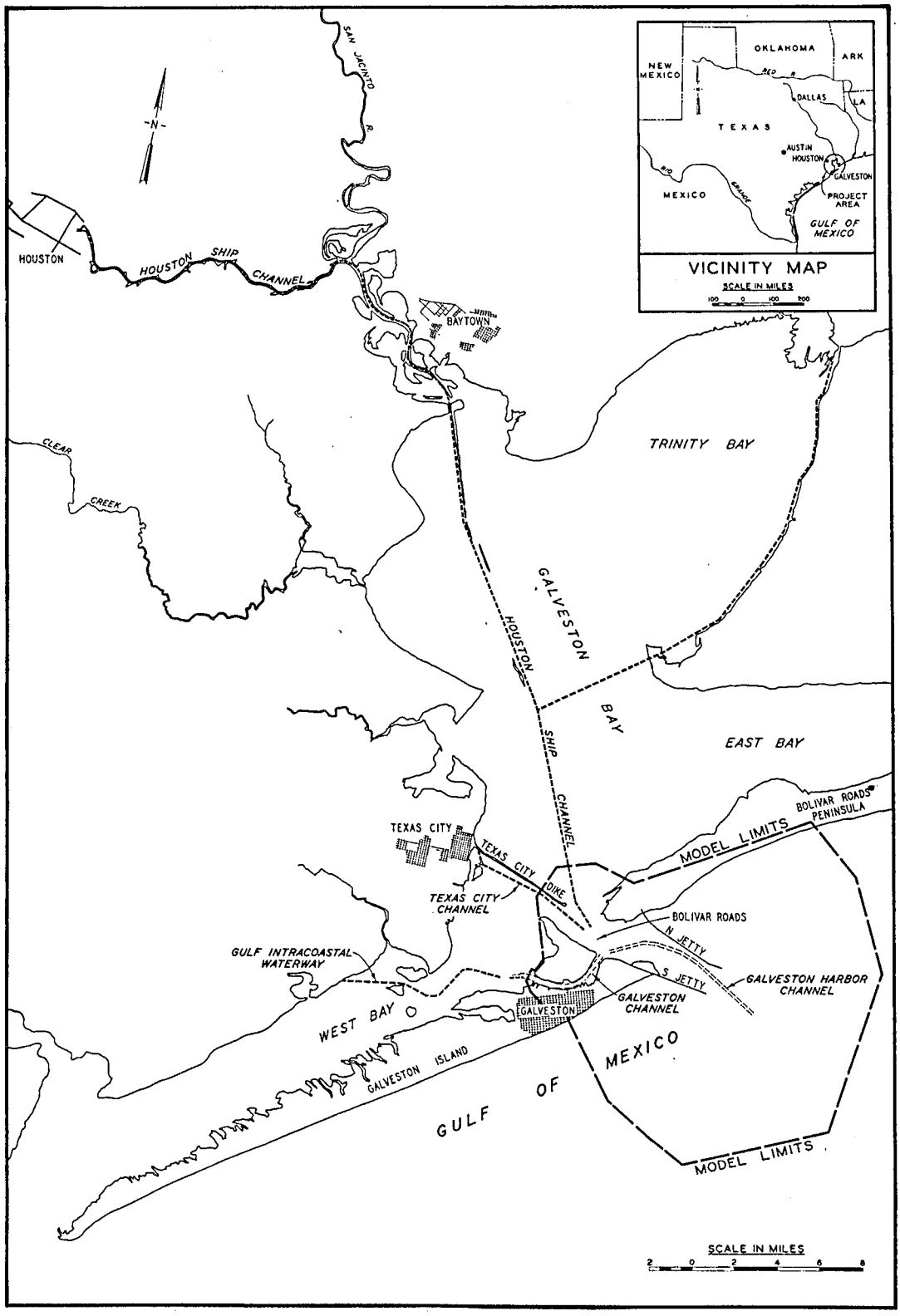

Figure 7-16. Galveston Bay location map.

the movement of prototype bed material by the prototype hydraulic forces. The coal used had a specific gravity of 1.4, a grain-size range of 0.1 to 5.0 millimeters, and a median grain diameter of 1.4 millimeters. Beyond the limits of the movable-bed section, the remainder of the model bed was molded of concrete to provide space for the wave generator and the inflow-outflow system required for the tide generator.

The model was constructed to linear scale relations, model-to-prototype, of 1:500 horizontally and 1:100 vertically. Other scale relations such as time, velocity, discharge, and volume were computed from these linear scales. The computed time scale of 1:50 was applied only to reproduction of prototype hydraulic forces in the model and had no relation to the time required for the model to reproduce observed changes in prototype hydrographic conditions. The model layout is shown in Figure 7-17.

The following model operating procedure was developed during trial verification tests:

(a) The first cycle (about 30 minutes) was a normal tidal cycle with waves.

(b) Operation of the model tide generator was stopped when ebb velocities reached a maximum, and the model was operated for 1 model hour with a sustained ebb flow and without waves.

(c) Operation of the tide generator was resumed, and a normal tidal cycle was run with waves.

(d) At the time of maximum flood velocity, operation of the tide generator was again suspended, and 1 model hour of sustained flood velocity was run without waves.

During the trial verification tests it was found that reproduction of two of the above sequences of operation (requiring a total of 3 hours each) resulted in an accurate reproduction of average annual shoaling of the inner and outer bars, as well as duplication in the model of the prototype locations of the bars or shoal areas. Thus, the empirical time scale for bed movement was 6 hours in the model to 1 year prototype. The characteristics of the waves used during the tests were derived by numerous trial-and-error experiments on the model. The waves developed empirically and in these tests were the results of progressive attempts to reproduce in the model the rates and directions of bed movement that occurred in the prototype, as indicated by hydrographic surveys and dredging records. The hindcast wave climate served as a guide in the selection of the model test waves, but could not be strictly adhered to because of the distortions previously discussed.

(8) Test Procedures. The five plans selected for testing in the model had as a combined objective to find a solution to the two most pressing problems for which the model study was authorized: relocation

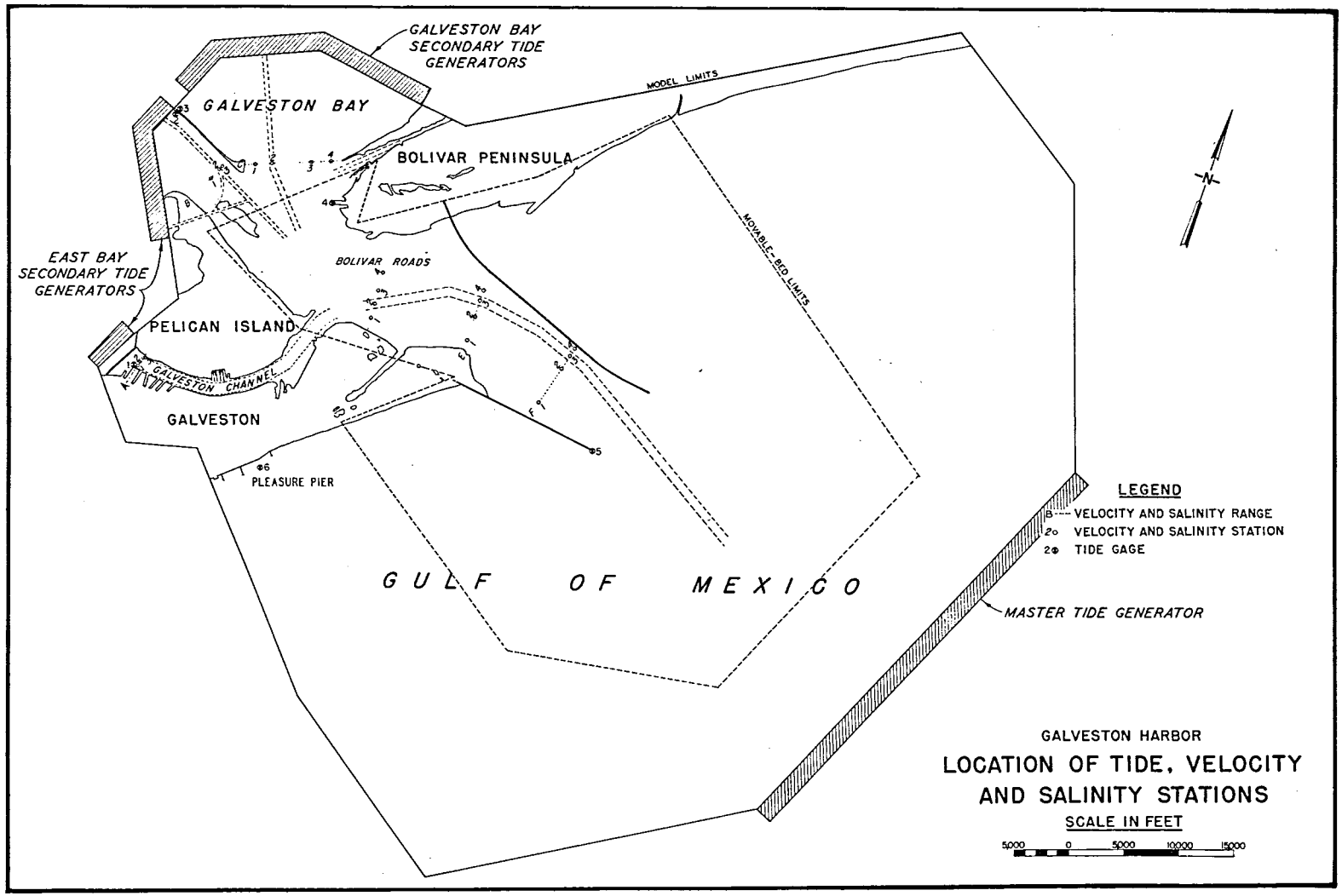

Figure 7-17. Galveston Harbor and entrance channel model limits.

and stabilization of the jetty channel designed to accommodate supertankers, and diversion of currents causing the undermining of the north jetty. For all plans tested, the entrance channel was maintained at the authorized project dimensions (800 feet wide and 42 feet deep for the inner bar channel, and 44 feet deep for the outer bar channel). The fixed procedures developed in the verification phase of the study were followed in the operation of all tests. The only variations between the various tests were in the features of the plans of improvement.

Before the beginning of each test, the movable bed of the model was molded to conform to the prototype survey of 1960, and the selected plan of improvement was installed in the model. The navigation channel was dredged to project dimensions along the proposed realinement, and the channel was maintained by annual dredging throughout the duration of the test. Each of the channel realinement tests consisted of the simulation of at least 12 prototype years in the model, 8 years of normal conditions, and 4 years after a simulated storm condition. Detailed studies of the paths of moving bed material were made during the various tests. The model bed was surveyed and mapped at the end of each simulated year of each test to determine the progressive changes in bed conditions, as well as the final results of each test. Analyses and interpretations of the results of the model tests were based on careful observations during model operations and on survey studies of the model bed, in relation to the qualifications and limitations of the model.

(9) Summary of Test Results. Conclusions based on results of the model tests were:

(a) Entrance channel realinement plan 2 was superior to the existing channel alinement because the plan provided a shorter and straighter channel for navigation by supertankers, diverted the strong ebb currents away from the north jetty and thus protected the jetty from the undermining action of these currents, and provided a 4-foot-deeper entrance channel for essentially the same maintenance dredging required for the existing channel.

(b) Construction of the plan 2 channel could be scheduled over as long as 2 years without affecting overall shoaling in an 8-year period. However, the shoaling rate during the first 2 years after completion of construction would probably be accelerated by normal adjustment of channel side slopes. An important element of the construction procedure is the disposal of dredged material in the abandoned part of the existing channel to avoid enlarging the total cross-sectional area between the jetties and thus reducing current strengths.

(c) The outer 3,000 feet of the north jetty could be permitted to degrade naturally to elevation -12.0 without detrimental effects on shoaling in the realined channel. However, deterioration of appreciably more than 3,000 feet of the north jetty would cause an undesirable change in the overall flow patterns in the entrance, which in turn would cause the inner shoal to again encroach on the inner bar channel.

(d) Sidecast dredging techniques should not be used in maintenance of the outer bar channel at the entrance to Galveston Harbor, because dredged material placed close to the channel will return quickly to the channel and increase the shoaling rate in the outer bar channel.

(e) Dredged material placed in the northeasterly one-third of the existing disposal area, 3 miles off the outer end of the south jetty, will return to the entrance channel; dredged material placed in the remaining two-thirds moves generally to the east beach area south of the south jetty and will not return to the channel.

(f) An anchorage area can be developed for deep-draft tankers with only a slight increase in annual maintenance dredging. Elimination of the western 2,000 feet of anchorage tested in the model would essentially eliminate maintenance dredging requirements.

(g) The addition of a spur dike to the north jetty would reduce shoaling in the outer bar channel by about 250,000 cubic yards per year as a result of the increased impounding capacity of the revised north jetty. This annual benefit would cease when the new impounding area is filled, and economic justification of the spur dike appears doubtful.

(h) Reducing the width of the entrance channel from 800 to 600 feet would significantly reduce annual maintenance dredging, and studies are necessary to determine if the lesser width would be satisfactory for navigation.

(i) Deepening the inner and outer bar parts of the entrance channel to 46 and 48 feet, respectively, would increase average annual maintenance dredging in the channel by about 100,000 cubic yards. This increase would be partially offset by a reduction in the shoaling rate in the anchorage area.

(j) All three jetty extension plans tested caused significant increases in the overall shoaling rate in the entrance channel.

The recommended changes were constructed in the prototype. Figure 7-18 shows the prototype existing channel condition before construction and the proposed channel relocation alinement. Figures 7-19 and 7-20 show the extent of scour and fill that occurred in model and prototype, respectively, from the initial construction to the end of the second year after construction. The navigation channel has been eliminated from this comparison, because the realined channel was constructed and two maintenance dredging operations were performed during this period. Major changes in depth are concentrated in the abandoned channel, and especially in the area used for dredged-material disposal. This comparison readily shows the increased tendency for shoaling of the abandoned channel in the prototype as compared to the model predictions. In the area between the abandoned channel and the relocated channel, the model indicates fill and the prototype indicates scour; however, all of

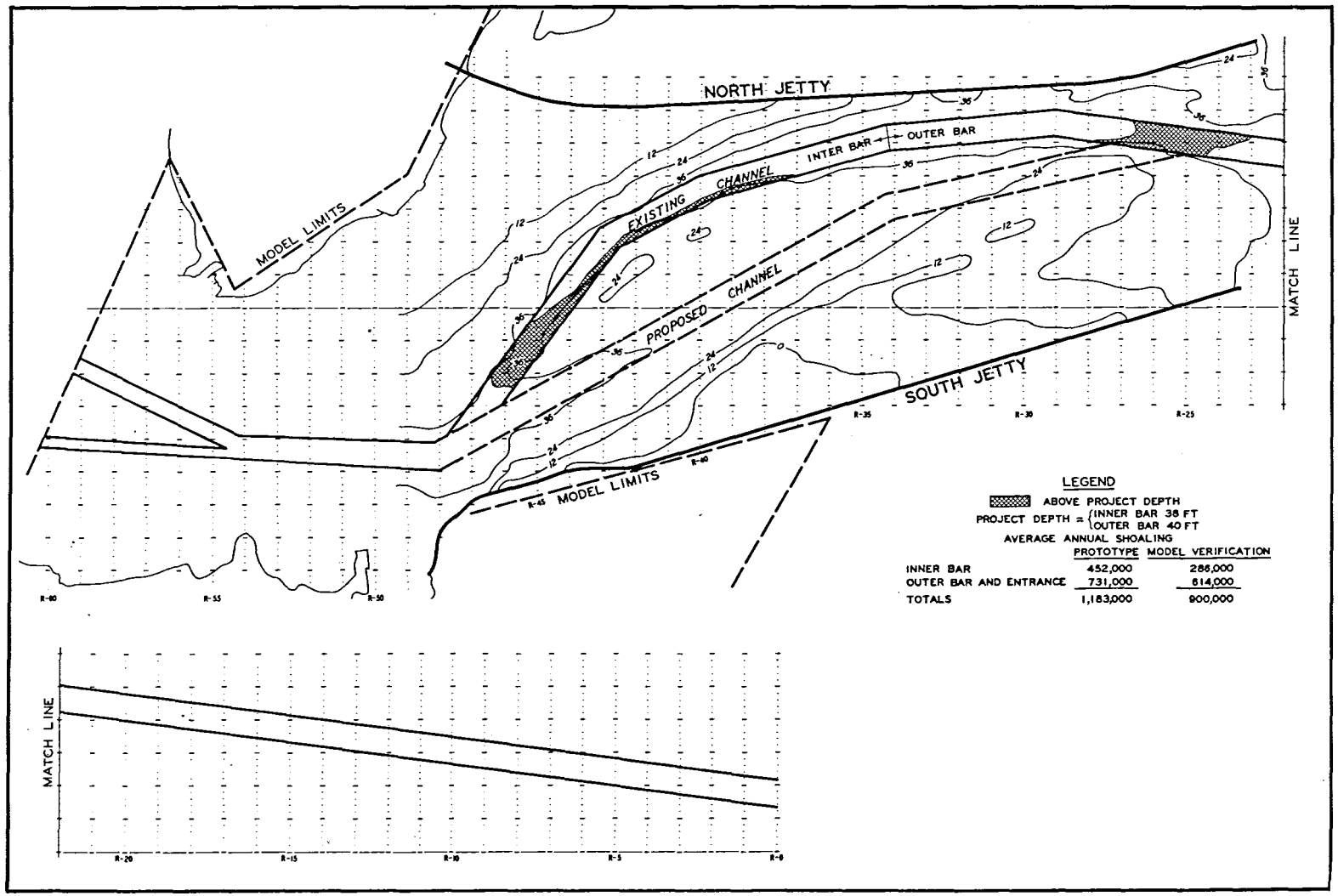

Figure 7-18. Prototype existing channel condition before construction of proposed channel relocation, Galveston Bay and Harbor Entrance Channel.

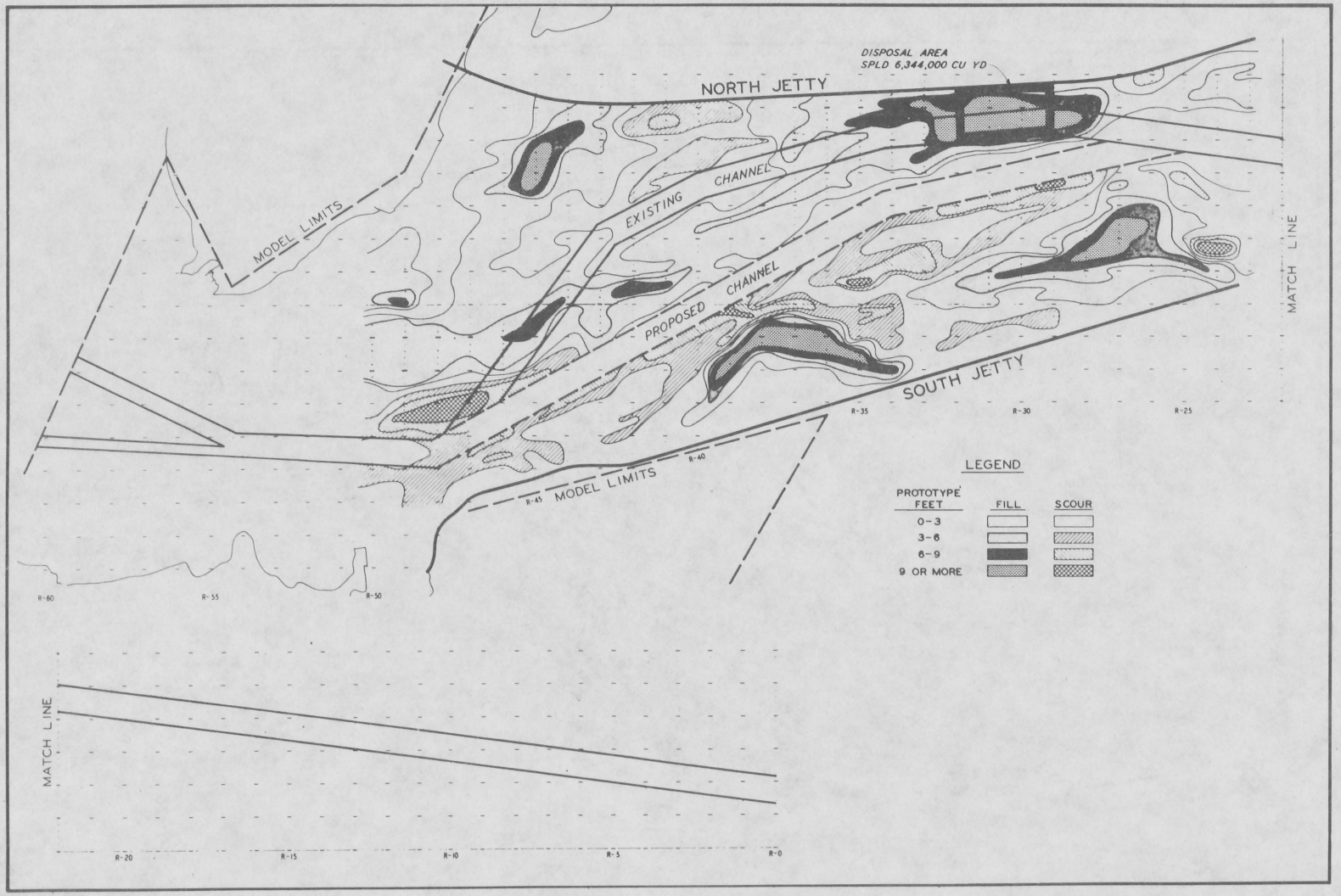

Figure 7-19. Model scour and fill occurring from the initial new channel construction to the end of second year after construction, Galveston Bay and Harbor Entrance Channel.

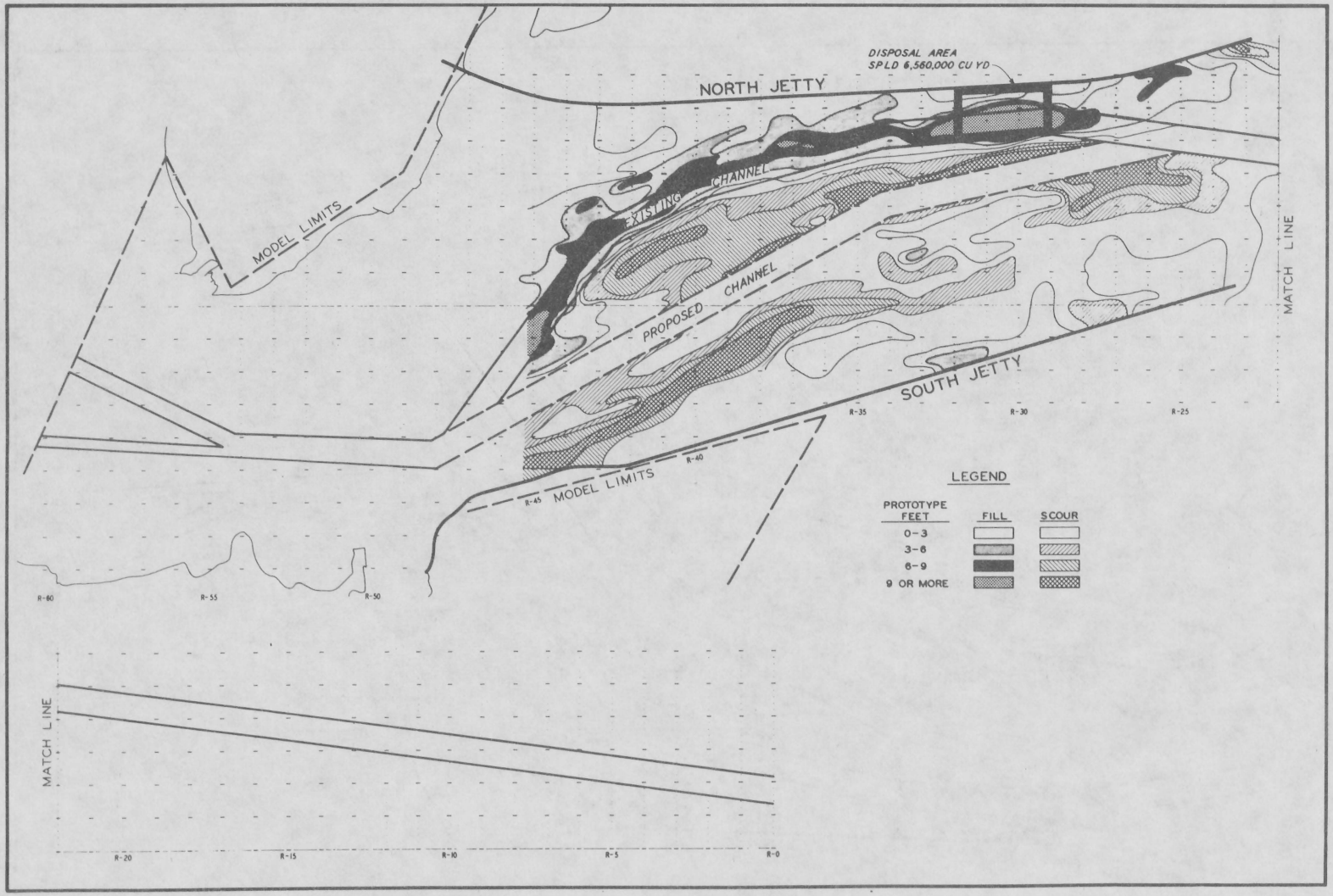

Figure 7-20. Prototype scour and fill occurring from the initial new channel construction to the end of second year after construction, Galveston Bay and Harbor Entrance Channel.

the indicated scour is attributable to an anchorage dredged in this area in the prototype. South of the abandoned channel, the model indicates two areas of rather substantial fill that are not borne out by prototype experience. The inner area is in extremely shallow water and is typical of the unnatural model-bed formations developed in shallow water when using crushed coals as bed material and with exposure to significant wave action.

The objectives of the original model study were to determine a means for protecting the north jetty from being undermined by tidal currents and to determine the shoaling characteristics of the inner and outer sections of a deepened entrance channel. One plan tested in the model was constructed in the prototype. The feasibility of the plan was partly judged on model results indicating that although a deepened channel along the proposed alinement would require increased maintenance dredging, the additional cost would be partially offset by a seaward shift in the shoaling distribution.

An analysis of pertinent data 6 years after construction of the plan by Letter and McAnally (1977) indicates that the model:

(a) Correctly predicted that the channel realinement and dredged-material disposal would halt undermining of the north jetty next to the outer bar channel;

(b) correctly predicted that total maintenance dredging volumes would increase for the proposed channel but underpredicted the magnitude of the increase;

(c) erroneously predicted that the inner bar channel would experience net erosion and require no maintenance dredging beyond the second year;

(d) correctly predicted the approximate absolute and relative increases in maintenance dredging volumes for the outer bar channel;

(e) correctly predicted that maintenance dredging volumes for the approach channel would increase, but underpredicted the magnitude of that increase due to a marked absence of shoaling in the seaward extension of the approach channel; and

(f) correctly predicted a seaward shift in the channel shoaling volume distribution but overpredicted the magnitude of the shift; this overprediction was due to the erroneous scour prediction for the inner bar channel.

Therefore, it is concluded that the model satisfied most qualitative objectives but failed to accurately meet some quantitative objectives.

9. Summary.

Although a current trend is toward computerization of the theoretical aspects of tidal inlet studies, the engineering researcher is required to continue experimentation since new or improved theories must be verified by sound testing programs. The scaled reproduction of the physical phenomenon occurring at an inlet is fundamental because the problem is too complex to be amenable to analytical solutions in its entirety, and empirical information is necessary. When properly scaled, the experimental model mirrors the true physical behavior of the inlet and relevant quantities measured in the scale model permit prediction of the corresponding quantities in the prototype.

An analysis of the forces governing the phenomena shows that both viscous and gravity forces are important and both should be satisfied simultaneously. However, since water is generally used as the model fluid in inlet studies, an approximate similarity requirement may be used based on empirical relationships which include the major effects of frictional forces, and the model is operated according to gravitational laws. Manning's formula is used as the controlling roughness similarity criterion when the flow is fully rough turbulent in both the model and prototype, and Froude scaling laws are applied since a surface wave is essentially a gravitational phenomenon.

The physical modeling of tidal inlets easily falls into one of four distinct catagories; i.e., fixed-bed, distorted- or undistorted-scale, or movable-bed, distorted- or undistorted-scale. Since similarity is not strictly adhered to in most movable-bed testing because of the difficulties involved in scaling sediment particles, the movable-bed models are, by implication, distorted. This distortion is empirically accounted for by a deliberate second distortion, usually a distortion of time or wave climate alterations. The specific type of model selected is determined by the problem which requires investigation; e.g., hydraulic characteristics such as currents and water circulation patterns are usually studied in fixed-bed models, and the results are frequently transferred to movable-bed models of the same region where littoral processes and sediment transport problems may exist. A fixed-bed model may also be useful in studying shoaling of entrance and interior inlet channels.

Sometimes an investigation of events occurring in or near the tidal inlet constitutes the predominant purpose of the model study. At other times the influence of wave energy flux or tidal flows carrying pollutants through the inlet into other parts of the bay or estuary may require analysis for optimal solutions. In this case the inlet becomes an integral part of the overall problem but does not become the exclusive concern of the researcher. For these reasons it is difficult to generalize on the cost and time required for inlet model studies. Recent experience at WES indicates that inlet models generally vary in size from about 3,000 to 25,000 square feet. Because of the wide variety of sizes and the amount of detail required for each, the cost of design and construction of the models also varies over a large range. The cost varies

with the complexity of the model geometry (on the order of $12 to $15 per square foot in 1976); however, this does not normally include the cost of major appurtenances such as tide and wave generators, pumps, shelter, and instrumentation.

Construction time also varies with both the size and complexity of the model. About 1 to 3 months are normally required, except in movable-bed models where the requirement exists for remolding the model bed after each test or series of tests. A short period of construction time is then required intermittently as the testing program is pursued; however, a substantial period of time is required for model verification after completion of construction. This is, in essence, a trial-and-error procedure and the amount of time necessary to verify the inlet model again can vary with the size and complexity. Depending on the personnel available, verification time can extend from 1 to 4 months.

The actual testing program of a single inlet can extend from a few weeks to as long as a year or more. Several different plans will probably be tested and occasionally it is necessary to conduct hydraulic tests of currents and water surface elevation changes in a fixed-bed model, and then convert a section of the area to a movable-bed variety to investigate the littoral effects produced by the various alternative plans. These are considered high-cost model studies since the entire construction, verification, and testing can extend over 2 or more years with a total cost exceeding $500,000 (in 1976 dollars).

LITERATURE CITED

BOBB, W.H., and BOLAND, R.A., Jr., "Channel Improvement, Fire Island Inlet, New York; Hydraulic Model Investigation," Technical Report H-69-16, U.S. Army Engineer Waterways Experiment Station, Vicksburg, Miss., Nov. 1969.

BOBB, W.H., and BOLAND, R.A., Jr., "Effects of Proposed Barriers on Tides, Currents, Salinities, and Dye Dispersion for Normal Tide Conditions," *Galveston Bay Hurricane Surge Study*; Report 2, Technical Report H-69-12, U.S. Army Engineer Waterways Experiment Station, Vicksburg, Miss., July 1970a.

BOBB, W.H., and BOLAND, R.A., Jr., "Effects of Plan 2 Alpha and Plan 2 Gamma Barriers on Tides, Currents, Salinities, and Dye Dispersion for Normal Tide Conditions; Hydraulic Model Investigation," *Galveston Bay Hurricane Surge Study*; Report 3, Technical Report H-69-12, U.S. Army Engineer Waterways Experiment Station, Vicksburg, Miss., July 1970b.

BROGDON, N.J., "Effects of Proposed Barriers on Hurricane Surge Heights; Hydraulic Model Investigation," *Galveston Bay Hurricane Surge Study*; Report 1, Technical Report H-69-12, U.S. Army Engineer Waterways Experiment Station, Vicksburg, Miss., Sept. 1969.

EINSTEIN, H.A., and CHIEN, N., "Similarity of Distorted River Models with Movable Bed." *Proceedings of the American Society of Civil Engineers*, Vol. 80, No. 566, Dec. 1954.

GESSLER, J., "Modeling of Fluvial Processes," *River Mechanics*, Ch. 21, Vol. II, Colorado State University Press, Fort Collins, Colo., 1971.

GRAF, W.H., *Hydraulics of Sediment Transport*, McGraw-Hill Book Co., New York, 1971, pp. 513.

KAMPHUIS, J.W. "Coastal Mobile Bed Model--Does it Work?" *Proceedings of the second Annual Symposium on Modeling Techniques*, 1975, pp. 993-1009.

LE MEHAUTE, B., "Comparison of Fluvial and Coastal Similitude," *Proceedings of the 12th Conference on Coastal Engineering*, 1970, pp. 1077-1096.

LETTER, J.V., Jr., and McANALLY, W.H., Jr., "Physical Hydraulic Models: Assessment of Predictive Capabilities; Movable-Bed Model of Galveston Harbor Entrance," Report 2, Research Report H-75-3, U.S. Army Engineer Waterways Experiment Station, Vicksburg, Miss., Nov. 1977.

McNAIR, E.C., Jr., and HILL, T.C., "Summary Report; Model Studies of Shrewsbury Inlet," Miscellaneous Paper H-72-2, U.S. Army Engineer Waterways Experiment Station, Vicksburg, Miss., Mar. 1972.

MIGNIOT, C., ORGERON, C., and BIESEL, F., "LCHF Coastal Sediment Modeling Techniques," *Proceedings of the second Annual Symposium on Modeling Techniques*, San Francisco, Calif., 1975, pp. 1638-1657.

SAGER, R.A., and McNAIR, E.C., Jr., "Effects of Proposed Barriers on Hurricane Surge Heights; Hydraulic Model Investigation; Appendix A; Calibration Tests; Hydraulic Model Investigation," *Galveston Bay Hurricane Surge Study*, Report 1, Technical Report H-69-12, U.S. Army Engineer Waterways Experiment Station, Vicksburg, Miss., Mar. 1973a.

SAGER, R.A., and McNAIR, E.C., Jr., "Effects of Proposed Barriers on Tides, Currents, Salinities, and Dye Dispersion for Normal Tide Conditions; Appendix B; Calibration Tests; Hydraulic Model Investigation," *Galveston Bay Hurricane Surge Study*, Report 2, Technical Report H-69-12, U.S. Army Engineer Waterways Experiment Station, Vicksburg, Miss., Mar. 1973b.

SCHURING, D.J., *Scale Models in Engineering; Fundamentals and Applications*, Pergamon Press, New York, 1977, pp. 299.

SIMMONS, H.B., and BOLAND, R.A., Jr., "Model Study of Galveston Harbor Entrance, Texas; Hydraulic Model Investigation," Technical Report H-69-2, U.S. Army Engineer Waterways Experiment Station, Vicksburg, Miss., Feb. 1969.

APPENDIX

SYMBOLS AND DEFINITIONS

Symbol	Definition	Dimension	Unit
A	Area	L^2	ft^2
$A_1, A_2, \ldots A_n$	A set of n variables in the π theorem	--	--
a	Acceleration	L/T^2	ft/sec^2
	•Moment arm of force P (Fig. 6-38)	L	ft
a,b,c	Parapet moment arms (Fig. 6-40)	L	ft
a,b,c,d	Linear dimensions necessary to define the geometrical boundary conditions	L	ft
a_1	Wave amplitude at input line	L	ft
B	Flume width	L	ft
b	Width	L	ft
	•Bottom width of wave generator plunger (Fig. 6-9)	L	ft
	•Moment arm of force W (Fig. 6-40)	L	ft
C	Coriolis force	F	lb
	•Constant (Eq 2-25)	--	--
C'	Constant (Eq 2-26)	--	--
C_{bm}	Acoustical velocity of shock front in breakwater material	L/T	ft/sec
C_D	Drag coefficient	--	--
C_d	Discharge coefficient for an orifice or inlet	--	--
C_h	Chezy coefficient	--	--
C_w	Acoustical velocity of shock front in water	L/T	ft/sec
c	Specific heat of water	--	Btu/lb/°F
	•Moment arm of uplift force U (Fig. 6-38)	L	ft
C_{at}	Velocity of sound in outside air	L/T	ft/sec
c.p.	Center of pressure distance (Fig. 6-16)	L	ft
D	Effective diameter of stone	L	ft
	•Sediment particle diameter (Section V only)	L	ft; mm
	•Damage to rubble-mound breakwater cover layer (Section VI only)	--	percent
	•Depth of narrowest part of pneumatic chamber nozzle (Eq 6-37; Fig. 6-10)	L	ft
$\overline{DF}$	Linear scale distortion factor	--	--
D_p	Effective stone diameter of prototype core material (Fig. 4-5)	L	cm

Symbol	Definition	Dimension	Unit
D_s	Sediment particle size	L	ft; mm
D_{50}	50-percent-finer-than particle diameter	L	ft; mm
D_*	Dimensionless sediment size (Section V only)	--	--
d	Depth	L	ft
d_1	Distance from stillwater level to crest of rubble-mound base of composite breakwater (Fig. 6-3)	L	ft
E	Energy	LF	ft-lb
	•Modulus of elasticity	F/L^2	lb/ft^2
	•Dispersion coefficient (Section III only)	L^2/T	ft^2/sec
E	Dispersion coefficient in salinity intrusion region	L^2/T	ft^2/sec
E_{bm}	Modulus of elasticity of breakwater material	F/L^2	lb/ft^2
E'_{bm}	Bulk modulus of elasticity of breakwater material	F/L^2	lb/ft^2
E_L	Longitudinal dispersion coefficient in uniform density fluid	L^2/T	ft^2/sec
E_N	Modulus of elasticity of nylon	F/L^2	lb/ft^2
E_n	Euler number	--	--
E_w	Modulus of elasticity of water	F/L^2	lb/ft^2
e	Base of natural logarithms (2.71828)	--	--
F	Force	F	lb
	•Reads "function of"	--	--
	•Froude number (Section V only)	--	--
	•Total horizontal wave force on vertical-wall parapet (Fig. 6-38; Eq 6-43)	F	lb
F_e	Elastic compression force	F	lb
F_f	Friction force between base of parapet and crest of rubble-mound breakwater	F	lb
F_g	Gravity force	F	lb
F_i	Inertia force	F	lb
F_n	Froude number	--	--
F_{pr}	Pressure force	F	lb
F_{st}	Surface tension force	F	lb
F_μ	Viscous force	F	lb
F_*	Densimetric Froude number	--	--
	•Boundary layer densimetric Froude number (Section V only)	--	--
f	Friction factor	--	--

Symbol	Definition	Dimension	Unit
f, f', f''	Reads "Function of"	--	--
$\overline{f}$	Friction factor (Section V only)	--	--
g	Gravitational acceleration (32.2 ft/sec^2)	L/T^2	ft/sec^2
H	Wave height	L	ft
	•Artificial heat input (Eq 3-20)	--	Btu/hr
$H_{D=O}$	Model-selected design wave height for no-damage criterion	L	ft
H_{dim}	Dimensionless wave height, defined as $\rho_w gH/p_{at}$	--	--
H_i	Incident wave height	L	ft
H_t	Transmitted wave height	L	ft
	•Wave height at time t (Eq 4-25)	L	ft
$H_{1/3}$	Significant wave height	L	ft
H_1	Wave height at x = O in a flume (Eq 4-28)	L	ft
H_2	Wave height at x > O in a flume (Eq 4-28)	L	ft
$\Delta H/\Delta L$	Gradient of head loss through voids in rubble-mound breakwater core material, where $\Delta H = H_i$	L/L	ft/ft
h	Distance from stillwater level to bottom of prismatic wave generator plunger in neutral position (Fig. 6-9)	L	ft
	•Water depth above parapet (Fig. 6-38)	L	ft
Δh	Hydraulic head across an inlet	L	ft
h_T	Elevation of pneumatic chamber ceiling (height of tank)	L	ft
h_w	Elevation of water in pneumatic chamber at start of wave formation	L	ft
I	Area moment of inertia	L^4	ft^4
I_M	Mass moment of inertia	FT^2L	lb-sec^2-ft
K	Dimensionless number, defined by Eq 2-41 (Eq 2-41 through 2-46)	--	--
	•Net surface heat exchange coefficient (Eq 3-20)	-	Btu/(ft^2-hr-^{o}F)
	•Coefficient (>1) (Eq 4-32, 4-40, 4-44; Tables 4-2, 4-4; Figs. 4-5, 4-6)	--	
	•Wave number ($2\pi/L$) (Section V only)	L^{-1}	ft^{-1}
	•Stability coefficient (Eq 6-4a, 6-4b, 6-5)	--	--
	•Dimensionless constant (Eq 6-7)	--	--
	•Constant defined by Eq 6-33	$L^{-2}T^{-1}$	ft^{-2}-sec^{-1}
K'	Dimensionless number, defined by Eq 2-71	--	--

Symbol	Definition	Dimension	Unit
K_K	Coefficient in Eq. 4-32 as determined by Keulegan method	–	–
K_L	Coefficient in Eq 4-32 as determined by LeMéhauté method	–	–
K_r	Surface heat exchange scale	–	–
K_Δ	Stability coefficient for a particular armor-unit shape	–	–
k	Number of fundamental dimensions in the variables of a problem (Section II)	–	–
	• Adiabatic constant of air (Eq 6-6)	–	–
	• Constant, the value of which depends on the distribution of a loading force (Eq 6-12)	–	–
	• Wave generator shape coefficient (Eq 6-24)	–	–
$k_{\Delta P}$	Experimental stone or armor unit shape-placing coefficient	–	–
k_v	Stone or armor-unit shape coefficient	–	–
k_1	Coefficient defined by Eq 6-30	–	–
k_2	Coefficient defined by Eq 6-28	T^{-1}	sec^{-1}
L	Length	L	ft
	• Wavelength (Section V only)	L	ft
	• Vertical component of resultant force on structure (Fig. 6-16)	F	lb
ΔL	Average width of core-material section of rubble-mound structure	L	ft
L_c	Characteristic horizontal length, e.g., width of a bay mouth	L	ft
L_r	Linear scale of an undistorted-scale model	–	–
ℓ	Length of pendulum (Eq 2-27, 2-28)	L	ft
	• Length of pneumatic chamber (Fig. 6-10; Eq 6-28, 6-29)	L	ft
ℓ, m, n	Direction cosines of a normal to a boundary (Eq 2-31b, 2-65)	–	–
$(\ell_c)_a$	Characteristic linear dimension of armor unit	L	ft
$(\ell_c)_G$	Characteristic linear dimension of wave generator	L	ft
M	Mass	FT^2/L	$lb\text{-}sec^2/ft$
	• Moment of resultant force about structure toe (Fig. 6-16)	LF	ft-lb
M_n	Mach-Cauchy number	–	–

Symbol	Definition	Dimension	Unit
M_p	Moment of resultant force about a fixed balance pivot (Fig. 6-16)	LF	ft-lb
M_2	Principal lunar semidiurnal tidal harmonic constituent	L	ft
m	Arbitrary exponent (Section V only)	--	--
N	The dimensionless ratio L_c/d_c	--	--
N_s	Rubble-mound breakwater stability number $(K \cot \alpha)^{1/3}$	--	--
n	Number of variables in a problem	--	--
	•Manning's coefficient of roughness	$T/L^{1/3}$	$sec/ft^{1/3}$
	•Unit vector normal to boundary (Eq 2-31a)	L	ft
	•Number of layers of armor units or underlayer stones in a rubble-mound breakwater (Eq 6-40)	--	--
n_{quan}	Scale ratio of specified quantity (Section V only)	--	--
P	Porosity of armor units, underlayers, or core material after placement on breakwater ($P < 1$)	--	--
	•Maximum horizontal wave force on parapet as determined by model tests (Figs. 6-34, 6-38, 6-40)	F	lb
P_t	Armor-unit placing technique	--	--
p	Pressure	F/L^2	lb/ft^2
	•Arbitrary exponent (Section V only)	--	--
p_o	Pressure in pneumatic chamber relative to atmosphere (Eq 6-32)	F/L^2	lb/ft^2
Δp	Increment of pressure	F/L^2	lb/ft^2
	•Suction pressure in pneumatic chamber during subsequent wave motion (Eq 6-30)	F/L^2	lb/ft^2
Δp_i	Suction pressure in pneumatic chamber at beginning of wave motion (Eq 6-30)	F/L^2	lb/ft^2
p_{max}	Maximum pressure on vertical wall (Eq 6-7)	F/L^2	lb/ft^2
Δp_o	Initial suction pressure in pneumatic chamber required to raise water to height h_w ($\Delta p_o > o$) (Eq 6-30 through 6-33)	F/L^2	lb/ft^2
p_t	Theoretical maximum shock pressure on vertical wall (Eq 6-8)	F/L^2	lb/ft^2
Q	Discharge	L^3/T	ft^3/sec
Q',Q''	Reads "function of"	--	--

Symbol	Definition	Dimension	Unit
Q_{air}	Discharge of air from the orifices of a submerged manifold, per ft of manifold	$L^3/T/L$	$ft^3/sec/ft$ length
$(Q_{air})_{at}$	Discharge of free air delivered by a compressor to a manifold, per ft of manifold	$L^3/T/L$	$ft^3/sec/ft$ length
Q_w	Discharge of water from the orifices of a submerged manifold, per ft of manifold	$L^3/T/L$	$ft^3/sec/ft$ length
q	Lateral discharge per unit of horizontal length	$L^3/T/L$	$ft^3/sec/ft$ length
	•Arbitrary exponent (Section V only)	--	--
R	Hydraulic radius	L	ft
	•Resultant force on structure (Fig. 6-16)	F	lb
	•Reynolds number (Section V only)	--	--
R_n	Reynolds number	--	--
$(R_n)_C$	Critical Reynolds number	--	--
R_*	Reynolds number for initiation of sediment motion (Section V only)	--	--
r	Arbitrary exponent (Section V only)	--	--
	•Radius of cylindrical plunger (Fig. 6-9)	L	ft
S	Wave generator stroke (Eq 6-23; Fig. 6-9)	L	ft
	•Channel slope (Eq 7-9)	L/L	ft/ft
S_a	Specific gravity of armor unit	--	--
S_E	Slope of energy gradient	L/L	ft/ft
S_2	Principal solar semidiurnal tidal harmonic constituent	L	ft
S_{11}, S_{12}	Maximum runup in x and y directions, respectively	L	ft
s	Salinity concentration •ppt = parts per thousand •p/m = parts per million; also abbreviated ppm	–	ppt; p/m
sg	Specific gravity (Section V only)	--	–
T	Time	T	sec
	•Wave period	T	sec
	•Period of pendulum (Eq 2-27, 2-28)	T	sec
	•Temperature (Eq 3-17, 3-20)	–	°F
	•Horizontal component of resultant force on structure (Fig. 6-16)	F	lb
T_e	Equilibrium temperature	–	°F
T_o	Turning moment about landside toe of parapet (Fig. 6-40)	LF	ft-lb
$T_{1/3}$	Significant wave period	T	sec
t	Time	T	sec
	•Thickness of n layers of armor units or underlayer stones in rubble-mound structure (Eq 6-40, 6-41)	L	ft

Symbol	Definition	Dimension	Unit
t'	Time required to reduce wave height 50 percent by internal friction	T	sec
U	Cross-sectional area tidal velocity (Section III)	L/T	ft/sec
	•Total uplift force on parapet due to waves (Fig. 6-38)	F	lb
U'	Dimensionless velocity in x direction defined as $u/(gd_c)^{1/2}$	--	--
u	Velocity in x direction	L/T	ft/sec
u_2	Velocity of wave particle at nozzle mouth (Eq 6-34)	L/T	ft/sec
u_2, v_2	Velocity components on the shoreline (Eq 2-66, 2-93)	L/T	ft/sec
u_*	Shear velocity (Section V only)	L/T	ft/sec
V	Velocity	L/T	ft/sec
	•Velocity of wave propagation (phase velocity) (Eq 4-10 through 4-17b; Fig. 4-1; Eq 6-24 through 6-26, 6-35, and 6-36)	L/T	ft/sec
V'	Dimensionless velocity in y direction, defined as $v/(gd_c)^{1/2}$	--	--
$\overline{V}$	Volume	L^3	ft^3
$(\overline{V}_{air})_o$	Initial volume of air in pneumatic chamber, per foot of chamber	L^3/L	ft^3/ft length
$\overline{V}_T$	Total volume	L^3	ft^3
$\overline{V}_v$	Volume of voids	L^3	ft^3
V_w	Velocity of water impinging on breakwater slope	L/T	ft/sec
$\overline{V}_w$	Volume of water displaced per foot length of generator in T/2 sec	$L^3/T/L$	ft^3/sec/ft of generator
$\Delta\overline{V}_w$	Volume of water leaking around ends and bottom of wave generator per foot length of generator in T/2 sec	$L^3/T/L$	ft^3/sec/ft of generator
v	Velocity in y direction	L/T	ft/sec
W	Weight	F	lb
W_a	Weight of individual armor units	F	lb
$\overline{W}_a$	Total weight of armor units in a cover layer of thickness t for a given surface area	F	lb
W_n	Weber number	--	--
W_p	Weight of parapet (Eq 6-43)	F	lb
w	Velocity in z direction	L/T	ft/sec
	•Settling velocity (Section V only)	L/T	ft/sec
X	Dimensionless length in x direction, defined as x/L_c	--	--

Symbol	Definition	Dimension	Unit
X_1	Dimensionless length in x direction along the input line	–	–
x	Longitudinal length	L	ft
x_p	Distance of wave travel for wave to be reduced by 50 percent by internal friction (Eq 4-27; Fig. 4-2)	L	ft
x,y	Horizontal and vertical distances, respectively, of the pivot from the structure toe (Fig. 6-16)	L	ft
x_1,y_1	Coordinates of a point on a given input line	L	ft
x_2,y_2	Coordinates of a point on a coastline	L	ft
x,y,z	Longitudinal, lateral, and vertical coordinates, respectively	L	ft
	•Exponents in π terms	–	–
x_o,y_o,z_o	Coordinates of a point on a solid boundary	L	ft
Y	Dimensionless length in y direction, defined as y/L_c	–	–
Y_1	Dimensionless length in y direction along input line	–	–
y	Lateral length	L	ft
Z	Dimensionless depth, defined as z/d_c	–	–
z	Vertical length	L	ft
	•Depth below water surface (Eq 6-20)	L	ft
α	Exponent, defined by Eq 4-29 (Eq 4-28 through 4-31; Figs. 4-3, 4-4)	L^{-1}	ft^{-1}
	•Angle of seaside slope of breakwater measured from the horizontal	–	degrees
	•Angle of wave-generator plunger face, measured from the vertical (Fig. 6-9)	–	degrees
	•Angular acceleration (Fig. 6-40)	T^{-2}	rad/sec^2
β	Angle of wave attack	–	degrees
γ	Specific weight	F/L^3	lb/ft^3
	•Ratio of specific heats (Eq 6-32, 6-33)	–	–
γ'	Relative specific weight of sediment in fluid, defined as $(\gamma_s - \gamma_f)/\gamma_f$ (Section V only)	–	–
Δ	Shape factor of armor units (Eq 6-1 through 6-5)	–	–
	•Deflection of cable (Eq 6-12)	L	ft
δ	Fall of water surface in pneumatic chamber during wave generation	L	ft
η	Surface displacement from the undisturbed water level	L	ft

Symbol	Definition	Dimension	Unit
η'	Dimensionless surface displacement, defined as η/d_c	--	--
η_1	Surface displacement from undisturbed water level along the input line	L	ft
η_1'	Dimensionless surface displacement from undisturbed water level along the input line, defined as η_1/d_c	--	--
Θ	Dimensionless depth, defined as d/d_c	--	--
θ	Angular displacement of pendulum from the vertical	--	radians
	•Angle of bottom slope seaward of structure, measured from the horizontal (Eq 6-1 through 6-6)	--	degrees
	•Angle of inclination of the resultant force, measured from the horizontal (Fig. 6-16)	--	degrees
	•Angle of rotation of parapet about the landside toe (Fig. 6-40)	--	radians
	•Angle of anchor chain from bottom, measured from the horizontal (Fig. 6-52)	--	degrees
λ	Wavelength	L	ft
	•Horizontal linear scale (Section V only)	--	--
$(\lambda_c)_{min}$	Wavelength at which the velocity of a surface tension wave is a minimum	L	ft
μ	Dynamic viscosity	FT/L^2	lb-sec/ft^2
	•Vertical linear scale (Section V only)	--	--
ν	Kinematic viscosity	L^2/T	ft^2/sec
$(\xi_c)_a$	Characteristic linear dimension of armor unit surface roughness	L	ft
π	Refers to the Buckingham theorem (usually referred to as the pi (π) theorem) in which $\pi = f(\pi_1, \pi_2, \ldots \pi_{n-k})$ and π_1, π_2, etc. are dimensionless products	--	--
ρ	Density	FT^2/L^4	lb-sec^2/ft^4
$\Delta\rho$	Density differential	FT^2/L^4	lb-sec^2/ft^4
σ	Surface tension	F/L	lb/ft
τ	Dimensionless time, defined as t/T_c	--	--
τ_*	Shields parameter	--	--
Φ	Dimensionless velocity potential, defined as $\phi T_c/L_c^2$	--	--
ϕ	Velocity potential (Eq 2-29 through 2-35)	L^2/T	ft^2/sec
	•Reads "function of" (Eq 2-22)	--	--
	•Latitude (Eq 3-23)	--	degrees

Symbol	Definition	Dimension	Unit
Ω	Scale distortion factor (Section V only)	--	--
ω	Angular velocity of Earth's rotation	T^{-1}	rad/sec
	•Angular frequency (Fig. 6-40)	T^{-1}	rad/sec

SUBSCRIPTS

Symbol	Refers to
a	Armor unit
air	Air
at	Atmosphere
bm	Breakwater material
C	Critical value
c	Characteristic value
D	Damage ($H_{D=o}$)
	•Drag (C_D)
	•Sediment diameter (Section V only)
d	Discharge
E	Energy
e	Elastic compression
	•Equilibrium (T_e)
F	Froude number (Section V only)
F_*	Densimetric Froude number (Section V only)
f	Fluid
	•Friction (F_f)
$\overline{f}$	Friction factor (Section V only)
G	Wave generator
g	Gravity
H	Wave height (Section V only)
h	Chezy (C_h)
	•Horizontal
i	Incident (H_i)
	•Inertia
	•Initial (Δp_i)
K	Keulegan
L	Le Mehaute (K_L)
	•Longitudinal (E_L)
	•Wavelength (Section V only)
M	Mass

Symbol	Refers to
m	Model
N	Nylon
n	Dimensionless quantity (such as Froude or Reynolds number)
	•Number of variables in a set or series
o	Reference value
P	Parapet
ΔP	Shape-placing
p	Pivot point (M_p)
	•Prototype
	•Prototype core material (D_p in Fig. 4-5)
pr	Pressure
r	Ratio
s	Sediment
	•Stability (N_s)
st	Surface tension
T	Pneumatic wave chamber ceiling (h_T)
	•Total ($\overline{V}_T$)
	•Wave period (Section V only)
t	Technique (p_t)
	•Theoretical (p_t in Eq 6-8)
	•Time
	•Transmitted (H_t)
u	Horizontal velocity (Section V only)
u_*	Shear velocity (Section V only)
v	Vertical
	•Voids ($\overline{V}_v$)
	•Shape (k_v)
w	Settling velocity (Section V only)
	•Water
x	Longitudinal direction
y	Lateral direction
z	Vertical direction
γ	Specific weight (Section V only)
γ'	Relative specific weight (Section V only)
Δ	Stability
λ	Wavelength
μ	Dynamic viscosity

☆ U. S. GOVERNMENT PRINTING OFFICE : 1979 629-744/2376

Hudson, Robert Y.

Coastal hydraulic models / by Robert Y. Hudson, Frank A. Herrmann, Jr. ...[et al.]. – Ft. Belvoir, Va. : U.S. Coastal Engineering Research Center, 1979.

531 p. : ill. (Special report – U.S. Coastal Engineering Research Center ; no. 5)

Includes bibliographies.

This comprehensive report describes the use of hydraulic models to assist in the solution of complex coastal engineering problems. The report provides information for use by both the laboratory research engineer and the field design engineer on the capabilities and limitations of coastal hydraulic modeling procedures.

1. Beach erosion. 2. Harbors. 3. Hydraulic models. 4. Inlets. 5. Movable-beds – Models. I. Title. II. Herrmann, Frank A., jt. auth. III. Series: U.S. Coastal Engineering Research Center. Special report no. 5.

Hudson, Robert Y.

Coastal hydraulic models / by Robert Y. Hudson, Frank A. Herrmann, Jr. ...[et al.]. – Ft. Belvoir, Va. : U.S. Coastal Engineering Research Center, 1979.

531 p. : ill. (Special report – U.S. Coastal Engineering Research Center ; no. 5)

Includes bibliographies.

This comprehensive report describes the use of hydraulic models to assist in the solution of complex coastal engineering problems. The report provides information for use by both the laboratory research engineer and the field design engineer on the capabilities and limitations of coastal hydraulic modeling procedures.

1. Beach erosion. 2. Harbors. 3. Hydraulic models. 4. Inlets. 5. Movable-beds – Models. I. Title. II. Herrmann, Frank A., jt. auth. III. Series: U.S. Coastal Engineering Research Center. Special report no. 5.

TC203 .U581sr no. 5 627

Hudson, Robert Y.

Coastal hydraulic models / by Robert Y. Hudson, Frank A. Herrmann, Jr. ...[et al.]. – Ft. Belvoir, Va. : U.S. Coastal Engineering Research Center, 1979.

531 p. : ill. (Special report – U.S. Coastal Engineering Research Center ; no. 5)

Includes bibliographies.

This comprehensive report describes the use of hydraulic models to assist in the solution of complex coastal engineering problems. The report provides information for use by both the laboratory research engineer and the field design engineer on the capabilities and limitations of coastal hydraulic modeling procedures.

1. Beach erosion. 2. Harbors. 3. Hydraulic models. 4. Inlets. 5. Movable-beds – Models. I. Title. II. Herrmann, Frank A., jt. auth. III. Series: U.S. Coastal Engineering Research Center. Special report no. 5.

TC203 .U581sr no. 5 627

Hudson, Robert Y.

Coastal hydraulic models / by Robert Y. Hudson, Frank A. Herrmann, Jr. ...[et al.]. – Ft. Belvoir, Va. : U.S. Coastal Engineering Research Center, 1979.

531 p. : ill. (Special report – U.S. Coastal Engineering Research Center ; no. 5)

Includes bibliographies.

This comprehensive report describes the use of hydraulic models to assist in the solution of complex coastal engineering problems. The report provides information for use by both the laboratory research engineer and the field design engineer on the capabilities and limitations of coastal hydraulic modeling procedures.

1. Beach erosion. 2. Harbors. 3. Hydraulic models. 4. Inlets. 5. Movable-beds – Models. I. Title. II. Herrmann, Frank A., jt. auth. III. Series: U.S. Coastal Engineering Research Center. Special report no. 5.

TC203 .U581sr no. 5 627